RUSSIAN ACADEMY OF SCIENCES

SECTION “MEMBRANES AND MEMBRANE TECHNOLOGIES” OF D.I. MENDELEEV
RUSSIAN CHEMICAL SOCIETY

RUSSIAN FOUNDATION FOR BASIC RESEARCH

RAS SCIENTIFIC COUNCIL ON PHYSICAL CHEMISTRY

RUSSIAN MEMBRANE NETWORK

KUBAN STATE UNIVERSITY

«MEMBRANE TECHNOLOGY» INNOVATION ENTERPRISE

N.S. KURNAKOV INSTITUTE OF GENERAL AND INORGANIC CHEMISTRY RAS

INTERNATIONAL CONFERENCE

Ion transport in organic and inorganic membranes

Conference Proceedings

2 - 7 June 2013

Krasnodar 2013

SCIENTIFIC/ORGANIZING COMMITTEE

YAROSLAVTSEV A.B.	**Chairman,** Corresponding Member RAS, Prof., Kurnakov Institute of General and Inorganic Chemistry, RAS, Moscow, Russia
ZABOLOTSKY V.I.	**Co-chairman,** Academician Int. Hi. Ed. Acad., Prof., Head of the Membrane institute, Kuban State University, Krasnodar, Russia
POURCELLY G.	**Co-chairman**, Prof., Institut Européen des Membranes, Université de Montpellier II, Montpellier, France
AGEEV E.P.	Prof., Moscow State University, Moscow, Russia
BEREZINA N.P.,	Prof., Kuban State University, Krasnodar, Russia
BILDYUKEVICH A.V.	Prof., Institute of Physico-Organic Chemistry NAS, Minsk, Belarus
DAMMAK L.	Prof., Institut de Chimie et des Matériaux – Université Paris-Est, Paris, France
FILIPPOV A.N.	Prof., Gubkin Russian State University of Oil and Gas, Moscow, Russia
GNUSIN N.P.	Prof., Kuban State University, Krasnodar, Russia
GRAFOV B.M.	Prof., Frumkin Institute of Physical Chemistry and Electrochemistry RAS, Moscow, Russia
KHOHLOV A.R.	Academician RAS, Prof., Moscow State University, Moscow, Russia
KONONENKO N.A.	**Scientific secretary**, Prof., Kuban State University, Krasnodar, Russia
LARCHET C.	Prof., Institut de Chimie et des Matériaux – Université Paris-Est, Paris, France
NIKONENKO V.V.	**Scientific secretary**, Prof., Kuban State University, Krasnodar, Russia
NOVAK L.	President, MEGA, Strazh pod Ralskem, Czech Republic
OZERIN A.N.	Corresponding Member RAS, Prof., Karpov Physical Chemistry Institute, Moscow, Russia
PISMENSKAYA N.D.	Prof., Kuban State University, Krasnodar, Russia
RUBINSTEIN I.	Prof., The Jakob Blaustein Institutes for Desert Research, Sede Boker Campus, Israel
SHAPOSHNIK V.A.	Prof., Voronezh State University, Voronezh, Russia
SHUDRENKO A.A.	General director., Noncommercial Partnership Innovation-Technology Centre "Kuban-Yug", Russia
SISTAT P.	Prof., Institut Européen des Membranes, Université de Montpellier II, Montpellier, France
STAROV V.M.	Prof., Loughborough University, Leicestershire, UK
TSKHAY A.A.	President, JSC Membrane Technologies, Almaty, Kazakhstan
VOLFKOVICH Yu.M.	Prof., Frumkin Institute of Physical Chemistry and Electrochemistry RAS, Moscow, Russia
VOLKOV V.V.	Prof., Topchiev Institute of Petrochemical Synthesis RAS, Moscow, Russia

International French-Russian **A**ssociated **L**aboratory
“**I**on-**E**xchange **M**embranes and **R**elated **P**rocesses” ***IAL IEMRP***

The beginning of the official activity of the ***IAL IEMRP*** is the January 2011 while collaboration of the partners occurs since 1994. This collaboration was made within several European (INTAS) and numerous bilateral projects.

The activity of the ***IAL IEMRP*** is aimed at the **generation of knowledge** needed for the enhancement of ion-exchange membranes (IEMs) and the optimization of the conditions of their use in different applications. It is known that these applications are based on the permselective properties of IEMs conditioned by their structure at the nanometer scale. The ability to control the membrane structure and the deep understanding of interfacial phenomena and transport properties act a fundamental role in the development of novel membranes. On the other hand, *physico-chemical conditions of operation* (electric and hydrodynamic) are also very important, hence they are in the field of interest of the French-Russian laboratory as well.

In the joint research program, four general axes are established:
1) Structure-properties» relations and impact on the trans-membrane transfer;
2) Role of the surface properties in overall membrane behavior;
3) Interfacial phenomena at the ion-exchange material/solution boundary;
4) Confrontation of mathematical modeling and experimental research.

High attention is paid to the development of theoretical mathematical models, following the well-known quote of Kurt Lewin: “There is nothing more practical than a good theory”.

In addition to joint scientific research, educational and organizational works are within the scope of the laboratory activity.

There are four teams in the structure of ***IAL IEMRP***: two ones from the French side, European Membrane Institute (**EMI**) CNRS-University Montpellier 2- High National School of Chemistry, Montpellier, and Institute of Chemistry and Materials -CNRS-University Paris-Est (**ICMPE**), Paris; and two ones from the Russian side: Kuban State University, Krasnodar, and Kurnakov Institute of General and Inorganic Chemistry of RAS, Moscow. The director of ***IAL IEMRP*** is Professor Gerald Pourcelly, the Russian co-director is Professor Victor Nikonenko.

Up to now, the main achievements of the laboratory are:

- 10 validated international collaboration projects (PICS, INTAS, PECO-CEI, PECO-NEI)
- 52 joint papers in international journals (Thomson data base)
- 3 book chapters
- 54 international communications
- 5 Ph-D (two on-going ones)
- 13 common organizations of conferences (mainly in Tuapse)

In Russia the collaboration is supported by Russian Foundation of Basic Research. There are 4 on-going projects and 1 project (M. Urtenov) recently submitted:

- **A. Yaroslavtsev** (***IGIC***): Effect of inorganic nanoparticles immobilized in nanopores on the transfer properties of organic ion-exchange membranes
- **V. Nikonenko** (***KubSU***): « Structure-properties » relationships for ion-exchange membranes; the effect of membrane nanostructure on ion and water transport
- **V. Zabolotsky** (***KubSU***): Effect of ion-exchange membrane surface heterogeneity on its electrochemical behavior
- **N. Pismenskaya** (***KubSU***): Ampholyte transfer in electrodialysis processing of dilute solutions
- **M. Urtenov** (***KubSU***): Electroconvective mechanism of overlimiting transfer in membrane systems: mathematical modeling and experiment.

A very appreciated support is provided by the **European Project Marie Curie FP7 IRSES People 2010 (2011-2015)** COTRAPHEN: “Coupled ion and volume transfer phenomena in heterogeneous systems: Experiment and applications in clean energy, micro-analysis and water treatment”. Its Coordinator is Prof Andriy Yaroshchuk (Catalunia University, Barcelona). **EMI (Montpelier), ICMPE (Paris)** and **KubSU (Krasnodar)** are involved in. Every year 5-6 young researchers participate in exchange among Barcelona, Montpellier, Paris and Krasnodar.

Activity of ***IAL IEMRP*** is growing out of the framework of French-Russian collaboration. In addition to Barcelona (a master student from the Catalunia University, Monica Reig, is staying now at KubSU for a 2-month traineeship), Laval University, Quebec, Canada, is a new partner of this cooperation. Seguei Mikhylin, the PhD student at this university makes his traineeship at KubSU.

On April, 8, 2013, a meeting of a Steering Committee, organized by the CNRS of France was held in order to overview the activity of the ***IAL IEMRP***.

The meeting in Paris in spring 2013

The activity of all teams was highly appreciated, and, in whole, this International Associated Laboratory was assessed as the best one over 27 on-going IAL supported by the Institut of Chemistry of CNRS, France. The next meeting will be scheduled in Moscow in spring 2014.

Physical Chemistry Department jubilees

Between the 38th (held in Agoy in 2012) and 39th (which is planned in 2013) conferences at the Physical Chemistry Department of Kuban State University professors Sheldeshov N.V., Berezina N.P. and Nikonenko V.V. had celebrated their jubilees (September 2012, October 2012 and February 2013 relatively). I would like to remember today how our young professors Kolya Sheldeshov and Vitya Nikonenko had become well-known, meritorious specialists in membrane science and technology. Truly they passed the famous school of membrane seminars which have been established by Professor N.P. Gnusin in 1975.

Kolya Sheldeshov came to the Department being a 3-course student and began to investigate bipolar membrane properties under supervision of Nikolay Petrovich Gnusin. Natasha Pismenskaya who measured impedance and volt ampere curves of domestic membranes was among his students. The membranes have been produced at NIIPM (Scientific Research Institute of Polymer Materials) and its functions were investigating at first by V. Greben in Vladivostok. Scientific shipping for bipolar electrodialyser test was organized by Gnusin N.P. at Far East in 80th. N.V. took part in this expedition along with Vladivostok scientists. In 1985 he maintained a PhD thesis titled: “Transport of ions and water dissociation in bipolar ion-exchange membranes”; in 2002 he did a DSc thesis titled: “Processes with participation of hydrogen and hydroxyl ions in systems with ion-exchange membranes”. Quite young doctor of science Zabolotskiy V.I. took the very active participation in supervising of this work. At that time electrochemistry of bipolar membranes was created in general, basic mechanisms of proton and hydroxyl ion generation in the border of contrary charged membrane joint in the electric field were revealed. N.V. Sheldeshov was the author of more than 40 fundamental papers and provide each our conference with new results about processes occurred in mono- and bipolar membranes. But the talent of Nikolay Victorovich is not only limited with academic research and development of the complex of precise methods of impedance and transport number measurements, methods of multichamber electrodialysers study.

A lot of technological approaches of Sheldeshov became a basis of the original schemes of electromembrane technologies (in cooperative with Gnusin and Zabolotskiy). The ones not only protected with patents but operates in real technological concentrating, water treatment, amino acid and biologic cleaning dividing processes. These schemes are consisted of a number of construction solutions developed by active participation of Nikolay Victorovich.

We all know N.V. Sheldeshov’s activity as a teacher. In the course of many years he read lectures dedicated physical chemistry and created the practice and the serie of calculating methods in all fields of physical chemistry. N.V. Sheldeshov always can maintain any scheme and measurement cell as known of all our teachers and laborants.

For the latest time Sheldeshov N.V. is the vice-dean of teaching at the Faculty of Chemistry and High Technology, works in Methodological Committee of Kuban State University. He supervises diploma, course and aspirant works. He is a head of the laboratory of electromembrane technology at the Department of Physical Chemistry. In 1996 N.V. Sheldeshov was awarded as “Meritorious Member of Kuban Science and Technique”, in 2012 he was honored by Ministry of Education and Science of the Russian Federation.

Vitya Nikonenko had appeared at Physical Chemistry Department of Kuban State University as a student of Math Department of KSU. He came from Maikop Pedagogical Institute – he was a 4-year student of Mathematic Department. Merry and handsome young man at Chemistry Faculty he attracted everybody's attention at first by passing the huge examination on all chemistry to professor Y.A. Afanasyev (who was the Head of Inorganic Chemistry Department in 70th). Besides N.P. Gnusin often charged him with scientific lectures on ion-exchange resin electrochemistry and mathematic modeling at the Physical Chemistry Department seminars and it was clear that Vitya Nikonenko will be a good teacher because he could make scientific reports easy and logically.

When our annual conferences in Dzhubga started N.P. Gnusin assigned Vitya as an organizer of theoretical direction inside of seminars along with Applied Mathematic Department M.H. Urtenov and K.A. Lebedev who penetrated into electromembrane phenomenon mathematic modeling. The scientific potential of V. Nikonenko was developing during contact with Yu. Gurevich and Yu. Kharkats from Institute of Electrochemistry (Moscow) and with S. Dukhin and his colleagues from Institute of Colloid Chemistry and Chemistry of Water (Kiev). Now they are Doctors of Mathematics and work successfully in touch with V.V. Nikonenko and other electrochemists in the field of mathematic modeling.

In 1980 he maintained a thesis of candidate titled: "Steady-state electrodiffusion in ion-exchange membrane system with a ternary electrolyte solution"; in 1996 he did a thesis of doctor titled: "Mathematical modelling of electrodialysis of dilute solutions". In the same year was published the book "Ion transport in membranes". Now they are Doctors of Mathematics and work successfully in touch with V.V. Nikonenko and other electrochemists in the field of mathematical modeling. In 1980 he defunded a PhD thesis titled: "Steady-state electrodiffusion in ion-exchange membrane system with a ternary electrolyte solution"; in 1996 he did a DSc thesis titled: "Mathematical modelling of electrodialysis of dilute solutions". In the same year was published the book "Ion transport in membranes". The total number of citations of his publications according to the Russian Science Citation Index is over 2000 (the highest citing index at Kuban State University). He is the head of 30 scientific projects.

Nowadays when professor V.V. Nikonenko organized cooperative Russian-French laboratory on the basis of the Laboratory of Electromembrane Phenomena we remember the first acquaintances and meetings with our French colleagues at the International Conferences in Moscow above all in 90th (very hard time for our country). Owing to fluent French Victor Vasilyevich set up contacts with professors in Montpellier (Claude Gavach, Gérald Pourcelly), Paris (René Buvet, Christian Larchet and Bernard Auclair), and Rouen (Michel Métayer). Sociability, professional records and charm of Victor Vasilyevich surely facilitated his regular multiannual cooperation with scientists in universities of Rouen and Paris, European Membrane Institute in Montpellier as well. Exchange of postgraduates and collaborators, their continual participation in our annual conferences and cooperative publications was organized. Two postgraduates of Physical Chemistry Department – E. Laktionov and S. Parshikov maintained theses in Paris in 1997-1998. And surely V.V. Nikonenko has a great part in these events. He had opened a door to France for all other professors of our Department – V. Zabolotsky, N. Pismenskaya, N. Kononenko, N. Berezina – and of other universities – V. Shaposhnik, O. Grigorchuk, A. Yaroslavtsev, A. Tskhay, K. Tastanov. In 2001 V.V. Nikonenko maintained in Paris a third thesis titled: "Ion transport in membrane systems".

This V.V. Nikonenko's activity is mostly in the shade of his other achievements (grants, publications, patents), but a foreign tour background connects the great tugs particularly already in France as well. I for instance am grateful to Victor Vasilyevich for friendly and interesting interaction during my business trips in Paris, Montpellier and Rouen, and for booking the amicable receptions with French coworkers and friends. I believe that admirable contacts with colleagues from such a beautiful country as France are as valuable as progress in membranes and membrane processes scientific exploration.

I from the rise of my years and recollections about fortunate making of our friends would like to wish Sheldeshov N.V. and Nikonenko V.V. to achieve new success in their researches. I wish our young people who have such examples in science good luck and prosperity.

Berezina N.P.
May 2013

Ninel P. Berezina is one of the pillars of the Department of Physical Chemistry. Berezina N.P. came to Kuban State University in 1970 from the Catalysis Institute of Siberian Science Department headed by academician Boreskov G.K. She had been a head of a new laboratory of metal catalysts. Academician Frumkin A.N., her scientific supervisor, wrote the special letter of recommendation to academician Boreskov concerning Berezina Ninel because she had maintained a PhD thesis titled: “Persulphate anion electroreduction kinetics” at the Electrochemistry Department of Moscow State University in 1967.

In 1989 the Membrane Materials Laboratory was established. Natalia Kononenko and Olga Dyomina became Ninel Berezina’s stable coauthors and close friends. They gathered a first collection of ion-exchange membrane materials and made comparative analysis of these materials. The complex of experimental membrane research methods was developed on the base of professor Gnusin N.P. works. It is still used in the practice for students and postgraduates. Berezina N.P. maintained a DSc thesis titled “Corellation between the electrochemical properties and structure of ion-exchange membranes” at Electrochemistry Institute in Moscow in 1991. The course of lectures on the membrane electrochemistry and physical chemistry of ionits were prepared on the foundation of monographs of professors Gnusin and Grebenyuk “Electrochemistry of Ionits” and “Electrochemistry of Granular Ionits”. The textbook by Berezina N.P. “Electrochemistry of Membrane Systems” was published at Kuban State University in Krasnodar in 2009.


Ninel Petrovna Berezina among her disciples

An impressive number of novel methods and measurement techniques for membrane characterization were developed at this laboratory. This work is highly appreciated by the world membrane community. The review by N.P. Berezina et al. Characterization of ion-exchange membrane materials: Properties vs structure published in Advances Colloid & Interface Science 139 (2008) 3, is now cited 56 times, according to Scopus. We think, it is the absolute record for the Nb citations/year in the Russian membrane community.

A number of other investigations devoted to the determination and interpretation of ion and water transport parameters in membrane systems, to the ion-exchange membrane modification, to the development of better understanding of membrane structure and its relationships with transport properties were carried out. The results are largely used in the practice of membrane characterization and in the interpretation of charged membrane behavior.

ORGANIZING COMMITTEE

Contens

FUNDAMENTAL ASPECTS OF PROCESSES OF HEAT AND MASS TRANSFER IN CHEMICAL TECHNOLOGY

Evgeny Ageev
Lomonosov Moscow State University, Moscow, Russia,
E-mail: ageev@phys.chem.msu.ru

Technology is sometimes defined as an instrumental way of rational activity. In chemical technology rational activity is associated with physicochemical transformations in the processing of raw materials for the purpose of production of various substances and materials.

The theoretical basis of modern chemical technology consists of thermodynamics, mechanics of continua, macrokinetics, material science, mathematical modeling.

The laws which describe heat and mass transfer match to the definition. The fundamental basic Fourier conduction law and the statement of the second law of thermodynamics by Carnot are obtained in the framework of notion of the material nature of heat (caloric theory).

The basis of theoretical treatment of the processes of chemical technology are differential equations of conservation of mass, momentum and energy. In macroscopic physics a high degree of generalization is achieved by using the term “substance” – an extensive property of a material system, for which such notions as quantity, density and flux nave a meaning. Then the generalized substance balance law (Umov equation) has the form

$$\frac{\partial \rho_k}{\partial t} = -div(J_k + \rho_k \vec{v}) + I_k, \tag{1}$$

where ρ_k is the density of the substance, J_k and $\rho_k \vec{v}$ are the conductive flux and the convective stream, I_k are the sources (the sinks). If $I_k = 0$, then the balance equation becomes the conservation law.

When analyzing many processes, it is often preferable to monitor the change of properties using a moving Cartesian coordinate system, i. e. fixed on the individual particle of the medium. Then the change of a scalar property a will be

$$\frac{da}{dt} = \frac{\partial a}{\partial t} + \vec{v}\ grad\ a, \tag{2}$$

where $\frac{da}{dt}$ is the substantial derivative, $\frac{\partial a}{\partial t}$ is the local derivative of function a, $\vec{v}$ is the velocity of the coordinate movement.

By applying the Umov equation to the process of diffusion, accompanying the mass transfer when $I_k = 0$ and in the absence of convection, we obtain the non-stationary Fick law

$$\frac{\partial c_k}{\partial t} = div(D_k\ grad\ c_k) = D_k \frac{\partial^2 c_k}{\partial r^2}, \tag{3}$$

where c_k is the molar concentration, r is the coordinate.

It is often forgotten that equation (3) is valid under the following assumptions: $T, p, D = \mathrm{const}$, external fields, sources, sinks are absent, the diffusion is one-dimensional, the diffusant is binary.

It is also implicitly assumed that:

1. the macroscopic media is locally equilibrium, continuous and isotropic (the continuity);
2. the disturbance (concentration wave) propagates infinitely rapidly (the long-range action).

The latter means that the process is described by an equation with a parabolic second-order partial derivative.

The dependence of the diffusion coefficient $D = f(p, c)$ will lead to the appearance of nonlinear terms

$$\frac{\partial c_k}{\partial t} = D_k\ div\ grad\ c_k + \frac{\partial D_k}{\partial c_k}(grad\ c_k)^2 + \frac{\partial D_k}{\partial p} grad\ p\ grad\ c_k \tag{4}$$

The process of heat and mass transfer in locally non-equilibrium media possesses the inertial property: the system responds to the action not in the same moment as in the locally equilibrium case, but by the relaxation time later, i. e. the fluxes are determined by the previous history of the process.

Locally equilibrium medium

$J_g = \lambda\ grad\ T$ – the Fourier law.

Locally non-equilibrium medium

$J_g + \tau \frac{\partial J_g}{\partial t} = -\lambda\ grad\ T$ – the Maxwell–Cattaneo law (τ is the relaxation time).

If diffusion is accompanied by a chemical reaction or if thermal conduction proceeds in a media with distributed heat sources, then the initial perturbation can evolve into progressive wave moving with the speed exceeding the diffusion speed. These processes are described by hyperbolic equations.

In the report also will be considered the mechanism of action of countercurrent columns, in which selective mass transfer takes place, and because of the “phase reversal” at the ends of the column the multiplication of the separation effect is achieved.

The majority of technological processes proceed at variable values of T and p and are often accompanied by heat supply or removal from the outside. These factors are taken into account by expressing the maximum work in terms of exergy

$$\Delta E_x = \Delta H - T_0 \Delta S \qquad (5),$$

where T_0 is the outside temperature.

Exergy is connected with Gibbs energy by the relation

$$\Delta E_x = \Delta G - (T - T_0)\left(\frac{\partial \Delta G}{\partial T}\right)_p , \qquad (6)$$

from which it follows that the values ΔE_x and ΔG can both higher or lower than one another depending on the temperatures of the process and the environment as well as the sign of the derivative in equation (6).

It can be shown that the relation of Gouy–Stodola

$$\Delta E_x = T d_i S \qquad (7)$$

reflects the intersystem entropy generation, which is equivalent to the energy quality loss.

In the report will also be considered modern approaches to enhancement of efficiency of energy-conserving thermodynamic cycles oxidative conversion of natural gas.

INFLUENCE OF TEMPERATURE AND AGGRESSIVE ENVIRONMENTS ON HYDROPHOBICITY OF HETEROGENEOUS MEMBRANES OF DIFFERENT NATURE

[1]Elmara Akberova, [2]Kseniya Nebavskaya, [1]Vera Vasil'eva, [2]Nataliya Pis'menskaya
[1]Voronezh State University, Voronezh, Russia, *E-mail*: *viv155@mail.ru*
[2]Kuban State University, Krasnodar, Russia

Introduction

The majority of electromembrane processes (high temperature electrodialysis, electrodialysis under intensive current regimes, electrolysis synthesis of acids and bases from corresponding salts, etc.) is conducted under elevated temperatures, in aggressive environments and under the action of the electrical current. It is known that during the continued use of the ion exchange materials in such conditions the irreversible changes of their surface properties can take place.

The aim of this work is to study the effect of thermochemical treatment on the morphology and surface hydrophobicity of commercial heterogeneous ion exchange membranes.

Experiments

The objects of study were commercial serial heterogeneous membranes: cation exchange MK-40 membrane and anion exchange MA-40 and MA-41 membranes, manufactured by JSC "ShchekinoAzot" (Shchekino).

The temperature treatment of membranes was conducted by their heating in water at different temperatures, as well as by their heating in 5.0M NaOH solution and 2.5M H_2SO_4 solution at 100^oC during 50 hours [1].

To evaluate the hydrophobicity of membrane the contact angles of swollen in distilled water (hydrated) membranes were measured using sessile drop method. The experimental methodics consisted of dosing the drop of test liquid at the various parts of the membrane surface. We have used the distilled water as a test liquid; the volume of drop was 7 μL. The shape of drop was registered with digital camera [2]. The contact angles were determined via analysis of images, obtained from not less than three repeated measurements at the moment of drop landing and after 20 s of this event.

The experimental studies of structure of hydrated membranes were conducted using the method of raster electron microscopy at JSM-6380 LV microscope (Japan) equipped with energy dispersive spectrometer and regulated pressure. Quantitative evaluation of pore size distribution of membrane surface was made with author program complex [3] with realized methods of digital processing of microphotographs of membranes, which allow automatizing the morphology analysis.

Results and Discussion

The relative changes of contact angles of surfaces, total exchange capacities and water contents of MK-40 membrane after its temperature treatment in water at different temperatures are shown in Fig.1. After the heating of MK-40 membrane in water at 100^oC during 50 hours its contact angle value decreased from 50 degrees (conditioned sample) to 30 degrees.

It is known that hydrophobic/hydrophilic balance of the surface of membrane is determined both by the chemical nature of the matrix of membrane or its inert binding, which usually is highly hydrophobic, and its hydrophilic polar fixed groups. The higher the content of fixed groups in the membrane and its water content, the more hydrophilic the surface of membrane will be. The presence of fixed groups in the membrane bulk is characterized by its exchange capacity. Since the data on the exchange capacity of MK-40 membrane indicate that the total concentration of dissociating fixed groups in it has decreased on 18% after the thermal treatment (Fig. 1), then the fact of decrease of contact angle is explained by the increase in the water content of the membrane.

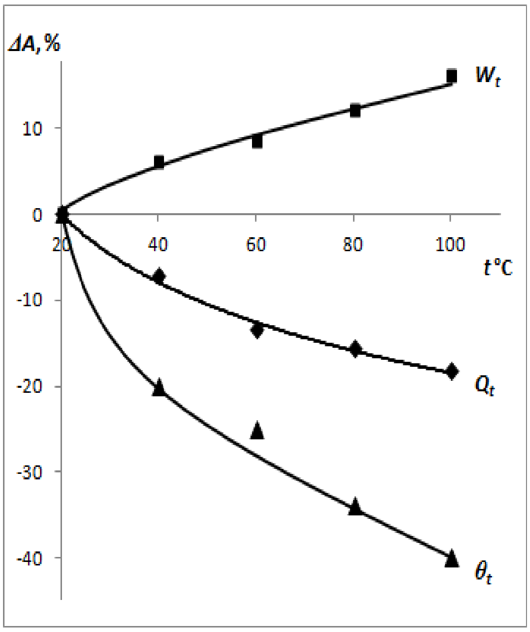

Figure 1. Temperature dependencies of relative changes in total exchange capacity (Q), water content (W) and contact angle of surface (θ) of MК-40 membrane after its temperature treatment in water during 50 hours

The reason of increase of water uptake of membrane is the broadening of space in pores occupied by the equilibrium electrical neutral solution. Comparison of electron microscopy images, obtained in low vacuum for the hydrated membrane samples after their thermal treatment in water and aggressive environments confirm the formation of the voluminous cavities at the boundary between ion exchange resin particles and polyethylene after the heating. The results of quantitative estimation reflect the twofold increase of porosity of MК-40 membrane surface and the increase in weighted mean of radii of macropores on 55% after its temperature treatment in water (Fig. 2).

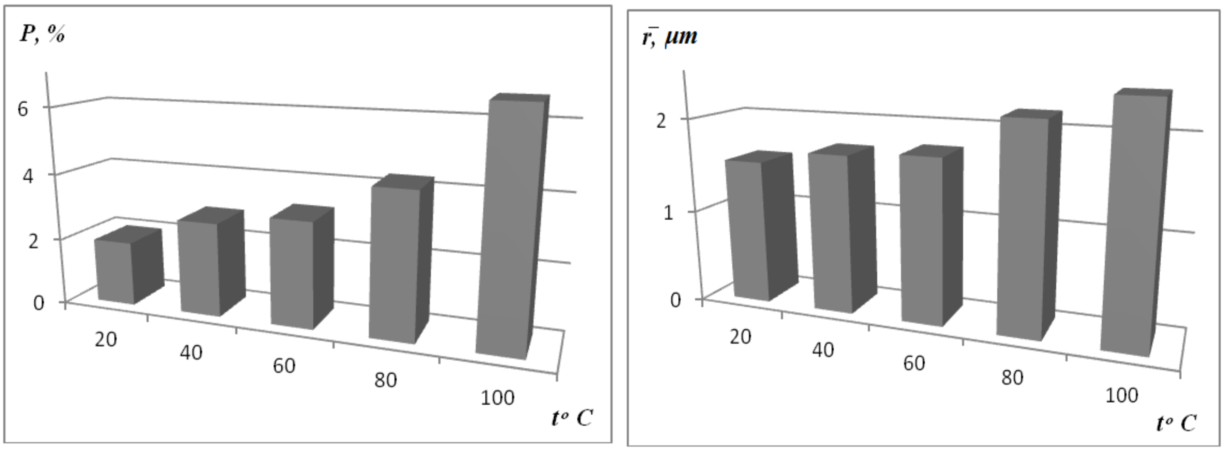

(a) *(b)*

Figure 2. Fraction (a) and weighted mean radius (b) of macropores at hydrated MК-40 membrane surface after its temperature treatment in water during 50 hours

The comparison of contact angle values of surface of MК-40membrane (Fig. 3*a*) show that magnitude of their changes lay within the experimental threshold (3°) for samples after the conditioning and temperature treatment in water and alkaline environments. The full permeation of the drop through the membrane after its thermal treatment in sulfuric acid solution indicates on the presence of voluminous hydrophilic pores at its surface.

The analysis of the effect of thermochemical treatment on the hydrophobicity of heterogeneous membranes of different nature (Fig. 3b) show that the maximal changes in contact angle values are found for the MК-40 and MA-40 membranes after their thermal treatment in acidic environment which are characterized by increasing in the porosity in 4.0-4.5 times in comparison with the conditioned samples.

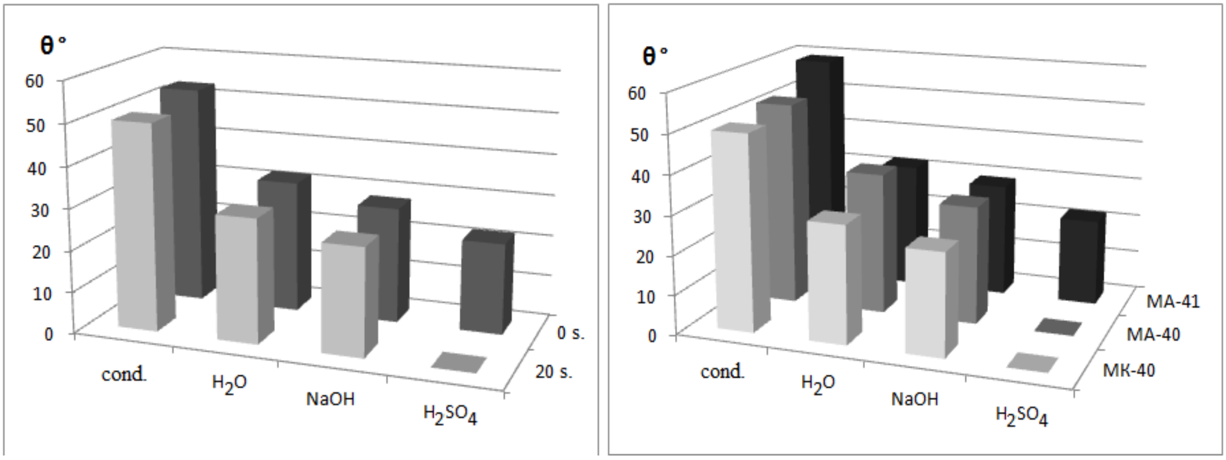

(a) *(b)*

Figure 3. Contact angles of MК-40 membrane surface at the moment of drop landing and after 20 s past this event (a) and contact angle of different membranes after 20 s past drop application (b). Designations: conditioned membrane (cond.), membrane after temperature treatment in water (H_2O), alkaline (NaOH) and acidic environments (H_2SO_4) at 100 °C during 50 hours

Such a way the correlation between the morphology changes and surface hydrophobicy changes of heterogeneous membranes of different nature after their temperature and thermochemical treatment is established.

Acknowledgements

Part of this investigation was realized within French-Russian laboratory "Ion-exchange membranes and related processes". The authors are grateful to RFBR, Russia (grants 12-08-00188-a, 13-08-01168)

References

1. Ion-exchangers. Methods of determining the stability of ion-exchange membranes to action of chemical environments. State Standard 10899-75. Introduced 1977-01-01. M.: Izdatelstvo Standartov, 1978. 3 p. (in Russian)
2. Patent № 124786, IPC (8) G01B11/26 (2006.01) G01N13/00 (2006.01). The set up for measuring the contact angles of surfaces / *Nebavskaya K.A., Nebavsky A.V., Nikonenko V.V., Belova E.I.* (Krasnodar, RF); the applicant and the patent owner: Kuban State University, RU; 20.09.2012 (in Russian)
3. *Sirota E.A., Vasil'eva V.I., Akberova E.M.* Certificate of state registration of computer program. 2012619723 (Ru). Calculation of porosity of ion exchange materials in the processing of SEM images / Voronezh State University. 26.10.2012. (in Russian)

THE EFFECT OF THERMOCHEMICAL IMPACT ON TRANSPORT-STRUCTURAL CHARACTERISTICS OF MK-40 MEMBRANE

Elmara Akberova, Vera Vasil'eva, Vladimir Shaposhnik, Mikhail Malykhin
Voronezh State University, Voronezh, Russia, *E-mail: viv155@mail.ru*

A comparative analysis of the effect of the temperature impact on the transport-structural characteristics of the sulfocation-exchange heterogeneous MK-40 membrane samples in aqueous, alkaline and acidic environments is carried out. By scanning electron microscopy differences in the surface and bulk microstructure of the hydrated membrane samples after chemical conditioning, temperature or thermochemical impact are visualized. it is found more significant increasing of porosity and the share of ion-exchanger on the surface in comparison with the cross section of membrane after heating in water and aggressive environments. The maximum changes in the structural and electrical transport properties is revealed for MK-40 membrane samples, exposed to thermochemical impact in a sulfuric acid solution.

Experiments

The object of the study is mass-produced by "Shchekinoazot" (Shchekino) heterogeneous cation-exchange MK-40 membrane, which is based on strongly acidic ion-exchanger KU-2, obtained by copolymerization of styrene and divinylbenzene with subsequent sulfonation.

The heat treatment is carried out by heating of the membrane samples in water, and 5.0 M solution of sodium hydroxide and 2.5 M sulfuric acid at 100 °C during 50 hours [1].

To characterize the electrical transport properties of the membrane it was applied contact-difference method, which consists in measuring of the electric resistance of two and one membranes in the cell with platinum electrodes and finding their difference, what is regarded as the true electrical resistivity of the membrane [2].

Experimental investigations of membrane structure in the hydrated state were carried out using scanning electron microscopy (SEM). Microscope model JSM-6380 LV (Japan) is pressure-regulated with energy dispersive analyzer of elemental content. Membrane samples for the study were square plates sized $(4\times5)\cdot10^{-3}$ m. SEM images of the membranes surface and cross section were performed at 500-fold magnification.

A quantitative estimation of the share of ion-exchange component and porosity on the membrane surface and cross section was carried out using author's software system [3, 4], in which digital processing of electron microscopic images of membranes that allow to perform automated analysis of their morphology were realized.

Results and Discussion

The results of determining the structural-kinetic properties of MK-40 membrane by the concentration dependences of the electrical conductivity (Fig. 1) are shown in Table 1. The parameter f_2, characterizing the volume fraction of intergel spaces filling with equilibrium electroneutral solution after temperature treatment increases twice in comparison with conditioned sample. Differentiating effect of aggressive environment on the intergel phase volume shows itself not so much. The obtained patterns remain for points of isoconductivity. The values of electrical conductivity in isoconductance point κ_{iso} grow with increasing of water content of the membrane samples.

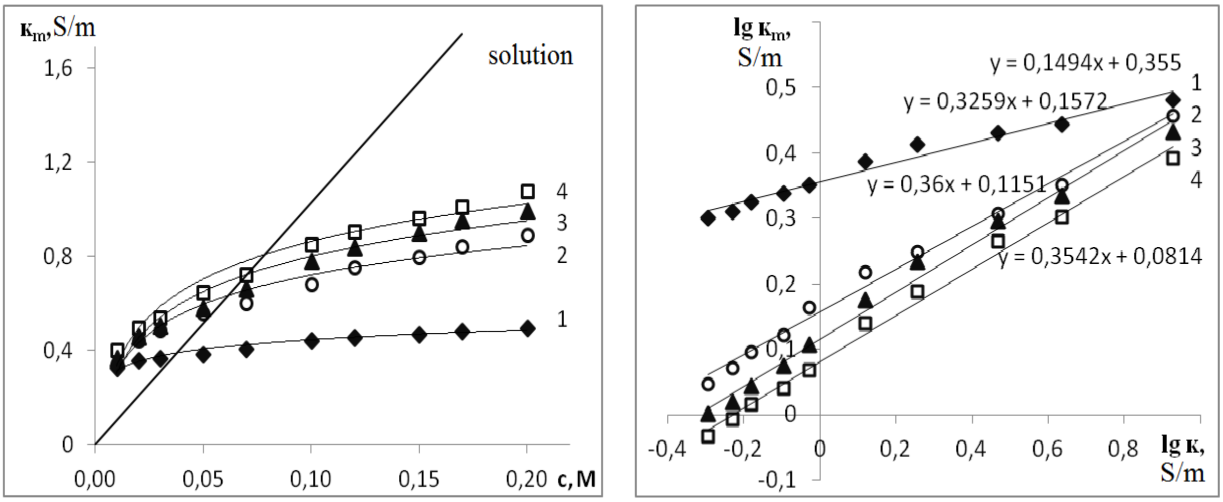

(*a*) (*b*)

Figure 1. Concentration dependence of the electrical conductivity (a) and dependence of MK-40 membrane conductivity on NaCl solution conductivity in bilogarithmic coordinates (b) after conditioning (1), the temperature impact in aqueous (2), alkaline (3) and acidic (4) environments

Table 1. Transport-structural characteristics of MK-40 membrane in NaCl solution

Characteristics	Membrane samples			
	after the conditioning	after the temperature impact		
		H_2O	NaOH	H_2SO_4
f_2	0.15	0.32	0.36	0.35
c_{iso}, M	0.032	0.050	0.054	0.064
κ_{iso}, S/m	0.38	0.58	0.65	0.74

Close physical meaning to the volume fraction of intergel spaces in structurally heterogeneous membrane has a share of macropores and structural defects in the hydrated sample. Comparison of the electron microscopic images of hydrated membrane samples performed in the regime of low vacuum after temperature treatment in water and aggressive environments confirms the formation of large cavities at the boundaries between the ion-exchanger particles and polyethylene under heating (Fig. 2).

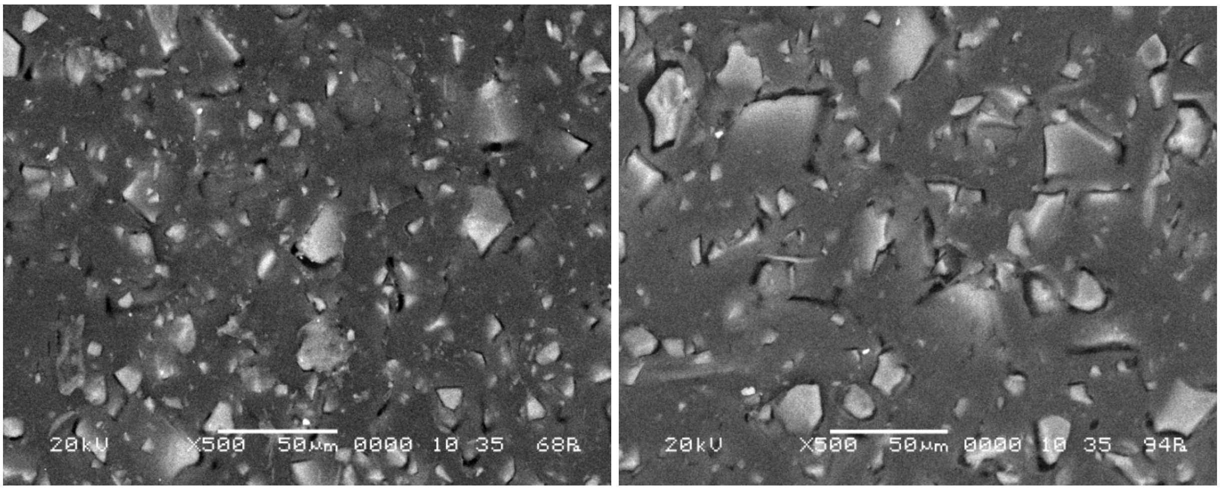

(*a*) (*b*)

Figure 2. SEM images of the surface of hydrated MK-40 membrane samples at 500-fold magnification after conditioning (a) and heating in water (b) at 100 °C during 50 h

Results of a quantitative estimation of the pore structure on MK-40 membrane surface and cross section (Fig. 3) reflect the growth of surface and bulk porosity of the membranes after the temperature and thermochemical impact and shows more significant changes in the structure of the surface in comparison with the cross section. On the surface of the samples subjected to the thermochemical effect, an increase in the total porosity of 2-3 times and in the average macropore radius of 40-70% is revealed. In the membrane bulk the maximum increase of macropores share and their average radius is 40% and 15% respectively. The increase in the total porosity and the average pore size is due to "decapsulation" of ion-exchanger particles as a result of volume changes in the membrane phase due to heating and an impact of aggressive environments.

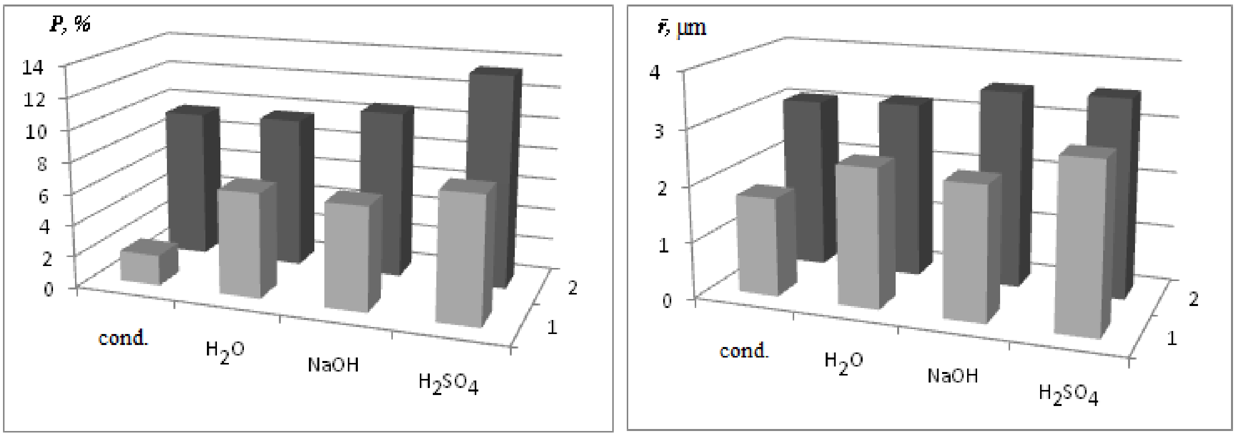

(a) *(b)*

Figure 3. The share (a) and the average radius (b) of macropores on the surface (1) and in the bulk (2) of MK-40 membrane in hydrated state: after conditioning (cond.), the temperature in aqueous (H_2O), alkaline (NaOH) and acidic (H_2SO_4) environments at 100 °C during 50 h

The correlation between changes in the structural and transport characteristics of the sulfocation-exchange MK-40 membrane after the temperature and thermochemical impact is established. By the scanning electron microscopy anisotropy of surface and cross section microstructure of the MK-40 membrane is visualized and more significant increasing in surface inhomogeneity in comparison with a cross section after heating of the membrane in water and aggressive environments is identified.

References

1. Ion-exchangers. Methods of determining the stability of ion-exchange membranes to action of chemical environments. State Standard 10899-75. Introduced 1977-01-01. M.: Izdatelstvo Standartov, 1978. 3 p. (in Russian)
2. *Shaposhnik V.A., Emel'yanov D.E., Drobysheva I.V.* // Kolloidnyy zhurnal. 1984. Vol.46. №4. P. 820. (in Russian)
3. *Sirota E.A., Kranina N.A., Vasil'eva V.I.* etc. // Bulletin of VSU, Series: Chemistry. Biology. Pharmacy. 2011. № 2. P. 53. (in Russian)
4. *Sirota E.A., Vasil'eva V.I., Akberova E.M.* Certificate of state registration of computer software. 2012619722 (Ru). Estimation of surface and bulk inhomogeneity of heterogeneous ion-exchange membranes by electron microscopic images / State educational establishment of higher professional education "Voronezh State University". 26.10.2012. (in Russian)

ASYMMETRIC LAYERED MEMBRANES

Lidia Annikova, Jan Krivcik, David Nedela, Jaroslav Hadrava
"MemBrain s.r.o.", Straz pod Ralskem, Czech Republic
E-mail: lidia.annikova@membrain.cz, Jan.Krivcik@membrain.cz, david.nedela@membrain.cz

Introduction

In our last article [1] we wrote about the wastewater treatment plant of uranium using bipolar membranes. There we used the laboratory type EDZ unit with 64 cm^2 of active membrane area. Membrane stack consisted of heterogeneous membranes 6 BM, 6 AM and 7 CM - three-compartment cell. We were able to reach up to 12 % acid and base solutions However, anion-exchange membranes degraded after four months (resistance increased 4 times, the selectivity dropped 3 times).

In this paper we use only two compartment cell without chemically less stable anion exchange membrane. This gives us more long term stable process but with a maximum hydroxide concentration not exceed 5 %. Therefore we try to modify both cation and bipolar membranes to increase its performance (preferentially its permselectivity).

Experiments

We have prepared multilayered cation or bipolar membranes from both heterogeneous ion-exchange membranes and combination of heterogeneous and homogeneous membrane layer [2]. For heterogeneous membrane layer we used AM-PES and CM-PES RALEX. The homogeneous layer was prepared from special triblock copolymer Nexar provided by Kraton Polymers Nederland B.V. (www.kraton.com). The Nexar is provided in both membrane foil and as a solution. For BM preparation we used both form of Nexar. In the Table 1 there are single membrane properties.

Table 1. The electrochemical properties of the initial samples

№	Polymer	t_{dry}, mm	*IEC*, meq/g$_{dry}$	*Δwt*, %	R_A [Ωcm^2]		*P*, %
					1	2	
1	Nexar MD9100$_l$ (liquid)		0,77				
2	Nexar MD9100$_s$ (solid membrane)	0,03	0,77	85,5	0,72	0,73	98
3	Heterogeneous cation membrane CM-PES	0,50	2,45	58,7	7,95	7,78	96
4	Heterogeneous anion membrane AM-PES	0,50	1,89	55,2	7,63	7,54	95

t_{dry} - thickness of the dry membrane; *IEC,meq*/g$_{dry}$ - dry membrane exchange capacity; *Δwt* % - wight of water per gram of dry membrane; R_A [Ω·cm^2] - membrane resistance measured at a constant current from one and then other side, in 0.5 M *NaCl:*1 – direction of current in positive; 2 – direction of current in negative; *P*, % - selective membrane in 0.1/0.5 M *KCl*

In the table 2 there are properties of surface modified cation and anion exchange membrane by liquid or solid Nexar MD9100. Nexar was applied only on one side. When layer of homogenous membrane are thick, resistant these membranes are very high (membranes No1 and No 4). In case of anion membrane modification by cation layer we can easily prepare the BM. If we want only modify the anion membrane selectivity than the cation layer needs to be very thin.

Results and Discussion

As you can see from Table 2. the Nexar membrane is too thick, therefore the bipolar membrane was prepared and therefore the areal resistance is too high. In case of using Nexar solution the very thin cation layer can be prepared without any strong negative influence on membrane resistance.

The membrane performace in electrodialysis was verified by model ED test with 20 g/l of natrium sulfate and natrium nitrate. In the Table 3. there are ED test results for modified membranes No3 and No6 (from table 2). The modified side was oriented into diluate loop for positive current polarity. All tests were in batch regime with a constant voltage of 1 V per cell pair. The ED tests were end when conductivity solution in duliate drops below 1 mS/cm.

Table 2. The electrochemical properties of multilayer membrane

№	**Composition**	t_{wet}, **mm**	Δwt, **%**	R_A [Ω cm^2]	
				1	***2***
1	CM-PES+MD9100$_s$	0,607	53,9	7,45	122,7
2	CM-PES+MD9100$_l$	0,505	55,3	11,85	234,7
3	CM-PES+MD9100$_l$	0,611	57,1	6,72	6,5
4	AM-PES+MD9100$_s$	0,653	48,2	693,19	10618,2
5	AM-PES+MD9100$_l$	0,570	47,9	6,53	104,9
6	AM-PES+MD9100$_l$	0,599	57,0	5,02	4,86

Table 3. The results of the electrodialysis desalination

No	**Solution**	**Current polarity**	**Time t, min**	**Maximum current I, A**
1	Na_2SO_4	Pozitive/negative	50	0,93
2	Na_2SO_4	Pozitive	70	0,72
3	Na_2SO_4	Negative	35	1,27
4	$NaNO_3$	Pozitive	55	0,82
5	$NaNO_3$	Negative	30	1,29

Current polarity – direction of current in membrane stack

Test No 1 is standard electrodialysis test with standard heterogeneous membranes Ralex. In this standard test there is no difference between current flowing in the forward (positive) and reverse (negative) direction. Modified membranes in electrodialysis process have asymmetric effect in orientation depending on the current flow. In the positive direction the current is lower than in the negative direction, respectively the time required for desalination solution is higher. At the same time resistance of modified membranes and standard heterogeneous membranes Ralex haven't big difference.

In addition it is clear that through desalination in $NaNO_3$ is faster than in the case of Na_2SO_4 due homogeneous layer of modified membranes, which have high permselectivity than initial heterogeneous membrane.

In the future we will use these modified membranes in bipolar electrodialysis to obtain a higher concentration and pure of the solutions.

References

1. *Annikova L.A., Krivcik J., Nedela D.* Investigation of bipolar membranes properties by electrodialysis method. Ion Transport in Membranes, abstracts book, Tuapse, 2012. P. 14.
2. *Elmidaoui A., Elhannouni F., Taky M., Chay L., Amine M., Sahli M., Echihabi L., Hafsi M.* Optimization of nitrate removal operation from ground water by electrodialysis. Sep. Purif. Technol. 2002. V. 29, № 3. P.235

HIGH PRESSURE MEMBRANE CONTACTORS FOR CO_2 CAPTURE: DESORPTION STAGE CHALLENGE

Stepan Bazhenov, Anastasiya Shutova, Georgiy Dibrov, Vladimir Vasilevsky, Valeriy Khotimsky, Alexey Volkov
Topchiev Institute of Petrochemical Synthesis, Moscow, Russia, *E-mail: sbazhenov@ips.ac.ru*

Introduction

Membrane gas absorption process (MGA) is one of the promising ways to reduce anthropogenic carbon dioxide emissions. This method based on porous hollow fiber membranes has been already successfully realized in pilot scale [1]. In spite of this, such a variant of process is difficult to implement in case of high pressure gas mixtures purification and membrane gas desorption (MGD) approach. In these processes membranes should meet certain requirements, specifically: i) high CO_2 permeability, ii) chemical and mechanical stability in CO_2 absorption solvents at high temperature, iii) absence of liquid leakage through the membrane at operated conditions. As it can be seen from our previous work [2], membrane based on nonporous high-permeable glassy polymers (such as poly[1-(trimethylsilyl)-1-propyne - PTMSP) are suitable for this purpose.

In this work we focused on development of CO_2 desorption (MGD) process with high pressure gas-liquid membrane contactor based on PTMSP and composite-type PTMSP membranes.

Experiments

The 50 % wt. aqueous solution of methyldiethanolamine (MDEA) was chosen as one of the most common solvent for high pressure absorption/desorption process. Absorbent was saturated with pure CO_2 until the required CO_2 loading (0.44 mol/mol amine) was achieved. The CO_2 concentration was measured by means of absorbent's electroconductivity. Both homogeneous and composite-type based on inorganic thermally stable material PTMSP-membranes were tested.

Results and discussion

The main result of MGD process with composite PTMSP-membranes is presented on Figure 1.

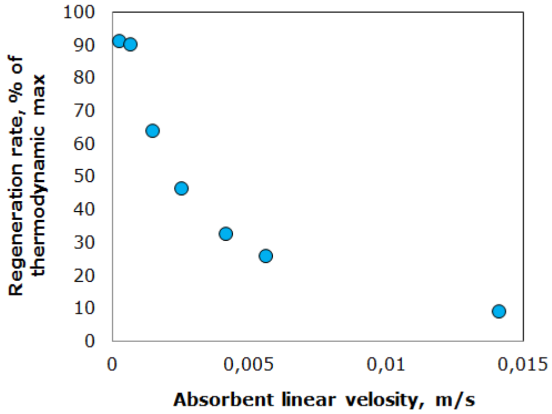

Figure 1. Absorbent regeneration rate (in % of thermodynamic maximum) vs. absorbent velocity in membrane contactor. Conditions: transmembrane pressure – 35 bar, T_{des} = 100 ℃, effective selective layer thickness – 2 µm

It can be concluded, that 90% of CO_2 are removed from absorbent for only one cycle in membrane contactor. The efficiency of process can be improved by increasing in number of cycles. To sum up, the results of our study allows to conclude that MGD using PTMSP-based membranes is a promising process which provides high regeneration efficiency of MDEA absorbent in combination with typical advantages of membrane process: large gas-liquid interfacial area, modularity and improved energy efficiency.

Aknowledgements

This research work was partially supported with the funding from FP7 project "DECARBit". This research cooperation is the part of the Dutch-Russian Centre of Excellence "Gas4S" (NWO-RFBR).

References

1. *Vogt M., Goldschmidt R., Bathen D., Epp B., Fahlenkamp H.* // Energy Procedia. 2011. V.4. P. 1471.
2. *Trusov A., Legkov S., van den Broeke L.J.P., Goetheer E., Khotimsky V., Volkov A.* // J.Membr.Sci.. 2011. V.383. P. 241.

NOISE ANALYSIS OF ION TRANSPORT THROUGH CHARGED MEMBRANES

[1]Ekaterina Belashova, [1]Philippe Sistat, [1]Stella Lacour, [1]Gérald Pourcelly
[2]Natalia Pismenskaya
[1]Institut Européen des Membranes, CNRS, Université Montpellier 2, ENSCM, France
[2]Membrane Institute, Kuban State University, Krasnodar, Russia
E-mail: ekaterina.belashova@iemm.univ-montp2.fr

Introduction

Some recent progress in ion transport analysis have shown that complex mechanisms can contribute to ion transport, for instance current induced chemical reaction like water splitting but also convection induced by ion transport. A battery of electrochemical techniques belong to the common toolbox of researchers in the field. The usual set includes voltammetry, chronopotentiometry, chronoamperometry, and electrochemical impedance spectroscopy (EIS). All theses techniques are complementary to other ones bring an information that is more or less easily interpreted. From a practical point of view, the very low frequency part of impedance spectra is often plagued by electrical noise and cannot provide a clear source for investigation. In all cases the contribution of a additional technique is needed and the technique of choice seems to be the electrical noise analysis.

Experiment

The experimental cell used for the study is a flow cell where the membrane works under electrodialysis conditions. This cell has been extensively described elsewhere [1]. The membranes used where MK-40 (cationic) heterogeneous; MA-41 (anionic) heterogeneous; AMX (anionic) homogeneous. Experiments have been carried out in differents solutions: NaCl 0,02 M; Lysine-HCl 0,02 M and $C_4H_4O_4$ malic acid 0,02 M.

Results and Discussion

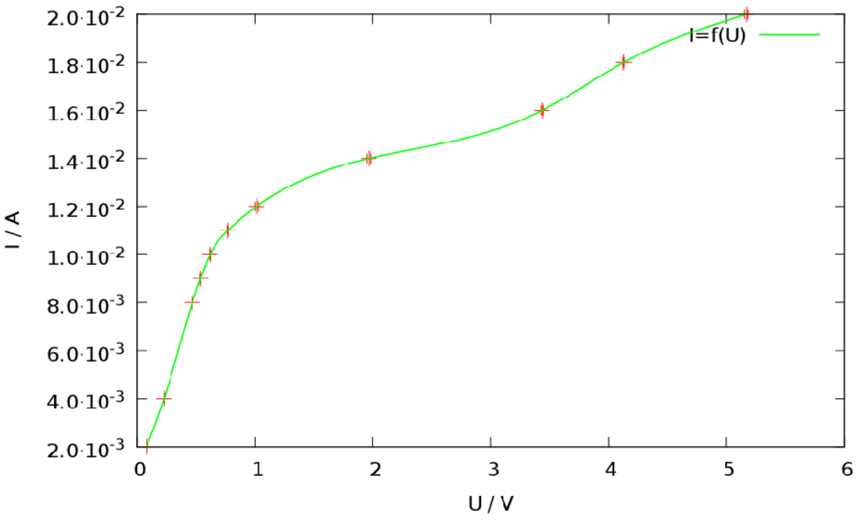

Figure 1. Current voltage curve in quasi steady-state conditions obtained by linear sweep voltammetry. The cross point shows the current intensity for which a chronopotentiogram has been recorded

Firstly, an experimental current voltage was obtained by linear sweep voltammetry in order to have a clear idea of the limiting current density, like in figure 1. Afterwards, a classical chronopotentiogram is recorded at a fixed current density. The first part of the chronopotentiogram is discarded since it represents the evolving part due to the establishment of concentration polarization. We are mostly interested in the steady state part of the chronopotentiogram. We assumed that steady-state is reached with after a transient time of almost 300 s. We keep this part for noise analysis through the computation of the spectral power density of the stochastic steady-state chronopotentiometric signal. An sample of such a signal is represented on the figure 2.

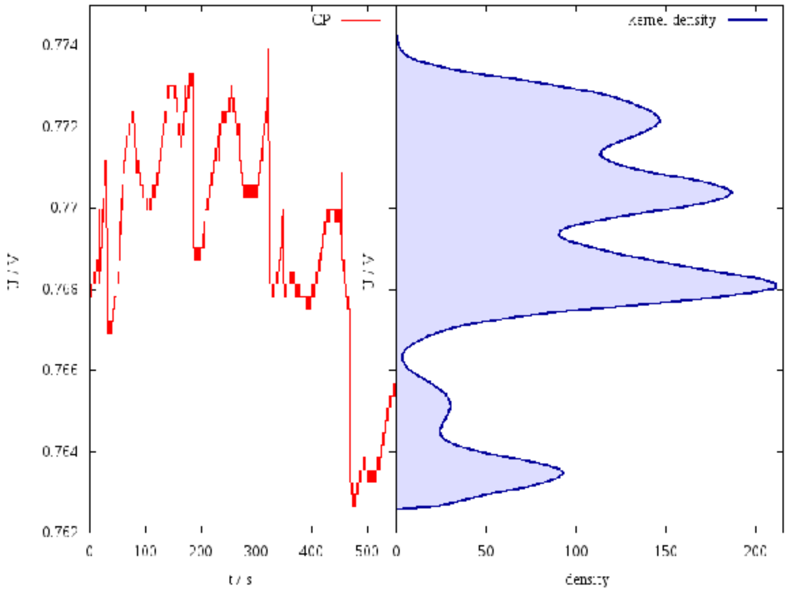

Figure 2: Chronopotentiometric record in quasi steady state and distribution of the voltage value

The spectral power density of the signal is then computed numerically. As it appears in the figure 3, we can distinguish three peculiarities of power spectra for ionic membranes bathed by aqueous solutions. A low frequency part (f<1Hz), linked to the diffusion phenomena and some of its instabilities. This low frequency part exhibits a frequency dependence for the intensity owing to a $1/f^{\alpha}$ law (Brown noise) explaining the difficulties to obtain well defined very low frequency part of impedance spectra. Another point is the increasing level of white noise at higher frequencies following the current density. The white noise is the constant background existing at frequency here higher than 1Hz. At last, there are some specific frequencies appearing as spike in the spectra, there are the evidence that some events take place periodically and can be related for instance to the development of convection vortexes or other sources. An intensive analysis of the data must be carried out in the future to relates the different peaks to their physical origin.

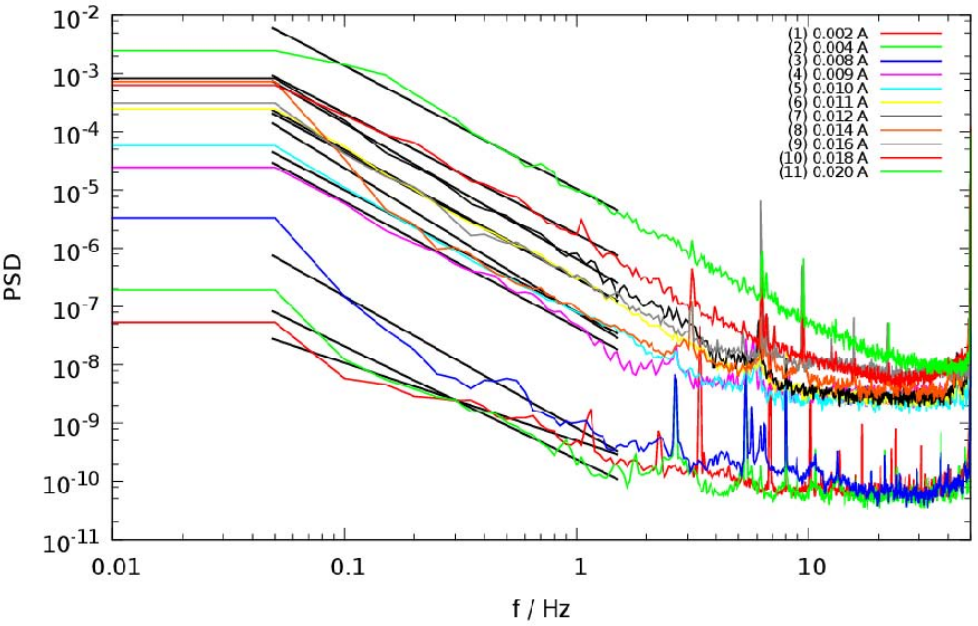

Figure 3: Power spectra density of the voltage across an AMX membrane bathed with a NaCl solution

Conclusion

The power law of noise at low frequencies (Brown noise) exhibits an α coefficient almost equal to 2. As a consequence it can be related to perturbed diffusion phenomenom. However for some specific samples a deviance to this behavior is noted. In this case we can think that a more complex mecanism is involved in ion transport. It can be seen that the amplitude of the noise depends strongly on current(/voltage) applied to the membrane system. The higher the voltage, the higher the noise intensity. The white noise depends on current(/voltage). An step in the noise intensity appears for a given value of the voltage. Nevertheless, for the time being we cannot be sure that this onset is due to the a new contribution of a specific transport mecanism or a change due to the automatic ranging of the potentiostat voltmeter(ampmeter). Further investigation must be carried out for a clear disambiguation of this effect. On the PSD, and for some specific frequencies depending on the current applied, some sharp peaks obviously appears. Mechanisms leading to such marked phenomena are still to identify, but known candidates for an explanation exists [2]: reaction, convection, coupled phenomena.

Acknowledgements

This investigation was realized within French-Russian laboratory "Ion-exchange membranes and related processes". The authors are grateful to CNRS, France, and to RFBR, Russia (grants 11-08-93107_NCNIL, 12-08-93106_NCNIL, 13-08-01168), as well as to FP7 Marie Curie Actions "CoTraPhen" project PIRSES-GA-2010-269135 (ENSCM) for financial support.

References

1. *Belova E., Lopatkova G., Pismenskaya N., Nikonenko V., Larchet C., Pourcelly G.* The effect of anion-exchange membrane surface properties on mechanisms of overlimiting mass transfer // J. Phys. Chem. B. 2006. V. 110. P. 13458-13469.
2. *Nikonenko V., Pismenskaya N., Belova E., Sistat Ph., Larchet Ch., Pourcelly G.* Intensive current transfer in membrane systems: Modelling, mechanisms and application in electrodialysis // Adv. Colloid Interface Sci. 2010. V. 160. P. 101-123.

PECULIARITIES IN THE BEHAVIOR OF MEMBRANE SYSTEM CONTAINING AMPHOLYTES SOLUTION

[1]Ekaterina Belashova, [1]Philippe Sistat, [1]Stella Lacour, [1]Gérald Pourcelly
[2]Natalia Pismenskaya
[1]Institut Européen des Membranes, CNRS, Université Montpellier 2, ENSCM, France
[2]Membrane Institute, Kuban State University, Krasnodar, Russia
E-mail: ekaterina.belashova@iemm.univ-montp2.fr

Introduction

Nowadays, the behavior of strong electrolyte solutions in the membrane systems is well known. A large number of researches was aimed to provide a better understanding of laws governing transport through ion-exchange membranes [1-2]. But number of studies describing the behavior of organic acids during electrodialysis process is much low. The difficulty to understand the transport mechanisms of ampholyte-containing solutions is due to the coupling of chemical reactions: ampholytes contain polar groups (carboxyl and / or amino groups) which react with the solvent to form H^+ and OH^- ions and change the charge according to pH.

The aim of this work is to reveal the peculiarities in the ampholyte transport through ion-exchange membranes.

Experiment

Two systems membrane/solution containing ampholytes were investigated:

- anion-exchange membrane AMX (Astom, Tokuyama Corp., Japan) with a solution of monosodium phosphate;
- cation-exchange membrane Nafion (DuPont, USA) with a solution of lysine hydrochloride.

Both membranes have also been studied with a strong electrolyte solution (sodium chloride).

The transport phenomena under electrodialysis conditions were investigated by conventional transient electrochemical methods such as: Voltammetry, Chronopotentiometry, and Impedance electrochemical spectroscopy. Studies were performed with a laboratory flow cell previously described in details in [3].

The ampholyte concentration and pH dependence of membrane electrical conductivity were determined under alternating current by differential method with a clip-cell [4].

The ionic form distributions were calculated thanks to a specially developed model based on the matter balance, electroneutrality and equilibrium reactions.

Results and Discussion

Difference in the behavior of ampholytes and NaCl solutions is pointed out in the analysis of the concentration dependence of membrane electrical conductivity. In the case of strong electrolyte solution, electrical conductivity of membranes decreased as the solution became more dilute (Fig. 1). The reason is the electroneutral solution, which is identical to the external one. Within the framework of the microheterogeneous model [5], an ion-exchange membrane together with nanopores, contains also macropores and wide channels filled with the electroneutral solution. At low concentrations of the external solution, the low electrical conductivity of the solution in the inter-membrane spaces also causes a low conductivity of the membrane as a whole. On the contrary, electrical conductivity of membranes in the ampholytes solution increased in the diluted solutions (Fig. 2). Calculation results of ionic forms distribution in the membrane solution of monosodium phosphate (Fig. 3) and lysine hydrochloride (Fig. 4) clearly exhibit those phenomena that occur on the diluate side of the external solution (where pC=-log10(C)).

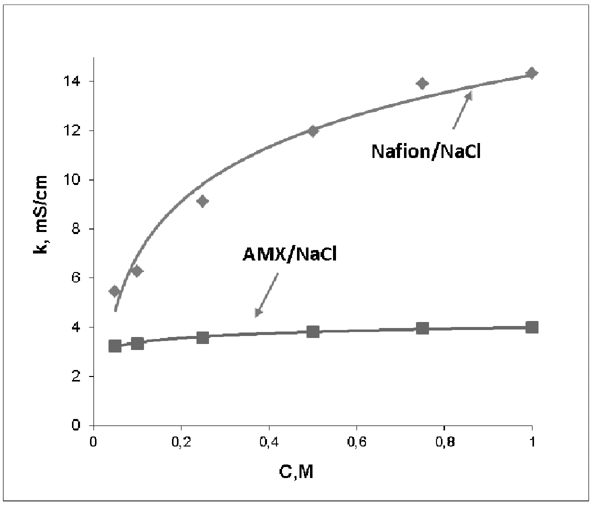

Figure 1. Sodium chloride concentration vs membrane electrical conductivity

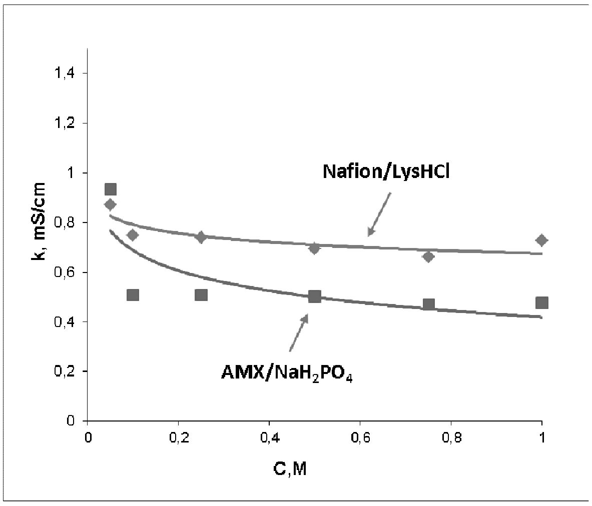

Figure 2. Ampholyte concentrations vs membrane electrical conductivity

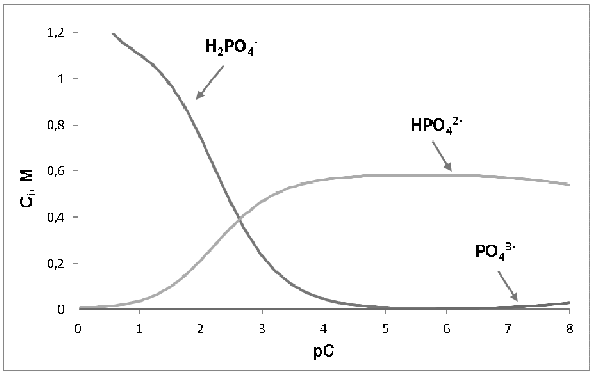

Figure 3. Monosodium phosphate solution: ionic forms distribution within the anion-exchange membrane as a function of the external solution concentration

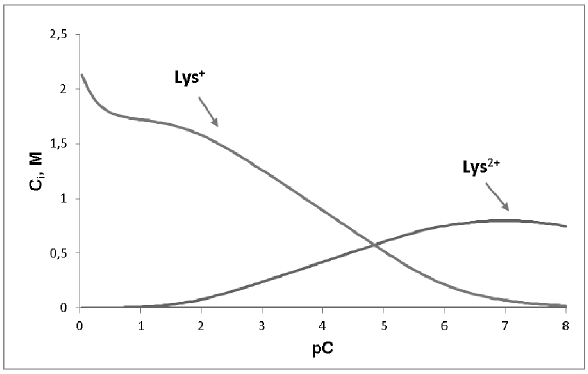

Figure 4. Lysine hydrochloride solution: ionic forms distribution within the cation-exchange membrane as a function of the external solution concentration

Experimental and theoretical observations are explained by the changing of internal pH solution of the membrane as the external solution becomes more dilute. As a consequence, the speciation of ionic forms within the membrane solution is modified (part of the single charged ions transforms into double charged ions). As a result, the electrical conductivity of the membranes increases for diluted solutions within a given concentration range.

The factors considered above describe the equilibrium systems – membrane/solutions (containing ampholytes). Transfer mechanisms of ampholytes solution under the influence of the electric current also demonstrate some features. As it can be seen from Figure 5 and 6, experimental limiting current for both ampholytes solutions is lower than the theoretical, which was calculated by the Leveque equation. Analysis of the current-voltage curves also shows the formations of the second plateau which indicate the emergence of the limiting state.

These effects possibly related with the chemical reactions at the membrane/solution boundary during electrodialysis process. Due to the changing of the pH solution near the membrane surface (as a result of Donnan exclusion or generation of H^+/OH^- ions) the part of the single charged ions transforms into neutral form, that leads to decrease of a real solution concentration into diluted diffusion layers. Molecules diffuse into bulk solution and dissociate again in single charged ions. As a consequence of this stepwise transformation, current-voltage curves of membrane systems containing ampholyte solutions demonstrate two limiting currents and two plateaus.

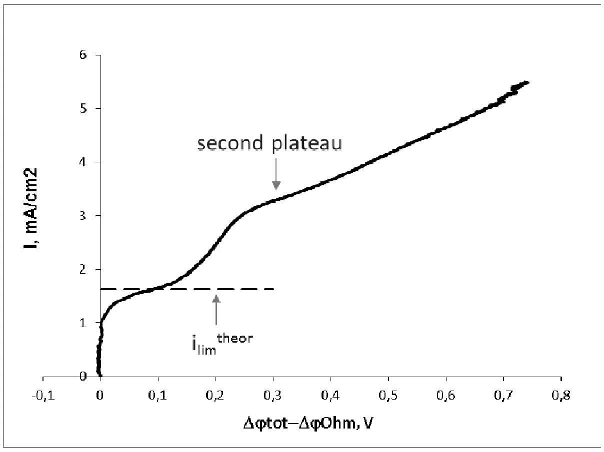

Figure 5. Current-voltage characteristics of system NaH2PO4/AMX

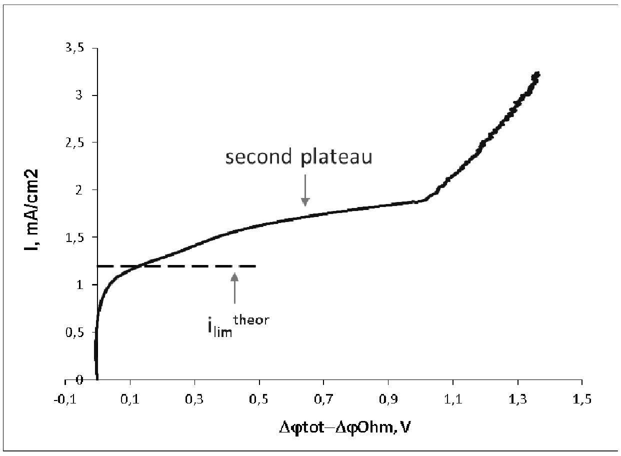

Figure 6. Current-voltage characteristics of system LysHCl/Nafion

Conclusion

Transport mechanisms for phosphoric acid anions through anion-exchange membranes and for lysine cations through cation-exchange membranes are quite similar to each other and differ from the mechanism for the ions of strong electrolytes. Such peculiarities relate with ionic forms repartition due to pH solutions changes.

Acknowledgements

This investigation was realized within French-Russian laboratory "Ion-exchange membranes and related processes". The authors are grateful to CNRS, France, and to RFBR, Russia (grants 11-08-93107_NCNIL, 12-08-93106_NCNIL, 13-08-01168), as well as to FP7 Marie Curie Actions "CoTraPhen" project PIRSES-GA-2010-269135 for financial support.

References

1. *Rubinstein I., Zaltzman B.* Electro–osmotically induced convection at a perm selective membrane // Physical review E. 2000. V. 62. №2. P. 2238 – 2251.
2. *Nikonenko V., Pismenskaya N., Belova E., Sistat Ph., Larchet Ch., Pourcelly G.* Intensive current transfer in membrane systems: Modelling, mechanisms and application in electrodialysis // Adv. Colloid Interface Sci. 2010. V. 160. P. 101-123.
3. *Belova E., Lopatkova G., Pismenskaya N., Nikonenko V., Larchet C., Pourcelly G.* The effect of anion-exchange membrane surface properties on mechanisms of overlimiting mass transfer // J. Phys. Chem. B. 2006. V. 110. P. 13458-13469.
4. *Karpenko L., Demina O., Dvorkina G., Parshikov S., Larcher C., Berezina N.* Comparative study of methods used for the determination of electroconductivity of ion-exchange membranes // Elektrokhimiya, 2001. 37. 328.
5. *Zabolotsky V.I., Nikonenko V.V.* Effect of structural membrane inhomogenity on transport properties // J. Membr. Sci. 1993.Vol.79. P.181-198.

PT AND PT-NI NANOPARTICLES ON DIFFERENT SUPPORTS AS ELECTROCATALYSTS FOR OXYGEN REDUCTION REACTION

Sergey Belenov, Vladimir Krikov, Larisa Visochina, Vladimir Guterman
Southern Federal University, Rostov-on-Don, Russia, *E-mail: serg1986chem@mail.ru*

Introduction

One of the key factors affecting the proton exchange membrane fuel cells (PEMFC) performance is the slow kinetics of the oxygen reduction reaction under PEMFC operating conditions. The composite materials containing Pt or Pt-alloy nanocrystals deposited onto highly developed surface of carbonaceous supports are most promising electrocatalysts. However, the catalyst activity depends on many factors such as preparation methods, precursor properties, support, nanoparticles size and so on. The stability of the catalyst support is of great importance in the development of new substrates. In addition to high surface area, porosity and electrical conductivity, corrosion resistance is also an important factor in the choice of a good catalyst support [1]. There are a lot of nanostructured materials including carbon metal oxides, conducting polymers and hybrid structures which were exhaustively researched over the past few decades to improve the existing and also develop novel PEMFC/DMFC catalyst supports [2].

The aim of this work was an investigation of different supports for catalytic materials.

Experiments

PtxNi alloys on different supports (nanodiamonds, Vulcan XC-72, TIMREX HSAG300, TiB2, Taunit, BP 2000) were prepared by simultaneous reduction of metal ions from water-organic suspension. $NaBH_4$ was used as a reducing agent. Prepared materials were investigated by X-ray diffraction (XRD), X-ray fluorescent method, trans-mission electron microscopy (TEM), thermal analysis (TA), BET, cyclic voltammetry on the rotating disc electrode in 1M H_2SO_4. The electrochemical active surface area (EAS) was measured by cyclic voltammetry based on the relationship between the surface area and charge expended to the H_{upd} desorption or to the oxidation of adsorbed on the electrode CO [3-4]. From Levich-Koutecky plots a number of electrons transferred to one O_2 molecule were estimated.

Results and Discussion

It was found how D_{aver} of the Pt nanoparticles, their GSD dispersion and EAS depended on the concentration of organic component (DMSO) in the matrix solution [5]. Pt and Pt-Ni nanoparticles with homogenous distribution were synthesized by borohydride method on Vulcan XC-72 (Fig.1) and nanodiamonds (Fig.2). The average nanopaticle size of PtNi material on nanodiamonds (5 nm) less than PtNi material on a carbon support Vulcan XC-72 (7 nm). According to the results of thermal analysis PtNi material on nanodiamonds shows more stability than PtNi material on Vulcan XC-72. But in the case of nanodiamonds there is a problem with poor electrical conductivity. The solution of this problem is doping nanodiamonds or using of mixtures nanodiamonds with other substances which characterized by high conductivity.

The number of electrons indicates that the four-electrons mechanism predominates for the ORR for catalysts. It’s in a good agreement with literature data.

The maximum mass activity and specific activity in oxygen reduction reaction was found for Pt on a carbon support Vulcan XC-72, but this material showed more decrease stability in compared some different supports.

Application of thermal analysis to the study of platinum based catalysts on the highly dispersed carbon carrier may provide additional information about the structure of such materials [6]. It was a comparative TG study of Pt/C materials on different carriers. With the model samples was shown as loading and uniform metal nanoparticles distribution on the surface of carbon carrier influence on high-temperature oxidation kinetics.

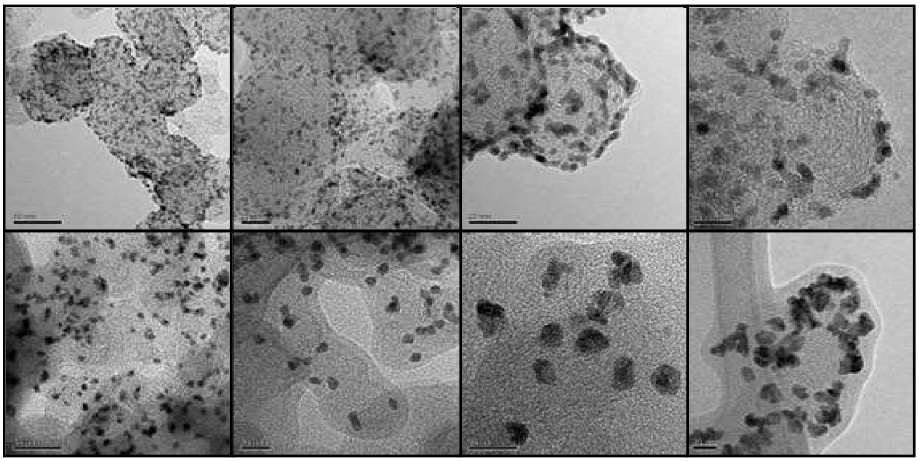

Figure 1. TEM images of Pt/C (Vulcan XC-72) (top) and PtNi/C (Vulcan XC-72) (down) materials prepared from water-glycerin (1:1) solutions

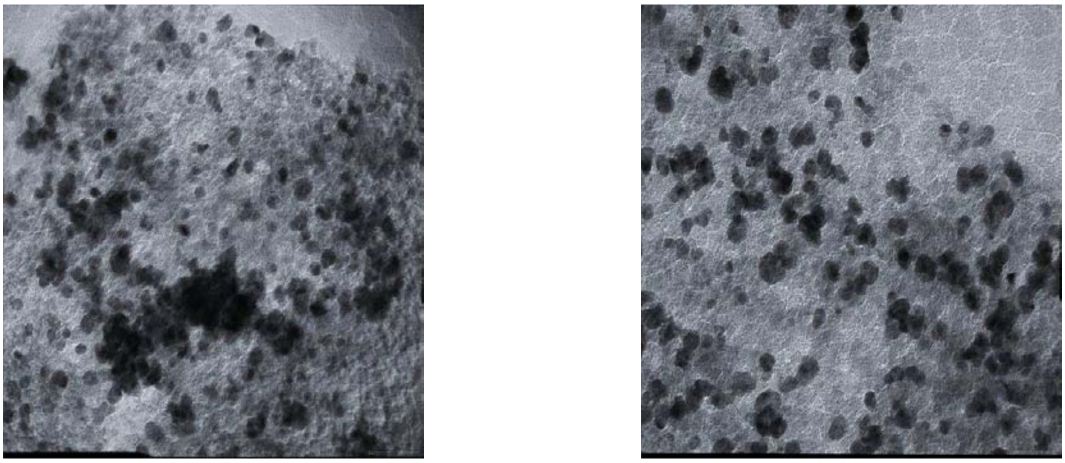

Figure 2. TEM images of Pt_3Ni nanoparticles on nanodiamonds

In summary, carbon-supported Pt catalysts with an average particle size of 1.8-5.4 nm and metal loading of 20 wt % were prepared by wet synthesis using $NaBH_4$ as a reduction agent. Electrochemical estimations indicate that the four-electrons mechanism predominates for the ORR for all Pt/C catalysts. For some PtxNi/C materials less number of electrons were estimated. This phenomenon can be explained by impact of two-electron reaction.

Acknowledgements

This work was made by supporting of Haldor Topsoe A/S grant «Control composition, microstructure, stability and activity in oxygen redaction reaction carbon carried Pt/C and PtxNi/C electrocatalysts»; Russian Foundation for Basic Research (grant №10-03-00474a and 11-08-00499a). The Ministry of education and science of Russia grant № 14.132.21.1468.

References

1. *Antolini E.* // Applied Catalysis B: Environmental. 2009. V.88. p. 1-24.
2. *Sharma S., Pollet B. G.* // Journal of Power Sources. 2012. V. 208. p. 96 -119.
3. *Guterman V. E., Belenov S. V., Lastovina T. A., Fokina E. P., Prutsakova N. V., and Konstantinova Ya. B.* // Rus. J. Electrochem. 2011. V. 47. P. 933 - 939.
4. *Gudko O. E., Lastovina T. A., Smirnova N. V., Guterman V. E.* // Nanotechnologies in Russia. 2009. V. 4. p. 309-318.
5. *Leontyev I., Belenov S., Guterman V., Haghi-Ashtiani P., Shaganov A., Brahim B.* // Rus. J. Electrochem. 2011. V. 115 p. 5429 -5434.
6. *Vysochina L. L., Belenov S. V., Guterman V. E.* // Fundamental Problems of Electrochemical Energy: Abstracts of the VIII International Conference 3-7 October 2011. Saratov, pp. 95-98.

REORGANIZATION OF THE MICELLAR STRUCTURE OF PERFLUORINATED SULFOCATIONIC MEMBRANES IN THE PROCESS OF NANOCOMPOSITE MATERIALS PREPARATION

Ninel Berezina, Svetlana Shkirskaya, Irina Falina, Olga Dyomina
Kuban State University, Krasnodar, Russia

It’s well known, that fluoropolymer ion selective membranes of Nafion type (USA) or MF-4SC (Russia) have specific cluster-channels structure that could be described in frames of inversed micelle model (fig. 1). The inversed micelle represents the combination of ion-dipole associates or inversed micelles and hydrophobic tetrafluoroethylene chains. Inherently this model considers the fact that ion-dipole clusters are formed during the polymer matrix swelling in water solutions. The clusters of 3-6 nm in diameter are bonded with channels of 1-1.5 nm in diameter. These structural fragments are surrounded by the hydrophobic flouroethylene chains.

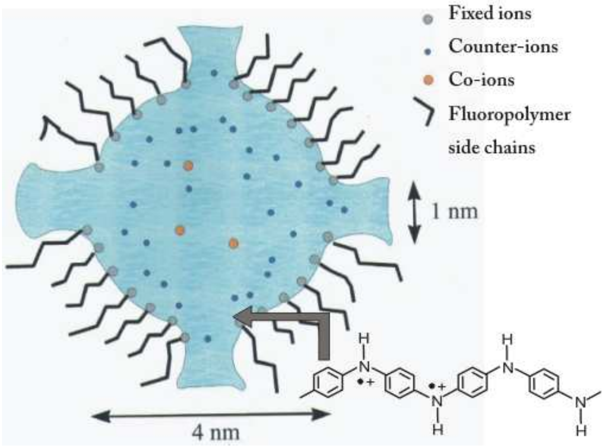

Figure 1. Micellar structure of the perfluorinated sulphocationic membrane nanosystem [1]

This process is caused by water desorption from clusters and strong electrostatic interaction between charges of fluoropolymer matrix side chains and modifiers charged centers. The effect of sorption – desorption during the MF-4SC/polyaniline nanocomposites preparation is the example of interactions above mentioned. Aromatic chains of polyaniline (PAn) intercalate into the amorphous zones of pristine membrane and significantly change ways of ions transfer in different processes. The localization of modificated components has a great importance on the stage of matrix synthesis conditions choosing. On the base of conductivity dependence on equilibrium solution concentration one can evaluate the complex of parameters (a,b,c,d,e) that reflects the structural changes in composite membrane during the modification in the frames of Gnusin model approach [2]. Model parameters correspond to fractions of current that flows through mixed channel of the gel and solution (a), gel (b) and solution (c) channels and the fractions of current that flow through gel (e) and solution (d) phases in mixed channel (fig. 2). Two-dimensional figures of such parameters demonstrate the reorganization of conducting ways which is caused by changes in composite’s morphology.

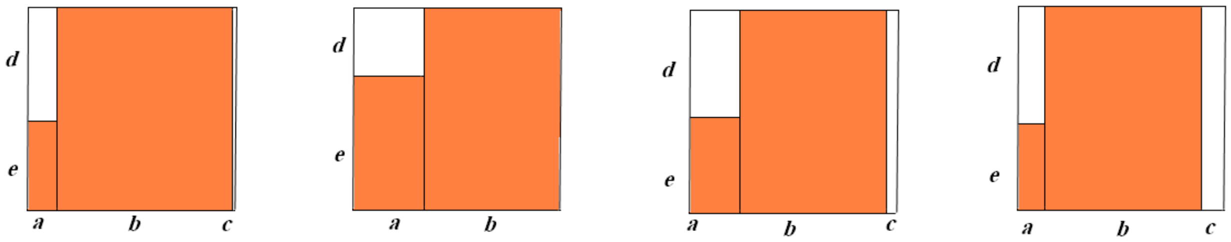

2a 2b 2c 2d

Figure 2. Two-dimensional figures of conducting ways in MF-4SC membrane before (a) and after modification by polyaniline (b,c,d). b,c,d correspond to the different thickness of polyaniline layer on the membrane surface (20, 32 and 36 mcm accordantly)

The analysis of the obtained results permitted to conclude that polyaniline chains in MF-4SC/PAn composite membrane are located near both the SO^-_3-groups and in the intermediate zone (fig. 3).

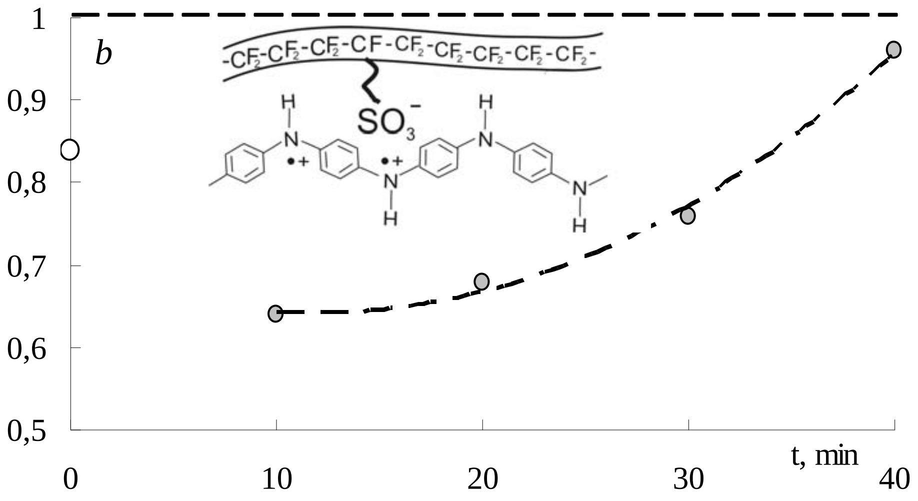

Figure 3. The dependence of the parameter b on the time of hydrolysis

So, during the matrix synthesis of composite materials by means of modifier intercalation into membrane the reorganization of micellar structure takes place. On the base of conductivity dependence on equilibrium solution concentration one can evaluate the complex of model parameters (a,b,c,d,e) that reflects the structural changes in composite membrane during the modification. The analysis of the obtained results permitted to conclude that polyaniline chains in MF-4SC/PAn composite membrane are located near both the SO^-_3-groups and in the intermediate zone.

Acknowledgements

The work was supported by Russian Foundation of Basic Research (project № 13-08-00544-a).

References

1. *Rollet, A.-L.* Etude des properiétés physico-chimiques d'ions dans un milieu poreux chargé exemple du Nafion. These de doctorat de I'Universite Pierre et Marie Curie (Paris VI). - Paris, Frans. - 1999.-179p.
2. *Berezina N. P., Gnusin N. P., Demina O. A., Annikova L. A.* Effect of Polyaniline on the Current Passing through Structural Fragments of Ion-Exchange Sulfonic-Cationite Resins and Membranes // Russian journal of Electrochemistry. 2009. Vol.45, No 11. P. 1226-1233

ELECTRODEPOSITION OF SOME METALS INTO THE PORES OF ETCHED TRACK NANOMEMBRANES

Vladimir Berezkin, Victor Korotkov, Dmitry Zagorsky, Alexander Vasiliev, Vladimir Kudriavtsev
Shubnikov Institute of crystallography RAS, Moscow, Russia.
Mendeleev state chemical technological university, Moscow, Russia, *E-mail: berezkin38@mail.ru*

It is known that track membranes could be used as template in the matrix synthesis. The main goal of this technique is to fill the pores with required substance. One of the best porous matrix version is track membrane. The track membrane application as porous matrix advantage is possibility to control the main geometric parameters of porous system at the stage of virgin film irradiation and at the stage of track chemical etching[1]. It is possible to fill the track membrane porous with various materials. But pores filling with metals is most prospective. The one is executed with metal plating into track membrane pores. The geometry of template structure may be controlled at this stage too. It must be noted that the electrodeposition (metal plating) is well-studied technological process, widely used in industry but it`s peculiarities in the low volume are investigated insufficiently.

In this work the Co and Ni electrodeposition into track membranes pores with diameters in range from 0.1 mcm to 0.5 mcm was carried out.(It must be mentioned that the first results for Co are given in [2]). Here the metals deposition was done in potentiostatic regimes and the dependence of current on time was measured. The obtained results are given in Fig.1 (for Co) and in Fig.2 (for Ni).

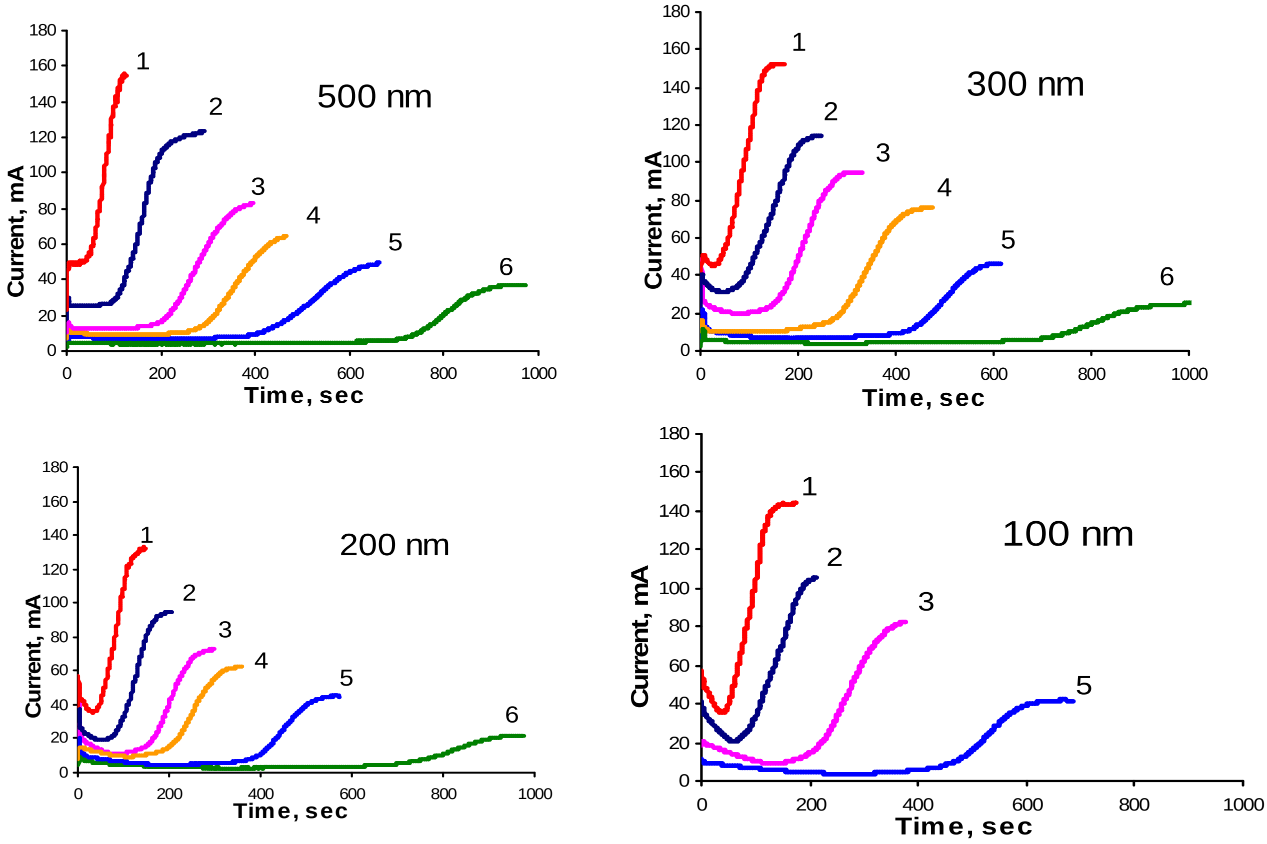

Figure1. I-t curves for deposition of Co for different pores diameters -500,300,200, and 100 nm and for different potentials:1: -680 mV, 2: -630 mV,3: -580 mV,4: -555 mV,5: -530 mV, 6: -505 mV

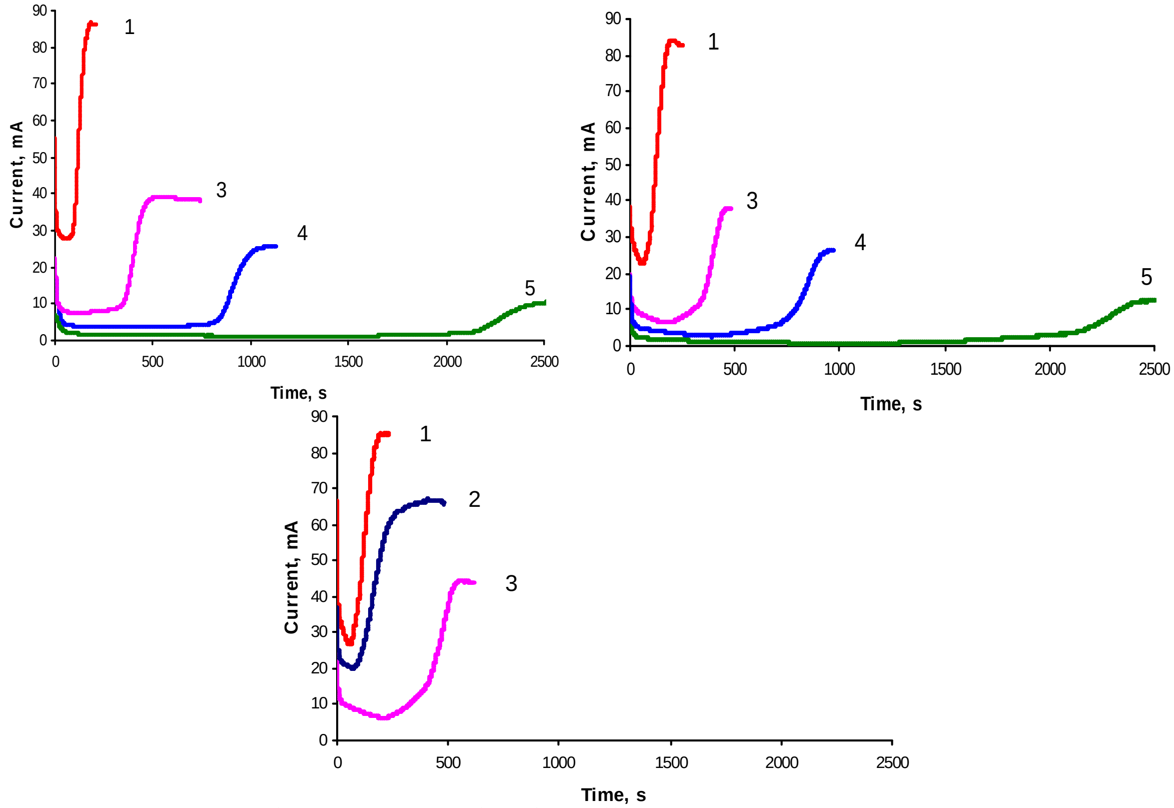

Figure 2. I-t curves for deposition of Ni for different pores diameters -500, 200 and 100 nm and for different potentials: 1: -700 мВ,2: -650 мВ,3: -600 мВ,4: -550 мВ,5: -500 мВ

Two effects are of great interest here: growth rate decrease (the one was observed clearly in initial stage of pores filling with metal) and current density increase.

In order to explain the first effect we should note that two processes competition takes place in the growth of metal replicas in the narrow pores – decrease of unfilled pore section length and decrease of electrolyte concentration owing to hindered ion transport in narrow channels (so called diffusion limits).The first results in electrical resistance decrease and the second – vice-versa. It is clearly that growth decrease proves second process dominance. This conclusion is suggested with the fact that effect is maximal for narrow pores and/or under high overvoltage.

The increase of current density was observed in metal replicas growth in matrix pores. It must be noted that increase of effective electrolyte conductivity in the track membranes pores was observed earlier. This fact was explained with gel layer formation at the pore surface [3,4]. It may be suggested that current density increase defined in work presented can be explained with gel layer existing at pore surface. The one's high conductivity results in increase of measured conductivity by several times with compare to standard one.

Aknowlegments. This work was supported by Grants OFN B-65 and RFBR 13-08-01448. We are also thankful to Dr. P. Yu. Apel for membrane preparations and for discussions.

References

1. *Martin C.R.* // Science, 1994. Vol.266, P.1961-1966.
2. *Korotkov V., Kudravtsev V., Zagorskiy D., Bedin S.* // Electroplating and Surface treatment., 2011, Vol. XIX, N 4, P.23-28.
3. *Berezkin V.V., Kiseliova O.A., Nechaev A.N., Sobolev V.D., Churaev N.V.* // Kolloidny Journ. 1994. Vol. 56. N 3, P. 319-325.
4. *Vilensky A.I., Gainutdinov R.V., Larionov O.G., Mchedlishvili B.V.* // Physical Chemistry Journ. 2001. N 12, P. 2278-2282.

INFLUENCE OF CHEMICALLY MODIFIED POLYSTYRENE ON BIPOLAR MEMBRANE CHARACTERISTICS

Alexander Bespalov, Tatyana Sorokoumova, Olga Shapovalova, Nicolai Sheldeshov, Victor Zabolotsky
Kuban State University, Krasnodar, Russia, *E-mail: sheld_nv@mail.ru*

Introduction

One of the promising areas of the electrochemical process is electrodialysis with bipolar membranes. It allows different processes with the participation of H^+ and OH^- ions such as preparation of inorganic and organic acids or bases, purification of the amino acids from salts and other processes.

Currently, bipolar membranes produced on a variety of homo-and heterogeneous monopolar membranes. Homogeneous bipolar membranes have a lower ions transport numbers and low operating voltage, however, are complex in the synthesis. The process of heterogeneous bipolar membranes preparation is simpler, but most of the known types of membranes have either low operating voltage, but the high number of co-ions transport, or high operating voltage, but low transport numbers of ions. Thus, the actual task is finding a simple approach to preparation heterogeneous bipolar membranes having improved characteristics.

Experiments

A convenient way to obtain heterogeneous bipolar membranes is pressing of heterogeneous cation-and anion-exchange membranes containing polyethylene as an inert binder. The modifies membrane preparation was carried out by dissolving the chemically modified polystyrene in acetone, and evaporation of the solution applied to the surface of cation-exchange membrane and further compacting it with an anion exchange membrane.

Frequency spectra of the membrane impedance were measured in four-chamber flow cell with active area of 2.27 cm^2 using four-electrode technique by virtual impedance meter-analyzer in 1 Hz – 1 MHz frequency range. Dependence of bipolar region resistance on the current density was determined from the frequency spectra of membrane. Then the partial current-voltage characteristic of the bipolar region was calculated using the formula $\eta_b = \int_0^{I^*} R_b dI$. Effective dissociation rate constant of water k_Σ and entropy factor β were calculated using equation $i_{H^+/OH^-} = k_\Sigma \frac{\varepsilon\varepsilon_0}{\beta}(\exp(\beta E_m(\eta_b)) - \exp(\beta E_m(0)))$ proposed in [1] for the partial voltage-current characteristics of bipolar regions of bipolar membranes. Current density of H^+ and OH^- generated in the space charge region of bipolar membranes was calculated using ion transport numbers of ions through bipolar membrane MB-2 and its analogues $i_{\mathrm{H^+,OH^-}} = iT_{\mathrm{H^+,OH^-}}$ [2].

Results and Discussion

It follows from the dependence of the resistance of a bipolar region of membranes on the current density that modified bipolar membranes have a substantially lower resistance than the original membrane (Figure 1). Comparison of the partial current-voltage characteristics (Figure 2) of the original and modified membranes shows that the overvoltage of the original membrane is greater than 20 V at 2 A/dm^2 and modified membranes at the same current have an overvoltage of 4 V (modified membrane 1) and 8 V (modified membrane 2).

Table shows that modified polystyrene as catalyst of water dissociation reaction exhibits strong catalytic effect on dissociation of water molecules in analog of MB-2 bipolar membrane as compared with original analog of MB-2. Effective rate constant increases more then ten times to the constant in original analog of MB-2.

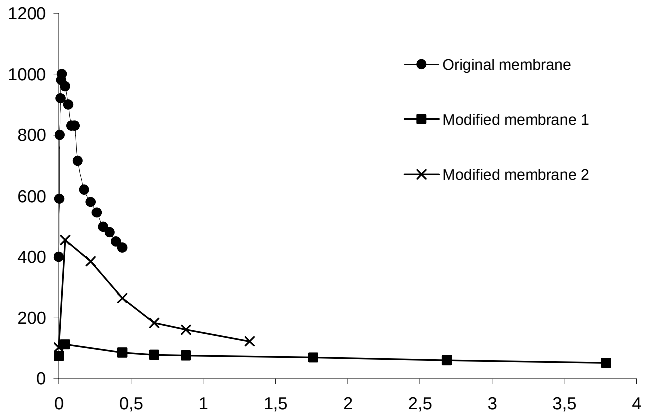

Figure 1. The resistance of a bipolar region of the original and modified membranes on the current density in the system of 0.5 M HCl | 0.5 M NaOH

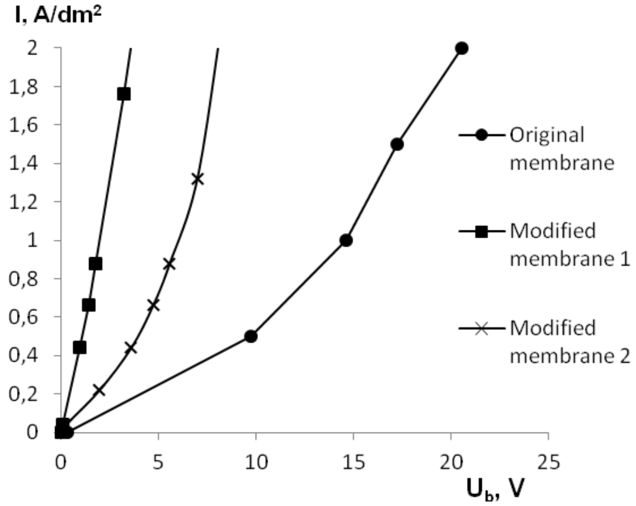

Figure 2. Partial overvoltage current-voltage characteristics of bipolar region of original and modified bipolar membranes in the system of 0.5 M HCl | 0.5 M NaOH

Table. Characteristics of water dissociation in the space charge region of analog of MB-2 with chemically modified polystyrene as catalyst and in original analog of MB-2

Membrane	**k_Σ,1/s**	**β, m/V**
Modified membrane 1	97	2,2
Modified membrane 2	9,0	3,3
Original analog of MB-2	6,8	2,1

Thus, the addition of chemically modified polystyrene as a polymer modifier significantly improves the electrochemical properties of industrial heterogeneous bipolar membranes.

References

1. *Umnov V.V., Shel'deshov N.V., Zabolotsky V.I.* The current-voltage characteristics of the space-charge bipolar membrane // Electrochemistry. 1999. Vol. 35. № 8. P. 871-878.
2. *O.V.Shapovalova, N.V.Sheldeshov, V.I.Zabolotsky.* Study of electrochemical characteristics of modified bipolar membranes // International Conference Proceedings “Ion transport in organic and inorganic membranes” 28 May – 2 June Krasnodar 2012. P. 201 – 203.

MASSTRANSFER, ELECTROPHYSICAL AND PHOTO-ELECTRIC PROPERTIES OF STRUCTURES ON THE BASIS MESOPOROUS SILICON WITH METALS NANOPARTICLES

[2]David Bilenko, [2]Victor Galushka, [2]Evgenia Hasina, [2]Inna Misenko, [1,2]Denis Terin, [2]Elvira Zharkova, [2]Sergey Venig

[1]Engels Technological Institute of Saratov State Technical University, Engels, Russia
[2]Saratov State University, Saratov, Russia

Metals nanoparticles intercalation in disorderded semiconductor layers allows to manufacture new composite structures, its possessing high catalytic, sensor and optoclectronic properties [1]. In this work influence nanoparticles of silver and iron on properties nanoporous silicon (SiMP) is discussed.

For the first time existence electrically controlled masstransfer of silver is revealed. Ag ions proceed from solid solution AgI and on channels SiMP are transferred to monocrystal silicon. Ions source is structure Ag-AgI, the temperature of phase transition is reduced at reduction of the particles size [2-4]. Change resistance of layer SiMP saturated Ag, occurs from electrically controlled moving Ag^+ from solid solution AgI in porous silicon channels. The sizes of porous silicon channels are tens nanometers.

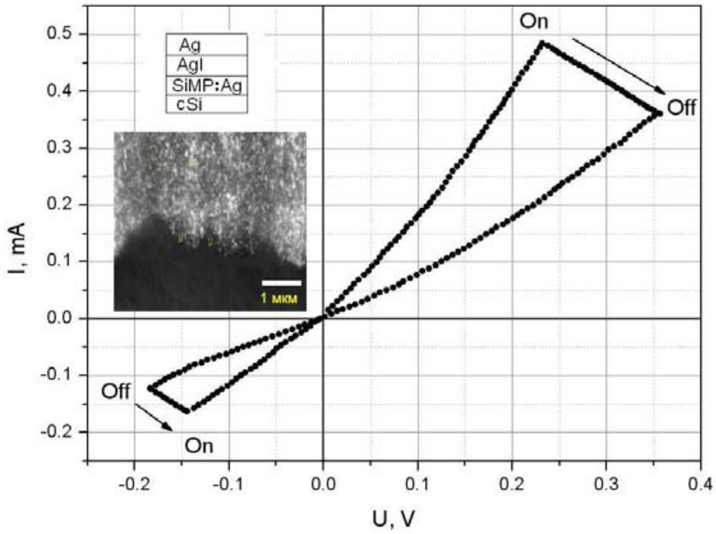

Figure 1. Voltage-current characteristic of structure Ag-AgI-SiMP:Ag-cSi

Experiments have shown, that switching of a current in structure with amplitude in some мA is observed at small voltage ~ 0.2 V. Researches photo-electric and photo-voltaic properties of structures with SiMP:Fe have allowed to establish, that these properties the same as also electrophysical [5], depend on concentration Fe ambiguously. Parameter $\mu\tau$, determed from photoconductivity, and order of current change at illumination AM-1 at concentration Fe ~ 0.1-0.2 at.% grow, and at Fe ~ 1 at.% order and $\mu\tau$ decrease, coming nearer to values in an initial material, and high permanent photoconductivity PPC ~ 10 is observed. Structures have high photosensivity so voltage of open circuit V_{oc}~16 mV at capacity of radiation AM-1 ~2 mW/cm^2. Results specify an opportunity of use such materials in sensitive photodetectors and elements of memory.

References

1. *Q.W. Chen, X. Li, Y. Zhang* // Chem. Phys. Lett. 2001. V. 343. P. 507.
2. *S. Yamasaki, T. Yamada, H. Kobayashi, H. Kitagawa* // Chem. Asian J. 2013. V. 8, P. 73.
3. *D. Bilenko, V. Galushka, I. Mysenko, K. Razumov, D. Uchaikin, A. Smirnov, D. Terin* // Ion transport in organic and inorganic membranes: Proc. Int. Conf., Krasnodar, 2012, P.30 – 33.
4. *V. Galushka, D. Terin, I. Mysenko, D. Bilenko* // Int. J. of applied and basic researches. 2012. V. 12, P. 91.
5. *D. Bilenko, V. Galushka, E. Zharkova, I. Mysenko, D. Terin, E. Hasina,* PhTP 2013. 47, P. 644

HYBRID PERFLUORINATED SULFOCATION-EXCHANGE MEMBRAINES – MATERIALS FOR POTENTIOMETRIC SENSORS

[1]Olga Bobreshova, [1]Anna Parshina, [2]Ekaterina Safronova, [2]Andrey Yaroslavtsev
[1]Voronezh State University, Voronezh, Russia, *E-mail: olga1@box.vsi.ru*
[2]Kurnakov Institute of General and Inorganic Chemistry RAS, Moscow, Russia

Introduction

Membrane modification can lead to a substantial change in their conductivity, permeability, strength and some other parameters [1]. The introduction of nanoparticles into membrane matrix makes it possible to enhance the ion transfer selectivity and to achieve asymmetry of transport processes [2]. Recently, we have proposed to use the hybrid membranes with zirconia nanoparticles as the electrodoactive material of potentiometric PD-sensors [3, 4]. In this report the dependences of sensitivity of PD-sensors based on hybrid membranes on the dopant concentration are considered. Particular attention is given to the possibility of such PD-sensors application for the determination of organic cations and anions in multiionic solutions.

1. Alternative membranes for sensors and PD-sensor device

The methods where sensors are applied are becoming widely used. The development of multifunctional potentiometric sensors using ion exchange membranes has become one of the main topics due to the prospects of their use in multiionic solutions.

Originally hydrocarbon membranes were already used for the potentiometric determination of polar organic electrolytes. However, these membranes have drawbacks: porous membranes containing water are low-selective. The composition of the membrane electrolyte in this case is therefore very sensitive to the composition of the solution. The use of perfluorinated membranes is more promising: hidrophophobicity of their matrix and macro pores absence provide their high selectivity to counterions. In addition, these membranes have high chemical stability.

A special feature of PD-sensors organization is that the distance between the boundaries of the membrane with the test and reference solutions corresponds to the membrane length, unlike the case of the known ion selective electrodes, in which it corresponds to the membrane thickness [5]. It does make the processes at the two sides in the membrane effectively independent from each other, because the membrane length, establishing of steady concentration profiles of the species in the membrane takes enormously long time. In other words, it is possible to neglect the diffusion potential. This reasoning proves the overall membrane potential being dominated only the interfacial potential difference. That is why, the external Donnan potential is the analytical signal of our potentiometric sensor.

2. The cation and anion sensitivity of PD sensors based on hybrid membrane

The perfluorinated membranes doped with zirconia were obtained as described elsewhere [6].

The use of membrane MF-4SC and Nafion with gradient ZrO_2 distribution for the determination of $NovH^+$ and $LidH^+$ cations in the solutions leads to a significant increase of sensor response values in comparison with initial membranes.

Increase in zirconia concentration in the membranes to 2,4 % leads to substantial increase in sensitivity of PD-sensors to $NovH^+$ and $LidH^+$ cations. At the same time sensitivity of the sensor to protons decreases.

Since zirconia particles in modified membranes give evidence of both cation- and anion-exchange properties it was found that the use of membrane with gradient zirconia distribution through the length leads to significant contribution of anions into analytical signal, in contrast to unmodified membrane samples. Increase of zirconia concentration in the membranes up to 2,4 - 5% results in the substantial increase in sensitivity of PD-sensors to CH_3COCOO^-, HS^- and Gly^- anions.

The essential sensitivity of PD-sensors based on hybrid perfluorinated membrane to organic cations and anions can be explained on the basis of the model according to which the dopant introduction into membrane pores leads to pores and channels expansion [1]. The presence of

ZrO_2 particles in membranes leads to replacement of «free» solution out of the pores. Furthermore, the presence of large organic ions into the pores of modified membrane reduces the interaction of the inorganic ions (including H_3O^+) with -SO_3^--groups. This explains the increase of sensitivity of PD sensors with hybrid membrane to $LidH^+$ and $NovH^+$ ions (in comparison with H_3O^+ ions) and to Gly^- and CH_3COCOO^- anions (in comparison with K^+ and NH_4^+ cations).

3. PD-sensors application for the determination of organic cations and anions in multiionic solutions

The result evidences the possibility of using hybrid perfluorinated membranes with gradient ZrO_2 distribution as electrodoactive material in PD-sensors which are sensitive to organic cations and anions. Such cross-sensitive PD-sensors were successfully used for quantitative analysis of multiionic solutions.

Acknowledgements

This present work was supported by the Russian Foundation for Basic Research (projects №12-08-00743-a, №12-08-31471/ mol_a).

References

1. *Yaroslavtsev A.B.* Correlation between the properties of hybrid ion-exchange membranes and the nature and dimensions of dopant particles // Nanotechnologies in Russia. 2012. V. 7, № 9-10. P. 8-18.
2. *Yaroslavtsev A.B., Karavanova Yu.A.,Safronova E.Yu.*, Ionic conductivity of hybrid membranes // Petr. chem. 2011. V. 51. №7. P. 493-479 (Membranes and membrane technologies. 2011. V.1, №1. P 3-10. In Russian).
3. *Bobreshova O.V., Parshina A.V., Polumestnaya K.A., Safronova E.Yu., Yankina K.Yu., Yaroslavtsev A.B.* Sensors based on zirconia-modified perfluorinated sulfonic acid membranes sensitive to organic anions in multiionic aqueous solutions // Petroleum Chemistry. 2012. V. 52, № 7. P. 499-504.
4. *Bobreshova O.V., Parshina A.V., Polumestnaya K.A., Safronova E.Yu., Yankina K.Yu., Yaroslavtsev A.B.* Perfluorinated sulfocation-exchange membranes modified with zirconia for sensors sensible for organic anions in multiionic aqueous solutions // Mendeleev Communications. 2012. V. 22, № 2. P. 83-84.
5. *Bobreshova O.V., Parshina A.V., Agupova M.V., Polumestnaya K.A*. Determination of amino acids, vitamins, and drug substances in aqueous solutions using new potentiometric sensors with Donnan potential as analytical signal // Russian Journal of Electrochemistry. 2010. V. 46, № 11. P. 1338-1349.
6. *Voropaeva E.Yu., Stenina I.A., Yaroslavtsev A.B. Ion* Transport in MF-4SK membranes modified with hydrous zirconia. // Russ. J. Inorg. Chem., 2008. v. 53, № 11, p. 1677-1680.

CHANGES AT THE STRUCTURE AND THE CHEMICAL COMPOSITION OF THE ANIONEXCHANGE MEMBRANES IN THE ELECTRODIALYSIS PROCESS

Ruslan Chermit, Mikhail Sharafan, Viktor Zabolotsky
Kuban State University, Krasnodar, Russia

Introduction

In a previous work [1] we have already studied the electrotransport characteristics of anion-exchange membranes with different nature of ion-exchange groups (MA-40 MA-41, Ralex AMH-PES), and an assessment of the modification's influence by polyelectrolyte complexes containing quaternary ammonium bases on the water dissociation rate, and electrolyte ions transport across heterogeneous anion-exchange membrane MA-40 using a device with a rotating membrane disk (RMD). The investigation methodology of EMS by RMD method was described in detail in [2]. It was found that for all considered commercially produced membranes reaction of water's dissociation actively occurs, while on the membranes AMH and MA-41, containing mainly quaternary ammonium groups, this process takes place with the greatest intensity. Such membranes behavior has been explained in [3], assuming a partial transition of quaternary ammonium bases in the reaction with hydroxyl ions to the tertiary amines, which, as in series (1) [4], accelerate the reaction of water dissociation at increasingly extent in comparison with secondary amines.

From the literature it is also known that the hydroxyl ions resulted in reaction of water dissociation lead to thermohydrolysis of quaternary ammonium groups, occurring at the anion exchange membrane / solution interface by the Hoffmann reaction, by changing the composition of the anionexchange membrane surface layer. During the Hoffmann's cleavage of quaternary ammonium bases are formed tertiary ammonium base, olefin and water [5].

$$[(C_2H_5)_2\overset{+}{N}(C_3H_7)_2]OH^- \rightarrow CH_2{=}CH_2 + C_2H_5N(C_3H_7)_2 + H_2O$$

Results and discussion

To better understand such behavior of the studied samples of anion-exchange membranes we determined the part of weak basic groups (tertiary and secondary amines) in the initial membranes. For this purpose the investigated anion-exchange membrane was kept for 48 hours in a 1M solution of copper sulfate at a pH 4. Later, the samples were properly washed with distilled water to the constancy of the chemical composition of the washing solution, then dried membrane's samples were examined for the presence of chemically bound copper with tertiary, secondary and primary amines by atomic absorption spectroscopy method, the results are reported in Table 1.

Table 1. The comparison of portion of weak basic ammonium groups in the anion-exchange membranes

Membrane	The part of copper in the membrane, %	The part of weak basic groups, %
MA-40	3,9	71
MA-40M	2,9	59
MA-41	0,042	7,4
AMH	0,0036	0,1

The table shows that the membrane MA-40 has the maximum quantity of weak basic groups – more than 70%, while the initial membrane AMH contains only quaternary ammonium groups which don't initiate water dissociation reaction according to series of catalytic activity of ionogenic groups in relation to the water dissociation reaction on the membrane / solution interface. Total and partial CVCs were measured by RMD method to study the stability of strongly basic anionexchange membranes under overlimiting current regimes during thermohydrolysis of quaternary ammonium bases from the time under the current (Fig. 1).

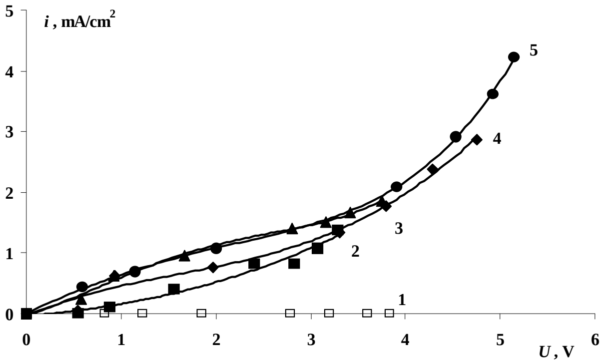

Figure 1. Partial by OH⁻ ions CVCs for EMS with the AMH in 0.01 M NaCl solution, under a membrane disk rotation velocity of 100 rpm: 1 – initial membrane, 2 –after 4 hours under the current, 3 - 8 hours, 4 - 12 hours, 5 - 16 hours

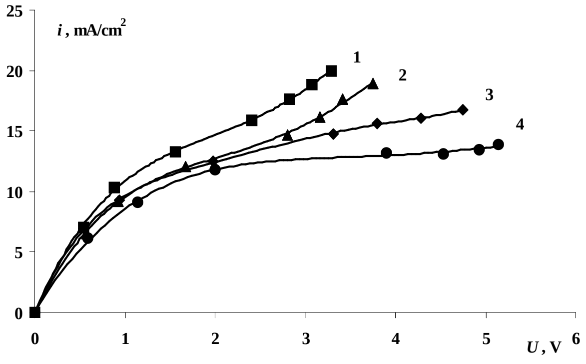

Figure 2. Partial by Cl⁻ ions CVCs for EMS with the AMH in 0.01 M NaCl solution, under a membrane disk rotation velocity of 100 rpm: 1- after 4 hours under the current, 2 - 8 hours, 3 - 12 hours, 4 - 16 hours

Fig.1 shows that water dissociation wasn't observed on the initial anion-exchange membrane AMH (curve 1), whereas after 4 hours (curve 2) the part of current carried by hydroxyl ions across the membrane has already been 10-15%, with respectively decrease mass transfer of salt ions, as evidenced from the partial by Cl⁻ ions CVCs for EMS with the AMH in 0.01 M NaCl solution, (Fig. 2).

Thus, it is experimentally shown that at high-intensive current modes of electrodialysis process thermohydrolysis of quaternary ammonium groups in strongly basic membranes occurs with the formation of catalytically active in the water dissociation reaction tertiary amines according the Hoffmann reaction. In presence of anodic reaction products (dissolved active chlorine), the rate of degradation increases. Problem of the structure and chemical stability of strongly basic anion-exchange membranes, as well as ways to enhance their stability at high densities of electric current in the membrane systems is opened question today.

This work was supported by RFBR grant № 12-08-93105-НЦНИЛ_a and grant № 12-08-31277 mol_a.

References

1. *Bugakov V.V., Sharafan M.V., Zabolotsky V.I., Nebavsky A.V.* Masstransfer mechanism and limiting state formation peculiarities at anionexchange membranes // Ion transport in organic and inorganic membranes. Conference proceeding. Krasnodar, 2010. P. 25-27.
2. *Sharafan M.V., Zabolotsky V.I.* Pat. №78577 RU. 27.11.2008.
3. *V.A. Shaposhnik, A.S. Kastyuchik, O.A. Kozaderova.* // Elektrokhimiya. 2008. V. 44. P. 1155.
4. *V.I. Zabolotsky, N.V. Sheldeshov, N.P. Gnusin.* // Uspehi khimii. 1988. V. 57. P. 1403.
5. *Ui-Son Hwang, Jae-Hwan Choi.* Changes in the electrochemical characteristics of a bipolar membrane immersed in high concentration of alkaline solutions. // Separation and Purification Technology. 2006. V. 48. P. 16.

ELECTROCHEMICAL STABILITY OF THE HOMOGENIOUS ANIONEXCHANGE MEMBRANE AMX IN THE OVERLIMITING CURRENT MODES

[1]Ruslan Chermit, [1]Mikhail Sharafan, [1]Victor Zabolotsky, [1]Svetlana Eterevskova, [2]Gerald Pourcelly
[1]Kuban State University, Krasnodar
[2]European Membrane Institute, Montpellier, France

Introduction

The transition to high-intensity electromembrane processes is one of the priorities of the membrane electrochemistry and electromembrane technology. The usage of intense current regimes, many times exceeding the limit diffusion current is often a prerequisite of modern electrodialysis to produce ultrapure deionized water, which in turn dictates new requirements for apparatus used in these ion-exchange membranes. Conducting processes desalination systems electro at high-current modes complicated one of the most important phenomena of conjugate concentration polarization - the process of dissociation of water molecules on the interface membrane / solution interface, which in turn leads to a change in pH in the membrane channel.

The dissociation of water and the pH change in alkaline and the acid side, is not only a decrease in current efficiency, but also a number of adverse events complicating the course electromembrane process. When a transition occurs alkalization solution carbonates and bicarbonates in the deposition of hardness salts, by acidification - polysilicic acids and loss transfer ampholytes in molecular form. Furthermore, the shift in the pH of the dissociation of water molecules flowing in EMC at current densities exceeding the current limit value can have a significant effect on the structure and the chemical composition of the surface of ion exchange membranes, in particular, to cause alkaline hydrolysis of quaternary amino groups in the surface layer of the membrane Hoffmann by reacting [1, 2] to form a tertiary amino flow accelerating dissociation of water [3].

Results and discussion

To study the effect of surface morphology of ion-exchange membranes and features of the mechanism of formation of overlimiting state, as well as assessing the impact of electroconvection, current-voltage characteristics were studied and the number of ion transport of salt and water dissociation products for a system with a homogenous anion exchange membrane AMX (Tokuyama Soda, Japan). We see that as for the heterogeneous anion exchange membranes form CVC membrane AMX is also different from the classical (Fig. 1).

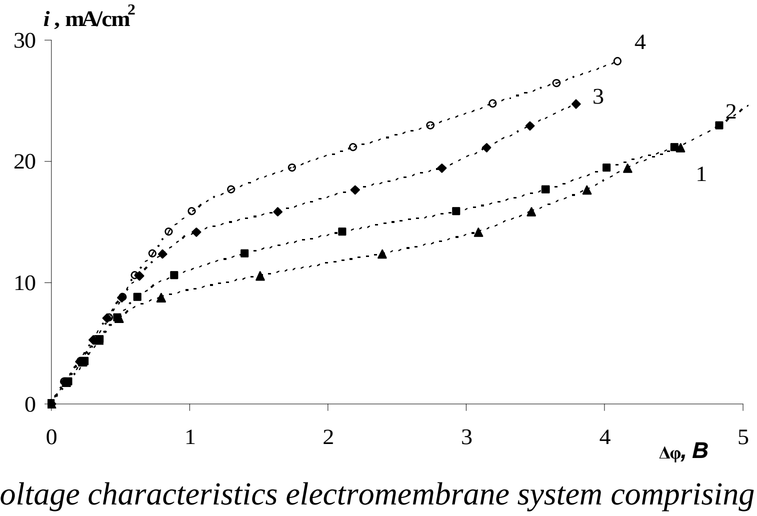

Figure 1. Total voltage characteristics electromembrane system comprising membrane AMX in 0.01 M NaCl solution at various rotation speeds of the membrane disc (rev / min):
1 - 100 2 - 200 3 - 300 4 - 500

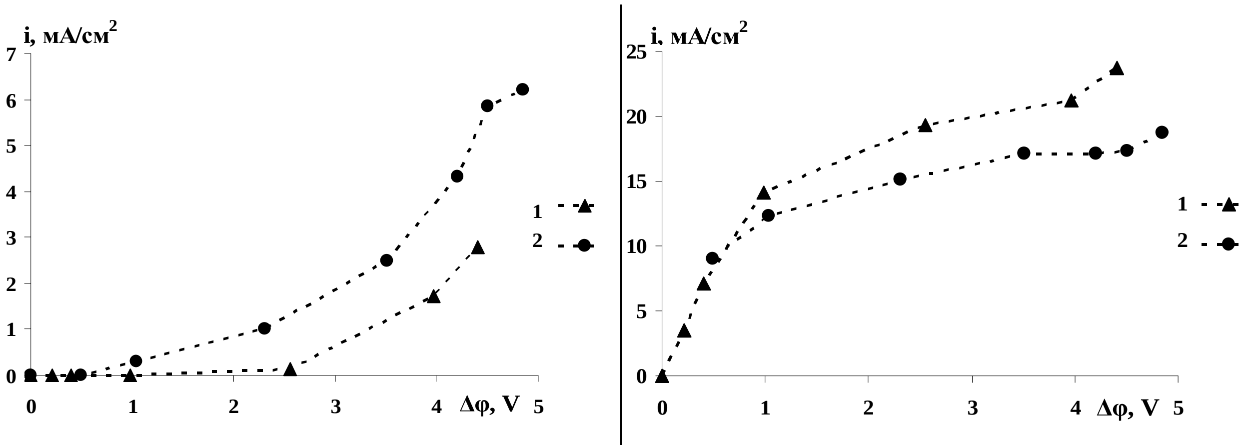

a

b

Figure 2. Partial CVC by OH^- ions (a) and Cl-(b) EMS containing membrane AMX in 0.01 M NaCl solution at a rotational speed of the membrane disc 100 rev / min: 1 - opening the membrane, 2 - after 10 hours; The electric current density at which the membrane is maintained, amounted to 2.5 i_{lim},, i_{lim}= 10,3 mA/cm^2

The partial CVC (Fig. 2) by chlorine and hydroxyl ions shows that the current in the OH-ions on the original membrane AMX when a potential jump Δφ = 2,7 In almost no growth and transport numbers by hydroxyl ions is observed only at high values of the potential drop . Transport numbers reach a value of T_{OH-}= 0.15 at a potential jump Δφ = 4,5 V. At the same time, the membrane AMX, spent 10 hours on the conditions of flow through her high current density i / i_{lim} = 2.5, the dissociation of water begins to manifest itself in the potential jump Δφ = 1V, and at Δφ = 2,7V in the transport numbers reach T_{OH-}value = 0.22, and a significant decrease in mass transfer of salt ions (Fig. 2b), similar to the heterogeneous strong base anion exchange membrane MA-41P [3]. It should be noted that the range of voltages in which the anion exchange membranes on the initial dissociation of water does not occur for a homogeneous membrane AMX wider than heterogeneous MA-41P.

This work was supported by RFBR grant № 12-08-93105-НЦНИЛ_a, grant № 12-08-31277 mol_a and №13-08-01460 A

References

1. *Sata T., Tsujimoto M., Yamaguchi T., Matsusaki K.* // J. of Membrane Science. 1996. V. 112. P. 161.
2. *U. Hwang, J.-H. Choi* // Separation and Purification Technology. 48 2006. P. 16.
3. *Zabolotskii V.I., Bugakov V.V., Sharafan M.V., Chermit R.Kh.* // Russ. J. Electrochem. 2012. V. 48. P. 650.

THE ELECTROOSMOTIC PERMEABILITY OF HETEROGENEOUS CATION-EXCHANGE MEMBRANES IN BASIC AMINO ACIDS SOLUTIONS

Mikhail Chernikov, Anastasia Silko, Elena Krisilova, Tatiana Eliseeva
Voronezh State University, Voronezh, Russia, *E-mail: mischa.vsu@gmail.com*

Introduction

The ion transport in electromembrane systems is always accompanied by solvent electroosmotic flux. This phenomenon becomes very significant for the electrodialysis with concentration chambers that have no flow through.

Experiments

The electroosmotic permeability and water transport numbers of heterogeneous cation-exchange membranes MK-40 and FTCM-E in arginine and histidine solutions were determined. The experiments were carried out at the constant current value 4.25 mA/cm^2. Amino acid feed solution flow velocity was 6 cm^3/min. The cell and the method for determination of electroosmotic permeability of ion-exchange membranes were described previously [1].

Results and Discussion

Figure. 1 shows the dependence of MK-40 membrane electroosmotic permeability on amino acid hydrochloride solution concentration. The maximum electroosmotic permeability values are characteristic of diluted solutions (C<0.05 mol/l). The electroosmotic permeability decreases with an increase of feed concentration. The comparison between solutions of amino acid hydrochlorides indicates that the electroosmotic permeability in arginine solutions is more than in histidine solutions.

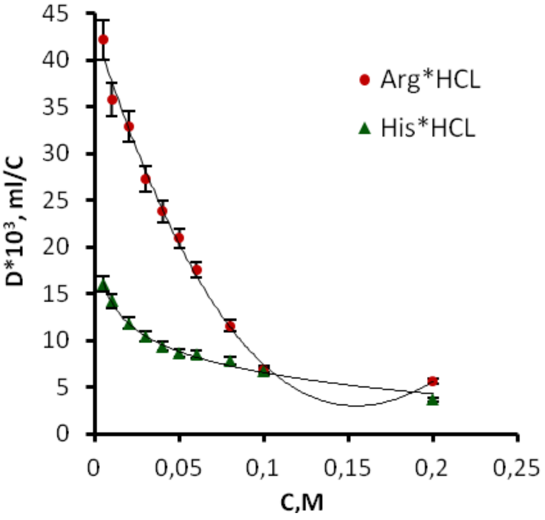

Figure 1. The dependence of MK-40 membrane electroosmotic permeability on amino acid hydrochloride solution concentration

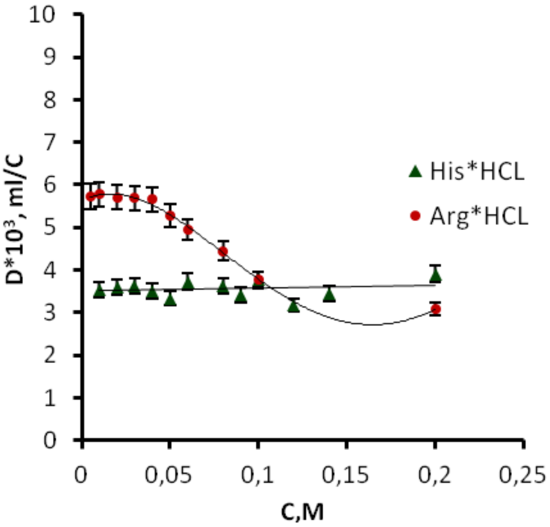

Figure 2. The dependence of FTCM-E membrane electroosmotic permeability on amino acid hydrochloride solution concentration

The electroosmotic permeability values for MK-40 membrane are more than those for FTCM-E membrane.

This difference is probably caused by pore size difference for these membranes. In diluted solutions there are more water molecules that are not comprised in hydration shells and they transfer convectively through the membrane [2]. Large pores can promote water electroosmosis flux increase. In addition, MK-40 membrane is characterized by more humidity value than FTCM-E.

In basic arginine and histidine solutions differences between the membranes under study regarding to electroosmotic flux are not so significant(Fig. 3-4).

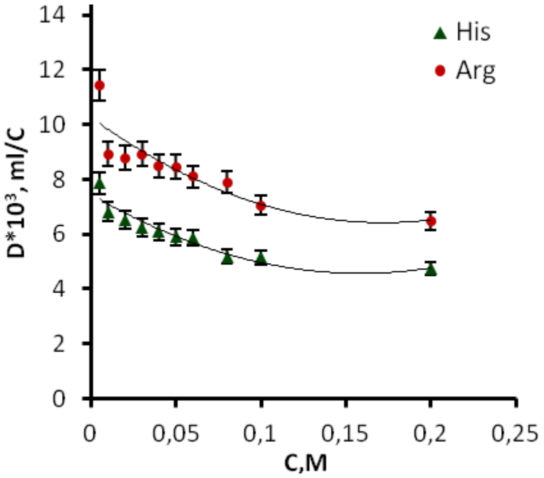

Figure 3. Effect of basic amino acid solution concentration on MK-40 membrane's electroosmotic permeability

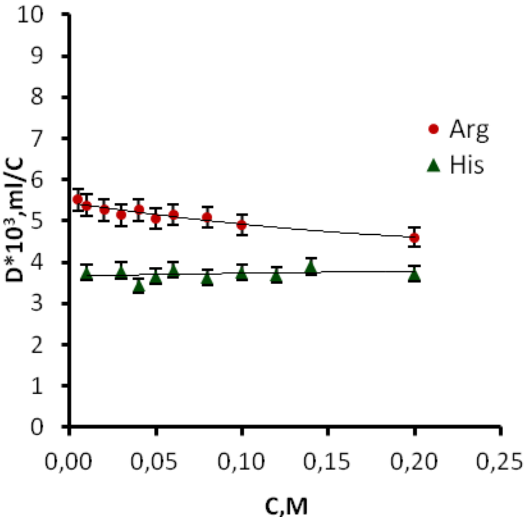

Figure 4. Effect of basic amino acid solution concentration on FTCM-E membrane electroosmotic permeability

In these diluted solutions MK-40 membrane electroosmotic permeability is sharply less than in hydrochlorides dilute solutions. Feed concentration has slight influence to water flux. Feed concentration of the both basic amino acids solutions does not affect FTCM-E membrane permeability regarding solvent in the studied range. This membrane is preferable for the concentration of histidine and arginine solutions in electrodialysis.

References

1. *T. V. Eliseeva, E. V. Krisilova, M. A. Chernikov* // Petroleum Chemistry. 2011. V. 51. P. 626.
2. *Protasov K.V.* Ph.D. Thesis. Krasnodar. 2010.

INVESTIGATION OF STRUCTURAL AND ELECTROTRANSPORT PROPERTIES OF COMPOSITE ION-EXCHANGE MEMBRANES WITH DIFFERENT FIBROUS TYPE

[1]Mariya Chernyaeva, [1]Natalia Kononenko, [1]Tatyana Berzon, [2]Marina Kardash
[1]Kuban State University, Krasnodar, Russia
[2]Engels Technological Institute (branch) of Saratov State Technical University, Engels, Russia

The impregnation of chemical fibrous by monomers with the subsequent reaction of polycondensation is the method of ion-exchange materials preparations. Thus the formation of phenolsulfocationic polymeric matrix is passed on a surface and inside fibrous structure. Fibrous composite ion-exchange membranes have complex structure and various electrotransport properties, which are dependent on the temperature, pressure and other conditions of synthesis, and also on the nature of a synthetic fiber [1].

The aim of this work is the study of structural characteristics and conducting properties of composite ion-exchange membranes on the base of different fibers: polyacrylonitrile (PAN), novolac phenol-formaldehyde (NPF) and polyester (PE). Samples were made at Engels Technological Institute in identical conditions of synthesis making use of 20 MPa pressing pressure. The porous structure of membranes was studied with method of standard contact porosimetry [2]. The integral and differential porosimetry curves are shown in Figure 1.

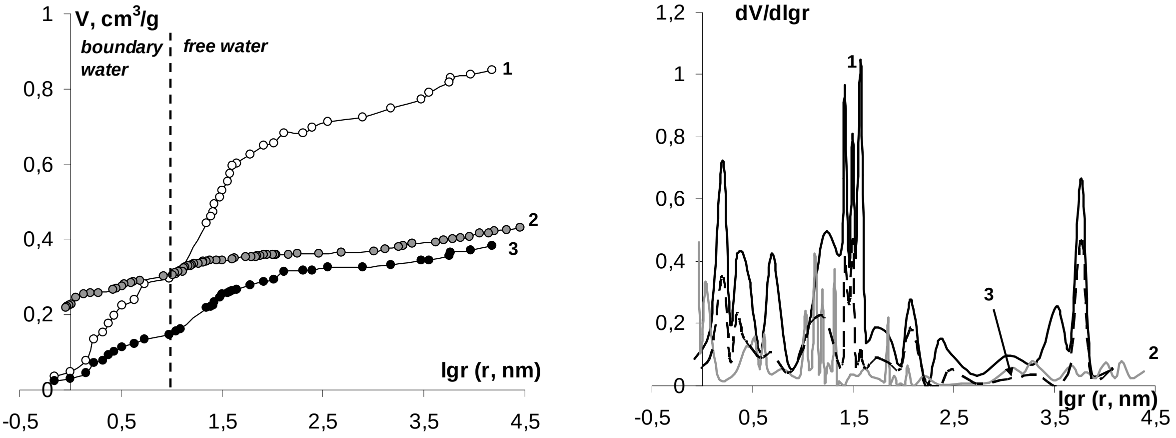

a *b*

Figure 1. The integral (a) and differential (b) functions of water distribution by the effective pore radii for composite membranes with different type of fibers: 1 –NPF, 2-PAN and 3-PE

As can be seen from the Figure 1a, all composite membranes have sufficiently large volume of macropores with effective radius of about 10 μm, irrespective of a fibrous type. The sample based on NPF has maximal volume of pores (V_0, cm^3/g), which is 2 times higher as compared with other membranes.

The specific internal surface area S (m^2/g), the volume of free water (V_{free}) and the volume fraction of the free water in swollen membrane (f_2) were calculated from the porosimetry curves of the relative water content V (cm^3 H_2O/g) as a function of the effective radii of pores r (nm) in the membrane.

$$S = 2\int_0^{\infty} \frac{1}{r^2}\left(\frac{dV}{d\ln r}\right)dr = 2\int_0^{\infty} \frac{dV}{r} \qquad f_2 = \frac{V_{free}}{V_{dry.m} + V_0}$$

where dV is the differential of aqueous volume, $V_{dry.m}=1/\rho$ – the volume of 1 g of dry membrane; ρ – the density of dry membrane.

The region of "bonded" water on the curve of water distribution along the pore radii corresponds to the energy of water bonding $A > 1$ kJ/mol and to the effective value of pore radii r < 100 nm. Table 1 presents structural parameters of membranes. As can be seen from the table, the parameter V_{free} has greater value in the case of membranes on the base NPF. The membrane on the base of PAN has a greater value of parameter S because this sample contains a lot of micropores with radii $r < 1$ nm.

Table 1. Structural parameters of fibrous composite membranes

Type of fibers	V_0, $g_{H2O}/g_{dry\ m}$	S, m^2/g	V_{free}, $g_{H2O}/g_{dry\ m}$	f_2 from V_{free}	f_2 from κ
NPF	0,85	355	0,55	0,39	0,15
PAN	0,43	539	0,12	0,12	-
PE	0,38	182	0,24	0,27	0,22

The parameter f_2, found from the porosimetry curves, has the same physical sense, as volume fraction of solution in structural-heterogeneous membrane within the framework of two-phase conducting model [3]. Calculation of the parameter f_2 is carried out by processing concentration dependence of specific conductivity of the membrane and solution in bilogaritmic coordinates $lg\kappa - lg\kappa_2$ according to the formula:

$$\kappa = \kappa_1^{f1}\,\kappa_2^{f2}$$

where κ_1 and f_1 are conductivity and volume fraction of the gel phase, appropriately; κ_2 and f_2 are conductivity and volume fraction of internal solution, which distributed in structural cavities and pores of the swollen membrane. The concentration dependence of membrane specific conductivity was obtained measuring membrane electroresistance in NaCl solution with the help of mercury-contact method. Figure 2 presents experimental data and also results of their processing in bilogaritmic coordinates. The values of parameter f_2 are given in the table.

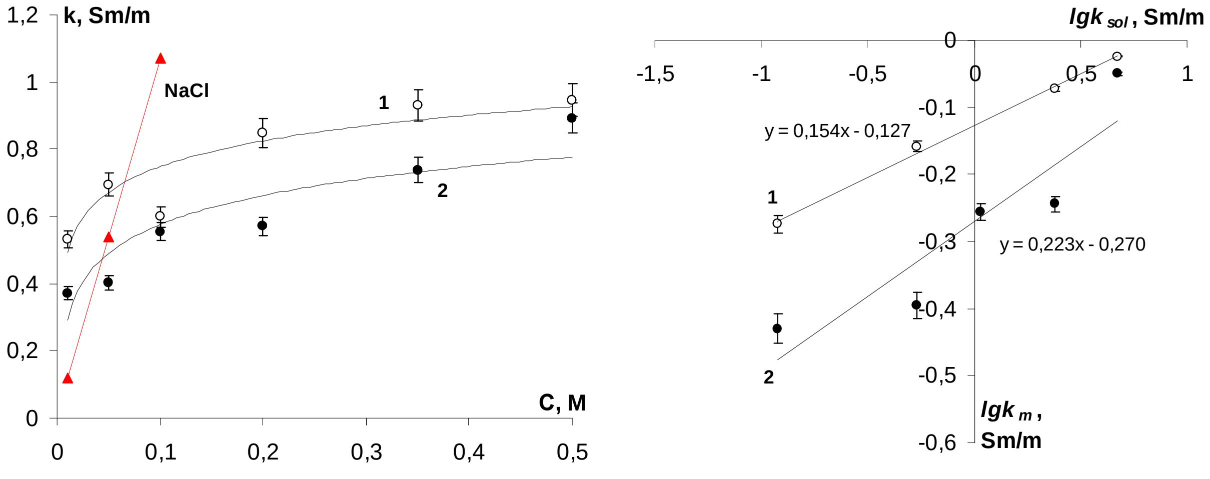

a *b*

Figure 2. Concentration dependence of conductivity of membranes on the basis of NPF fibers (1) and PE fibers (2) in solution of NaCl (a) and the results of the experimental data in bilogarithmic coordinates (b)

The analysis of the table shows, that conductivity of NPF membrane is less sensitive to concentration of an equilibrium solution despite of greater volume of free water in its эstructure.

Thus, the type of fibrous base influences the structural and conducting properties of composite membranes.

The present work is supported by the RFBR (project № 12-08-31006-mol_a).

References

1. *Kardash M.M., Pavlov A.V., Shkabara A.I.* // Chemical fibers. 2007. № 1. P. 30-33.
2. *Volfkovich Yu.M., Bagotzky V.S., Sosenkin V.E., Blinov I.A.* // Colloids and Surfaces A: Physicochemical and Engineering Aspects. 2001. V. 187–188. P. 349-365.
3. *Berezina N.P., Kononenko N.A., Dyomina O.A., Gnusin N.P.* // Advances Colloid Interface Sci., V. 139. 2008. P.3-28.

ROLE OF POLYANILINE BARRIER LAYER IN ASYMMETRY OF CURRENT-VOLTAGE CURVES

[1]Sergey Dolgopolov, [1]Natalia Loza, [1]Natalia Kononenko, [1]Ninel Berezina, [2]Sergey Lakeev
[1]Kuban State University, Krasnodar, Russia, *E-mail: svd888@mail.ru*
[2]Karpov Institute of Physical Chemistry, Moscow, Russia

The availability of anisotropic composites based on MF-4SC membrane and polyaniline (PAn) an applied electric field was investigate. Composites MF-4SC/PAn had asymmetric transport properties. The potassium dichromate was used as a polymerization reaction initiator. Electrochemistry behavior of obtained samples and composite MF-4SC/PAn, prepared by successive diffusion polymerization solutions (aniline + HCl and $(NH_4)_2S_2O_8$+HCl) into the water was compared. The asymmetry of current-voltage curves (CVC) for the composite MF-4SC/PAn, prepared in static conditions was observed and thoroughly investigated in HCl, NaCl, NaOH and series of isomolar solutions HCl–NaCl [1, 2].

Current-voltage curves for anisotropic composites prepared by different conditions show in fig.1. CVC was obtained with different direction polarizing current. The limiting current density (i_{lim}) decrease about 75% on the orientation of the membrane PAn layer to the flow of counter ion in comparison the initial membrane was observed. A significant decrease in the slope of ohmic part in this case indicates an increase in the resistance of these samples. Also observe increase potential of transition to the limiting and overlimiting state. The same effect always occur for the electromembrane system with PAn.

CVC have unusual character on the orientation of the unmodified side to the flow of counter ion. At low potentials observed inhibition of the flow counter ions, but if the potential rise up to 50 - 150 mV, conductivity of the electromembrane system begins to increase linearly (fig. 1b). One of the possible reason for this is the appearance of the internal electric field due to anion-exchange properties of the PAn layer. There is no limit current state in this case.

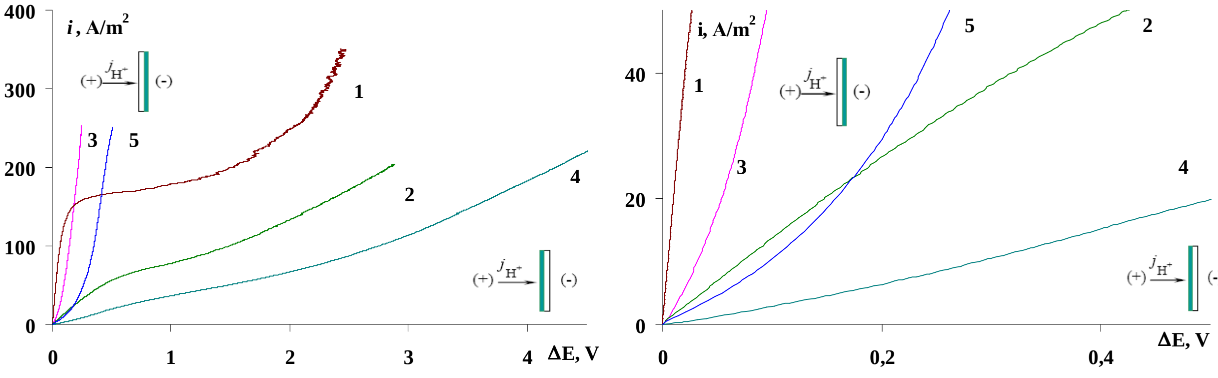

a *b*

Figure 1. The current-voltage curve (a) and ohm section of current-voltage curve (b)of the MF-4SC/PAn composite membrane in the 0,05 M HCl *solution: 1 – initial membrane, 2-5 – MF-4SC/PAn composite, was prepared in electric field (2, 3) and in the static conditions (4, 5); 2, 4 –orientation of the PAn layer in the counter ions flow; 3, 5 – and the second orientation*

Thus the composites with anisotropic properties was obtained due to the PAn chains self-organization during the synthesis on the both sides of the initial membrane. Changes at the surface morphology of both sides of the membrane are observed, that causes changes of CVC in both orientations for composite in the electric field. This effect does not depend on the preparation methods of the anisotropic composite and on the oxidant type which initiate aniline polymerization in the membrane phase.

The present work is supported by the RFBR (project № 12-08-01092).

References

1. *Berezina N.P., Kononenko N.A., Sytcheva A.A.-R., Loza N.V., Shkirskaya S.A., Hegman N., Pungor A.* // Electrochimica Acta. 2009. V.54. P. 2342-2352.
2. *N.A. Kononenko, N.P. Berezina S. Dolgopolov, N. Loza, S. Lakeev* // Elektrokhimiya. 2012. V. 48. №8. P. 940.

COMPOSITE HOLLOW FIBER MEMBRANES WITH DIFFUSION LAYERS FROM POLY[1-(TRIMETHYLSYLIL)-1-PROPYNE]

[1]Georgiy Dibrov, [2]Alexandr Bildukevich, [2]Vadim Usoskiy, [2]Victor Kasperchik, [1]Vladimir Vasilevsky, [1]Eduard Novitsky, [1]Elena Litvinova, [1]Valeriy Khotimsky, [1]Vladimir Volkov

[1] Topchiev Institute of Petrochemical Synthesis RAS, Moscow, Russia
[2] Institute of Physical Organic Chemistry, National Academy of Sciences, Minsk, Belarus
e-mail: george.dibrov@ips.ac.ru, vvvolkov@ips.ac.ru, ednov@ips.ac.ru

Introduction

The application of membrane gas-liquid contactor is a new promising way in regeneration technology of absorbents saturated with carbon dioxide. The main element which determines the effectiveness of these devices is the membrane, hollow fiber in the first place, as it allows to create the most advanced devices with a high surface area (≥ 10 000 m^2/m^3 of the apparatus). In this work the results of the elaboration of hollow-fiber composite membranes are described. Asymmetric polysulfone (PSf) and polyethersulfone (PES) ultrafiltration membranes were used as supports, poly[1-(trimethylsylil)1-propyne] (PTMSP) as a diffusion layer.

Experiments

Methods of asymmetric hollow fiber ultrafiltration membranes formation from PS and PES were developed. These membranes were used as supports for the composite gas separation membranes formation. Samples of hollow fibers with the water permeability of 150-200 (PS-50), 500-600 (PES) and 700-800 (PS-100) $l\cdot(m^2\cdot h)^{-1}$ were developed. Inner diameter of fibers was 950-1050 μm, average thickness of walls – 280 μm. Pores size on the bore side of the fiber was not more than 0.02-0.05 μm, on the shell side – 10 μm. According to calibration by model solutions of a polyvinylpyrrolidone, the molecular weight cut-off of membranes was 50 and 100 kDa, respectively. The composite membranes were obtained by pumping the PTMSP solution through the bore side of the hollow fibers. Pure nitrogen and carbon dioxide permeance was measured at pressures up to 2 bar and temperature 23^oC using constant pressure/variable volume technique.

Results and Discussion

Composite membranes with highest carbon dioxide permeance were obtained when PS-100 sample with high water permeability was used as a porous support. PTMSP solution in hexane was used for the formation of the selective layer of composite hollow fiber membranes (PTMSP molecular weight was $1.2\cdot10^6$ g/mole). The choice of solvent was defined by the fact that polysufone is insoluble in hexane. This provided the preservation of internal pores sizes and configuration of the hollow fiber support. After the selective layer deposition selectivity $\alpha(CO_2/N_2)$ increased up to 3.5 and was equal to that of PTMSP indicating that composite membrane was defect-free (Table 1) while carbon dioxide permeance was 0.26 $m^3\cdot(m^2\cdot h\cdot bar)^{-1}$.

Table 1. Nitrogen and carbon dioxide permeance (P/l) and selectivity (α) of initial hollow fibers PS-100 and composite PTMSP membranes.

Permeance and selectivity	Initial hollow fibers PS-100	Composite PTMSP membranes
P/l(N_2), m^3(STP)· (m^2·h·bar)$^{-1}$	26.90	0.07
P/l(CO_2), m^3(STP)· (m^2·h·bar)$^{-1}$	23.94	0.26
$\alpha(CO_2/N_2)$	0.89	3.5

The authors gratefully acknowledge the support RFBR grant # 12-08-90010_Bel_a.

NITROGEN SELECTIVE POLY(2-METHYL-5-VINYL TETRAZOLE)-ZEOLITE MIXED MATRIX MEMBRANES

[1]Georgiy Dibrov, [2]Elena Knyazeva, [1]Alexandr Malakhov, [1]Eduard Novitsky, [3]Vladimir Ostrovsky, [3]Rostislav Trifonov, [1]Alexey Volkov

[1]Topchiev Institute of Petrochemical Synthesis RAS, Moscow, Russia, *E-mail: george.dibrov@ips.ac.ru*
[2] Lomonosov Moscow State University, Moscow, Russia
[3] State Institute of Technology, St. Petersburg, Russia

Introduction

Modern membrane industry allows to obtain oxygen enriched air in the permeate and oxygen depleted air (technical nitrogen) in the retentate. This is achieved by using oxygen-selective membranes. In this work an attempt to obtain nitrogen-selective membranes is made. Poly(2-methyl-5-vinyl tetrazole) (PMVT) is distinguished from other polymers by its unique chemical composition $–[C_4N_4H_6]_n–$. The backbone of its macromolecule is decorated with side groups which are heterocycles primarily composed of nitrogen atoms. Filling PMVT with zeolites that have nitrogen-selective sorption was employed to increase the transfer of nitrogen through the membrane.

Experiments

The effect of synthesis conditions on the properties of zeolite NaA was studied. Zeolites were synthesized in the form of isolated crystals of small size for further modification and application as components of mixed matrix membranes (MMMs). The resulting crystalline products were characterized using X-ray diffraction analysis and scanning electron microscopy (SEM). PMVT with M_w~ $7\cdot10^4$ g/mole was synthesized by method described elsewhere [1]. Permeability and diffusion coefficients of nitrogen, oxygen and carbon dioxide for the PMVT film with a thickness of 50 μm were measured at a feed pressure of 0.6 - 0.8 bar and at temperatures of 25-45°C using a constant volume/variable pressure experimental setup (GKSS Time-Lag Machine) [2].

Results and Discussion

Using aerosil, hydroxide and sodium aluminate zeolite samples with various sizes of crystals were prepared at 90 ℃ (fig. 1). The mixture of NaAII: Na2O- Al2O3 - SiO2 (3:1:2) crystallized into the material with the smallest crystal size (fig. 1) and appeared as the most promising for molding PMVT-zeolite MMMs. Optimal concentration of polymer was found to be 2.5 wt% to form homogeneous PMVT membranes. For a sample of the membrane with thickness 50 μm nitrogen and oxygen permeability coefficients were 0.05 and 0.17 Barrer respectively. The ideal gas selectivity was 3.4 indicating that membranes were defect-free. Therefore it was proven that this method may be applied to form PMVT-zeolite MMMs.

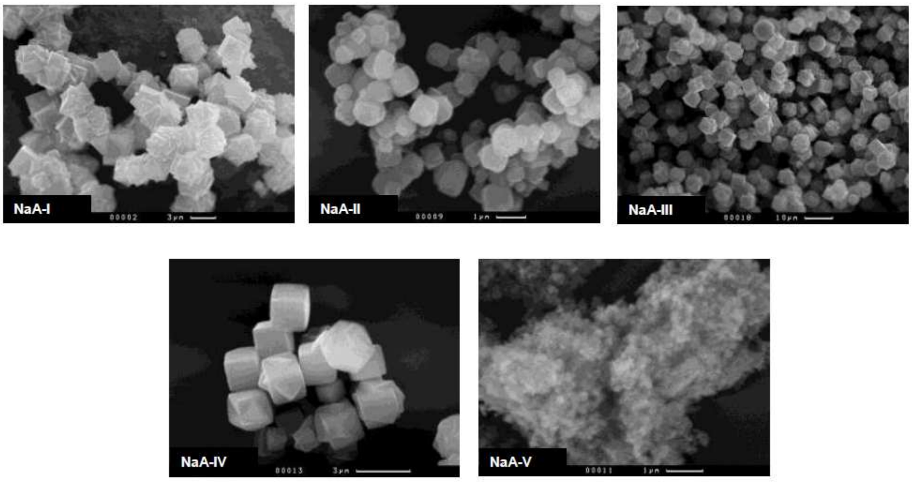

Figure 1. SEM micrograph of zeolite crystals synthesized

The authors gratefully acknowledge the support RFBR grant # 12-08-00275-a.

References

1. *M. Uspenskaya*, Tetrazole containing polymers, St. Petersburg (2008)
2. *S.M. Shishatskiy, Yu.P. Yampolskii, K.V. Peinemann* // J. Membr. Sci. 112 (1996) 275–285.

INFLUENCE OF IONOGENIC GROUPS AND POLYMER MATRIXES TYPES AND MANUFACTURING TECHNOLOGY ON THE STRUCTURE ORGANIZATION OF THE ION-EXCHANGE MEMBRANES

Olga Dyomina, Ninel Berezina, Natalia Kononenko, Nikolay Gnusin
Kuban State University, Krasnodar, Russia

Introduction

The data listed in catalogs [1-8] indicate that the basic ion-exchange membranes equilibrium characteristics which determine their electrotransport properties: ion-exchange capacity and water content, depend both on the membranes manufacturing technology and nature of ionogenic groups and polymer matrixes due to their different hydratability and hydrophilic nature.

The aim of this study is to investigate effect of nature of ionogenic groups and polymer matrixes on the structure organization of ion-exchange membranes and on the mechanisms of current passing through their structural fragments.

Experiments

The objects of the study were the commercial heterogeneous and homogeneous membranes which were manufactured in different countries (Table 1). Model parameters which reflect the structure organization of ion-exchange materials: the volume fractions of conductive phases (f - of the gel phase, $(1-f)$ - of intergel solution) and their relative position (parameters α), were calculated using an extended three channel model [9]. Model parameters that reflect the current parts flowing via three parallel channels: sequentially through gel and solution (*a*), only through gel (*b*), only through solution (*c*), were also calculated by this way. Parameters *d* and *e* are the current parts flowing via solution (*d*) and gel (*e*) in the channel of their serial combination (*a*). Calculations were performed on the basis of the experimentally obtained concentration

Table 1: Commercial ion-exchange membranes

Membrane	Matrix	Fixed groups	Q, $\frac{mmol}{g_{dry}}$	n_m, $\frac{mol.H_2O}{mol.groups}$	κ_{iso}, $\frac{Sm}{m}$
MK-40 (Russia)	polystyrene (PS), divinylbenzene (DVB)	$-SO_3^-$	2.24	11.8	0.35
MA-41 (Russia)	PS, DVB	$-N^+(CH_3)_3$	1.50	22.1	0.58
MA-40 (Russia)	epichlorhydrine, polyethylenepolyamine	$\equiv N, = N,$ $-N^+(CH_3)_3$ (<20%)	3.60	14.0	0.40
CR 67-HMR-412 (USA)	vinyl monomer	$-SO_3^-$	1.94	16.7	0.52
AR 204-SZRA-412 (USA)	vinyl monomer	$-N^+(CH_3)_3$	1.27	33.0	0.89
CM-1 (Japan)	PS, DVB	$-SO_3^-$	2.15	9.7	0.52
AM-1 (Japan)	PS, DVB	$-N^+(CH_3)_3$	2.00	8.3	0.22
3361-BW (China)	PS, DVB	$-SO_3^-$	3.15	10.9	0.58
3362-BW (China)	PS, DVB	$-N^+(CH_3)_3$	1.75	15.3	0.62
Nafion 117 (USA)	trafluorethylene, polyfluorvinyl ether	$-SO_3^-$	0.91	11.3	0.73
Nafion 425 (USA)	trafluorethylene, polyfluorvinyl ether	$-SO_3^-$	0.83	12.9	0.37
MF-4SC (Russia)	trafluorethylene, polyfluorvinyl ether	$-SO_3^-$	0.79	12.7	0.47
MF-4SC$_{rein}$ (Russia)	trafluorethylene, polyfluorvinyl ether	$-SO_3^-$	0.62	18.5	0.54

dependences of the studied membranes conductivity according to the procedure described in [10]. NaCl solutions were used as equilibrium ones.

Results and Discussion

The range of values of model parameters of the commercial heterogeneous and homogeneous membranes of Russian and foreign production are shown in Table. 2. We can see that the model parameters of the heterogeneous membranes produced by a mechanical technique by mixing powdered ion-exchange resins and polyethylene, with a subsequent pressing of the obtained mixture and reinforcement as a rule with a Nylon mesh (MК-40, MA-40, MA-41, CR 67-HMR-412, AR 204-SZRA-412, 3361-BW, 3362-BW) are changing in a fairly narrow range. The parameters of polystyrene CM-1 and AM-1 membranes manufactured by paste method are changing in the same range. Consequently, the nature of the ionogenic groups and the polymer matrixes of heterogeneous membranes as well as manufacturing technology have slight effect on their structure organization and the mechanisms of current passing through their structural fragments: the general current part (≈ 70%) is transferred through gel by counterions (*b*), and the channel of the solution (*c*) is practically absent.

Table 2. The range of values of model parameters of the heterogeneous and homogeneous perfluorinated membranes of Russian and foreign production

Membranes	Model parameters						
	f	α	*a*	*b*	$c\times10^2$	*d*	*e*
Heterogeneous	0,85±0,05	0,44±0,08	0,29±0,09	0,70±0,08	0,02 ± 0,01	0,45±0,06	0,55±0,06
Homogeneous perfluorinated	0,93±0,03	0,46±0,02	0,14±0,07	0,85±0,06	0,30±0,20	0,47±0,01	0,53±0,01

Table 2 also shows the value range of the parameters of homogeneous commercial perfluorinated membranes such as Nafion and MF-4SC. As we can see, the distinguishing feature of this membranes type is higher gel phase volume fraction compared with the heterogeneous membranes which provides a significant increase in the contribution of the channel clear gel (*b*) in the overall current transport through the membrane. The second distinguishing feature of the unlinked perfluorinated membranes is the presence of pure solution channel (*c*). The contribution of channel (*c*) in the overall current transport in the commercial homogeneous membranes is much higher than in heterogeneous samples.

Thus, the nature of ionogenic groups, the polymer matrixes and the manufacturing technology have a significant influence on the equilibrium and transport characteristics of the homogeneous and heterogeneous membranes (Table 1). At the same time the above mentioned factors have a little influence on the relationship and relative position of the conductive phases in commercial ion-exchange membranes and the current transport through their structural fragments.

The present work was supported by the Russian Foundation for Basic Research

References

1. Ion-exchange membrane. Granulates. Powders. Catalogue. NIITEKHIM. 1977.
2. Neosepta. Ion-exchange membranes. Tokuyama Sda. Co. Ltd. 1979.
3. Aldrich. Germany catalogue. Handbook of fine Chemicals. 1999-2000.
4. Ionics. Bulletins. Cation-Transfer Membranes. Anion-Transfer Membranes. USA. 1990.
5. Selemion. Ion-exchange membranes. Japan: Asahi Glass Co., 1984.
6. Data Sheet Membrane. RALEX MEGA, 2005.
7. *Mazanko A.F., Kamaryan G.M., Romashin O.P.* Industrial membrane electrolysis. Khimiya, 1989.
8. PE heterogeneous ion-exchange membrane. The Factory standard HU Q/G-HPA87-94. Shanghai chemical plant.
9. *Gnusin N.P., Berezina N.P., Kononenko N.A., Demina O.A., Annikova K.A.* // Zh. Fiz. Khim. 2009. Vol. 83 № 1. P. 122.
10. *Gnusin N.P., Demina O.A., Annikova K.A.* // Elektrokhimiya. 2009. Vol. 45. № 4. P. 522.

THE EFFECT OF COMPLEX FORMATION ON THE SORPTION OF Hg (II) BY ION-EXCHANGE MEMBRANE

[1]Alexander Dyukov, [2]Svetlana Shishkina, [2]Evgeniya Zhelonkina
[1]"KCKK Mineral Fertilizer Plant" OJSK, Kirovo-Chepetsk, Russia, *E-mail: Aleksandr.Dyukov@kckk.ru*
[2]Vyatka State University, Kirov, Russia, *E-mail: vgu_tep@mail.ru*

Despite worldwide reduction of usage of highly toxic mercury its application in chlorine industry, measuring and lighting device productions is still in use. To decrease ecological danger of such productions it is necessary to find effective methods which lower mercury losses from a production cycle and exclude mercury containing wastes. One of these methods is the electrodialysis. However physicochemical properties of ion-exchange membranes in water solutions containing mercury compounds are studied insufficiently.

In present work physicochemical properties of ion-exchange membranes heterogeneous ion-exchange membranes MC-40, MA-40 and MA-41 made in Russia in sodium chloride solutions of 85 millimoles concentration containing different amount of mercury ions (from 0.25 millimoles to 100 millimoles) were studied.

In solution containing inorganic ligands mercury ions form complicated particles of various composition.

With the use of methodology written in [1] we calculated the concentration of such particles present in water solution. For the calculation we take into account, firstly, equilibrium equations of mercury for stepped chloride complex formation, secondly, mercury hydrating equations, thirdly, material balances for chloride and mercury ions and at last, a proton equilibrium equation which is derived from electro neutrality condition and material balances. In is show that depending on concentration of the solution nearly 50 percent of mercury ions may exist as negatively charged complex ions $HgCl_3^-$ and $HgCl_4^{2-}$. The quantity of positively charged mercury particles such as $HgCl^+$ and Hg^{2+} is negligible.

It should be noted that the quantities of mercury absorbed by anion-exchange membranes exceed their exchange capacities [2]. Therefore, as an addition to the exchange mechanism there takes place a chemical one between mecury ions and functional groups.

Are studied mercury sorbtion by the membranes in pure mercury (II) cloride solutions in which, as it was calculated according to the methodology [1], mercury exists mostly in neutral molecules of $HgCl_2$. It is stated that MA-40 absorbs mercury from pure mercury chlorides in practically the same amounts as from sodium together with mercury cloride solutions. MA-40 also absorbs mercury from such solutions in comparable amounts. This fact indicates that there exist a chemical mechanism of mercury sorbtion.

D-metal ions including mercury ones are able to coordinate protonless secondary and tertiary aminogroups around them with chelate structure formation [3]. Therefore MA-40 the functional groups of which are secondary and tertiary amines may absorb mercury both ways according to coordination mechanism (chemically) and exchange one.

It is known [4] that during changing of state of ion-exchange materials (changing of counter ions, complex ions formation with functional groups, unexchange sorbtion) the shape of their IR-spectra also changes.

Thus the presence of changes in IR-spectra of MA-41 may be explained by the $HgCl_3^-$ и $HgCl_4^{2-}$ ions taking part in the exchange process.

Appearance of new maximums may be the result of coordination interaction between mercury ions and functional secondary and tertiary aminogroups. As a visual conformance of the process of complex formation with the participation of functional groups may be the fact that the membrane changed its colour to a grey one.

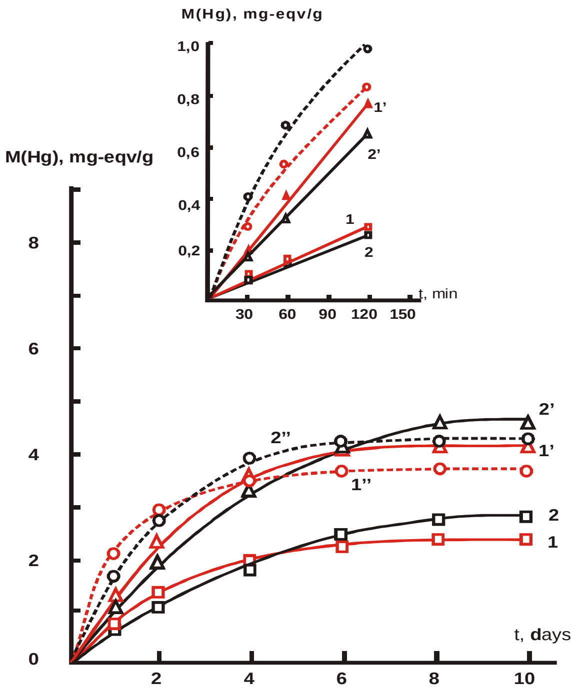

Figure 1. Saturation curves of MA-41 in solutions under studying and pure mercury (II) chloride solutions. Mercury concentration is (in M 10^{-3}): 1,2 - 2,5; $1^{'}$,$2^{'}$ – 5; 3,3’ – 10

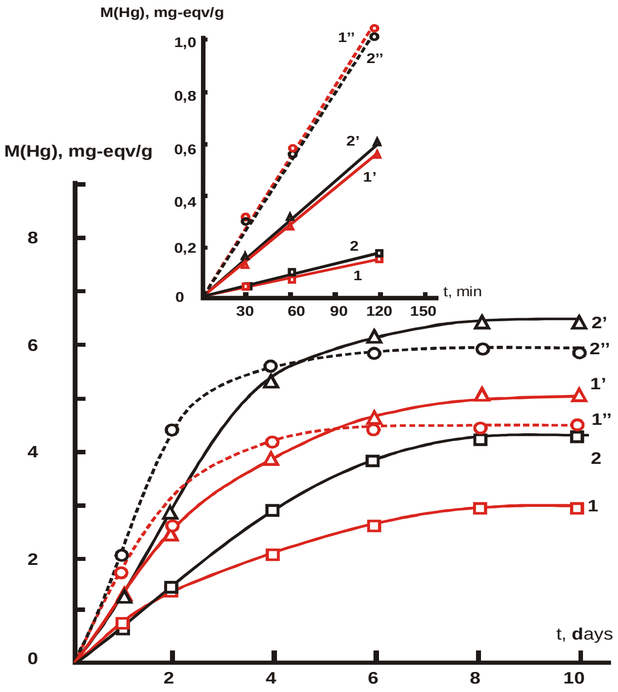

Figure 2. Saturation curves of MA-40 in solutions under studying and pure mercury (II) chloride solutions. Mercury concentration is (in M 10^{-3}): 1,2 - 2,5; $1^{'}$,$2^{'}$ –5;3,3’–10

Resistance of the membranes equilibrated with solutions under studying was measured as a combined one with marking out ohmic resistance by means of Impedancemeter Z-2000. Concentration dependences of electrical conductivity of the membranes in solution under studying correlate completely with the conception of interaction of the membranes with mercury containing particles.

MA-40 has the smallest electrical conductivity because chloride counter-ions to the most degree are immobilized in the chelate structures and complex ions which have low mobility. MC-40 in its turn are in sodium ions form and its electrical conductivity correlate with literature data. Significant part of mobility in case of MA-41 belongs to low mobility complex ions of $HgCl_3^-$ and $HgCl_4^{2-}$.

References

1. *Butler J.* Ionic Equilibrium. (A Mathematical approach), Reading, Massachusetts, 1964.
2. *Zabolotskiy V.I., Nikonenko V.V.* Ion Transport in Membranes. –M.: Nauka, 1996.-392 p.
3. *Shishkina C.V., Petchenkina E.S., Dyukov A.V.* Transport properties of anion-exchange membranes: Effect of the formation of complexes // Russian J. Electrochemistry. 2006. T.42. N 12. P.1457-1465.
4. *Semushin A.M., Yakovlev V.A., Ivanova E.V.* IR absorption spectra of ion-exchange materials. Chemistry, 1980. 96 p.

STRUCTURAL TRANSFORMATION OF POLYMER AND COMPOSITE ION-EXCHANGE MATERIALS INFLUENCED BY ORGANIC SOLVENT

[1]Yuliya Dzyazko, [1]Ludmila Ponomaryova, [2]Yurii Volfkovich, [2]Valentin Sosenkin, [3]Vladimir Trachevskii, [1]Alexey Palchik, [1]Sergey Vasilyuk, [4]Nikolay Scherbatyuk
[1]Vernadskii Institute of General & Inorganic Chemistry of the NAS of Ukraine, Kiev, Ukraine
E-mail: dzyazko@ionc.kiev.ua
[2] Frumkin Institute of Physical Chemistry & Electrochemistry of RAS, Moscow, Russia,
E-mail: yuvolf40@mail.ru
[3]Kurdyumov Institute of Metal Physics of the NAS of Ukraine, Kiev, Ukraine
[4]Kholodny Institute of Botany of the NAS of Ukraine, Kiev, Ukraine

Introduction

Organic-inorganic ion-exchange materials are more attractive comparing with polymer ones due to their considerable protonic conductivity under low humidity conditions, stability against fouling with organic substances and bacteria, selectivity towards d-metal ions etc. [1]. They are used for low-temperature fuel cells, electromembrane separation, ion exchange. However some processes, which require organic-inorganic materials, involve organic solvents. They are able to change structure of the polymer constituent (matrix). Inorganic particles can be located in different pores of the matrix: in clusters, empties between gel fields, structure defects [2]. Thus transformation of porous structure of the swollen polymer probably results in a change of particle location. The aim of this work was to investigate this possible effect.

Experiments

Strongly acidic gel-like cation-exchange resin Dowex HCR-S (Dow Chemical) containing 8-10 % DVB has been chosen as a model matrix (sample 1). The resin was immersed in a $ZrOCl_2$ solution followed by treatment with H_3PO_4. Sample 2, which contains zirconium phosphate (ZrPh) in forms of single nanoparticles and their aggregates, has been obtained by this manner [2]. Both initials and modified resins were immersed in acetone (samples 3 and 4 respectively). Finally the inorganic constituent was incorporated into the resin, which had been treated previously with organic solvent (sample 3→sample 5). The materials were investigated with a method of standard contact porosimetry, which can be applied to polymers [3, 4]. Water was used as a working liquid, the samples were previously vacuumized at 353 K. Removal of bonded and free water from ZrPh phase is impossible under these conditions. Thus structure of the polymer has been mainly recognized. The resins were investigated using NMR, FTlR and imedance spectroscopy, scanning and transmission electron microscopy, Analogues resin, namely KU-2-8 (Schekinoazot), was also researched for a comparison.

Results and Discussion

Both non-aggregated nanoparticles and their aggregates (up to several μm) have been found in the matrix of sample 2 (Fig. 1a).

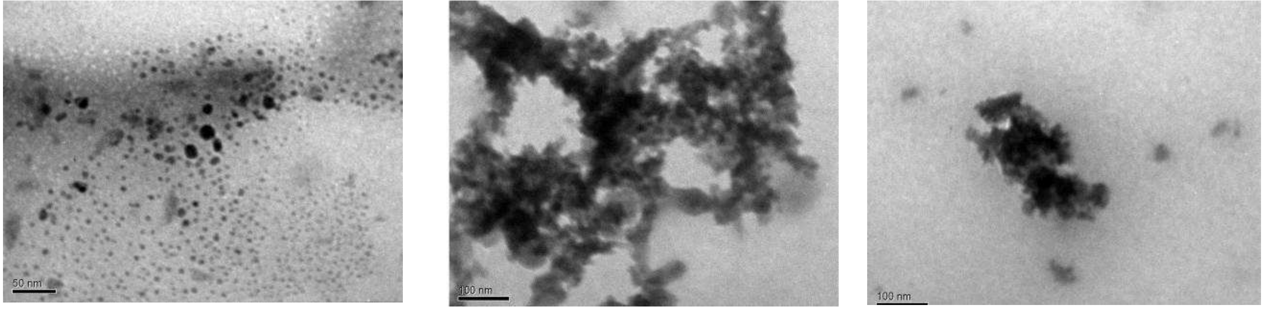

a *b* *c*

Figure 1. TEM images of samples containing ZrPh: no acetone treatment (a), immersed in acetone after (b) and before (c) insertion of inorganic constituent

The nanoparticles, which are stabilized with the polymer, are placed inside the clusters and probably channels of gel phase, the aggregates can be located between gel fields and inside structure defects. No single nanoparticles were found for the samples, which had been immersed in acetone both before and after modification with ZrPh (Figs. 1b, c). In these cases the nanoparticles form aggregates of different size.

Insertion of ZrPh into the matrix causes an increase of macropore size and volume evidently due to stretching of the polymer influenced by the aggregates (Fig. 2). Simultaneously the volume of mesopores decreases as a result of their corking with the nanoparticles. If no acetone treatment is used, the pores with a radius of 10 nm, which are attributed to clusters, have been found. As for resins treated with organic solvent, the cluster radius decreases up to 2 nm. Decrease of size of the transport pores, where functional groups are located, causes diminution of electrical conductivity of H-forms of the ion-exchangers. For instance, these values are 0.42 and 0.23 Ohm^{-1} m^{-1} for samples 1 and 3 respectively.

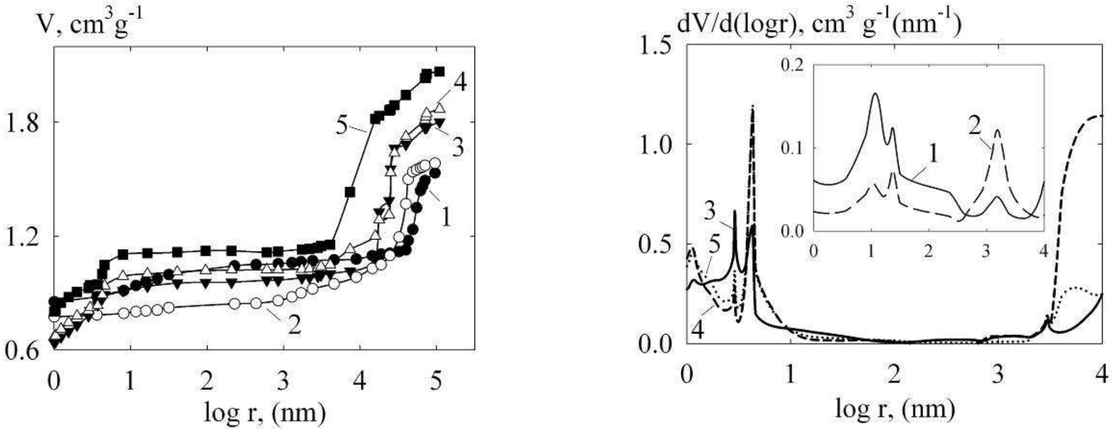

Figure 2. Integral (a) and differential (3-5) pore volume distributions. The numbers are related to corresponding samples

It should be stressed, that all the resins demonstrate anomalous microporosity, which is much higher comparing to that for known polymer ion-exchange materials [4]. However functional properties of Dowex HCR-S and well-known KU-2-8 (ion-exchange capacity, swelling, electrical conductivity etc.) are rather close. This is probably caused by hydrophilic fields of hydrocarbon chains: these fields are involved in the clusters, which are formed with functional groups. The pores, which are caused by these fragments, evidently provide extremely high microporosity, which is recognized with a method of standard contact porosimetry. Hydrophilic fields are free from –SO$_3$H groups but contain polar fragments. According to elementary analysis data, H-form of Dowex HCR-S contains additions of sodium (≈1-2 %), which are outside ion exchange. This is confirmed by NMR ^{23}Na spectra, corresponding signal is observed at –1 ppm (Fig. 3). No signal for KU-2-8 sample has been found. After conversion of the ion-exchanger into Na-substituted form, a shift of the signal to weak field is observed, the peak becomes wider.

Fig. 4 illustrates FTIR spectra both for KU-2-8 and Dowex HCR-S ion-exchangers in the fields, where the stripe caused by vibration of C-O bond (here C atom is attributes to benzene ring or linear hydrocarbon chain), was expected. However the stripes for these ion-exchangers are similar, thus the amount of hydrophilic fragments (probably C-ONa) is rather small. Acetone is adsorbed by both hydrophilic and hydrophobic fields of polymer chains. As a result, the clusters are reorganized and some hydrophilic fragments, which do not contain functional groups, remove them.

In the case of organic-inorganic ion-exchangers, the nanoparticles also leave clusters (sample 4) and form aggregates in the empties between gel fields or in the macropores (see Fig. 1 b). At the same time the single nanoparticles are not formed in the matrix, which has been immersed previously with organic solvent (see Fig. 1 c). This is caused by a small size of the reorganized clusters and state of zirconium in a solution, which is used for modification procedure.

Zirconium exists in aqueous solutions as polymerized hydroxocomplexes of different composition. Penetration of them inside reorganized clusters is evidently difficult.

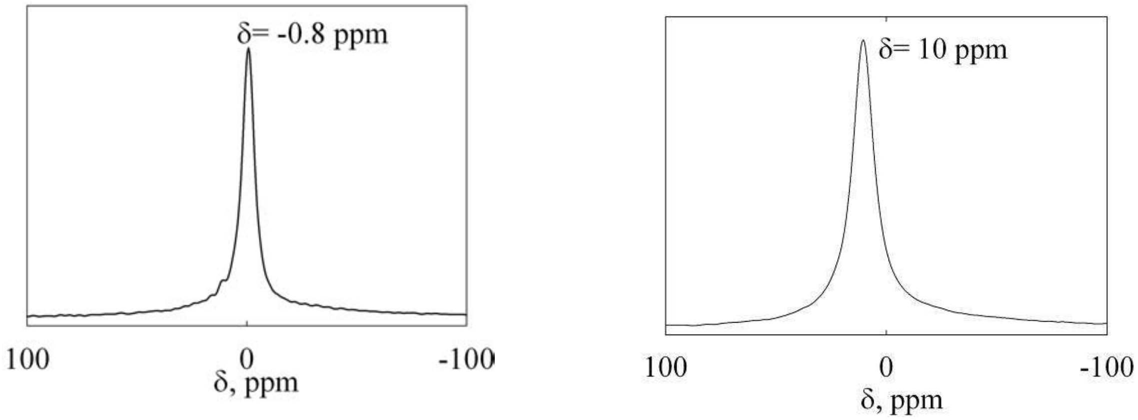

a *b*

Figure 3. NMR ^{23}Na spectra for H- (a) and Na- (b) forms of Dowex HCR-S resin

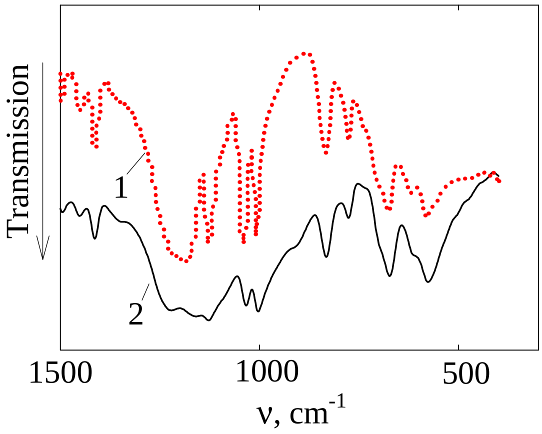

Figure 4. FTIR spectra of Dowex HCR-S (1) and Ku-2-8 (2) resins

Conclusions

Since the nanoparticles in clusters provide high electrical conductivity of the ion-exchange materials and low percolation threshold [2], reorganization of the clusters in organic media undoubtedly leads to degradation of this characteristics. The polymer matrix must be treated with organic solvent before insertion of inorganic particles. It is possible to assume, that a decrease of polymerization degree of zirconium hydroxocomplexes in a solution, which is used for nanocomposite preparation, would give a possibility to obtain the nanoparticles inside reorganized clusters.

References

1. *Yaroslavtsev A.V., Nikonenko V.V.* // Nanotechnologies in Russia. 2009. V. 4. P. 137-159.
2. *Dzyaz'ko Yu.S., Ponomareva L.M., Volf'kovich Yu.M., Sosenkin V.E., Belyakov V.N.* // Rus .J. Electrochem. 2013. V. 49. P. 209-215.
3. *Volfkovich Yu.M., Sosenkin V.E., Bagotzky V.S.* // J. Power Sources. 2010. V. 195. P. 5429.
4. *Berezina N. P., Kononenko N. A., Dyomina O.A., Gnusin N. P.* // Adv. Colloid Interface Sci. 2008. V. 139, P. 3-28.

ANION EXCHANGE RESIN, BASED ON EPOXIDIZED MONOETHANOLAMINE VINYL ETHER, ALLYL GLYCIDYL ETHER, POLYETHYLENE IMINE FOR THE SORPTION OF RHENIUM (VII) IONS

Edil Ergozhin, Katira Serikbaeva, Tolegen Chalov, Tatyana Kovrigina, Anna Nikitina
JSC "Institute of Chemical Sciences A.B.Bekturova", Almaty, Kazakhstan: *E-mail: katira_87@mail.ru*

Introduction

Among the materials that have a great strategic importance, a special place is occupied rare and refractory metals such as rhenium[1]. The richest source of its raw materials are copper-molybdenum ores from which it is taken incidentally during their processing for the main components [2,3].

Belonging to rare metals rhenium, and as a result, small concentration in raw material sources determine the complexity of the extraction of metal [4]. Go to effective processes for recycling rhenium containing solutions is a technology based on the use of ion-exchange sorption methods [1]. Basic requirements to ionits are selectivity to rhenium in general, high capacity characteristics and the ability to complete desorption of these rhenium solutions of ammonia [2]. Such requirements are met only weakly basic anion exchangers with certain functional groups, including industrial resins AN-21H16, AN-82 and AM-14G-14KR produced by the Soviet Union, previously used for the extraction of rhenium from washes of wet dust collecting molybdenum production. However, at the present time in Russia they discontinued. In this connection is to provide new topical ion exchangers having a high sorption and kinetic properties with respect to the ion ReO_4^-.

New anion exchanger (EVEMEA-AGE-PEI) was synthesized by usage of the epoxidizedmonoethanolamine vinyl ether(EMEAVE), allylglycidyl ether(AGE) and polyethylene imine(PEI), static exchange capacity of this anion exchanger is respectively 14.73 $mg \cdot eq \cdot g^{-1}$ (of 0.1 N HCl solution).

By potentiometric titration, it was found thatEVEMEA-AGE-PEI in the OH-form is a weak base anion exchanger.

Objects and methods

Sorption of rhenium (VII)anion EVEMEA-AGE-PEI in the OH form (particle size 0.5-1.0 mm) was studied under static conditions at a ratio of sorbent: solution equal to 1:400, at room temperature of 20 ± 20S, varying the concentration of rhenium in the solution NH_4ReO_4 from 0.102 to 1.024 $g \cdot l^{-1}$, and their acidity in the pH range from 1.2 to 6.2 by addition of 0.1 n solution of H2SO4. The contact with the sorbent solution is from 15 minutes to 7 days. For the preparation of model solutions used NH_4ReO_4 salt production firm «ALDRICH» (USA).

Sorption capacity (CE) was calculated from the difference between the initial and equilibrium concentration of the solution, which was determined by the method of classical polarography against 0.5 n H_2SO_4 solution on the recovery in Re^{7+} ($E_{1/2}$ = - 0.50 V). Polarogram shot at universal polarograph PU-1 in a cell thermostated at 25 ± 0.50S, using the dropping mercury electrode. Oxygen from the test solutions were removed by blowing argon for 5 minutes. As the reference electrode is a saturated calomel electrode.

Structure of the surface anion before and after sorption of rhenium was examined by electron microscopy scanning electron microscope JSM 6510LA company JEOL (Japan) at a resolution of the microscope 30 Å cm^{-1}.

Results and Discussion

The influence of the concentration of model solutions NH_4ReO_4 on the sorption of perrhenate ion anion EVEMEA-AGE-PEI is shown in Figure 1,2.

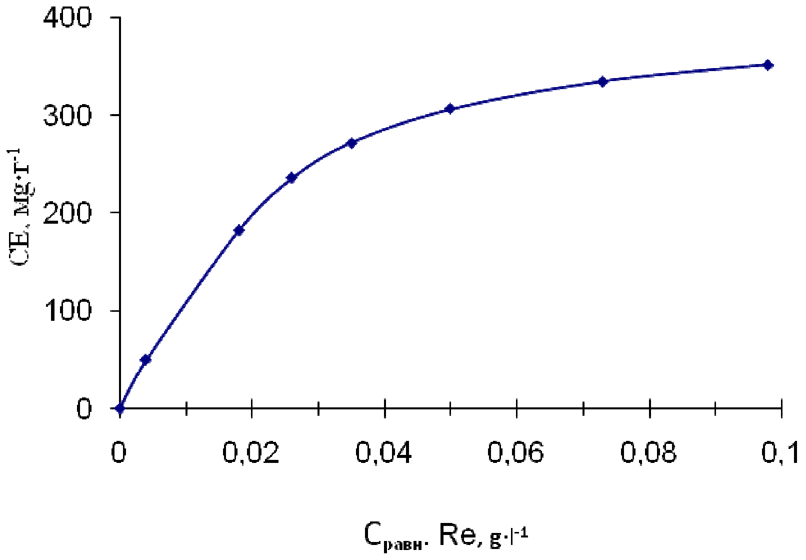

Figure 1.Sorption isotherm ReO_4^- anion exchange resin based on EVEMEA-AGE-PEI. The contact 7 days

From Figure 1 shows that it increases with CE ion content ReO_4^- and when removed from the solution containing 1.02 g · l^{-1}rhenium and having a pH of 6.2, equal to 33.2 mg·g^{-1}. The extent of their recovery (A) of NH_4ReO_4 solutions having a concentration of rhenium by 0.1-0.7 g · l^{-1} remains constant up to 88.0% (Figure 2). With an increase of its content in the solution to 1.02 g · l^{-1}it reduced to 80.8%.

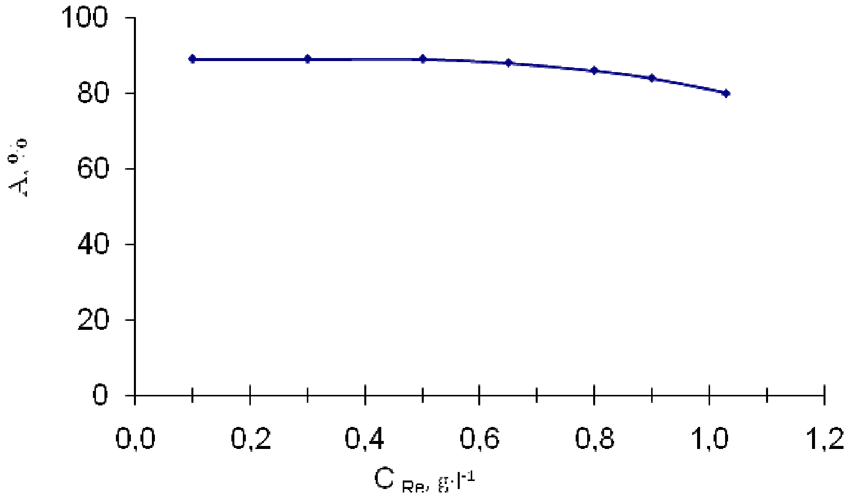

Figure 2. The degree of extraction of the perrhenateanion ion-based EVEMEA-AGE-PEI solution concentration of NH_4 ReO_4.The contact 7 days

Literature data show that we obtained a new anion exchanger has high sorption properties compared to the known ion exchangers. This is obviously due to the chemical structure of the polymer matrix EVEMEA-AGE-PEI and the structure of its surface (Figure 3).

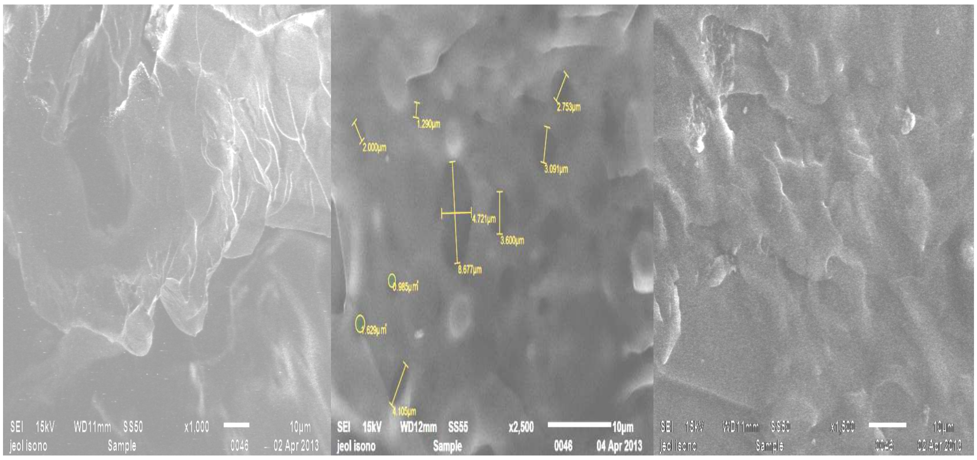

a *b* *c*

Figure3. Electron micrographs of the surface of the anion exchanger EVEMEA-AGE-PEIbefore (a, b) and after sorption (c) perrhenate ions

These electron microscopy show that the anion exchange resin EVEMEA-AGE-PEI has developed a folded surface, cut by many macropores ranging in size over a wide range from 0.985 to 8.677 mkm (Figure 3 a, b). The rhenium content in its surface layer is 8.61-21.40 wt%.

Conclusions

Study of the sorption of rhenium (VII) based on the new anion epoxidizedmonoethanolamine vinyl ether, allylglycidyl ether and polyethylene imine. Found that it has high absorption properties with respect to the perrhenate ions during the recovery of the individual solutions.

References

1. *Peganov V.A., Molchanov T.V., Smirnov K.M.* Sorption processes in technology hydrometallurgical processing molybdenum concentrates // Non-ferrous metals. 2010. N 12. P. 56-59.
2. *Blokhin, A.A., Maltsev E.E., Panchishina L.B., Murashkin Y.B.* Ion exchange extraction of rhenium from molybdenum sulphate solutions // Non-ferrous metals. 2009. N 7. P. 53-56.
3. *Abisheva Z.S., Rural A.N., Bekturganov N.S., Ospanov E.A., Ospanov N.A.* Sorption of rhenium from industrial solutions of sulfuric acid leaching of the Balkhash smelter on the anion A 170 // Non-ferrous metals., 2012. N 7. P. 57-61.
4. *Troshkina I.D., KhaingZawNaing, Ushanova O.N., Wei Pyo, Abdusalomov A.A.*Extraction of rhenium from sulfuric acid solutions active carbons // Zh. butt. chemistry. 2006. T. 79. V. 9. P. 1435-1438.

COMPOSITION AND PROPERTIES OF WHEY SALT CONCENTRATE AND PROSPECTS FOR ITS USE

[1]Ivan Evdokimov, [1]Irina Kulikova, [2]Dmitry Volodin, [2]Artem Bessonov
[1]North-Caucasian Federal University, Stavropol, Russia, *E-mail: eia@ncstu.ru*
[2]Ltd "Mega ProfiLine", Stavropol, Russia, *E-mail: vdn@mpline.ru*

Introduction

Preparation of dry milk mineral salts enables their wide application in the food industry. The molasses [1] received during the lactose production from UF- permeate or salt solution that remains after whey nanofiltration are used as raw materials [2]. Whey contains some minerals that are molecular or colloidal solutions as the salts of organic and inorganic acids. The share of inorganic salts makes up 67% of phosphorus, 75% of calcium, 80% of magnesium. Table 1 shows the macro-element mineral composition of the whey.

Table 1. Whey mineral composition

Minerals,	Ca, mg/100 g	K, mg/100 g	Mg, mg/100 g	Na, mg/100 g	P, mg/100 g
Whey	358	1427	45	513	472

For preparation of whey mineral concentrate we proposed to use the solution, which is received during whey electrodialysis. In the initial period of desalting mainly monovalent ions of sodium, potassium, and chloride are removed from whey. The anions of phosphoric acid and citric acid start to remove simultaneously as whey is being desalted. It causes partial dissociation of complexes that bind calcium and magnesium ions. Therefore as the whey desalting level goes up the rate of divalent cations removal also increases. As a result, two products are produced after electrodialysis: demineralized whey and whey salt concentrate.

Experiments

Composition and properties of demineralized whey and whey salt concentrate depend on the demineralization level. At the 90% level 5,248 g / l of anions and 2,991 g/l of cations go into the salt concentrate from the cheese whey. The macroelement composition of the concentrate after the cheese whey demineralization is shown in Table 2.

Table 2. Salt Concentrate Composition After Cheese Whey Electrodialysis

Title	DS, %	Ash, %	Ca, mg/100 g	K, mg/100 g	Mg, mg/100 g	Na, mg/100 g	P, mg/100 g	pH
Salt Concentrate	2,2	1,2	969	2783	166	868	797	5,65

The study of curd (acid) whey demineralization shows the possibility to remove 90% of minerals with the pass of some whey proteins (2-3%), lactose (4-5%) and non-protein nitrogen (23-25)%. The pH doesn’t change, titratable acidity is reduced by 70%. The degree of some ions pass into the whey concentrate is 97% of chlorine, 90% of potassium, 86% of sodium, 75% of calcium, 56% of magnesium at the 90% demineralization level.

Results and Discussion

The disposal of calcium and phosphorus ions is the most problematic as it requires the application of chemicals and complicates the production of dry salt concentrate due to the significant energy costs. We have developed technologies of whey salt concentrate usage in the production of table water with different mineral compositions [3] and meat and sausages production for stable color formation [4] as an alternative to the use of sodium nitrite.

References

1. Patent 5185166 (USA).
2. WO 99/40798.
3. *Kornilov N.I., Evdokimov I.A., Kudinov R.A.* // Bulletin of the North Caucasus State Technical University. № 5 (9). 2006.
4. Patent 2468586 (RF).

DIFFUSION CHARACTERISTICS OF COMPOSITES ON THE BASE OF DIFFERENT MF-4SC MEMBRANES AND POLYANILINE

Irina Falina, Ninel Berezina, Alisa Kulikova,
Kuban State University, Krasnodar, Russia, *E-mail: Irina_falina@mail.ru*

Introduction

The application of composite membranes on the base of perfluorinated sulfocationic membranes and polyaniline which forms a barrier layer on the membrane surface permits to rise the concentration degree of electrolyte solution in the electrodialysis in comparison with heterogeneous membranes [1]. The aim of this work was the investigation of diffusion permeability asymmetry effect of the membranes with barrier layer of the polyaniline on the surface prepared in different synthesis conditions.

Experiments

To explore the influence of membrane composition on the diffusion permeability asymmetry we prepared the series of composite membranes, where the polyaniline (PAn) is located in the surface layers of the MF-4SC membranes. Membranes modifying was performed as described in [2] by chemical polymerization with ammonium peroxydisulfate, oxidant solution contacted with membrane different time periods 1,2,3 hours. The two types of base membranes MF-4SC were used: as received (MF-4SC №1, ion-exchange capacity IEC=0.56 mmol/g_{sw}, Water content = 0.20) and pretreated with ethylene glycol (MF-4SC №2, IEC=0,68 mmol/g_{sw}, Water content = 0,24). Diffusion permeability concentration dependencies were measured in HCl solutions for the initial and composite membranes by means of periodic action cell.

Results and discussion

After modification the diffusion permeability of the membranes considerably decreases: by 10-40% for MF-4SC/PAn №2 and four times for MF-4SC/PAn №1. To explore the influence of surface modification on the transport properties of the composites the diffusion permeability was measured when membrane meets the electrolyte flux with modified (P_m) and unmodified (P_u) surfaces. On the base of diffusion permeability data the coefficient of asymmetry was calculated by division the diffusion permeability in case when modified surface meets flux by the diffusion permeability in the opposite side.

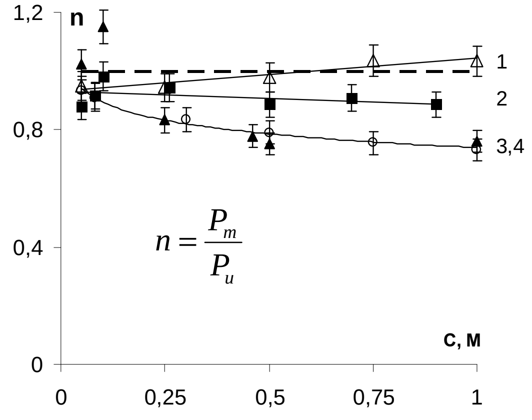

Figure 1. Concentration dependencies of diffusion permeability asymmetry coefficient in HCl solutions for membranes MF-4SC №1 (curve 1) and №2 (curve 2-4), 1,3 – 2 hours of synthesis, 2,4 –1 and 3 hours correspondingly

One can see that for the composite MF-4SC/PAn №1 membrane orientation to the electrolyte flux doesn't affects on diffusion permeability, hence asymmetry coefficient is near 1. While for the composite on the base MF-4SC №2 the asymmetry coefficient decreases with the concentration growth and achieves 0,7 in 1M HCl solution for the composites after 1 and 2 hours of synthesis. Since polyaniline is anion-exchange material, modified and unmodified surfaces of the membrane have different charge state and possess different diffusion resistance towards the electrolyte flux. This distinction of surfaces leads in effect of diffusion permeability asymmetry.

On the base of diffusion permeability data the estimation of parameter β was carried out. This parameter β determines the shape of concentration profile inside the membrane (fig. 2a) as it was shown in [3].

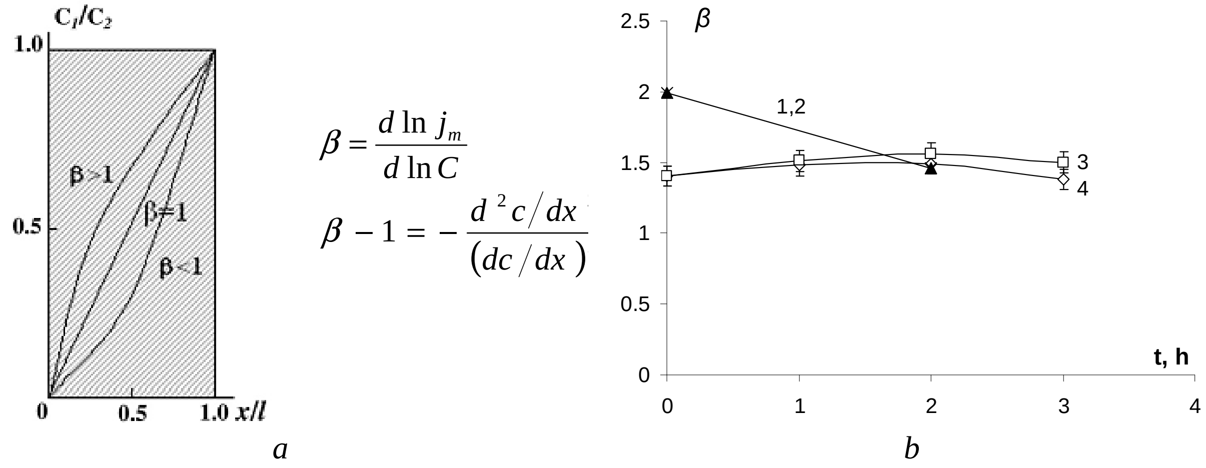

$$\beta = \frac{d \ln j_m}{d \ln C}$$

$$\beta - 1 = -\frac{d^2 c / dx}{(dc/dx)}$$

a *b*

Figure 2. Dependence of parameter β value on the synthesis time of the composite and it's orientation towards the electrolyte flux: membrane meets the electrolyte flux with modified (1,3) and unmodified (2,4) surfaces. 1,2 – MF-4SC №1, 3,4 – MF-4SC №2

Fig. 2b shows the dependence of parameter β value on the synthesis time of the composite membranes. One can see that both for initial and composite membranes concentration profiles have convex shape and β value doesn't depend on the membrane orientation towards the electrolyte flux. For composites MF-4SC/PAn №2 parameter β retains the magnitude, close to initial membrane. At the same time for MF-4SC №1 membrane β value decreases after modification that point to the reduction of the membrane diffusion resistance due to appearance of positive charged centers (anion-exchange groups) of the polyaniline chains. In present work for the first time parameter β was calculated for membrane diffusion properties before and after modification.

The value of parameter β reflects the peculiarities of membrane structural organization. It is demonstrated that parameter β determined from the diffusion experiment permits to compare the diffusion behavior before and after the modification in frames of conceptions of concentration profile formation inside the membrane.

The work was supported by Russian Foundation for Basic Research (Project No 13-08-00544).

References

1. *Protasov K. V., Shkirskaya S. A., Berezina N. P., Zabolotskii V. I.* Composite sulfonated cation-exchange membranes modified with polyaniline and applied to salt solution concentration by electrodialysis // Russ. J. Electrochemistry. 2010. V. 46. № 10. P. 1131.
2. *Berezina N. P., Kononenko N. A., Filippov A. N., Shkirskaya S. A., Falina I. V., Sycheva A. A.-R.* Electrotransport properties and morphology of MF-4SK membranes after surface modification with polyaniline // Russ. J. Electrochemistry. 2010. V. 46. № 5. P. 485.
3. *Gnusin N.P,. Berezina N.P., Shudrenko A.A., Ivina O.P.* Electrolyte diffusion through the ion-exchange membranes // Jurnal fizicheskoy chimii. 1994. V. 68. №3. P. 565-570.

CORRELATION BETWEEN EQUILIBRIUM PHYSICAL-CHEMICAL CHARACTERISTICS, WATER DISTRIBUTION AND ELECTROCHEMICAL BEHAVIOUR OF MF-4SC MEMBRANES

[1]Irina Falina, [1]Mariya Chernyaeva, [1]Sergey Dolgopolov, [1]Svetlana Shkirskaya, [2]Sergey Timofeev
[1]Kuban State University, Krasnodar, Russia; *E-mail: irina_falina@mail.ru*
[2]JSC «Plastpolymer», St.-Petersburg, Russia

Introduction

The content and energy state of water is an important factor for electrochemical behavior of ion exchange membranes. In the process of the perfluorinated membrane MF-4SC (JSC «Plastpolymer», St.-Petersburg) modification it was established that modificator intercalates mainly into the structural cavities of the swollen membrane, filled with water [1].

The current-voltage curve for the set of perfluorinated membranes MF-4SC, which differ in water content and ion-exchange capacity (IEC) (Table 1), in HCl solutions are presented on Fig. 1. One can see that polarization curves have different parameters. The decrease in IEC on 25% causes the reduction of limit current value on the same value. The measurements of concentration dependencies of electroosmotic permeability for the membranes in NaCl solutions showed, that for the MF-4SC №2 it doesn't depend on the electrolyte concentration and maintains low and constant value (t_w =8-7 molH_2O/F), while for the MF-4SC №1 t_w changes from 12 to 7 molH_2O/F when the concentration of NaCl solution increases from 0.1 to 1 M. The difference of electroosmotic properties of researched membranes is concerned with difference in water content.

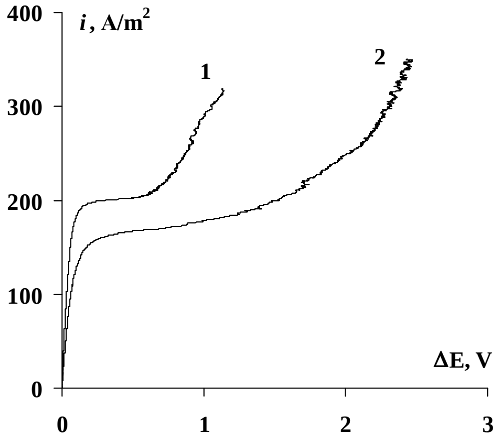

Figure 1 – Current-voltage curves of different MF-4SC membranes. 1 and 2 – MF-4SC №1 and 2 according to Table 1

Table 1. Physical-chemical parameters of MF-4SC membranes

	Water content	IEC, mmol/g_{sw}	n, mol H_2O/mol SO_3^-
MF-4SC №1	0,23	0,72	17,7
MF-4SC №2	0,20	0,56	19,8

The energy state of water was explored by differential scanning calorimetry / termogravimetry[1] (DSC/TG) and contact standard porosimetry. For the ion-exchange materials on the DSC there are two endothermic peaks (fig. 2a), which correspond to removal of water with different energy states. On the first stage (peak I on DSC) of the dehydration the swelling water is removed. The water molecules that interacts with the fixed groups [SO3--H2O-H+], are removed at higher temperatures (peak II on DSC). The third region corresponds to desulfonation of the perfluorinated matrix [2]. The increase of absorbed water quantity in the membrane volume causes the decrease of I transition temperature due to the plasticizing effect of water – extension of free volume inside the membrane provokes the chains mobility growth. At the same

---

[1] Authors gratitude prof. Z.A. Temerdashev, Ph.D. J.N. Konshina and Ph.D. student. A. Turmasova for DSC/TG mearurements.

time less value of specific water content for MF-4SC №1 membrane indicates the higher stability of ion clusters and strengthening of hydrogen bonds, that affects the greater area of the first peak.

The contact standard porosimetry data for the membranes are presented on fig. 2b. The maximum water content according to DSC/TG and porosimetry are similar. The distance between fixed ions is greater on 15% and inner specific surface area is lower on 15% for the MF-4SC №2 that is caused by the lower water content and IEC.

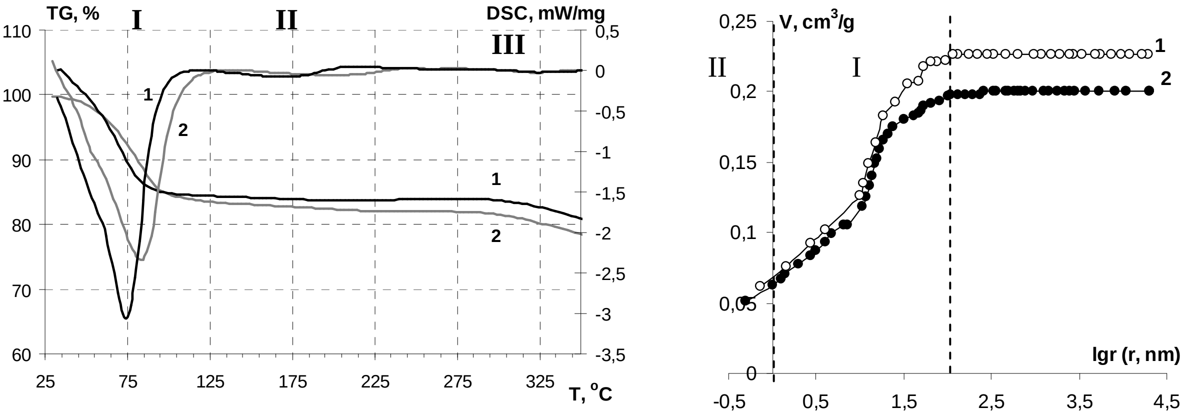

a *b*

Figure 2 – DSC/TG (a) and porosimetry curves (b) for the membranes MF-4SC. 1 and 2 – MF-4SC №1 and 2 according to Table 1

According to the standard contact porosimetry method the water located in pores with radii r >1 nm is bound freezable water (peak I on DSC), in pores r < 1 nm – cluster water, which enters into the near hydrate shell of fixed ions and counter-ions (peak II on DSC). The quantity of water located into the pores r < 1 nm by porosimetry is 5 times greater, then appropriate area by DSC/TG. By DSC/TG data the cluster water amounts to ~1 molH_2O/molSO_3^-, while the limitation of contact standard porosimetry methods is r ≥ 1 nm which corresponds 4-5 molH_2O/molSO_3^-.

In this work the correlation between equilibrium physical-chemical, electrotransport and structural properties of the ion-exchange material was shown. The comparison of structural characteristics for different perfluorinated membranes indicated the fact that the electrochemical properties are defined by the hydrophility of the charge transfer ways and water energy state in the polymer matrix.

The work was carried out in frames of Strategy Development of Higher Education Institutes Program (Project No 12/5c-1.2).

References

1. *Yaroslavtsev A.B.., Nikonenko V.V.* Ion-exchange membrane materials: properties, modification and practical application // Rossiyskie Nanotechnologii. 2009. V. 4. №3–4. P. 8-29.
2. *de Almeida S. H., Kawano Y.* Thermal behaviour of Nafion membranes // J. Thermal Analysis and Calorimetry. 1999. V. 58. P. 569-577.

THEORY OF DYES REJECTION IN THE PROCESS OF AQUEOUS-ALCOHOL MIXTURES NANOFILTRATION

[1]Anatoly Filippov, [2]Tamara Philippova
[1]Gubkin Russian State University of Oil and Gas, Moscow, Russia, *E-mail: a.filippov@mtu-net.ru*
[2]Moscow State University of Food Production, Moscow, Russia, *E-mail: filippova.tam@yandex.ru*

Introduction

The nanofiltration (NF) cleaning of hydroalcoholic mixtures from dissolved dyes requires selection of the optimal filtering modes in order to provide the best dye rejection by a membrane and acceptable system productivity. This kind of optimization problems can not be solved without a mathematical model of the process. However, the problem is complicated by the fact that by using nanoporous polymeric membranes based on poly (trimethylsilyl propyne) – PTMSP and poly (4-methyl-2-pentyne) – PMP, the flow through the membrane is detected at the alcohol concentration not less than 45% (in the case of ethyl alcohol, for example) [1] up to the pressure of 100 atmospheres.

Theory

The model of gradual opening of hydrophilizing pores of originally hydrophobic membrane and increasing flow of solvent which is an aqueous solution of various alcohols, by increasing the pressure drop across the membrane, was previously developed [2]. Feature of the model is highly non-linear dependence of the membrane permeability k on the applied differential pressure p, so that the filtration rate is determined by the following Darcy-like equation:

$$V\left(p\right)=\frac{k\left(p\right)}{\mu}\cdot p\,, \tag{1}$$

where μ is the mixture viscosity having an extreme dependence on the concentration of alcohol. The characteristic dependence of *V (p)* in dimensionless coordinates for approximating triangular distribution of membrane pores on the dimensionless radius (Fig.1) is shown by a curved line in Fig.2 [3]. The straight-line relationship in the same figure gives the dependence of the filtration rate on the pressure in the hypothetical case where all the pores of the membrane are open to filtration.

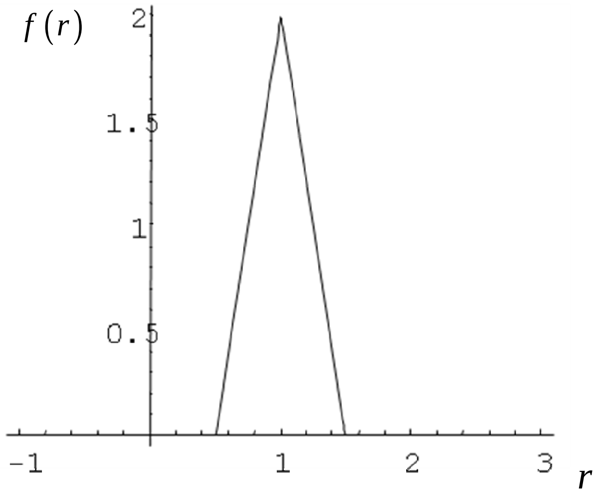

Figure 1. Triangle Distribution of Pore Radii

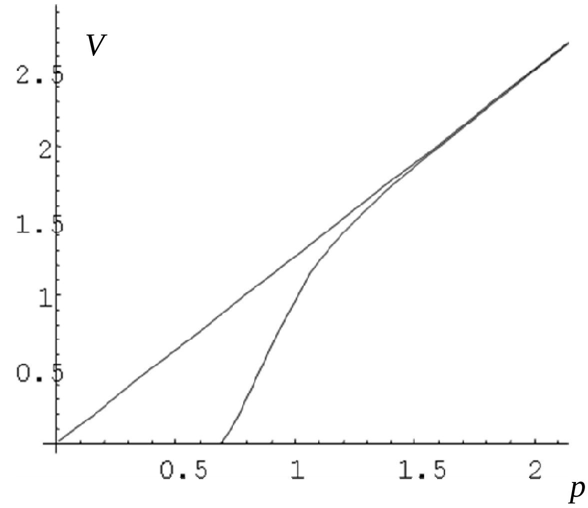

Figure 2. Dimensionless Dependence of V(p)

If the mixture filtered is non-electrolyte solution, then the charge effects can be neglected. In this case, solute (in our case – a dye) retention (rejection coefficient of the membrane) can be calculated by the formula obtained earlier [4]:

$$R = 1 - \frac{1}{1 + \left(\frac{\gamma_m}{\alpha_m} - 1 \right) \exp\left[-Pe\Delta \right] \left(1 - \exp\left[-Pe\alpha_m \nu_m \right] \right)} \qquad (2)$$

where we introduced the dimensionless Peclet number $Pe = \frac{Vh}{D}$, h – the thickness of the membrane, $\Delta = \frac{\delta}{h}$, $\nu_m = \frac{D}{D_m}$, D, D_m – the diffusion coefficients of the dye molecule in the bulk solution and the membrane, respectively, δ – the thickness of the diffusion layer, α_m – special coefficient which takes into account the deviation of average speed of solute molecules in the membrane from the filtration rate V, γ_m – coefficient of the equilibrium distribution of solute molecules in the membrane pores. On substitution of (1) in equation (2) we obtain $R(p)$ – the dependence of the rejection coefficient on the dimensionless pressure drop, which is graphically shown in Fig.3 for the general case.

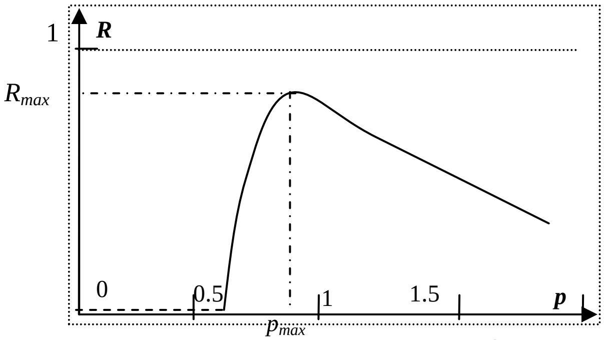

Figure 3. Schematic Dependence of R(p)

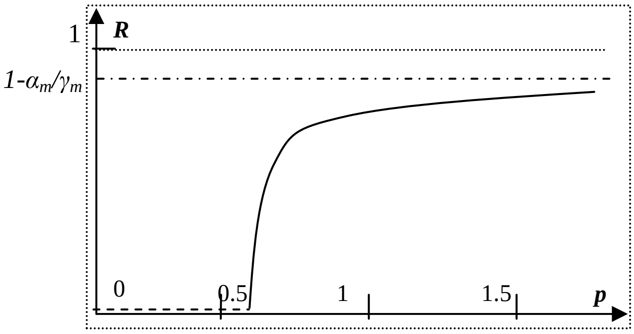

Figure 4. Asymptotic Dependence of R(p) for Δ=0

As can be seen from Fig.3 the function $R(p)$ has a maximum R_{max}, which is reaching by Peclet number Pe ~ 1. At the same time there is a sloping part on the curve $R(p)$ with almost zero retention, which corresponds to the first branch of the curve in Fig.2 (up to p=0.7). In the experiments, as a rule, we can not commit to the sharp point of the ascending branch of the curve $R(p)$ to the value $p = p_{\max}$, but we can only determine its descending part, which can be very shallow. In this case the false hypothesis of independence of the rejection coefficient on the pressure drop is sometimes putting forward, especially when this coefficient is close to unity. In the case of a very intensive mixing of the solution when we can approximately set $\Delta = 0$, the first exponential factor in the denominator of the formula (2) is equal to 1 and the dependence $R(p)$ is monotonically increasing, asymptotically approaching its limit value $1 - \frac{\alpha_m}{\gamma_m}$, which is closer to unity, the greater the distribution coefficient γ_m (the parameter α_m is not much different of 1):

$$R = 1 - \frac{1}{1 + \left(\frac{\gamma_m}{\alpha_m} - 1 \right) \left(1 - \exp\left[-Pe\alpha_m \nu_m \right] \right)} \qquad (3)$$

It is known that for reverse osmosis (RO) membranes that the parameter γ_m is hundreds, and for ultrafiltration (UF) membranes – tens of dimensionless units. Since the NF membranes, as compared to the level of surface interaction of solute molecules with their matrix, are between the RO and UF membranes, for them intermediate values of γ_m – from a few tens to hundreds of units to be expected. Note that the dependency of $R(p)$ tends to the asymptote $1-\frac{\alpha_m}{\gamma_m}$ (Fig. 4) and it provides an independent way to evaluate γ_m using the experimental curve. The diffusion coefficient of the solute molecules (in our case – a dye) can be obtained from the processing of diffusion experiments [5]. Then there is in the theory the only adjustable parameter α_m, which is in addition close to 1. The behavior of the entire curve $R(p)$ is described by a system of formulas (1) and (3). Note also that using ion-exchange membranes (IEM) for the nanofiltration purification of water-alcohol mixtures from dyes the negative values of the rejection coefficient can be observed, as positive solute adsorption in the pores is typical for the IEM, which leads to the values $\gamma_m < 1$ [5]. The same phenomenon was observed during NF of neutral dye – Solvent Blue 35 by PTMSP-based membrane [6]. In the latter case, the horizontal asymptote in Fig.4 becomes negative, so for R=-0.046 we have $\gamma_m/\alpha_m = 0.956$. It means that there is an absence ($\gamma_m = 1,\ \alpha_m = 1.046$) or a very weak interaction of Solvent Blue 35 with the membrane (positive specific adsorption of the dye in the membrane matrix). When using electrolyte solutions of non-neutral dyes, anybody must take into account the charge density of the membrane that leads to a more complex problem which requires numerical calculations applying analytical formulas [7].

Conclusion

Hence the model suggested here for nanofiltration of dyes dissolved in aqueous-alcohol mixture using nanoporous PTMSP and PMP based membranes allows us qualitatively imagine and quantitatively evaluate the behavior of the rejection coefficient as function of dimensionless applied pressure under given concentration of alcohol using only one fitting parameter.

This work is supported by the Russian Foundation for Basic Research (project no 11-08-01043_a).

References

1. *Volkov A.V.* Transport of wetting/non-wetting mixtures through hydrophobic high permeability glassy polymers. Third International Conference on Organic Solvent Nanofiltration. 2010. September 13-15. Imperial College London. UK.
2. *Ivanov V.I.* Investigation of the Process of Disclosing of the Pores of Hydrophobic Nanoporous Membranes at the Filtration of Water-Organic Mixtures // Vestnik Nizhegorodskogo Universiteta. 2011. No. 4(2). P. 438-439.
3. *Filippov A., Ivanov V., Volkov A., Yushkin A., Bogdanova Yu., Dolzhikova V.* Influence of Hydrophobicity of PMP and PTMSP Nanoporous Membranes on a Flow Rate of Aqueous Alcohol Mixtures under Applying of External Pressure Drop. Int. Conf. on Ion transport in Organic and Inorganic Membranes. 2012. May 28 – June 02. KSU Krasnodar. Russia. Conference Proceeding, P. 71-74.
4. *Martynov G.A., Starov V.M., Churaev N.V.* To the Theory of Membrane Separation of Solutions // Colloid J. of the USSR. 1980. V. 42. No. 3. P. 402-410.
5. *Kolechko M.V., Filippov A.N., Shkirskaya S.A., Timofeev S.V., Berezina N.P.* Synthesis and Diffusion Permeability of MF-4SK/Polyaniline Composite Membranes with Controlled Thickness of the Modified Layer // Colloid J. 2013. V. 75. No. 3. P. 289–296.
6. *Volkov A.V., Stamatialis D.F., Khotimsky V.S., Volkov V.V., Wessling M., Plate N.A.,* Poly[1-(trimethylsilyl)-1-propyne] as a solvent resistance nanofiltration membrane material // J. Membr. Sci. 2006. V. 281. P. 351–357.
7. *Gorsky V.G., Starov V.M., Filippov A.N., Nigmatullin R.R., Bryk M.T.* Partitioning of Aqueous Solutions of Binary Inorganic Electrolytes Using Chemically Modified Charged Ultrafiltration Membranes. Theory and Experiment // Soviet J. Water Chemistry and Technology. 1992. V. 14. No. 2. P.93-100.

THE MODEL OF A CHARGED BILAYER MEMBRANE FOR COMPOSITE MEMBRANES MF-4SC/POLYANILINE WITH CONTROLLED THICKNESS OF THE MODIFIED LAYER

[1]Anatoly Filippov, [2]Svetlana Shkirskaya, [2]Ninel Berezina, [2]Mariya Kolechko
[1]Gubkin Russian State University of Oil and Gas, Moscow, Russia
[2]Kuban State University, Krasnodar, Russia

Introduction

At present, nanocomposites based on sulfocationite membranes and polyaniline (PAn) are widely used in fuel cells and sensing mechanisms, as well as for selective separation of electrolyte solutions. The choice of the conditions for the synthesis of PAn in a membrane matrix, which would ensure the production of composites with desired nanostructure and properties, is an urgent problem. The goal of this study was the development of a method for the formation of a PAn layer with a fixed thickness near the membrane surface and the production of an MF-4SC/PAn composite with a high conductivity. This method is based on modification of a layer-by-layer sulfated hydrophobic fluoroplast-4SF (F-4SF) film.

Experiments

Inert nonconducting polymer F-4SF was used as the basic matrix. This material does not possess ionexchange properties, but acquires them as a result of alkaline hydrolysis of sulfonylfluoride groups ($–SO_2F$). The thickness of the charged sulfated layer can be controlled by varying the duration of alkaline hydrolysis. Films with different thicknesses of the charged layers were obtained by boiling in a 10% NaOH solution for 10, 20, 30, and 40 min. Then, the matrix synthesis of PAn in the charged sulfocationite layer of the matrix were performed. In this case, one of the sides of a hydrolyzed sample was subjected to modification with PAn in a two chamber cell. As a result, PAn occupied the entire charged layer. No further intergrowth of PAn chains into the bulk of the membrane occurred, because the dense hydrophobic uncharged unsulfonated inner region consisting of F-4SF was impermeable to the modifying solutions. For all samples, the chemical synthesis of PAn was carried out via consecutive diffusion of an aniline solution in the presence of hydrochloric acid and $(NH_4)_2S_2O_8$ as a polymerization initiator into water for 2 h, as was described in [1]. Thus modified samples were boiled in an aqueous ammonia solution for soft alkaline saponification of the film region that had remained uncharged. The following parameters of the basic membrane and the membranes modified with PAn were determined: membrane thickness (l_m), modified layer thickness (l_1), exchange capacity (Q), moisture content (W), and specific moisture capacity (n_m) (Table 1).

Table 1. Physicochemical characteristics of the studied membranes

Membrane, hydrolysis duration	l_m, μm	l_1, μm	Q, mg-equiv/g	W, g_{H2O}/g	n_m, mol H2O/mol SO_3^-
MF-4SC	200	–	0.57	0.19	18.5
MF-4SC/PAn, 10 min	200	20	0.59	0.19	17.9
MF-4SC/PAn, 20 min	200	32	0.60	0.19	17.6
MF-4SC/PAn, 30 min	190	36	0.60	0.20	17.6
MF-4SC/PAn, 40 min	180	40	0.64	0.20	15.6

Results and Discussion

Figure 1 shows the concentration dependences of the integral coefficient of diffusion permeability and conductivity for the initial membrane and MF-4SC/PAn composites. Note that no effect of asymmetric diffusion permeability was observed for MF-4SC/PAn composite membranes when concentration of the HCl solution was varied within a wide range (0.1–1 M). It is seen from Fig. 1 that, as the thickness of the Pan modified layer increases, the diffusion permeability coefficient and specific conductivity synchronously decrease to compare with the values obtained for the initial membrane.

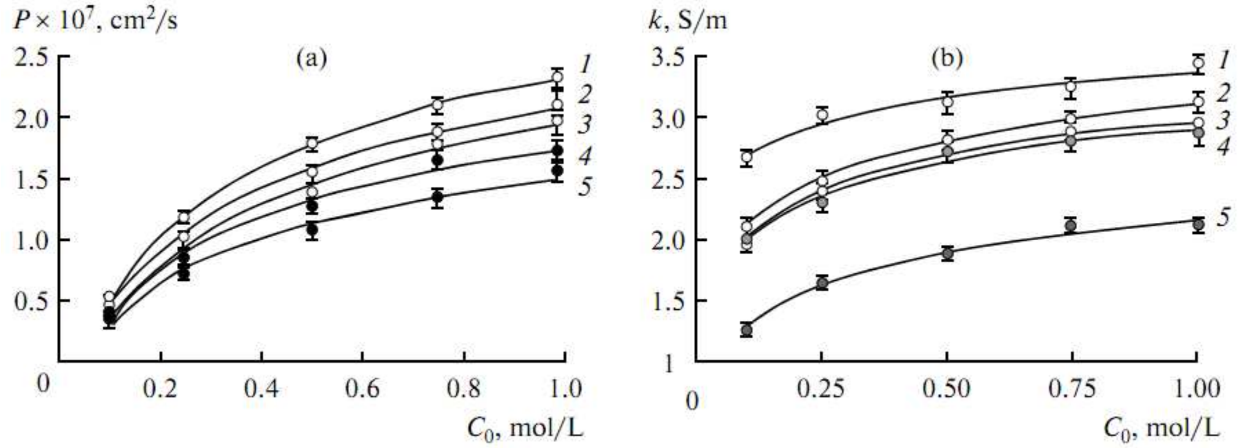

Figure 1. Diffusion permeability (a) and conductivity (b) as functions of HCl solution concentration for (1) MF-4SC membrane and MF-4SC/PAn composites resulting from matrix hydrolysis for (2) 10, (3) 20, (4) 30, and (5) 40 min. Symbols and curves denote the experimental data and the theoretical calculations based on the bilayer model, respectively

The maximum thickness of the PAn modified layer, which was reached using this method, was 25% of the total thickness of the membrane. This thickness of the modified layer corresponds to a 35% decrease in both conductivity and diffusion permeability relative to these parameters of the initial membrane. It was established that the composite membranes with a fixed thickness of the PAn modified layer are characterized by a high selectivity to protons (1–0.98) in a wide range of variations in the concentration of HCl solutions.

The experimental data were processed according to the “bilayer charged membrane” model [2] (hereinafter, “bilayer model” for short). The model was based on the dependence of the diffusion permeability of the initial unmodified membrane on electrolyte concentration (Fig. 1a, curve 1). This dependence was described by the following analytical formula:

$$P_0 = \frac{D_2|\rho_2|}{2C_0}\left(\sqrt{1+\left(\frac{2C_0}{\rho_2\gamma_2}\right)^2}-1\right) \equiv \frac{2C_0\, {}^{D_2}\!/\!_{\gamma_2}}{\sqrt{(\rho_2\gamma_2)^2+4C_0^{\;2}}+|\rho_2|\gamma_2} \tag{1}$$

where D_2 is the effective (averaged) diffusion coefficient of cation and anion, ρ_2 is the volume charge density, γ_2 is the equilibrium distribution coefficient, and C_0 is the electrolyte concentration on one side of the membrane (hereinafter, subscripts 2 and 1 attribute the corresponding parameter to the unmodified and modified regions of the membrane, respectively).

The effective diffusion coefficient and volume density of charges fixed in the initial membrane were determined from comparison of the experimental dependence $P_0(C_0)$ and formula (1) using the least squares method. The following values were obtained: $\tilde{D}_2 \equiv {}^{D_2}\!/\!_{\gamma_2} = 30.75,\ \tilde{\rho}_2 \equiv \rho_2\gamma_2 = -0.57$. The exchange capacity of the initial swollen membrane ρ_2 = –0.57 mol/L was determined in an independent experiment. From these data, for the initial membrane, it is easy to find the coefficient of equilibrium distribution $\gamma_2 = 1$ (there is no specific adsorption of ions in this membrane) and integral coefficient of HCl diffusion in the membrane D_2 = 30.8 μm^2/s, which turned out to be 110 times lower than that for this electrolyte in a dilute solution (3.3 × 103 μm^2/s).

The bilayer model, which was proposed in [2] for describing the asymmetry effects of the transport properties of bilayer membranes, can also reproduce the symmetry of the diffusion permeability of the composites with fixed thicknesses of the PAn modified layer. Two relationships must be fulfilled between the physicochemical and geometrical parameters: $\tilde{\nu} \equiv \frac{D_1 h_2 \gamma_2}{D_2 h_1 \gamma_1} = 1$, $\tilde{\rho} \equiv \tilde{\rho}_2 = \tilde{\rho}_1$ (i.e., effective exchange capacity $\tilde{\rho} \equiv \rho_2 \gamma_2 = \rho_1 \gamma_1$ is constant over the entire thickness of the membrane). In this case, in spite of the different exchange capacities of the layers, the diffusion permeability is the same at different orientations of the membrane in a measuring cell; i.e.,

$$P \equiv P_w = P_s = \frac{2C_0 \left(D_2 / \gamma_2 \right)(1+H)}{\sqrt{(\tilde{\rho})^2 + 4C_0^2} + |\tilde{\rho}|} \equiv \frac{2C_0 \left(D_1 / \gamma_1 \right)(1+1/H)}{\sqrt{(\tilde{\rho})^2 + 4C_0^2} + |\tilde{\rho}|} \tag{2}$$

where H = h_1/h_2 is the relative thickness of the modified layer. It follows from the condition $\tilde{\nu} \equiv \frac{D_1 h_2 \gamma_2}{D_2 h_1 \gamma_1} = 1$ obtained above that the diffusion coefficients of electrolyte molecules in the membrane layers are related via the following equation:

$$H \cdot D_2 / \gamma_2 = D_1 / \gamma_1 \tag{3}$$

The described algorithm was used to calculate the physicochemical parameters of the modified membranes (Table 2). As can be seen from Fig. 1a, the concentration dependences calculated for the diffusion permeability are in good agreement with the experimental data. Determining factor $\Delta = |\tilde{\rho}_1| - |\tilde{\rho}_2|$ is equal to zero for all studied samples of composite membranes regardless of the modified layer thickness. The zero value of this factor explains the absence of asymmetry of diffusion permeability for the composites with fixed thicknesses of the modified layer in the direct experiment.

Table 2. Physicochemical parameters of initial MF-4SC membrane and MF-4SC/PAn composite membranes

Modification duration, min	γ_1	γ_2	ρ_1, mol/l	ρ_2, mol/l	$\tilde{\rho}_1$, mol/l	$\tilde{\rho}_2$, mol/l	D_1, μm^2/s	D_2, μm^2/s	$\tilde{D}_1$, μm^2/s	$\tilde{D}_2$ μm^2/s
0	-	1	-	-0.57	-	-0.57	-	30.8	-	30.8
10	0.73	1	-0.78	-0.57	-0.57	-0.57	1.80	22.8	2.5	22.8
20	0.81	1	-0.70	-0.57	-0.57	-0.57	3.54	23.0	4.4	23.0
30	0.89	1	-0.64	-0.57	-0.57	-0.57	3.95	18.5	4.4	18.5
40	0.70	1	-0.82	-0.57	-0.57	-0.57	2.99	15.4	4.3	15.4

It was ascertained in [1] that, for MF-4SC membranes subjected to the surface modification, Δ < 0, which is typical for composite membranes with a gradient distribution of PAn. Such membranes exhibit asymmetry of the diffusion permeability with respect to HCl solution. In the experiments performed in [1], asymmetry coefficient η varied from 0.73 to 0.95 depending on duration of PAn synthesis and electrolyte concentration. Thus, the bilayer model is applicable for describing the asymmetry effect of the transport properties of bilayer membranes, as well as can also describe the symmetry of the diffusion permeability of the composites with fixed thicknesses of the PAn modified layer as it was shown in this study.

This study was supported by the Russian Foundation for Basic Research (#13-08-00544-a).

References

1. *Berezina N.P., Kononenko N.A., Filippov A.N., Shkirskaya S.A., Falina I.V., Sycheva A.A.-R.* // Elektrokhimiya. 2010. Vol. 46, P. 515.
2. *Filippov A.N., Starov V.M., Kononenko N.A., Berezina N.P.* // Adv. Colloid Interface Sci. 2008. Vol. 139, P. 29.

FORMATION OF VORTICITY PLUGS IN MICROCHANNELS

Elizaveta Frantc, Michail Chernov

Kuban State University, Krasnodar, Russia: *E-mail: gandizel@mail.ru, chernov_math@mail.ru*

Introduction

The experiments described in [1] show the existence in microchannels "vorticity plugs" when in the laminar flow appears localized areas of vortex patterns, see Fig.1.

Figure 1. Vorticity plug in a micro-channel, experiments [1], Re=0.12

This phenomenon occurs at very low Reynolds number, Re <0.2 in micro-channels. In the present work we do not discuss physical mechanism of this phenomenon and only present a mathematical algorithm to find such solutions on the basis of the Navier-Stokes equations.

Formulation

In two dimensional case, the Navier-Stokes equations can be written as one equation with one unknown variable, the stream function Ψ (x, y), which defines a two-dimensional liquid flow, namely,

$$-c\frac{\partial\nabla^2\Psi}{\partial x}+\frac{\partial\Psi}{\partial y}\frac{\partial\nabla^2\Psi}{\partial x}-\frac{\partial\Psi}{\partial x}\frac{\partial\nabla^2\Psi}{\partial y}=\frac{1}{\mathrm{Re}}\nabla^4\Psi \tag{1}$$

$$y=\pm1:\ \Psi=\frac{\partial\Psi}{\partial y}=0 \tag{2}$$

$$\Psi=y-\frac{1}{3}y^3 \tag{3}$$

Function (3) is a trivial laminar solution of the equations (1)-(2). For the application of our numerical method it is necessary to shift velocity to the value of U = 1 - y ²:

$$\begin{gathered}\frac{1}{\mathrm{Re}}\left(\frac{\partial^4\psi}{\partial y^4}+2\frac{\partial^4\psi}{\partial y^2\partial x^2}+\frac{\partial^4\psi}{\partial x^4}\right)-(U-C)\left(\frac{\partial^3\psi}{\partial x^3}+\frac{\partial^3\psi}{\partial x\partial y^2}\right)+U''\frac{\partial\psi}{\partial x}=\\ \frac{\partial\psi}{\partial y}\left(\frac{\partial^3\psi}{\partial x^3}+\frac{\partial^3\psi}{\partial x\partial y^2}\right)-\frac{\partial\psi}{\partial x}\left(\frac{\partial^3\psi}{\partial x^2\partial y}+\frac{\partial^3\psi}{\partial y^3}\right)\end{gathered} \tag{4}$$

The equation (4) is equivalent to equation (1). In order to find a numerical solution, let us get rid of one of the independent variables for this function and decompose ψ in Fourier series in the variable x. Thus, we obtain the following system of nonlinear ODE's, in which there is only a dependence on y:

$$\begin{gathered}\frac{1}{\mathrm{Re}}\left(\frac{d^4\psi_k}{dy^4}-2k^2\alpha^2\frac{d^2\psi_k}{dy^2}+k^4\alpha^4\psi_k\right)-ik\alpha(U-C)\left(\frac{d^2\psi_k}{dy^2}-k^2\alpha^2\psi_k\right)+ik\alpha U''\psi_k=\\ \sum_{p=-\infty}^{+\infty}ik\alpha\frac{d\psi_{k-p}}{dy}\left(\frac{d^2\psi_p}{dy^2}-p^2\alpha^2\psi_p\right)-i(k-p)\alpha\psi_{k-p}\left(\frac{d^3\psi_p}{dy^3}-p^2\alpha^2\frac{d\psi_p}{dy}\right)\end{gathered} \tag{5}$$

$$y=\pm1:\ \psi_k=\frac{d\psi_k}{dy}=0$$

To find a solution of this system is rather complicated problem, in particular, because of the fact of the dependence of the left hand side of the equations on y. In order to get rid of it, let us multiply both sides of this equation by the solution of the linear adjoint problem. Since the differential operator is a linear operator, we can say that the original equation is reduced to a system of algebraic equations. The question arises: how to solve this system of nonlinear algebraic equations with quadratic nonlinearity? Newton's method in this case does not work, as we need a fairly accurate initial guess. Therefore, we will use the Petviashvily method [2]. Briefly describe its essence.

Consider a system of nonlinear algebraic equations with quadratic nonlinearity:

$$x_k = \sum_{i,j=1}^{N} a_{ij}^{(k)} x_i x_j = F_k, \; k = 1, ..., N \tag{6}$$

Each equation is multiplied by the corresponding $x_k, \; k = 1, ..., N$. Then let us sum the right and left hand sides of the equations of the system. The sum of the left hand sides denote $I_1 = x_1^2 + x_2^2 + ... + x_N^2$, while the sum of right hand sides is $I_2 = x_1 F_1 + x_2 F_2 + ... + x_N F_N$. Instead of the system to solve the following:

$$x_k = \left(\frac{I_1}{I_2} \right)^2 F_k, \; k = 1, ..., N \tag{7}$$

where I_1, I_2 are stabilizing factors. It is known [2], that in many cases there is a convergence to the largest by absolute value root. The convergence of this process has not been proved yet, but it was not given a single example in which this method diverges.

Let us return to the original problem. Let us denote the linear left part of the equation (5) by L, and the right hand side by N and write down the system in the following form, skipping subscript k:

$$L\psi = N \tag{8}$$

Further we will write down ψ, assuming one of the functions $\psi = (\psi_1, \psi_2, ...)$.

If we multiply (8) by the adjoint eigenfunction φ_m, we will get $(\varphi_m, L\psi) = (\varphi_m, N)$. By definition, for the adjoint operator $(\varphi, L\psi) = (L^* \varphi, \psi)$, hence, eventually, we will obtain a dot product in L_2:

$$\int_{-1}^{1} \overline{\varphi}_m L\psi dy = \int_{-1}^{1} \overline{\varphi}_m N dy$$

$$\int_{-1}^{1} \overline{L^*} \overline{\varphi}_m \psi dy = \int_{-1}^{1} \overline{\varphi}_m N dy$$

$$\lambda_m \int_{-1}^{1} \overline{\varphi}_m \psi dy = \int_{-1}^{1} \overline{\varphi}_m N dy$$

Let us present ψ as a superposition:

$$\psi = \sum_{s=1}^{+\infty} H_s \psi_s(y)$$

where H_s - are unknown coefficients and $\psi_s(y)$ - are eigenfunctions of the linear problem, which satisfy the boundary conditions(2), and, hence,

$$\int_{-1}^{1} \overline{\varphi}_m \psi_s dy = (\varphi_m, \psi_s) = \delta_{ms}$$

Eventually, we will obtain,

$$\lambda_m \int_{-1}^{1} \overline{\varphi}_m \psi_s dy = \int_{-1}^{1} \overline{\varphi}_m N dy$$

$$\lambda_m H_m = (\varphi_m, N) = \int_{-1}^{1} \overline{\varphi}_m N dy$$

So, in order to find the unknown coefficients of the expansion of ψ, we have to know the eigenvalues H_m and eigenfunctions ψ, and adjoint functions of the problem. And in order to find the function ψ, must also find eigenfunctions ψ_s.

Results of calculations

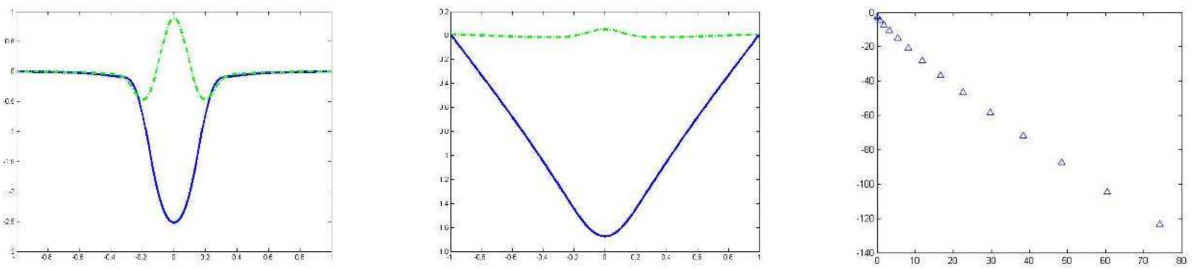
a *b* *c*

Figure 2. First (a) and second (b) eigenfunctions of the linear problem along with first 15 first eigenvalues (c)

In Fig. 2b and Fig. 2a dependence of the real and imaginary parts of the first eigenfunction for the eigenvalue problem and the adjoint problem, are presented, respectively. The first 15 eigenvalues are shown in Fig. 2c.

The solution of the problem is, as follows,

- Partial differential equation is reduced to a system of ordinary differential equations, and then – to a system of nonlinear algebraic equations.
- The resulted nonlinear algebraic system is solved by Petviashvily method [2], the functions ψ_k, also are found.
- The coefficients of the equations are found with the help of the ajoint problem.
- The unknown steam function is built up using these coefficients.

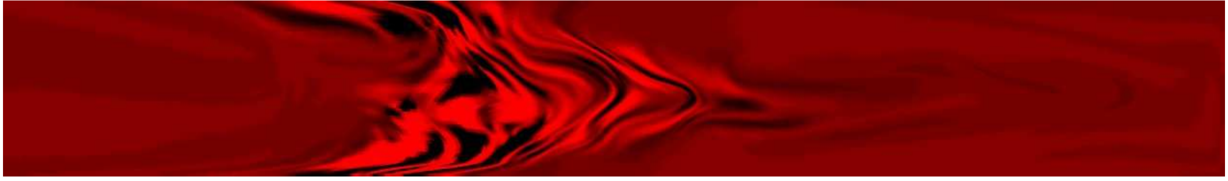

Figure 3. Our numerical vorticity plug, Re=0.2

In Fig 3 we present the numerical solution, obtained by Petviashvily method.

As a result of this work, we numerically solved the Navier-Stokes equations, and found localized coherent structures which corresponds to the localized area of the vortex structures in microchannels. There is a qualitative correspondence to the experiments of [1].

References

1. *Nguyen N.-T., Wereley S.T.* // ARTECH HOUSE. 2006. p. 497.
2. *Petviashvily V. I., Tsvelodub O.Yu.* // DAN USSR, v.328 - 1978. P.1321-1324.

THEORETICAL AND EXPERIMENTAL STUDY OF AQUEOUS SUSPENSION FILTRATION THROUGH MODEL OF A POROUS MEDIUM

[1]Anastasiya Gabova, [1]Georgiy Belyakov, [1]Nikolay Baryshnikov, [1]Aliya Tairova, [2]Anatoly Filippov
[1]Institute of Geospheres Dynamics RAS, Moscow, Russia,
[2]Gubkin Russian State University of Oil and Gas, Moscow, Russia, *E-mail:* a.filippov@mtu-net.ru

Introduction

One of the main problems of rational development of hydrocarbon fields is to select the optimal mode of intrusion of the particles (proppant) in the hydraulic fracture and to determine the conditions of their uniform filling, as well as the destruction of formed "plugs" of proppant. Cracks filled with large particles (proppant) have a high permeability compared to the surrounding rocks, which can significantly increase the recovery of oil from their surfaces.

Experiments

In filtration experiments (Fig.1) we used aqueous suspension containing solid particles of silicon carbide (moissanite) of 10 micron average diameter and concentration 84g/liter that corresponds ~ 0.5×10^6 particles per cm^3. The sheet of 0.9 mm x 24 cm x 15 cm foam rubber, compressed between the plates of polished glass mirrors, which is a braiding of polyurethane filaments with thickness of 100 microns with an average pore size of 600 microns (Fig.2), was used as a porous medium (initial thickness of the sheet was 5 mm and initial porosity – 0.98). The porosity of the compressed foam rubber decreased to 0.93, and its permeability – 150 Darcy. Before each experiment, the porous layer was filled with water. Dissemination of the suspension into the reservoir model occurs under differential pressure created at the ends of the reservoir model using a vacuum pump. Monitoring the area of penetration of the suspension into the porous medium was conducted using a camera that records the light coming through different parts of the medium with different concentrations of filtered particles. The density distribution of the particles deposited in the pores was correlated with the distribution of brightness on the obtained photographs. The experimental dependences of the volumetric filtration rate Q(t) which is monotonically decreasing with time t and the concentration profiles n(x,t) of the particles deposited in the foam rubber at different time were obtained.

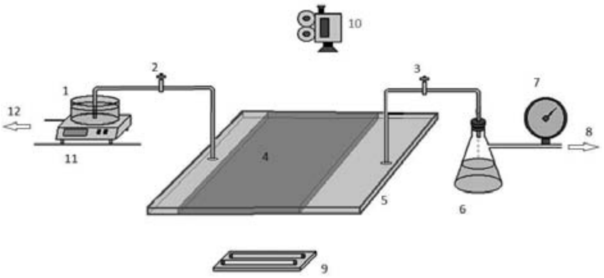

Figure 1. The experimental setup:
1 - container with aqueous suspension, 2,3 - tubes, 4 - sheet of foam rubber, 5 - cell, 6 - buffer capacity, 7 - gauge, 8 - to the vacuum pump, 9 - backlight, 10 - camera, 11 – weighing-machine, 12 - to the computer interface

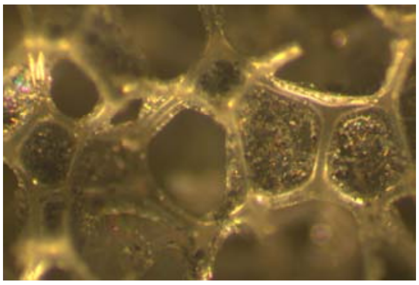

Figure 2. Foam rubber cells with retained particles: polyurethane fibers diameter - 100 μm, average pore size - 1 mm, average particle size of silicon carbide - 10μm

Theory

To describe the pore blocking process the probabilistic-sieve model of microfiltration [1, 2] has been applied, which allowed us to determine physicochemical parameters of non-stationary process of aqueous suspension filtering. According to this model the linear filtration rate $u(t)$ has the following form:

$$u(t) \equiv \frac{Q(t)}{S} = \frac{Q_\infty / S}{1-(1-Q_\infty/Q_0)\,\mathrm{e}^{-\omega t}}\,, \tag{1}$$

where $Q_\infty = \lim\limits_{t\to\infty} Q(t)$, $Q_0 = Q(0)$, S is the cross-sectional area of the medium and ω – parameter which depends on particle concentration and Q_∞. In our experiments we had $Q_0 = 12.96\,\mathrm{cm}^3/\mathrm{sec}$ and S=2.16 cm^2. The values of $Q_\infty = 3.67\times10^{-3}\mathrm{cm}^3/\mathrm{sec}$ and $\omega = 2.7\times10^{-6}\mathrm{sec}^{-1}$ were fitted using (1) by the least square method. Fig.3 presents experimental (symbols) and theoretical (curve) dependencies of Q(t).

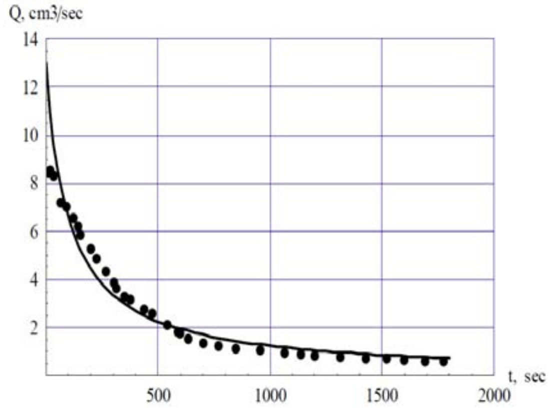

Figure 3. Volumetric filtration rate Q as function of running time t

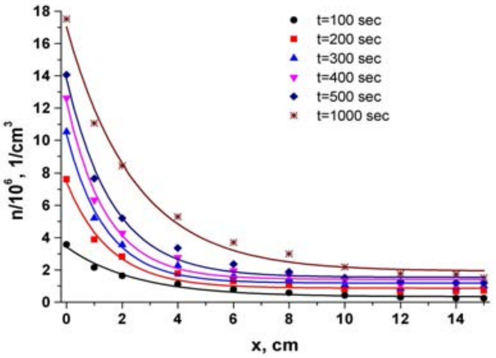

Figure 4. Profiles of numerical concentration at different moments of time

In order to describe behavior of numerical particle concentration $n(x,t)$ we need to employ the law of mass balance in the form:

$$\frac{\partial n}{\partial t} = -\frac{\partial J}{\partial x} + q(x,t)\,, \tag{2}$$

where x is the coordinate which is directed along the pressure gradient (in our experiments the pressure difference $\Delta p = 0.6\,\mathrm{bar}$ was applied at 15 cm deepness of the filtration bed), q(x,t) is the sink density of the particles due to blockage of the pores and J is the flux of the particles. We evaluated the particle diffusion coefficient as ~ 10^{-10}cm^2/sec, so characteristic Peclet number ~ 10^8>>1. It means that we may neglect the diffusive part of the flux and consequently write

$$J = \alpha u(t)\, n(x,t)\,, \tag{3}$$

where α – correcting factor which takes into account the difference between mean velocity of the particles in the pores and filtration rate. We assume also that the sink density is proportional to the excess of number of particles (at given point and on given time) over some critical value n_* ($H(x)$ – Heaviside function, β=const – coefficient of proportionality):

$$q(x,t) = -\beta\left(n(x,t)-n_*\right)H(n-n_*)\,. \tag{4}$$

On substitution of (3) and (4) in (2) we get the transport equation and its solution takes the form:

$$n(x,t) = n_*\left(1+\mathrm{e}^{-\beta t}\cdot f\left(x-\alpha\frac{Q_\infty}{S\omega}\ln\left(\mathrm{e}^{\omega t}-\left(1-\frac{Q_\infty}{Q_0}\right)\right)\right)\right), \tag{5}$$

where $f(x)$ is an auxiliary function which should be determined from initial and/or boundary conditions. In our case experimental values of numerical concentration of the particles can be approximated by the following simple formula:

$$n(x,t) = n_0(t) + n_1(t)\cdot \mathrm{e}^{-x/x_0(t)}, \qquad (6)$$

So, in order to match (5) and (6), we should choose for $f(x)$ an appropriate decay law: $f(x) = A + B\,\mathrm{e}^{-\gamma x}$ (A, B, γ=const). (7)

Table 1 gives dependencies of coefficients in formula (6) as functions of running time, which were fitted by the least square method. Fig.4 shows experimental (symbols) and theoretical (curves) behaviors of these coefficients. It is seen that there is a good agreement between them.

It is necessary to mention that from (2)-(4) we can extract the stationary distribution of the particles concentration $n_\infty(x)$ along the deepness of the filtration layer. Really, assuming $t \to \infty$, we arrive at the ordinary differential equation for $n_\infty(x)$:

$$\alpha u_\infty \frac{dn_\infty}{dx} = -\beta(n_\infty - n_*), \qquad (8)$$

where $u_\infty = Q_\infty / S = 1.7\cdot 10^{-3}\,\mathrm{cm/sec}$. General solution of Eq (8) has the form:

$$n_\infty(x) = n_* + C\cdot \mathrm{e}^{-\frac{\beta}{\alpha u_\infty}x}, \qquad (9)$$

where C is unknown constant. We can evaluate n_* and C, as well as ratio β/α comparing Eqs (6) and (9) under supposition that t=1000 sec is almost infinite characteristic time for the system under consideration. From Table 1 we conclude $n_* \approx 1.92\cdot 10^6\,\mathrm{cm}^{-3}, \beta/\alpha \approx 7\cdot 10^{-4}\,\mathrm{sec}^{-1}$ and $C = 15.1\cdot 10^6\,\mathrm{cm}^{-3}$.

Table 1. Time-dependent coefficients in formula (6)

t, sec	$n_0(t)\mathrm{x}10^{-6}$, 1/cm^3	$n_1(t)\mathrm{x}10^{-6}$, 1/cm^3	$x_0(t)$, cm
100	0.34	3.08	2.50
200	0.87	6.58	1.55
300	1.18	9.18	1.40
400	1.41	11.01	1.43
500	1.55	12.26	1.67
1000	1.92	15.10	2.44

Conclusion

The model for calculation of concentration profiles of the suspended particles along the deepness of the filtration bed in running time is developed. A good agreement between experimental and theoretical values of numerical concentration of the proppant particles as functions of coordinate and time is established. The model can be applied for evaluation of dynamic porosity of the rocks as well as changing of their specific permeability.

This work is supported by the Russian Foundation for Basic Research (project no 12-08-01091).

References

1. *Filippov A., Starov V., Lloyd D., Chakravarti S., Glaser S.* Sieve Mechanism of Microfiltration // J. Membr. Sci. 1994. V. 89. P. 199-213.
2. *Filippov A.N., Iksanov R.Kh.* Mathematical Modeling of Microfiltration of Polydisperse Suspension on Heterogeneous Membranes // Petroleum Chemistry. 2012. V.52. №7. P.520-526.

VALIDITY OF THE BOLTZMANN EQUATION TO DESCRIBE DONNAN EQUILIBRIUM AT THE MEMBRANE-SOLUTION INTERFACE

[1,2]Oane Galama, [1,3]Jan Post,[1]Martien Cohen Stuart, [1,2]Maarten Biesheuvel
[1]Wageningen University, WG Wageningen, The Netherlands.
[2]Wetsus, centre of excellence for sustainable water technology, CJ Leeuwarden, The Netherlands.
[3]KWR Watercycle Research Institute, PE Nieuwegein, The Netherlands.

Introduction

Densely charged nanoporous membranes are found throughout science and technology. To describe the transport fluxes of ions across the membrane, one of the key elements is a model for the ion partitioning, or ion distribution, at the membrane/solution interface [1-6]. This is the Donnan equilibrium, or Donnan layer. Here the ion concentration changes from its value in the external salt solution, to a different value just within the membrane matrix. The simplest approach, describing the Donnan equilibrium uses the classical Boltzmann equation.

Experiments

In this research sorption experiments where performed with densely charged anion exchange membranes (Neosepta AMX) and cation exchange membranes (Neosepta CMX). These membranes were soaked in a NaCl solution with a concentration varying from 0.01-3 M. After equilibrating the membranes were put in demineralized water, to release the absorbed ions or were put in a divalent exchange solution ($MgSO_4$) to exchange the absorbed ions. The released/exchanged co-ion and counterion concentrations were measured.

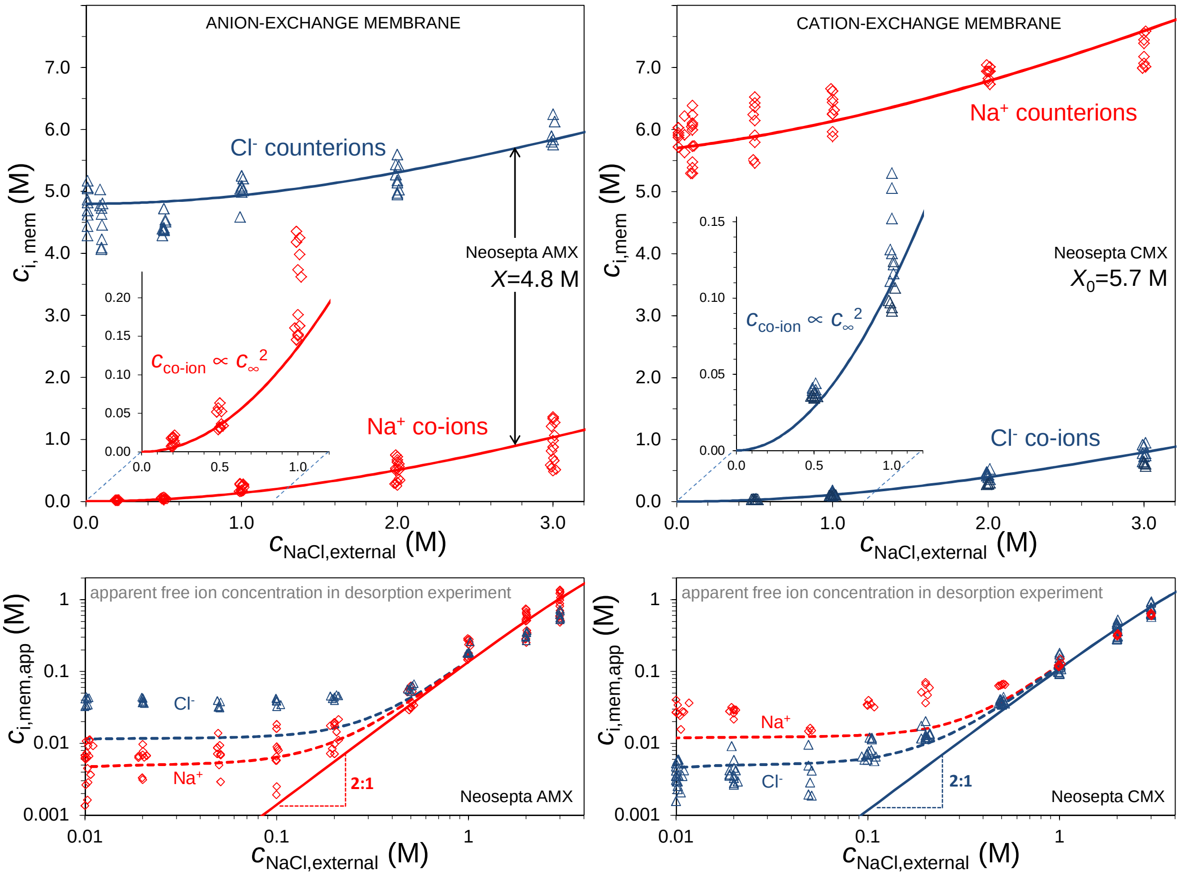

Figure 1. Measured co-ion and counterion concentration (markers) as function of the external soaking solution concentration and modified Donnan theory (lines). Dashed lines in the lower panels describe theoretical prediction for apparent 'free ion' concentration

Results and Discussion

To obtain a good fit of data it was found necessary to express the membrane charge and ion concentrations per volume of aqueous solution phase in the membrane, and to include a volume-exclusion term in the Boltzmann relation. A discrepancy between theory and experiment data is found at low external NaCl concentrations. Similar deviations from the Donnan model have been reported for over half a century [7-10], but do not yet have a convincing explanation. Agreement between experiment data and theory at low external NaCl concentrations is obtained when we model the desorption experiment taking into account the role of H^+ and OH^- ions in closing the charge balance, and postulating the presence in the membrane of a tiny amount of fixed groups with a charge opposite to overall fixed membrane charge.

References

1. *F.G. Donnan* The theory of membrane equilibria // Chemical Reviews, 1 (1924) 73-90.
2. *F.G. Donnan* Theorie der Membrangleichgewichte und Membranpotentiale bei vorhandensein von nicht dialysierenden elektrolyten, Ein beitrag zur Physikalisch-chemischen Physiologie., Zeitschrift Für Elektrochemie, 17 (1911) 572-581.
3. *E.H. Cwirko, R.G. Carbonell* // Ionic equilibria in ion-exchange membranes: a comparison of pore model predictions with experimental results // Journal of Membrane Science, 67 (1992) 211-226.
4. *D. Gillespie, R.S. Eisenberg* Modified Donnan potentials for ion transport through biological ion channels // Physical Review E - Statistical, Nonlinear, and Soft Matter Physics, 63 (2001) 061902.
5. *J.R. Bontha, P.N. Pintauro* Water orientation and ion solvation effects during multicomponent salt partitioning in a Nafion cation exchange membrane // Chemical Engineering Science, 49 (1994) 3835-3851.
6. *T. Xu, W. Yang, B. He* Partition equilibrium between charged membrane and single electrolyte aqueous solution // Chinese Journal of Chemical Engineering, 9 (2001) 326-330.
7. *F.G. Helfferich* Ion Exchange, McGraw-Hill, New York, (1962).
8. *D.H. Freeman* Electrolyte uptake by ion-exchange resins // Journal of Physical Chemistry, 64 (1960) 1048-1051.
9. *E. Glueckauf, R.E. Watts* The Donnan law and its application to ion exchanger polymers // Proceedings of the Royal Society A, 269 (1962) 339-349.
10. *G.M. Geise, B.D. Freeman, D.R. Paul* Sodium chloride diffusion in sulfonated polymers for membrane applications // Journal of Membrane Science, 427 (2013) 186-196.

HYBRID NANOMATERIALS BASED ON TITANIA AND CELLULOSE FIBERS

[1]Olga Galkina, [2]Anna Sycheva, [3]Artem Blagodatski, [4,5]George Kaptay,
[3,6] Vladimir Katanaev, [1]Alexander Agafonov
[1]Institute of Solution Chemistry of the Russian Academy of Sciences, Ivanovo, Russia,
E-mail: olgalgalkina@mail.ru
[2]Materials Science Research Group, Hungarian Academy of Sciences, Miskolc, Hungary,
E-mail: a.sycheva@uni-miskolc.hu
[3]Institute of Protein Research, Russian Academy of Sciences, Pushchino, Russia;
[4]Department of Nanotechnology, University of Miskolc, Miskolc-Egyetemvaros, Hungary;
[5]Bay Zoltan Applied Research Nonprofit Ltd, Miskolc, Hungary, *E-mail: kaptay@hotmail.com*
[6]Department of Pharmacology and Toxicology, University of Lausanne, Switzerland

Introduction

Titanium dioxide (titania) has unique photophysical and chemical properties that define the new range of its practical use. Titania-based coatings with high specific surface area and narrow pore size distribution range have provided great prospects for practical application in solar energy transformation, photocatalysis [1], water and air cleaning and processing as self-cleaning, photochromic, and superhydrophobic/hydrophilic coatings [2] and just recently as matrices for bioencapsulation and drug delivery. The significant interest is in obtaining new types of photoactive materials based on titania, which, on the one hand, would allow to extend the range of its practical application, and, on the other hand – to derive new fundamental knowledge about the influence of the structure of materials on their photocatalytic and biological activity. Of importance are developments devoted to obtaining "smart textiles" showing a self-cleaning ability from organic pollutions under the influence of light as well as high bactericidal activity. The present work reports the new method of obtaining TiO_2-modified cotton fibers possessing the high photocatalytic activity and antibacterial properties.

Experiments

Titania particles have been obtained using a low-temperature sol-gel synthesis, which leads to the TiO_2 formation of anatase – brookite modification in solution bypassing the drying stages [3]. A stable sol contained ultrafine TiO_2 nanoparticles with an average hydrodynamic radius of 20 nm. Further treatment of cellulose fiber by nanocrystalline titania hydrosol with 1,2,3,4 – butanetetracarboxylic acid (BTCA) as cross-linking agent showed a strong fixation of nanoparticles on the surface of a cotton fiber by covalent bonding. The physical and chemical properties of hybrid nanomaterials were investigated by Fourier-transform infrared spectroscopy, thermogravimetric analysis, low-temperature adsorption/desorption of nitrogen and scanning electron microscopy. The antibacterial properties of the modified samples were also investigated.

Results and Discussion

The surface morphology of pure and modified cotton fibers is shown in Fig. 1. It can be seen from Fig. 1a that pure cotton fibers are not contaminated. After modifying with titania hydrosol the cotton fibers are coated with a quite irregularly distributed white precipitate; there is “gluing” of fibers and in some areas the coating is absent (Fig. 1b). The sample obtained using the cross-linking agent also contains titania (Fig. 1c). The coating is composed of particles from a fraction of micrometer to 50 micrometers in size. Here the particles are distributed more uniformly over the fibers. After five washing cycles (Figure 1d, e) a considerable reduction in the quantity of titania precipitate is observed in the SEM images. According to thermogravimetric analysis, the TiO_2 content of the sample without cross-linking agent is 9.4%, which is almost twice as low as that of the sample with cross-linking agent (17.1%). During washing about 50% of non-bonded adsorbed titania leaves the surface of cotton fibers. It has been established that TiO_2 nanoparticles are cross-linked to the surface of a cotton fiber by the formation of transverse ester bonds with BTCA (Fig. 2). Sodium hypophosphite, in this case, acts as a catalyst of the reaction, increasing the rate of cross-linking the cellulose macromolecules to BTCA and $TiO_{2.}$

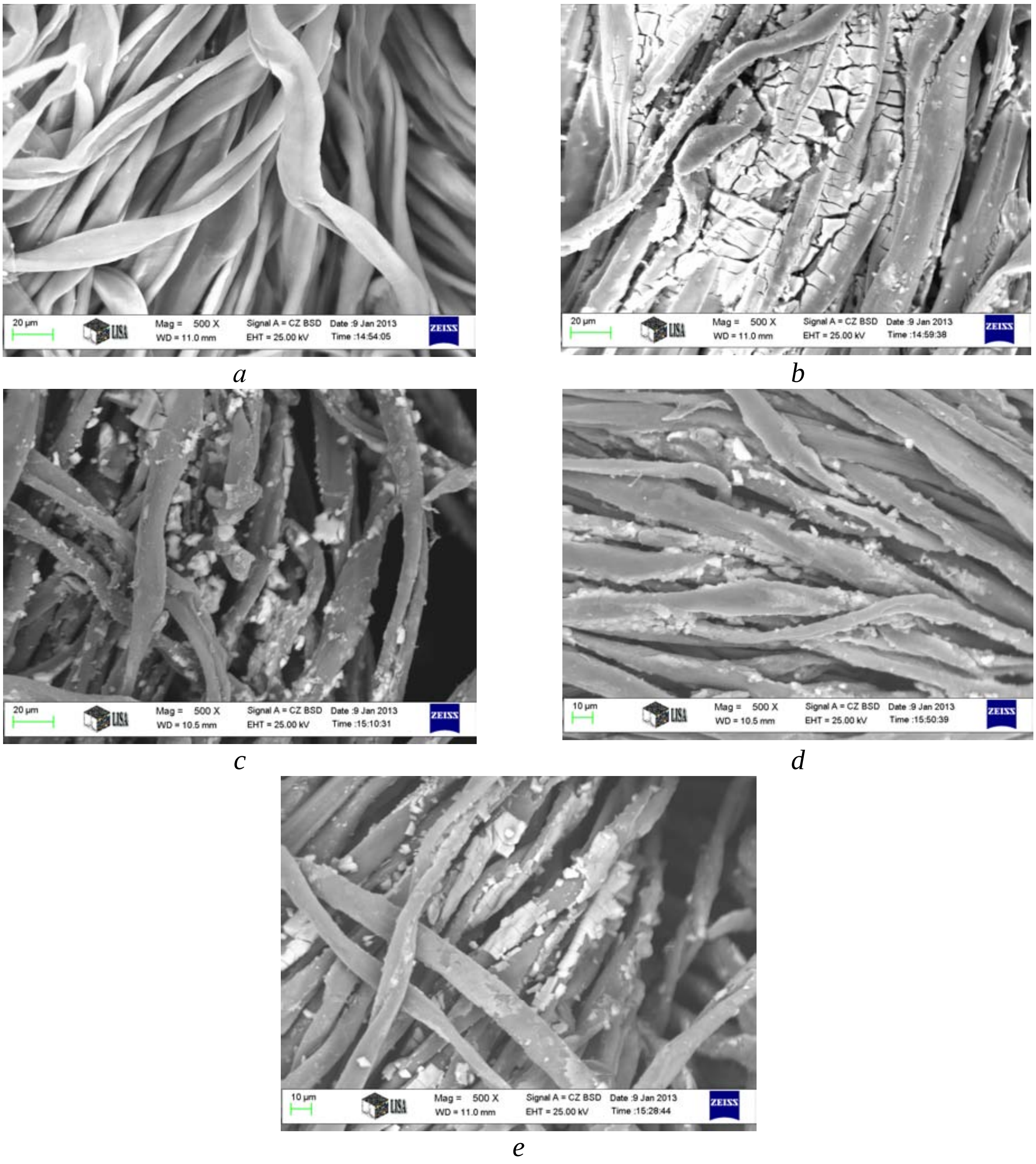

a *b* *c* *d* *e*

Figure 1. SEM micrographs of cotton fabrics before (a) and after modification with TiO_2 hydrosol (b), TiO_2 hydrosol and BTCA (c) and the same composite samples after 5 cycles of washing (d, e), respectively

It was revealed that NaH_2PO_2 weakens hydrogen bonds between carboxylic acid functional groups in BTCA, promoting the accelerated formation of cyclic anhydride at low temperatures. Based on IR spectroscopy data, it was found that the addition of a BTCA cross-linking agent and sodium hypophosphite as a cross-linking catalyst to TiO_2 hydrosol leads to the shift of the absorption band from 1642 to 1660 cm^{-1}, which testifies to the formation of Ti–O–C bond. Therefore, the use of cross-linking agent allows obtaining composite fabric with higher TiO_2 content even after 5 washing cycles.

The self-cleaning properties of the fabrics without washing, as well as after 5 cycles of washing, were estimated by the rate of decomposition of a model dyeing agent, namely, Rhodamine B under the action of UV irradiation. The degradation of an organic dyeing agent in non-modified sample is almost not observed, which is associated with its high stability. At the same time, upon the introduction of titania nanoparticles (an effective photocatalyst) into a cotton fabric, this process can be intensified. The efficiency of operation of such a composition depends on a lot of factors, including the amount of reactive centers and the strength of their bonding with the carrier surface (cotton cellulose). In this case, the problem of the degree of interaction, the cross-linking of these nanoparticles with the fiber surface, remains of particular importance. Sample derived using BTCA, manifests higher photoactivity, since nanoparticles of titania are cross-linked with the surface of cotton fiber with covalent bonds, which causes the retention of reactive centers with an increasing number of washing cycles.

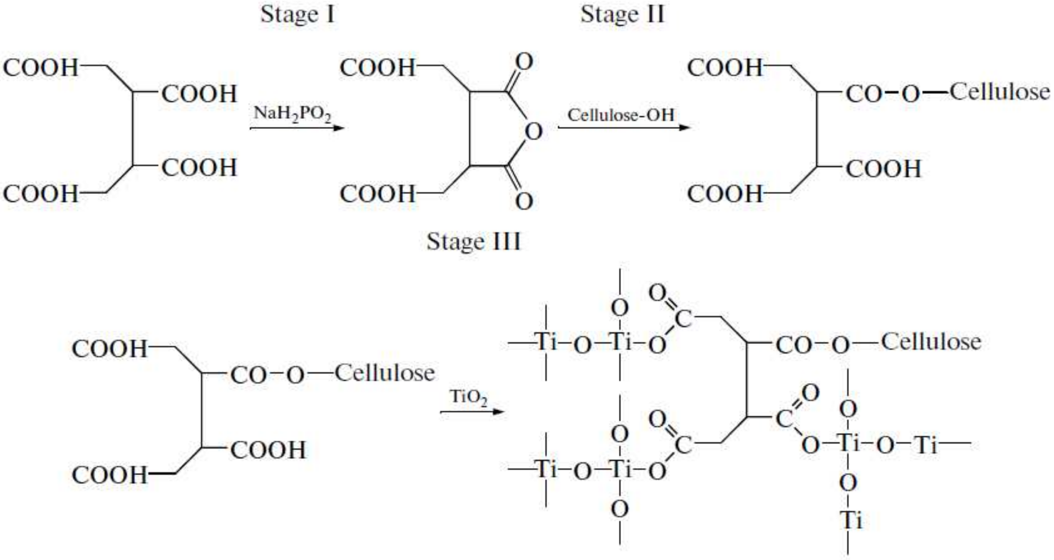

Figure 2. Mechanism of interaction of cotton fibers with BTCA and TiO$_2$

In the case of Gram-negative bacteria E. coli, fabric processing with nanocrystalline titania hydrosol with and without using a cross-linking agent results in a significant reduction of the microorganism survival. The bactericidal activity of samples is primarily due to photocatalytic properties and crystal structure of the synthesized titania described in detail in [3]. As a result of UV-irradiation, reactive oxidative species, such as OH•, O_2•, HO_2• are generated on the surface of TiO_2, of which the hydroxyl radical OH• is considered the most important oxidizing agent that ensures cell inactivation. The modified TiO_2 fibers have bacteriostatic effect, inhibiting the growth of bacterial culture and can be potentially used as aid in the fight against pathogen microorganisms.

Acknowledgements

This research was (partially) carried out in the framework of the Center of Excellence of Applied Materials Science and Nano-Technology at the University of Miskolc.

References

1. *A.V. Agafonov, A.V. Vinogradov* Catalytically active materials based on titanium dioxide: Ways of enhancement of photocatalytic activity// High Energy Chemistry. 2008. V. 42. No 7. P. 578-580.
2. *O.L. Galkina, V.V. Vinogradov, A.V. Agafonov and A.V. Vinogradov* Surfactant-Assisted Sol-Gel Synthesis of TiO_2 with Uniform Particle Size Distribution // Int. J. Inorgan. Chem. 2011. V. 2011. doi:10.1155/2011/108087. Article ID 108087. 8 pp.
3. *O.L. Galkina, V.V. Vinogradov, A.V. Vinogradov, and A.V. Agafonov* Development of the Low Temperature Sol-Gel Synthesis of TiO_2 to Provide Self-cleaning Effect on the Textile Materials // Nanotech. in Russia. 2012. V. 7. Nos. 11–12. P. 604–614.

STABILITY OF A THIN FILM UNDER A DC ELECTRIC FIELD

Georgy Ganchenko, Ekaterina Gorbacheva
Kuban State University, Krasnodar, Russia, *E-mail: ganchenko.ru@gmail.com; katya1911@list.ru.*

Introduction

In this paper we study the stability of a thin film electrolyte of an external dc electric field. A similar problem was studied in [1], [3] and [4], but they use the assumption of no mobile charge at the gas-liquid interface, although it was the main cause instability. Also in these studies considered only nanofilms, which does not give a complete picture of the phenomenon, because the microscale instability arise for other reasons [2, 5]. In this paper, we consider the cases as microfilm and nanofilms, which allows you to compare the cases and study the transition from one to another. In this paper the curves of neutral stability, critical values of parameters in the transition to instability.

Theoretic Approach

The mathematical model described by the system Nernst-Planck-Poisson-Stokes equations:

$$\frac{\partial c^{\pm}}{\partial t}+\boldsymbol{u}\cdot\nabla c^{\pm}=\nabla\cdot(c^{\pm}\nabla\Phi)+\nabla^2 c^{\pm}, \qquad (1)$$

$$\nu^2\nabla^2\Phi=(c^+-c^-), \qquad (2)$$

$$-\nabla p+\nabla^2\boldsymbol{u}=\frac{\kappa}{\nu^2}(c^+-c^-)\nabla\Phi, \qquad (3)$$

$$\nabla\cdot\boldsymbol{u}=0, \qquad (4)$$

$$y=0: \quad \nu\frac{\partial\Phi}{\partial y}=q, \qquad (5)$$

$$c^+\frac{\partial\Phi}{\partial y}+\frac{\partial c^+}{\partial y}=0 \qquad -c^-\frac{\partial\Phi}{\partial y}+\frac{\partial c^-}{\partial y}=0 \qquad (6)$$

$$\mathrm{v}=0, \quad u=0. \qquad (7)$$

$$y=h(x,t): \quad c^+\frac{\partial\Phi}{\partial n}+\frac{\partial c^+}{\partial n}=0, \quad -c^-\frac{\partial\Phi}{\partial n}+\frac{\partial c^-}{\partial n}=0, \quad (8)$$

$$\Phi=\varphi, \quad \nu\frac{\partial\Phi}{\partial n}=\delta\nu\frac{\partial\varphi}{\partial n}+\sigma, \qquad (9)$$

$$\frac{\partial\sigma}{\partial t}+\frac{\partial(u_s\sigma)}{\partial x}=0, \qquad (10)$$

$$p-\frac{We}{R}+[nT^f n]+[nT^e n]=P_{ATM} \qquad (11)$$

$$[nT^f n]+[nT^e n]=0, \qquad (12)$$

$$\mathrm{v}=\frac{\partial h}{\partial t}+u\frac{\partial h}{\partial x}. \qquad (13)$$

In the gas model is described by the Laplace equation for the electric potential:

$$\nabla^2\varphi=0, \qquad (14)$$

With boundary conditions: $y=H:\dfrac{\partial\varphi}{\partial y}=0.$ (15)

The boundary conditions (5) - (7) are given on a hard surface. (6) - the condition of impermeability of the ions.

The boundary conditions (8) - (13) are defined on the free surface. (8) - the condition of impermeability of positive and negative ions, (10) - the condition of conservation of charge, (11) - a condition for normal stress, (12) - a condition for shear stresses (fig. 1). Square brackets denote the jump in the value in going through the interface (value minus the value of the gas to liquid), P_{ATM} – pressure in the gas, which is then without loss of generality assumed to be zero, T^f – hydrodynamic stress tensor, T^e – tensor of the Maxwell-Wagner.

$c^{\pm}$ – concentration of positive and negative ions;
Φ – electric potential; p – pressure;
(u,v) – velocity components $\boldsymbol{u}$;
φ – electric potential in the air;
q – charge on the solid surface; σ – mobile charge at the gas-liquid.

Parameters:

$$\nu = \frac{\tilde{\lambda}_D}{\tilde{h}_0}, \quad \tilde{\lambda}_D = \left(\frac{\tilde{\varepsilon}\tilde{\Phi}_0}{\tilde{F}\tilde{c}_0} \right)^{1/2} = \left(\frac{\tilde{\varepsilon}\tilde{R}\tilde{T}}{\tilde{F}^2\tilde{c}_0} \right)^{1/2}.$$

Parameter κ characterizes the physical properties of the electrolyte solution, and fixed for a given fluid and electrolyte. We – is the Weber number, $\tilde{\varepsilon}$ – dielectric constant of the medium, $\tilde{\gamma}$ – coefficient of surface tension, λ_D - number of Debye, $\tilde{h}_0$ - the characteristic size of the problem.

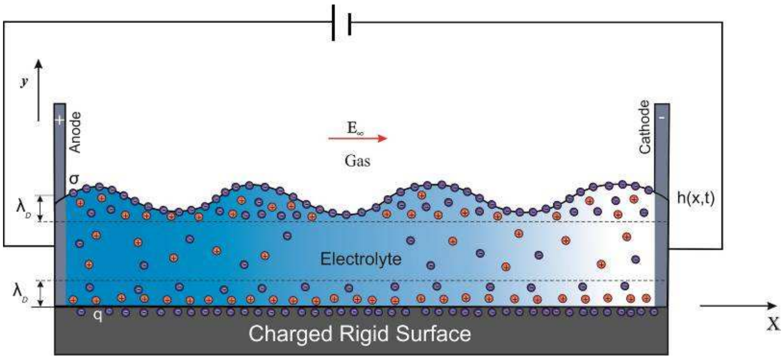

Figure 1. Illustration problem statement

To study the problem of the stability of one-dimensional steady-state solution (fig. 2) are superimposed small periodic perturbation along the spatial coordinate x. Due to small perturbations in the problem will only be considered a linear stability.

$$\begin{aligned} &c^\pm = c_0^\pm + \hat{c}^\pm(y)\exp(i\alpha x + \lambda t), \quad \Phi = \Phi_0 + \hat{\Phi}(y)\exp(i\alpha x + \lambda t), \quad \Psi = \Psi_0 + \hat{\Psi}(y)\exp(i\alpha x + \lambda t) \\ &U = U_0 + \hat{U}(y)\exp(i\alpha x + \lambda t), \quad h = 1 + \hat{h}\exp(i\alpha x + \lambda t), \quad \sigma = \sigma_0 + \hat{\sigma}\exp(i\alpha x + \lambda t) \end{aligned} \tag{16}$$

As a result of the substitution of the functions (16) in (1-4) is obtained by a linear homogeneous system of ordinary differential equations with an unknown parameter lambda and with unknown functions $\hat{K}, \hat{\rho}, \hat{\Phi}, \hat{\Psi}$, where $K = c^- + c^+$, $\rho = c^+ - c^-$. K - ion concentration, ρ - charge density, Ψ – stream function or velocity potential, with appropriate boundary conditions (5-13) In addition to the unknown functions, there are two unknown numbers: $\hat{h}, \hat{\sigma}$, where $\hat{h}$ – perturbation of the surface and $\hat{\sigma}$ is induced charge.

$$\lambda\hat{K} + i\alpha U\hat{K} - i\alpha K'\hat{\Psi} + i\alpha E_\infty\hat{\rho} = \frac{\partial}{\partial y}\left(\rho\hat{\Phi}' + E\hat{\rho} + \hat{K}'\right) - \alpha^2\rho\hat{\Phi} - \alpha^2\hat{K}, \tag{17}$$

$$\lambda\hat{\rho} + i\alpha U\hat{\rho} - i\alpha\rho'\hat{\Psi} + i\alpha E_\infty\hat{K} = \frac{\partial}{\partial y}\left(K\hat{\Phi}' + E\hat{K} + \hat{\rho}'\right) - \alpha^2 K\hat{\Phi} - \alpha^2\hat{\rho}, \tag{18}$$

$$\nu^2\left(\hat{\Phi}'' - \alpha^2\hat{\Phi}\right) = -\hat{\rho}, \tag{19}$$

$$\hat{\Psi}^{IV} - 2\alpha^2\hat{\Psi}'' + \alpha^4\hat{\Psi} = i\alpha\frac{\kappa}{\nu^2}\left(\rho'\hat{\Phi} - E\hat{\rho}\right) - \frac{\kappa}{\nu^2}E_\infty\frac{\partial\hat{\rho}}{\partial y}. \tag{20}$$

The number λ is chosen so that the system to have a nontrivial solution. After application of the Galerkin expansion of functions in series of Chebyshev polynomials and the τ-method, obtained a generalized eigenvalue problem for the linear algebraic system: $\det(A - \lambda B) = 0$. The matrix A is composed of the operator of the differential system. Eigenvalue problem is solved by QR algorithm.

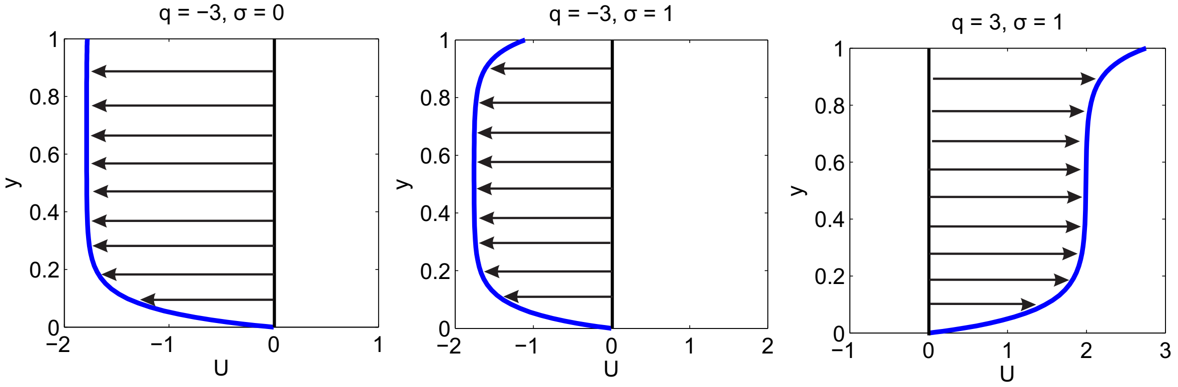

Figure 2. Illustration of the one-dimensional velocity (u) solutions for different parameters

If $\mathrm{Re}(\lambda) > 0$, then the one-dimensional solution loses its stability (or instability), i.e. film can curl up into droplets. If $\mathrm{Re}(\lambda) < 0$, then there is no loss of stability. The point α where $\mathrm{Re}(\lambda) = 0$ is the bifurcation point (or imbalance).

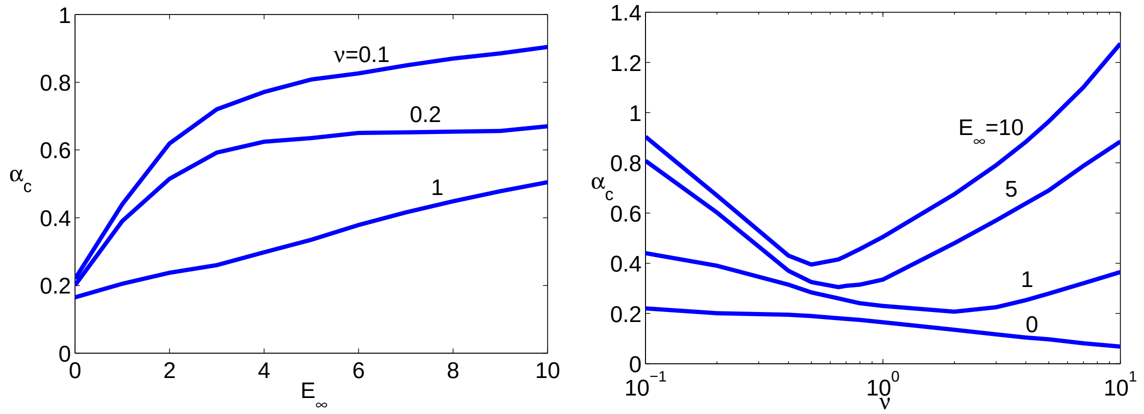

Figure 3. Illustration α_c depending on E_∞ and ν

Results and Discussion

Curves of neutral stability for the various parameters of the problem for micro- ($\nu << 1$) and nano-films ($\nu = O(1)$)(fig. 3). From the results it is clear that, as the characteristic dimension of the problem volatility is reduced. In addition, found that the system is stable in the absence of mobile charge at the interface, which is confirmed by the analytical solution of the system (17-20) derived from the assumption that ν .

References

1. *S. W. Joo* // Microfluid Nanofluid 2008. V. 5. P. 417.
2. *B. Zaltzman and I. Rubinstein* // J. Fluid Mech. 2007. V. 579, P. 173.
3. *B. Ray, P. D. S. Reddy, D. Bandyopadhyay, S. W. Joo, A. Sharma, S. Qian and G. Biswas* // Theor. Comput. Fluid Dyn. 2012. V. 26. P. 311.
4. *M. Mayur, S. Amiroudine and D. Lasseux* // Physical Review E. 2012 V. 85, P. 046301.
5. *Schibauer J., Demekhin E.A., Ganchenko G.* // Physical Review E. 2012. V. 85. P.055302.

PHYSICOCHEMICAL, STRUCTURAL AND MECHANICAL AGEING OF ANION-EXCHANGE MEMBRANES DURING INDUSTRIAL ELECTRODIALYSIS AND ITS CAUSES

[1]Wendy Garcia-Vasquez, [1]Lasaad Dammak, [1]Christian Larchet, [2]Victor Nikonenko, [2]Nataliya Pismenskaya, [1]Daniel Grande

[1]Institut de Chimie et des Matériaux Paris-Est UMR 7182 CNRS – Université Paris-Est, Thiais, France.
[2]Kuban State University, Krasnodar, Russia.

Introduction

It is known that the efficiency of electrodialysis (ED) processes depends in a large part on the properties of the ion exchange membranes (IEMs) used. The evaluation of IEM lifetime is an important aspect in the control of the operation, as membranes tend to lose their physico-chemical and separative properties during ED, which is accompanied by lower yields and increasing costs due to the replacement of IEMs and the growth of energy consumption.

In this communication, physico-chemical, structural and mechanical properties of an anion-exchange membrane (AEM) were investigated throughout their lifetime in a full scale ED stack used for whey demineralization, in order to get a deeper insight into the understanding of IEM ageing. This fundamental investigation reveals significant issues concerning IEMs properties and their long-term behavior. The approach is based upon the interpretation of the membranes characterization in actual ED for whey demineralization by means of a systematic analysis of new samples and samples used at different times.

Experiments

Samples AMX-SB, were taken from an industrial ED stack at 45%, 70% and 100% of their lifetime in whey demineralization (several thousands of hours). They are made of functionalized polystyrene crosslinked with (DVB) and finely powdered poly(vinyl chloride) (PVC), which were coated onto a PVC cloth used as reinforcing material To take out every sample it was necessary to stop the production and disassembly the ED stack; a fresh sample was also studied to compare a new membrane with the used ones and to establish the evolution of membrane characteristics with time. Membranes were characterized through their physicochemical properties (conductivity, permeability, ion-exchange capacity, thickness, water uptake, contact angle, etc.); structural and morphological properties (by SEM, EDX, FTIR, ICP, nitrogen sorption porosimetry, etc.) and mechanical properties (assessed by the tensile strength test). The microheterogeneous model was applied to describe the samples relations between structure and properties.

Finally an ageing protocol was performed in new samples, to simulate the acid-basic cleaning procedure in ED, and conclude about the causes of IEM ageing. Ageing protocol consisted in a cycle of 30 minutes in 0.1M HCl at 40°C, rinse with deionised water at room temperature, 30 minutes in 0.1M NaOH at 40°C, and finally, rinse with deionised water at room temperature before restarting the cycle. This was repeated at least 8 times per day until membranes spent 300 hours in each solution; normally, this is the total time that membranes would spend in cleaning solutions during its lifetime, in whey demineralization ED.

Results and Discussion

With increasing time of operation, the membranes became darker and more fragile. There is not a significant loss of the ion-exchange capacity or degradation of the functional poly(styrene-*co*-divinylbenzene) (PS-DVB). However, fouling (observed by FTIR) causes a decrease in the counter-ion mobility within the membrane which produces a reduction of the electrical conductivity (Fig 1).

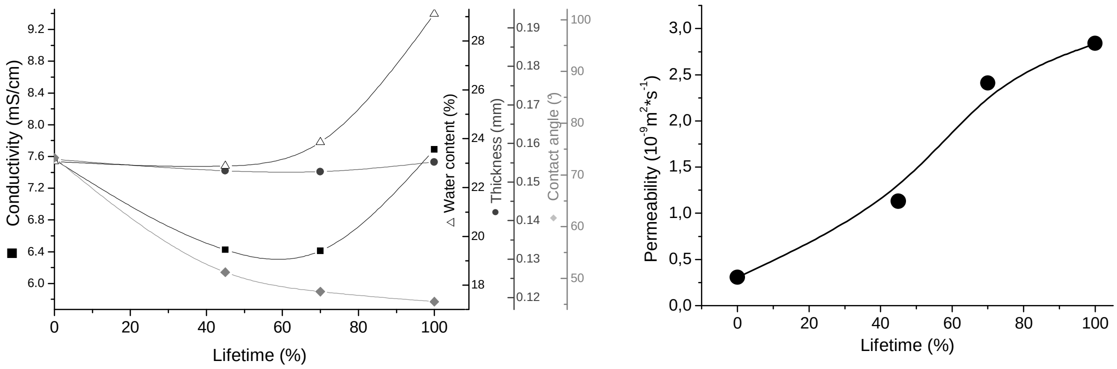

Figure 1. Physico-chemical properties of AEM samples as a function of their lifetime. Conductivity, water uptake, thickness and contact angle (left). 0.1M NaCl permeability (right)

By means of SEM images and specific surface area measurements (BET method) it was possible to acknowledge that the membrane porosity increased gradually with the time of operation. This accounts for the increase in permeability through the appearance of new pores which form channels for non-selective electrolyte transfer. A Soxhlet extraction with THF permitted to extract, 44% of the new membrane as soluble fraction. This decreased gradually up to 11.4% for the membrane at 100% of lifetime. Extractables were identified by FTIR to be PVC. Accordingly, new pores in the used membranes were left by PVC washed out from the membrane during the cleaning-in-place process in ED.

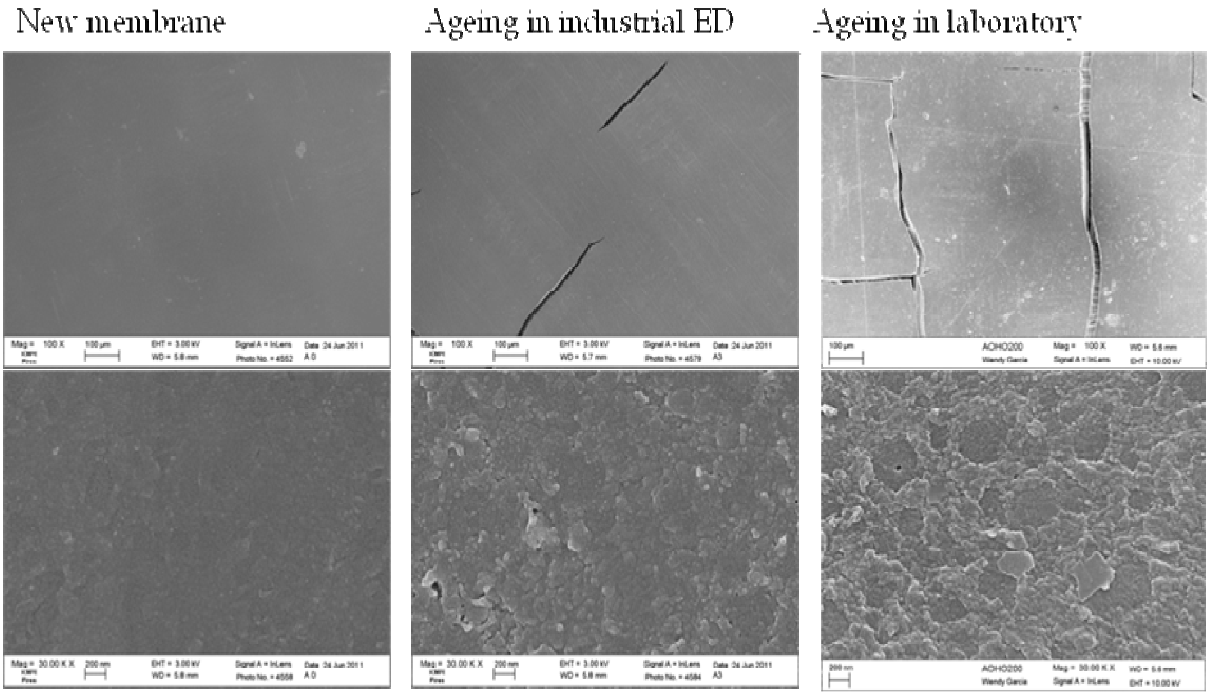

Figure 2. SEM images of new and aged membranes in industrial ED and through the ageing protocol in laboratory. (Magnification: First row x100; second row x 30 000)

These new pores not only contribute to increasing electrolyte permeability, but also to growing conductivity in the last stage of ED. The latter is due to the fact that there is a substitution of non-conductive regions occupied by PVC for pores filled with electrolyte solution apparently containing also organic components of whey. The new AEM presented a combination of the mechanical properties associated with the two polymeric components, *i.e.* the rigidity of PS-DVB and the toughness of PVC. However, the loss of PVC had severe consequences in the mechanical properties of the AEM. As it was seen in the stress-strain curves, the Young modulus, which indicates the rigidity of a material, decreased by 20% from 0% to 100% of lifetime. Likewise, the breaking strength, which represents the membrane plasticity, decreased by 45% and the area under the stress-strain curve decreased of almost 80%, which strongly indicated a loss of the material toughness. Characterization of sample that underwent the ageing protocol in laboratory shows that it has the same behaviour, and it has suffered the same changes than membranes in industrial ED. It is noteworthy that there is a formation of similar macroscopic cracks and microscopic porosity (Fig. 2).

A Soxhlet extraction with THF permitted to extract only the 17% of the membrane, accounting for a PVC loss. The sample lost 23% of Young modulus, 62% of strain at break and 85% of area under the stress-strain curve.

Conclusion

We have found that there are several events accompanying the process of membrane ageing in ED. Fouling occurs from the beginning of the operation leading to a decrease in the counterion mobility. The following phases of membrane deterioration are apparently due to the loss of PVC which results in formation of non-charged pores within the membrane matrix, available for electroneutral electrolyte solution and for large molecules coming from whey. In addition, membrane toughness decreases. Gradually the AEM membrane converts from a rigid and tough material to a rigid and brittle one. This results in the formation of cracks and tears leading to the final failure in the ED stack.

The cause of AEM ageing in ED for whey demineralization, is more likely to be, the traditional acid-basic cleaning protocol.

Acknowledgements

This investigation was realized within French-Russian laboratory "Ion-exchange membranes and related processes". The authors are grateful to CNRS, France, and to RFBR, Russia (grants 11-08-93107_CNRSL, 12-08-00188_CNRSL, 13- 8-96508r_yug), as well as to FP7 Marie Curie Actions "CoTraPhen" project PIRSES-GA-2010-269135 for financial support.

Pt/CNF COMPOSITE MATERIALS FOR H_2 AND CO POTENTIOMETRIC SENSORS: SIZE EFFECT

Ekaterina Gerasimova, Andrey Belmesov, Ekaterina Zolotukhina, Yuriy Dobrovolsky
Institute of problems of chemical physics of RAS, Chernogolovka, Russia, *E-mail: lyramail@mail.ru*

Introduction

Information about composition of gas phase and specially about concentration of detrimental impurities is usually needed for work optimization of modern devices and to maintain the purity of environment. The principle problem in this case is the determination of concentration of carbon monoxide and hydrogen because of toxicity of CO and explosion hazard of H_2. That is why the development of high-effective real-time sensor devices is so important.

Electrochemical sensors response to gas phase composition changes due to electrochemical reactions occur on interface working electrode/electrolyte. Such type of sensors is referred to potentiometric sensors with possibility to choose the selective electrocatalyst for working electrode.

In this work we study the influence of platinum clusters size on operating efficiency and sensitivity of platinum/carbon materials as potentiometric sensors of H_2 and CO.

Experiments

As a platinum clusters carrier were chosen carbon nanofibers (CNF) with diameter 100-200 nm. Deposition of platinum clusters was realized by reduction H_2PtCl_6 with ethylene glycol in conditions of microwave treatment. Clusters size was determined by XRD and TEM analyses. Synthetic procedure of Pt/CNF catalysts was described in details in [1]. Electrocatalysts with platinum content from 4% to 61 wt % and with average size of Pt particles from 1 nm to 2.6 nm were used as an electrode material of sensors.

Investigation of sensor behaviours was studied in electrochemical cells:

Working electrode (WE) | Solid-state electrolyte (SSE) | Reference electrode (RE)

Synthesized composite materials were used as WE, $(NH_4)_2HPW_{12}O_{40}\cdot nH_2O$ played the role of proton-conductive SSE and PbO_2 was used as RE.

Such sensors were tested in gas mixtures with 400-4000 ppm of H_2 and/or CO.

Results and Discussion

In H_2-containing atmosphere the dependence of potential (emf), E, of investigated sensors on H_2-concentration is semi-logarithmic in the whole range of analyzed concentration, c, (Eq. 1):

$$E = E_0 + K\cdot \lg[c], \qquad (1)$$

where K is an empirical coefficient.

Reproducibility of obtained data by repeated measurements of identical concentration is very high ($R^2>0.99$). The slope of sensor potential dependence on logarithmic concentration (Eq. 1) varied from 42 to 116 mV. Moreover, there is a dependence on composition of working electrode notable on the size of platinum clusters. It should be mentioned, that the obtained slope (table 1) is not even close to theoretical slop of hydrogen oxidation reaction (59 mV). Such behaviour can be explain with possibility of several competitive electrochemical reactions, e.g. hydrogen oxidation and oxygen reduction. In this case the potential of working electrode is compromise.

As follows from the analysis of potential-concentration dependences for H_2 and CO sensors in air all investigated materials showed sufficient sensibility. Pt/CNF electrocatalyst with clusters size 2.1 nm has the highest sensibility. However, in the inert argon atmosphere with CO the platinum is quickly poisoned.

Table 1. Electrocatalysts Pt/CNF Characteristics and Parameters of Equation (1) in H_2-Air Atmosphere

Platinum content, wt %	Platinum surface in CO-method, S_{CO}, m^2/g	Platinum surface in H_2-method, S_H, m^2/g	Platinum geometrical surface, by TEM, S_{TEM}, m^2/g	Average size of Pt clusters by TEM, nm	Average size of Pt clusters by XRD, nm	Slope in Eq. (1), -K, mV	$-E_0$, mV
4	30	55	250	1.0	-**	42,3	718
7	90	105	120	2.1	2.5(40°)	116,5	950
23	90	100	155	1.7	2.3(40°)	74,8	782
49	30	30	85	2.4	3.4(67°)	72,5	826
61	40	50	70	2.6	3.7(67°)	70,3	724

** - Pt reflection and background noise are commensurable.

In conclusion it should be noted, that potentiometric sensors Pt/CNF | $(NH_4)_2HPW_{12}O_{40}\cdot nH_2O$ | PbO_2 type can be used for H_2 and CO concentration detection in air. The sensitivity of such sensors shows direct dependence on size of platinum particles in electrocatalyst.

This work is supported by RFBR (№ 12-03-31746).

References

1. *Gerasimova E. V., Bukun N. G., Dobrovolsky Y. A.* // Russian Chemical Bulletin. 2011. V. 60(6). P. 1045-1050.

AGEING OF ION-EXCHANGE MEMBRANES IN ELECTRODIALYSIS: STRUCTURAL AND PHYSICOCHEMICAL INVESTIGATION

Rim Ghalloussi, Lobna Chaabane, Christian Larchet, Daniel Grande, Lasâad Dammak

Institut de Chimie et des Matériaux Paris-Est UMR 7182 CNRS – Université Paris-Est, 2 Rue Henri Dunant, Thiais, France. *E-mail: dammak@u-pec.fr*

Introduction

It is well known that the efficiency of electrodialysis (ED) processes depends in a large part on the properties of the ion-exchange membranes (IEMs) used. The evaluation of IEM lifetime is an important aspect in the control of the operation, as membranes tend to lose their physico-chemical and separative properties during ED, which is accompanied by lower yields and increasing costs due to the replacement of IEMs and the growth of energy consumption.

In this context, the understanding of ageing processes occurring in IEMs used in ED for food industry applications, and the investigation of their long-term behavior are necessary to enhance the progress of this advantageous technology.

The deterioration of IEMs is intimately related to the modification of two parts of the membrane, namely the polymer matrix and the nature and concentration of the functional sites. In this paper, we will focus on the evolution of physicochemical and structural properties of IEMs after their use in a full scale ED stack.

Experiment

Two Neosepta® ion-exchange membranes, produced by Astom (Japan), were studied at two crucial moments in their lives: before and after use for 2 years in ED for food industry. The cation-exchange membranes are noted CEMN (fresh sample) and CEMU (used sample). The notations AEMN and AEMU are used for anion-exchange membrane.

The conductivity (CDM92 from Radiometer-Tacussel), ion-exchange capacity (French standards NF X 45-200), water content (French standards NF X 45-200), contact angle (FM40 EasyDrop goniometer from Krüss) and ion transport number (French standards NF X 45-200) were determined for each new and used membrane. Scanning electron microscopy (LEO 1530 microscope) and EDX analysis were also carried out.

Results and Discussion

SEM microphotographs, at different magnifications, of fresh and used membranes are shown in Fig. 1. The first line corresponds to sections and the two others for membrane surfaces. As it can be seen, the surface of a fresh Neosepta® membrane is smooth and homogeneous (at least at the scale of the order of several microns). The surface of used CEM presents some “scales”. They are due to the fact that the membrane becomes fragile: the surface of used swollen membrane is smooth, but when the membrane is drying, the scales appear. The surface of AEM shows important structural defects. The cavities on its surface can be so great that the reinforcing cloth, normally located at about ten microns from the surface, is exposed.

Such strong deterioration of membrane structure should be accompanied with no less significant changes in membrane properties. The main static and transport characteristics of the IEMs under study are shown in Table 1.

In Table 1 we remark that the exchange capacities drop significantly after 2 years of use in ED treatment of solutions containing weak organic acids, in a food industry application. The CEM sample showed a dramatic variation in its contact angle, exchange capacity, and Na^+ transport number, but it displays a moderate decrease in its water content and thickness.

The AEM appeared to be the most affected membrane by the decrease in exchange capacity and contact angle, accompanied by a large increase in water content and thickness.

From EDX analysis given by Figure 2, we can remark a significant decrease in the intensity of the peaks corresponding to sulfur and sodium in the used CEM. This confirms that some of the sulfonic functional sites of CEMU ($SO_3^-Na^+$) are completely removed from the membrane. The magnitude of this decrease is comparable to that of E_C (see Table 1).

An increase of the peaks corresponding to sulfur and oxygen is observed in the two MEAs. This can be explained by the poisoning of MEAs by sulfur polyvalent ions such as sulfate ion SO_4^{2-}or SO_3^{2-}sulfite ion, and / or transfer sites sulphonic lost by MECs.

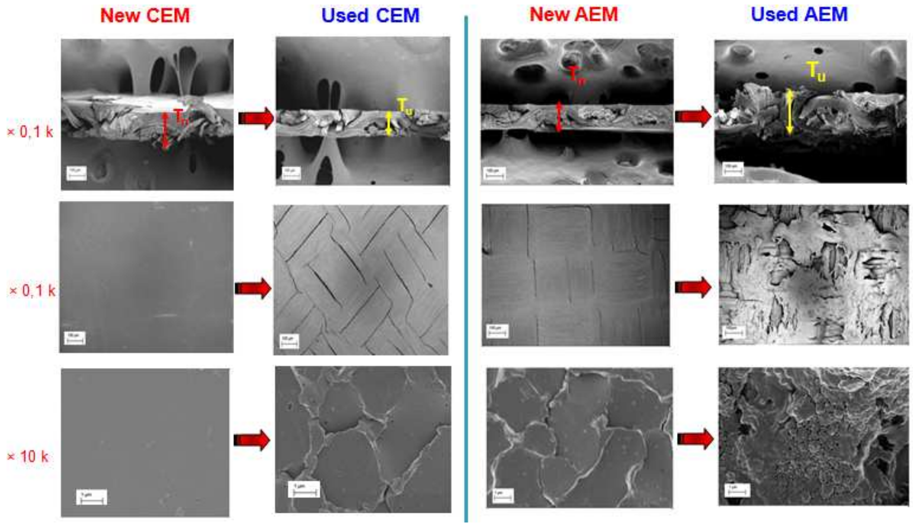

Figure 1. SEM micrographs of new and used CEM and AEM

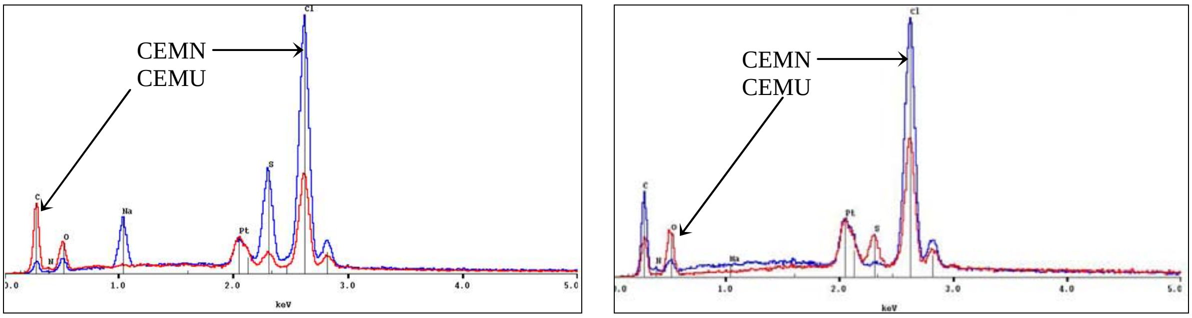

Figure 2. EDX analysis of new and used CEM and AEM

Table 1. Static and dynamic characteristics of the studied membranes

Membrane		**E_C (meq.g^{-1} of dry IEM)**	**%W**	**T (µm)**	**θ (°)**	**κ_m (S.cm^{-1})**	**f_2**	**$t_{counterion}$**
CEM	***CEMN***	2.66	28.2	176	38 ± 2	6.1	0.12	0.97
	CEMU	0.77	23.7	160	79 ±2	2.3	0.10	0.60
AEM	***AEMN***	1.45	28.7	148	69 ± 2	5.6	0.11	0.99
	AEMU	0.23	40.3	344	52 ± 2	5.0	0.30	0.99

The CEM suffered significant degradation; nonetheless, it was generally more robust and resistant than the anion-exchange counterparts, which was more unstable. A significant degradation in the polymer matrix of both membrane types was found. The CEM and the AEM lost a part of ion exchange sites and their specific electrical conductivity decreased. However, the CEM becomes denser with lower water content and higher surface hydrophobicity, while the water content and the thickness of AEM increased in about two times. The permselectivity of CEM decreased, while that of AEM was not deteriorated.

We have used the microheterogeneous (fig. 2) model [1-3], on which we have made some changes, to analyze the ageing process. This model was used to explain the evolution of the totality of static and transport properties, and in particular, the apparent contradiction between the loss of exchange capacity and the increase in permselectivity of used AEMs.

Organic and inorganic compounds found in the used CEM in excess as compared with the unused one are present there in too small amounts to contribute noticeably to the water content and swelling. The loss of exchange sites leads to increasing concentration of co-ions in CEM and deterioration of its permselectivity.

In contrast to CEM, the water content in the AEM and its thickness increase essentially during its use in ED. Consequently, the surface hydrophobicity decreases. This behaviour is explained by sorption of organic colloidal particles within membrane nanopores. As these particles are generally hydrophilic, they attract water which leads to higher swelling. At the same time, these particles replace electroneutral solution in the pore center. As a result, the effective radius of ion conducting channels decreases, the DELs occupy a more important volume fraction of the pore solution that favours permselectivity. However, the higher swelling of the AEM leads to rupture of some bonds and polymer chains. As a result, structure macro-defects (fissures, cavities, caverns) filled with external solution appear in the membrane. In the long run, these defects may form through unselective en passages meaning full unfitness of the membrane.

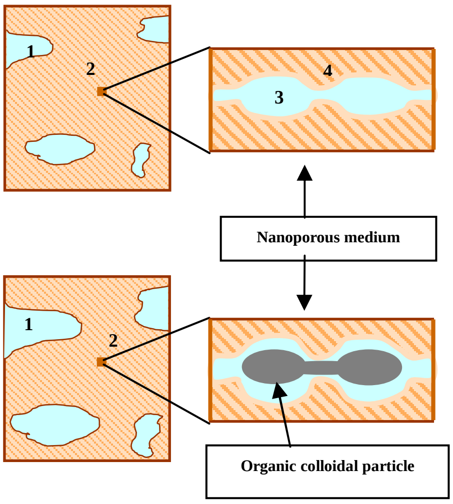

Figure 2. Possible structure variation of an AEM: (a) before and (b) after the use in ED of organic acid containing solutions; 1: macro-defects of structure, 2: nanoporous media, 3: nanopore filled with a charged solution, 4: hydrophobic matrix

Conclusion

Both types of membranes lose a part of ion-exchange sites; their specific electrical conductivity decreases. However, the CEM is generally more robust and resistant than the anion-exchange counterparts. The structure and properties of CEM and AEM vary in different ways. The CEM become denser, its water content and thickness decrease, and the surface becomes more hydrophobic. Apparently, it is due to the loss of hydrophilic ion-exchange sites. Organic and inorganic compounds found in the used CEMs in excess as compared with the fresh ones are present there in too small amounts to contribute noticeably to the water content and swelling.

The loss of ion-exchange sites leads to an increasing concentration of co-ions in CEMs and a deterioration of their permselectivity.

References

1. *V. Compan, E. Riande, F.J. Fernandez-Carretero, N.P. Berezina, A.A.-R. Sytcheva*, Influence of polyaniline intercolations on the conductivity and permselectivity of perflyorinated cation-exchange membranes, J. Membr. Sci., 318 (2008) 255-263.
2. *S. A. Novikova, E. Y. Safronova, A. A. Lysova, A. B. Yaroslavtsev*, Mendeleev Commun, 20 (2010) 156.
3. *V.V. Nikonenko, A.B. Yaroslavtsev, G. Pourcelly,* Ion transfer in and through charged membranes, Structure, properties, theory. Chapter 9 in Ionic Interactions in Natural and Synthetic Macromolecules, edited by A. Ciferri and A. Perico, John Wiley & Sons, Inc., 2012, pp. 267-336.

DONNAN DIALYSIS OF THE MIXTURE OF PHENYLALANINE AND SODIUM CHLORIDE WITH PROFILED MEMBRANE MK-40P

Elena Goleva, Vera Vasil'eva, Kristina Chegereva, Anastasia Moshkina
Voronezh State University, Voronezh, Russia, *E-mail: vorobjeva_ea@mail.ru*

Introduction

Ions extraction from solutions with other substances using dialysis as compared with other separation methods is recognized efficient and competitive [1, 2]. Its advantages over the methods of electrodialysis, sorption and extraction are primarily in the low energy cost, ease of equipment design and maintenances. Donnan dialysis is a separation process that uses interdiffusion of two or more counterions through the ion-exchange membrane [2]. This type of dialysis, when using electrically charged membranes, in fact, is a continuous ion-exchange process. The ions of the solution continuously exchange for another ions of the same charge sign in the other solution, separated from the first one by ion-exchange membrane.

The preparative production of amino acids from mixtures with mineral electrolytes is one of the main problems of applied biochemistry. The aim of this work is the study of the possibility of selective extraction of sodium ions from the mixture with bipolar ions of amino acid by Donnan dialysis with profiled sulfocation-exchange membrane.

Experiments

Donnan dialysis of solutions was carried out using two-compartment flowing dialyzer of continuous action. The height and width of the working area of the membrane were 4.2 and 1.7 cm., respectively. Examined solution (dialysate) was passed in section 1 of the dialyzer, while hydrochloric acid solutions of different concentrations (diffusate) were passed in the counterflow mode through the adjacent section 2. Examined solutions were passed at the rate of $4{,}5 \cdot 10^{-2}$ m/s, diffusate solution – at the rate of $5{,}8 \cdot 10^{-3}$ cm/s.

Solutions of alkylaromatic nonpolar amino acid phenylalanine and mineral salt sodium chloride were studied. Since the pH of the examined solutions were 5,20-5,60, the amino acid that was an ampholyte (pJ=5,91), was in the form of bipolar ion. Concentrations of sodium chloride and phenylalanine in their individual solutions and in the mixture were 0.025 M. The range of concentrations of hydrochloric acid solutions in the diffusate was $2{,}5 \cdot 10^{-5}$-2,5 M.

At a dialysis used a heterogeneous sulphocation-exchange membrane MK-40P with geometrical-nonuniform (profiled) surface. Zabolotsky V. I. et al. developed the technique of ion-exchange membranes profiling by wet hot pressing, which is patented in RF [3], and defined conditions which are not degrading physical, chemical, transporting and structure characteristics of membranes.

Results and Discussion

The dependence on the diffusion fluxes of the components of the concentration of hydrochloric acid in the diffusate (Fig. 1) has shown that at the range of high acid concentrations for both individual and mixed solutions in dialysis sodium ions fluxes significantly exceeded the phenylalanine fluxes. Reduction of hydrochloric acid concentration in the diffusate $C(HCl)<4{,}0 \cdot 10^{-3}$ M caused an inversion of the membrane selectivity: the amino acid fluxe exceeded the mineral ion fluxe. The reason of it is the features of mechanisms of transport of mineral and organic ions through the sulfocation-exchange membrane in the H-form.

Equivalent ion-exchange reactions occur between hydrogen counterions of sulfocation-exchange membrane and cations of metal in Donnan dialysis of mineral component solutions. Sodium ions from the dialysate solution pass through the membrane into the diffusate solution, and acid hydrogen ions are transferred in the opposite direction. Basically, the receiving diffusate solution acts as solution for regeneration by normal ion exchange.

The mechanism of transport of phenylalanine through the sulfocation-exchange membrane is determined by the ionic composition of the amino acid solution. Protonation of bipolar ions of amino acid by hydrogen ions, located in the membrane as counterions, increases the mass transfer rate because cations of amino acid diffuse in the membrane phase more easily. Cations of phenylalanine in the solution can be exchanged with hydrogen counterions of the membrane by reaction of equivalent ion exchange in which counterions of the membrane are displaced into the external solution.

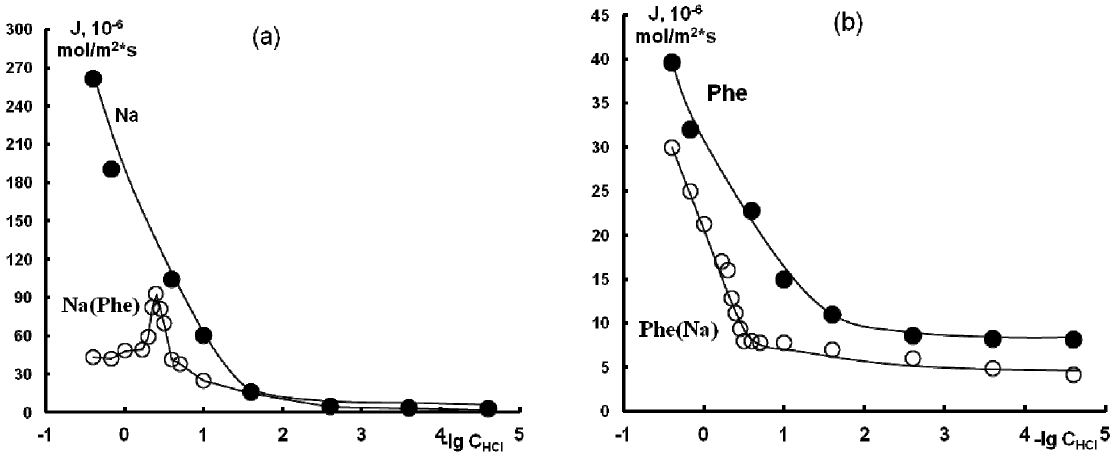

Figure 1. The dependences of the diffusion fluxes of sodium ions (a) and phenylalanine ions (b) in Donnan dialysis of individual NaCl, Phe and equimolar solutions NaCl(Phe), Phe(NaCl) on the concentration of hydrochloric acid in the diffusate

The competitive kind of interaction of the components fluxes is carried out by Donnan dialysis of mixed solutions, and it results in great reduction of the rate of mass transfer of sodium ions compared with phenylalanine ions (Fig. 1). The effect of amino acid’s influence increases with the growth of the concentration of hydrochloric acid in the diffusate. The sodium ions fluxes exceed the phenylalanine fluxes 10 times when the concentration of hydrochloric acid is 0,3-0,4 M, when C(HCl)=2,5 M the rate of mass transfer of the components is practically identical. The reason is associated with an increase of the amount of cation form of amino acid by reduction of the pH of the solution in section 1 because of the transfer of hydrogen ions from the diffusate.

The dependences on the separation factor S_F of the concentration of hydrochloric acid in the diffusate during Donnan dialysis of equimolar solution (a) and of the ratio of the components concentrations in the mixture solution of phenylalanine and sodium chloride (b) through the profiled membrane MK-40 P in the H-form are shown in Fig. 2.

The experimental dependence of the separation factor for the Donnan dialysis can be divided into three sections (Fig. 2a). In the first section separation factor S_F had a value of less than one, which is caused by acceleration of the diffusion of bipolar ions of amino acid when using cation-exchange membrane in H-form and electrolyte transport limitation due to the Donnan exclusion. The second section at $C(HCl)>4,0\cdot 10^{-3}$ M was characterized by growth of S_F due to increase of amount of elimination of sodium ions with growth of the concentration of acid in the diffusate. The separation efficiency maximum was observed at the acid concentrations range of 0,3-0,4 M, that corresponds cation form of phenylalanine content 40-56%. With further increase of the concentration of hydrochloric acid (the third section) the decrease of separation factor was observed due to competitive transfer of cations of phenylalanine produced by protolysis of bipolar ions of amino acid in both solution and membrane phases.

The dependence on the separation factor of the ratio of components concentrations in the dialysate solution has shown that separation factor increases with reduction of portion of amino acid: salt concentration’s increase of 200 times led to separation factor growth of 8 times (Fig. 2b).

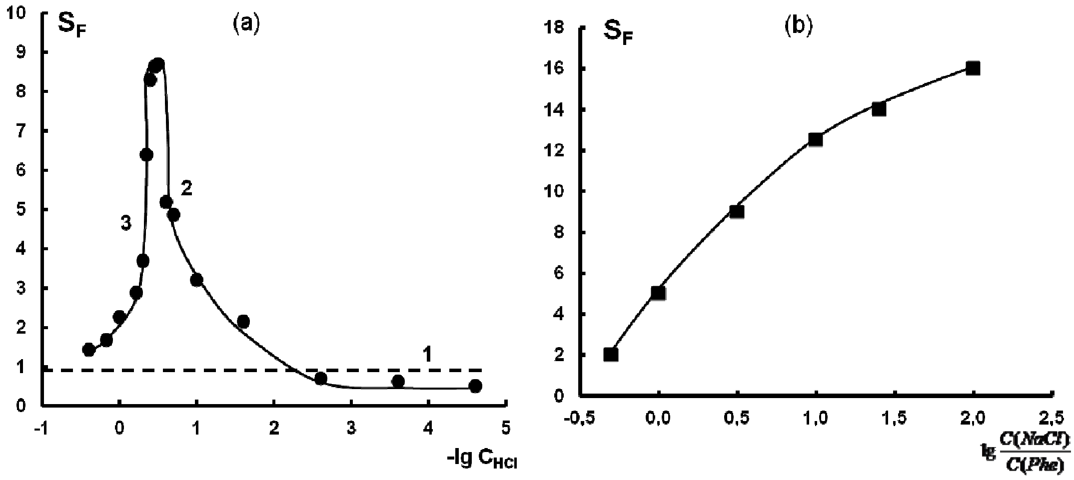

Figure 2. The dependence of separation factor on the concentration of hydrochloric acid in the diffusate in Donnan dialysis of equimolar solutions of sodium chloride and phenylalanine (a) and on the ratio of the components concentrations in the mixture solution for C_0*(NaCl)=0,025 M when C(HCl)=0,25 M (b)*

Thus, by varying the concentration of hydrochloric acid in the diffusate and, accordingly, the values acidity index and the ratio of different ion forms of amino acid in the dialysate can create the conditions for selective transport of sodium cations or phenylalanine ions through the sulfocation-exchange membrane.

The experimental results have shown the possibility of application of Donnan dialysis with sulfocation-exchange membrane for selective extraction of metal cations from a mixture of phenylalanine with mineral salts.

Acknowledgments

We are grateful prof. V.I. Zabolotsky (Kuban State University) for the provided samples of a profiled cation-exchange membranes.

References

1. *Mulder M.* Basic principles of membrane technology. M.: World, 1999. 513 p.
2. *Hwang S.-T., Kammermeyer K.* Membranes in separations. M.: “Chemical”, 1981. 464 p.
3. *Zabolotskii V. I., Loza C. A., Sharafan M. V.* Method of profiling of ion-exchange membrane. Pat. RF 2284851, BO1D 61/52, 10.10.2006.

MATHEMATICAL DESCRIPTION OF MASS TRANSFER IN ELECTRO-BARO MEMBRANE PROCESSES

Vladislav Golovashin
Tambov State Technical University, Tambov, Russia, *E-mail: vvvtam@inbox.ru*

Introduction

One promising area of membrane technology are electro-baro membrane processes, which are the driving forces of the pressure field and the electric field. To describe the mass transfer in the electro-baro membrane separation, it is possible using the Navier-Stokes equations and the continuity of flow, the Nernst-Planck equation, and the Poisson equation, written for inter-membrane channels and membrane, and extended the appropriate boundary conditions. In this paper, the influence of the electric field on the separation of the aqueous solution of hexamine, which is present in the wastewater of pharmaceutical companies.

Theory

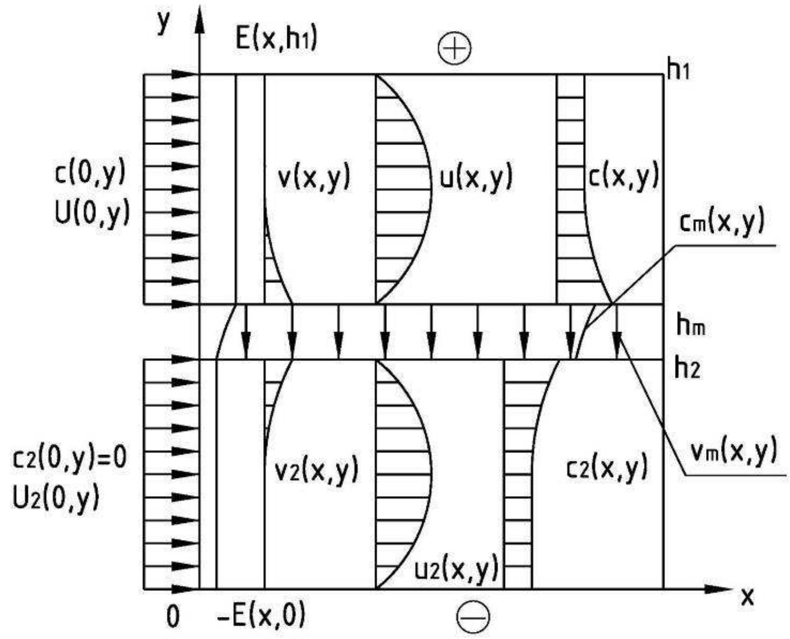

Figure 1. Scheme of mass transfer

Stationary mass transfer permeate in the channels parted by the semipermeable membrane, it is possible to feature system of the differential equations including equations of motion of a fluid and the equation of electro-convective diffusion [1], noted for the intermembranous channel, and the fluid and electro-convective diffusion equations of motion, noted for a membrane:

For the first channel:

$$\nabla\cdot\left[\eta\cdot\left(\nabla\boldsymbol{u}+(\nabla\boldsymbol{u})^T\right)\right]+\rho\cdot(\boldsymbol{u}\cdot\nabla)\cdot\boldsymbol{u}+\nabla P=0 \quad (1)$$

$$\nabla\cdot\boldsymbol{u}=0 \quad (2)$$

$$\nabla\cdot(-D\cdot\nabla c-z\cdot u_e\cdot F\cdot\nabla E)=-\boldsymbol{u}\cdot\nabla c \quad (3)$$

$$-\nabla\cdot(h_1-h_m)\cdot\varepsilon_0\cdot\varepsilon_r\cdot\nabla E=0 \quad (4)$$

With boundary conditions:

$$u(0,y)=u_0;\ u(x,h_1)=0;\ u(x,h_m)=0;\ P(L,y)=P_0 \quad (5)$$

$$v(0,y)=0;\ v(x,h_1)=0;\ v(x,h_m)=k\cdot P(x,h_m) \quad (6)$$

$$c(0,y)=c_0 \quad (7)$$

$$-D\cdot\nabla c(x,h_1)-z\cdot u_m\cdot F\cdot\nabla E+\boldsymbol{u}\cdot c(x,h_1)=0 \quad (8)$$

$$-D\cdot\nabla c\left(x,h_m\right)-z\cdot u_m\cdot F\cdot\nabla E+\boldsymbol{u}\cdot c\left(x,h_m\right)=-R\cdot c\left(x,h_m\right)\cdot v\left(x,h_m\right) \tag{9}$$

$$E\left(x,h_1\right)=E_0;\ E\left(0,y\right)=0;E\left(L,y\right)=0 \tag{10}$$

For the second channel:

$$\nabla\cdot\left[\eta\cdot\left(\nabla\boldsymbol{u}_2+\left(\nabla\boldsymbol{u}_2\right)^T\right)\right]+\rho\cdot\left(\boldsymbol{u}_2\cdot\nabla\right)\cdot\boldsymbol{u}_2+\nabla P_2=0 \tag{11}$$

$$\nabla\cdot\boldsymbol{u}_2=0 \tag{12}$$

$$\nabla\cdot\left(-D\cdot\nabla c_2-z\cdot u_e\cdot F\cdot\nabla E\right)=-\boldsymbol{u}_2\cdot\nabla c_2 \tag{13}$$

$$-\nabla\cdot h_2\cdot\varepsilon_0\cdot\varepsilon_r\cdot\nabla E=0 \tag{14}$$

With boundary conditions:

$$u_2(0,y)=u_0;\ u_2(x,0)=0;\ u_2(x,h_2)=0;P_2(L,y)=P_2 \tag{15}$$

$$v_2(0,y)=0;\ v_2(x,0)=0;\ v_2(x,h_2)=v_m(x,h_2) \tag{16}$$

$$c_2(0,y)=0 \tag{17}$$

$$-D\cdot\nabla c\left(x,0\right)-z\cdot u_e\cdot F\cdot\nabla E+\boldsymbol{u}_2\cdot c\left(x,0\right)=0 \tag{18}$$

$$c_2(x,h_2)=c_m/\gamma \tag{19}$$

$$E\left(x,0\right)=-E_0;\ E\left(0,y\right)=0;E\left(L,y\right)=0 \tag{20}$$

With membrane:

$$\nabla\cdot\left[\eta\cdot\left(\nabla\boldsymbol{u}_m+\left(\nabla\boldsymbol{u}_m\right)^T\right)\right]+\rho\cdot\left(\boldsymbol{u}_m\cdot\nabla\right)\cdot\boldsymbol{u}_m+\nabla P_m=0; \tag{21}$$

$$\nabla\cdot\boldsymbol{u}_m=0 \tag{22}$$

$$\nabla\cdot\left(-D_m\cdot\nabla c_m-z\cdot u_e\cdot F\cdot\nabla E\right)=-\boldsymbol{u}_m\cdot\nabla c_m \tag{23}$$

$$-\nabla\cdot h_m\cdot\varepsilon_0\cdot\varepsilon_m\cdot\nabla E=0 \tag{24}$$

With boundary conditions:

$$u_m(0,y)=0;\ u_m(L,y)=0;u_m(x,h_m)=0;P_m(x,h_m)=P(x,h_m) \tag{25}$$

$$v_m(0,y)=0;\ v_m(L,y)=0;v_m(x,h_m)=v(x,h_m) \tag{26}$$

$$c_m(x,h_m)=c\cdot\gamma \tag{27}$$

$$-D\cdot\nabla c\left(x,h_2\right)-z\cdot u_e\cdot F\cdot\nabla E+\boldsymbol{u}_m\cdot c\left(x,h_2\right)=0 \tag{28}$$

$$E\left(0,y\right)=0;E\left(L,y\right)=0 \tag{29}$$

The Poisson equation is written simultaneously to both channels and membrane.

Where: $\boldsymbol{u}$, $\boldsymbol{u}_{m,2}$ - a field of velocities of a solution in a diaphragm and channels, m/s; η - kinematic viscosity of a solution, m²/s; ρ - solution density, kg/m^3; P, $P_{m,2}$ - pressure in a membrane and channels, Pa; $c_{m,2}$ - concentrations of permeate in a membrane and channels, kg/m^3; u, $u_{m,2}$ - a dilatational component of a vector of velocity in a membrane and channels, m/s; v, $v_{m,2}$ - a cross component of a vector of velocity in a membrane and channels, m/s; D, D_m - a diffusion constant in a solution and a membrane, m^2/s; E -electric potential, V; ε_0 - the dielectric constant;$\varepsilon_{1,2,m}$ - the dielectric constant; $h_{1,2}$ - a thickness of a membranous channel, m; L - length of the membranous channel, m. h_m - a thickness of a membrane, m; R - rejection; γ- an equilibrium distribution.

It should be noted that the above proposed a mathematical model of heat transfer in electricbaromembrane processes is a fairly simplistic because it does not take into account the heat on the electrodes and the heat transfer in inter-membrane channel, as well as in membranes, as well as the reactions occurring at the electrodes. However, for “small' current density calculations performed on this mathematical model showed good agreement with experimental data.

Results and Discussion

Approximating expression for the equilibrium distribution coefficient gained experimentally looks like:

$$\gamma = 0,018 \cdot c^{-0,32} \cdot \left(\frac{T_0}{T}\right)^{2,45} \cdot \left(\frac{P_0}{P}\right)^{0,98} \tag{30}$$

Approximating expression for coefficient of diffusive permeability of the diaphragm, gained of experiments on diffusion looks like:

$$D_m = 3{,}3 \cdot 10^{-10} \cdot c^{-0{,}0011} \cdot \left(\exp\left(-0{,}021 \cdot c\right)\right) \cdot \exp\left(\frac{-1632}{T}\right) \tag{31}$$

$$R = 1 - \frac{1}{1 + \left(\frac{1}{\gamma} - 1\right)\left[1 - \exp\left(-\frac{v(x,h_m) \cdot h_m}{D_m}\right)\right] \cdot \exp\left(-\frac{v(x,h_m) \cdot \delta}{D}\right)} \tag{32}$$

The combined equations (1-32) were solved by a finite element method with a net thickening on boundaries. Adequacy of the offered mathematical model was checked on laboratory installation equipped with the module of flat chamber type with use of membrane ESPA1. Concentration three methenamine in permeate and penetrate was spotted by the photocalorimetric method [2]. Results experiments and calculation are presented in table 1. Experimental and calculation datas are gained at P=4·10^5 Pa. As a modelling solution water solution three methenamine of mark CP, prepared on distilled water was used.

Influence of concentration of permeate on a separation process was explored, at initial velocity of a solution in the intermembranous channel of 0,25 m/s. Apparently the discrepancy of experimental and calculation datas makes of the table no more than 10% that testifies to adequacy of the offered mathematical exposition of process. The concentration of the solution was 1,2 kg/m^3. Table 1 shows the experimental and calculated data for the anode membrane.

Table 1. Experimental and calculated data for the anode membrane

The electric Potential *E*, V.	**The specific Productivity, J·10^6, m/s**		**Concentration in Permeate, c_2, kg/m^3**	
	Experimental	**Calculation**	**Experimental**	**Calculation**
1	6,32	6,33	0,070	0,071
10	6,39	6,41	0,071	0,070
20	6,42	6,43	0,068	0,068
30	6,47	6,50	0,066	0,065

References

1. *Rubinstein I.* Electro-diffusion of ions. SIAM:11 Philadelphia. 1990 – 263p.
2. *Peregud E.A.* Air Chemical analysis's rebuzzing (new and advanced methods). L: Chemistry, 1976.

SYNTHESIS AND DIFFUSION PROPERTIES OF MEMBRANES AMEX MODIFIED BY CERIA

Daniil Golubenko, Yulia Karavanova, Andrei Yaroslavtsev
Kurnakov Institute of General and Inorganic Chemistry, Moscow, Russia, *E-mail: yuka@igic.ras.ru*

Introduction

Waste water treatment is in the focus of government programs in different countries. One of the most complex problem in water treatment area is nitrates removing [1]. There is no economical technology abled to output nitrate anion nowadays [2]. The solution of problems of water medium purification is related, to a considerable extent, to the use of diverse membrane materials [3], which do not always satisfy increasing demands of science and industry. So work of membrane modification, and especially preparation of membranes containing inorganic and macromolecular components extensively developed. Membrane composite materials with enhanced selectivity and transfer rate of nitrate ions were obtained from heterogeneous AMEX membranes. The modification of membrane pores by ceria nanoparticles increases the transfer numbers with respect to anion and enhances the mobility of NO_3^- ions.

Experiments

For the synthesis of modified samples anion-exchange membrane AMEX (MEGA) was saturated with cerium ions by keeping in cerium (III) nitrate and cerium (IV) ammonium nitrate solutions, and then the precursor was hydrolysed. To determine the transport properties of the obtained membranes ionic conductivity and diffusion of membrane in different ionic forms (hydroxyl, nitrate and chloride) were investigated. Ionic conductivity was measured by impedance spectroscopy.

Results and Discussion

No crystalline ceria was observed in the obtained membrane using X-ray phase analysis. At the same time, the X-ray diffraction pattern of the residue obtained after membrane annealing at 600 °C is identical to the CeO_2 diffraction pattern (Fig. 1).

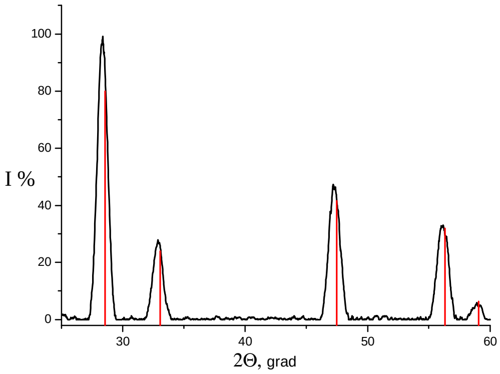

Figure 1. X-ray diffraction pattern of the AMEX membrane modified by ceria and annealed at 600 °C; the bar chart diagram corresponds to ceria (card 34-0394, PDF-2)

In order to estimate the transfer numbers of the membranes (t_+), the values of diffusion coefficients D_{Na^+} and $D_{NO_3^-}$ were calculated from experiments on determination of the diffusion permeability and mutual diffusion coefficients of the membranes.

$$t_+ = D_{Na^+} / (D_{Na^+} + D_{NO_3^-})$$

where D_{Na^+} and $D_{NO_3^-}$ are the diffusion coefficients for sodium cation and nitrate anion (cm^2/s), respectively.

Modification substantially decreases the cations transfer number. The diffusion coefficients for the sodium cation correlate (table 1) with the water content, which can indicate the partial displacement of the intrapore solution from the modified membranes. Probably, this is a reason for a decrease in the mobility of the cation, because the cation can penetrate through the anion-exchange membrane only through the phase of the solution.

Table 1. Diffusion permeability, moisture content, interdiffusion coefficients, and transfer numbers of the modified membranes

Membrane	D(Na^+) , cm^2/s	% H_2O	D(OH^-/NO_3^-) cm^2/s	t_+ %
AMEX	8,1·10-7	25,7	1.2·10-5	4,6
Ce3-1	1,4·10-7	19,1	2.9·10-5	0,2
Ce3-2	5,9·10-8	18,5	2.1·10-5	0,2
Ce4-2	6,2·10-8	18,3	2.0·10-5	0,2
Ce4-4	1,4·10-7	19,7	7.2·10-6	1,3

As a result of insertion of small amounts of ceria, the nitrate ion conductivity of the samples increases substantially compared that of the initial membrane (see Fig. 2). This is probably related to an increase in the concentration of the carriers (NO_3^-), which can be sorbed on the CeO_2 surface. Moreover, for the AMEX_3_01 sample, the nitrate ion conductivity is not only higher than the chloride ion conductivity, but also ~25% exceeds the conductivity of the hydroxo form (which is maximum for other samples).

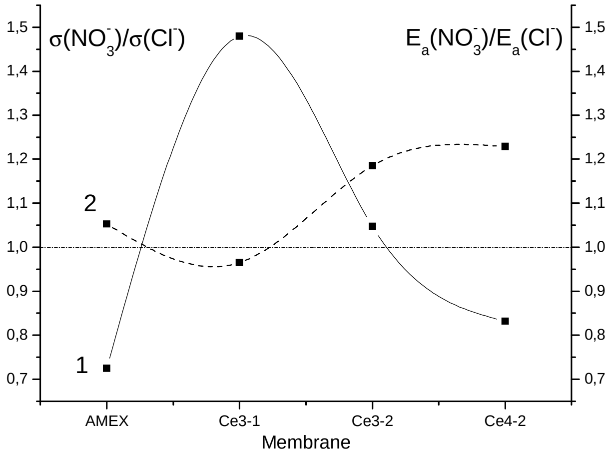

Figure 2. Relations of conductivity for membrane in Cl^--form and NO_3^--form (1) and activation energy (2) for the transport of nitrate anion for membrane

This work was financially supported by RFBR grant № 13-08-01259a.

References

1. *DeZuane J.,* Handbook of Drinking Water Quality, 2nd ed., John Wiley & Sons., New York., 1997.
2. *Amit Bhatnagar, Mika Sillanpaa,* Review of emerging adsorbents for nitrate removal from water // Chem. Eng. J. 2011. V. 168. P. 493–504.
3. *Yaroslavtsev A. B., Nikonenko V. V.* // Ross. Nanotekhnologii [Russian Technologies]. 2009. V. 3. P. 8.

OXYGEN REDUCTION BY CATHODE POLARIZED DISPERSED METALS INTO ION-EXCHANGE MATRIX

Vladislav Gorshkov, Tamara Kravchenko, Lev Polyanskiy
Voronezh State University, Voronezh, Russia. *E-mail: vgorsh88@gmail.com*

Bifunctional nature of metal-polymer nanocomposites (NCs) is determining in considering with a number of chemical and electrochemical systems [1]. The carrier of nanoscale metal particles becomes an important because the size distribution by volume of the polymer material, the pH of the internal medium, and chemical resistance of NCs are depends on its status. The aim of this study was to resolves a question of the limiting diffusion current of oxygen to the metal ion exchanger NCs, which differ in the nature of the metal (Ag, Cu) component, size and distribution of metal particles and the ionic form of the polymer matrix.

Studying the process of cathodic reduction of oxygen was performed on granular NCs of silver and copper based on the macroporous sulfonic cation-exchanger KU-23. Metal reduction was carried out by various reducing agents by known methods [2]. Given the percolation threshold of the electronic conductivity of nanocomposites with particles of silver and copper for electrochemical studies were selected materials with 7 and 10 landings of these metals respectively.

Analysis of the morphology and microstructure of the samples was carried out by scanning electron microscope (SEM) JSM 6380LV and X-ray diffraction analysis (XRD). The diffraction patterns were obtained on a DRON-3.

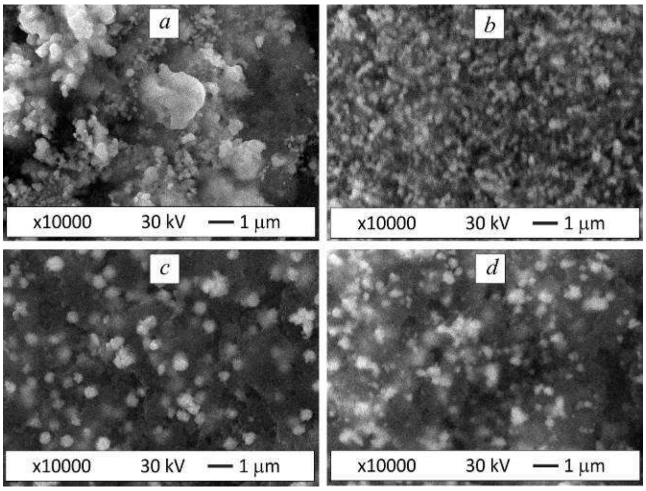

Figure 1. Micrographs of cuts of metal-containing grains NCs: a) $Ag^0 \cdot$KU-23, reducing agent $N_2H_4 \cdot H_2O$; b) $Ag^0 \cdot$KU-23, reducing agent $NaBH_4$; c) $Cu^0 \cdot$KU-23, reducing agent $Na_2S_2O_4$; d) $Cu^0 \cdot$KU-23, reducing agent $NaBH_4$ (surface layer)

Microscopic studies of the samples showed that the metal particles within the ion-exchange matrix are different in size and have a globular shape. Their average size is on the order of hundreds of nanometers.

The X-ray (Fig. 2) is found peak that corresponds to a line (111) of copper oxide (I). The average crystallite size of metals in XRD calculated by the Selyakov equation. XRD gives the average size of 50-60 nm. Comparison of SEM and XRD data allow to conclude that the observed microscopic globules are agglomerates consisting of the basic structures of smaller radius on the order of tens nanometers. The capacitance values of NCs by metals and their particle size are shown in table 1.

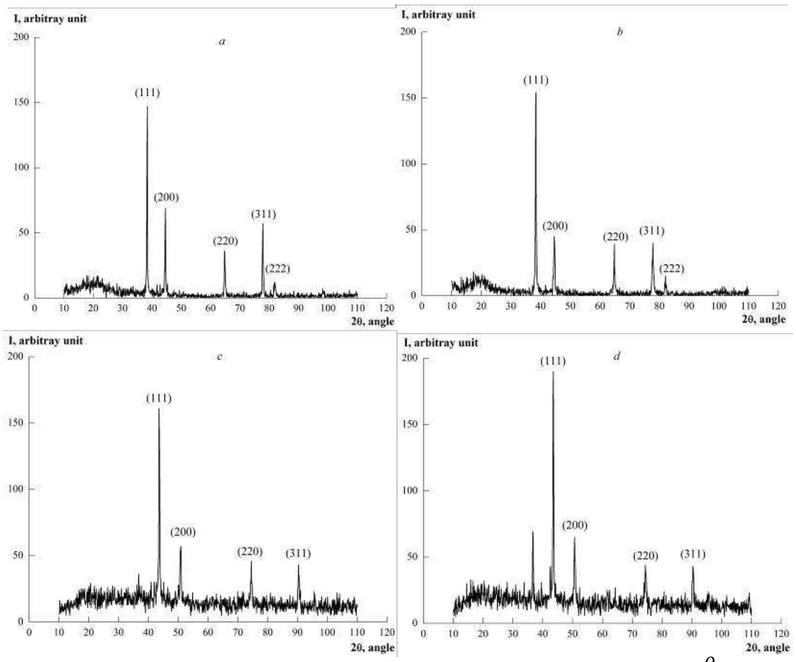

Figure 2. X-ray diffraction patterns for the metal-containing NCs: a) Ag^0·KU-23, reducing agent $N_2H_4 \cdot H_2O$; b) Ag^0·KU-23, reducing agent $NaBH_4$; c) Cu^0·KU-23, reducing agent $Na_2S_2O_4$; d) Cu^0·KU-23, reducing agent $NaBH_4$ (surface layer)

For the electrochemical studies of single grains nanocomposite was used a rotating disk electrode with original design. The measurements were made in temperature-controlled three-electrode cell with separate work and support section.

Table 1. The capacity of NCs by metals and their particle size.

Nanocomposites	The reducing agent for metal	The capacity by metals ε_{Me^0}, mmol-eqv/cm^3	The average particle size of metal *d*, nm	
			SEM	XRD
Ag^0·КУ-23	$N_2H_4 \cdot H_2O$	4.9±0.1	150±50	104
Ag^0·КУ-23	$NaBH_4$	5.2±0.2	300±100	63
Cu^0·КУ-23	$Na_2S_2O_4$	9.5±0.1	400±100	62
Cu^0·КУ-23	$NaBH_4$	9.0±0.2	400±150	55

The metal in the process of chemical deposition in the ion-exchange matrix is usually deposited in greater quantity on the surface of the granule. Its content is slightly reduced in depth. The radial distribution of the metal particles, obtained by the energy dispersive analysis (EDA), was shown in fig. 3.

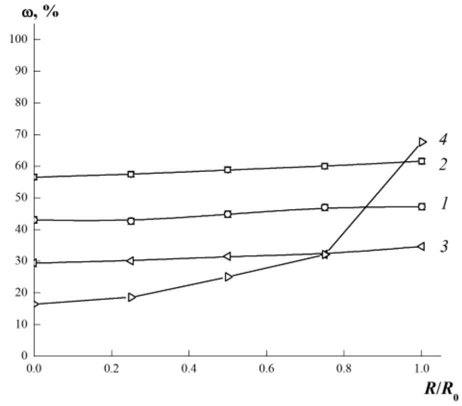

Figure 3. Metal distribution along the radial coordinate of the metal-containing grain NC with radius R_0: 1) Ag^0·KU-23, reducing agent $N_2H_4 \cdot H_2O$; 2) Ag^0·KU-23, reducing agent $NaBH_4$; 3) Cu^0·KU-23, reducing agent $Na_2S_2O_4$; 4) Cu^0·KU-23, reducing agent $NaBH_4$ (surface layer)

By the nanocomposites in H^+ and Na^+ ion form were obtained cyclic voltammetric and chronoamperometric curves of the electroreduction of oxygen dissolved in aqueous 0.1 M sulfuric acid and sodium sulfate. Because the limiting diffusion current of oxygen are strongly depends on the hydrodynamic conditions, the curves were recorded on a rotating disk electrode with a grain of nanocomposite at a constant speed ω = 600 rpm. Chronoamperometric curves clearly indicate the absence of significant phase changes in NC and allow to define the limiting diffusion current.

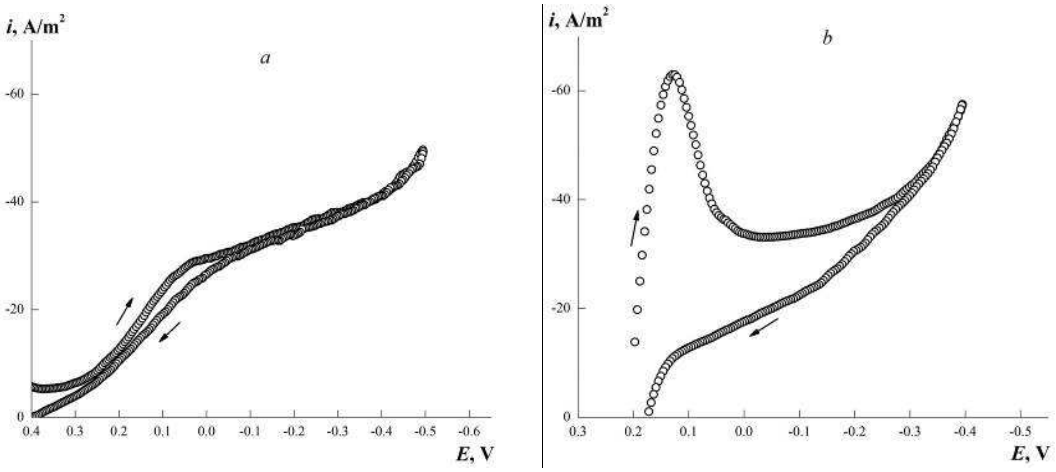

Figure 4. The cyclic potentiodynamic curves of molecular oxygen electroreduction on the grain of metal-containing NCs: a) Ag^0·KU-23, reducing agent $NaBH_4$; b) Cu^0·KU-23, reducing agent $NaBH_4$

In most cases, the limiting currents are in the range 30-40 A/m^2 (table 2). Higher values are obtained on silver NCs that is most chemically resistant to the active oxygen environment. For such electrodes nor the size of the metal particles nor ionic form of the matrix does not substantially influence the current limit.

Table 2. Dimensional maximum diffusion current density of the electroreduction of oxygen on metal NCs.

Reducing agent/ Ionic form	**Dimensional maximum diffusion current density i_{max} , A/m^2**			
	Ag^0·KU-23		**Cu^0·KU-23**	
	H^+	**Na^+**	**H^+**	**Na^+**
N_2H_4·H_2O	35.4	37.5	-	-
$Na_2S_2O_4$	-	-	31.2	19.3
$NaBH_4$	38.5	10.2	30.1	10.5

Current decrease caused by transition from the external diffusion of oxygen to mixed the external and internal kinetics in connection with macroporous structure of the matrix and chemical reactivity of metal nanoparticles component. Self-dissolution of the metal takes place with the formation of passivating layers of product or impurity components which reduce the intensity of oxygen electroreduction.

This work was supported by the RFBR (project № 11-08-00174_a).

References

1. Ion Exchange Technologies. Ed. by Ayben Kilislioglu. InTech. 2012. P. 366.
2. *Kravchenko T.A., Polyanskii L.N., Kalinichev A.I., and Konev D.V.* Metal–Ion–Exchanger Nanocomposites (Nauka, Moscow, 2009) [in Russian].

PLATINUM-BASED ELECTROCATALYSTS FOR LOW-TEMPERATURE FUEL CELLS: PROBLEMS OF ACTIVITY AND STABILITY

[1]Vladimir Guterman, [1]Sergey Belenov, [1]Tatiana Lastovina, [1]Andrey Paharev, [2]Natalia Sobgaida[2]

[1]Southern Federal University, Rostov-on-Don, Russia. *E-mail: gut57@mail.ru*
[2]Saratov State Technical University, Saratov, Russia

Introduction

Nanoparticles (NPs) of platinum or its alloys deposited on the surface of carbon microparticles, nanofibers or nanotubes are, by far, the most effective electrocatalysts for reactions occurring in low-temperature fuel cells (PEMFC, DMFC). Commercial production of low-temperature fuel cells (LTFC) is not possible without reducing the amount of precious platinum in catalyst layers of membrane electrode assembly and/or increased corrosion and morphological stability of catalysts in LTFC operation. The implementation of these tasks, in turn, requires innovative solutions in the field of optimization of the composition and multi-level microstructure of electrocatalysts (EC). The main areas for improvement of supported platinum ECs are: platinum alloying with some d-metals, optimizing the size and shape of nanocrystals, the formation of multi-component nanoparticles with M-core - Pt-shell architecture, strengthening the adhesion of nanoparticles to the surface of the support and increase its stability, improving the uniformity of size and spatial distribution of platinum NPs. The problem, however, is not only to find the best solution within each of the directions. The problem is to provide the entire set of optimal characteristics for the preparation of a catalyst.

Experiments

Pt/C and Pt-M/C catalysts were prepared by methods of sequential or simultaneous chemical reduction of the corresponding metal in the carbon suspension prepared on the basis of solutions of their salts and H2PtCl6. Water-organic two-component system or a mixture of organic solvents generally was used as the solvent. As the reducing agent NaBH4 (aqueous solution) at 20 - 40 oC was used. Characterization of the composition and structure of the catalysts was carried out by methods XRD, X-ray fluorescence analysis, TEM, thermal analysis (DSC and TG). Determination of the electrochemically active surface area (ECSA) and the study of the electrochemical performance of the materials were carried out on a stationary and rotating disk electrode by cyclic voltammetry.

Results and Discussion

The nature of the carbon support has little effect on the conditions of nucleation and growth of metal nanoparticles, which may be due mainly physical nature of their adhesion to the surface and in the pores of the carrier. The most important factor to optimize the morphology of Pt/C and Pt-M/C catalyst is a variation of a nature and composition of the two-component solvent. The composition of the solvent may influence considerably on average size formed nanoparticles (crystallites), their spatial dispersion and size distribution, degree of NP agglomeration [1-6]. For example, for the synthesis of Pt/C in water-dimethylsulfoxide solution, an average platinum crystallite size (Dav) is directly proportional to the volume concentration of water in the mixed solvent [1]. Found that changing the size of nanocrystals, which occurs due to changes in solvent composition, may be accompanied by a change in their shape and as a result, the catalytic activity of Pt/C [3]. Reducing the size of the NPs is usually accompanied by increased agglomeration processes. As a result, catalyst ECSA not always correlate with the value of Dav [5].

Catalysts containing M@Pt/C (M = Cu, Ag) nanoparticles with core-shell structure were prepared by the method of successive chemical reduction of metals. [6] The need for direct confirmation of core-shell structure by TEM techniques required to form quite thick platinum shell, whereby no essential differences in the mass activity of the catalysts with similar composition based on “alloy” nanoparticles and core-shell structures. Nevertheless, M @ Pt / C catalysts were sufficiently resistant to hot acid solutions and were not subjected to substantial degradation in the course of repeated cycling in the potential range 0.05 - 1.2 V.

For some catalyst systems, including samples of commercial production, it was investigated their stability during repeated cycling. In fact, the variation of ECSA values during voltage cycling was studied. As result, catalysts that exhibit improved stability as compared with analogs with close composition were found.

It is known that the oxidation of the carbon surface adjacent to the nanoparticles under the action of high-active oxygen-containing species (radicals OOH*, H2O2, etc.) formed on the cathode, is one of the main causes of degradation of metal-carbon catalysts. Similar localization of the oxidation process takes place during heating Pt/C nanostructured materials in an oxygen containing atmosphere. In fact, the platinum nanoparticles are a heterogeneous catalyst whose boundary with carbon is a place of redox reaction. Although the kinetics and mechanism of the carbon support oxidation in the fuel cell (temperature of about 100 °C, the electrolyte) and high-temperature oxidation in the gas phase can vary significantly, we cannot exclude the possibility of the same type of influence of various factors on the corrosion resistance of the metal-carbon composite at low and high temperatures. We conducted a comparative study of the kinetics of high-temperature oxidation of metal-platinum electrocatalysts, which revealed the specific role of alloying component nature and composition of the platinum alloy in the process of degradation. It is shown that more or less uniform distribution of platinum nanoparticles on the surface and in the pores of carbon microparticles, the presence or absence of appreciable amount of weakly coupled to a carrier aggregates composed of a plurality of nanoparticles of Pt, have a regular effect on the kinetics of carbon thermal oxidation.

This work was supported by Russian Foundation for Basic Research, projects nos. 10-03-00474a and 11-08-00499a.

References

1. *V. E. Guterman, S. V. Belenov, O. V. Dymnikova, T. A. Lastovina, Ya. B. Konstantinova, and N. V. Prutsakova* Influence of Water-Organic Solvent Composition on Composition and Structure of Pt/C and Pt_XNi/C Electrocatalysts in Borohydride Synthesis // Inorganic Materials. 2009. V. 45. P. 498–505.
2. *I. N. Leont'ev, V. E. Guterman, E. B. Pahomova, A. B. Guterman, and A. S. Miheikin* Particle Size Effect in Nanoscale Pt_3Co/C Electrocatalysts for Low-Temperature Fuel Cells // Nanotechnologies in Russia. 2009. V. 4, Nos. 3–4. P. 170–175.
3. *I.N. Leontyev, S. V. Belenov, V. E. Guterman, etc.* Catalytic activity of carbon supported Pt/C nano-electrocatalysts. Why reducing the size of Pt nanoparticles is not always beneficial. // J. of Physical Chemistry C. 2011. V. 115. P. 5429–5434.
4. *V.E. Guterman, S.V. Belenov, T.A. Lastovina, E.P. Fokina, N.V. Prutsakova, Ya.B. Konstantinova* Microstructure and Electrochemically Active Surface Area of PtM/C Electrocatalysts // Russian J. of Electrochemistry, 2011, Vol. 47, No. 8, pp. 933–939.
5. *V.E. Guterman, A.Y. Pakharev, N.Y. Tabachkova* Microstructure and Size Effects in Pt/C and Pt3Ni/C Electrocatalysts Synthesised in Solutions Based on Binary Organic Solvents // Applied Catalysis A: General. 2013. V. 453. P. 113-120.
6. *Lastovina T.A., Guterman V.E., Manokhin S.S.* Influence Of Different Types of $(CuPt_{0,1})_2$@Pt/C Posttreatment on Their Composition, Microstructure and Electrochemical Active Surface Area // Int. Scientific J. for Alternative Energy and Ecology. 2011. i.9. P. 111 – 115.

ION TRANSPORT IN HYBRID MATERIALS BASED ON PERFLUORINATED SULFOCATION-EXCHANGE MEMBRANES CONTAINING SILICA AND ZIRCONIA WITH SYMMETRIC AND ASYMMETRIC DISTRIBUTION

[1]Yulia Karavanova, [1]Alexandr Mikheev, [1]Ekaterina Safronova, [2]Gerald Pourcelly, [1]Andrey Yaroslavtsev
[1]Kurnakov Institute of general and inorganic chemistry RAS, Moscow, Russia,
[2]Institut Européen des Membranes (CNRS, UM2, ENSCM), Monpellier, France
E-mail: safronova@igic.ras.ru

Introduction

The perfluorinated sulfo cation-exchange membranes such as Nafion (Du Pont, USA), Dow (Dow, USA) and MF-4SC (LTD Plastpolymer, Russia), which are widely used in the development of alternative energy sources and water treatment systems, are of keen interest [1]. To improve the properties of such membranes hybrid materials doped by nano-sized additives, for example, hydrated silica and zirconia [2], are developed. Change of hydrophobicity, proton donor and proton acceptor properties of oxides surface by chemical bonding of various groups is promising trend to obtain hybrid materials with given properties and to investigate the mechanism of ion transport process in these materials [1]. Bi-layer membranes with gradient dopant distribution through the thickness of the sample are very promising and innovation materials also. The main feature of them is ion transport asymmetry that is typical for the biological objects.

In this report the properties of hybrid materials based on MF-4SC membrane with symmetric and asymmetric distribution of hydrated SiO_2 and ZrO_2 including oxides with modified surface contained proton donor and proton acceptor groups and hydrophobic fragments are described.

Experiments

The hybrid materials were prepared by casting from a polymer solution containing a calculated amount of precursors for further synthesis of dopants with modified surface followed by precursor's hydrolysis as described in [3]. Bi-layer membranes were prepared by consecutive casting at first by a pure polymer solution and then by a polymer solution containing a calculated amount of precursors. All membranes were treated one after another by 5% solution of HCl and twice by bidistilled water at 80°C.

Hybrid membranes with symmetric silica and zirconia distribution

Influence of incorporation into MF-4SC membrane matrix of silica and zirconia particles with modified surface contained various groups (hydrophilic proton donor and proton acceptor groups, hydrophobic groups) that impart different properties was investigated. It was established the correlation between the nature of dopant particles and water uptake, sorption ability and ion transport of hybrid membranes. It was observed non-typical for ion-exchange membranes phenomenon in the case of MF-4SC membranes contained silica with proton acceptor groups on the surface. This modification results in a decrease in ion exchange capacity, water uptake and diffusion permeability of the membranes, whereas the ionic conductivity of the membranes with low content of modifying groups increases in comparison with the membrane that contains pure SiO_2. An explanation was given on the basis of the model of the semielasticity of membrane pores and channels [4].

Hybrid membranes with asymmetric silica and zirconia distribution

Asymmetry coefficient (X) of transport properties of obtained membranes was established via diffusion permeability coefficients determination in two directions: when ion diffuse from modified ($P_{mod.}$) and unmodified ($P_{unmod..}$) side as $X=(P_{unmod.}-P_{mod.})/P_{mod.}*100\%$. Increase in the thickness of modified surface is accompanied by the asymmetry reduction and maximal effect was obtained for the material with the thickness of modified layer is 20%.

Diffusion permeability coefficients and asymmetry coefficients of NaCl and HCl solutions through the membranes with gradient silica and zirconia distribution are presented in table (the thickness of modified layer is 20%). The diffusion rate is higher when the ions diffuse from the unmodified side of membrane. Asymmetry coefficients are varied from 5 to 65 % depending on the diffusion solution and dopant type and it`s concentration in modified layer. Asymmetry effect is more pronounced in HCl solution than in NaCl. Asymmetry coefficients are grown with the increase in the dopant concentration in the modified layer. Membranes with silica incorporated into modified layer results in higher asymmetry coefficients of hybrid membrane than that with zirconia. Thus maximal asymmetry effect is observed for membrane with 10 wt.% of SiO_2 and reaches 65% in the case of 0.1M HCl solurtion (table).

Table. Diffusion permeability coefficients (cm^2/s) and asymmetry coefficients (%) of hybrid membranes with gradient SiO_2 and ZrO_2 distribution through the thickness of the sample

Diffusing solution **Modified layer composition**	**0.1 M HCl / H_2O**		**X (HCl)**	**0.1 M NaCl / H_2O**		**X (NaCl)**
	$P_{unmod.}$	**$P_{mod.}$**		**$P_{unmod\ ..}$**	**P_{mod}**	
MF-4SC	$2.16 \cdot 10^{-7}$		-	$2.06 \cdot 10^{-7}$		-
MF-4SC+1.5 wt.% SiO_2	$2.46 \cdot 10^{-7}$	$2.21 \cdot 10^{-7}$	11	$2.80 \cdot 10^{-7}$	$2.67 \cdot 10^{-7}$	5
MF-4SC+3 wt.% SiO_2	$2.61 \cdot 10^{-7}$	$2.25 \cdot 10^{-7}$	16	$2.21 \cdot 10^{-7}$	$2.08 \cdot 10^{-7}$	6
MF-4SC+5 wt.% SiO_2	$2.66 \cdot 10^{-7}$	$2.30 \cdot 10^{-7}$	16	$2.85 \cdot 10^{-7}$	$2.75 \cdot 10^{-7}$	4
MF-4SC+7 wt.% SiO_2	$2.76 \cdot 10^{-7}$	$2.33 \cdot 10^{-7}$	18	$2.36 \cdot 10^{-7}$	$2.19 \cdot 10^{-7}$	8
MF-4SC+10 wt.% SiO_2	$4.26 \cdot 10^{-7}$	$2.58 \cdot 10^{-7}$	65	$2.71 \cdot 10^{-7}$	$2.32 \cdot 10^{-7}$	17
MF-4SC+2.5 wt.% ZrO_2	$1.70 \cdot 10^{-7}$	$1.46 \cdot 10^{-7}$	16	$1.45 \cdot 10^{-7}$	$1.37 \cdot 10^{-7}$	6
MF-4SC+5 wt.% ZrO_2	$1.55 \cdot 10^{-7}$	$1.28 \cdot 10^{-7}$	21	$1.51 \cdot 10^{-7}$	$1.41 \cdot 10^{-7}$	7
MF-4SC+7 wt.% ZrO_2	$3.84 \cdot 10^{-7}$	$3.22 \cdot 10^{-7}$	19	$1.44 \cdot 10^{-7}$	$1.29 \cdot 10^{-7}$	12
MF-4SC+10 wt.% ZrO_2	$4.65 \cdot 10^{-7}$	$3.37 \cdot 10^{-7}$	38	$2.49 \cdot 10^{-7}$	$2.19 \cdot 10^{-7}$	13

On the basis of literature and obtained data it can be proposed two main reasons of the ion transport asymmetry phenomenon in the investigated membranes. The first one is origin of the gradient of mobile ions concentration within the membrane due to the presence of dopant particles, and the second one is asymmetry of pores within the membrane. Therefore, asymmetry depends on the dopant concentration and their nature. Thus incorporation of oxides with various sorption-exchange properties of the surface into modified layer may has great influence on the transport asymmetry.

Acknowledgements

This work was financially supported by the Russian Foundation for Basic Research (project 11-08-93105).

References

1. *Yaroslavtsev A.B.* // Nanotechnologies in Russia. 2012. V. 7, № 9-10. P. 8-18.
2. *D. J. Jones and J. Roziere,* Inorganic/organic Composite Materials. Handbook of Fuel Cells – Fundamentals, Technology and Applications, John Wiley & Sons, Ltd., Chichester, UK, 2003, p. 2826.
3. *Safronova E.Yu., Yaroslavtsev A.B.* // Solid state ionics. 2013. In press.
4. *Novikova S.A., Safronova E.Yu., Lysova A.A., Yaroslavtsev A.B.* // Mend. Comm. 2010. V. 20. P. 156-157.

CFD AVL FIRE INVESTIGATION OF THE INFLUENCE OF THE MATERIALS´ PARAMETERS ON POLYMER ELECTROLYTE FUEL CELL PERFORMANCE

[1]Larisa Karpenko-Jereb, [1]Christof Sternig, [1]Andreas Theiler, [2]Clemens Fink, [2]Reinhard Tatschl
[1]Graz University of Technology, Graz, Austria, *E-mail: larisa.karpenko-jereb@tugraz.at*
[2]AVL List GmbH, Graz, Austria

Introduction

The goal of the investigation was to conduct the parameter study – an investigation of the influence of single physical and transport characteristics of the fuel cell components such as polymer electrolyte membrane (PEM), catalyst layer (CL) and gas diffusion layer (GDL) on PEMFC performance.

Experiments

The simulations of PEMFC behavior were carried out using the CFD code AVL FIRE. The fuel cell module of AVL FIRE was developed in 2009, it includes comprehensive 3D modeling coupled thermal, electric, fluidic and electrochemical phenomena [1-2]. In 2012 the new developed membrane transport model was implemented in the module, which additionally considers the dependences of water sorption isotherm and electro-osmotic coefficients of PEM on the temperature [3-4]. The thorough validation of the fuel cell models of AVL FIRE carried using the fuel cell geometry (Fig. 1a) demonstrated the good agreement between simulation and experiment. Some of the validation results are presented in Figure 2. To save the computing time the parameter study was performed on the single channel fuel cell (Fig. 1b). The calculations were conducted for 70°C, symmetric humidification RH=90% and gas pressure 1 atm.

In general 25 parameters were tested as listed below. It should be mentioned that the tested characteristics are required input parameters of the interface of AVL FIRE fuel cell module.

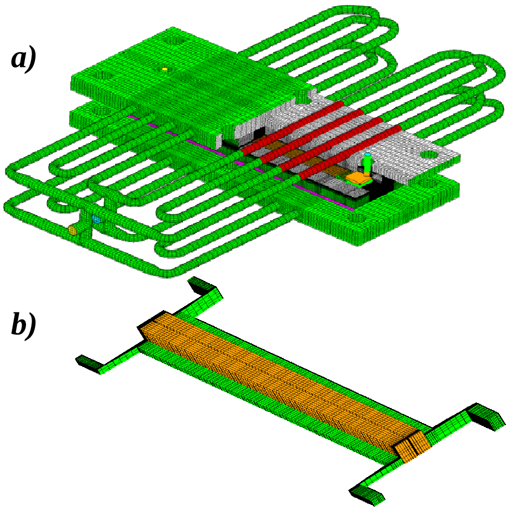

*Figure 1. Simulation geometries of PEMFC used to validate the developed PEM Model: **a)** Full Coupled Cell; **b)** Single Channel Cell*

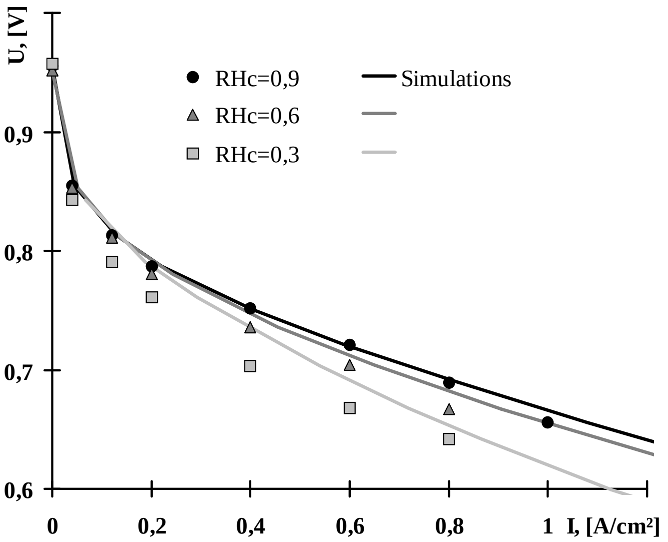

Figure 2. Polarization curve of the PEMFC, $\lambda a/\lambda c$=2,2/1,5; T=70°C; P=101,325kPa at different relative humidity in the cathode. Measurements were carried out using MEA Gore Primea 5620; GDL SGL-35BC Intelligent Energy

PEM parameters: thickness, acid group concentration, ionic conductivity, electro-osmotic coefficient, water diffusion coefficient, Henry coefficients as well as diffusion coefficients of H_2, O_2, N_2.

Cathode and anode CLs parameters: thickness, exchange current density, transfer coefficient.

GDL parameters: thickness, porosity, inplane permeability, throughplane permeability, tortuosity, contact angle, thermal conductivity and throughplane electrical conductivity.

Results and Discussion

The AVL FIRE calculations were performed at voltages from 0.420 to 0.855 V for three variations of each parameter: first one – for the reference value (***rv***), which corresponds to the realistic magnitude; second and third ones – for the reference value multiplied by 0.5 and 1.5 factors correspondently. In order to investigate the changes in PEMFC performance at the variation of each tested parameter we analyzed in detail polarization curves and dependencies of the power density, membrane over-potential, mean water concentration in PEM, total water flux in PEM as well as relative humidity at the interface PEM/CCL on the current density.

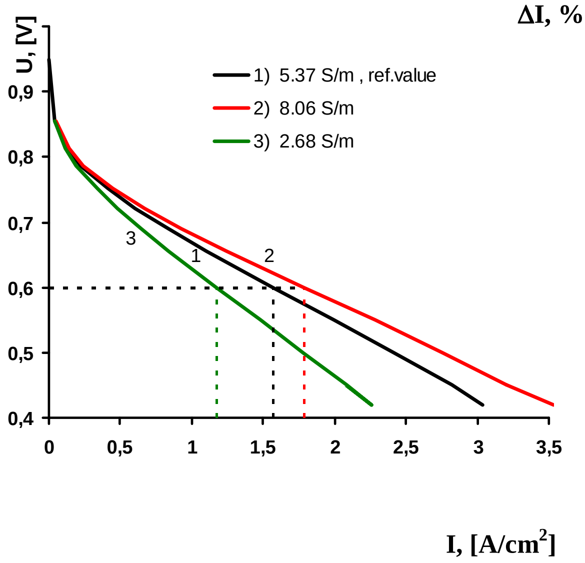

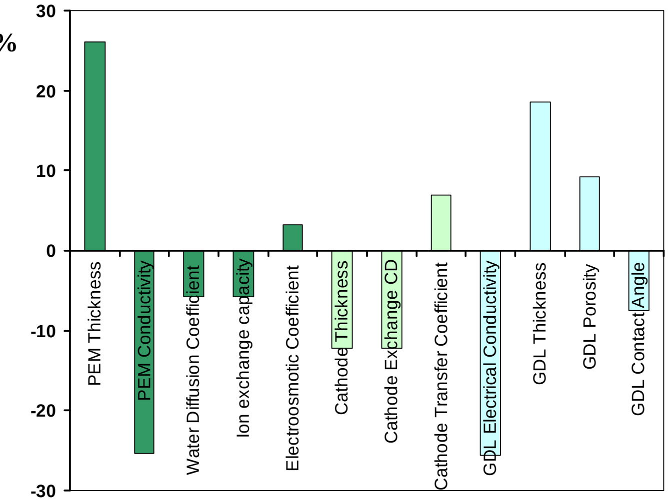

*Figure 3. Polarisations curves simulated for the various PEM conductivity, for: 1) reference value (**rv**); 2) **rv***1.5; 3) **rv***0.5*

*Figure 4. The relative changes in the current density of PEMFC at the decreasing of the tested material parameter in two times **(rv*0.5)***

Figure 3 demonstrates the polarization curves calculated for three different values of conductivity of the polymer electrolyte membrane. The increasing of the membrane conductivity causes the changes in the polarisation curve slope and growth of the current density of the fuel cell.

In order to summarize and compare the numerous obtained data we calculate the relative changes of the current density at 0.6 V for investigated variations of the parameters. For example at the decreasing of the tested parameter, the relative change of the current density ΔI is calculated by the expression:

$$\Delta I = \frac{I_{rv*0.5} - I_{rv}}{I_{rv}} \cdot 100\% \qquad (1),$$

where I_{rv} - the current density (CD) calculated from the reference value of the tested parameter, $I_{rv*0.5}$ - CD from the reference value multiplied by factor 0.5.

Figure 4 presents the selected results of the relative changes in CD at the decrease of the reference parameterby the factor 0.5. The declines in the membrane thickness, electro-osmotic coefficient in PEM, transfer coefficient in cathode CL as well as GDL thickness and porosity lead to increasing CD of the fuel cell. Decreasing the PEM conductivity, water diffusion coefficient, ion-exchange capacity, cathode thickness and exchange current density as well as GDL contact angle are causing CD´s drop.

The variations of the characteristics of the anode catalyst layer showed practically no changes in the fuel cell performance.

The changes of the water diffusion and electro-osmotic coefficients in PEM lead to insignificant alterations of the voltage-current characteristics of the fuel cell, but influence the total water flux.

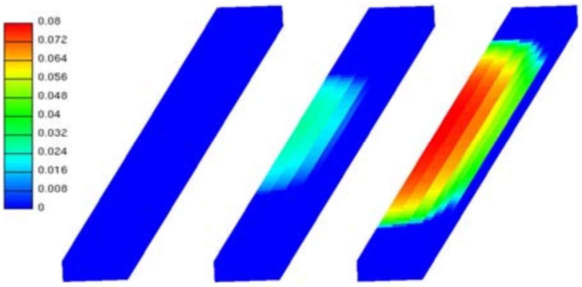

a) b) c)

Figure 5. Liquid water volume fraction (-) in anode GDL at interface to bipolar plate/ channel for different water diffusion coefficients [m^2/s] in PEM: a) 1.34E-11; b) 2.68E-11 (rv); c) 4.02E-11

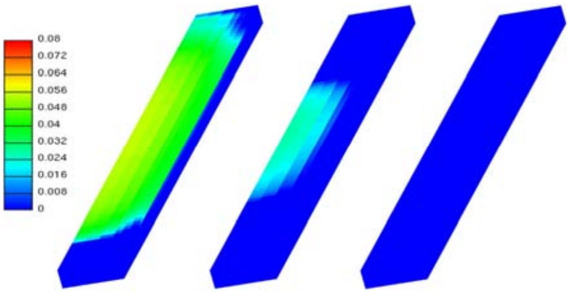

a) b) c)

Figure 6. Liquid water volume fraction (-) in anode GDL at interface to bipolar plate/channel for different drag coefficients in PEM: a) 0.054; b) 0.108 (rv), c) 0.160

The analysis of the distribution of the liquid water in GDL showed that the growth of the water diffusion coefficient in PEM leads to increasing the back water diffusion from the cathode to the anode side (Fig.5). Figure 6 demonstrates the decreasing in the concentration of the condensed water when the electro-osmotic coefficient in the polymer electrolyte membrane increases.

Acknowledgement. The work has been financially supported by the Austrian Promotion Foundation (FFG) and AVL List GmbH, **Project A3 FALCON**, Advanced 3D Fuel Cell Analysis and Condition Diagnostics. Project No. 835811.

References

1. Manual AVL FIRE version 2010. Edition 11/2010. AVL List GmbH, 2010. 91 pp.
2. *Fink C., Fouquet N.* Three-dimentional simulation of polymer electrolyte membrane fuel cells with experimental validation // Electrochimica Acta. 2011. V. 56 (28). P.10820-10831.
3. *Karpenko-Jereb L., Innerwinkler P., Kelterer A.-M., Fink C., Prenninger P., Tatschl R.* Parametric study of membrane transport model for PEMFC // 9th Symposium on Fuel Cell and Battery Modeling and Experimental Validation, Switzerland, April 2-4, 2012. P. 101-102.
4. *Karpenko-Jereb L., Innerwinkler P., Kelterer A.-M., Fink C., Prenninger P., Tatschl R.* Development of The Membrane Transport Model For PEMFC Simulations // Procedia Engineering. 2012. V. 44. P. 388 – 390.

PREDICTING EFFECTIVE TRANSPORT PROPERTIES OF MICROPOROUS MEMBRANES USING STOCHASTICALLY RECONSTRUCTED 3D IMAGES

[1]Marina Karsanina, [2,1]Kirill Gerke, [3]Roman Vasilyev, [3]Dmitry Korost
[1]Institute of Geospheres Dynamics of Russian Academy of Sciences, Moscow, Russia,
E-mail: mary_o_kors@list.ru
[2]CSIRO Land and Water, Urrbrae, South Australia
[3]Lomonosov Moscow State University, Moscow, Russia

Introduction

One of the main factors defining main physical properties and numerous flow phenomena in porous media, including fluid and solute movements, is pore structure, e.g., pore sizes and their connectivity [1]. Filtration characteristics can be predicted using different numerical methods if detailed 3D structure and surface properties are known. X-ray microtomography can be used for rapid assessment of structural information, however, this method has significant resolution limitations. FIB-SEM and BIB-SEM techniques can be useful for micro and meso-structure characterization [2], but are extremely expensive and time-consuming. High-resolution 2D SEM images are usually readily available and can be used for 3D structure reconstruction using different methods: 1) statistical methods (correlation functions and simulated annealing [3,4], multi-point statistics [5,6], entropy methods [7]), 2) sequential methods (sphere or other granular packs) [8] and 3) morphological methods [9]. Stochastic reconstructions using correlation functions possess some important advantage - they provide a statistical description of the structure, which is known to have relationships with all physical properties. In addition, this method is more flexible for other applications to characterize porous media. The main aim of this work was to predict filtration properties of microporous membranes (ceramic filters) based on 3D structural information obtained by stochastic reconstructions using 2D images.

Materials and methods

Three ceramic samples were scanned using SkyScan 1772 microtomography scanner with a resolution of 2.5 μm, which was enough to capture all major pore sizes to exclude any under-resolution porosity effects, which was verified using high-accuracy SEM imaging. Subcroppings from the obtained 3D images are shown on Fig.1. From each of these one representative 2D image with porosity closest to the mean value for the whole cube was chosen for stochastic reconstructions. For each 2D cut numerous 3D realizations were obtained using different configurations of correlation functions and simulated annealing (modified Yeong-Torquato algorithm). Original and resulting 3D images were used for detailed analysis of filtration properties (permeability) and morphology (pore-size distributions, connection numbers, local porosity and percolation distributions, etc.). Pore-size statistics and connectivity numbers were obtained by pore-network extraction using maximal inscribed ball algorithm. Extracted pore-network model and finite-difference Stoke's equation solver were used to calculate effective permeabilities, relative permeabilities for two-phase flow and dimensionless electrical conductivity. Overall scheme of the current study is presented on Fig.2. The quality of reconstructions was evaluated using all aforementioned quantities.

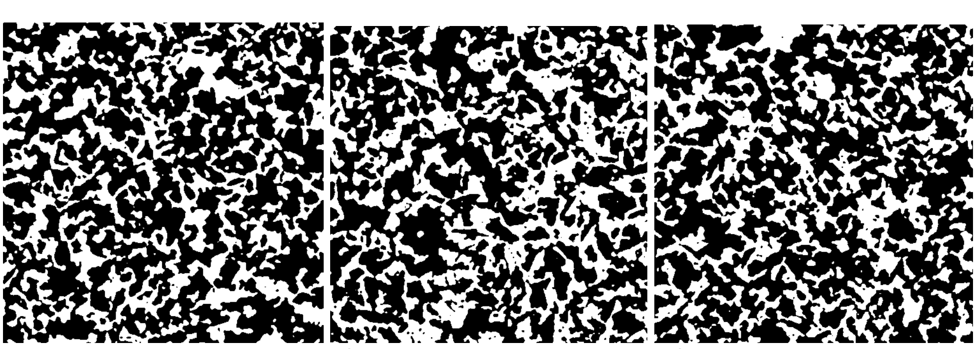

Figure 1. 2D images of ceramics structure used for reconstruction

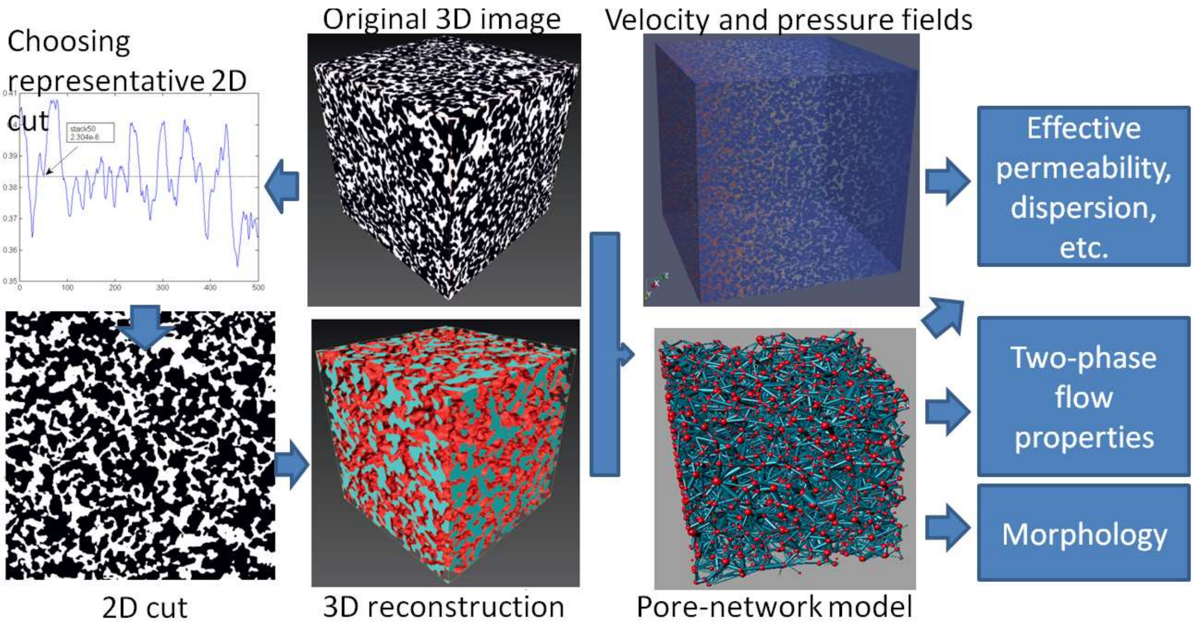

Figure 2. Study flowchart

Results and Discussion

Our results suggest that morphology and structure depend significantly on the amount of statistical information used for reconstruction. However, for relatively simple pore structures representing most artificial membranes and filters, accurate 3D reconstructions (Fig.3) and predictions of transport properties can be obtained using stochastic methods.

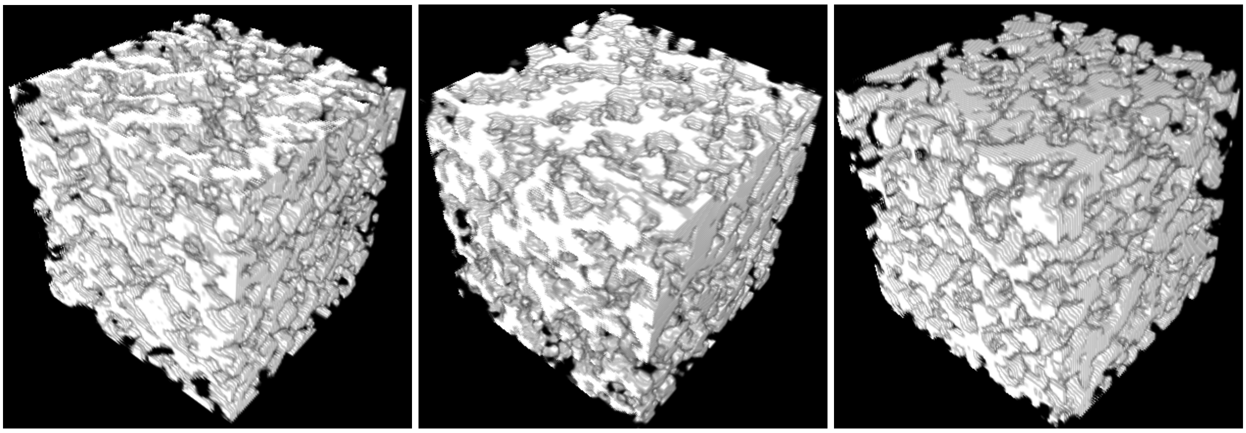

Figure 3. Resulting 3D reconstructions

References

1. *Torquato S*. Random Heterogeneous Materials: Microstructure and Macroscopic Properties (Springer-Verlag, New York, 2002).
2. *Joos J., Carraro Th., Weber A., Ivers-Tiffee E.* // Journal of Power Sources, 2011, 196: 7302-7307.
3. *Yeong C.L.Y., Torquato S.* // Phys. Rev. E. 1998a. 57: 495-506.
4. *Yeong C.L.Y., Torquato S.* // Phys. Rev. E, 1998b, 58: 224-233.
5. *Okabe H., Blunt M.J.* // Water Resour. Res., 2007, 43:0043-1397.
6. *Tahmasebi P., Hezarkhani A., Sahimi M.* // Computational Geosciences, 2012, 16: 779-797.
7. *Piasecki R.* // Proc. R. Soc. A. 2011. 467: 806 – 820.
8. *Øren P.E., Bakke S.* // Transport in Porous Media., 2002, 46, 311-314.
9. *Biswal B., Øren P.-E., Held R.J., Bakke S., Hilfer R.* // Phys. Rev. E. 2009. 80: 041301.

INVESTIGATION OF PORE SIZE DISTRIBUTION FOR ULTRAFILTRATION MEMBRANE: ATOMIC-FORCE MICROSCOPY AND STATISTICAL TREATMENT

Daria Khanukaeva, Anatoly Filippov

Gubkin Russian State University of Oil and Gas, Moscow, Russia, *E-mail: khanuk@yandex.ru*

Introduction

Such an important characteristic of membranes as the pore size distribution (PSD) was investigated for the ultrafiltration (UF) membrane PA-100, registered trademark “Mifil” (Institute of Physico-Organic Chemistry, National Academy of Sciences, Belarus). The samples of the membrane were scanned by atomic force microscope (AFM) SmartSPM-1000 of AIST-NT company, the images were processed using the Gwyddion software. The statistical treatment of the data was fulfilled; several smoothing curves and their parameters were obtained and estimated using two fitting criteria. The lognormal curve was proved to be the best one for small samples of the membrane under investigation. The comparison of this distribution law with PSD obtained by the method of hydrodynamic liquid squeezing [1, 2] showed good agreement.

Experiments

The semi-contact mode of scanning was used for the AFM investigation of the UF membrane PA-100. Two series of images were selected for further statistical treatment. One of the images obtained is shown in Figure 1.

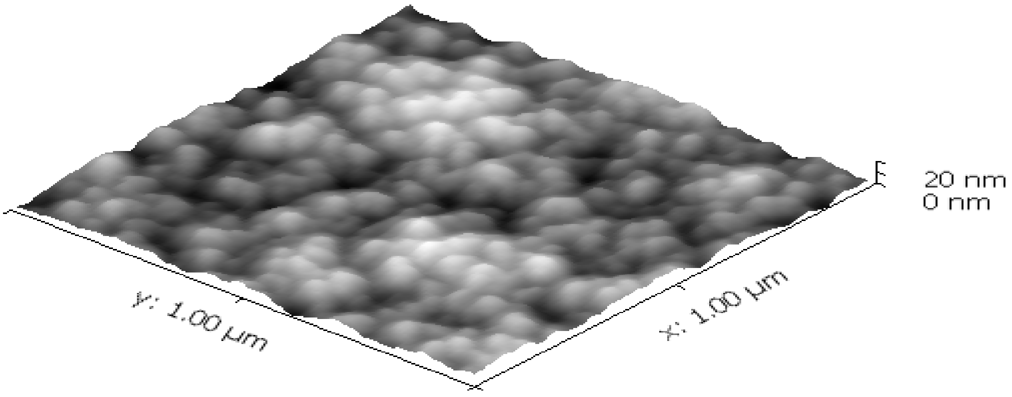

Figure 1. AFM image of UF membrane PA-100

The 2D images were processed using Gwyddion software in the following way. The darkest regions of the image, i.e. regions lower than some threshold, were interpreted as pores and selected for further analysis. The choice of the threshold value was defined by the corresponding range of pores sizes for the investigated membranes, which is about 3÷60 nm. The pore size was treated as the radius of the circle with the area equal to the area of the pore projection.

Mathematical treatment

In contrast to many papers dealing with PSD, in the present work no assumption of the distribution law is made. The method of Pearson curves [3] is applied to the interpretation of statistical data obtained.

The idea of the method consists in the search of the distribution law $y(x)$ as the solution of the differential equation

$$\frac{dy}{y} = -\frac{x + b_1}{b_2 x^2 + b_1 x + b_0} dx, \tag{1}$$

where the origin of variable x is the mean value of the variate and coefficients b_0, b_1, b_2 are calculated using central moments of the considered sampling.

Depending on coefficients in equation (1) its solution gives curves of several types. It is worth mentioning that Gaussian distribution can be obtained as one of the limit cases. In order to check the most wide spread hypothesis of lognormal PSD law, we applied the method of Pearson curves to the logarithms of pores sizes. As a result we obtained the values of parameters corresponding to the limit case of normal law with high accuracy. After that we applied the technique of least squares for the calculation of normal distribution parameters for logarithms of pores sizes. The curves of both distributions are shown in Figure 2 along with the group experimental data. As one can see the curves are very close to each other and the experimental data. The assumption-free of distribution law Pearson curve almost coincides with Gaussian curve for logarithms of pores radii. This fact is the first mathematical confirmation of lognormal nature of PSD for the UF membrane.

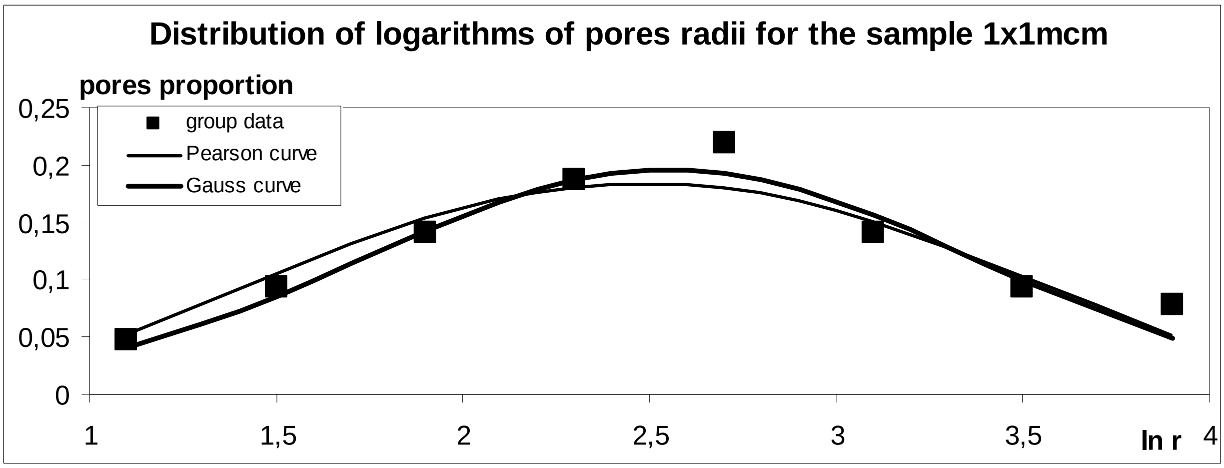

Figure 2. Pearson and Gauss curves fitting group experimental data

As an alternative hypothesis of the PSD law we used Rayleigh law in its original form with one parameter a_{1R}: $f(r) = \frac{r}{a_{1R}^2} e^{-\frac{r^2}{2a_{1R}^2}}, \quad (r > 0)$ and in modified form $f(r) = \frac{r - b_{2R}}{(a_{2R} - b_{2R})^2} e^{-\frac{(r - b_{2R})^2}{2(a_{2R} - b_{2R})^2}}, \quad (r > b_{2R})$, where a_{2R} is the parameter and b_{2R} = 2 nm [4]. Figure 3 demonstrates both these curves along with Pearson and lognormal curves plotted as the functions of pores radii. Original experimental data are also presented in Figure 3.

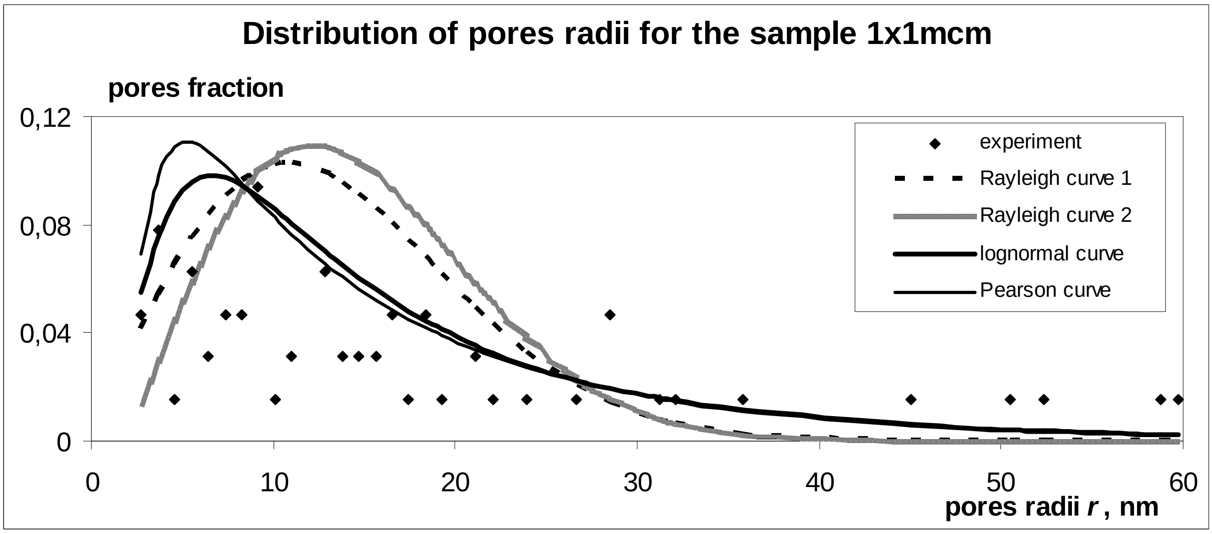

Figure 3. Rayleigh, Pearson and lognormal curves for the original experimental data

Only qualitatively, basing on various pictures, it is sometimes rather difficult to decide, what curve fits experimental data better. Therefore quantitative analysis of the obtained fitting laws is required. Pearson and Kolmogorov fitting criteria were applied to all the obtained laws for all the investigated samples. The significance level was chosen to be 0.1. The data will confirm the hypothesis of the distribution law with the reliability no less than 0.9, if $\chi^2 < \chi^2_{cr}$ and $\lambda < \lambda_{cr}$ for Pearson and Kolmogorov criterion correspondingly. Table 1 presents the statistics of both criteria and the corresponding critical values for one of the investigated samples. It is easy to see, that the values of χ^2 much exceed the critical level for both Rayleigh curves, which must be rejected in favor of Pearson and lognormal curves. Being a lighter one, Kolmogorov criterion allows accepting Rayleigh law with one parameter on the chosen significance level. But for Pearson and lognormal curves it gives smaller values of the statistics λ. This means that inequality $\lambda < \lambda_{cr}$ is held with higher reliability in this case. The choice between Pearson and lognormal curves is not obvious for different samples. But keeping in mind that these curves are very close to each other for all samples, we may take that one, which is more convenient for applications. This is lognormal law.

Table 1. Results of fitting criteria application

Criterion / **Distribution**	**Pearson** χ^2		**Kolmogorov** λ, $\lambda_{cr} = 1.2$
	χ^2	χ^2_{cr}	
Pearson curve	1.7	2.7	0.2
lognormal	1.5	7.8	0.2
Rayleigh law with one parameter	147	6.2	0.7
Rayleigh law with two parameters	182	4.6	1.3

Results and Discussion

The method of Pearson curves was applied to all the investigated samples of the UF membrane PA-100. It demonstrated that the distribution curve remains the same for different parts of the membrane. For all samples the curve obtained was a limit case of Pearson curves corresponding to lognormal law. Quantitative analysis also showed the lognormal curve to be the best fitting curve among considered. And this is the second mathematical confirmation of its validity.

The obtained lognormal curve was plotted on the same graph with the PSD of the investigated membrane, obtained by the method of hydrodynamic liquid squeezing [1, 2]. The curves showed very good agreement.

Thus, the combination of AFM and thorough statistical treatment presents a mathematical proof of the lognormal law of PSD for the investigated small samples of the UF membrane. The method used is verified by a good agreement of the curve obtained with the analogous data from another method. So, the suggested technique gives good results for PSD study of the UF membranes and, perhaps, can be applied to investigation of other types of membranes.

This work was supported by the RFBR (projects nos. 11-08-01043, 12-08-90010).

References

1. *Svyatchenko V.V.,Bildukevich A.V.* // J. Applied Chem. 1991.N1. P.101-106.
2. *Filippov A.N., Kononenko N. A., Vasin S. I., Kasperchik V. P., Jaskevich A. L., Chernyaeva M. A.* // Colloid J. 2010. V.72. N 6. P.839-850.
3. *Cramer H.* Mathematical methods of statistics, Uppsala, Princeton University Press, 1945.
4. *Mourhatch R., Tsotsis T. T., Sahimi M.* // J. Membr. Sci. 2011. V.367. P.55-62.

AMINO ACID INFLUENCE ON CURRENT-VOLTAGE CHARACTERISTICS OF ANION-EXCHANGE MEMBRANE MA-41 IN ELECTRODIALYSIS OF MINERAL SALT SOLUTIONS

Anastasiya Kharina, Bui Thi Phuong Hai, Victoria Kabanova, Tatyana Eliseeva
Voronezh State University, Voronezh, Russia, *E-mail:aukharina@gmail.com*

Introduction

Amino acids can be produced by microbiological and chemical synthesis as well as by hydrolysis of proteins. Requirements for target product demineralization become important after microbiological synthesis of amino acids. In order to solve this problem at the final stage of production it is often advisable to use electrodialysis (ED) as an efficient and ecologically clean technology [1]. Application of this technology supposes the necessity to investigate electrochemical behavior of membranes in the model solutions. Current-voltage characteristics (CVC) of anion-exchange membranes being more susceptible to fouling in ED of solutions containing mineral salts and amino acids are studied in this work.

Experiments

Experiments are carried out in a seven-compartment ED stack with alternating cation- and anion-exchange membranes MK-40 and MA-41 accordingly (“Shchekinoazot”, Russia). ED stack has AgCl electrodes placed on both sides of the studied anion-exchange membrane to obtain its CVC.

Phenylalanine (Phe), tyrosine (Tyr), α-alanine (α-Ala) in the solution of sodium sulphate or sodium chloride are used throughout this study for comparison with individual mineral salt solutions. The main characteristics of amino acids are shown in Table 1.

Table 1. Characteristics of tested amino acids

Amino acids	Structural formula	Molecular mass	pI	pK		
				$pK_{1,}$	pK_2	pK_R
Phe	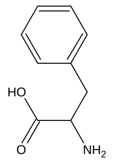	165.19	5.91	2.58	9.24	-
Tyr	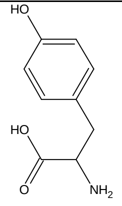	181.19	5.63	2.20	10.07	9.40
α-Ala	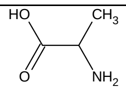	89.10	6.01	2.34	9.69	-

Results and Discussion

The shape of the obtained CVC (Fig.1) is close to that described in numerous publications and that can be called classical. At low currents, there is a linear region (region 1) that seems as a vertical straight line in coordinates i - U. This region is followed by an inclined plateau (region 2) replaced then by a region (3) where the slope is much higher than that of plateau [2].

It appears that the existence of an amino acid in the solution does not affect significantly the value of limiting current density because the solution pH is close to the isoelectric point. This renders most of the amino acid ions are in the bipolar form so they do not take part in transferring the current through the membrane. This situation, however, changes after exceeding the limiting current density. Water splitting at the membrane–solution interface changes the pH in the solution boundary layer as well as in the membrane phase. In the membrane phase bipolar ions can be recharged into anions that are able to migrate through the membrane [3]. It leads to higher values of current density at the same voltage in the system including amino acid in comparison with a single salt solution.

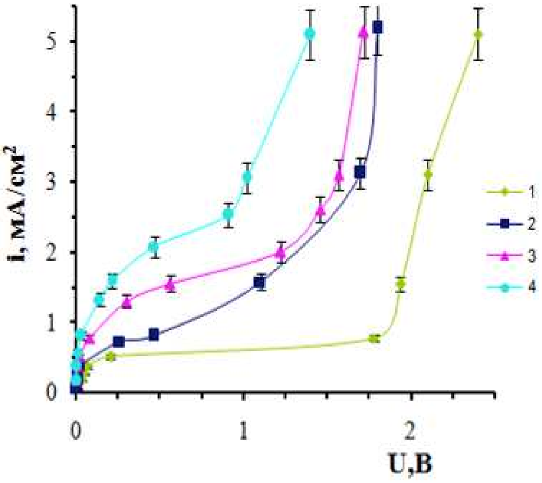

Figure 1. Current-voltage curves of MA-41 membrane measured for different solutions: NaCl 0.01M - 1, Phe 0.02M+NaCl 0.01M - 2, Phe 0.05M+NaCl 0.01M - 3, Phe 0.1M + NaCl 0.01M - 4

Thus, it is found that the presence of alkyl amino acids in the used concentration range in NaCl solution does not affect the i_{lim} in the CVC of anion-exchange membranes. In addition, similar results are obtained in the mixed solution amino acid - sodium sulphate.

Difference in shape of CVC for heterogeneous membranes using in ED of NaCl (Na_2SO_4) solution and mixed solutions of NaCl (Na_2SO_4) with the test amino acids is detected at the current densities above the limit.

At the overlimiting conditions of electrodialysis the reduction of the “plateau” length is found in the mixed solutions. It deals with the two reasons. On the one hand, the presence of amino acid in solution can increase the generation rate of OH^- и H_30^+ ions during water splitting process. Besides the intensity of water splitting will increase in proportion to the concentration of amino acids in solution. On the other hand, the possible adsorption of amino acids on the membrane alters the structure of the surface and contributes to its hydrophobicity. It leads to an increase of electroconvection contribution into mass transfer when the current density is higher than the limiting one.

References

1. *Bukhovets A., Eliseeva T., Dalthrope N., Oren Y.* // Electrochimica Acta. 2011. V.56. P. 10283– 10287.
2. *Belova E.I., Lopatkova G. Yu., Pismenskaya N. D. et. al.* // J. Phys. Chem. 2006. V. 110. P. 13458-13469**.**
3. *Bukhovets A., Eliseeva T., Oren Y.* // J. Membr. Sci. 2010. – V.364. P. 339-343.

PHYSICO-CHEMICAL EVOLUTION OF METAL NANOPARTICLES IN ION-EXCHANGING MATRIX IN OPEN SYSTEM

Svetlana Khorolskaya, Lev Polyanskiy, Tamara Kravchenko
Voronezh State University, Voronezh, Russia, *E-mail: krav@chem.vsu.ru*

Introduction

Composite polymers, in which metal nanoparticles (or their compounds) are introduced into the porous matrix with fixed ion-exchanging centers, can increase the effectivity of wide variety of chemical processes [1, 2] due to the high reactivity of the particles with excess energy at the expense of their size decreased till the nanolevel. It is noted [3] that, starting from the certain critical metal content, its state ceases to be a set of isolated particles. Metal forms an ensemble of clusters, in which the charge transfer is possible with the optimal distance between the particles. This factor must be taken into account, because it leads to the dramatic change of rates of stages, including the charge transfer and ion transport. Consequently, it is very important to find relation between the metal particle content in the ion-exchanging matrix and kinetic mechanism of the chemical reaction with their participation. This information will allow to make a correct choice about the metal capacity in the composite.

The purpose of this paper consists in the study of the rate and interaction mechanism of the molecular oxygen dissolved in water with copper–ion exchanger nanocomposites depending on the capacity of incorporated metal in it.

Experiments

As a result of chemical deposition of copper into the sulfonic type cation exchanger KU-23, the set of nanocomposites (NC) with copper amount within the range 1 – 10 meq/cm^3 per bulk material weight is obtained. According to X-ray experiment crystallite size varies from 30 to 50 nm, that is the evidence of the nanostructured dopant nature, which particles are joint into agglomerates up to 500 nm. Higher content of the metal incorporated into the support results in the increase of copper particles tightness in the matrix pores, while the particle size remains almost the same.

Results and Discussion

Regarding reduction reaction of molecular oxygen dissolved in water, which presents steadily in the open systems as an active corroding agent, the following steps occur in the NC grain: internal diffusion of oxygen in the nanocomposite pores, oxygen adsorption on the copper centers, redox reaction of oxygen with copper particles. Oxidation of copper-containing NC in H$^+$- ion form with one metal loading, when its particles and matrix hydrogen counter-ions are in the equivalent ratio, proceeds with formation of soluble products of copper oxidation:

$$[\text{R-SO}_3^- \text{H}^+]_2 \cdot \text{Cu}^0 + {}^1\!/_2\,\text{O}_2 = (\text{R-SO}_3^-)_2\text{Cu}^{2+} + \text{H}_2\text{O} \tag{1}$$

The process takes place by electrochemical mechanism and consists of two partial charge-transfer reactions – anodic oxidation of copper and cathodic recovery of oxygen molecules:

$$\text{Cu}^0 \rightarrow \text{Cu}^{2+} + 2\text{e}^- \tag{2}$$

$${}^1\!/_2\,\text{O}_2 + 2\text{H}^+ + 2\text{e}^- \rightarrow \text{H}_2\text{O} \tag{3}$$

In whole, the process is limited by cathodic half-reaction of oxygen reduction, occurring in a pore-diffusion regime in subsurface granule layer at the initial oxidation period.

In the case of two loadings and more, at the time when protons disappear in the grain and ionogenic sites are occupied by copper counter-ions, in oxidation product composition copper oxides become to prevail:

$$\left[(\text{R-SO}_3^-)_2\text{Cu}^{2+}\right]_2 \cdot \text{Cu}^0 + {}^1\!/_2\,\text{O}_2 = \left[(\text{R-SO}_3^-)_2\text{Cu}^{2+}\right]_2 \cdot \text{CuO} \tag{4}$$

$$2\text{Cu}^0 + 2\text{OH}^- \rightarrow \text{Cu}_2\text{O} + \text{H}_2\text{O} + 2\text{e}^- \tag{5}$$

$$\text{Cu}_2\text{O} + 2\text{OH}^- \rightarrow 2\text{CuO} + \text{H}_2\text{O} + 2\text{e}^- \tag{6}$$

The source of OH^- ions involved in the partial oxidation reactions (5) and (6) is oxygen reduction reaction, proceeding in the neutral solution in pores of ion-exchanging matrix:

$$\frac{1}{2}O_2 + H_2O + 2e^- \rightarrow 2OH^- \qquad (7)$$

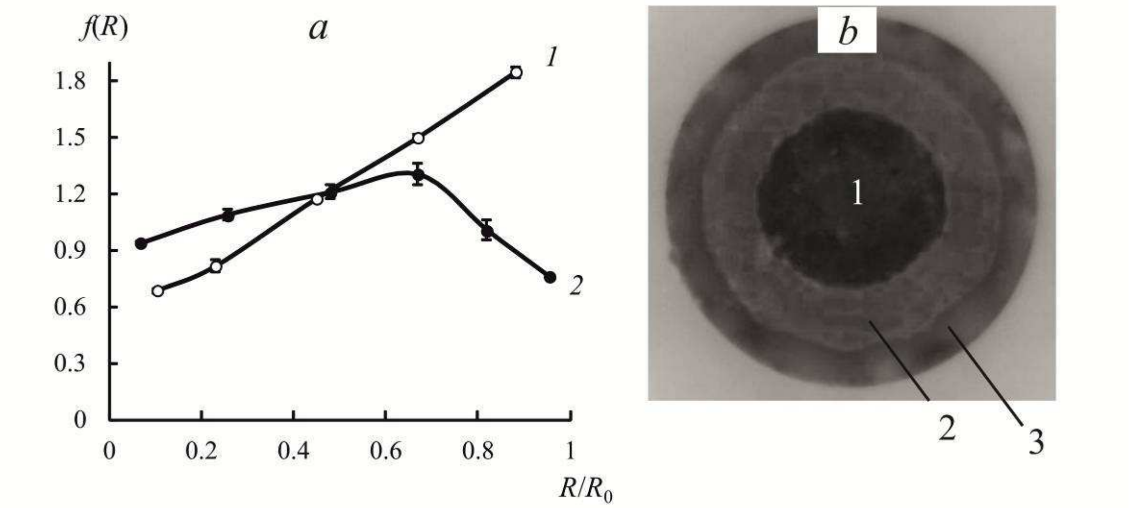

Figure 1. (a) Relative content f(R) of copper on the radial coordinate R of NC grain with radius R_0 according to the data from elemental microanalysis before oxidation process start (1) and after completion (2). (b) NC grain slice after oxidation. The layers of copper oxidation products: 1 – Cu^0, 2 – Cu_2O, 3 – Cu^{2+}. Capacity by copper ε_{Me^0} = 1.99 meq/cm^3

It can be seen from Figure 1, how the self-organization of metal nanoparticles takes place in the polymeric matrix. After oxidation of copper nanoparticles their partial dissolution from external layers of granule is occurred. Outside copper particles are ionized at the start of oxidation process, and copper ions, formed in result of reaction (1) and (2), spread over matrix volume and occupy ion-exchanging sites. It leads to lower content of metallic copper at the peripheral grain layer.

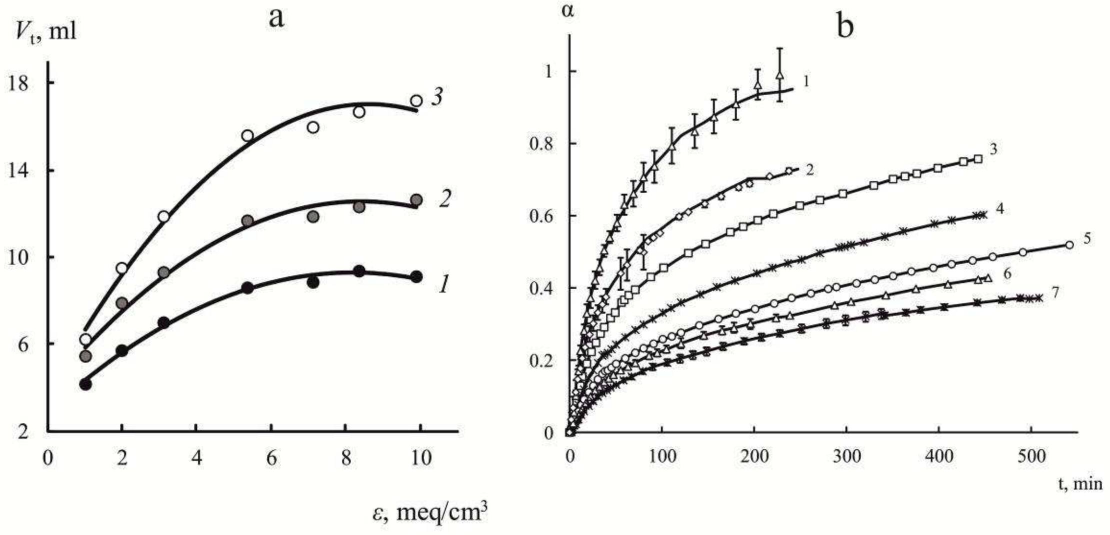

Figure 2. (a) Quantity V of sorbed oxygen depending on the capacity of NC by metal to the process time 60 (1), 120 (2), 240 (3) min. (b) Completeness degree α of the oxygen reduction by NC with different copper capacity ε_{Cu^0}, meq/cm^3: 1 – 1.02; 2 – 1.99; 3 – 3.11; 4 – 5.38; 5 – 7.11; 6 – 8.38; 7 – 9.89

The experimental kinetic curves of oxygen reduction have shown (Figure 2b), that the dependence of the oxygen reduction rate on the metal component content in NCs has characteristic form. As content of metal particles increases, quantity of oxygen sorbed grows, rate and completeness degree of the process decrease respectively.

The process is the most intensive, when interaction takes place between metal nanoparticles and chemically active matrix, which is a source of hydrogen ions involved in the reaction. In this case practically complete oxidation of separate nanoparticles proceeds, accompanied by their ionization to copper (II). Further, as the content of metal particles raises, barely the part of them dissolves completely, while that part of particles increases, whose core is being covered with an oxide layer. At the same time with increasing particle concentration, the distance therebetween decreases, so that electron transfer between them is made easier. The assemblage of particles begins to be electronically associated collective of particles, which can transfer the charge by a tunneling mechanism. At a critical metal content (from 6.2 meq/cm^3 of copper content) at the percolation threshold current transport in the composite is similar to a massive metal.

It is significant for high-capacity nanocomposites that the oxidation rate is higher in pre-percolation area than after the percolation threshold. As copper content in the matrix volume increases and the distance between the oxidized and unoxidized particles decreases, before the percolation threshold in the system Cu_2O – O_2 more complex donor-acceptor cooperative interactions are possible. It is known [4], that the copper oxide (I) is semiconductor with p-type conductivity, which in the presence of oxygen can increase its conductivity, that promotes the formation of an additional conductive volume. This means that repeated metal doping adds some conductivity and cooperativity to the isolated islands of metal clusters, however, it promotes active passing of the oxidation process to a certain limit. After the percolation threshold, higher density of the metal particles only restricts diffusion path of oxygen, as dominating oxidation product – copper oxide (I) has more than three times greater molar volume than copper (23,46 cm^3/mol and 7,12 cm^3/mol, respectively). Therefore, the amount of oxygen sorbed after the percolation threshold is at a constant level (Figure 2a), and further increase of the metal capacity in order to enhance the process speed is not reasonable.

References

1. *Kravchenko T.A., Polyanskiy L.N., Kalinichev A.I., Konev D.V.* Metal-ion exchanger nanocomposites, Nauka, Moscow, 2009.
2. *Domènech B., Bastos-Arrieta J., Alonso A., Macanás J., Muñoz M., and Muraviev D.N.* Bifunctional Polymer-Metal Nanocomposite Ion Exchange Materials, in Ion Exchange Technologies, ed. Kilislioğlu A., InTech, 2012, DOI: 10.5772/51579. Available from: http://www.intechopen.com/books/ion-exchange-technologies/bifunctional-polymer-metal-nanocomposite-ion-exchange-materials
3. *Rostovshchikova T.N., Smirnov V.V., Kozhevin V.M., Yavsin D.A., Gurevich S.A.* // Ross. Nanotekhnol. 2007. V.2 (1-2). P.47-60.
4. *Gul V.E., Shenfil L.Z.* Electroconductive polymeric compositions, Khimiya, Moscow, 1984.

INFLUENCE OF CONDUCTIVE AREA FRACTION AND OF WATER SPLITTING ABILITY UPON ELECTROCHEMICAL CHARACTERISTICS OF HETEROGENEOUS ANION EXCHANGE MEMBRANES

[1]Ekaterina Knyaginicheva, [1]Ekaterina Belashova, [1]Natalia Pismenskaya,
[2]Philippe Sistat, [2]Gérald Pourcelly
[1]Kuban State University, Krasnodar, Russia;
[2]European Membrane Institute, CNRS-ENSCM-UMII, Montpellier, France

Introduction

In recent years, the electrodialysis became broadly applied in fining of wines, juices, in processing of dairy products, waste waters, and also in synthesis, purification and fractioning of precursors for biodegradable polymers. As a consequence, the demand arose for creation of novel anion exchange membranes with suppressed generation of H$^+$, OH$^-$ ions and high capability of initiation of electroconvection. The aim of this work was to study the effects of size of conductive area of membranes and chemical nature of polar groups on the development of electroconvection near the surface of experimental heterogeneous membranes.

Experiments

Commercial MA-41 membranes, as well as experimental samples of MA-41P$_{\mathrm{I}}$ membranes with increasing microporosity were modified with two different strong bifunctional polyelectrolytes (modifier M$_1$ and modifier M$_2$), containing quaternary ammonium bases. Photomicrographs of surface of dry and swollen MA-41 and MA-41P$_{\mathrm{I}}$ membranes were obtained using SEM (Jeol) and optical microscopy (Zeiss Imager.Z1, Axio software and 63x.1.4 oil DICI lens). Electrochemical impedance spectra, chronopotentiograms and current-voltage curves were obtained using the method described in [1] (PI-50-1.1 potentiostat or Autolab-100 with FRA2 module). The intermembrane distance was 6.5 mm, the average linear flow velocity of 0.02 M NaCl solution was equal to 0.4 cm/s. The limiting current density was calculated using the convection-diffusion model [2].

Results and Discussion

Analysis of images of dry (Fig.1) and swollen (Fig.2) membranes shows that the fraction of conductive area and surface irregularity of MA-41P$_{\mathrm{I}}$ is higher than that of MA-41.

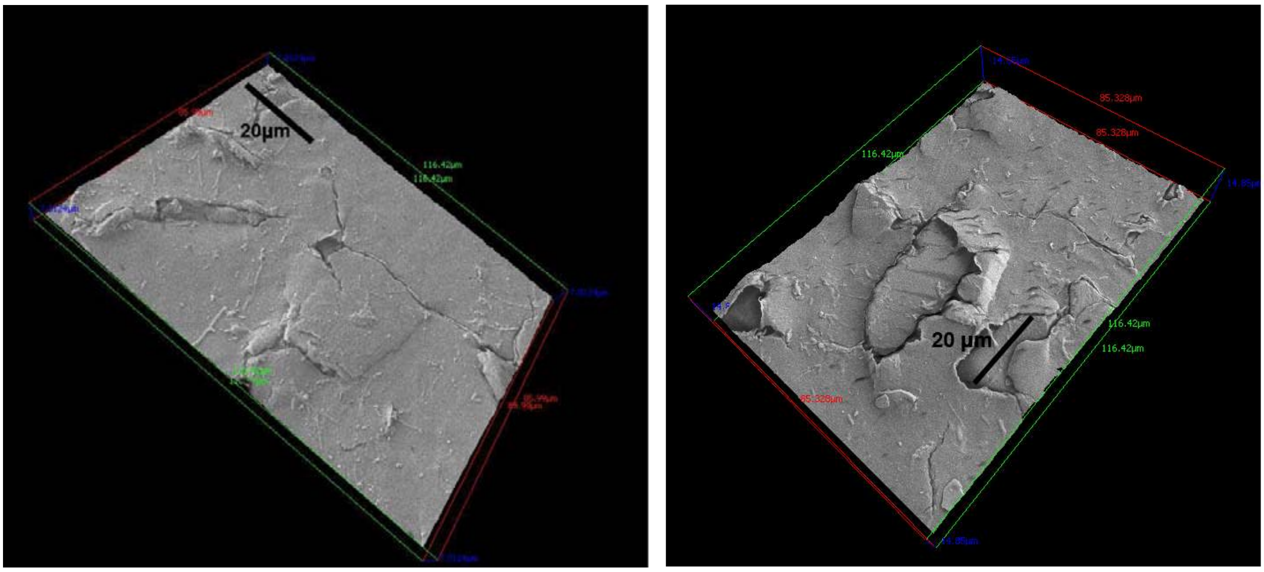

a *b*

Figure 1. 3D SEM image of dry MA-41 (a) and MA-41P$_{\mathrm{I}}$ (b) membranes

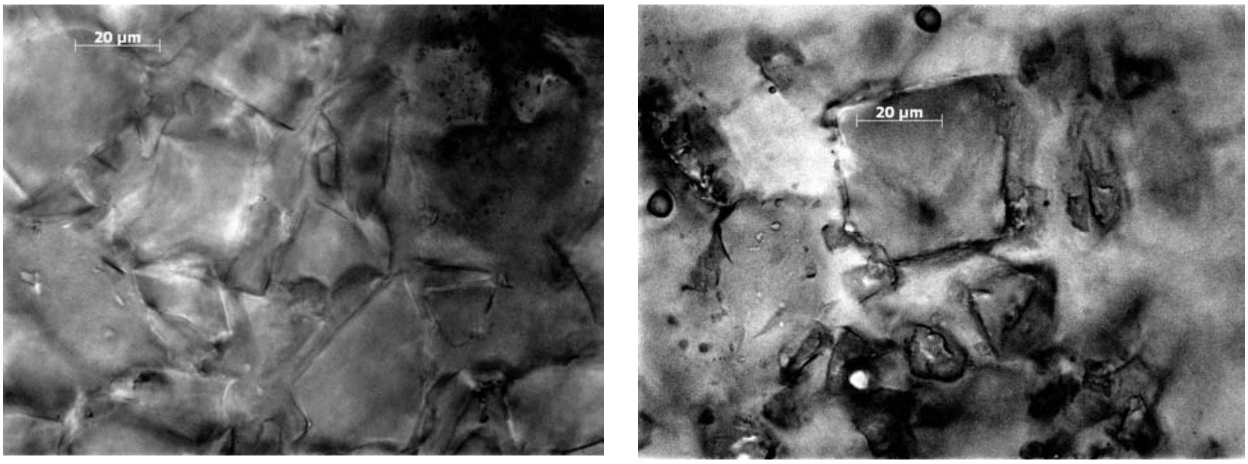

a *b*

Figure 2. Optical image of swollen MA-41 (a) and MA-41P_I (b) membranes

An increment in the fraction of conductive surface leads to increased transition time values on MA-41P_I chronopotentiograms in comparison with MA-41 (Fig.3).

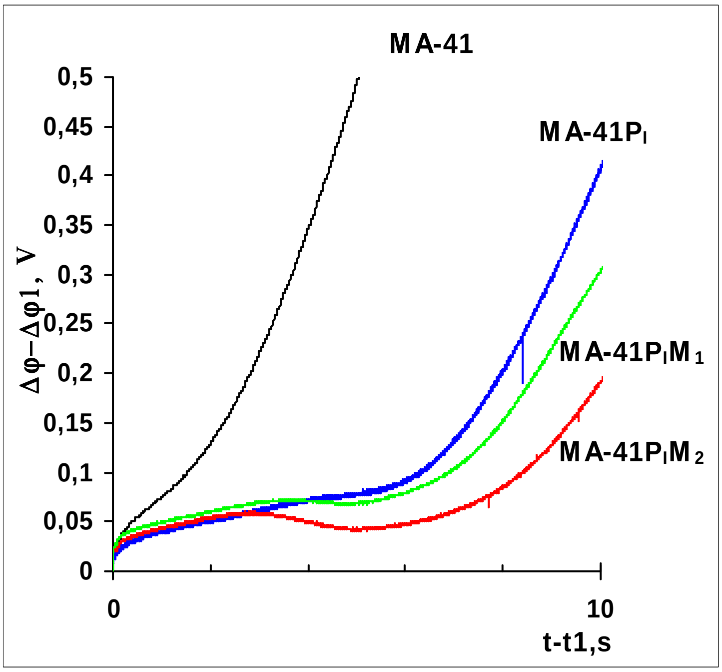

Figure 3. Initial parts of chronopotentiograms of studied membranes at current density 20 mA/cm^2

Analysis of shapes of electrochemical impedance spectra (Fig. 4) evidences that the increase in the size of conductive area leads to a decrease of water splitting on MA-41P_I compared to the MA-41 membrane. If the fraction of the conductive area is kept constant (MA-41Π_I, MA-41$\Pi_I M_1$, MA-41$\Pi_I M_2$ membranes), the treatment with strong electrolytes suppresses the generation of H^+ and OH^- ions. The most visible effect is found with the M_2 modifier.. The impedance spectroscopy data are confirmed by the pH measurements in desalination channels, formed by the studied membranes and MK-40 membrane.

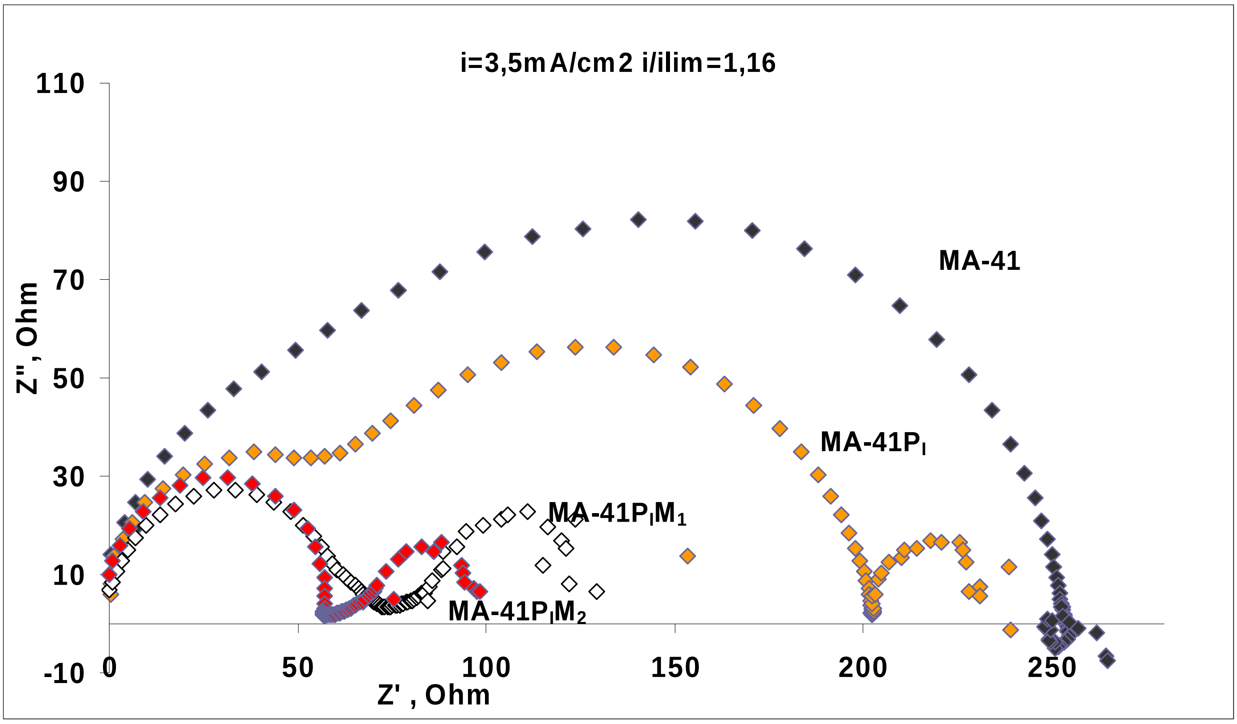

Figure 4. Electrochemical impedance spectra of the studied membranes

The unusual form of the initial part of chronopotentiograms of modified membranes and the increase in the transition time (Fig. 3) suggest that electroconvection starts at lower values of potential drop and it develops more intensively on the MA-41P$_{I}$M$_{1}$ and MA-41P$_{I}$M$_{2}$ membranes in comparison with the MA-41 and MA-41P$_{I}$ membranes. The development of electroconvection leads to a decrease of potential drop, registered in overlimiting current modes in chronopotentiograms and current-voltage curves.

Acknowledgements

This investigation was realized within French-Russian laboratory "Ion-exchange membranes and related processes". The authors are grateful to CNRS, France, and to RFBR, Russia (grants 12-08-00188, 13-08-01168), as well as to FP7 Marie Curie Actions "CoTraPhen" project PIRSES-GA-2010-269135 for financial support.

References

1. *Pismenskaya N.D., Nikonenko V.V., Melnik N.A., Shevtsova K.A., Belova E.I., Pourcelly G., Cot D., Dammak L., Larchet C.* Evolution with Time of Hydrophobicity and Microrelief of a Cation-Exchange Membrane Surface and Its Impact on Overlimiting Mass Transfer // J. Phys. Chem. B. 2012. V. 116. P. 2145–2161.
2. *Zabolotsky V.I., Nikonenko V.V.* Ion transfer in membranes. Moscow: Nauka, 1996. - 391 p.

INFLUENCE OF EXTERNAL ELECTRICAL FIELD ON THE ANILINE POLYMERIZATION IN THE MF-4SC MEMBRANE AND PROPERTIES OF PREPARED COMPOSITES

Natalia Kononenko, Ninel Berezina, Natalia Loza, Sergey Dolgopolov, Mariya Chernyaeva
Kuban State University, Krasnodar, Russia, *E-mail: kononenk@chem.kubsu.ru*

Introduction

Chemical template synthesis of polyaniline (PAn) in membrane matrix allows to prepare the composites, which are perspective for application both in electromembrane processes of water purification and solutions processing, and in fuel cells. The properties of these materials essentially depend on conditions of realization of polyaniline synthesis: concentration of polymerization solutions, potential of redox systems for electron acceptors during the oxidative polymerization of aniline; duration of synthesis and other parameters [1-3]. Even the sequence of membrane treatment by monomer solutions and polymerization initiator influences on conductive and diffusive properties of composites [4]. We may expect that samples obtained in an electrical field, will have the special set of properties. The matrix synthesis of polyaniline has made possible to prepare a lot of composite materials, however only samples with bulk distribution of polyaniline in a membrane were prepared in an electrical field [5]. At the same time the surface modified composites with anisotropic structure and asymmetric transport properties have most interesting properties. Till now such type composites were not prepared in an external electrical field. More detailed study is necessary to use an external electrical field for realization of polyaniline synthesis and for specification of the localization place of polyaniline in a membrane. It is interesting to reveal, whether the barrier properties of the polyaniline layer and stabilization of membrane nanostructure will state previous, or new functional properties will appear for samples which are prepared in an electrical field. The aim of this work is to prepare composites, having bulk distribution of polyaniline in the MF-4SC membrane or having polyaniline layer on membrane surface in an external electrical field. One of the tasks of this work is to investigate the conducting properties and structural characteristics of the prepared materials.

Experimental

Template synthesis of polyaniline in MF-4SC as a basic matrix was carried out in an electrical field with the help of electrodialysis cell. 0.01 M solution of aniline (An) and 0.005 M solution of H_2SO_4 were used as the monomer solution. The polymerization initiator was 0.01 M $FeCl_3$+0.01 M HCl solution in the case of bulk modification and 0.002M $K_2Cr_2O_7$+0.01 M HCl in the case of surface modification of MF-4SC membrane. The bulk modification samples were prepared in two stages. The surface modification samples were prepared in one stage. Series of samples were prepared in static conditions according to [3, 5]. Concentration dependences of the conductivity of samples in HCl solutions were measured by mercury-contact method. The porous structure of membranes was studied by method of standard contact porosimetry [6].

Results

The aniline polymerization in MF-4SC membrane leads to decrease of conducting properties in any conditions of preparation. As can be seen from Figure 1, the decrease of conductivity is minimal for samples which were prepared in an electrical field. The decrease of conducting properties of anisotropic samples which are prepared in static conditions depends on solutions concentration of monomer and polymerization initiator. The conductivity decreases on the average by the order in comparison with the initial membrane when making use of 1 M solution of An. A type and concentration of the initiator (0.5 M $(NH_4)_2S_2O_8$ or 0.2 M $K_2Cr_2O_7$ solutions) do not play an essential role.

The conductivity in isoconducting point (κ_{iso}) and the volume fractions of conducting phases (f_1 and f_2) were found from concentration dependences of composites within the framework of two-phase microheterogeneous model of conductivity. The results of calculation are shown in Table 1. The analysis of the model parameters of composite membranes confirmed, that samples prepared in an external electrical field have the highest κ_{iso} value. The parameter f_2 characterizes the volume fraction of internal solution in a membrane and its value was calculated also independently from integral porosimetry curve.

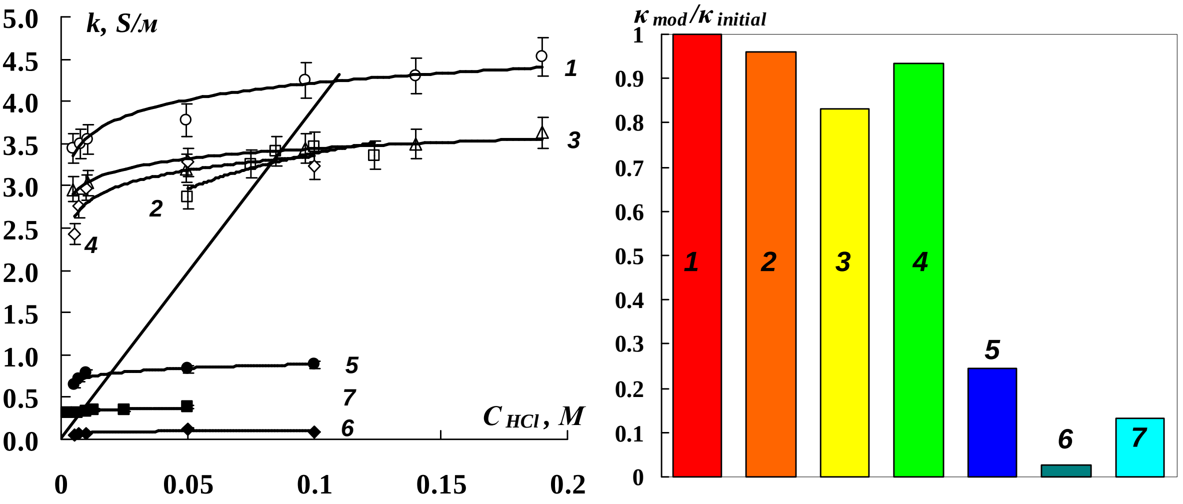

a *b*

Figure 1. Concentration dependences of the conductivity of MF-4SC (1) and MF-4SC/PAn (2-7) in HCl solutions (a) and relative conductivity of composites in 0.1 M HCl solution (b). Numbers of samples are the same as in the Table 1

Table 1. Transport-structural parameters of MF-4SC/Pan composites, which are prepared in different conditions

Number of sample	**Solutions concentration of monomer and initiator**	**Conditions of preparation**	**Type of modification**	V_0, cm^3/g	κ_{iso}, *S/m*	f_2 *from conductivity*	f_2 *from porosimetry*
1	–	-	-	0.23	3.65	0.11	0.13
2	0.01M An 0.01M $FeCl_3$	electric field	bulk	0.21	3.40	0.23	0.10
3	0.01M An 0.01M $FeCl_3$	static	bulk	0.22	3.41	0.05	0.11
4	0.01M An 0.002M $K_2Cr_2O_7$	electric field	surface	0.25	3.36	0.08	0.14
5	0.1M An 0.02M $K_2Cr_2O_7$	static	surface	0.23	0.79	0.09	0.12
6	1M An 0.2M $K_2Cr_2O_7$	static	surface	0.21	0.06	0.10	0.10
7	1 M An 0.5M $(NH_4)_2S_2O_8$	static	surface	-	0.33	0.04	-

The minimal value of the parameter f_2 is observed for the sample which was prepared using concentrated polymerization solutions (1 M An and 0.5 M $(NH_4)_2S_2O_8$). It is related with reduction of total volume of water in a membrane (the parameter V_0) after matrix synthesis of PAn under such conditions (Table 1). From porosimetry curves (Fig.2) follows that this decrease is not such significant as it could be possible to expect from the analysis of the conducting data. The competing action of two factors can be the reason of these effects: a circuit of PAn can not only replace water from membranes, but also render disjoining action on a polymeric matrix of a base membrane [7]. However, the changes in a structure of transport channels of a membrane do not leave the nanosize level, because the formation of macropores with effective radius more than 100 nm in the porosimetry curve is not observed.

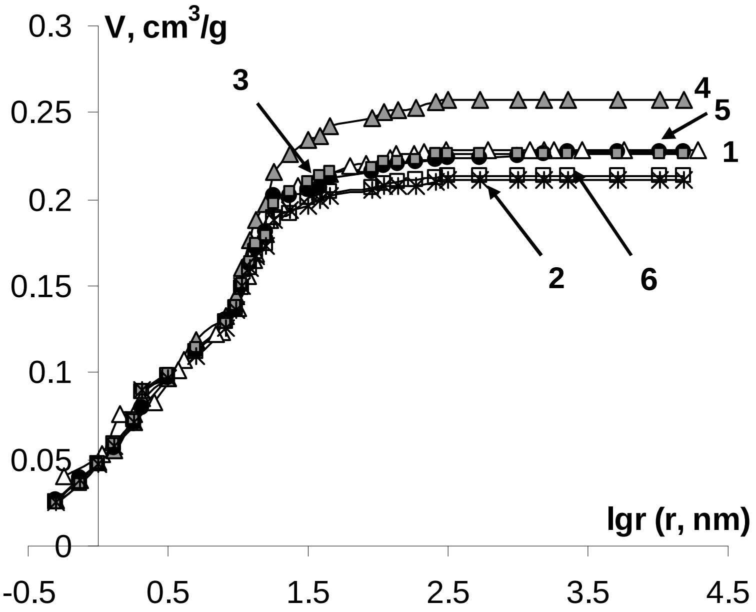

Figure 2. The integral functions of water distribution by the effective pore radii for composites, which are prepared in different conditions. Numbers of samples are the same as in the Table 1

Conclusions

Thus, the method of polymerization of aniline in the MF-4SC membrane matrix in an external electric field is faster and more resource-saving as compared with static conditions. The smaller concentration of polymerization solutions in this case promotes preparation of composites with more balanced set of the transport characteristics. It is shown, that the realization of aniline polymerization process in an external electrical field allows to prepare composites with higher proton conductivity, which is in fact by the order higher in comparison with composites prepared in static conditions. It is related with increasing of maximal water-content in samples and that promotes the greater mobility of proton. Thus the nanostructure of polymer is saved, and macropores are not forming. The effect of conductivity increase depends on the concentration of monomer and does not depend on type of the initiator.

Acknowledgments

The present work is supported by the Russian Foundation for Basic Research (project № 12-08-01092-a).

References

1. *Nagarale R.K., Gohil G.S., Shahi Vinod K., Trivedi G.S., Rangarajan R.* // J. Colloid Interface Sci. 2004. V.277. P.162-171.
2. *Tan S., Bélanger D.* // J. Phys. Chem.. 2005. V.109. P. 23480-23490.
3. *Berezina N.P., Kononenko N.A., Sytcheva A.A.-R., Loza N.V., Shkirskaya S.A., Hegman N., Pungor A.* // Electrochimica Acta. 2009. V.54. P. 2342–2352.
4. *Lysova A.A., Stenina I.A., Gorbunova Yu.G., Yaroslavtsev A.B.* // Vysokomolekularnye soedineniya. B. 2011. V.53. P. 130-136.
5. *Kononenko N.A., Berezina N.P., Dolgopolov S.V., Polovinko T.P., Falina I.V.* Patent RF, № 2011149509/05(074299), 05.12.2011.
6. *Volfkovich Yu. M., Bagotzky V.S., Sosenkin V.E., Blinov I.A.* // Colloids and Surfaces A: Physicochem. Eng. Aspects. 2001. V.187–188. P. 349-365.
7. *Compan V., Riande E., Fernandez-Carretero F.J., Berezina N.P., Sytcheva A.A.-R.* // J. Memb. Sci. 2008. V.318. P. 255-263.

ELECTRO-MEMBRANE REGENERATION OF CHLORINE-HYDROGENE ACID FROM ITS PECTINE SOLUTIONS

Vladimir Kotov, Irina Bodyakina, Alexey Lukin, Galina Netyesova
Voronezh State Agricultural University, Voronezh, Russia, *E-mail: irina.bodyakina@inbox.ru*

Introduction

Pectin is polysaccharide, whose molecules consist of polygalacturonic acid. Pectin is extracted from vegetational waste by using acid for extraction and ethanol for precipitation. [1]. However, one of the disadvantages of such method is acid pollution of the precipitator and inevitable loss of the extracting agent.

Experiments

On order to regenerate the extracting agent from acid pectin extracts we used a method of ion-selective electrodialysis. The latter was used for 0.3 % apple pectin solutions in 0.05 M chlorine-hydrogene acid. The solution composition was due to average concentration of substances typical of pectin solutions. The process took place in four-section apparatus according to the scheme: anode – anode section – cation-exchange film MK-40 – concentration section – anion-exchange film MA-40 or MA-41 – deionization section – anion-exchange film MA-40 or MA-41 – catelectrode section – catelectrode, during an hour with the current density 1-6 mA/sm^2. The initial solution was placed in the deionization section. During the electrodialysis there was formed chlorine-hydrogene acid as the result of chlorine ions transition through anion-exchange film, and hydrogene ions, generated on the anode, through cation-exchange film. In the deionization section there was deacidification process due to hydroxide ions, generated on the catelectrod and transferred through another anion-exchange film. The results of alkalimetric potentiometric titration of the composition of concentration and deionization sections were used for estimation of acid extract, the degree of its regeneration as well as the degree of deionization of the initial solution.

Results and Discussion

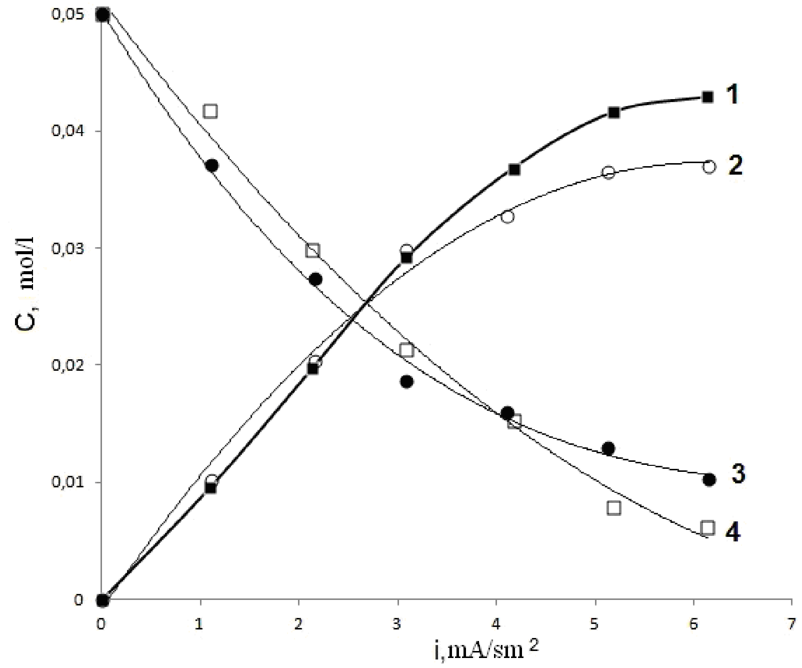

Figure 1. Dependence of concentration of chlorine-hydrogene acid (C) from current density (i) in the comcentration section (1, 2) and chloride-ions in the deionisation section (3, 4) during electrodialysis with membranes MA-40 (1, 3) and MA-41 (2, 4)

Fig. 1 shows profiles of process performance in regard to current density. The amount of acid in the concentration section as well as its regeneration degree grow along with growing current density up to 4 mA/sm^2 in case of usung membranes MA-40 and 3 mA/sm^2 – membranes MA-41. Similarly, the amount of the acid decreases in the deionization section, which means the degree of deionization of the solution increases. With higher current density the profiles growth slows down, which means supermaximum performance

The results demonstrate the lower limiting current density if we use membranes MA-41 in contrast with MA-40. If we use membranes MA-41, the performance is high with relatively low current density, and in case of MA-40 the performance is high with high current density (Fig. 1, chart 1).

Table 1. The amount of extracted chlorine-hydrogene acid (η) in the case of various current density in the concentration section

Membrane MA-40		Membrane MA-41	
i, mA/sm^2	η	i, mA/sm^2	η
1.10	0.759	1.11	0.799
2.14	0.805	2.16	0.822
3.09	0.812	3.09	0.812
4.17	0.768	4.11	0.692
5.19	0.697	5.13	0.619
6.14	0.608	6.15	0.523

Difference in the dialysis profiles when using various chemical membranes is due to a number of reasons. It is known that the number of counter-ions transference in membranes MA-40 and MA-41 differ slightly [2]. However, there is pectin involved in the process. Functioning as electrolyte it can become sorbed on membranes. Also, the aliphatic character of the matrix of the membrane MA-40 and location on it of groups with similar polarity, unlike hydrophobic aroma matrix of MA-41, increases pectin sorption. It is commonly known [3] that during electrodialysis the on receiving side of the anion-exchange film there appears dipolar layer between positively charged fixed ions and the pectin polyanion, in which there is a process of additional water dissociation inducted by the electric field. As a result, there is not only useful transference of chloride-ions, but also that of hydroxide-ions, which deacidify acid in the concentration section. This in its turn leads to lower current profile (chart 1) in comparison with traditional profiles concerning chloride-ions in the systems with no pectin involved. Since the dipolar layer at the membrane surface (MA-40) is stronger, with low current density the profiles are lower tnan in cases with the membranes MA-41. Higher deionization of the solution with membrane MA-41 will very soon bring about maximum current. Yet, as we think, there is another, more important reason for that. Fig. 2 shows the photos of the anion-exchange membranes involved in the research. The considerable part of MA-41 is occupied with current-proof lavsan reinforcement thread (about 16 %), so the real surface size occupied for transference is much less than that of MA-40. Hence, the maximum current density for MA-41.

Similarly, membranes MA-41 demonstrate lower profiles with the current density over 3 mA/sm^2 (Fig. 1), due to the fact that real current density is higher than established and the negative process of water decomposition on the pre-membrane layer is more intensive than in case of MA-40. Yet, we should take into account the fact that with the maximum current density the generated hydroxide-ions can react with methyl group of fixed ion of benzyltrialkilammonium of MA-41[4] with formation of methanole and tertiary amine group. The latter function as catholytes during the process of water dissociation, which also causes the low profiles.

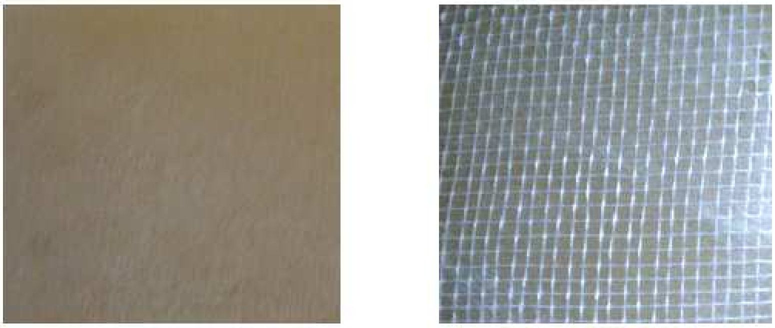

1 2

Figure 2. The surface of anion-exchange membranes: 1 – MA-40, 2 – MA-41

If we use the profiles shown in Fig. 1, we will see that the degree of deionization of the solutions with current density of 5 mA/sm^2 is 84-88 % for the membranes MA-40 and 74-79 % for the membranes MA-41. The degree of the acid regeneration is correspondingly 83-86 and 73-74 % with the current profiles of 0.70-0.61 и 0.62-0.52.

All in all, the results obtained in the research reveal good prospects for using the method of electrodialysis with anion-exchange films MA-40 to generate chlorine-hydrogene acid from acidic pectin extracts for reusing in the technology of pectin production.

References

1. *Donchenko L.V.* Pectin Technologies. M.: DeLи, 2000. 256 p.
2. Ion-exchange films. Granulates. Powders. Catalogue. M.: Mir, 1977. – 16 p.
3. *Bodyakina I.V., Bagryantsev V.A., Kotov V.V., Lukin A.L.* // Vestnik of VSU. Series: Chemistry. Biology. Pharmacia. 2012. № 2. P. 9-13.

ELECTROCONDUCTIVE PROPORTIES OF PECTIN SOLUTIONS IN TERMS OF THEOTY OF GENERALIZED CONDUCTIVITY AND MICRO HETEROGENEOUS MODEL

Vladimir Kotov, Irina Bodyakina, Alex Lukin, Galina Netyesova
Voronezh State Agricultural University, Voronezh, Russia, E-mail: irina.bodyakina@inbox.ru

Introduction

Pectins are polyelectrolytes of plant origin. Their molecules consist of polygalacturonic acid chains. The characteristic feature of pectin solutions is gelation, thanks to which the more is its concentration, the higher is its viscosity. Rheologic properties of pectin have been studied quite well, while more information needs to be discovered about their electroconductive properties. Thus, the latter is the focus of the article.

Experiments

The object of the study is apple pectin and natrium pectate with the concentration of 0.05-0.50%. Molecular weight of the pectin was 30.1 kDa and the amount of carboxy group 2.30 mM/gr. To determine the electric conductivity slide wire bridge was used temperature of 298 K.

Results and Discussion

Figure 1 shows the dependence of electroconductive properties of pectins under study on their concentration.

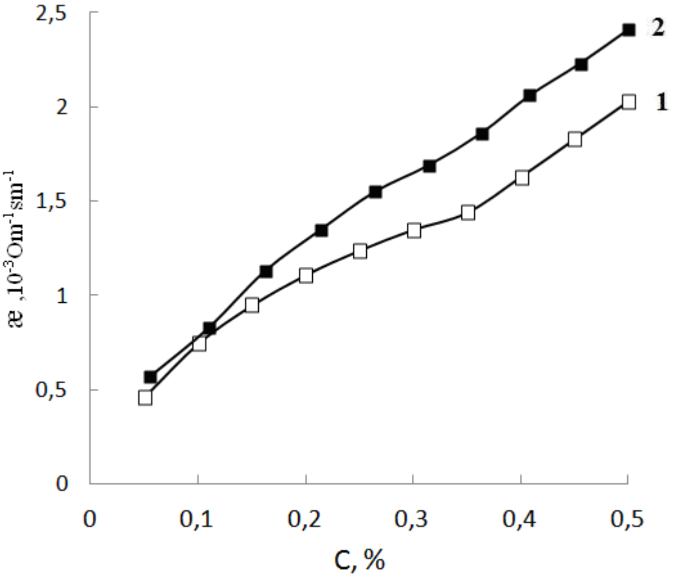

Figure 1. Dependence of electric conductive properties (æ) of pectin solutions (1) and natrium pectate (2) on their concentration (C)

The curves look quite typical of those for electrolytes: the higher the concentration, the lower is the growth of electric conductivity. But curve 1 (pectin) shows a slight bend at the point of 0.30-0.35%. This is due to [1] structural changes described in the work. The growth of electric conductivity of the above mentioned concentrations is due to formation of conductive channels in the gel microphase of the solution and abnormally high proton conductivity.

The next stage was the evaluation of how each of the microphases contributed to the conductivity properties of the solutions. For this we used sample pectin solutions with weakly connected ion exchangers consisting of two microphases – hydrated pectin polyanions or oectate (gel) and uncomplexed solution containing products of polyelectrolyte dissociation (nongel parts). To find out the electric conductivity of the microphases we used the terms of the generalized theory of heterogeneous conductivity and microheterogeneous two-phase model [2, 3].

For estimation of electric conductivity of nongel microphase(æ) we used the results of pH estimation (for pectin) or experimental data on general electric conductivity(æ), considering that ionization of polyelectrolyte was total (for pectate). Also, we took into account table values of ion mobility for hydrogen and natrium.

Electric conductivity of gel microphase ($\ae^{/}$) was estimated with help of equation:

$$\bar{\ae} = \ae^{*f_1} \cdot \ae^{f_2} \qquad (1),$$

here f_1 and f_2 correspond to the parts of gel and nongel microphases. Value f_2 was estimated in relation to the slope of curve of linear dependences and $f_1 = 1-f_2$. Values f_1 and f_2 correspond to 0.25 and 0.75 (for pectin solutions), and 0.35 and 0.65 (for natrium pectate).

Figure 2 demonstrates concentration dependences of electric conductivity gel microphase.

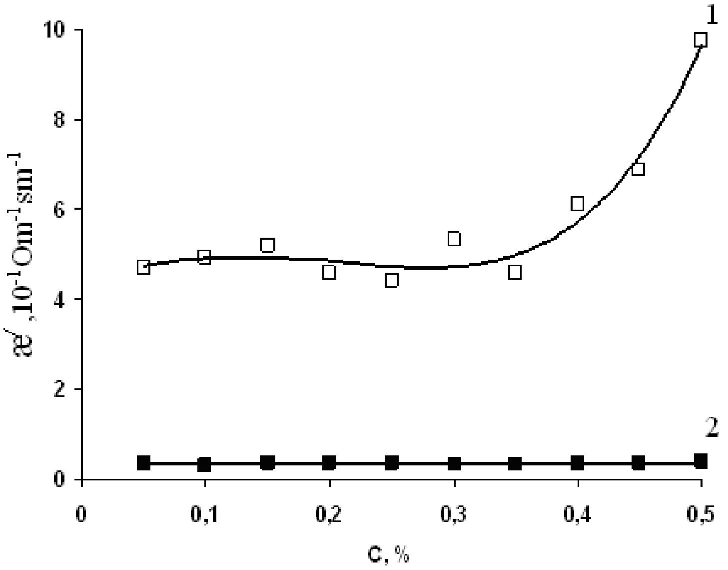

Figure 2. Dependances of specific electric conductivity of gel ($\ae^{/}$) pectin solutions (1) and pectate (2) on concentration (C)

Curve 1 (for pectin) has a horizontal part (C = 0.05 – 0.35%) after which we can observe high rise of electric conductivity. This proves the above mentioned assumption about a high speed of protons in conductive channels of gel microphase. Curve 2 (for natrium pectate) is linear all way through and is parallel in relation to axis of abscissas, which proves the lack of structuring. It seems due to electrostatic repulsion of carboxylate ions fixed on molecules and due to formation of fibrillous structure of the solution.

Absolute values of ($\ae^{/}$) are higher by two in pectin solutions and by one in natrium pectate in comparison with ion resins and ion exchange membranes. This confirms the assumption about abnormal proton mobility in conductive channels in gel microphase. The higher values of gel microphase ($\ae^{/}$) of pectin in comparison with pectate are due to the fact that conductive channels on the surface of pectin molecules alongside other different components contain strongly ionized carboxyl groups. By contrast, conductive channels of pectate molecules contain only weakly ionized hydroxide groups and water.

References

1. *Netyesova G. A. Kotov V. V., Bodyakina I.M. Lukin A.L.* // Journal of physical chemistry. 2012. T. 86. No. 9. P. 1569-1572.
2. *Gnusin N.P., Zabolotsky V. I. is mean. Nikonenko V. V., Meshenkov A.I.* // Magazine of physical chemistry. 1980. T. 54. No. 6. P. 1518-1522.
3. *Gnusin N.P., Berezina N.P., Meshenkov A.I.* // Electrochemistry. 1988. T. 24. No. 3. P. 364.

CAUSES AND FEATURES OF ELECTROCONVECTION SYSTEMS WITH HETEROGENEOUS ION-EXCHANGE MEMBRANES

[1]Anna Kovalenko, [1]Victor Zabolotsky, [1]Victor Nikonenko, [1]Makhamet Urtenov, [1]Konstantin Lebedev

[1]Kuban State University, Krasnodar, Russia

E-mail: *savanna-05@mail.ru, nikon@chem.kubsu.ru, urtenovmax@mail.ru, klebedev.ya@yandex.ru*

Introduction

This study is a continuation of our earlier works [1, 2]. It is devoted to the theoretical research of the basic laws of electroconvection (EC) in electromembrane systems (EMS) with non-uniform ion-exchange membranes (IEM). Heterogeneity of IEM (natural or artificial) is the factor which affects the non-uniformity conduction of segments on a membrane surface. As a result, electric current flowing in the system, gives rise to body forces providing EC.

The purpose of this work is to study the reasons and features of EC caused by a non-uniform structure of an IEM. With this purpose, the stationary and non-stationary mathematical 2D models of EC in the desalination cell of EMS with non-uniform membranes are constructed. The electrodialysis of binary electrolyte in overlimiting regime is studied. The model consists of the Nernst-Planck-Poisson and Navier-Stokes equations added by the necessary boundary conditions. The statics and dynamics of the arising and development of the rotational structures appearing as a result of heterogeneity IEMs are investigated. The various phenomena and processes affecting the ion mass transfer are studied by calculation of I-V characteristics.

Theory

The reason of any movement of a fluid is a pressure gradient, ∇P. The influence of electrochemical processes on hydrodynamics occurs through the body force $\vec{f}$ in the Navier-Stokes equation. If this force is potential ($rot\vec{f} = 0$), there is such a function ψ that $\vec{f} = \nabla\psi$. If a new value ("modified pressure") $\tilde{P} = -P + \psi$ is introduced, and Navier-Stokes equations containing P are transformed to new variables “stream function - curl”, it can be seen that the fluid current-lines do not vary (but the fluid velocity varies). For this reason, the first kind electroosmosis does not lead to formation of the electroconvective whirlwinds. In EMS the electric body force $\vec{f}$ is determined by the space charge density ρ and the electric field intensity $\vec{E}: \vec{f} = \rho\vec{E}$. The cause of EC (electroosmosis of the second kind) is the vortex character of the field of electric force ($rot\vec{f} \neq 0$), namely, when $rot\vec{f}$ reaches a certain significant value. Electric field is a potential field since $\vec{E} = -\nabla\varphi$, where φ is the electric potential: $rot\vec{E} = 0$. Consequently, $rot\vec{f} = \rho rot\vec{E} + \nabla\rho \times \vec{E} = \nabla\rho \times \overline{E}$. Therefore, the vortex character of the electric force field is defined by the charge density gradient, i.e. by $\nabla\rho$. Besides for the occurrence the EC vortices, it is necessary $\left\| rot\vec{f} \right\| \geq P_0$, where P_0 is the threshold of pressure necessary to overcome a viscous resistance. This pressure is connected with linear velocity of solution V_0.

In the case of ED cells with homogeneous IEMs, $\nabla\rho$ is caused by non-uniform desalination of solution on width and length of the channel [2, 3].

In this work the other mechanism of occurrence EC is studied. This mechanism is caused by (natural or artificial) non-uniform surface conductivity of IEM. Actually, there are studies aimed at the formation of non-uniform conductivity of the membrane surface in order to enhance mass transfer. Various levels of heterogeneity are formed: from micro-heterogeneity (of micron size) up to macro-heterogeneity [3]. Heterogeneity is observed both on the membrane surface and on the membrane cross-section. Distinction in a structure of a surface and internal structure of different types of membranes is reflected on their electrochemical properties which are observed in chronopotentiograms. During the preparation of these membranes, the original microstructure of resins with the effective radius of ~100 nm remains unchanged and a secondary structure forms that contains coarse pores with the effective radius of ~1000 nm and mainly consists of gaps between resin particles and polyethylene [4]. Thus, on the heterogeneous membrane surface, one can distinguish conducting domains with the characteristic size of ~20–30 µm, the nonconducting domains with the size of ~ 70–120 µm and the transition regions filled with equilibrium solution with the size of about 1 µm.

If the membrane surface is homogeneous, the current streamlines are regularly distributed. The electrolyte concentration at the membrane surface is approximately identical along the surface. If the surface is non-uniform, current streamlines are condensed near well conducting domains (funnel effect). The local current density here is essentially higher than its average value over the surface. Dukhin and Mishchuk consider this effect as the main reason of EC in membrane systems. However as it has been shown above, the cause EC is the gradient of space charge density. The funnel effect causes higher heterogeneity in distribution of electrolyte concentration near the membrane surface. This leads to a higher gradient of space charge density. The charge has significant size and creates the vortex electric force which can lead to EC. The mathematical model presented here describes the transport of ions of binary electrolyte in a desalination cell with a homogeneous anion-exchange and a heterogeneous cation-exchange membranes.

Results and discussions

In the proposed model, the heterogeneity of IEMs is described by alternation of conductive and non-conductive domains between which there are intermediate domains where the conductivity varies from zero to the value corresponding to the conductive domains.

The numerical experiments are made for a NaCl solution. The following parameters were specified: the initial concentration, the mean forced flow velocity V_0, the intermembrane distance h, the length of the channel L, the electric potential drop $\Delta\varphi$. Several special cases are studied:

1) **A single non-conductive domain**. In this case. EC arises at some ratio of solution velocity and the potential drop. A vortex is formed before the non-conductive domain. The solution velocity in the vortex is higher than the average velocity of the forced flow. With reducing the size of the non-conductive domain, the size of the electroconvective vortex increases. The EC vortex, even having the small size, brings a more concentrated solution from the solution bulk to the membrane surface quite effectively.

2) **Two non-conductive domains** of 70 microns in length each. If the distance between these domains is sufficiently large, higher than 500 microns, two vortices arise before each domain; there is no interaction between the vortices. If the distance is less than 500 microns, the vortices interact. No vortex arises before the second domain. It is explained by the fact that the first vortex increases the solution velocity. At a greater solution velocity, a higher potential drop is needed to create an EC vortex.

3) **Periodic alternation of conductive and non-conductive domains**. The streamlines calculated in this case are represented in Fig. 1. An anion exchange membrane is situated from above, and a cation-exchange one, from below. The solution flows from the left to the right.

EC vortices arise near both membranes, but at the cation-exchange membrane the onset of EC occurs at a lower potential drop, and the size of vortices is much higher. It is due to the difference in the diffusion coefficients of sodium and chloride. In a numerical experiment where the diffusion coefficients were taken identical, the streamlines were symmetrical.

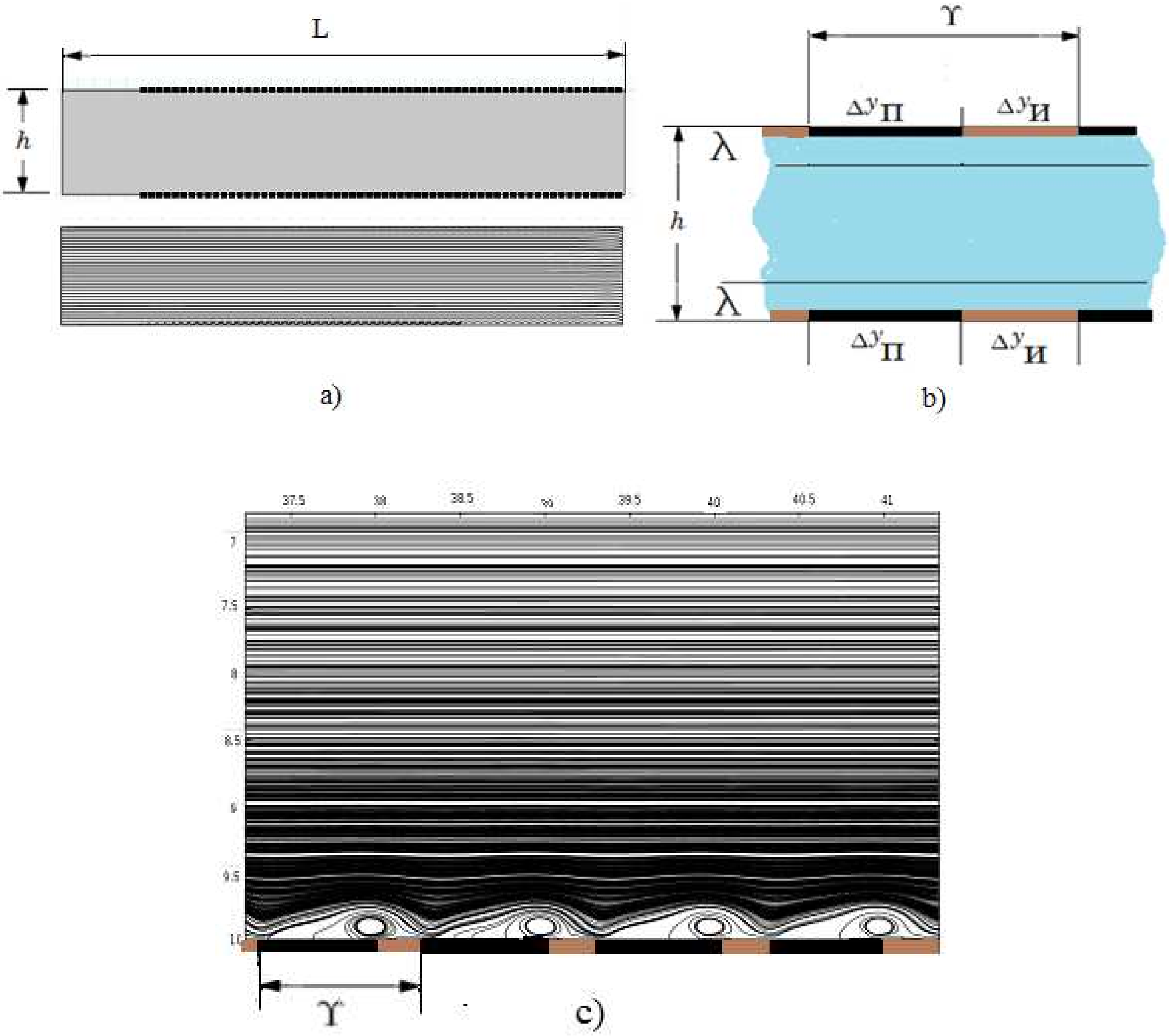

Figure 1. a) The scheme of desalination channel with heterogeneous membranes. Each membrane contains 120 non-conductive domains representing the spots of polyethylene on the surface. b) Magnification of a): the length of conductive and non-conductive domains is $\Delta y u=30$ microns and $\Delta y n=70$ microns, respectively. c) Streamlines in a fragment of the channel. Calculation parameters: $L= 14$ mm; $h=2$ mm; $V_0 = 1.3$ mm/s; $\Delta\varphi = 0.3$ V

References

1. *Kovalenko A.V., Urtenov M.K., Shaposhnikova T.L.* Modelling electroconvection in electromembrane systems of the water-preparation caused heterogeneity ionexchange of a membrane // Energy supply and water-preparation. №1 (75), 2012, P.15-20
2. *Uzdenova A.M., Kovalenko A.V., Urtenov M.K.* Mathematical of model electroconvection in electromembrane systems. − Karachaevsk: KGU , 2011.-156 p.
3. *Zabolotskii V.I., Nikonenko V.V., Urtenov M.Kh., Lebedev K.A., Bugakov V.V.* Electroconvection in Systems with Heterogeneous Ion-Exchange Membranes // Rus. J. Electrochem. 2012, V. 48, №. 7, pp. 692–703.
4. *Berezina, N.P., Kononenko, N.A., and Volfkovich, Yu.M.* // Russ. J. Electrochem. 1994. Vol. 30. P. 329.

2D – SIMULATION OF THE GALVANO-DYNAMIC MODE OF THE TRANSFER OF THE BINARY ELECTROLYTE IN ELECTRO-MEMBRANE SYSTEMS

[1]Anna Kovalenko, [2]Emil Zholkovskiy, [1]Makhamet Urtenov
[1] Kuban State University, Krasnodar, Russia
E-mail: savanna-05@*mail.ru, urtenovmax@mail.ru*
[2] Institute of Bio-Colloid Chemistry, Kiev, Ukraine

For the simulation of the transfer of the binary electrolyte in electro-membrane systems, micro-fluids, etc, in electro-neutrality solution conditions, the classical system of electro-diffusion equations, which consists of Nernst - Plank equations, material balance, electro-neutrality conditions and current flow is used [1].

Electro-membrane systems, as well as other electrical systems, work in two equitable in the physical sense modes: potentio-dynamic, when a fall of the potential in a circuit is specified or in galvano-dynamic mode, when the average density of the current in the circuit is specified.

These conditions are the alternatives to each other, namely, the specification of the fall of potential determines the average density of current in the circuit, and, vice versa.

It is well known [1], that if the conditions of electro-neutrality are executed, the local equivalent concentration of the electrolyte meets the equation of convective diffusion: $\frac{\partial C}{\partial t}+(\vec{u},\nabla C)=D\Delta C\cdot$

For the simulation of galvano-dynamic and galvano-static modes, we derived the new equation for the current density $\vec{I}$ [2]: $\Delta\eta=(\nabla \ln C,\nabla\eta)$, where the function η is a function of current for the current density, so $\frac{\partial\eta}{\partial x}=I_y$, $\frac{\partial\eta}{\partial y}=-I_x$.

Thus, for simulation of galvano-dynamic mode, we have a system of 2 scalar equations with 2 unknown scalar functions C and η. The rest of the physico-chemical characteristics can be found by formulas. From the results of item 2, it can be seen that the simulation of galvano-dynamic modes, is not fundamentally different from the simulation potentio-dynamic modes.

We derived the natural boundary conditions for the function η [3].

The above results allow to introduce the concept of the integrated potential of the electro-membrane system: $P=\varphi+i\cdot\eta$, that is a function of the coordinates of any point within the object and, therefore, the function describes the internal properties of the object. So, unlike the electrochemical impedance, this allows us to analyze the internal properties of the object.

Conclusions

In this research, the system of equations is derived from Nernst - Plank equations and from electro-neutrality conditions. The system of equations is convenient for the simulation of galvano-dynamic (and galvano-static) mode, and, it is a complete analogue of the corresponding system of equations, now used for the simulation of potentio-dynamic (and potentio-static) modes. The basis of this system is a new equation for the stream function for the density, for which the corresponding boundary conditions were derived. Results of our work can be used for theoretical studies of the galvano-dynamic (and galvano-static) mode of electro-membrane systems.

Acknowledgments

We are grateful to RFBR (grant 13-08-00464) as well as to FP7 Marie Curie Actions "CoTraPhen" project PIRSES-GA-2010-269135 for financial support.

References

1. *Newman D.* Electro-chemical systems, M.: The world, 1977, 463p.
2. *Pismenskiy A., Nikonenko V., Sistat Ph., Pismenskaya N., Kovalenko A., Urtenov M.* / Rus. J. Electrochem. 2012. №.7. P. 756-766
3. *Kovalenko A., Zholkovskiy E., Urtenov M.* // Proceedings of Kuban state University. The natural Sciences. - Krasnodar: Kuban state University, №3, p. 52-57.

ESTIMATION OF SURFACE CONDUCTING AREA OF AN ION-EXCHANGE MEMBRANE BY ELECTROCHEMICAL IMPEDANCE SPECTROSCOPY METHOD

[1]Anton Kozmai, [1]Isaac Rubinstein, [1]Boris Zaltzman, [2]Nataliya Pismenskaya

[1]Ben Gurion University of the Negev, Sede Boqer Campus, Israel, *E-mail: kozmay@yandex.ru,*

[2]Kuban State University, Krasnodar, Russia

Introduction

Membrane surface morphology, in general, and the surface conductivity of the membrane, in particular, is the major factor affecting the physico-chemical characteristics of a membrane system [1, 2, 3]. Mechanisms of ionic transport through ion-selective membrane systems can be efficiently studied by electrochemical impedance spectroscopy (EIS) method. The first attempt to assess the effect of membrane surface electrical heterogeneity on impedance spectra was made by Moya [4]. It was found that the diffusional arc of impedance spectra increases with increasing heterogeneity. But the width of the diffusional arc also depends on diffusion boundary layer (DBL) thickness near the membrane surface [5]. Thereby, distinguishing between the contributions of concentration polarization process and surface conducting area in diffusional arc width becomes a truly delicate problem.

In the case when a membrane has conductive and non-conductive sections on its surface, a tangential component of the flux must arise near conductive sections. This phenomenon should occur on definite time scales corresponding to certain frequencies, depending on the sizes of the conductive and insulating parts of the membrane surface. According to these arguments, the electrical heterogeneity of the membrane surface should affect not only the width of Warburg spectrum, but it should become apparent through affecting the shape of its major EIS characteristics in a suitable frequency range.

The main purpose of this work is to test this general idea that is to find out whether the EIS technique allows assessing the electrical heterogeneity of a membrane surface and whether this method is sensitive enough for practical applications.

Theory

In order to assess the surface conductivity we developed a 2D mathematical model of low-frequency membrane impedance response. The system studied consists of an ideal ion-exchange membrane flanked by two diffusion boundary layers (DBLs). Electrolyte concentration in DBLs varies under the action of small harmonic perturbations of the electrical current.

We consider the case when the depleted DBL is adjacent to the heterogeneous surface of the membrane ($x=\delta$), which for the sake of simplicity is modeled by a periodic sequence of alternating 1D conducting and insulating segments (Figure 1). The dimensionless length of each conducting interval, h, is a control parameter in our study. The side of the membrane adjacent to the enriched DBL ($x=d+\delta$) is assumed to be perfectly conducting.

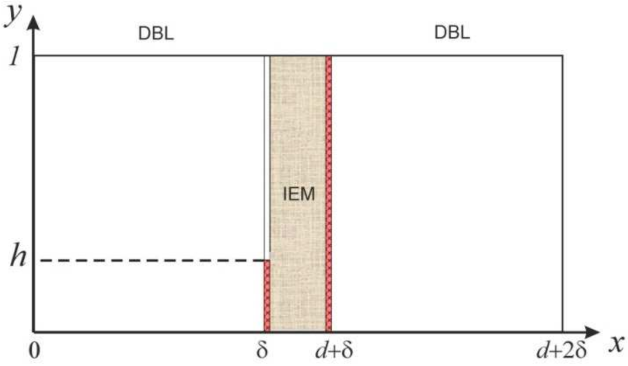

Figure 1. Scheme of the membrane system under study

Mathematically, the model consists of dimensionless Nernst–Planck equations combined with the local electro-neutrality condition valid for the under-limiting current regime.

$$(c_x + c\varphi_x)_x + (c_y + c\varphi_y)_y = c_t,$$

$$(c_x - c\varphi_x)_x + (c_y - c\varphi_y)_y = c_t,$$

$$c = c_- = c_+.$$

Here, c is the electrolyte concentration, φ is the electric potential, lower indexes “+” and “–“ refer to cations and anions concentrations, respectively.

Considering the time-dependent perturbations of the boundary value problem of the form

$$c(x,y,t) = c_0 + \alpha C(x,y)e^{i\omega t}, \qquad (2)$$
$$\varphi(x,y,t) = \alpha \Phi(x,y)e^{i\omega t},$$

and linearizing the governing equations with respect to small harmonic electric current perturbation with amplitude $\alpha \ll 1$, we obtain

$$C_{xx}(x,y) + C_{yy}(x,y) = i\omega C(x,y), \qquad (3)$$
$$\Phi_{xx}(x,y) + \Phi_{yy}(x,y) = 0,$$

where ω is the perturbation frequency.

Application of the boundary conditions and solution of the problem resulted in the following analytical expression for the impedance of the system

$$Z = \delta + \sum_{n=1}^{\infty} \frac{\sin^2(\pi n h)\tanh(\pi n \delta)}{h^2 (\pi n)^3} + \frac{\tanh(\delta\sqrt{i\omega})}{\sqrt{i\omega}} + \sum_{n=1}^{\infty} \frac{\sin^2(\pi n h)\tanh\left(\delta\sqrt{(\pi n)^2 + i\omega}\right)}{h^2 (\pi n)^2 \sqrt{(\pi n)^2 + i\omega}}. \qquad (4)$$

The first two terms in (4) correspond to the Ohmic resistance of DBLs. The second term relates to the membrane heterogeneity. The third term is frequency dependent and represents the Warburg impedance of the system. Finally, the last term corresponds to the deviation from the Warburg-type behavior due to electrical heterogeneity of the membrane surface.

Results and Discussion

The results of our study stand in a good agreement with experimental data for the heterogeneous cation-exchange membrane, MK-40, homogeneous anion-exchange membrane, AMX, and homogeneous cation-exchange membrane, Nafion-117 (see Figure 2).

To summarize, in our study we have shown that electrical heterogeneity of the membrane surface is a source of deviation of impedance spectra from the linear Warburg-type dependence.

The proposed model is sensitive to the variation of the control parameter h, characterizing the membrane surface conductivity (Figure 2c). In particular, our study predicts that homogeneous cation-exchange membrane Nafion-117 (based on a conducting polymer matrix) has a very high, but still not perfect, 90% surface conductivity.

The predicted conductivity of the homogeneous anion-exchange membrane AMX is lower and equal to about 70%. This prediction stands in a fair agreement with experimental measurements, with the membrane non-uniform composition (45% of AMX membrane is non-conducting polyvinylchloride) constituting the likely source of the estimated membrane surface heterogeneity (in industrial applications the AMX membrane is commonly viewed as practically homogeneous).

The predicted surface conductivity for MK-40 is low and varies between 5-7%.

In conclusion we can state that in our study we generalized the EIS method to the analysis of the membrane surface structure. Our method stands in a fair agreement with the existing experimental data.

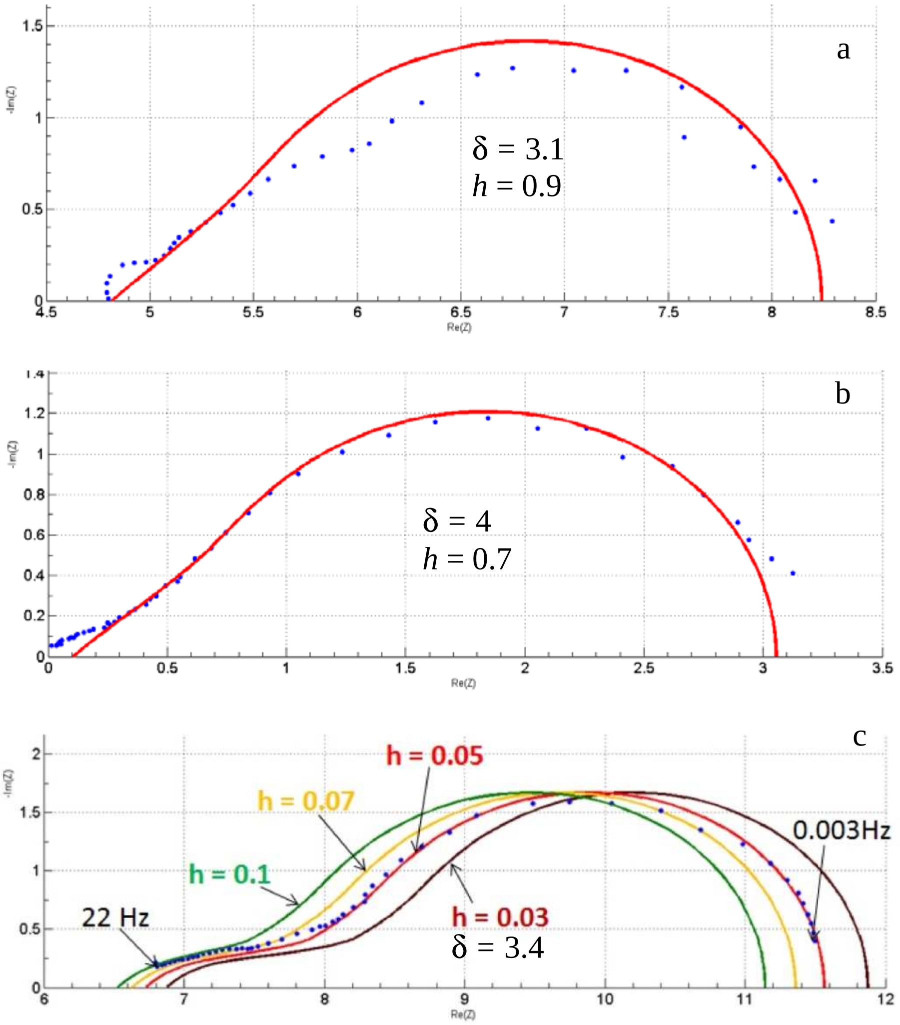

Figure 2. Calculated (solid lines) and experimental (dots) spectra for membranes: a) Nafion-117; b) AMX; c) MK-40. Parameters of the model (DBL thickness (δ) and part of conducting area (h)) are shown on the figure

Acknowledgement

The study was funded by Blaustein Center for Scientific Cooperation, Blaustein Institutes for Desert Research and by Israel Science Foundation, Project 65/07 and RFBR, Project 13-08-01168.

References

1. *Lukáš J., Tyáčková V.* J. Membr. Sci., 58 (1991) 49-57.
2. *Volodina E., Pismenskaya N., Nikonenko V., Larchet C., Pourcelly G.* J. Colloid Interface Sci., 285 (2005) 247-258.
3. *Ibanez R., Stamatialis D.F., Wessling M.* J. Membr. Sci., 239 (2004) 119-128.
4. *Moya A.A.* Electrochim. Acta, 55 (2010) 2087-2092.
5. *Sistat P., Kozmai A., Pismenskaya N.* Electrochim. Acta, 53 (2008) 6380-6390.

EFFECT OF THE CARBON SUPPORT TYPE FOR THE CATALYTIC ACTIVITY OF THE PLATINUM-CARBON CATALYSTS

Alexandra Kuriganova, Kseniya Novikova, Marina Kubanova, Nina Smirnova
South-Russian State Technical University, Novocherkassk, Russia,
E-mail: kuriganova_@mail.ru

Introduction

The efficiency of the low-temperature fuel cell (FC) is determined by a combination of many parameters. Among these parameters are important design and engineering decisions, properties of the proton-exchange polymer membrane, the gas diffusion layer, the temperature and corresponding water management in the system. But one of the important factors is an activity of the metal-carbon catalyst that is use as active component in the cathode and anode of the FC. As a rule, metal-carbon catalyst is a nanosized platinum particles deposited on the surface of larger particles of carbon support.

In turn, the efficiency of the nanosized Pt/C catalyst depends on the two parameters: catalyst morphology (size and shape of the platinum nanoparticles) and a carbon support structure (grain size, porosity, specific surface). The use of the carbon materials as a support for the FC catalysts determined by some of its characteristics: high specific surface area, chemical inertness, thermal stability and high electrical conductivity [1]. In addition, the use of the carbon materials makes it easy to extract platinum from spent catalysts by burning its.

Experiments

In this paper we investigated the series of the carbon materials (Timrex, Taunit, carbon nanotubes produced by Institute of Problems of Chemical Physics (Chernogolovka) – CNT1 and Ivanovo State University (Ivanovo) – CNT2) as a support for the nanosized platinum particles. For the catalysts prepare the method of the electrochemical dispergation was used [2]. It guaranteed the continuity of the catalyst morphology. Platinum loading in all samples was 40%.

Catalytic activity of the Pt/C was assessed using CO oxidation reaction. The mechanism of this reaction is well known, and simplicity of CO molecule to avoid ambiguity of the electrochemical measurements results, that related to the influence of the molecular structure and the difficulty of the mechanism of its oxidation. In addition, oxidative desorption of CO (CO-stripping) is the most reliable method for the determining of the electrochemically active area of the Pt/C catalysts [3].

Results and Discussion

In the literature we can find some information about a correlation between potential of CO oxidation on the Pt/C catalysts and the size of the platinum nanoparticles [4,5]. It is know, that the smaller size of the particle, the more anodic potential the process of CO oxidation have place. Using the same method for the catalysts preparing (electrochemical dispergation) and produce catalysts with identical structure of the platinum nanoparticles, we eliminated the influence of the particle size on CO oxidation process.

As shown in Figure 1a the value of CO oxidation potential peak depending on different type of the carbon supports. CO pre-adsorption was performed in deaerated 0,5M H_2SO_4 solution at the potentials 0,1 V, 0,3 V and 0,5 V (RHE). As shown in Figure 1b the highest value of the specific area observed when platinum nanoparticles deposited on carbon fibers Taunit and carbon nanotubes CNT2. Probably this is due to the more uniform distribution of the platinum nanoparticles on the surface of carbon support and the positive influence on the catalytic layer structure, such as the use of the carbon materials fibers and nanotubes.

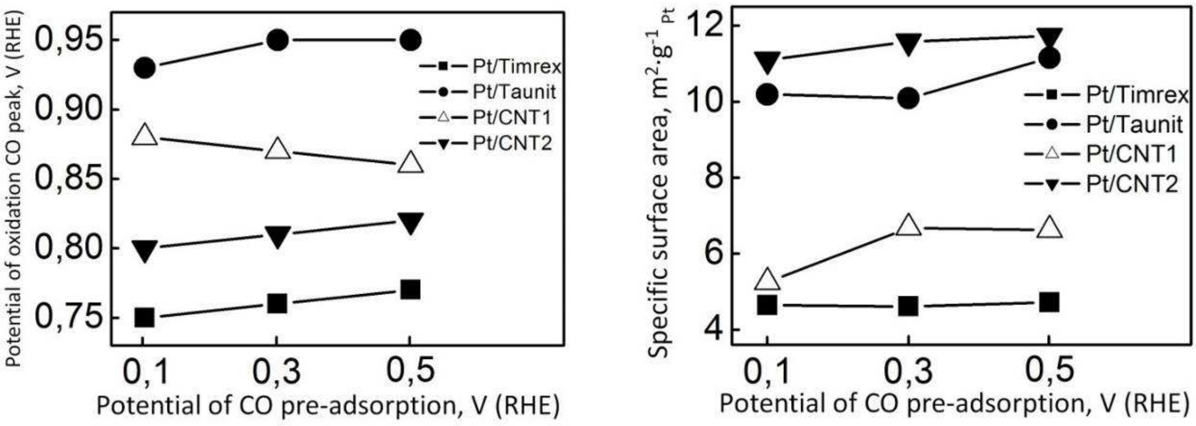

a *b*

Figure 1 – a) Dependence of CO oxidation potential peak on the different carbon support type and potential of CO pre-adsorption;
b) Dependence of the specific surface area of the catalyst on different carbon support type and potential of CO pre-adsorption

References

1. *Ermete Antolini*. // Appl. Catal. B: Environmental. 2009. V. 88. P. 1-24.
2. *I. Leontyev, A. Kuriganova, Yu. Kudryavtsev, B. Dkhil, N. Smirnova*. // Applied Catalysis A: General. 2012. V.431-432. P.120-125.
3. *Cooper, K.R., Ramani, V., Fenton, J.M., and Runz, H.N.* Experimental Methods and Data Analyses for Polymer Electrolyte Fuel Cells, Southern Pines, N.C.: Scribner Associates, 2005.
4. *M. Shao, A. Peles, K. Shoemarker*. // Nano. Lett. 2011. V. 11. P.3714-3719.
5. *F. Godínez-Salomón, E. Arce-Estrada and M. Hallen-López*. // Int. J. Electrochem. Sci. 2012. V. 7. P. 2566 - 2576

NUMERICAL INVESTIGATION OF MICROPARTICLES’ BEHAVIOR UNDER ELECTRIC CURRENT

Alexandr Kuzepalov, Vladimir Shelistov
Kuban State University, Krasnodar, Russia, *E-mail: alex.kuzepalov@gmail.com, shelistov_v@mail.ru*

Introduction

The problem of movement of conducting micro- and nanoparticles in an electric field, electrophoresis, is a well-known phenomenon that is widely used in industry and biology (paint spraying on metals; separation of mixtures, particularly proteins and charged macromolecules in biochemistry and medicine). Interest to this problem has recently increased due to its applications in nanotechnology; it also arises in space biotechnology.

For small electric fields, according to Smoluchowsky’s theory, the particle’s velocity is proportional to the strength of the field and does not depend on the particle’s size; for strong fields, it is proportional to the radius and to the square of the field’s strength. This phenomenon is called electrophoresis of the second kind.

Despite the abundance of both theoretical and experimental works, a review of which can be found in [2–3], many questions concerning electrophoresis remain open.

Statement and Results

The movement of a conducting microparticle in a solution of a binary electrolyte under an electric field is described by a closed system of Nernst-Planck-Poisson-Stokes equations. The particle is assumed impermeable to anions; a constant concentration of cations is assumed on its surface. The potential of the conducting surface remains constant, adhesion conditions for the fluid are assumed on it. Far from the particle, both ions’ concentrations tend to an equilibrium concentration; the fluid’s velocity, to that of the particle; the electric field, to that externally imposed.

In the present work, a closed solution to the problem is obtained numerically for the first time. The difficulties of obtaining such a solution arise due to a number of factors: the Nernst-Planck-Poisson-Stokes equations are a strongly coupled partial differential equations system; the problem has a small parameter at the higher-order derivative. Several characteristic spatial scales exist in the problem and each of them features its own rather complex phenomena, so the electrophoresis of the second kind is an integral result of those factors’ interaction. The problem is described by three dimensionless parameters: the strength E_∞ of an external field, the coupling coefficient κ of hydrodynamics and electrostatics, and the dimensionless Debye number ν.

Since the solution of the system has singularities on the particle’s poles (corresponding to the direction of the electric field), an eigenfunction expansion has been used in the numerical algorithm, namely, Legendre and Gegenbauer polynomials. Quasi-spectral method has been utilized to carry out nonlinear operations; its realization required developing of Fourier transforms with respect to those polynomials. A finite-difference method has been applied in the radial direction, which has allowed using arbitrary mesh stretching. Formation of large concentration gradients near the particle required thickening of the mesh in this area. To the contrary, a sparse mesh can be used at a distance of several particle’s radii without a significant loss in accuracy. Semi-implicit third-order Runge-Kutta method has been used to solve the system in time.

Figure 1 depicts the particle and main regions of the solution, the existence of which has been confirmed with our calculations: I — space charge region, II — diffusion region, III — a region, in which space charge and diffusion boundary layer are absent. The latter region is separated from regions I and II by the point x_0 having the polar angle θ_0. The arrows denote the direction of cations’ flow to the particle’s surface. Velocity, electric potential, ions’ concentrations and charge density fields have been obtained in the calculations.

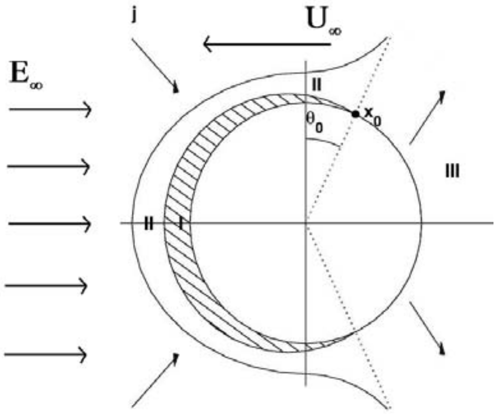

Figure 1. Schematic statement of the problem

Immediately after the equator, $\theta > 90^\circ$, the velocity changes its direction, which leads to formation of a vortex on the rear side of the particle. Figure 2 illustrates a typical distribution of the tangential velocity component along the particle with respect to the polar angle ($E_\infty = 30$, $\nu = 0{,}001$, $\kappa = 0{,}2$). There is a very thin region near the particle's surface where the velocity increases rapidly from zero to the slip velocity; it is not shown in the figure.

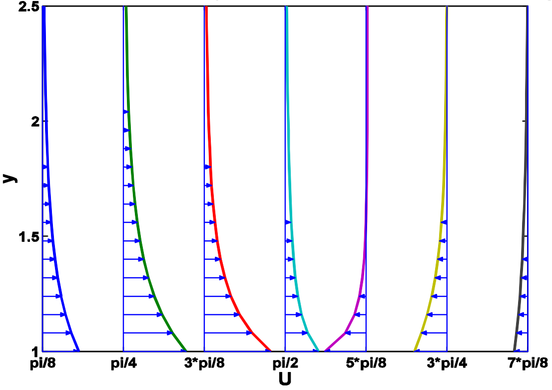

Figure 2. Tangential velocity distribution along the particle

Analysis of the calculations has revealed the following features of the system:

1) very high gradient of anions' concentration (which do not pass through the surface) in a small vicinity of the particle;

2) small changes in concentration at a distance of about 4-5 times the particle's radius;

3) development of vortices behind the particle.

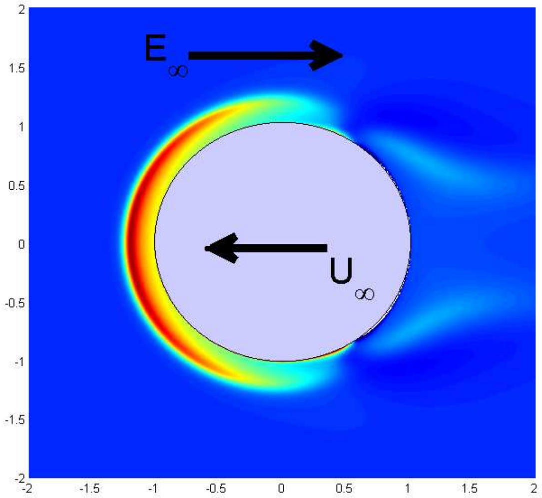

Figure 3. Charge density distribution for $E_\infty = 30$, $\nu = 0{,}001$, $\kappa = 0{,}2$

The calculations have shown a good agreement with theoretical results (see Figure 4).

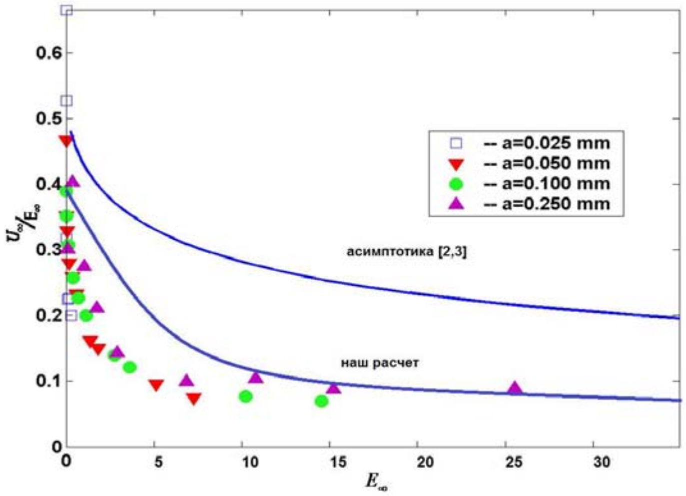

Figure 4. Comparison with analytics

To conclude, a transition from a regular flow to a chaotic one for sufficiently large external fields has been found for the first time in the present work.

Acknowledgements

The work was supported by Russian Foundation for Basic Research, projects No 11-08-00480, 12-08-00924, 12-08-31544.

References

1. *Dukhin S. S.* // Adv. Colloid Interface Sci. 1991. V. 35. Pp. 173–196.
2. *Ben Y., Demekhin E. A., Chang H.-C.* // J. Colloid Interface Sci. 2004. V. 276. Pp. 483–497.
3. *Kalaidin E. N., Demekhin E. A., Korovyakovskiy A. S.* // Doklady Physics. 2009. No. 4. P.210–214.

STRUCTURE OF QUANTUM MECHANICS AND VOLCANO TASK

Konstantin Lebedev, Evgeniy Tymaev, Marina Kyzakina
Kuban State University, Krasnodar, Russia, *E-mail: klebedev@fpm.kubsu.ru;tumayev@phys.kubsu.ru; kuzzyashka@yandex.ru*

Introduction

Interest to Quantum Mechanics (QM) grows in connection with fast development of nanotechnology [1]. For example a researches of transmembrane carry of quantum particles along a molecular chains [2] and a works of creation of quantum computers, descriptions of the phenomena “confiment” in rings, such as ”potentials Hill”. In particular there is the important and difficult Volcano problem [3] which was solved while for the only one electron [4], though greater interest the problem with pair particles “electron-dot” and “electron-electron” represent. The clear and exact understanding of the physical fundamentals QM is possible only on the basis of the axiomatic method. The strict statement of mathematical bases QM has been given in [5]. A bit later the mathematics had included concept of "structure" [6]. In particular the elementary mathematics [7] and some mathematical disciplines [8] can be considered as hierarchies of mathematical structures.

Structure

The QM can be considered, in full conformity with [5, 6] as a structure which consist of two structures QM = {H, A}, here H is a structure of Gilbert space H = { Ψ , $\boldsymbol{C}$, ψ+φ, a·φ, <ψ,φ>, ‖ψ‖}, Ψ – set of vectors above the field complex numbers C with operations of addition ψ +φ vectors and multiplication of vectors a·φ on a numbers, with scalar product <ψ,φ> and norm ‖ψ‖ generated by scalar product. Axioms H are given in [5, 6]. Second structure *A*(H,H) is a structure of linear Hermitian operators A which with ranges of definition and area of values are set of H. The structure *A* is set *A* = {A, A+B, a·A, AB, {A,B}, H, Ut , S } , where A - set of Hermitian operators. In structure A the reflections are contained: A+B addition of operators; a·A - multiplication of operators on numbers of field C, axioms are given in [5, 9]; AB – the multiplication (superposition) of operators which together with A+B submits axioms of associative algebra with unit [5]; {A,B} – the quantum operator of Poisson (containing the h - Planck constant), which together with AB submit to axioms of the Li algebra [5]. Thus the structure A contains i) linear space of associate algebra and ii) Li algebra. The basic physical maintenance of QM is determined by six axioms [10]: 1) State of the quantum system are described by vectors ψ of Gilbert structure H; 2) Dynamic variables (DV) are corresponded to operators of structure A; 3) Results of measurement DV in a state of ψi is an own values ai in equations Aψi = aiψi,; 4) The probability to receive value ai is given by formula P(ai) = |<ψi, ψ>|2; 5) Operators Xj and Pj correspond coordinates xj and impulses pj satisfying to commutative equality {Xj , Pk} = δjk I, where δjk - Kronekera symbol, I - the single operator. The concrete choice of operators (so-called “representation”) can be various, that reflects arbitrariness in a choice of Gilbert basis. So, in the coordinate representation Xj = xj and Pj $= -ih\frac{\partial}{\partial x_j}$. By means of the given axioms the theorem that the average value DV of *A* in a condition ψ is given by formula $\langle A\rangle$ = < ψ, *A*ψ > had been proved [5]. In structure ***A*** there is special operator H - operator Schrödinger, for example, for oscillator $(P^2 + m\varpi X^2)/2m$). Operator U_t is connected with dynamics of system with help of the equation $\frac{dA}{dt} = \frac{\partial A}{\partial t} + \{\mathrm{H}, A\}$ and U_t preserve all operations *A*+*B*, *AB*, {*A*,*B*} in structures that it is automorphism two algebras. The axiom 6) confirms that change of the average value $\langle A\rangle$ in a condition ψ to be given by equation $\frac{d\langle A\rangle}{dt} = \left\langle \frac{\partial A}{\partial t} \right\rangle + \langle\{\mathrm{H}, A\}\rangle$ from which the equation Schrödinger $ih\frac{d\psi}{dt} = \mathrm{H}\psi$ [10] is followed. The spin operator S is entered into structure A [10] else. Further all positions of

QM are developed as the theorems following of the given axioms: the indeterminate relationship is the fundamental fact confirmed experimentally, statements of the theory of representations, etc.

Model and Discussion

To assign a task for quantum object Volcano with free pair particles: “electron-dot” and “electron-electron” in a bidirectional ring which is described by radial potential Volcano $V(r)=\frac{a_1}{\boldsymbol{r}^2}+a_2\boldsymbol{r}^2$, where $\boldsymbol{r}$ – radius-vector of a particle in the polar system of coordinates, a_1, a_2 - parameters of system. Schrödinger H operator for two quantum particles is

$$H(\boldsymbol{r}_1,\boldsymbol{r}_2)=-\frac{h^2}{2m}\nabla^2_{r_1}+V(r_1)-\frac{h^2}{2m}\nabla^2_{r_2}+V(r_2)\pm\frac{e^2}{|\boldsymbol{r}_1-\boldsymbol{r}_2|},\quad \text{where}\quad \nabla^2_r=\left[\frac{1}{r}\frac{\partial}{\partial r}\left(r\frac{\partial}{\partial r}\right)+\frac{1}{r^2}\frac{\partial^2}{\partial\varphi^2}\right]\text{-}$$

Laplas operator in cylindrical coordinates (r,φ); sign plus " + " is for “electron- electron” system, minus " – " for “electron-dot” system. In case of “electron – electron” interaction the weights of particles are identical and Schrödinger operator is invariant concerning rearrangements. Levels of energy for a considered two-partial problem are the solutions of a stationary problem on own values $H\psi(r_1,r_2)=\lambda\psi(r_1,r_2)$. Problem is the differential equation in private derivatives of the second order of elliptic type. In the equation is added the zero boundary conditions on infinity $\psi(r_1,\infty)=\psi(\infty,r_2)=0$. As a result of noted above invariance of operator Schrödinger concerning rearrangements in case of the two-electronics Volcano problem, wave function will possess the certain quality, i.e. will be either symmetric or antisymmetric in relation to rearrangements. The “two-electronic” wave function should be antisymmetric then symmetric wave function $\psi(r_1,r_2)$ correspond singlet spin condition at which spins of electrons are antiparallel. Similarly, antisimmetric wave function correspond triplet spin condition with parallel spins of electrons. For system an “electron-dot” two-partial wave function $\psi(r_1,r_2)$ does not possess the certain parity even for singlet and triplet spin conditions. The potential in Volcano model was successfully used in an explanation experimentally observable biting in oscillators Aaronov – Bom which were experimentally observed in a bidirectional semi-conductor ring [11]. As thickness of a ring is much less, than internal and external radiuses of a ring, in such rings movement electrons along one direction (axis Oz), perpendicular than a plane of the ring is "frozen" in the basic condition in strong superficial potential. Therefore in a plane of a ring bidirectional circulating electronic gas and a problem is formed has two dimensions that allows to hope for reception on occasion analytical decisions of the magnetic moment dependences and the continuous current in a thin ring from cyclotron frequency.

References

1. Surface chemistry and electrochemistry of membranes. New York. 1999. V.75. 1021 p.
2. *Serikov A.A., Xarkenian V.N.* // The theoretical and mathematical physics. V. 78, №1. 1989. P. 116.
3. *Tan W.-C., Inkson J.C.* Phys. Rev. B60, 5626 (1999). 5626-5635.
4. *Margulis V.A.* The magnetic moment of Volcano ring // Physics of a firm body. V. 50. 2008. P. 148-153.
5. *Neumann J*. Mathematical of Quantum Mechanics. Berlin 1932. 368 p.
6. *Bourbaki N.* // Les grands courants de la pensée mathématique. 1948. P. 35-37.
7. *Lebedev K.A.* Architecture of elementary mathematics. Krasnodar. 2000. 34 p.
8. *Lebedev K.A.* Architecture of mathematics. Topology, algebra and the functional analysis. KubGU. Krasnodar. 2001. 18 p.
9. *Trenogin V.A.* The Functional Analysis. M. 1980. 495 p.
10. *Shpolskia E.V.* The Atomic Physics. V.II. M. 1974. 444 p.
11. *Liu J., Gao W.X., Ismail K., Lee K. Y., Hong J. M., Washburn S.* Phys. Rev. B 48. 1993. P. 5148.

ELECTROCHEMICAL PREPARATION OF ELECTRODE COMPOSITE MATERIALS BASED ON PT AND NI: PROPERTIES AND APPLICATIONS IN ELECTROCHEMICAL ENERGETIC

[1]Darya Leontieva, [2]Igor Leontiev, [1]Nina Smirnova

[1]South-Russian State Technical University, Novocherkassk, Russia, *E-mail: da.leontyva@mail.ru*

[2]Southern Federal University, Rostov-on-Don, Russia

Introduction

The development of electrochemical power engineering in many respects depends on advances in the elaboration of active and stable nanomaterials for the cathodes and anodes of devices of energy storage and conversion, such as supercapacitors and fuel cells. The structure and properties of such nanomaterials depend on the way of preparation. Electrochemical methods provides the high active and contamination-free materials.

Low temperature fuel cells (FC), in which the oxidation of hydrogen or simple organic molecules (for example, methanol) occurs on the anode and the reduction of oxygen, on the cathode, are considered highly effective and environment friendly energy sources [1]. Platinum containing metal–carbon composites are the best materials for preparing anodic (Pt-NiO/C) and cathodic (Pt_3Ni/C) catalysts as the constituents of FC [2, 3].

Electrochemical capacitors (also known as supercapacitors), combining the advantages of the high power of dielectric capacitors and the high energy of rechargeable batteries. Currently, the anode material in asymmetric supercapacitors are such materials as composites which consist of conductive carbon black and transition metals oxides (for example NiO/C).

Experiments

Methods for the preparation of NiO/C [4], Pt-NiO/C [5] Pt_3Ni/C [6] electrode materials by the electrochemical dispersion of metals (Ni, Pt and Pt_3Ni alloy) foil under the action of alternating current in alkaline solution were proposed.

For the preparation of NiO/C composite (electrode material for supercapacitors), were used an asymmetric pulse alternating current with the amplitudes ratio of the cathode and anode pulses j_c: j_a = 4:1. A commercial nanosized carbon black powder Vulcan XC-72 was used as a support, which was introduced with stirring into a solution before placing the Ni-electrodes. Introduction of carbon black immediately into the electrochemical cell was found to be of critical importance. It allows obtaining the NiO nanosheets uniformly distributed over the carbon support surface with small or no agglomeration. NiO/C composite

The concentration of NiO in the composite were determined based on the duration of the synthesis, knowing the preliminarily measured rate of the dispersion of electrodes. After the synthesis, the suspension was filtered, and the composites was washed with distilled water to a neutral pH value of wash water and dried at 80°C for 1 h.

As prepared NiO/C composite was used as a support for Pt nanoparticles. For the preparation Pt nanoparticles were used a symmetric pulse alternating current. The result of two step desperation of Ni and Pt foils is Pt-NiO/C composite which could be used as anode electrode material for Direct methanol FC.

Pt_3Ni/C catalyst for cathode material of PEM FC was prepared by electrochemical dispersion of Pt_3Ni alloy foil under symmetric pulse alternating current as in previous case.

Results and Discussion

1. NiO/C composite electrode material

The X-ray diffraction and Raman scattering investigations of the prepared NiO/C composite confirmed the β-NiO crystallites formation. The morphology of synthesized NiO/C can be described as well dispersed on carbon support nano-leaves consisting of tight-packed array of nanoparticles (D111 = 7.7 nm) with 500-2000 nm sheet length and 20 nm thickness. NiO/C composite exhibits the high specific surface area of 137 $m^2 \cdot g^{-1}$ and a micro-meso-macroporous structure with a narrow distribution of the pore size from 1 to 200 nm.

The electrochemical properties of the nanostructured NiO/C was investigated using cyclic voltammetry (CV) and galvanostatic charge-discharge studies. The synthesized NiO/C composite exhibited pseudocapacitive behavior with the mass capacitance value as high as 1012 $F\cdot g^{-1}$ and 750 $F\cdot g^{-1}$ measured from CV and discharge curves, respectively. NiO/C composites could be promising for use as electrode material in supercapacitors.

2. *Pt-NiO/C composite electrode material*

Using X-ray diffraction, scanning electron microscopy investigation was established that Pt-NiO/C catalyst contain β-NiO crystallites (D111 = 7.7 nm) which are agglomerated into thin plates (average size ~ 2000 nm). Pt particles (D111 = 10.6 nm) are uniformly distributed over the surface of the carbon support and the β-NiO plates. Pt-NiO/C as anode catalyst have high electrocatalytic activity toward methanol electrooxidation reaction (more over 30%) than Pt/C catalyst which was prepared in a similar way. So it could be promising for use as anode material in the Direct methanol FCs.

3. *Pt_3Ni/C composite electrode material*

The structural properties of Pt_3Ni/C material were studied using X-ray diffraction analysis and scanning electron microscopy, it was found that the synthesized Pt_3Ni/C catalyst containing the particles of a stoichiometric metal phase of Pt_3Ni (D111 = 9.6 nm) and also Pt_xNi particles ($x > 3$) enriched in platinum (D111 = 8.1 nm). ORR activity of Pt_3Ni/C catalyst was studied in the three-electrode electrochemical cell with rotating disk electrode method. The rate of the oxygen reduction reaction (ORR) at the Pt_3Ni/C higher than at the Pt/C. The presence of Ni in the catalyst reduces the overvoltage of the ORR. Studies of current-voltage and power characteristics of Membrane electrode assemble showed that Pt_3Ni/C catalyst at the cathode are provided to obtain high power density.

References

1. *Barbir, F.,* PEM Fuel Cells: Theory and Practice, New York: Elsevier, 2005.
2. *Gottesfeld, S. and Zawodzinsk, T.A.,* Advnces in Electrochemical Science and Engineering, Alkire, R.C., Gerischer, H., Kolb, D.M., and Tobias, C.W., Eds., Weinheim: Wiley_VCH, 1997. V. 5, P. 195.
3. *Thompsett, D.,* Platinum Met. Rev. 2002. V. 46. P. 3.
4. *Smirnova N.V., Leontieva D.V., Kuriganova A.B.* // RU. Appl. No. 2010140535/02(058106). filed Oct. 10. 2010.
5. *Leont'eva D.V., Smirnova N.V.* // Int. Science J. «Alternative Energy and Ecology». 2012. № 10. P. 59-63.
6. *Smirnova N.V., Kuriganova A.B., Leont'eva D.V., Leont'ev I.N., Mikheikin A.S.* // Kinetics and Catalysis. 2013. N.2. P. 255–262.

THE APPLICATION OF POTASSIUM DICHROMATE TO PREPARE ANISOTROPIC MF-4SC/POLYANILINE COMPOSITES

Natalya Loza, Sergey Dolgopolov, Julia Korshikova, Irina Falina, Sergey Loza, Marina Andreeva
Kuban State University, Krasnodar, Russia, *E-mail: Nata_Loza@mail.ru*

The composites based on the perfluorinated MF 4SC membranes and polyaniline (PAn) have a set of unique electrochemical and optical properties [1]. Nowadays we have methods that have been developed to obtain composites in static conditions and in external electric field [1-3]. Saturation of perfluorinated MF-4SC matrix with phenylammonium ions is the necessary condition for obtaining polyaniline. Subsequently under the influence of initiator the polymerization of aniline is happened. To obtain composites with uniform distribution of the PAn in base polymeric MF-4SC matrix is used ferric chloride (III) or ultraviolet radiation [4]. Materials, in which polyaniline is distributed mainly on the surface of the composite, are obtained by the action of initiators such as peroxydisulphate-, permanganate or dichromate-anionand etc, which are co-ions with respect to the MF-4SC membrane. The most perspective for practice in different devices and electrochemical processes are the anisotropic composites with asymmetric transport properties. However in the presence of peroxydisulphate ammonium the aniline (An) polymerization proceeds both in the membrane phase and in the solution, which leads to contamination of the cell.

The aim of this work is selection of the redox-system, which satisfies the requirement of obtaining an anisotropic composite without a parallel formation of polyaniline in the solution phase. For this aim was the analysis of the series of oxidants formed by ions having the same charge with the sulfonic acid groups in the base matrix: NO_3^-/NH^{4+}, $Cr_2O_7^{2-}/Cr^{3+}$, MnO^{4-}/Mn^{2+}, $SO_3^{2-}/S_2O_3^{2}$, which ranges ΔE from 0.705 V to 1.51 V. Selected initiators were used for obtaining MF-4SC/PAn composites in static conditions in two steps. On the first step the membrane was placed in the 0.01M aniline and 0.01 M HCl solution for the saturation with phenylammonium ions for 10 hours, on the second step - into the equimolar initiator solution for 3 hours.

In the case of using sodium sulfite and sodium nitrate as an initiator of the reaction polymerization of aniline the membrane remained colorless. When using potassium permanganate and potassium dichromate samples acquired green color typical of polyaniline in the emeraldine form. Availability of polyaniline layers on both sides of the membrane was determined visually by microscopic assay of sections with 35 fold magnification. In this study was chosen $K_2Cr_2O_7$ for preparation anisotropic composite MF-4SC/PAn, because in this case polyaniline layer on the composite surface is more homogeneous and coloration is more uniform.

Anisotropic MF-4SC/PAn composites were prepared by the method of successive diffusion polymerizing solutions into the water. Work solutions were 1M An – 0.2M $K_2Cr_2O_7$ and 0.1M An- 0.02M $K_2Cr_2O_7$. The concentration ratio of hydrochloric acid to aniline was 1:1 in all the solutions. Synthesis was carried out in a cell consisting of two chambers of equal size, separated by a polymer film. One of the chambers was filled with polymerizing solution, the other – with distilled water. Synthesis was carried out in two steps, the duration of each step was 60 min. On the first step the membrane was saturated with phenylammonium ions, and on the second step polymerization of aniline was occurred under the dichromate anion action. The kinetic curves of diffusion transfer of acidic $K_2Cr_2O_7$ solution through the membrane is shown in *Fig. 1*.

The diffusion of an acid solution of potassium dichromate is accompanied by the formation of aromatic polyaniline chains in the basic matrix of the membrane and has a two-stage process (*fig.1*). At the first stage (*I*) is a diffusion of $K_2Cr_2O_7$ solution through a membrane that is saturated with phenylammonium ions. The second stage (*II*) is the formation of the barrier PAn layer on the membrane surface. As the result the diffusion rate of the oxidant solution is reduced to 2 and 1.5 times depending on the concentration of polymerizing solutions. Similar effects were observed for the modification of the MF-4SC/PAn in the presence of ammonium peroxydisulphate.

The diffusion permeability of the MF-4SC/PAn composites are decreased as compared with initial membrane in all investigated concentrations (*fig.2, a*). At the same time asymmetry of diffusion permeability was observed on the sample prepared using 0.1M An- 0.02M $K_2Cr_2O_7$ solution. The diffusion permeability decreases with increasing concentration of hydrochloric acid solution (*fig.2, b*). This is adjusting with previous data on the change of the asymmetry effect with the concentration of membranes modified by tetrabutylammonium cations [5].

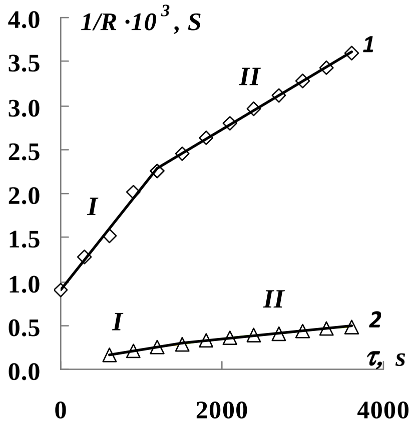

Figure. 1. The kinetics curves of solution conductivity in the chamber with water in the process of solution polymerization initiator diffusion through the membrane MF-4SC into the water 1 – 0.2M $K_2Cr_2O_7$ +3M HCl; 2 – 0.02M $K_2Cr_2O_7$ +0.3M HCl

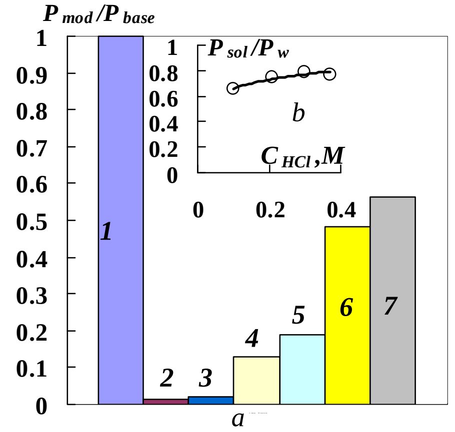

Figure 2. Relative coefficients of diffusion permeability (a) in the HCl solutions depend on orientation composites to the HCl flow: 2, 4, 6 – modified side to the HCl flow; 3, 5, 7 – other side to the HCl flow. 1 – initial MF-4SC; 2, 3 - MF-4SC/PAn -1M An – 0.2M $K_2Cr_2O_7$; 4, 5 - MF-4SC/PAn -0.1M An- 0.02M $K_2Cr_2O_7$; 6, 7 - MF-4SC/PAn –1 M An – 0.5M $(NH_4)_2S_2O_8$[2]. *The relation of diffusion permeability asymmetry coefficient to the HCl concentrations (b) for the MF-4SC/PAn-0.1M An- 0.02M $K_2Cr_2O_7$ composite*

Thus, as initiator of aniline polymerization was selected the potassium dichromate which redox–potential value is softer than ammonium peroxydisulphate. The anisotropic MF-4SC/PAn composites were obtained by the method of successive diffusion of polymerizing solutions with the $K_2Cr_2O_7$. The optimum concentration of the initiator and monomer solutions was found (0.1M An and 0.02M $K_2Cr_2O_7$). It was shown that the diffusion permeability of the composite is significantly reduced in comparison with the initial membrane. The asymmetry effect of the diffusion permeability for the composite depends on the concentration of hydrochloric acid.

The present work is supported by the Russian Foundation for Basic Research (project № 12-08-01092).

References

1. *Berezina N.P., Kononenko N.A., Sytcheva A.A.-R., Loza N.V., Shkirskaya S.A., Hegman N., Pungor A.* // Electrochimica Acta. 2009. V.54. P. 2342-2352.
2. *Berezina N.P., Kubaisi A.A.-R., Alpatova N.M., Andreev V.N., Griga E.I.* // Rus. J. Electrochem. 2004. V.40. P. 286-293.
3. *Shkirskaya S.A., Sytcheva A.A.-R., Berezina N.P., Timofeev S.V., Krishtopa M.V.* Patent RF № 2411070, 10.02.2011.
4. *Berezina N.P., Kononenko N.A., Loza N.V., Sytcheva A.A.-R.* // Rus. J. Electrochem. 2007. V.43. P. 1340-1349.
5. *Gnusin N.P., Berezina N.P., Kononenko N.A.* // Elektrokhimiya. 1987. V. 23. P. 142-146.

---

[2] Diffusion permeability data were obtained by Ph.D. Shkirskaya S.A.

ELECTROCHEMICAL BEHAVIOUR OF THE PROFILED MEMBRANES

Sergey Loza, Natalya Loza
Kuban State University, Krasnodar, Russia, *E-mail: S_Loza@mail.ru*

The current-voltage characteristic of individual membrane can provide information about the electrochemical behavior of ion-exchange materials under the polarization of a constant electric current. Measurement of current-voltage characteristics was performed in a flow cell with platinum polarization electrodes by the method described in [1]. Investigated cation-exchange membrane was separated from the electrode chambers by anion-exchange membranes. The polarizing current was supplied by potentiostat, the membrane potential was measured with silver-chloride electrodes. The working solution was 0.05M sodium chloride.

Profiled membranes were made by the patented method [2] comprising that before pressing the membrane become to a swollen state, thereby reducing the temperature and pressure to eliminate the effect of encapsulation resin grains by the film of inert polyethylene. Profiling membrane in the swollen state under mild conditions can significantly develop their surface (both visible and active) and to increase the electrical conductivity, moisture content and porosity. It should be noted that the improved transport characteristics of the profiled membranes accompanied by an increase of the diffusion permeability which may result in some loss of selectivity.

Figure 1 shows the current-voltage characteristics of the source and the profiled membranes MC-40. Membrane MC-40P has a significant asymmetry current-voltage curves. In case of orientation of the membrane profile to depleted diffusion layer leads to a shift of the potentials of limiting currents to lower values, indicating an increase of mass transfer. It can be assumed that the cause of earlier onset of overlimiting state at such an orientation of the membrane is that the heterogeneity of the surface (geometrical and electrical) creates favorable conditions for the development of conjugate effects of concentration polarization.

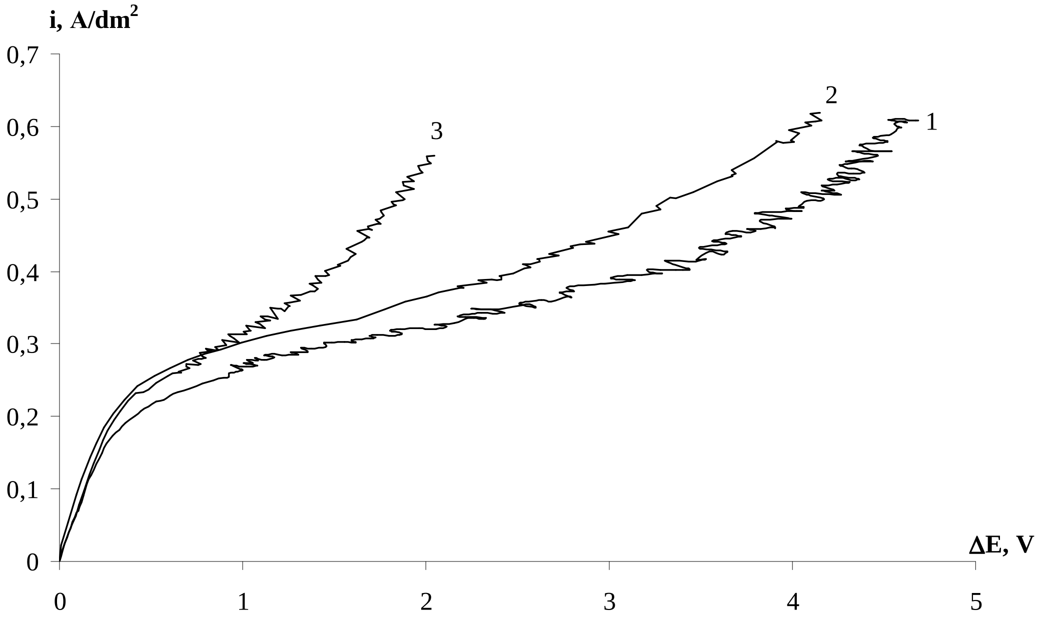

Figure 1. Current-voltage characteristics of ion-exchange membranes in 0.05M solution NaCl (linear flow rate of solution 0.3 cm/c): 1 – MC-40; 2 - MK-40P (profile faces in the concentrate chamber); 3 - MK-40P (profile faces in the diluate chamber)

Moreover, the membrane shows an increase in the limiting current density, which may be due to some reduction in its selectivity. However, it should be noted that in the case it is profiled membranes we can obtain “pseudo limiting” current as the surface area of these membranes is not defined and i_{lim} observed increase may be due to increased work surface of shaped membrane. The current-voltage characteristics shown in Figure 1 are obtained at a relatively low linear velocity of the solution. It can be assumed that an increase in flow rate in several times (up to linear speeds used in electrodialysis apparatus) will cause to increase the difference of overlimiting mass transfer between the smooth and profiled membranes even more.

The obtained samples of the profiled membranes possess a complex mechanical and electrical transport properties which make them promising materials for practical applications in electromembrane devices.

The present work is supported by the Russian Foundation for Basic Research.

References

1. *Loza N.V., Kononenko N.A., Shkirskaya S.A., Berezina N.P.* // Russian Journal of Electrochemistry. 2006. T. 42. № 8. C. 815-822.
2. *Zabolotsky V.I., Loza S.A., Sharafan M.V.* Method of profiling of heterogeneous ion-exchange membranes / Pat. 2284851 Russian Federation, MKI6 B01D61/52. № 2005101531/15; appl. 24.01.2005, publ. 10.10.2006, Bull. Number 28.

ELECTROHYDRODYNAMIC REGULATION OF PH AND ELECTROOSMOTIC VELOCITY IN DISPERSE SYSTEMS

Larysa Lysenko, Nikita Borovitskiy, Nataliya Mishchuk
Institute of Colloid and Water Chemistry, Kyiv, Ukraine, *E-mail: nat_mis@ukr.net*

Introduction

The methods based on the electroosmotic movement of liquid and electromigration of ions are widely used for decontamination of natural and artificial disperse and porous systems from different ionic and nonionic pollutants, stabilization and dewatering of soils and clay minerals, drying of wood, sludge and walls of the buildings, intensification of oil recovery from exhausted oil deposits, extraction useful or harmful admixtures from anthropogenic wastes and so on.

The ability of electrical treatment of different moist disperse and porous systems is substantially limited by accompanying chemical and electrochemical processes, the features of which depend both on the nature of treated dispersions and on the conditions of developed processes. In particular, in a number of investigations it was shown that one of the most important factors, which affect the efficacy of electrical purification and dewatering of different materials, is initial pH of a material, which affects its electrokinetic potential and, correspondingly, the electroosmotic mobility of liquid. However, even if the initial value of pH is favorable for electroosmosis, it can be changed by water electrolysis on electrodes. In this case the electroosmotic mobility of liquid in the region of high pH increases and the region of low pH goes down (Fig.1). From another side, the electrolysis can pay the positive role, since the electrodes as sources of H and OH ions can be used for pH regulation of disperse materials.

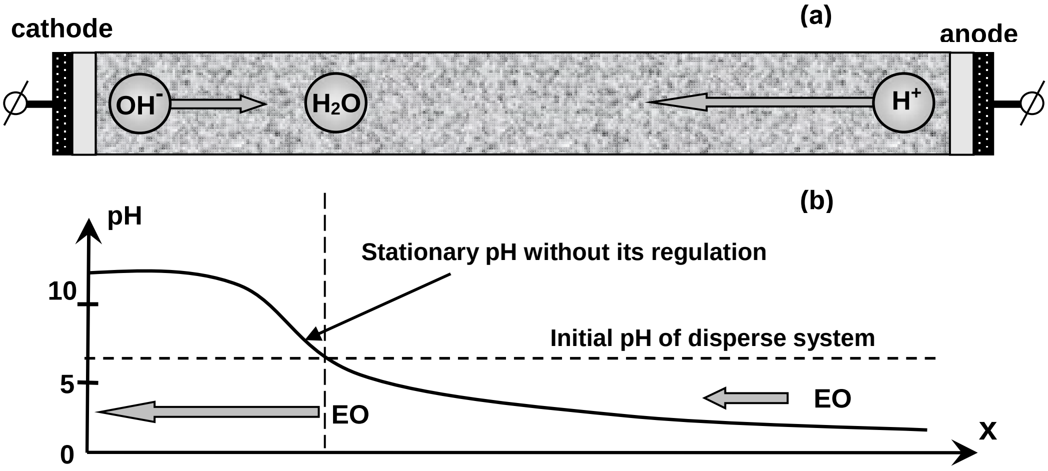

Figure 1. The scheme of ion transport through kaolinite (a) and the change of pH and electroosmotic velocity EO (b) after the treatment of disperse system at constant electric field

Experimental results and discussions

The change of pH is strongly related with ion-exchange capacity of investigated disperse material. As a model system we used kaolinite (the specific surface area is 20m^2/g (argon), and the cation exchange capacity is 0.075 mg-eq/g) the pH regulation and as a result the electrokinetic properties of which depend on unequal conditions for desorption and removal of ions in clay soils. For clay minerals, two types of active sorptive sites can be described on the basis of their location (basal or edge surface of flat clay particles). The first type results from the occurrence of isomorphous substitution of Si^{4+} by Al^{3+} in the tetrahedral sheet. The second type is hydroxyl groups located on undercoordinated structural ions (Si^{4+},Al^{3+}) on broken edges and terraces on clay particle surfaces. Such surface silanol and aluminol functional groups are responsible for the development of a pH-dependent charge in clay minerals. For nonexpendable 1:1 phyllosilicate kaolinite, made of a succession of gibbsite and siloxane sheets, acid–base reactions may also take place on the gibbsite basal planes (Al–O–Al groups).

The electrokinetic potential of kaolinite after regulation of its pH by addition of the necessary amount of NaOH and HCl is shown in Fig. 2 and demonstrates the change of its value and sign. The investigation of electroosmosis at optimum pH value of kaolinite during its electrical treatment demonstrates rather stable electroosmotic velocity and current (Fig. 3), which are required for effective decontamination of disperse system from non-charged pollutants and for its dewatering.

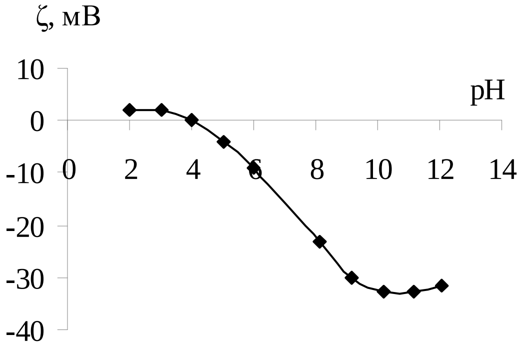

Figure 2. Dependence of electrokinetic potential on pH of pore liquid

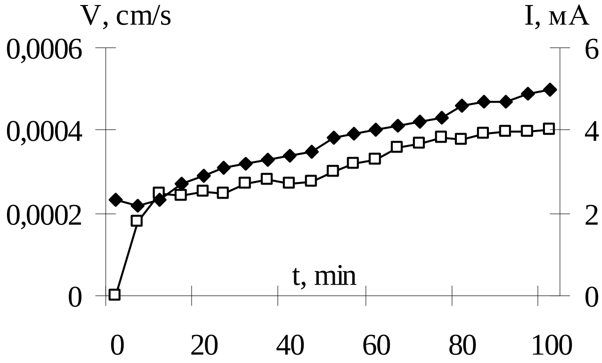

Figure 3. Electroosmotic velocity (◆) and current (□) at treatment of kaolinite. pH = 10,5. E= 3 V/cm

Electrohydrodynamic method of regulation of pH and electroosmotic permeability of moist disperse and porous systems is proposed and theoretically substantiated [1, 2]. The proposed idea is based on the creation of such hydrodynamic conditions, that undesirable ions are removed from given electrode chamber and cannot migrate to the treated dispersion. In the same time in opposite electrode chamber the hydrodynamic conditions must allow the easy movement of the necessary ions to and through a disperse system, creating at its volume the necessary value of pH.

Since the majority of disperse systems have negative surface potential, the maximum electroosmotic velocity can be reached at high pH values. That is why the used technique must support the transport of OH ions and prevent the ingress of H ions into the treated disperse system.

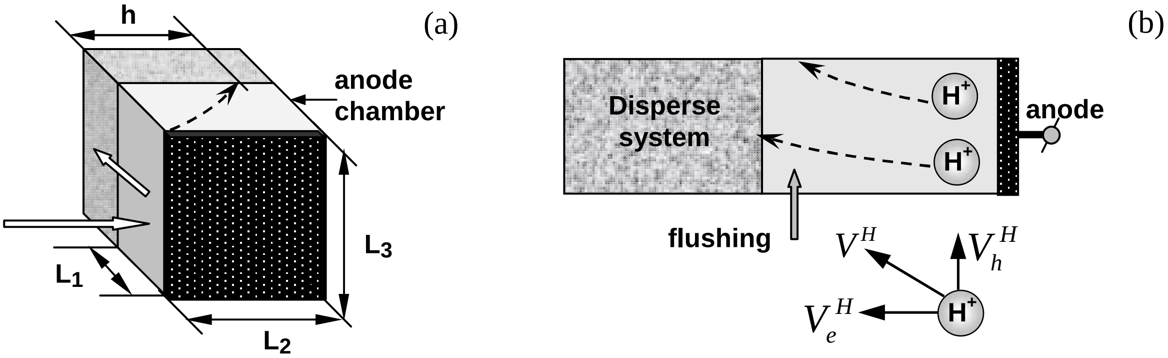

Figure 4. Scheme of anode chamber (a) and ion movement in electric and hydrodynamic fields (b)

The ion movement consists of two components: a) hydrodynamic movement with the velocity of liquid flow v_h along the electrode and b) electromigration perpendicularly to the electrode with the velocity v_e, which is defined by the local electric field strength and electromigration mobility of ions.

H ions definitely do not enter the disperse system, when during the movement of ions from electrodes to the disperse system the hydrodynamic flow through the anode chamber provides their hydrodynamic shifting on the distance h, which is larger than the size of the anode chamber L_2 in the direction of liquid flow: $h > L_2$ or $V_h > FD^{OH} E / RT$ (V_h is the averaged hydrodynamic velocity, F is the Faraday constant, D^H is the coefficient of diffusion of H ions, E is the electric field strength, R is the gas constant, T is the absolute temperature). Correspondingly, the liquid flow through the cathode chamber must be pumped with relatively low velocity at which OH ions are not carried out from a cathode chamber and reach the disperse system. According to the theoretical analysis the critical volume liquid velocities for the anode chambers with account of the experimental cell characteristics is defined as $Q_h^{cr} = (FE / RT) D_H L_2 L_3$ and take values 220 cm^3/h.

The experimental verification of the developed method for argilliferous wastes and different types of soil and the theoretical analysis of the obtained data are conducted. The samples of pH distribution along the disperse system from the cathode to the anode (dotted line shows the initial value of pH) and dependence of electroosmotic velocity through disperse system on the time, counted from the beginning of treatment, are shown in Figs. 4 a, b.

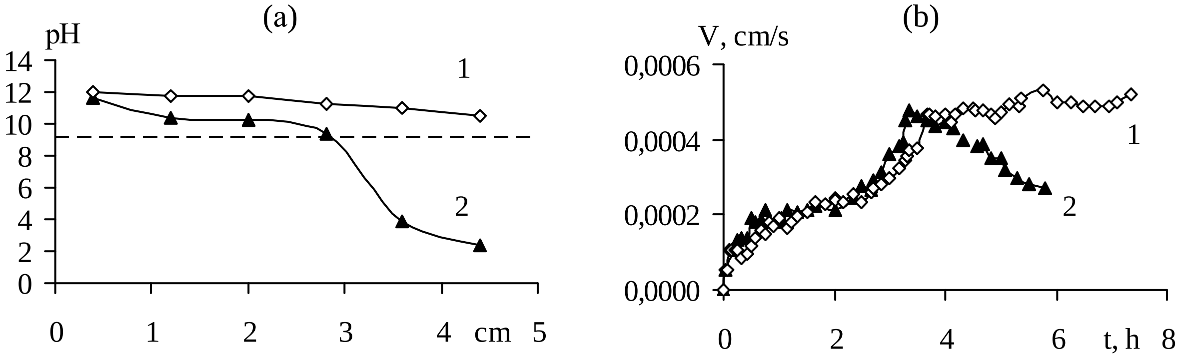

Figure 5. Distribution of pH in kaolinite in the direction from cathode to anode (a) and dependence of electroosmotic velocity on the time (b) without (curves 1) and with (curves 2) pH regulations

E = 3 V/cm, the thickness of treated kaolinite layer - 4.5cm, 1- liquid velocity in anode and cathode chambers - 30 cm^3/h, 2 - liquid velocity in anode and cathode chambers 250 cm^3/h and 30 cm^3/h, correspondingly. Dashed line shows the initial pH of dispersion

In the first case (curves 1) the investigation was conducted at the flushing velocities lower than critical values, i.e. without pH regulation. In the second case (curves 2) the conditions for the reduction of pH were created. The obtained experimental data corroborated the performed theoretical calculations. The obtained pH profiles correspond to the estimated ones: in the first case the velocity of electroosmosis decreases up to its complete cessation; in the second case due to the low pH at the anode region the velocity demonstrate the tendency to its reduction; in the third case high pH values provide maximum and stable velocity of electroosmosis.

The influence of surfactants on the electroosmotic mobility of non-charged contaminants was also analyzed. It is shown that the efficiency and the regulation rate of pH and electroosmotic permeability strongly depend not only on different characteristics of disperse or porous systems (total exchange and buffer capacities of materials, its porosity and initial surface potentials and pH), but also on the treatment mode.

References

1. *Lysenko L.L., Mishchuk N.A.* // Colloids and Surfaces, A. 2009. V. 333. P. 59-66.
2. *Lysenko L.L., Mishchuk N.A.* // J. Water Chemistry Technology. 2009. V. 31. P. 245-261.
3. *Lysenko L.L., Mishchuk N.A., Rynda E.F.* // J. Water Chemistry Technology. 2011. V. 33. P. 243-255.

2D SIMULATION OF THE CHRONOPOTENTIOMETRIC CURVES FOR A HETEROGENEOUS MEMBRANE SYSTEM AND MAPPING THE DISTRIBUTION OF POTENTIAL IN SPACE

[1]Semyon Mareev, [1]Mahamet Urtenov, [1]Anna Kovalenko, [1]Victor Nikonenko, [2]Christian Larchet
[1]Kuban State University, Krasnodar, Russia; *E-mail: semyon-mareev@bk.ru*
[2]Institut de Chimie et des Matériaux CNRS - Université Paris-Est, Thiais, France

Introduction

It is known, that analysis of chronopotentiograms gives an important information about the mechanisms of ion transport in the membrane and in the adjacent diffusion boundary layers [1, 2]. In this paper we propose a 2D simulation of the chronopotentiometric curves based on the numerical solution of unsteady transport equations to show the effect of membrane surface heterogeneity on the electric current and concentration distribution near the interface.

Theory

We consider time-dependent model of ion transport through the membrane separating two identical solutions of single electrolyte. The system under study consists of a heterogeneous membrane with two adjacent diffusion boundary layers (DBLs) and the two mixed solutions with a constant bulk concentration. The transport of ions in the DBLs is described by the Nernst-Planck and material balance equations. A new variable, the current function, η, is introduced via the current density $\vec{I}$:

$$\frac{\partial \eta}{\partial x} = I_y , \ \frac{\partial \eta}{\partial y} = -I_x$$

This definition of the function η constrains the current density to satisfy the charge conservation (continuity) equation:

$$\frac{\partial I_x}{\partial x} + \frac{\partial I_y}{\partial y} = 0$$

The use of the new function allows essential simplification in the formulation of the 2D mathematical problem.

Results and discussions

The distribution of the concentration near the membrane surface and the current streamlines are presented in Fig. 1. In the case of the heterogeneous surface, the current lines are distributed nonuniformly over the membrane surface: they are concentrated in the regions with good conductivity (Fig. 2b). The solution near the conductive part is more diluted (a), but due to the tangential current (b), the decrease in the average limiting current density is not so great: it is equal to 2.8 mA cm^{-2} in the case of full conductive surface and to 2.5 mA cm^{-2} in the case where only a half part of the surface is conductive. As a consequence of non-uniform current distribution, the local current density through the conductive regions is higher, in comparison with the case of homogeneous interface and the same average current density. Hence, if the DBL thickness is the same in two systems under comparison, the concentration polarization of the heterogeneous membrane is higher: the interface concentration near the conductive regions is lower and the potential drop is greater. The results of comparing the calculated chronopotentiometric curves for the case of homogeneous and heterogeneous membranes is presented in Fig. 2. Curve 1 is the result of the calculation for the case of homogeneous membrane with the DBL thickness δ=240 microns, and curve 2 is calculated for the case of heterogeneous membrane. The DBL is the same in both cases, the size of the conductive part is 40 microns and the nonconductive one is 200 microns.

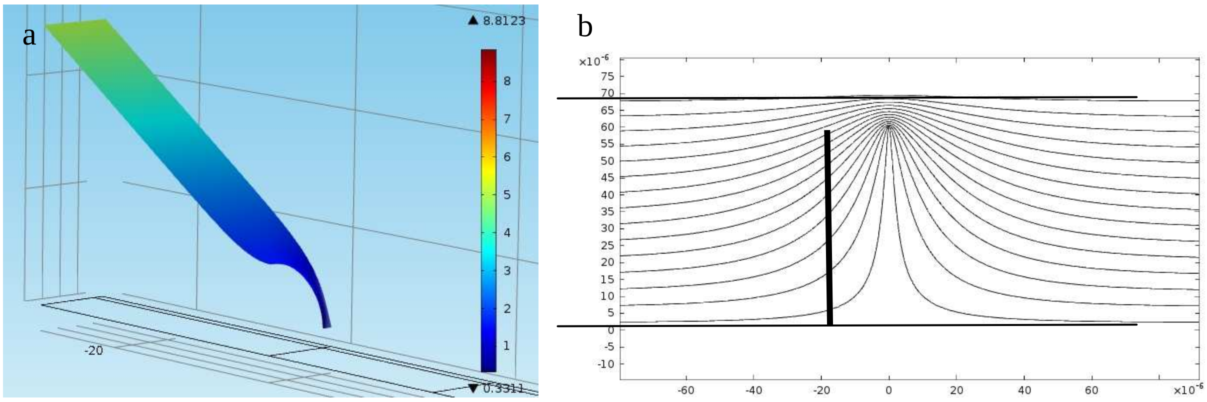

Figure 1. The concentration distribution in the left (depleted) DBL (a) and electric current streamlines (b) near heterogeneous membrane surface

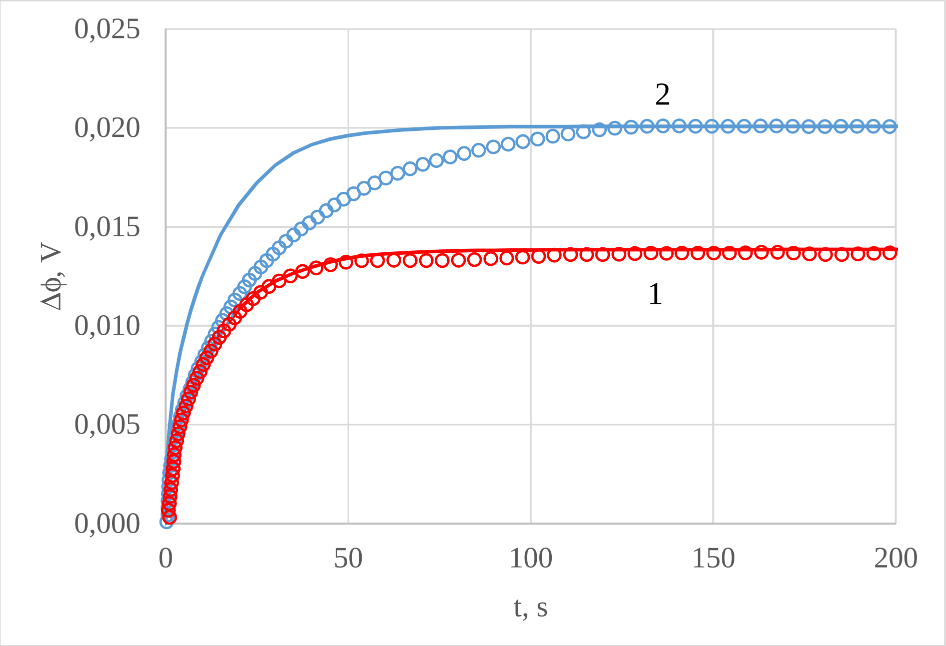

Figure 2. Experimental (points) and calculated (lines) chronopotentiometric curves of the membrane AMX (1) and MA-40 (2) in a 0.1 M NaCl solution at a density of DC $i = 5$ *mA cm*$^{-2}$

Acknowledgments

Part of the work was carried out within the framework of joint French-Russian laboratory “Ion-Exchange Membranes and Related Processes”. The authors are grateful to the CNRS, RFBR (Grant No. 12-08-93108-NCNIL-a, 12-08-00188-a, 13-08-01168), and FP7Marie Curie Actions “CoTraPhen” Project PIRSES-GA-2010-269135.

References

1. *Belova E.*, Lopatkova *G.*, *Pismenskaya N.*, *Nikonenko V.*, *Larchet Ch.*, *Pourcelly G.* Effect of Anion-exchange Membrane Surface Properties on Mechanisms of Overlimiting Mass Transfer // J. Phys. Chem. B. 2006. V. 110. P. 13458-13469
2. *Larchet C.*, *Nouri S.*, *Auclair B.*, *Dammak L.*, *Nikonenko V.* Application of chronopotentiometry to determine the thickness of diffusion layer adjacent to an ion-exchange membrane under natural convection // Adv. Colloid Interface Sci. 2008. V. 139. P. 45-61

THE EQUILIBRIUM OF ORNITINE AND LYSINE SORPTION BY CATION-EXCHANGE MEMBRANE

Nina Maygurova, Anastasiya Sholokhova, Tatiana Eliseeva, Elena Krisilova
Voronezh State University, Voronezh, Russia, *E-mail: nina.vsu@gmail.com*

Introduction

Membrane methods are the most promising for the separation of amino acids. Electrodialysis with ion-exchange membranes can be used for the concentration, purification and extraction of amino acids from various solutions. Knowledge of ion-exchange membranes' sorption characteristics is required to optimize the parameters of electrodialysis. Studies of amino acids' sorption are very important for the description of their mass transfer processes in membranes [1-2]. At the same time published data on amino acids sorption by ion-exchange membranes are limited [3-4]. The aim of this work is to study sorption characteristics of cation-exchange membranes Fumasep® FTCM in the solutions of ornitine and lysine hydrochlorides.

Experiments

The objects of this study are amino acids – lysine (2,6-diaminohexanoic acid) and ornitine (2,5-diaminopentanoic acid) as well as heterogeneous sulfocation-exchange membrane Fumasep® FTCM (produced by "Fuma-Tech", Germany).

The solutions of lysine and ornitine are analyzed by the method of photometry based on cooper complexes formation [5]. The membranes are prepared and converted into H^+-form according to the procedure described in [6].

Amino acids sorption by membrane is studied in the static conditions. The initial concentrations are 0.10 and 0.02 mol/dm^3. The membrane peaces immersed in amino acid solution are shaked, and the samples are taken and analyzed periodically. The amount of absorbed amino acid is calculated from the changes in its concentration in solution. The kinetic curves are presented in the coordinates of the process completion degree (F) as a function of time (t).

Sorption isotherms are measured by the method of variable concentrations. The absorbed amount of the amino acid is determined from the change in its concentration in the solution. The distribution coefficient (K_d) for the system cation-exchange membrane – amino acid solution is calculated as the ratio of amino acid concentrations in the membrane and in the solution.

Results and Discussion

The kinetic curves of basic amino acids' sorption on FTCM membrane are shown in the Figure 1.

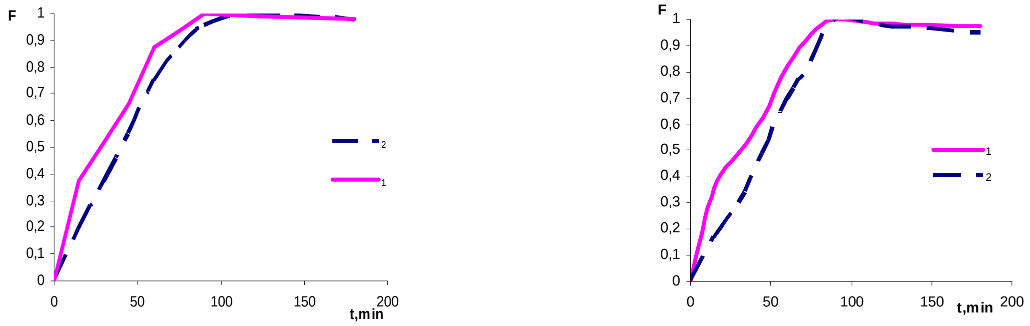

a *b*

Figure 1. Kinetic sorption curves: a – ornitine hydrochloride sorption b – lysine hydrochloride sorption (1- c=0.10M; 2 – c=0.02M)

The dependencies are of saturation curves type. The equilibrium in the both systems ornitine and lysine solution – the Fumasep FTCM membrane is reached in circa 90 minutes.

It is found that the sorption isotherms of aliphatic basic amino acids are of S-shaped form and can not be described by the Langmuir equation. The maximum capacity of sorption was 1.94 and 1.95 mmol / g for ornithine and lysine, respectively.

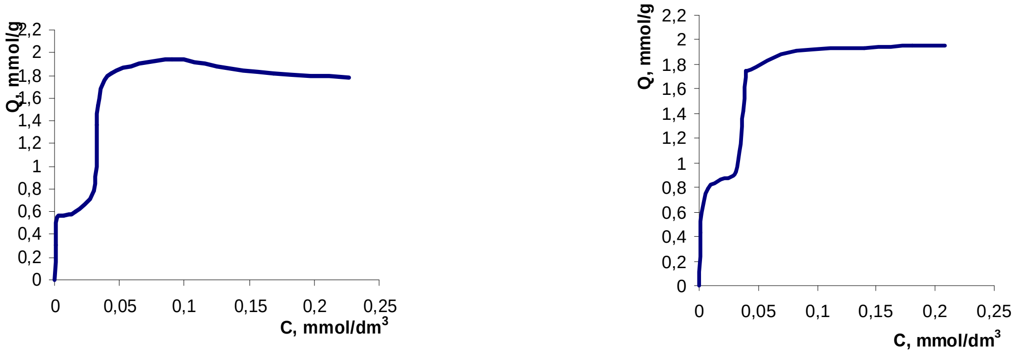

a *b*

Figure 2. Sorption isotherms for the cation- exchange membrane Fumasep ® FTCM a) ornithine hydrochloride and b)-lysine hydrochloride

Total exchange capacity of the membrane is not reached at low equilibrium concentrations, this may be due to the fact that basic amino acid in the acidic solution exists as a doubly charged ion, wherein two amino groups are protonated and each one can react with a fixed group. The competing sorption of hydrogen ions along with amino acid ions is also possible. At higher equilibrium concentrations total exchange capacity is fully realized, as the hydrogen ions sorb less than the amino acid.

The equilibrium distribution coefficients determining the affinity of membrane to amino acid are presented in Figure 3 as a function of equilibrium concentration.

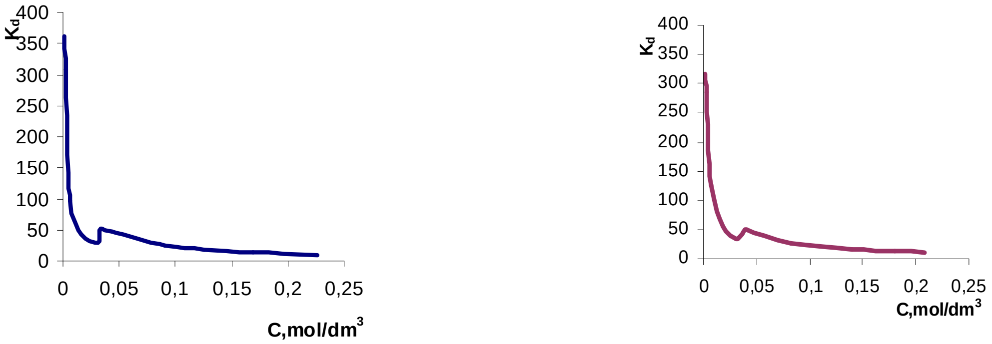

a *b*

Figure 3. The dependence of the distribution coefficient for ornithine monohydrochloride (a) and lysine monohydrochloride (b) on the equilibrium concentration

The distribution coefficients fall with an increase of the equilibrium solution concentration because of the saturation of the ion-exchange active sites as well as swelling decrease and free water amount decline in membrane phase. Changes of hydration are confirmed by the data if IR-spectroscopy.

This work was supported by Russian Ministry of Education and Science in the frame of scientific project № 11.7136.2013.

References

1. *Timashev S. F.* Physicochemistry of Membrane Processes. Moscow: Khimiya, 1988. 240 p.
2. *Zabolotskii V.I., Nikonenko V.V.* Ion Transfer in Membranes. Moscow: Nauka, 1996. 392 p.
3. *Kikuchi K. et al.* // J. Chem. Eng. Jap. 1994, V. *21*. P. 391-398.
4. *Gotoh T., Kikuchi K.* // Bioseparation. 2000, V. *9*. P. 37-41.
5. *Roshal E.R. et al.* // Russian Chem.-Pharm. J. 1988. V. *6*. P. 30.
6. *Berezina N.P. et al.* Physicochemical Properties of Ion-Exchange Materials: Practical Course, Krasnodar: Kuban. Gos. Univ., 1999.

USE OF CONDUCTIVITY AS A MONITORING PARAMETER IN ION-EXCHANGE BASED TECHNOLOGIES OF AMMONIUM REMOVAL

Andriy Malovanyy, Myroslav Malovanyy
Lviv Polytechnic National University, Lviv, Ukraine, *E-mail:mmal@polynet.lviv.ua*

Introduction

Removal of ammonium from municipal wastewater using ion-exchange processes is a perspective way of recovering nitrogen from waste streams which allows further its use as a valuable product. In such technologies spent ion exchange material can be used directly as a fertilizer [1] or be regenerated with salt solution with further its processing in order to get fertilizer with higher nitrogen content. Regenerant treatment technologies include pH elevation followed by ammonia stripping [2,3] or precipitation as struvite in REM NUT process [4]. For all the named technologies it is important to detect the breakthrough of ammonium ions in order to assure high efficiency of wastewater treatment. The aim of this work was to assess the possibility of using conductivity measurement as a tool for detecting ammonium breakthrough.

Experiments

Three laboratory scale ion exchange columns, filled with strong acid cation (SAC) resin KU-2-8, synthetic zeolite NaA and natural zeolite of clinoptilolite type, were used in this study. Experiments were done using real pretreated municipal wastewater and synthetic wastewater with ammonium concentration ranging from 26.6 to 40.4 mg NH_4-N/dm^3 and pH in the range 7.35-7.77.

Electric conductivity was measured in inflow (EC_{in}) and outflow (EC_{eff}) of ion exchange columns in a number of runs. Ammonium concentration in the outflow was analyzed spectrophotometrically.

Results and Discussion

It was observed that the outflow EC was always lower than in inflow using any type of ion exchange material. This is explained by different conductance of ions involved in ion exchange. The parameter that representsthe contributions to the total solutionconductivity made per mole of eachion present in aninfinite dilution is known as a limiting molar ionic conductivity λ^0. Limiting molar ionic conductivities of Na^+, NH_4^+, Ca^{2+} and Mg^{2+} at 25 °C are 50.1, 73.5, 106.0 and 119.0 S·cm^2/mol[5]. When 1 meq/L of NH_4^+, Ca^{2+} or Mg^{2+} ions changes for Na^+ in ion exchange column, conductivity should drop by 23.4, 2.9 or 9.4 µS/cm respectively. However, these valuescannot be expected to obtain precisely in experimental conditions, since the criterion of infinite dilution was not met and temperature was not 25 °C. EC_{eff} was stable until breakthrough and with rise of ammonium concentration it increased correspondingly. Such behavior was observed for all of the materials. Initial drop of conductivity (EC^0) was different in all cases when different ion exchange materials and wastewater types were used because the concentration of ammonium and other ions was different as well.

For experiments with SAC resin EC drop, recalculated per 1 mmol NH_4-N removed, was in the range 26.7-28.4 S·cm^2/mol. These values are higher than 23.4 S·cm^2/mol which shows than not only ammonium, but other ions (including Ca^{2+} and Mg^{2+}) are removed from wastewater. If selectivity of SAC resin was the same for all the ions that are removed from wastewater, then change of conductivity per 1 mmol NH_4-N removed would be constant and coefficient k_{EC} would be equal to 1 in equation:

$$C_{eff} = k_{EC} \frac{EC_{eff} - EC^0}{EC_{in} - EC^0} \cdot C_{in} \tag{1}$$

whereC_{in} and C_{eff} – concentrations of ammonium in inflow and outflow.

However, when data of 5 runs (with both synthetic and real wastewater as inflow) was plotted on single graph (Fig. 1), coefficient k_{EC} was determined to be 0.65. Lower value of k_{EC} can be explained by different breakthrough of ammonium and other ions. With equation 1 and determined coefficient k_{EC} ammonium concentration in the effluent from the SAC resin column can be predicted using conductivity measurements. The coefficient k_{EC} is expected to be different for different wastewater, where the main influence should have the ratio between concentration of ammonium and other ions in it.

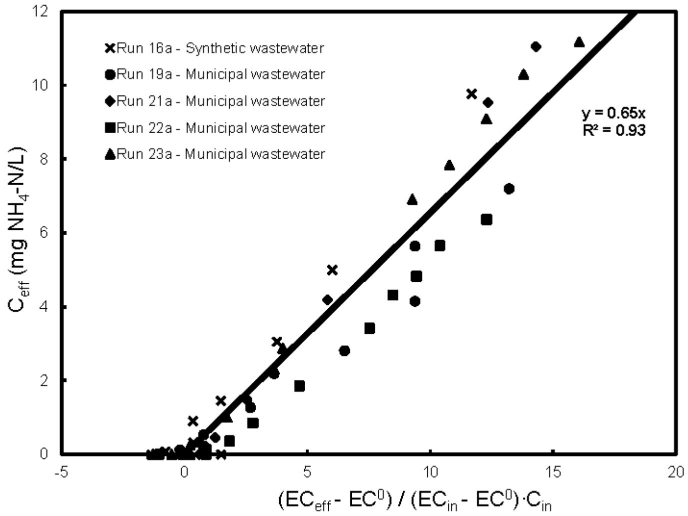

Figure 1. Correlation of EC and effluent ammonium concentration in experiments with SAC resin

References

1. *Strelcov O.A.* Use of clinoptilolite to improve the properties of mineral fertilizers. Conference “Application of natural zeolites in animal and plant”, Tbilisi, Georgia, 1984:P.243.
2. *SuhrL.G.* Experience with ammonia removal by selective ion exchange and closed-cycle air stripping regenerant renewal. International Seminar on Control of Nutrients in Municipal Wastewater Effluents, California, USA, 1980: pp. 137–184.
3. *RahmaniA.R., SamadiM.T., EhsaniH.R.* Investigation of clinoptilolite natural zeolite regeneration by air stripping followed by ion exchange for removal of ammonium from aqueous solutions. Iranian Journal of Environmental Health Science & Engineering. 6 (2009) 167–172.
4. *Liberti L., Petruzzelli D., De Florio L.* REM NUT ion exchange plus struvite precipitation process. Environmental Technology. 22 (2001) 1313–24.
5. Coury L., Conductance Measurements Part 1 : Theory. Current Separation. 18 (1999) 91–96.

INFLUENCE OF COUNTERION HYDRATION ON DEVELOPMENT OF ELECTROCONVECTION IN MEMBRANE SYSTEMS

[1]Nadezhda Melnik, [1,2]Ekaterina Belashova, [1]Natalia Pismenskaya, [1]Victor Nikonenko, [2]Philippe Sistat, [2]Gerald Pourcelly
[1]Kuban State University, Krasnodar, Russia, *E-mail: v_nikonenko@mail.ru*
[2]European Membrane Institute, CNRS - Université Montpellier 2/ENSCM, Montpellier, France,
E-mail: gerald.pourcelly@univ-montp2.fr

Introduction

It is known that electroconvection can significantly increase the mass transfer of salt ions in overlimiting currents modes. This work is aimed at better understanding of the effect of the counterion mobility and its hydration degree on the patterns of electroconvection at ion exchange membrane/solution boundary in intensive current modes.

Experiments

Overlimiting behavior of a Nafion 117 membrane is studied in LiCl and KCl electrolyte solutions. Some characteristics of electrolytes are given in the table.

Table. Some characteristics of the studied electrolytes [1]

Electrolyte	Electrolyte diffusion coefficient at infinite dilution, D, 10^5, $cm^2\ s^{-1}$	Transport number at infinite dilution		Hydration number (primary hydration shell)		Radius of the hydrated ion, nm	
		Cation, t_+	Anion, t_-	cation	anion	cation	anion
KCl	1.99	0.49	0.51	1.9	2.3	0.24	0.12
LiCl	1.37	0.33	0.67	7.0	2.3	0.13	0.12

The Nafion 117 membrane is known as a homogeneous cation exchange membrane characterized by a low rate water splitting (generation of H^+ and OH^- ions) at overlimiting currents. This membrane is pre-operated under current for 25-30 hours. A Nafion 117 forms a desalting channel with an anion exchange MA-40PM membrane, which is a heterogeneous membrane specially modified in order to suppress the function of H^+ and OH^- ions generation.

The studies were carried out in a four-chamber flow-thruogh electrodialysis cell [2] with the polarized membrane surface area 4 cm^2, the intermembrane spacing 0.65 cm and the linear flow velocity of solution 0.4 cm/s. The limiting current density (when assuming the absence of electroconvection), $i_{lim\ theor}$, was calculated with help of the convection-diffusion model. [3].

Results and Discussion

As it might be expected, the transition from LiCl to KCl is accompanied by an increase in the experimental limiting current, which is determined by the intersection of the tangents to the initial and the plateau regions of the current-voltage curves, CVC (Fig. 1). This increase is due to higher values of the diffusion coefficient and the transport number of the K^+ ion compared to the Li^+ ion (Table). The limiting current densities found from the experiment are 10-20% higher than the values calculated using the convection-diffusion model. Electroconvective vortices deliver a more concentrated solution from the bulk to the membrane surface and partially remove diffusion restrictions in the studied system. Dilution of the solution leads to increase in the experimental limiting current and reduction of the CVC plateau length (Fig. 2), eventually because of higher thickness of space charge region at the membrane surface.

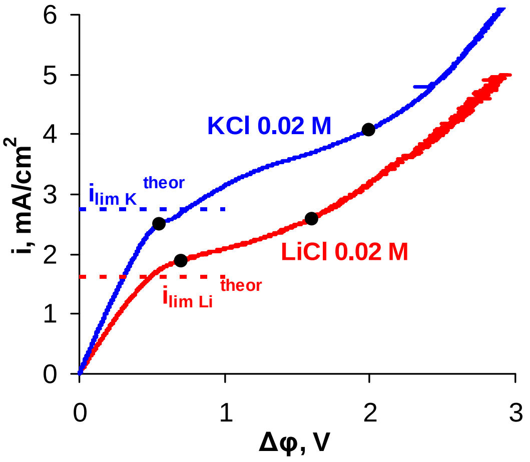

Figure 1. Current-voltage curves of the Nafion 117 membrane in 0.02 M LiCl and KCl solutions. The points delimit the sloped plateau

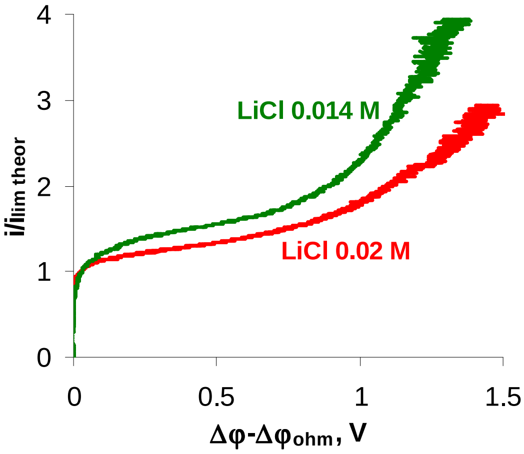

Figure 2. Reduced current-voltage curves of Nafion 117 membrane in 0.02 M and 0.014 M LiCl solutions

The effect of electroconvection on the CVC and chronopotentiograms (ChP) is more prominent in case of LiCl solutions compared to KCl solution. One of the evidences of this fact is the reduction of the plateau region length in the CVC of the Nafion 117/0.02 M LiCl system (Fig.1) compared with the Nafion 117/0.02 M KCl system. The difference in the ChP form is another manifestation of a more important role of electroconvection in the case LiCl. An inflection point appears in the initial part of ChP of Nafion-117 in 0.02 M KCl when the ratio $i / i_{\text{lim theor}} = 0.9$ (Fig. 3). This point shows transition from one ion transfer mechanism (controlled by diffusion) to another one (controlled by current induced convection) in the system. However, this point does not exist in the case of 0.02 M LiCl at the same ratio $i / i_{\text{lim theor}}$ (Fig. 3). A possible reason for this is the development of electroconvection locally already at very low values of potential difference. Namely, oscillations on the ChP curve for LiCl are seen at rather small values of the corrected potential difference $\Delta\varphi'$ ($\Delta\varphi' = \Delta\varphi - \Delta\varphi_{\text{ohm}}$, where $\Delta\varphi_{\text{ohm}}$ is the initial ohmic potential drop) (Figs. 3, 4). In the system with KCl, oscillations appear at much higher values of $\Delta\varphi'$. First, single potential oscillations are observed (better seen in the case of LiCl). They transform into regular and then into irregular oscillations, according to te theory by Rubinstein and Zaltzman.

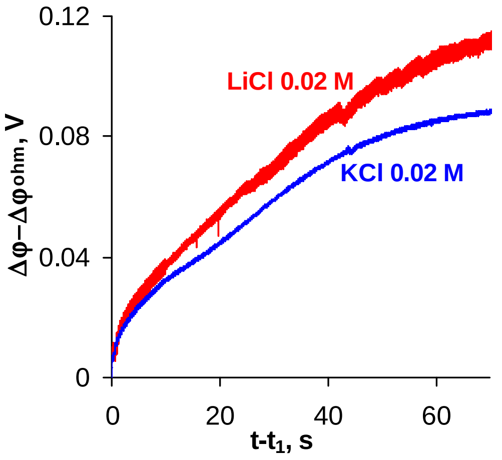

Figure 3. Initial part of chronopotentiograms of a Nafion 117 membrane in a 0.02 M LiCl and KCl solutions at $i/i_{\text{lim theor}}$=0.9

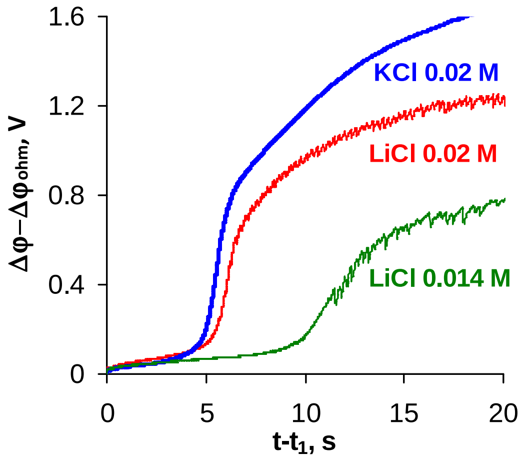

Figure 4. Initial part of chronopotentiograms of the Nafion 117 membrane in KCl (0.02 M) and LiCl (0.02 M and 0.014 M) solutions at $i/i_{\text{lim theor}}$=2.2

More intensive electroconvection in LiCl solutions leads to decrease of $\Delta\varphi'$ under the same ratio $i/i_{lim\ theor}$ (Fig. 4). The observed differences in the electrochemical behavior of the studied systems are due to the fact that the Li^+ ion is higher hydrated than the K^+ ion (Table). The higher hydration number (and the bigger Stokes radius), the greater volume of fluid in the solution space charge region is involved in movement.

Acknowledgments

Part of the work was carried out in accordance with the cooperation programme of International Associated French-Russian Laboratory "Ion-Exchange Membranes and Related Processes" The authors are grateful to the CNRS, RFBR (Grant No. 12-08-31535mol_a) and FP7 Marie Curie Actions "CoTraPhen" Project PIRSES-GA-2010-269135.

References

1. *Robinson R.A., Stokes R.H.* Electrolyte Solutions. Butterworths: London. 1968. 571 p.
2. *Belova E.I., Lopatkova G.Yu., Pismenskaya N.D., Nikonenko V.V., Larchet Ch., Pourcelly G.* The effect of anion-exchange membrane surface properties on mechanisms of overlimiting mass transfer // J. Phys. Chem. B. 2006. V 110. P. 13458-13469.
3. *Gnusin N.P., Zabolotsky V.I., Nikonenko V.V., Urtenov M.Kh.* Convective-diffusion model of electrodialytic desalination *// Elektrokhimiya* 1986. V. 22. P. 298

BILAYER ION EXCHANGE MEMBRANES FOR SELECTIVE NITRATE TRANSFER

[1]Stanislav Melnikov, [1]Aslan Achoh, [1,2]Victor Zabolotsky
[1]Kuban State University, Krasnodar, Russia
[2]LLC «Innovative Enterprise «Membrane Technology», Krasnodar, Russia

Introduction

The demineralization of whey is considered as one of the most promising application of membrane electrodialysis. The main task of electrodialysis treatment of whey is the removal of mineral salts to demineralization degree of 70-90%. Membrane electrodialysis allows the highly effective purification of liquid food products, significantly improving their characteristics and ensuring the toxicological safety.

Excessive levels of salts in food products cause undesirable changes in their quality that can cause serious poisoning of consumers. Ions responsible primarily include sodium cations, chloride and sulfate anions and, especially, nitrate ions. Nitrate ions are carcinogens; hence, their levels in products, first of all, in products for child nutrition, are strictly regulated.

The main goals of whey treatment with electrodialysis is the adjustment of salt balance (balance of sodium ions, chlorides, dihydrophosphates and sulfates) of final product and removal of dangerous for a human health nitrates.

Experiments

Among entire assortment of anion exchange membranes, the most readily available on Russian market are heterogeneous anion exchange membranes MA-40, MA-41, manufactured by JSC "Shchekinoazot" (Russia), and Ralex AMH-PES, manufactured by JSC "Mega" (Czech Republic). The electrochemical characteristics of the chosen membranes are represented in Table 1.

Table 1. Electrochemical properties of original heterogeneous anion exchange membranes

Type	MA-40	MA-41	Ralex AMH-PES
Use	Electrodialysis	Electrodialysis	Electrodialysis
Ion exchange groups	$\equiv N^+, =N^+, -N^+$	$R-N^+(CH_3)_3$	$R-N^+(CH_3)_3$
Inert binding	polyethylene	polyethylene	polyethylene
Reinforcing cloth	Nylon 6	Nylon 6	Polyethersulfone
Thickness (mm) **dry** **swollen**	0,3÷0,5	0,3÷0,5	max. 0,45 max. 0,75
Resistance **surface ρ_n, Ohm·cm²** **specific ρ, Ohm·cm**	< 10,0 < 150	< 10,0 < 150	< 7,5 < 120
Counterion transfer number (1,0/0,5 M NaCl)	> 0,94	> 0,94	> 0,95
Hydrodynamic permeability, mL/(h·m²)			0
Ion exchange capacity, mmole/g	4÷5	1,4	1,8

To study the separation of ions with same charge magnitude (chloride and nitrate) with industrial and developed developed membranes, the electrodialyser with two chamber elementary cell, membrane stack of which was composed with interchanging anion exchange membranes (both commercial and developed for this research) and MK-40 cation exchange membranes, was used. Characteristics of said module are represented in Table 2.

Table 2. Characteristics of laboratory electrodialysis module

Type of elementary cell	Two-chamber
Number of elementary cells	10
Solution flow	Parallel
Type of membranes	
anion exchange membranes	MA-41, Ralex AMH, MA-41C*
cation exchange membranes	МК-40
Material of	
anode	ruthenium oxide coated titanium
cathode	stainless steel
Dimensions of polarized area in channel	
length	400 mm
width	100 mm
height	0,9 mm

* MA-41 membrane with cation exchange MF-4SC coating on one side.

To prevent the membrane incurvating caused by the pressure difference in the chambers and to increase the limiting electrodiffusion current density (as a result of the decrease of diffusion layer thickness by the membranes) the chambers were supplemented with net-type separator-turbulator. The free, not occupied by the spacer volume of each camera was 80% of its total volume.

Linear flow velocity in concentration and desalination chambers was kept constant and equal to 30 L/h; in electrode compartments – sufficient to remove gases produced during exploitation.

The studies were conducted with sodium chloride solution, concentration of which was10 g/L, and with sodium chloride / sodium nitrate (5 g/L / 5 g/L) mixed solutions. This way the molar ratio was 1:1,75.

The concentration of studied ions was determined using ion exchange chromatography with simultaneous detection of all ions of interest in one sample.

Results and Discussion

The results of electrodialysis desalination study of sodium chloride solution show that all the studied anion-exchange membrane possess relatively close properties. Results exhibited by Ralex AMH membranes are slightly better, that can be explained by the higher fraction of its conductive surface compared to MA-41. MA-41C exhibits slightly worse properties (fig. 1), its differential current efficiency is 10-20% lower compared to not modified membranes (fig. 2). It seems that this effect is caused by the damping of both diffusion and migration mechanisms of anion transfer through the cation exchange film at the anion exchange membrane surface.

At the same time, integral current efficiency calculated using the starting and finish points of process are 0,94; 0,88 and 0,87 for the Ralex AMH, MA-41 and MA-41c membranes, respectively (fig. 2). Hence, in the chosen experimental conditions the modified membrane is almost identical to not modified ones, allowing its future use in electrodialysis.

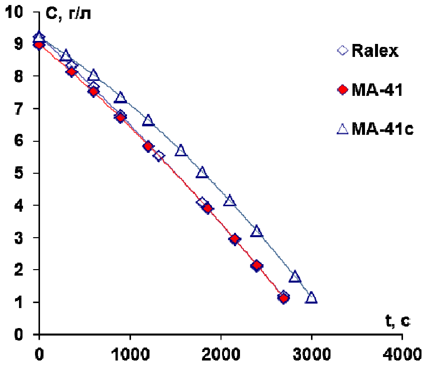

Figure 1. Dependence of sodium chloride concentration in studied solution on the duration of electrodialysis process for the studied membranes

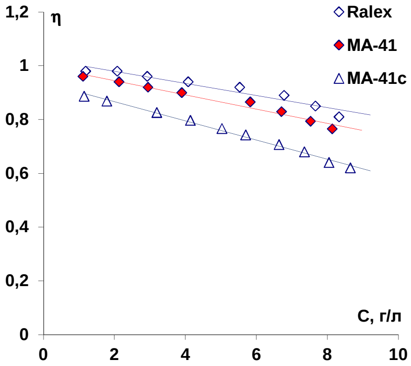

Figure 2. Dependence of current efficiency on the sodium chloride concentration in the studied solution

During treatment of chloride/nitrate mixture, some drop in current efficiency by chloride ions can be seen for all investigated membranes (fig. 3*a*). This effect appears due to presence of two anion types in the solution, so a concurrent transport of both species is observed during the experiment. This effect appears especially strong in the case of developed membrane MA-41C, that happens due to its higher selectivity towards nitrate ions compared to other membranes (fig. 3*b*).

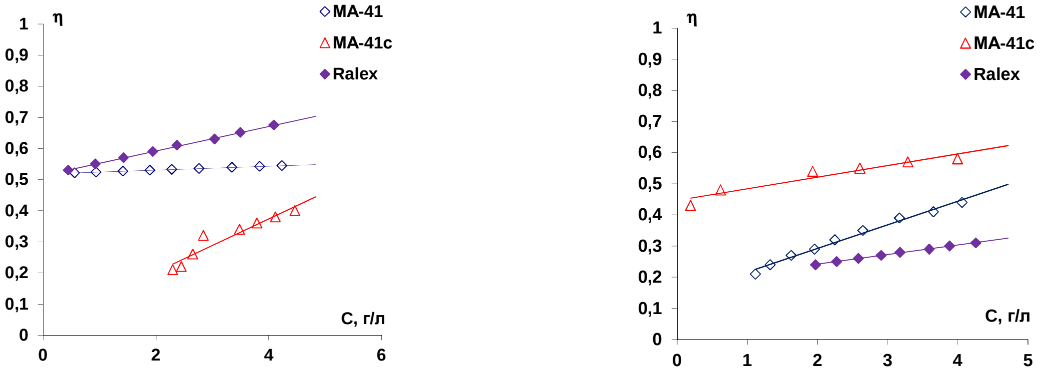

a *b*

Figure 3. Current efficiency by chloride (a) and nitrate (b) ions in the chloride/nitrate mixture

This selectivity increase happens due to change in hydrophilic-hydrophobic balance of the developed membrane surface, according to [1]. Increase in hydrophobicity facilitating the transfer of less hydrate anions (nitrates).

However, such membrane (MA-41C) allows treating only mixtures with high concentration of components. From the data obtained in the experiment it can be seen, that summary transport numbers of chloride and nitrate ions becomes lesser than 1 when chloride concentration becomes lesser than 2,1 g/L and nitrate concentration – 0,2 g/L. In this conditions the summary transport number equals to 0,64. From the data obtained earlier for asymmetric bipolar membranes in such conditions water dissociation products transport numbers can be 0,5-0,6 at the same current density which was used in the experiment in the present work.

Acknowledgements

The reported study was partially supported by Russian Foundation for Basic Research, research projects No. 11-08-708 00718-a, 12-08-31277-mol_a.

References

1. *Sata T.* // J. Membr. Sci. 2000. Vol. 73. P. 1–31.

CO-ION LEAKAGE THROUGH BIPOLAR MEMBRANES. INFLUENCE ON CURRENT-VOLTAGE CHARACTERISTICS AND WATER SPLITTING EFFICIENCY

[1]Stanislav Melnikov, [1]Nicolay Sheldeshov, [1,2]Victor Zabolotsky
[1]Kuban State University, Krasnodar, Russia
[2]LLC «Innovative Enterprise «Membrane Technology», Krasnodar, Russia

Introduction

High influence of bipolar membrane (BPM) monopolar layers thickness on its selectivity had been shown recently [1]. This fact is nontrivial in relation to monopolar ion exchange membranes as their selectivity does not depend on the thickness. At the same time increase or decrease in the thickness of BPM monopolar layers can increase products purity, or on the contrary, combine ion transport and pH shift functions. This work is aimed at studying the influence of co-ion leakage through a BPM on two of the essential membrane characteristics: current-voltage characteristic (CVC) and current efficiency of water dissociation.

Experiments

To study the effect of cation-exchange layer thickness on the electrochemical and transport characteristics of BPM asymmetric bipolar membranes with cation-exchange layer (CEL) thickness of 30 μm were investigated. Anion-exchange layer thickness remained equal to 450 μm. Ralex AMH-Pes was used as an anion-exchange layer and Nafion™ type membrane as an cation -exchange layer. The procedure used for creation of these membranes is described in [2].

The current-voltage characteristics measurements were carried out in a electrochemical cell with working membrane surface of 2.27 cm^2 in the HCl | BPM | NaOH system. Cation-exchange layer was facing towards the cathode and was washed in acid, and anion-exchange layer was facing towards the anode and was washed in alkali. The concentration of all solutions was 0,01, 0,1 and 0,5 M. For the measurement of current-voltage curves (CVC) Luggin-Haber capillaries connected to Ag/AgCl electrodes were used. In the present study dynamic method was used for measuring the current-voltage characteristic of asymmetric bipolar membranes. Linearly increasing and decreasing current was applied to the cell and CVC recorded. Current sweep rate was set at 2×10^{-5} A/s that gives a minimal hysteresis sweep between forward and backward CVCs. Transport numbers of co-ions (Na^+ and Cl^- ions) were measured by the modified Hittorf method [3]. The essence of the method is to determine the total flux of sodium cations into the acid from alkali and total flow of chlorine anions into the alkali from acid.

Results and Discussion

The CVCs measured in various conditions for studied membrane shows that asymmetric bipolar membrane withoiut any type of catalyst introduced into its bipolar region shows very low water splitting activity. Also oa ohmic region on the general CVC can be seen in solutions with concentrations of 0,1 and 0,5 M. Its presence shows that a high co-ion flux through membrane is observed. The shift of the potential at zero current from zero value for the VCV measured in 0,01 M solutions is due to non-equilibrium water dissociation potential usually observed on BPMs. Its theoretical value can be calculated from Nernst relation:

$$\Delta\varphi_{eq} = \frac{2{,}3RT}{F}\left(pH^{alkaly} - pH^{acid}\right) \quad (1)$$

That gives 0,51 V for the case of 0,01 M solutions. This value is very close to the experimentally obtained 0,48 V.

The shifts of said potential in case of higher concentrations of acid and alkali solutions occurs due to Donan potential drop across bipolar region, which produce some small electrical potential shift at zero current depending on the ion concentration of the external solutions.

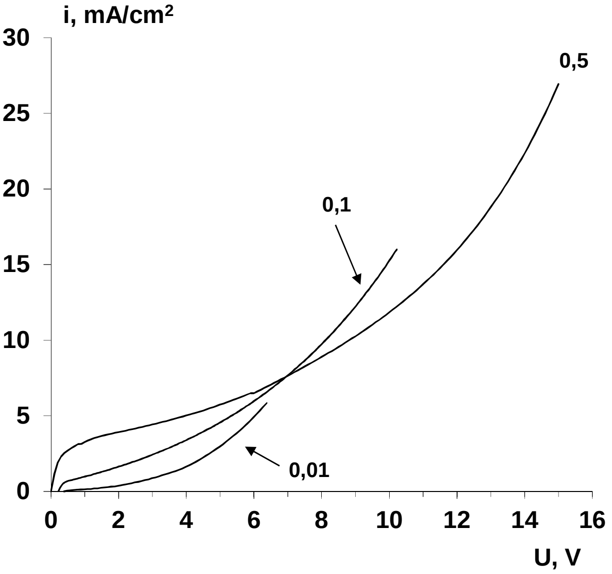

Figure 1. Current-voltage curves of asymmetric bipolar membrane with CEL thickness of 30 μm in solutions with various concentrations. Numbers near curves – concentrations of acid and alkali solutions

The water splitting potential, i.e. potential at which water splitting reaction starts, is basicly the same for 0,01 and 0,1 M solutions, but slightly increases in the case of 0,5 M solution. This can be explained as follows, diffusion of chloride anions to bipolar border reduces the electric field strength and BPM water splitting capability.

Sodium ion leakage through the AEL of the BPM, characterized by its transport number remains constant at 3±2 % in all investigated systems, because sodium ion transport is completely determined by AEL properties which are the same (Table).

On the contrary, the amount of chloride ion leakage through the CEL is significant. It is therefore reasonable to assume that Cl^- ion transfer across the CEL becomes a rate-limiting step.

Table. Electromigration transport numbers

Concentration	0,01	0,1	0,5
t_{Cl^-}	0,07±0,02	0,17±0,02	0,22±0,02
t_{Na^+}	0,04±0,02	0,02±0,02	0,03±0,02
t_{H^+/OH^-}	0,86±0,02	0,81±0,02	0,76±0,02

It is also interesting to note that, with increasing concentration of the external solutions, electromigration transport numbers of co-ions and water dissociation products through the membrane is virtually unchanged (fig.2). For example, the electromigration transport number of hydrogen and hydroxyl ions with increasing solutions concentration from 0.01 M to 0.5 M decreases from 0.86 to 0.82. In solutions with concentration of 0.5 M at low current densities water dissociation doesn't occur in bipolar region and the asymmetric bipolar membrane behaves as monopolar one, however, at current density of 10 mA/cm^2 transport numbers of hydrogen and hydroxyl ions are 0.4, while in the more dilute solutions at the same current density they are equal to 0.7-0.9. It can be concluded that at high current densities, concentration of the external solution does not matter but at the same time, current density at which water dissociation plays a significant role in the overall mass transfer increases with the concentration of the external solutions.

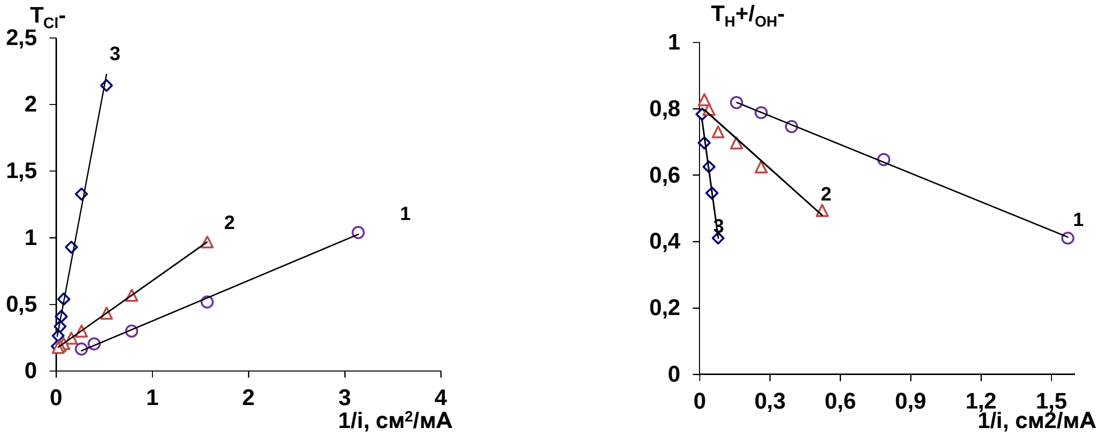

a *b*

Figure 2. Transport numbers of chloride ion (a) and water dissociation products (b) vs. Reversed current density. Concentration of acid and alkali solutions equals to, M: 1 – 0,01, 2 – 0,1, 3 – 0,5

It is also worth noting, that in solutions with higher concentration (0,5 M) the effective transport number exceeds 1. This suggests that a significant role of co-ion diffusion in the overall transport through bipolar membrane. Hence, one can obtain such experimental conditions when such membranes are capable of simultaneous ions removal and water splitting process.

Acknowledgments

The reported study was partially supported by Russian foundation for basic research, research projects No. 11-08-00718-a, 12-08-31277-mol_a.

References

1. *Wilhelm F.G.* // J. Membr. Sci. 2001. Vol.182. P.13.
2. *Melnikov S.S.* // Condensed matter and interphases 2010. №2. P.143.
3. *Sheldeshov N.V., Zabolotskii V.I., Shadrina M.V., Solov'eva M.V.* // J. applied. chem. 1990. Vol.63. №4. P.892.

DECREASE OF MINERAL FOULING AND INTENSIFICATION OF DEMINERALIZATION PROCESS BY APPLICATION OF PULSE ELECTRIC FIELD WITH SHORT PULSE/PAUSE CONDITIONS

[1]Sergey Mikhaylin, [2]Victor Nikonenko, [3]Gérald Pourcelly, [1]Laurent Bazinet
[1]Institute of Nutraceuticals and Functional Foods (INAF) and Dairy Research Center (STELA)
Université Laval, Sainte-Foy, Canada
[2]Kuban State University, Krasnodar, Russia
[3]Institut Européen des Membranes, Université Montpellier 2, Montpellier, France

Introduction

Electrodialysis (ED) is widely used in modern industrial processes such as demineralization of water, concentration, purification and modification of food, production of acids and bases. ED allows increasing the product quality with decreasing the costs. However, fouling on the ion-exchange membranes decreases the effectiveness of ED [1]. Recently it has been found that application of pulse electric field (PEF) can decrease membrane fouling [2, 3]. Thus, the objective of this research is to study the influence of special regimes of PEF on the membrane fouling and effectiveness of the demineralization, in order to find the best conditions of PEF.

Experimental methods

The electrodialysis cell was a Microflow-type cell described by Cifuentes-Araya et al. [3]. ED was carried-out in batch process at a constant current density of 40 mA/cm^2. The model salt solution was composed of Na_2CO_3 (1000 mg/L), KCl (800 mg/L), $CaCl_2$ (800 mg/L) and $MgCl_2$ (452 mg/L) in order to respect a Mg/Ca ratio of 2/5 [3]. The model salt solution was prepared just before the beginning of ED process. The ED treatments were stopped after the maximum voltage capacity of the power supply was reached (62.5 V) [3]. To find the optimal PEF conditions the following regimes were performed: T_{on}/T_{off}=3s/1s (PEF ratio 3), T_{on}/T_{off}=2s/0.67s (PEF ratio 3), T_{on}/T_{off} =1s/0.33s (PEF ratio 3), T_{on}/T_{off} =3s/0.3s (PEF ratio 10), T_{on}/T_{off} =2s/0.5s (PEF ratio 4) and T_{on}/T_{off} =1s/1s (PEF ratio 1). Four repetitions were carried-out for each PEF condition. After ED treatment, membrane thickness and fouling content were determined. On a 4-cm^2 dried membrane sample, electron microscopy photographs and X-ray elemental analysis were taken on the CEM and AEM surfaces in contact with the concentrate and diluate solutions in order to visualize the presence or not of fouling.

Results and discussion

Concerning the demineralization rate (DR) it can be seen that the optimum is at T_{on}=2s and there are no significant difference between both treatments at T_{off}=0.67s and T_{off}=0.5s (Fig.1).

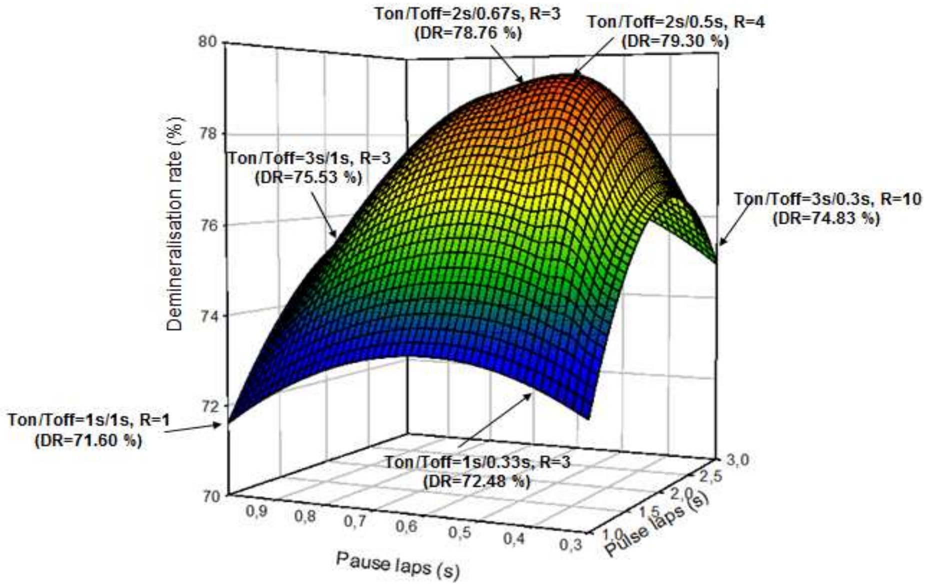

Figure 1. Demineralization rate in the different PEF conditions

Application of PEF regimes with T_{on}=1s decreased DR of approximately 7 units of percentage with no real difference according to the pause lapse duration (T_{off}=1s and T_{off}=0.33s). Increase of PEF modes to 3s/1s and 3s/0.33s led to similar intermediary DRs values around 75 %.

The good effectiveness of PEF modes with T_{on}=2s is presumably related to the special frequencies which accelerate the mass transfer from the bulk solution to the membrane surface decreasing the concentration polarization (CP).

Additionally, for the conditions 2s/0.67s et 2s/0.5s it was noted that the fouling on the CEM consisting principally of $Mg(OH)_2$. For other PEF conditions the presence of $CaCO_3$ and $Mg(OH)_2$ was detected. Moreover, quantities of CEM fouling observed for all T_{on}/T_{off} modes were less than the ones in previous studies. It is important to mention, in this study, the absence of fouling on the AEM for all PEF conditions. This absence of fouling on the AEM represents an important improvement comparing with all other studies in the literature.

Thereby, the results of the present work demonstrated the success in the intensification of the demineralization process by decreasing the membrane fouling. The best condition among the six conditions tested were T_{on}=2s with the highest DR.

Acknowledgements

This investigation was realized partly within French-Russian laboratory "Ion-exchange membranes and related processes".

References

1. *L. Bazinet, D. Montpetit, D. Ippersiel, J. Amiot, F. Lamarche* // J. Colloid Interface Sci. 237 (2001) 62-69.
2. *B. Ruiz, P. Sistat, P. Huguet, G. Pourcelly, M. Araya-Farias, L. Bazinet* // J. Membr. Sci. 287 (2007) 41–50.
3. *N. Cifuentes-Araya, G. Pourcelly, L. Bazinet* // J. Colloid Interf. Sci. 361 (2011) 79.

ESTIMATION OF CONTACT ANGLES FOR THE NUMBER OF FLUOROPOLYMER MEMBRANES

[1]Ekaterina Nazyrova, [1]Svetlana Shkirskaya, [1]Ninel Berezina, [1]Victoriya Ganych, [2]Sergey Timofeev
[1]Kuban state university, Krasnodar, Russia, *E-mail:* ninel_berezina@mail.ru
[2]JSC «Plastpolymer», St.-Petersburg, Russia

Introduction

The purpose of this work was comparison of contact angles of the number of composite membranes which are made on the basis of fluoropolymer membranes and various modifying agents. As it is well known the measurement of contact angles allows to receive valuable information about hydrophilic and hydrophobic properties of surface of polymeric films. Preparation of the nanocomposite materials on the basis of modifiered perfluorinated MF-4SC membranes lead to formation of anisotropic samples which have different properties in volume of the polymer due to modifying agents. It results in different values of transport properties and electrochemical characteristics depending on the direction of the transferable ions fluxes. Estimation of hydrophilic and hydrophobic properties of the polymeric film surface can be carried out by means of the known technique of contact angles measurement [1].

The contact angle θ or cos θ is the characteristic of hydrophilicity (hydrophobicity) membranes surface. It is defined as angle between the tangent AB (fig. 1a) which has been drawn to a surface of wetting liquid and the wetted surface of solid body AA, at that θ is always counted from tangent towards a liquid phase. The tangent is drawn across the point of three phases contact: solid phase (membrane), liquid (distilled water) and gas (air).

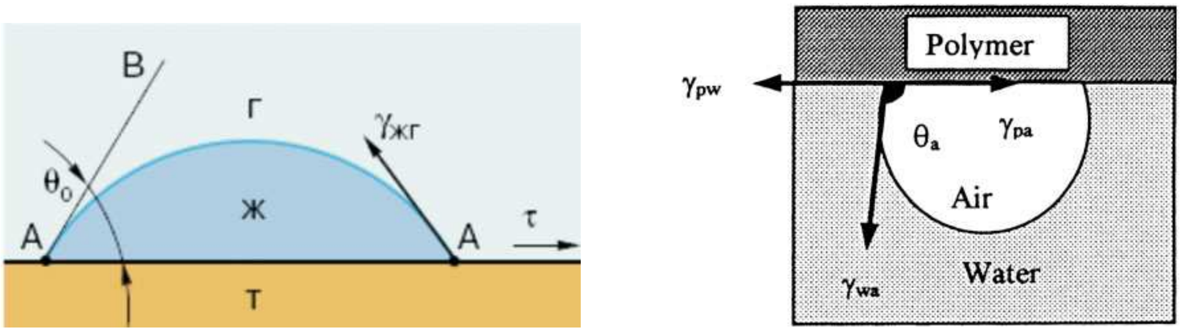

a *b*

Figure 1. Sessile Drop Method (a): Contact Angle θ_0 of Liquid Drop on Solid Surface; the Third Phase is Gas; Captive Bubble Method (b)

Experiments

The anisotropic composites obtained from modification of MF-4SC membrane by various modifying agents (F-4SF, MF-4SC (batch 29), MF-4SC/PAn, MF-4SC/Ag, MF-4SC cast film, MF-4SC cast film after modification by carbon nanotubes) were objects for comparison of contact angles.

The captive bubble method was used in this work (fig.1 b). The basic components of the installation are the cathetometer, measuring cell and the lighting device providing the contrast image of drop and studied surface. Measurements of contact angles were made in the three phase system consisting of water, a surface of membrane and a bubble.

Results and Discussion

Table 1 presents contact angles values measured during the course of this study. Contact angles for the studied membranes have close values from both sides. The exceptions are F-4SF and MF-4SC/CNT membranes which are connected with conditions of its preparation. It may be noted that membrane MF-4SC (s. 29) has higher contact angles in comparison with uncharged F-4SF film.

Table 1. Results of contact angles definition of the fluoropolymer membranes

Fluoropolymer membranes	Production conditions	cos θ		θ	
		1 side	**2 side**	**1 side**	**2 side**
F-4SF	The hydrophobic fluoropolymer film which doesn't contain sulfo-groups ("Plastpolymer", St. Petersburg)	-0,175 ± 0,03	-0,260 ± 0,04	100º	105º
MF-4SC (b.29)	The perfluorinated sulfocation membrane ("Plastpolymer", St. Petersburg)	-0,312 ± 0,03	-0,314 ± 0,04	108°	108°
MF-4SC/PAn	The composite obtained by sequential diffusion method of aniline on acid and $(NH_4)_2S_2O_8$ oxidant [2]	-0,370 ± 0,01	-0,394 ± 0,05	112°	113º
MF-4SC/Ag	The composite obtained by chemical reduction method of metallic silver from $AgNO_3$ and $C_6H_5NH_3NO_3$ solutions [3]	-0,262 ± 0,01	-0,278 ± 0,03	105°	106°
MF-4SC cast film	The membrane obtained from mixture of liquid MF-4SC ("Plastpolymer", St. Petersburg)	-0,306 ± 0,01	-0,286 ± 0,03	108°	107°
MF-4SC cast film/CNT	The membrane obtained from mixture of liquid MF-4SC containing carbon nanotubes ("Nanotechcentre", Tambov)	-0,314 ± 0,02	—	108°	—

This indicates on the hydrophilicity of its surface due to the presence of sulfo-groups. Modification of this membrane with polyaniline leads to increase of the contact angle due to surface distribution of polyaniline aromatic chains. At the same time distribution of metallic silver particles in the MF-4SC membrane has resulted in decrease of angle θ approximately on 3º from both sides because of covering of the surface with more hydrophobic metallic particles.

Thus the surfaces of polymer films studied have own microrelief which is characterized by the respective value of the contact angle.

The present work was supported by the Russian Foundation for Basic Research

References

1. *Roldugin V.I.* Physics and chemistry of a surface. TSUP Intelligence. 2008. P.568.
2. *Berezina N.A., Kononenko N.A., Filippov A.N., Shkirskaya S.A., Falina I.V., Sycheva A.A.-R.* Electrotransport properties and morphology of MF-4SC membranes after surface modification with polyaniline // Russian J. Electrochem. 2010. V. 46. № 5. P. 485.
3. *Blinova N., Stejskal J., Trchova M., Sapurina I., Ciric-Marjanovic G.* The oxidation of aniline with silver nitrate to polyaniline-silver composites // Polymer. 2009. V. 50. P. 50-56.

EFFECT OF DIFFUSION LAYER THICKNESS ON THE ELECTROLYTE PERMEABILITY OF A NAFION MEMBRANE

Ekaterina Nevakshenova, Elizaveta Korzhova, Victor Nikonenko
Kuban State University, Krasnodar, Russia. *E-mail: lizelotavocal@mail.ru*

Introduction

In view of the multiple applications of membrane technologies in recent years, there is a need in development of new ion-exchange membranes with more specified properties. To predict their characteristics, it is necessary to improve understanding of the impact of structural and kinetic parameters of the membranes upon their transport behavior in separation processes.

Theory

A non-stationary multi-layer model [1], which takes into account the membrane, the adjacent diffusion layers and bulk solutions, is considered. The ion and water transport in the membrane and the adjacent diffusion layers are described by the Kedem-Katchalsky equations. The phenomenological coefficients for these equations are found by using the microheterogeneous model [2, 3].

Experiments

The study was carried out in NaCl solutions with a Nafion-117 membrane, which underwent a heat pretreatment in order to increase the pore size. The ion exchange capacity, the sorption isotherm (Fig.1), the concentration dependence of specific electrical conductivity (Fig.2) and the diffusion permeability (Fig.3) of the membrane were measured in different experiments. We have measured also the dependence of the diffusion permeability on the diffusion layer thickness (Fig.4) The results of measurements were used to find the parameters of the microheterogeneous model: the volume fraction of the inter-gel solution, f2, the Donnan constant, KD, the diffusion coefficients of counter-ions, D1, and that of co-ions, D2, as well as the structural parameter □□

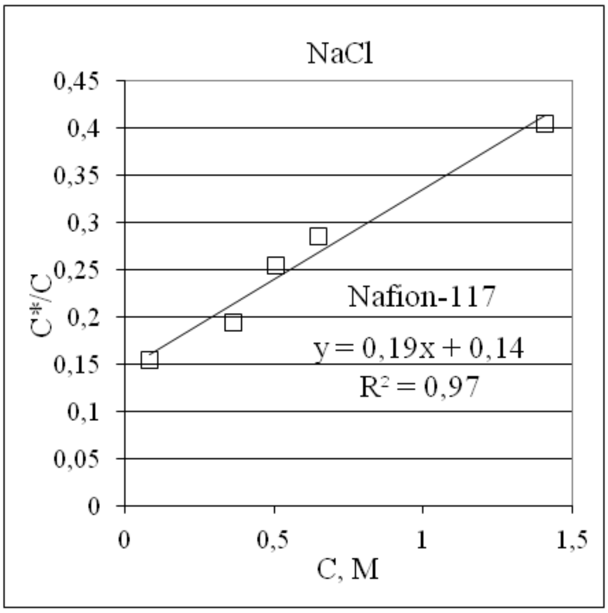

Figure 1. Sorption isotherm of Nafion-117 / NaCl

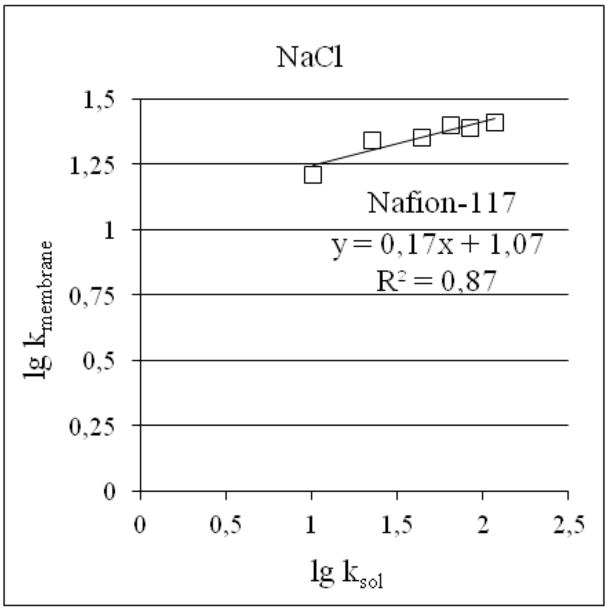

Figure 2. Logarithm of the Nafion-117 conductivity as a function of the logarithm of NaCl solution conductivity

The parameters (Table 1) were used in calculations of the effective diffusion permeability coefficient taking into account the contribution of the adjacent diffusion layers [1].

Table 1. Parameters of microheterogeneous model for a Nafion-117 membrane

Parameter / Membrane	$\overline{Q}$, $mmole\ cm^{-3}$	K_D	f_2	$D_1 10^9$, m^2/s	$D_2 10^9$, m^2/s	α
Nafion-117	1,68	0,38	0,17±0,01	0,28	0,05	0,28

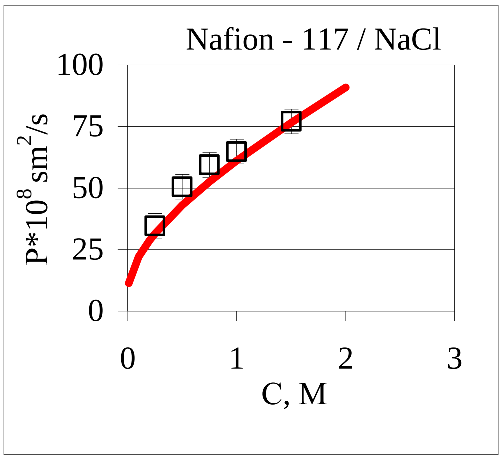

Figure 3. Concentration dependence of the integral constant of diffusion coefficient

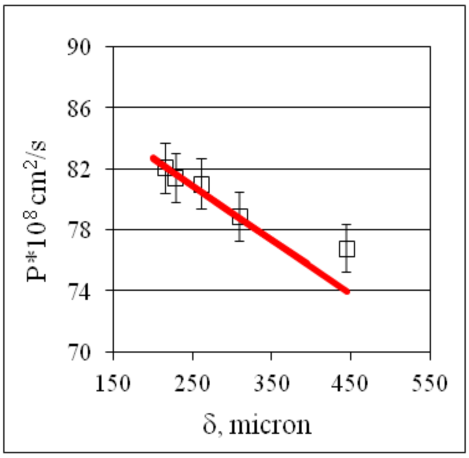

Figure 4. Dependence of the effective integral coefficient of Nafion-117 diffusion permeability on the thickness of the diffusion layer

Results and Discussion

The results presented in Figs. 1-4 show that there is a good accordance between experimental data (points) and theoretical curves. In particular, Fig. 4 shows that the effective diffusion permeability of Nafion decreases with increasing diffusion layer thickness. This effect is explained by the fact that not only the membrane, but the diffusion layers also contribute in the diffusion resistance of the system. In the case of a thick (550 μm) heterogeneous MK-40 this contribution was essentially lower [4].

Acknowledgement

The study was realized within French-Russian laboratory “Ion-exchange membranes and related processes”. We are grateful to CNRS, France, and to RFBR (grants 11-08-93107, 12-08-93106), Russia, and to FP7 Marie Curie Actions “CoTraPhen” project PIRSES-GA-2010-269135 for financial support.

References

1. *Larchet, C., Nouri, S., Auclair, B., Dammak, L., Nikonenko, V.* Application of chronopotentiometry to determine the thickness of diffusion layer adjacent to an ion-exchange membrane under natural convection // Advances Colloid Interface Sci. 2008. V. 139. P. 45-61
2. *Zabolotsky V.I., Nikonenko V.V.* Effect of structural membrane inhomogeneity on transport properties // J. Membr. Sci. 1993. V. 79. P 181-198
3. *Gnusin N.P., Kononenko N.A., Parshikov S.B.* Electrodiffusion through a mixed ion-exchange membrane with adjacent diffusion layers // Elektrokhimiya 1994. V. 30, № 1. P. 35 - 40.
4. *Vedernikova E.E., Nikonenko V.V., Pismenskaya N.D.* Accounting of the diffusion layer in the interpretation of the electrolyte diffusion permeability of ion-exchange membranes Proceedings of the international conference “Ion transport in organic and inorganic membranes”, June 7-12. Krasnodar. 2010. P. 204-205.

DIFFUSION PERMEABILITY OF SOME ANION EXCHANGE MEMBRANES IN THE SOLUTIONS OF SALTS OF PHOSPHORIC AND TARTARIC ACIDS

Ekaterina Nevakshenova, Evgeniya Shutkina, Natalia Pismenskaya
Kuban State University, Krasnodar, Russia, E-mail: nevakshenova-ekaterina@yandex.ru

Introduction

In many application of electromembrane technology in the food industry (high quality potable water, wine, juices, dairy products and products of biochemical synthesis) ampholytes, and in particular, hydrotartrates and hydrophosphates, are treated.

This work is aimed to study the diffusion permeability of several commercial anion exchange membranes in solutions containing these anions, and to analyze the mechanism of ampholyte transport and its similarities and differences with chlorides transport.

Experiments

The subjects of study were anion exchange membranes (AEM) MA-40, MA-41 («ShchekinoAzot», Russia); FTAM-E, FTAM-EDI (Fumatech, Germany); AMX, (Astom, Japan); AX; Ralex-AMH PES (MEGA, Czech). For each membrane the diffusion permeability coefficients were obtained using flow cell with controlled thickness of diffusion layer [1] in NaCl (pH=6,5), $KHC_4H_4O_6$ (pH=4,1), NaH_2PO_4 (pH=4,4) solutions. Several characteristics of studied membranes are presented in Table 1.

Table 1. Several characteristics of studied membranes

Membrane	Fixed groups	Thickness*, μm	Density, g/cm^3	Exchange capacity**, mmole/cm^3
FTAM-EDI	$-N^+(CH_3)_3$	560±10	1.01	3.02
FTAM-E	$-N^+(CH_3)_3$	570±10	1.08	1.85
MA-40	$=NH^+$, $-NH_2^+$, $\equiv N$	545±10	1.09	3.5
MA-41	$-N^+(CH_3)_3$	545±10	1.16	1.25
Ralex AMH-PES	$-N^+(CH_3)_3$	560±10	1.05	1.92
AMX	$-N^+(CH_3)_3$	170±10	1.14	1.74
AX	$-N^+(CH_3)_3$	170±10	1.06	3.05

*in 0,02M NaCl solution

**Cl^- form of swollen membrane

Results and Discussion

The comparison of concentration dependences of integral diffusion coefficient of AEM in NaCl (Figure 1), KHT and NaH_2PO_4 (Figure 2) solutions in concentration range from 0.1M to 1M shows that in NaCl solution there is a decrease of the membrane diffusion permeability (*P*) with dilution of solution. This behavior is in agreement with modern theories [2] and literature data [3]. However, in KHT and NaH_2PO_4 solutions, a noticeable growth of *P* with decreasing solution concentration is observed.

The observed effect agrees with the data presented in Ref. [4] for another ampholyte, phenylalanine, and is connected with occurring of the following phenomena. When diluting solution, H^+ ions, which are co-ions in an AEM, are excluded from the membrane by the Donnan effect.

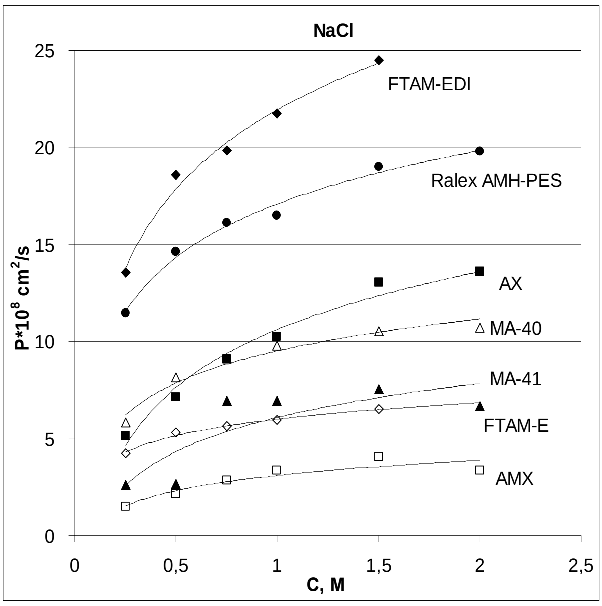

Figure 1. Concentration dependence of diffusion permeability of some anion exchange membranes in NaCl solutions

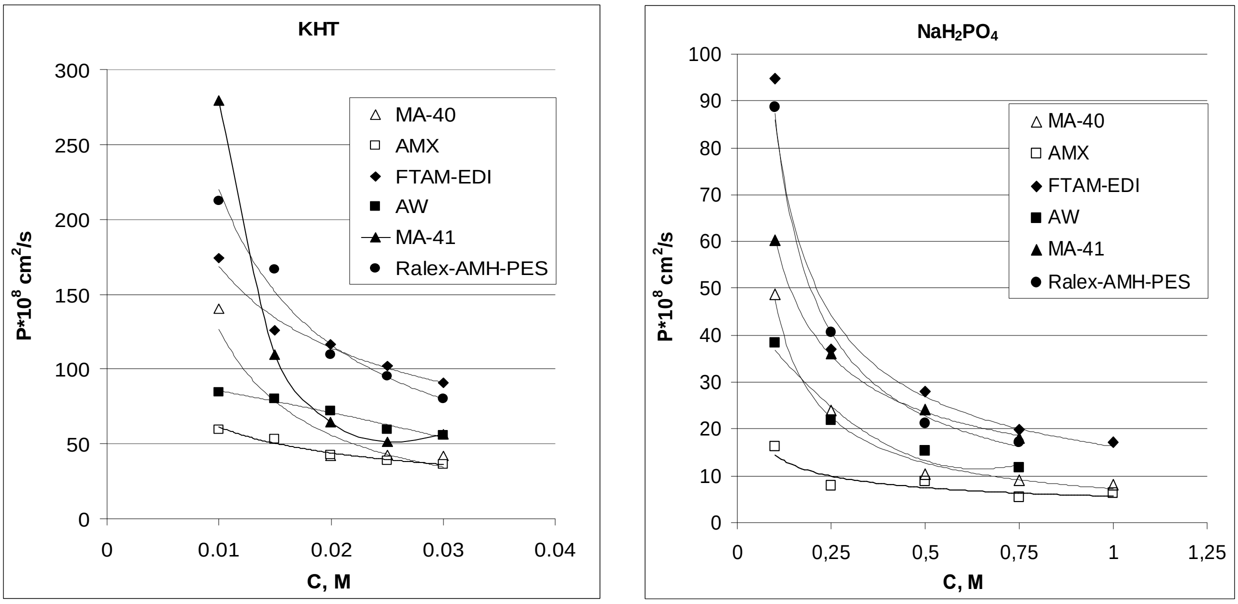

a *b*

Figure 2. Concentration dependence of diffusion permeability of some anion exchange membranes in KHT (a) and NaH_2PO_4 (b) solutions

As a result, pH of the internal membrane solution increases. In ampholyte solutions the membrane becomes enriched in multi-charged anions. In sufficiently diluted solutions, the increase in the charge of counterion leads to an increase in the electrolyte uptake by the membrane, as it follows from the Donnan equation, written as:

$$\frac{\bar{c}}{c} = K_D^{|z_A|}\left(\frac{c}{\bar{Q}}\right)^{|z_A/z_1|}$$

Here z_A is the charge of co-ion (Na^+ or K^+), z_1 is the charge of counterion (ampholyte anion), K_D is the Donnan constant, $\bar{Q}$ is the exchange capacity, $\bar{c}$ is the co-ion concentration in the membrane. Let us assume that $\frac{c}{\bar{Q}} = 0{,}01$, and consider two cases: when $z_1 = 1$ and when $z_1 = 2$.

Then, under other equal conditions, in the second case the co-ion concentration in the membrane will be 10 times higher than in the first case. The increase of co-ion concentration in the membrane internal solution is the *causa proxima* of the membrane diffusion permeability growth with decreasing ampholyte solution concentration.

Acknowledgement

The study was realized within French-Russian laboratory "Ion-exchange membranes and related processes". We are grateful to CNRS, France, and to RFBR (grants 11-08-93107_CNRSL, 12-08-93106_CNRSL), Russia, and to FP7 Marie Curie Actions "CoTraPhen" project PIRSES-GA-2010-269135 for financial support.

References

1. Pat. 100275 RF, IPC[51] G01N27/40 (2006.01). Device for measurements of diffusion characteristics of membrane / *Nikonenko V.V., Vedernikova E.E., Pismenskaya N.D.* (Krasnodar, RF); the applicant and the patent owner: GFO HPE Kuban State University (RF); №2010121195/28; Claimed 25.05.2010; Published 10.12.2010.
2. *Zabolotsky V.I., Nikonenko V.V.* Effect of structural membrane inhomogeneity on transport properties // J. Membr. Sci. 1993. V. 79. P 181-198.
3. *Berezina N.P., Kononenko N.A., Dyomina O.A., Gnusin N.P.* Characterization of ion-exchange membrane materials: properties vs structure // Advances Colloid Interface Sci. 2008. V.139. P.3-28.
4. *Shaposhnik V.A., Vasil'eva V.I., Grigorchuk O.V.* Transport phenomena in ion exchange membranes, M., MFTI. 2001. 199 P.

TRANSPORT PROPERTIES OF MEMBRANES BASED ON SULFONATED POLYCARBONATEMETHACRYLATE (SPCM)

[1,2]Stanislav Novikov, [2]Svetlana Novikova, [2]Anton Sanderov, [1]Andrey Yaroslavtsev
[1]Kurnakov Institute of general and inorganic chemistry RAS, Moscow, Russia,
E-mail: snovikov@syner-tech.ru
[2]Ltd. “Synergetic technologies", Moscow, Russia.

Introduction

Nowadays ion-exchange membranes have a wide range of applications: from water treatment and alternative energy supplies to high selective concentration, separation and extraction of target components both in laboratories and in industry with significant technical and commercial impact [1]. Today most of ion-exchange membranes are produced of sulfonated aromatic polymers such as copolymers of polystyrene with divinylbenzene, polysulfones and others. These materials have a lot of advantages, such as chemical and thermal resistance, simplicity of manufaction with high yield of product. But these materials have some disadvantages which limit the industrial application - relatively low ion-exchange capacity, high cost, and nearly poor mechanical properties, especially, high degree of swelling.

In this paper we report some transport characteristics of membranes based on SPCM.

Experiments

Producing membranes based on SPCM was carried out by the method of phase inversion [2]. SPCM was dissolved in ethanol with obtaining solution 1% by mass. The solution has been put on the horizontal glass plate and evaporated with heating 50°C during 24 hours. The membrane obtained has been separated from the glass plate and has been conditioned at room temperature consequentially for 3 hours in 3% mass solution of hydrochloric acid and then for 3 hours in deionized water. The measurements of conductivity have been produced in water media by two-electrode two-contact method with using «2B-1» and «Agilent-4285A» (7,5x104 − 3x107 Hz) conductometers (10 − 6x106 Hz) in temperature range 25 − 100°C. The conductivity was calculated by extrapolation of impedance hodographs on the axis of active resistance. The water content of samples was measured using thermal weight analyzer «Netzsch TG 209 F1» with heating speed 10°C/min. in temperature range 25÷150°C. The diffusion permeability was measured by the use of two-chambers diffusion cell. The sample was fixed in chambers channel and separated two water phases: the salt solution and the deionized water. The experimental data were obtained by measuring specific conductivity change with conductometer «Expert-002» and digital PC registration of output signal every 5 sec.

Results and Discussion

The increase in the sulfonation time results in the increase of the functional groups concentration, so the water uptake of the SPCM membranes and its conductivity increase also.

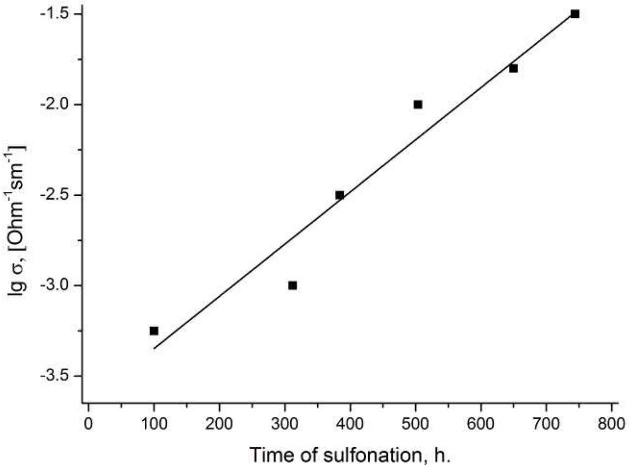

Figure 1. The influence time of sulfonation on conductivity of SPCM

Table 1. Diffusion permeability of chloride alkali metals water solutions and water uptake of SPCM membrane with IEC = 3,2 meq/g

Solution	Diffusion coefficient, sm^2/sec	Water uptake of membrane in salt form, % by mass
0,1M HCl – H_2O	$1,41 \times 10^{-6}$	152,7
0,1M $LiCl$ - H_2O	$1,50 \times 10^{-7}$	75,2
0,1M $NaCl$ - H_2O	$1,20 \times 10^{-7}$	71,8
0,1M KCl - H_2O	$1,11 \times 10^{-7}$	69,4
0,1M $RbCl$ - H_2O	$9,17 \times 10^{-8}$	50,5
0,1M $CsCl$ - H_2O	$8,12 \times 10^{-8}$	53,3

Diffusion permeability of SPCM membranes slightly exceeds the same permeability for membranes MF-4SC. The increase of cation radii causes progressive decrease of diffusion permeability. The high value of proton diffusion permeability is determined by specific relay transport mechanism, which is differs from the same mechanism for alkali metals cations. The extremely high water content of SPCM membrane in acid form can be explained by specific properties of high crosslinked structure of SPCM modificated with hydrophilic sulfonate functional groups [3].

In conclusion, should be noted, that the ion-exchange membranes based on high crosslinked sulfonated polymer SPCM have a good conductivity and high ion-exchange capacity which allows to propose in future such applications of this material as solid polymer electrolyte and as covering for filtration and composite membranes in industrial water supply technologies.

References

1. *A.B. Yaroslavtsev, V.V. Nikonenko* // Russian Nanotechnology, 2009, V.4.№3. P.44–65.
2. *W.-J.-Lee, Y.-J. Kim, M.-O. Jung, D.-H. Kim, D. Cho, S. Kaang* // Synth. Met. 123 (2001). P.327-333.
3. *G.V. Korolyov, M. Mogilevich* // Heidelberg: Verlag von Julius Springer, 2009. P.282.

OXYGEN ELECTROREDUCTION ON NANOCOMPOSITE SILVER / ION – EXCHANGING MEMBRANE (MF–4SC) / DISPERSED CARBON

Viktoriya Novikova, Mikhail Chayka, Tamara Kravchenko
Voronezh State University, Voronezh, Russia, *E-mail: viktoriya.novikova.85@list.ru*

Introduction

Molecular oxygen electroreduction reaction is in interest because it plays a determining role in the overall range of electrochemical processes in fuel cells, sensor devices, as well as in receiving deoxygenated water of high purity. The rate of this reaction and its selectivity depend to a large extent on the choice of the nanostructured electrode. Despite the variety of the electrode materials synthesized, creation of the composites with dispersed metal particles is the challenging task at the present time. It is convenient to use the ion-exchanging membranes as matrixes for particle stabilization and carriers for the nanoparticle formation [1].

Experiments

In the present work the silver-containing nanocomposite (NC) Ag/MF-4SC/C based on the homogeneous perfluorinated sulfonic acid membrane and carbon was studied. Before the nanocomposite synthesis, 7 wt% membrane (MF-4SC) solution in the isopropyl alcohol was mixed with the carbon black UM-76 and homogenized by ultrasonic machining. The suspension with volume of 0.02 ml was applied to the carbon electrode and dried until the complete removal of the solvent. The coated layer thickness δ was 3-4 µm. Electrochemical deposition of silver on the MF-4SC/C was carried out from aqueous solution 2.2 mM $AgNO_3$ + 1 M KCl + 0.2 M NH_4OH, deaerated with argon at the potential $E = 0.125$ V [2]. Chemical precipitation of silver into the ion-exchanging matrix consisted in the saturation of silver ions from 3% $AgNO_3$ solution, followed by the reduction with an alkaline solution of sulfuric hydrazine (0.34 M $N_2H_4{\cdot}H_2SO_4$ in the 1 M NaOH solution).

Microstructure analysis of the Ag/MF-4SC/C was conducted by using Scanning Electron Microscope (SEM, JSM 6380LV) and Transmission Electron Microscope (TEM, JEM-101).

To study molecular oxygen electroreduction at the composite electrodes, the potentiodynamic method was used. The polarization was carried out in 0.1 M H_2SO_4 solution, presaturated with oxygen for 40 minutes.

Results and Discussion

It was detected by SEM (Fig. 1a-c) that the size of silver particles, electrodeposited at the surface of the composite MF-4SC/C, equals to 620 – 920 nm. It was revealed that during oxygen cathodic reduction metal particles are dissolved, therefore, the particles size changes from 740 nm to 480 nm for 5 s of deposition (Fig. 1b, d). It should be noted that after the potentiodynamic cycling of the process in the inert atmosphere, particle size in the Ag/MF-4SC/C (Fig. 1e) does not change, as metal dissolution at the cathodic polarization in acid medium is observed only in the presence of oxygen [3].

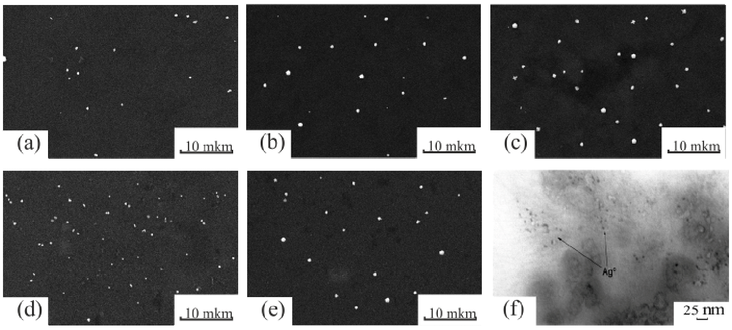

Figure 1. Electron micrographs of Ag/MF-4SC/C: SEM of composite with the electrodeposited silver particles to the time of deposition t_{depos} = 2 s (a), 5 s (b, d, e) and 10 s (c); a, b, c – after silver deposition; d – after the cycling in oxygen medium; e – after the cycling in the inert atmosphere; f – TEM of NC with silver particles chemically deposited

It was detected by TEM that the size of silver particles, chemically deposited into the composite MF-4SC/C, equals to 2 – 4 nm (Fig. 1f). The silver particles are formed in the membrane pores, which limit their size [4].

The polarization curves of oxygen electroreduction at the Ag/MF-4SC/C with chemically and electrochemically deposited silver particles are presented at Fig. 2. Theoretical values of the limiting diffusion current for two- and four-electron process are 19 Am^{-2} and 38 Am^{-2}, respectively, at electrode rotation rate ω = 600 rpm. Experimental values of the limiting diffusion current for observable electrodes are shown in Table 1. The increase of current at Ag/MF-4SC/C in comparison with MF-4SC/C can be explained by the presence of silver nanoparticles, which lead to the acceleration of molecular oxygen electroreduction reaction due to the catalytic effect. The possible reason of the limiting current increase is not only the rising contribution of the four-electron process in comparison with two-electron, typical for carbon-base materials, but also the increase of the real surface due to dispersed silver particles.

Table 1. The values of limiting diffusion current $i_{\lim}$ on investigated electrodes in 0.1 M H_2SO_4 solution. The electrode rotation rate ω = 600 rpm

Electrode	Ag particles deposition method	m_{Ag}, μg	$-i_{\lim}$, Am^{-2}
MF-4SC/C	-	-	33
Ag/MF-4SC/C, *d* = 620 nm	electrochemical deposition tdepos = 2 s	0.53	34
Ag/MF-4SC/C, *d* = 740 nm	electrochemical deposition tdepos = 5 s	1.41	38
Ag/MF-4SC/C, *d* = 920 nm	electrochemical deposition tdepos = 10 s	3.46	39
Ag/MF-4SC/C, *d* = 3 nm	chemical deposition	1.44	40

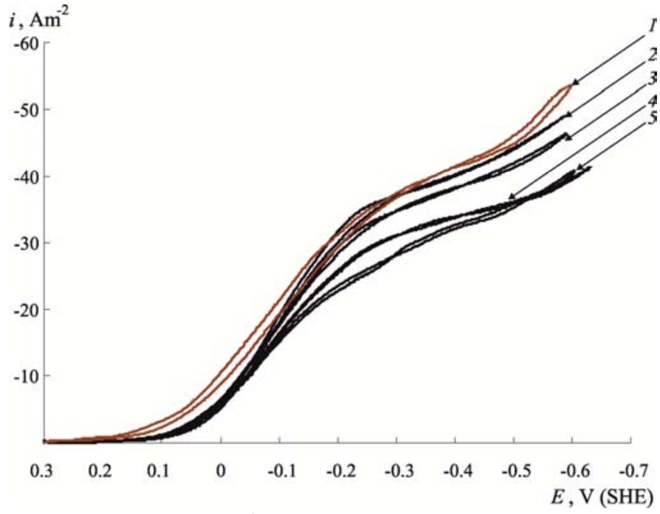

Figure 2. Potentiodynamic curves of molecular oxygen electroreduction in 0.1 M H_2SO_4 solution on investigated electrodes at electrode rotation rate ω = 600 rpm: 1- Ag/MF-4SC/C, d = 3 nm (chemically deposited particles); 2 - Ag/MF-4SC/C, d = 920 nm (t_{depos} = 10 s); 3 - Ag/MF-4SC/C, d = 740 nm (t_{depos} = 5 s), 4 - Ag/MF-4SC/C, d = 620 nm (t_{depos} = 2 s); 5 - MF-4SC/C

For MF-4SC/C and Ag/MF-4SC/C with electrodeposited silver particles the linear dependence of oxygen electroreduction diffusion current $i_{\lim}$ versus the square root of disk electrode rotation rate ω is extrapolated to the coordinate origin (Fig. 3), that indicates the process limitation by oxygen external diffusion. Whereas, for Ag/MF-4SC/C NC with chemically deposited silver particles this dependence does not observe, that can be connected with internal diffusion impact in result of metal particles formation in the membrane pores and reaction occurred in the film volume.

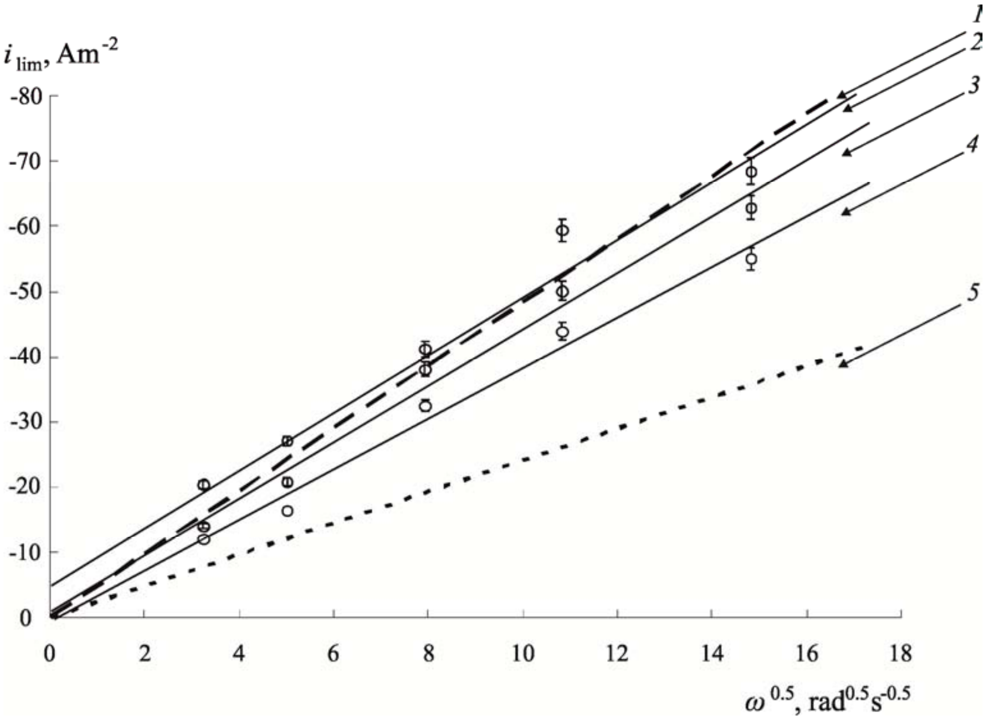

Figure 3. Dependence of molecular oxygen electroreduction limiting current i_{lim} versus the square root of disk electrode rotation rate ω in 0.1 M H_2SO_4 solution: 1 - four-electron process (theoretical); 2 - Ag/MF-4SC/C, d = 3 nm (chemically deposited particles); 3 - Ag/MF-4SC/C, d = 740 nm (t_{depos} = 5 s); 4 - MF-4SC/C; 5 - two-electron process (theoretical)

Conclusion

During cathodic polarization in the presence of dissolved oxygen, particle redistribution by sizes takes place as a result of silver particles self-dissolution reaction proceeding with inverse deposition simultaneously with oxygen electroreduction. The presence of silver particles explain the transition from two- to four-electron process of oxygen electroreduction.

The work is supported by the Russian Foundation for Basic Research (№ 10-08-00847, № 11-08-00174_a).

References

1. *Sheldeshov N.V., Melnikov S.S., Soloveva T.T., Bespalov A.V., Levchenko V.F., Buikliskii V.D., Zabolotskii V.I.* // Russ. J. Electrochem. 2011. V. 47, № 2. P. 200-208.
2. *Abdirisak A. Isse, Gottardello S., Maccato C., Gennaro A.* // J. Electrochem. Communications. 2006. V. 8. P. 1707-1712.
3. *Kreizer I.V., Marshakov I.K., Tutukina N.M., Zartsyn I.D.* // Protection of Metals. 2004. V. 40, № 1. P. 23-25.
4. *Novikova S.A., Yurkov G.Yu., Yaroslavtsev A.B.* // Inorganic Materials. 2010. V.46, №7. P. 793-798.

MECHANISM OF ELECTROCONVECTION IN ELECTRODIALYSIS FLOW-THROUGH CELL

[1]Victor Nikonenko, [1]Mahamet Urtenov, [1]Aminat Uzdenova, [1]Anna Kovalenko,
[1]Natalia Pismenskaya, [2]Vera Vasil'eva, [3]Philippe Sistat, [3]Gerald Pourcelly
[1]Kuban State University, Krasnodar, Russia, *E-mail: v_nikonenko@mail.ru*
[2]Voronezh State University, Voronezh, Russia*, E-mail: viv155@mail.ru*
[3]European Membrane Institute, CNRS - Université Montpellier 2/ENSCM, Montpellier, France,
E-mail: gerald.pourcelly@univ-montp2.fr

Introduction

For about 50 years, it is known that "limiting current" density does not really limit the current density in electrodialysis (ED). It is also clear that the use of high currents allows one to decrease the area of expensive ion-exchange membranes, hence to obtain more compact ED plants with lower investment costs. Now it is established that the main effect providing overlimiting transfer in dilute solutions is electroconvection. However, the mechanism of this phenomenon remains a major challenge.

Theory

The analysis presented here is founded on a first-principles “basic” model, which involves the Nernst-Planck-Poisson (NPP) equations fully coupled to the Navier-Stokes (NS) equations and does not contain any empirical assumptions or fitting parameters [1].

Results and Discussion

For the first time, a realistic I-V curve having the same main features as the experimental ones is calculated for an ED flow-through cell (Fig. 1). A linear initial part of the curve is followed by a sloping plateau situated over the value defined as “limiting” current in the classical theory based on the electroneutrality assumption. The initial part of the plateau is smooth, while the final part characterized by a higher slope is oscillating. This behaviour is in a very good qualitative accordance with this of CMX membrane. In the cases of Nafion and MK-40 the oscillations are higher, their beginning is nearly after exceeding the limiting current density.

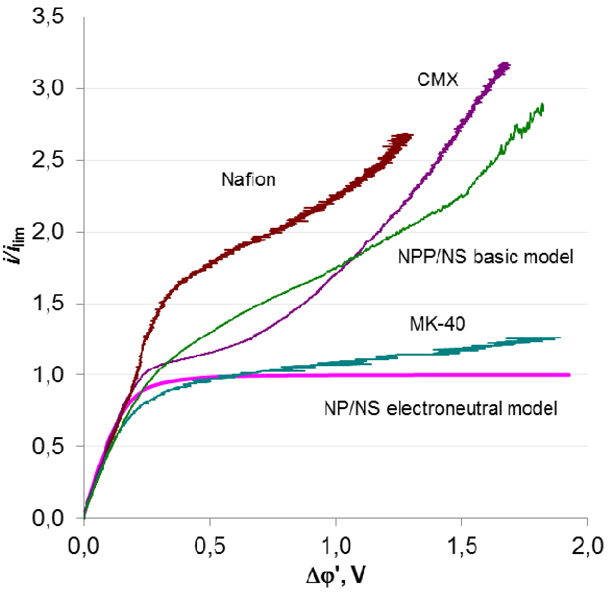

Figure 1. Ratio $i / i_{\lim}$ *as a function of the potential difference per cell pair (*$\Delta\varphi'$*) “corrected” for the ohmic losses in membranes. Experimental data for different cation-exchange membranes (heterogeneous MK-40, homogeneous CMX and Nafion®-117) in 0.02 M NaCl solutions, and calculations according to the NP/NS model under the LEN assumption and to the “basic” NPP/NS model*

To produce electroconvective mixing of depleted solution, which could enhance overlimiting transfer, two conditions should to be fulfilled: (i) an extended space charge region (SCR) should be formed, far beyond the equilibrium EDL, and (ii) the distribution of electric field lines should be inhomogeneous to give rise to a spatially inhomogeneous electric bulk force. According to Dukhin and Mishchuk [2], the occurrence of tangential component of electric field within the induced SCR at a (curved) membrane surface is a primordial condition for producing electroconvection. In this case, electroconvective vortices may be stable. The mechanism is named electroosmosis of the second kind, to emphasize the difference with the “classical” electroosmosis (of the first kind) where no induced SCR is formed. Rubinstein and Zaltzman [3] have shown that the cause of the onset of electroconvection and its further development may be hydrodynamic instability. A fluctuation in velocity or concentration leads to emergence of a spatially inhomogeneous electric field resulting in appearance of vortices, which, in turn, contribute to electric field inhomogeneity. These two modes of electroconvection are recognised in literature and sometimes are shortly called ‘Dukhin's and Rubinstein's electrokinetic modes’ [4].

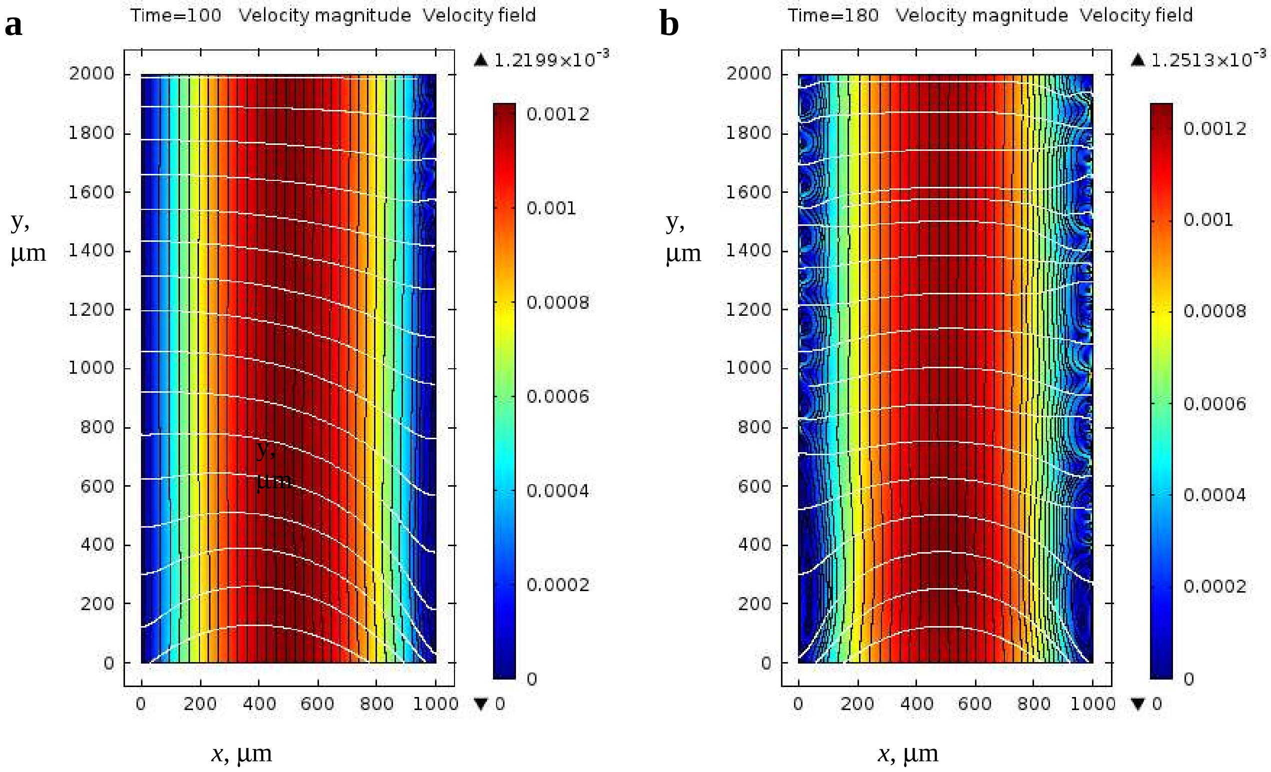

Figure 2. The distribution of electric current (white lines) and fluid velocity streamlines at two different voltages (times), $\Delta\varphi = 1.0$ V (a) and $\Delta\varphi = 1.8$ V (b). The first picture corresponds to emergence of unstable vortices at the CEM near the outlet, while a long vortex near the inlet remains stable. The second picture shows unstable vortices at both membranes

In the case of flat homogeneous membranes where there is no forced convection, only the Rubinstein-Zaltzman mode of electroconvection is possible. The flowing of solution through the ED cell results in essentially complicated behaviour. The initial part of the plateau of the I-V curve is smooth and relates to stable electroconvective vortices occurring. They are due to the Dukhin-Mishchuk electroconvection mode: inhomogeneous distribution of electric current density and appearance of tangential electric field are caused by partial desalination of the solution flowing through the cell: electric current stream-lines are concentrated near the inlet to the cell (Fig. 2). Onset of unstable electroconvection at higher voltages (the Rubinstein-Zaltzman mode) results in appearance of oscillations on the I-V curve and in increasing its slope. Initially, unstable vortexes emerge near the outlet of the desalination channel; then, at higher voltages, they occupy the entire channel. In the case of NaCl solution, electroconvective vortices emerge firstly at the cation-exchange membrane, and with increasing voltage, they appear at the anion-exchange membrane where their evolution follows the same scenario as at the cation-exchange membrane (Fig. 2b).

The basic model gives a new insight on the generalities and some important details of electroconvection enhancement of ion transfer in flow-through ED cells. However, as shown Fig. 1, there is great diversity in membrane behaviour at overlimiting currents. In addition to factors varying in Fig. 1 (membrane heterogeneity and degree of hydrophobicity), there are a number of other possibilities for affecting electroconvection and enhancing ion transfer: the use of profiled surface, ion-conductive spacers, membranes with supressed water splitting and other including novel types of water treatment devices.

Acknowledgements

This investigation was realized within French-Russian laboratory "Ion-exchange membranes and related processes". The authors are grateful to CNRS, France, and to RFBR, Russia (grants 11-08-00599-a, 11-08-93107_NCNIL, 12-08-00188-a, 13-08-01168), as well as to FP7 Marie Curie Actions "CoTraPhen" project PIRSES-GA-2010-269135 for financial support.

References

1. *Urtenov M.K., Uzdenova A.M., Kovalenko A.V., Nikonenko V.V., Pismenskaya N.D., Vasil'eva V.I., Sistat P., Pourcelly G.* // J. Membr. Sci. 2013, submitted to publication.
2. *Dukhin S.S., Mishchuk N.A.* // Kolloid. Zh. 1987. V. 49. P. 1197
3. *Rubinstein I., Zaltzman B.* // Phys. Rev. E 2000. V. 62. P. 2238
4. *Chang H.-C., Demekhin E.A., Shelistov V.S.* // Phys. Rev. E 2012. V. 86. P. 046319

PERFLUORINATED SULFONATED CATION-EXCHANGE MEMBRANES IN MULTISENSORY SYSTEMS FOR DETERMINATION OF ORGANIC AND INORGANIC IONS

Anna Parshina, Olga Bobreshova
Voronezh State University, Voronezh, Russia, *E-mail:parshina_ann@mail.ru*

Introduction

Perfluorinated sulfonated cation-exchange membranes (for example, Nafion, DuPont USA and MF-4SC, OSS «Plastpolymer», St.-Petersburg, Russia) can be effective electrodoactive materials for potentiometric sensors [1, 2]. The first advantage of these membranes is electrochemical stability. Other advantage is the system of the hydrophilic fixed groups (sulfonate groups) and hydrophobic perfluorinated walls which form nanostructure of membranes. The sizes of pores and pipes of membrane are equal 5 nm and 1 nm [3]. These parameters are comparable to the sizes of organic ions. Therefore variation of ion-molecular composition of such membranes influences on sensitivity of potentiometric PD-sensors to organic components in aqueous solutions [1, 2].

Experiments

The following analytes of interest were dissolved in aqueous solutions: glycine (Gly), α-, β-alanine (α-, β-Ala), leucine (Leu), nicotinic acid (Niacin), pyridoxine hydrochloride (PyridoxinHCl), thiamine chloride (ThiaminCl), novocaine hydrochloride (NovHCl), lidocaine hydrochloride (LidHCl), cysteine (Cys). Concentrations of test solutions ranged from $1.0\cdot10^{-4}$ to $1.0\cdot10^{-1}$ M. The pH values of Gly+HCl, α-Ala+HCl, β-Ala+HCl, Leu+HCl, Niacin+PyridoxinHCl+ThiaminCl, NovHCl, LidHCl solutions were <7. The pH values of Gly+KOH, Cys+KOH solutions were >7.

The samples of membranes MF-4SC containing organic ions were obtained by two procedures. In the first procedure the membranes were treated in solutions of amino acids and vitamins at boiling temperature of solution. In the second procedure the membranes were treated by keeping in ethylene glycol at glass transition temperature of membrane (110^{o}C) and than in solutions of amino acids and vitamins respectively at boiling temperature of solution.

The samples of membranes MF-4SC and Nafion with 2.0-5.0 wt.% of ZrO_2 were investigated. One half of membrane contains nanoparticles of ZrO_2. This half of membrane contacted with test solution. Other half of a membrane was not modified and contacted with reference solution of PD-sensor [4]. The samples of modified membranes were given by cand.ch.sc. Ekaterina Yu. Safronova and corresponding member RAS, dr.ch.sc., prof. Andrey B. Yaroslavtsev (N.S. Kurnakov Institute of general and inorganic chemistry of RAS, Moscow, Russia).

Results and Discussion

For effective quantitative determination of organic components (amino acids, vitamins, drugs) into the multiionic solution to eliminate some of the problem was necessary. First, the decrease of influence of the ion H_3O^+ on the sensitivity and stability of the response of PD sensors in multiionic solutions is important. Second, the increased sensitivity of the PD sensors to large organic ions is important. Third, the sensitivity to both the cations and the zwitterions of organic ampholytes is necessary.

Cross-sensitive PD-sensor based on membranes containing organic ions. Membranes with low sensitivity to ions of H_3O^+ and high sensitivity to cations and zwitterions of amino acids and vitamins were necessary for quantitative determination of components in solutions Gly+HCl, α-Ala+HCl, β-Ala+HCl, Leu+HCl, Niacin+PyridoxinHCl+ThiaminCl.

Membranes containing ions H_3O^+ and cations of amino acids were chosen for determination of amino acids. Decrease of concentration of ions H_3O^+ in a membrane became the reason of decrease of sensitivity of PD-sensors to H_3O^+ ions in solutions of amino acids. Sensitivity to cations and zwitterions of amino acids was increased. Increased concentrations of cations of amino acids in the membrane and the variation in the mechanism of protolysis reactions near the interface involving zwitterions were the reasons.

The greatest sensitivity of PD-sensors to PyridoxinH$^+$ in comparison with ions H_3O^+ was for the membranes containing ions K^+ and PyridoxinH$^+$. The greatest sensitivity of PD-sensors to NiacinH$^+$ and Niacin$^\pm$ in comparison with ions H_3O^+ was for the membranes containing ions H_3O^+ and PyridoxinH$^+$. Decrease of the «free» solution into the pores and the reduction the interaction of the ions H_3O^+ with -SO_3^--groups due to sorption of large organic ions were reasons of low sensitivity to H_3O^+. The sensitivity of the PD-sensors to zwitterions Niacin$^\pm$ is due to protolysis reactions involving ions H_3O^+ from the membrane. Size of cations Thiamin$^+$ and ThiaminH^{2+} similar in size to the membrane pore. These cations can block the pores of the membrane. Therefore the dependence of the sensitivity of the PD-sensors to Thiamin$^+$ and ThiaminH^{2+} from ion-molecular composition of the membrane and from the concentration of ions H_3O^+ in solution was weak.

Quantitative determination of amino acids and vitamins in solutions Gly+HCl, α-Ala+HCl, β-Ala+HCl, Leu+HCl, Niacin+PyridoxinHCl+ThiaminCl is executed with use cross-sensitive PD-sensors.

Cross-sensitive PD-sensor based on membranes containing nanoparticles of ZrO_2. Results of the study of cross-sensitivity of PD-sensor based on membranes with ZrO_2 were discussed using a model limited elasticity of the walls of the membrane pores [3]. Modification of the membranes nanoparticles leads to a decrease of the «free» solution into the pores. [3]. Therefore, the electrochemical potential of large organic ions into the pores of modified membrane is very different from their electrochemical potential in the solution. Furthermore, the presence of large organic ions into the pores of modified membrane reduces the interaction of the inorganic ions (including H_3O^+) with -SO_3^--groups. This explains the increase of sensitivity of PD sensors to ions LidH$^+$ and NovH$^+$ in comparison with ions H_3O^+ in solution NovHCl and LidHCl for membranes with 2.0-2.4 wt.% of ZrO_2. The same reasons explain the increase of sensitivity of PD sensors to anions Gly$^-$ and CH_3COCOO^- in comparison with cations K^+ and NH_4^+ in alkaline solution for membranes with 5.0 wt.% of ZrO_2.

Cross-sensitive PD-sensor in multisensory systems for qualitative analysis of foods. Cross-sensitive PD-sensor in multisensory systems for control of the degree of freshness of beer and analysis of reconstituted milk was used.

Acknowledgements

This present work was supported by the Russian Foundation for Basic Research (projects №12-08-00743-a, №12-08-31471/ mol_a).

References

1. *Bobreshova O.V., Parshina A.V., Agupova M.V., Polumestnaya K.A.* Determination of amino acids, vitamins, and drug substances in aqueous solutions using new potentiometric sensors with Donnan potential as analytical signal // Russ. J. of Electrochem. 2010. V. 46, № 11. P. 1338-1349.
2. *Bobreshova O.V., Parshina A.V., Polumestnaya K.A., Timofeev S.V.* A new type of potentiometric sensors based on perfluorinated, sulfonated cation-exchange membranes for quantitative analysis of multicomponent aqueous solutions // Petr. Chem. 2011. V. 51. N.7. P. 496-505 (Membranes and membrane technologies. 2011. V. 1, № 1. P. 27-36. In Russian).
3. *Yaroslavtsev A.B.* Correlation between the properties of hybrid ion-exchange membranes and the nature and dimensions of dopant particles // Nanotechnologies in Russia. 2012. V. 7, № 9-10. P. 8-18.
4. *Bobreshova O.V., Parshina A.V., Polumestnaya K.A., Safronova E.Yu., Yankina K.Yu., Yaroslavtsev A.B.* Perfluorinated sulfocation-exchange membranes modified with zirconia for sensors sensible for organic anions in multiionic aqueous solutions // Mendeleev Communications. 2012. V. 22, № 2. P. 83-84.

1D MODELLING OF NON-STATIONARY OVERLIMITING ION TRANSFER IN MEMBRANE SYSTEMS

Alina Petukhova, Aminat Uzdenova, Victor Nikonenko
Kuban State University, Krasnodar, Russia, *E-mail: v_nikonenko@mail.ru*

Introduction

In accordance with established to contemporary theoretical concepts, the main mechanism for the development electroconvection in membrane systems is electroosmotic slip of the second kind. A basic model involving the Nernst-Planck-Poisson equations coupled to the Navier-Stokes equations (NPP-NS) and not containing any adjustable parameters is proposed [1]. The model for the first time allows calculation real I-V curves taking into account electroconvection. The objective of the present work is comparison of 1D and 2D models of ion transfer in membrane system in overlimiting current regimes.

Theory

A 1D transient mathematical model of ion transfer in ion-exchange membrane system is proposed. The model is based on the Nernst-Planck-Poisson equations and the Nernst concept of the diffusion layer. However, in contrast to conventional similar models assuming local electroneutrality, the diffusion boundary layer (DBL) is supposed a function of current density and the time. It is assumed that electroconvective vortices formed near the membrane surface affect the DBL thickness. The mechanism of action is similar to the demographic model by Verhulst [2]. We put in the assumption that the thickness of the DBL is a function of the body electric force, but its action is manifested with a certain delay. The body force produces a vortex (that demands a certain time); the vortex results in decreasing the DBL thickness. To describe the fluctuations of potential drop, we assume that the development of one factor (electroconvective vortices) leads to the inhibition of the second factor (concentration polarization and body force), which is the cause of the first one.

Results and Discussion

1D Simulation allows us to describe the process, to identify the main factors that determine the behavior of the system and show them in a simplified form.

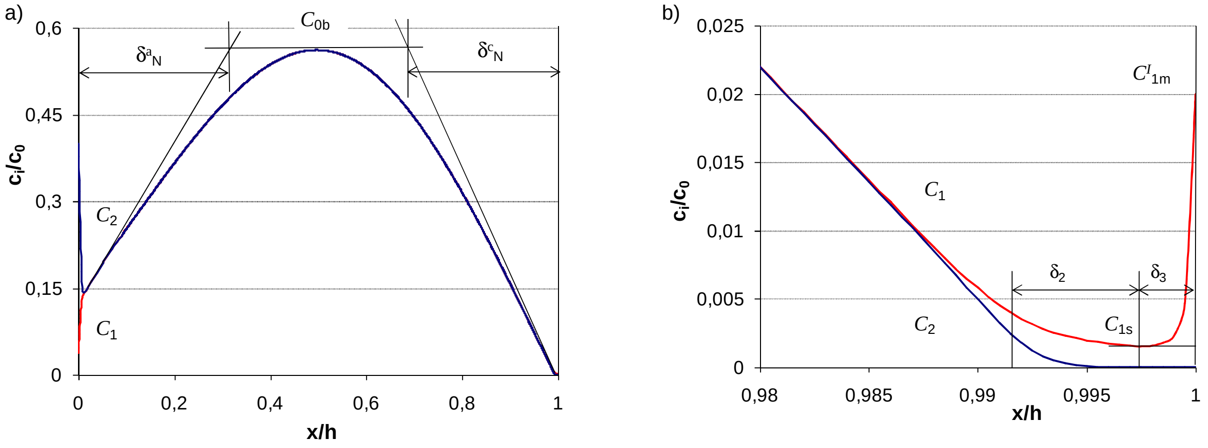

Figure 1. Concentration profiles of cation (C_1) and anion (C_2) calculated using the basic 2D NPP-NS model. a) shows the whole profiles, b) their part near the CEM, the arrows show the values of the extended (δ_2) and quasiequilibrium (δ_3) space charge regions found using the 1D model

We have compared the potential drop oscillations calculated with help of both models. As well, the comparison of the main characteristics of concentration profiles is carried out (Fig. 1). It is shown, that for small potential drops the process occurring in the DBL can be approximately described by using the 1D model.

Acknowledgements

This investigation was realized within French-Russian laboratory "Ion-exchange membranes and related processes". The authors are grateful to CNRS, France, and to RFBR, Russia (grants 11-08-93107_NCNIL, 12-08-93106_NCNIL, 13-08-01168), as well as to FP7 Marie Curie Actions "CoTraPhen" project PIRSES-GA-2010-269135 for financial support.

References

1. *Urtenov M.K., Uzdenova A.M., Kovalenko A.V., Nikonenko V.V., Pismenskaya N.D., Vasil'eva V.I., Sistat P., Pourcelly G.* Basic mathematical model of overlimiting transfer in electrodialysis membrane systems enhanced by electroconvection // J. Membr. Sci. 2013, submitted to publication.
2. *Verhulst, P.F.* Recherches mathématiques sur la loi d'accroissement de la population // Nouv. mém. de l'Academie Royale des Sci. et Belles-Lettres de Bruxelles 1845. V.18. P. 1-41

BIO / AMPHOLYTE MOLECULES AND IONS TRANSFER IN ION-EXCHANGE MEMBRANE SYSTEMS

[1]Natalia Pismenskaya, [1]Ekaterina Belashova, [1]Ekaterina Nevakshenova, [1]Veronika Sarapulova, [1]Semyon Mareev, [1]Victor Nikonenko, [2]Gerald Pourcelly, [2]Philippe Sistat
[1]Kuban State University, Krasnodar, Russia, *E-mail: n_pismen@mail.ru*
[2]European Membrane Institute, CNRS - Université Montpellier 2/ENSCM, Montpellier, France,
E-mail: gerald.pourcelly@univ-montp2.fr

Introduction

Processing of biomass and other kinds of primary products is developing most rapidly now due to the issues of green chemistry. Carbonic, phosphonic and amino groups are very typical for biomolecules and they very often present together (amino acids, proteins, etc). Biomolecules are ampholytes, as a rule. They take part in protolysis (proton-transfer) reactions in aqueous solutions and thereby change the charge or become electrically neutral depending on the pH of solution. This property is common also for inorganic ampholytes such as carbonic or phosphoric acid. The transformations of singly charged ampholyte ions in other forms resulted from addition of H^+ or OH^- ions can be represented for example as

$$H_2T \xleftarrow{H^+} HT^- \xrightarrow{OH^-} T^{2-}$$

$$H_2Lys^{2+} \xleftarrow{H^+} HLys^+ \xrightarrow{OH^-} Lys^{\pm} \xrightarrow{OH^-} Lys^-$$

$$H_3PO_4 \xleftarrow{H^+} H_2PO_4^- \xrightarrow{OH^-} HPO_4^{2-} \xrightarrow{OH^-} PO_4^{3-}$$

where T is the acid residual of tartaric acid and Lys denotes lysine amino acid.

These substances consist of several atoms and have larger size in comparison with Na+, K+, Cl- and other “simple” ions. All ampholyte ions have groups that form hydrogen bonds with water and work purely as a hydration center without altering the nature of the bulk H2O away from the hydration shell.

Electrodialysis is actively used for purification, separation, concentration and conversion of ampholytes. This membrane process allows the separation of particles using the difference in their charge sign and magnitude as well as the difference in their mobility. The possibility to control solution pH by governing water splitting in membrane system allows effective treatment of ampholyte-containing solutions via adjusting the desirable charge of particles. A large number of different levers, which can be used, present an important advantage of electrodialysis in comparison with other membrane methods. For example, ultrafiltration separation is based on the difference in size (mobility) of particles. Hence their charge is irrelevant: we cannot separate positively and negatively charged particles of similar size. In reverse osmosis, all charged particles, regardless of their sign of charge, are rejected.

Transport of ampholytes inside ion exchange membrane

The mechanism of ampholyte counter-ion transport through ion-exchange membranes differs from that of strong electrolytes containing cations and anions such as Na^+ and Cl^- [1]. Regardless of whether the transported singly charged ampholyte ion is of organic or inorganic nature, an increase in electrical conductivity (Fig.1a) and diffusion permeability (Fig.1b) of homogeneous ion-exchange membranes is observed with diluting solutions.

This growth is unusual as in the presence of strong electrolytes (such as NaCl) the membrane conductivity and permeability decreases with decreasing solution concentration (Fig.1). In the case of ampholyte solutions, the effect is caused by an increase in doubly charged ampholyte ion fraction in the gel phase of the membrane (Fig.2) due to variation of the pH of internal solution with diluting external solution. The pH of the internal solution decreases in the case of cation-exchange membrane, and increases in the case of anion-exchange membrane when the external solution becomes more dilute. This variation of pH is explained by the shift in the ionic equilibrium between the salt and the water counter-ions, which is due to increasing fraction of water ions in solution when it is diluted at a constant pH. Otherwise, this effect can be interpreted as a consequence of co-ion Donnan exclusion (OH^- ions in the case of cation-exchange membrane and H^+ ions in the case of anion-exchange membrane), which becomes stronger in dilute solutions. The microheterogeneous model [2] allows prediction of membrane transport characteristics both for strong electrolytes and for ampholytes (Fig.1a).

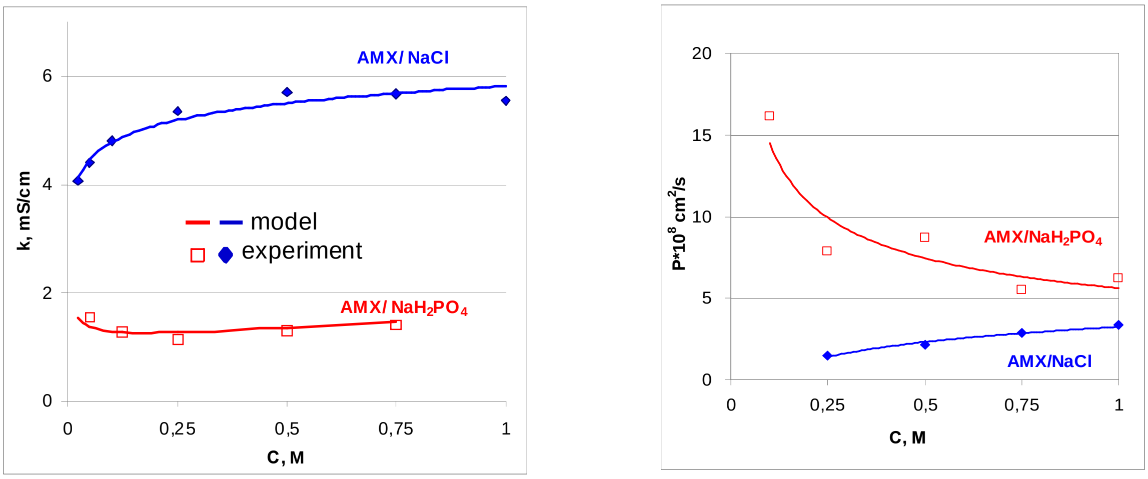

a *b*

Figure 1. Concentration dependences of specific electrical conductivity (a) and diffusion permeability (b) of AMX membranes in NaCl and some ampholyte solutions

The microheterogeneous model [2] assumes that the solution filling the membrane macropores is identical to the equilibrium external solution. The phase providing functional properties to the membrane is the charged gel, which incorporates microporous charged domains with fixed groups and mobile counterions and co-ions, which counterbalance the charge of the matrix. In the case of ampholyte solutions, we further developed the model [2] while taking into account protolysis reactions. As Fig. 1 shows, there is a good accordance of the updated model with experimental data.

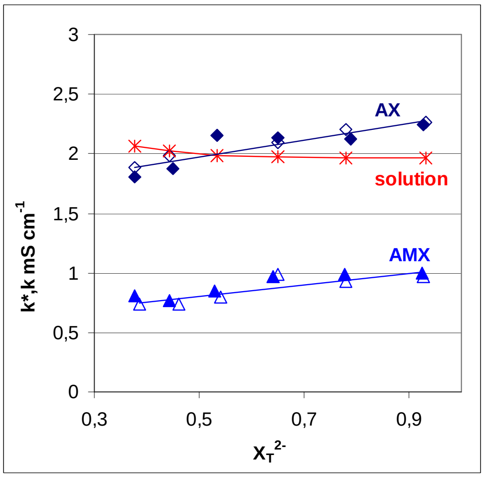

Figure 2. Electrical conductivity of AX and AMX membranes and solutions vs the equivalent ionic fraction of T^{2-} in the mixed KHT − K$_2$T external solution in the cases of constant total equivalent concentration, $C_{K^+} = C_{HT^-} + 2C_{T^{2-}}$ *=0.02 eq* L^{-1}

Another general property observed when conversing an IEM from a strong electrolyte to an ampholyte counter-ion form is a lost in conductivity. The main reasons seems to be the fact that ampholyte ions consist of many atoms and have larger size in comparison with Na$^+$, K$^+$, Cl$^-$ or other “simple” ions. Besides, the ampholyte ions are essentially more hydrated. Consequently, the water is more structured in the membrane internal solution, this solution contains less unbound water and the osmotic pressure is higher. In addition, chemical interactions of polar groups of the ampholyte ion with the membrane fixed groups are possible. All these factors result in decreasing ampholyte counter- ion mobility.

Transport of ampholytes in adjoining to membrane diffusion layer

The difference in the values of pH in the external and the internal (gel phase) solutions leads to occurrence of proton-transfer reactions at the membrane interface (Fig. 3). As a result, the depleted diffusion layer at the AEM becomes more acid and enriched with the molecular form of a weak acid. Similarly, at the CEM, this layer becomes enriched with the zwitterion of an amino acid (Fig.3). Our calculations using the values of pH, which are measured at the surface of membranes, indicate that the fraction of acid neutral molecules in the diffusion layer can reach 10% of the total amount of phosphor-containing species (Fig.4). The transfer of ampholyte species can be simulated using Nernst-Planck equations as well as equations of protolysis reactions and the assumption of electrical neutrality [3].

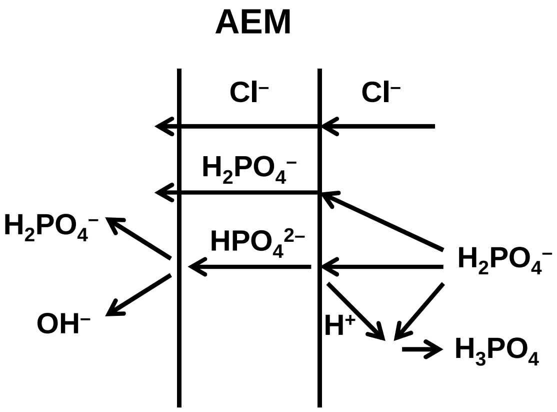

Figure 3. Scheme of ampholyte transport in membrane system

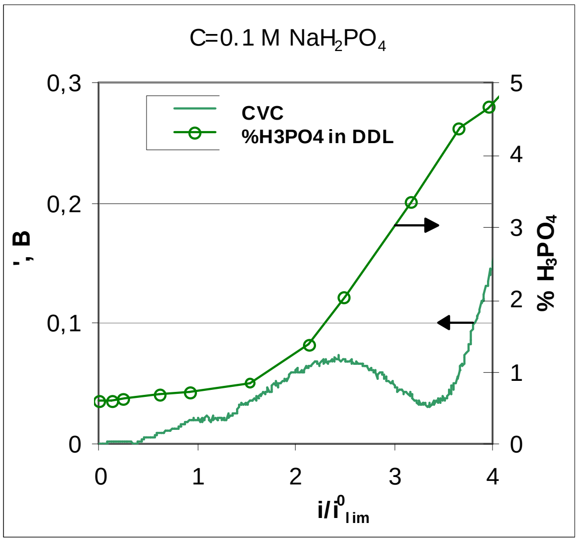

Figure 4. Current voltage characteristic of the membrane system and the corresponding molecular fraction of phosphoric acid in the depleted diffusion layer (DDL)

Acknowledgements

This investigation was realized within French-Russian laboratory "Ion-exchange membranes and related processes". The authors are grateful to CNRS, France, and to RFBR, Russia (grants 11-08-93107_NCNIL, 12-08-93106_NCNIL), as well as to FP7 Marie Curie Actions "CoTraPhen" project PIRSES-GA-2010-269135 for financial support.

References

1. *Pismenskaya N. D., Belova E. I., Nikonenko V. V., Larchet C.* Electrical Conductivity of Cation- and Anion-Exchange Membranes in Ampholyte Solutions // Russ. J. Electrochemistry. 2008. V. 44, No.11. P. 1285–1291.
2. *Zabolotsky V.I., Nikonenko V.V.* Effect of structural membrane inhomogeneity on transport properties // J. Membr. Sci. 1993.Vol.79. P.181-198.
3. *Nikonenko V., Lebedev K., Manzanares J.A., Pourcelly G.* Modelling the transport of carbonic acid anions through anion-exchange membranes // Electrochim. Acta 2003. V.48, No 24. P.3639-3650.

COMPARATIVE STUDY OF ELECTRODIALYSIS DESALINATION OF RED AND WHITE WINE WITH ION EXCHANGE MEMBRANES

Mikhail Porozhnyi, Veronika Sarapulova, Natalia Pismenskaya
Kuban State University, Krasnodar, Russia

Introduction

Electrodialysis (ED) is one of the most effective methods of wine stabilization from the tartrate sedimentation. This sediment is the potassium salt of tartaric acid, hence the main goal of the electrodialysis process is to reduce the content of potassium and hydrotartrates to certain concentrations. The efficiency of this process and its production validity are determined by using a pilot ED stack. To improve characteristics of the electrodialysis stabilization of wine, commercial and experimental anion exchange membranes were used.

Experiments

The process of ED desalination of a wine was studied by using commercial Japanese (Astom) anion-exchange membranes AMX and experimental anion exchange membranes MA-41PM produced by OAO ShchekinoAzote and modified by Membrane Technology IE. In both cases Japanese (Astom) cation-exchange membranes CMX were used. The membrane stack consisted of 5 anion-exchange membranes and 7 cation-exchange membranes forming 5 cell pairs.

Experiment was conducted in two stages, first, with the AMX membranes, and then with MA-41PM membranes. Both of the stages were managed under the same operation conditions:

- a constant current density was maintained at a value of 8 mA/cm^2;
- the flow rate in the concentration loop, CL, and in the desalination loop, DL, was 90 L/h ;
- the flow rate in the electrode loop, EL, was 200 L/h ;
- 5 L of a 5 g/L NaCl solution circulated in the concentration loop, 5 L of a 30 g/L KNO_3 solution circulated in the electrode loop.

5 L of a wine (red or white) circulated in the desalination loop at each stage of the experiment.

The desalting process was stopped, when the electrical conductivity κ_i decreased by 30 % in comparison with its initial quantity κ_0.

Kinetic dependences of the electrical conductivity, pH and temperature of the desalting solution, as well as the voltage across the membrane stack were registered during the experiment. Sampling for the following analysis of the component composition of the desalted wine was carried out at three different values of its electrical conductivity $\kappa_1 = 0{,}9\ \kappa_0$; $\kappa_2 = 0{,}8\ \kappa_0$ and $\kappa_3 = 0{,}7\ \kappa_0$.

After each run, all loops of the ED module were rinsed with distilled water. Before each subsequent run, each loop was rinsed with an appropriate solution: NaCl (CL), KNO_3 (EL), the wine (DL), in order to achieve a constant electrical conductivity of the circulating solution in each loop.

Results and Discussion

The analysis of the obtained data shows that the power consumptions of the desalting process of the wine are different when using commercial AMX or experimental MA-41PM membranes.

Acknowledgement

The study was realized within French-Russian laboratory “Ion-exchange membranes and related processes”. We are grateful to CNRS, France, and to RFBR (grants 11-08-93107, 12-08-93106), Russia, and to FP7 Marie Curie Actions “CoTraPhen” project PIRSES-GA-2010-269135 for financial support.

INTERMEDIARE PROTON CONDUCTING MEMBRANES BASED ON CsH_2PO_4

Valentina Ponomareva, Elena Shutova
Institute of Solid State Chemistry and Mechanochemistry, SB RAS, Novosibirsk, Russia
E-mail: ponomareva@solid.nsc.ru

Introduction

Fuel cells have attracted worldwide attention as a clean power source for electric vehicles, power generation systems, portable electronic devices etc. CsH_2PO_4 is perspective as an intermediate temperature proton membrane for electrochemical devices and in particular fuel cells [1,2]. The great scientific interest and large progress in electrochemical characteristics of solid acid fuel cells are observed today. However membranes of individual CsH_2PO_4 functions at ~250^{o}C only in high humidity conditions due to their specific chemical and thermal properties. The increasing of the conductivity in low temperature phase makes CsH_2PO_4 more attractive and perspective for application.

Experimental

The investigation was carried out using a.c. impedance method, Infrared spectroscopy, Xray diffraction, high resolution electron microscopy and differential scanning calorimetry. A phosphor and silica containing high dispersed matrix were synthesized by sol gel method.

Results and Discussion

Development of composite electrolytes is the effective approach to improvement of transport, thermal and mechanical properties. Proton composite electrolytes based on $M_mH_n(XO_4)_p$ acid salts are characterized by high conductivity values at intermediate temperatures and differed by transport, structural and thermodynamic parameters, depending on their phase composition [3,4]. The type of oxide, its' morphology, pore sizes and acid-basic properties influence significantly on the structural deformation of the salt in composites and as a result, various disordered states of the salt (superionic, amorphous or nanocrystalline) are stabilized in composite systems.

Various types of heterogeneous additives such as TiO_2, SiO_2, SiP_2O_7 and phosphosilicate gels with different morphology and surface acidity have been used. As for composites based on CsH_2PO_4, their transport and structural properties were shown to be determined by acid-basic properties of the oxide and its' surface to a greater extent than for other systems. The acid-basic characteristics of dispersed oxide influence significantly on the energy of interface interaction up to formation of the new low-conductive phases. In CsH_2PO_4 - SiO_2 systems a strong interface interaction of salt and SiO_2 makes easier the structural deformation of CsH_2PO_4 in the composites resulting in destruction of strong two-dimensional hydrogen bond network and salt dehydration at the intermediate temperatures [4,5].

The hydrogen bonds play an important role in the interfacial interactions in the proton-conducting systems and their formation involves a partial sorption of the part of salt protons by the surface OH–groups of the oxide. The management of transport and structural properties for systems based on acid salts has been shown by changing the bulk salt characteristics and properties of the grain boundary. The modification of heterogeneous additive surface by additional acid centers could decrease the interface interaction and obtain the composite systems with high proton conductivity and defined thermal stability.

A phosphor and silica containing high dispersed matrix differ by different Si:P content, chemical, thermal properties and specific surface areas (5 to 580 m^2/g). The relation Si:P was varied from 2 up to 7. The conductivity of $(1\text{-}x)CsH_2PO_4\text{-}x(SiO_2\text{-}qP_2O_5)$ composites, structural and thermal characteristics were shown to depend markedly both the salt and gel-additive concentration and Si:P content. In composites to be investigated the conductivity increases more than 3.5 orders of magnitude, exceeds significantly the conductivity of the parent salt and has maximal value at ~30-60 vol% of SiO_2-qP_2O_5. The composites were shown to exhibit the high proton conductivity ~10^{-3} -$3*10^{-2}$ S/cm at ~130-230^{o}C, and the temperature of superionic phase transition decreases and disappears with x increase. The phase composition of these composite systems depended on the composition and markedly on the P_2O_5 content in matrix. Thermodynamic and thermal stability of these systems also change markedly depending on composition and P_2O_5 content. The best transport, structural and thermal characteristics of composites were obtained for Si:P =1:0.14 due to the optimal energy of interface interaction. In these systems the highly disordered phase of CsH_2PO_4 is observed up to high x values. Whereas the formation of less thermal stable $CsH_5(PO_4)_2$ phase was observed in the systems based on silica with the higher P_2O_5 content. The thermal stability of at 180-200 ^{o}C was estimated for different systems during long term storage at low humidity and was shown to differ significantly. The systems with the higher P_2O_5 content have less thermal stability during prolong heating.

Besides the high proton conductivity in wide temperature range and low electron conductivity, the synthesized systems demonstrate increased thermal stability at low H_2O partial pressure (0.5-1 mol %) and T~200^{o}C, enhanced mechanical strength, low hydrogen permeability (< 10^{-14} m^2/s×Pa. These unique properties create perspectives of their using in electrochemical devices.

The work has been carried out with the partial financial support from grant RFBR №12-08-01339.

References

1. *Boysen D.A., Uda T., Chisholm C.R.J., Haile S.M.* // Science 2004, 303**,** 68.
2. Haile S. M., Chisholm C. R. I., Sasaki K., Boysen D. A., Uda T. // Faraday Discussions, 2007, 134, 17.
3. *Ponomareva V.G., and Lavrova G.V.* // Solid State Ionics, 2001, 145, 197.
4. *Ponomareva, V.G., and Shutova, E.S.* // Solid State Ionics*, 2005, 176, 2905.*
5. *Ponomareva V.G., and Lavrova G.V. J.* // Solid State Electrochemistry, 2011, 15, 213.

MEMBRANES FOR THE HYDROGEN ECONOMY. PROSPECTS FOR THE FUTURE

Gérald Pourcelly
European Membrane Institute, Montpellier, France, *E-mail: Gerald.Pourcelly@univ-montp2.fr*

Summary

An affordable, clean and reliable energy supply is a major global concern as the world's fuel consumption increases rapidly due to the increased industrialization and a growing human population. Among the various energy alternatives, hydrogen may be the most promising given that it is a "green fuel" *i.e.* the only combustion product is water (depending on which way hydrogen is further produced).

So, the emergence of hydrogen economy appears inevitable driven by the concerns of fossils resources and the consequence of the global warming. Such developments require the development of hydrogen production separation technologies with significantly improved energy and cost efficiencies. Membrane technology appears as the best choice for hydrogen purification.

Besides, before purification, hydrogen must be produced. Membranes and membrane reactors for pure hydrogen production are widely investigated not only because the wide scope of application areas of hydrogen, but especially because mechanically and chemically stable membranes with high selectivity towards hydrogen are now available and are continuously further improved in terms of stability and hydrogen flux. Membrane reactors are multiphase reactors integrating catalytic reactions and separation through membranes in a single unit.

Although metallic membranes produce high-purity hydrogen, the significantly higher material and fabrication costs together with hydrogen embrittlement under certain operating conditions limit its extensive use on the industrial scale. Similarly, other inorganic membranes (*e.g.* carbon ones) are generally brittle, difficult to process and hence increase fabrication costs. If the purity requirement is not stringent (H_2 purity < 99.5 v/v %) and the operating temperature relatively low, polymeric membranes are preferred over other alternatives based on economic considerations

The aim of this presentation is to highlight recent advances in hydrogen selective membranes (from palladium-based to silica, proton conductors and polymeric ones) along with the advances for the different types of membrane reactors available [1-5].

References

1. *F.Gallucci, E.Fernadez, P.Corengia, M. van Sint Annaland* Recent advances on membranes and membrane reactors for hydrogen production // Chem. Eng. Sci., 92 (2013) 40-66
2. *L.Shao, B.T.Low, T.S. Chung, A.R.Greenberg* Polymeric membranes for the hydrogen economy. Contemporary approaches and prospects for the future // J. Membr. Sci. 327 (2009) 18-31
3. *M.T.D.Nguyen, A.Ranjbari, L.Catala, F.Brisset, P.Millet* Implementing molecular catalysts for hydrogen production in proton exchange membrane water electrolysers. // Coord. Chem. Rev., 256 (2012) 2435-2444
4. *S.Kumar, A.Sharma, B.Tripathi* Enhancement of hydrogen gas permeability in aligned MWCNT-PMMA composite membranes // Micron, 41 (2010) 909-914
5. *S.Yun, S.T.Oyama* Correlations in Pd membranes for hydrogen separation // A review., *J.* Membr. Sci., 375 (2010) 28-45

ADSORPTION-ELECTROCHEMICAL INTERACTION OF POLYMERIC POROUS FILLED WITH CARBON MEMBRANES WITH AMINO ACIDS SOLUTIONS

Marina Pozdeeva, Valetine Sedelkin, Olga Chirkova, Ekaterina Gorocholinskaya
Engels Technological Institute (branch) of Saratov State Technical University named after
Yuri Gagarin, Engels, Russia, *E-mail: Pozdeevamg@mail.ru*

Introduction

The results of amino acid transfer research (of glycocoll and β-alanine) are displayed with regard to systems of solutions membrane filtration. It is established, that mechanism and quantitative indicators of amino acids interaction with hard electrodes of different structure determine by diffusion, electrochemical and adsorption processes in the system.

Experiments

Membrane separation processes and fractionation of polydisperse liquid mixtures with a wide range of pH, containing proteins and amino acids are used increasingly in the food, pharmaceutical, biochemical and other industries. Molecules and atoms such mixtures polarized and are positive and negative charges. The behavior of proteins and amino acids not studied in such mixtures - electrolytes in the presence of porous polymer membranes.

The results of the potentiometric study of the mechanism of interaction between two amino acids (glycine and β-alanine) in 2M NaCl solution with a platinum working electrode and a polymer cellulose acetate membrane with carbon filler presented in this paper.

Cyclic potentiodynamic curves (CPDC) for 2M NaCl solution with glycine in the potential area of +1 to the -1B in Figure 1.

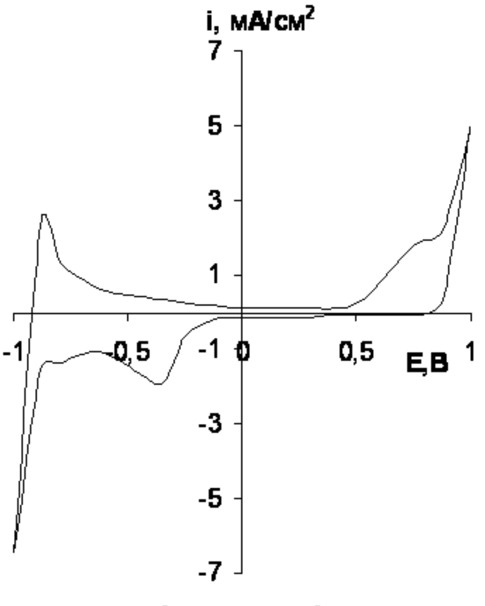

Figure. 1. Cyclic potentiodynamic curves for the system: 2M NaCl solution with glycine - Pt-electrode at the scan rate 80 mV/s

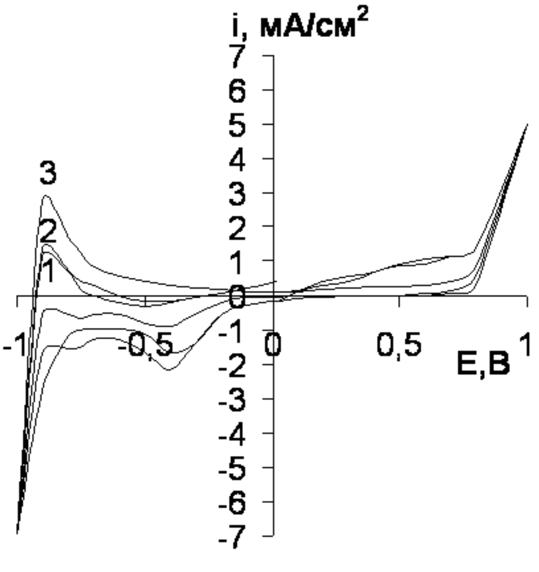

Figure. 2. Cyclic potentiodynamic curves for the system: 2M NaCl solution with glycine - Pt-electrode at the scan rate 80 mV/s and different pH: 1 –pH=2; 2 – pH=7; 3 – pH=11

CPDC first shot in the anode direction of potential Eb/t (no current) to +1B in which there is a sharp jump in the current, probably associated with the collapse of the water molecules by the scheme:

$$H_2O - 2e^- \rightarrow 2H^+ + O_{ads} \rightarrow 2H^+ + \frac{1}{2} O_{2ads}$$

and formation of the adsorbed oxygen. Reverse did and fixed peak current, connected, apparently, with the adsorption-desorption of oxygen.

Subsequent displacement potential in the cathode region is accompanied by the appearance on CPDC the site current limit ilim , and then the maximum and minimum current in the potential range -0.8 ... -0.9 V. These current peaks at CPDC likely connected with the intense adsorption-desorption of hydrogen. Current reversal in increments change of potential ΔE = 0.1 V in the cathodic and anodic potential region. The experience ends with the Eb/t.

CPDC in 2M NaCl solution with glycine at various pH values are shown in Figure 2. Current peaks captured in the cathodic direction of the current in the potential area Ea = -0.4 V and Ek = -0.8 V increase with increasing pH, which can be explained by the accumulation on the electrode of adsorbed molecules amino acids.

A distinctive feature of transport of amino acids from depth of the solution to the electrode surface for the system is a significant concentration gradient dc/dx with little potential gradient dE/dx, which indicates the intensity of molecular-diffusion flux.

The process of transfer of ions in the solution to the electrode of the cellulose acetate (CA) membrane is characterized by a high degree of reversibility (Figure 3,4). It is seen that CPDC forward and reverse on the membrane electrode not form hysteresis.

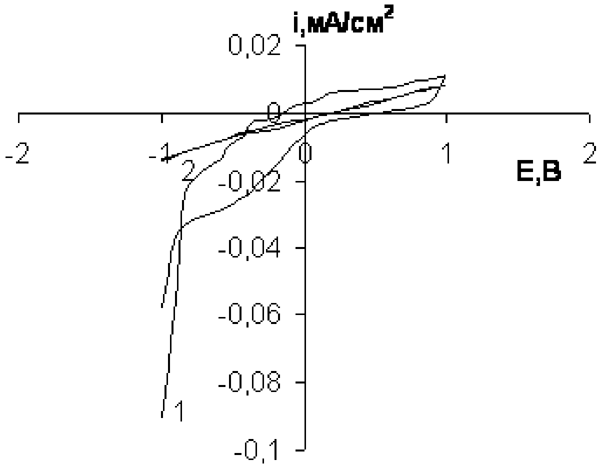

Figure. 3. Cyclic potentiodynamic curves for the system: a solution of β-alanine - electrode. 1 - Pt-electrode, 2 - CA electrode membrane (5% of CA, the carbon filler fines 85 microns). A solution of β-alanine – 0,005% by weight. Potential sweep rate - 80 mV/s

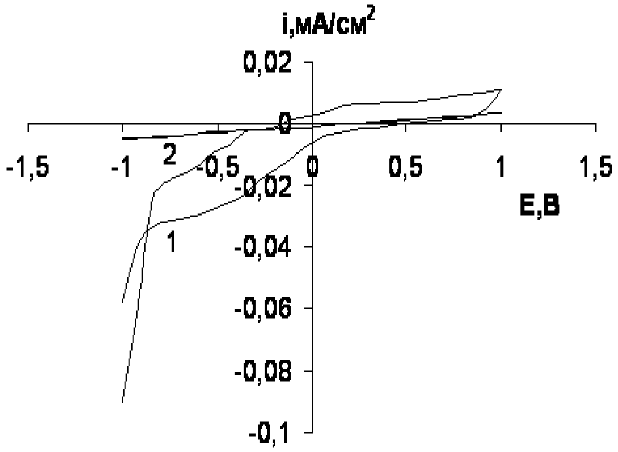

Figure. 4. Cyclic potentiodynamic curves for the system: a solution of β-alanine - electrode. 1 - Pt-electrode, 2 - CA electrode membrane (5% of CA, the carbon filler coarse 160 microns). A solution of β-alanine – 0,005% by weight. Potential sweep rate - 80 mV/s

Linear dependence of the i - E indicates a diffusion-migration mechanism of ion transport to membrane electrode.

Established that for CA of the membrane electrode with a carbon filler fines characteristic nearly linear increase Δi / ΔE with increasing concentration of β-alanine in solution. For membrane electrode with a carbon filler coarse experience stronger deviation of Δi / ΔE of linear, which is apparently connected with a non-uniform distribution of pore sizes in the structure of the electrode and the consequent difficulty of ion transport through the electrode.

These results should be used in the calculation and design of membrane modules to extract proteins from multicomponent solutions.

Conclusion

Thus, the experimental data suggest that in systems: solutions of amino acids -filtration membranes porous polymer are adsorption and electrochemical processes, accompanied by intense molecular diffusion and ion transfers.

Results of the study recommended used in the calculation and design of membrane modules for separation of amino acids and proteins from multicomponent solutions.

TRANSPORT PROPERTIES OF HYBRID NAFION MEMBRANE MATERIALS DOPED BY SILICA AND $H_{(3-X)}M_XPW_{12}O_{40}$ (M – K, Rb, Cs)

Ivan Prihno, Ekaterina Safronova, Andrey Yaroslavtsev
Kurnakov Institute of general and inorganic chemistry RAS, Moscow, Russia,
E-mail: safronova@igic.ras.ru

Introduction

Perfluorosulfonic cation-exchange membranes, such as Nafion, are widely used in electrochemical synthesis, water purification and fuel cell applications [1]. Incorporation of inorganic additives into such membranes is promising way to improve the conductivity of membrane and it's water management. It was founded that hybrid membranes contained dopants with high concentration of acid protons are the most promising materials for low and middle temperature fuel cells [2] because dissociated protons participate in ion transport process and promote sorption and retention of additional water molecules in the membrane. From this point of view incorporation of inorganic heteropolyacids such as phosphotungstic acid $H_3PW_{12}O_{40}$ (PWA) should leads to the considerable conductivity increase. However there is a need to stabilize PWA in the membrane matrix in order to prevent its high solubility. It is to prevent PWA washing out by its sorption on silica oxide surface or by its conversion into the insoluble salts.

In this work the results of Nafion+SiO_2+$H_{(3-x)}M_xPW_{12}O_{40}$ (M – K, Rb, Cs) membranes investigations are presented.

Experiments

The hybrid materials were prepared via in situ method as described in [3]. Nafion 117 membranes (thickness 230-250 µm) were pre-treated by tetraethoxysilane (≥98 %, Fluka) with the followed treatment by diluted NH_4OH solution to cause silica formation in membrane pores. PWA was incorporated into membrane matrix by membrane treatment with diluted PWA solution. To converse PWA into acid salts membrane was immersed into corresponding solution (M_2CO_3). All membranes were treated one after another by 5% solution of HCl and twice by bidistilled water at 80°C.

Results and Discussion

Incorporation of dopants into Nafion results in the increase in water uptake from 19.5% for the initial Nafion to 21.0-22.6 % for hybrid membranes. Proton conductivity at 100 % relative humidity (RH) of membranes Nafion+SiO_2+$H_{(3-x)}M_xPW_{12}O_{40}$ is less than that of Nafion+SiO_2 membrane (fig. 1a). At the same time it is equal or slightly less than conductivity of pure Nafion. As Nafion modification by acid PWA salts is accompanied by the water uptake and acid protons concentration increase it can be proposed that conductivity of three component Nafion+SiO_2+$H_{(3-x)}M_xPW_{12}O_{40}$ systems should be higher than Nafion+SiO_2. However, experimental data shows the reverse. The most probable reason for this is the simultaneous presence of proton and alkaline cations in the membrane that results in their deceleration. Furthermore, bulky cations are slow-moving and can block up the conductivity channels in the membrane.

Considerable increase in conductivity in comparison with Nafion membrane is observed at low relative humidity (fig. 1b). At RH=32% conductivity of Nafion+SiO_2+$H_3PW_{12}O_{40}$ membrane consists $9.5 \cdot 10^{-3}$ S/cm while conductivity of Nafion is $6.4 \cdot 10^{-4}$ S/cm. PWA conversion into insoluble salt form results in some decrease in conductivity. The ion conductivity mechanism at low RH differs from that at 100% RH. At high water uptake proton diffuse via Grotthuss mechanism between water molecules. As RH decreases the distance between the nearest oxygen atoms increases and transfer is limited by the frequency of protons jumps. In hybrid membranes dopant particles participate in the proton transport at low RH and the presence of additional acid protons in the membrane makes a contribution into conductivity.

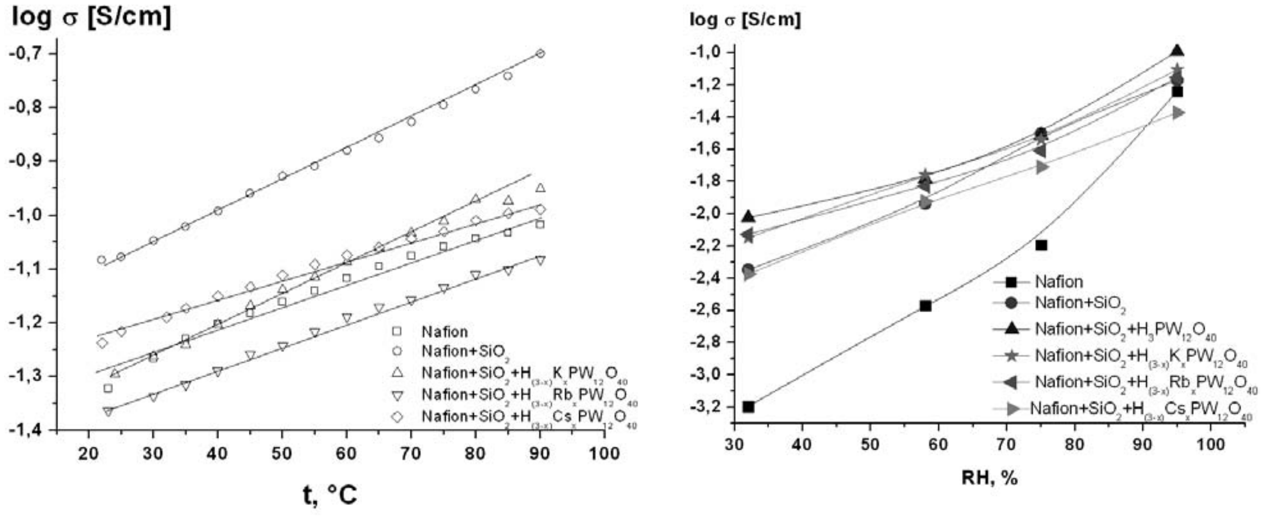

a *b*

Figure 1. Ion conductivity as a function on temperature (a) and relative humidity (b) for the investigated membranes

Diffusion permeability (P, cm^2/s) of 0.1M HCl solution through the membranes was investigated. Incorporation of SiO_2 into Nafion leads to the P increase in 3 times (from $2.52\cdot10^{-7}$ to $5.6\cdot10^{-7}$ cm^2/s). At the same time diffusion permeability of three component systems Nafion+SiO_2+$H_{(3-x)}M_xPW_{12}O_{40}$ is less than of Nafion+SiO_2 and gradually reduces with ion radius increase from $4.81\cdot10^{-7}$ for Nafion+SiO_2+$H_{(3-x)}K_xPW_{12}O_{40}$ to $3.2\cdot10^{-7}$ cm^2s for Nafion+SiO_2+$H_{(3-x)}Cs_xPW_{12}O_{40}$ and approaches to the diffusion permeability of Nafion. The reason of this phenomenon is decrease in the free space inside of membrane due to the presence of bulk dopant particles and bulk alkaline cations.

Acknowledgements

This work was financially supported by the Russian Foundation for Basic Research (project 12-08-91161).

References

1. *B. Yaroslavtsev, Yu. A. Dobrovolsky, N. S. Shaglaeva, L. A. Frolova, E. V. Gerasimova and E. A. Sanginov* // Russ. Chem. Rev., 2012, 81, 191).
2. *Yaroslavtsev A.B.* // Nanotechnologies in Russia. 2012. V.7, № 9-10. P. 8-18.
3. *Safronova E.Yu., Stenina I.A., Yaroslavtsev A.B.* // Russ. J. Inorg. Chem., 2010. V. 55. № 1. P. 13-17.

MATHEMATICAL MODEL FOR IONIC TRANSPORT THROUGH NANOPORES WITH AMPHOTERIC FIXED CHARGE GROUPS

[1]Patricio Ramirez, [2]Konstantin Lebedev, [2]Marina Kyzakina
[1]Polytechnic University of Valencia, Spain, *E-mail: patraho@fis.upv.es*
[2]Kuban State University, Russia, *E-mail: klebedev@fpm.kubsu.ru; kuzzyashka@yandex.ru*

Introduction

We have studied theoretically the effects of pH on the ion transport through amphoteric polymer membranes composed of weak polyelectrolytes where the charged groups are randomly distributed along the axial direction of the membrane. This system serves as simplified model for the pH controlled ion transport and drug delivery through membranes of biological interest. The theoretical approach employed is based on the Nernst-Planck equations [1-3]. The complete system of electrical charges is formed by: (1) the pH dependent amphoteric membrane fixed charge, and (2) the four mobile charges (the two salt ions and the hydrogen and hydroxide ions), that have been taken into account without any additional assumption. The model predictions show that the ionic fluxes and the membrane potential are very sensitive to the external pH, and the potential utility of these predictions for the analysis of experiments involving pH dependent passive transport through membranes is emphasized.

Model

Figure 1 shows schematically a polymeric film extending from $x = 0$ to $x = d$ which separates two electrolyte solutions (KCl in our case). The film contains a single cylindrical pore with radius a. The pH of the external solutions is controlled by adding either HCl or KOH. Therefore, the ionic mobile species present in the system are the salt ions (K^+ , Cl^-), and the hydrogen (H^+) and hydroxide (OH^-) ions. In Fig. 1, $c_{S,j}$ is the KCl concentration in solution j (j= L for the left solution and j= R for the right solution). Also, $c_{i,j}$ is the concentration of the species i in the bulk of the external solution j. In the following we use i = 1 for K+ ions, 2 for Cl^- ions, 3 for H^+ ions, 4 for OH^- ions, and 0 for the water mulecule. φ_j and pH_j refer, respectively, to the electric potential and the pH value of the solution j. $c_i(x)$ and $\varphi(x)$ are the local concentration of the species i and the local electric potential within the pore. $\Delta\varphi_L = \varphi(0) - \varphi_L$ and $\Delta\varphi_R = \varphi_R - \varphi(d)$ denote, respectively, the Donnan potential drops through the left and right pore/solution interfaces, and $\Delta\varphi_D = \varphi(d) - \varphi(0)$ is the diffusion potential within the pore. I is the total electric current passing through the membrane under an applied potential difference $V = RT(\varphi_L - \varphi_R)/F$. Finally, $X_F(x)$ is the total membrane fixed charge concentration at a point of coordinate x. The solutions are assumed to be perfectly stirred, and the whole system is isothermal.

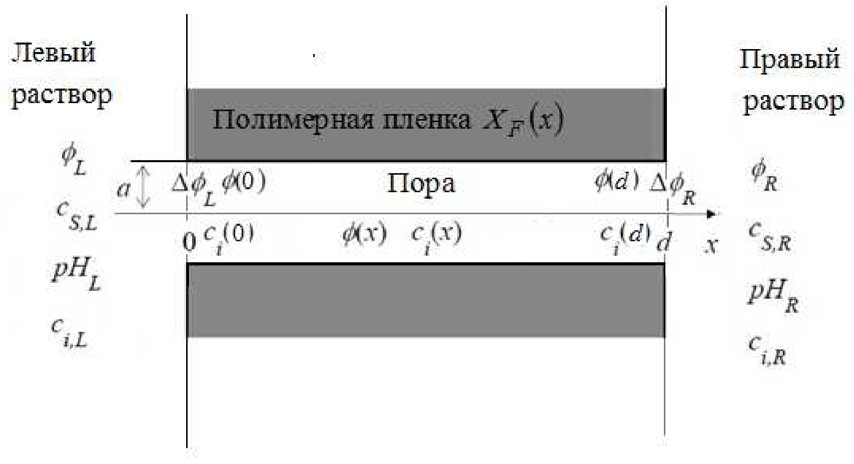

Figure 1. Sketch of the system under study

The nanopore contains amphoteric groups attached to the pore walls. We assume that these groups are homogeneously distributed on the pore surface, and can be charged or not depending on the local value of the pH within the pore solution. We denote by X_N^- and X_N^0 the (molar) concentrations of the charged (N–) and neutral (N0) acidic groups, and by X_P^+ and X_P^0 the concentrations of the charged (P+) and neutral (P0) basic groups, respectively. We assume also the following equilibrium between neutral charged groups $N^0 \xleftrightarrow{\Leftrightarrow K_N} N^- + H^+$, $P^+ \xleftrightarrow{K_P} P^0 + H^+$ where K_N and K_P are the respective equilibrium constants. From these equilibriums we obtain the total fixed charge concentration profile along the pore

$$X_F(c_3, c_4) = \frac{X_P^T}{1 + \frac{c_4}{K_P}} - \frac{X_N^T}{1 + \frac{c_3}{K_N}}.$$

Bulk solution and pore solution concentrations are connected through the following Donnan equilibrium conditions at the interfaces $x = 0$ and $x = d$:

$$\frac{c_1(0)}{c_{1,L}} = \frac{c_{2,L}}{c_2(0)} = \frac{c_3(0)}{c_{3,L}} = \frac{c_{4,L}}{c_4(0)}, \quad \frac{c_1(d)}{c_{1,R}} = \frac{c_{2,R}}{c_2(d)} = \frac{c_3(d)}{c_{3,R}} = \frac{c_{4,R}}{c_4(d)}.$$

The electroneutrality condition in the pore solution gives

$$c_1 + c_3 + X_F = c_2 + c_4.$$

The basic equations describing the ionic transport across the nanopore are the Nernst-Planck equations. The equations of mass balance for all mobile species are

$$\frac{\partial j_i}{\partial x} = 0 \text{ , } (i=1, 2) \text{ ; } \frac{\partial j_i}{\partial x} = v_i \text{ , } v_3 = v_4 = -v_0 = k_d c_0 - k_r c_3 c_4 \text{ , } (i=0, 3, 4).$$

The basic equations describing the ionic transport across the nanopore are the Nernst-Planck equations

$$j_i = -D_i \left(\frac{dc_i}{dx} + \frac{z_i F}{RT} c_i \frac{d\phi}{dx} \right), \quad i = 1 \div 4,$$

the Poisson equation

$$-\frac{\varepsilon\varepsilon_0}{F} \frac{d^2\phi}{dx^2} = c_3 - c_4 + c_1 - c_2 + X_F(c_3, c_4),$$

and the boundary conditions for the electric potential potential

$$\phi_L = \phi^I = 0, \; \phi_R = \phi^{II}, \; -1 \le \phi^{II} \le 1, \qquad \Delta\phi_L + \Delta\phi + \Delta\phi_R = \phi_R .$$

In our numerical solution we used a finite differences scheme together with the Newton's method, with initial guess given by the Goldman constant field approximation [4, 5]. The equations were linearized for the five mobile species, and written using the difference operator Δ. The functions without the operator Δ are considered as known from the previous iteration.

The above scheme results in six second order differential equations with unknown variables *H_2O(X), Cl(X), K(X),H(X) OH(X),* $\phi(X)$ and twelve boundary conditions. Considering a vector of unknown variables $Y = (C_0, C_1, C_2, C_3, C_4, \phi)$. There is a system of linear equations with a three-diagonal matrix

$$\begin{aligned} &-d_i \Delta C_i'' - z_i d_i \psi_i' \Delta C_i' - z_i d_i C' \Delta \psi_i' - z_i d_i \psi'' \Delta C_i - z_i d_i C_i \Delta \psi'' - \\ &- L_i (K_d \Delta C_{HA} - K_r C_{HA} \Delta C_H - K_r C_H \Delta C_A) = \\ &= (d_i C_i'' + z_i d_i C' \psi' + z_i d_i C_i \psi'') + L_i (K_d C_{HA} - K_r C_H C_{OH}) \text{ , } (i = 0 \div 5). \; (L_0 = -1, L_1 = L_2 = 0, L_3 = L_4 = 1) \end{aligned}$$

$$\bar{\varepsilon}\Delta\psi'' + \sum_{i=0}^{4}\Delta C_i - \frac{X_P^T}{K_P}(1+\frac{c_A}{K_P})^{-2}\Delta C_A + \frac{X_N^T}{K_N}(1+\frac{c_A}{K_N})^{-2}\Delta C_A =$$

$$\bar{\varepsilon}\frac{d^2\psi}{dX^2} + \sum_{k=0}^{4} z_k C_k + \bar{X}_F(C_1, C_2)$$

Iterations proceeded until

$$\sum_{i=0}^{5}\left\|(\Delta Y_i)_{p+1} - (\Delta Y_i)_p\right\| < \varepsilon$$

Results and Discussion

Figure 2 shows the comparison between our theoretical model and available experimental data. The results of Fig.2 (a) correspond to the biological ion channel Outer Membrane Porin F, OmpF [6, 7]. The charge distribution within the ion channel changes from symmetrical, nonpolar to asymmetrical, bipolar because of an externally imposed pH difference. The curves in Fig. 2 (b) correspond to the results of the above model. Remarkably, the *I-V* curve of the ion channel in Fig.2(b) resembles that of a bipolar junction when $pH_L = 3$ and $pH_R = 12$ because of the protonated positively charged groups and deprotonated negatively charged groups placed at the respective ends of the nanopore (see Fig.3). As expected, this externally induced bipolar nature is virtually lost when the pH values of the bathing solutions are identical. This $pH_L = pH_R = 3$ at 2(a) and our calculation $pH_L = pH_R = 7$ at 2 (b).

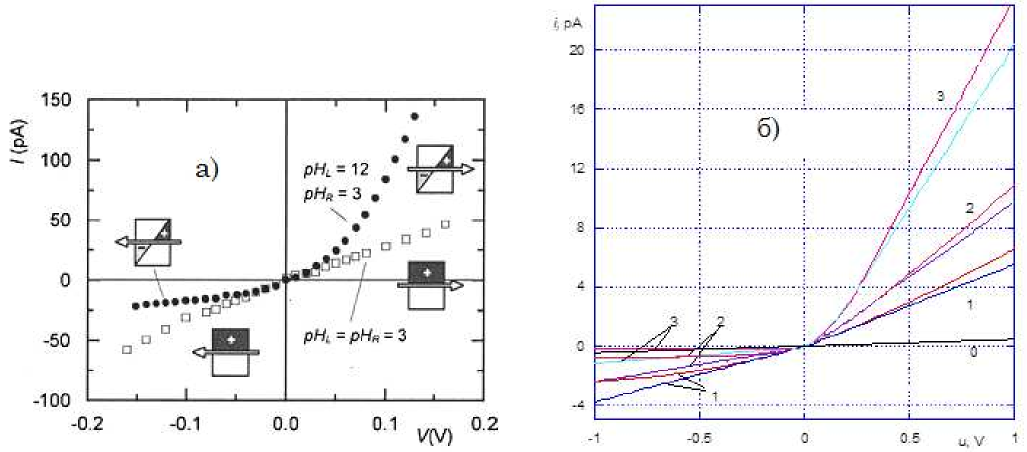

Figure 2. a) Experimental data of a biological ion channel: 1) pHL= pHR=3 2)pHL=12, pHR=3 [6,7] b) Theoretical I-V curves at different pH_L-pH_R values: 0-(7-7); 1-(8-6); 2-(9-5); 3-(10-4). Red curves are numerical calculations on full model, dark-blue curves are analytical approximations given by the Goldman constant field assumption

The results of the fixed charge membrane distribution X_F obtained by the above procedure in the case $pH_L = 10$ and $pH_R = 4$ are shown in Figure 3. For this pH configuration, zones with negative fixed charge close to the left boundary and positive fixed charge close to the right boundary are obtained. The thickness of these zones is controlled by the ratio K_N / K_P. This bipolar distribution explains the rectifying *I-V* curves of Fig. 2(b)

Our theoretical allows for the calculation of the pore charge distribution as well as the ionic transport numbers at any applied voltage. In all the model equations we have taken into account that the pH within the membrane may be very different from the external pH because of the membrane fixed charge *XF* .

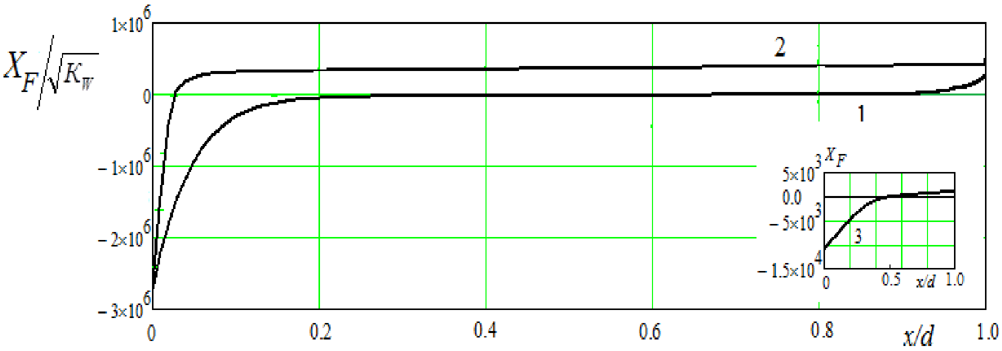

Figure 3. Concentration of fixed groups X_F *at* $pH_L=10$ *and* $pH_R=4$ *, u=1 V at different ratios* K_N/K_P *:1 -* 10^4*; 2-10 , u=1. Curve 3 at* $K_N/K_P=1$ *and u=0*

We have presented a theoretical model for ion transport through nanopores with amphoteric fixed charges. The results have been compared with available experimental data. Although we have introduced some crude approximations in order to keep the model reasonably simple, the calculations follow the experimental trends. The Goldman constant fiel assumption allowed receive some calculus of approximations enough accuracy of *I-V* curves, but should it is recognized insufficient for the description of distribution concentration, potential on length of a capillary. The model predictions could be useful for the analysis of future experiments.

References

1. *Ramirez P., Mafe S., Tanioka A., Saito K.*//Polymer 1997. Vol. 38 N19, PP. 4931-4934.
2. *Nikonenko V.V., Lebedev K.A., Сулейманов S.S.* Influence convective summand in equation of Nernst-Plank on characteristics of carry of ions through a layer of a solution or a membrane // Electrochemistry, 2009. T.45. №2. P. 170-179.
3. *Sulejmanov S.S., Kurilenko A.K., Lebedev K.A.* Iinfluence convectiv composed in equation of Nernst-Plank on characteristics of carry of ions through in the charged capillary of a synthetic membrane // The Ecological bulletin of center of science. 2009. № 2. C.56-64.
4. *Goldman D. E.* Potential, impedance, and rectification in membranes J. Gen. Physiol. 1943. V. 27. P. 37.
5. *Pellicer J., Mafe S., and Aguilella V. M.* // Ionic transport across porous charged membranes and the Goldman constant assumption. Ber. Bunsenges. Phys. Chem. 1986. V. 90. P. 867-872.
6. *Alcaraz A., Ramírez P., García-Giménez E., López M. L., Andrio A., Aguilella V. M.*, J. Phys. Chem. B110, 21205, 2006.
7. *Alcaraz A., Nestorovich E. M., Aguilella-Arzo M., Aguilella V. M., Bezrukov S. M. Salting* out the ionic selectivity of a wide channel: The asymmetry of OmpF. Biophys. J. 87:943-957. Biophys. J.87,943, 2004.

VOLTAMMETRY OF NANOPOROUS CHARGED GLASSES MEMBRANES

[1]Mònica Reig, [2]Semyon Mareev, [1,3]Andriy Yaroshchuk, [2]Victor Nikonenko

[1]Catalonian Polytechnic University, UPC, Barcelona, Spain; *E-mail: monica.reig@upc.edu*
[2]Membrane Institute, Kuban State University, KubSU, Krasnodar, Russia
[3]ICREA, Barcelona, Spain

Introduction

Porous glasses are leaching products of phase-separated alkali borosilicates. The first phase is an alkali-rich borate phase, soluble in hot mineral acids, water or alcohols. The second phase is almost pure silica. The pores can be formed during the phase separation process in a wide size range from 0.3 to 1000 nm in diameter, depending on glass composition, time and temperature of phase separation and leaching conditions. A quenching of the initial glass melt followed by a short-time treatment at lower temperatures results in microporous materials. Their surface is characterized by hydroxyl groups with concentration between 4 and 8 OHs nm^{-2}. This kind of membranes possesses, in comparison with other porous inorganic solids, high thermal stability, chemical resistance, high optical transparency, very flexible geometric forms, very reactive surface and good accessibility to eventually available active sites inside the porous structure. Moreover, this type of membranes are characterized by low permeability of air, a low surface acidity caused by very weakly acidic silanol and weakly acidic boranol groups. They are of interest for molecular sieve applications. Porous glasses are applied in biotechnology, membrane technology, micro-reaction engineering, dental industry, in heterogeneous catalysis between others applications.

Experiment

Nanoporous glass membranes properties are studied with help of an electrodialysis cell. There are 4 different porous sizes available: 15, 30, 50 and 100 nm. The cell includes 4 compartments: 2 electrode rinse ones, 1 dilute and 1 concentrate stream compartments. There is a cathode and an anode in each of the ends of the cell followed by an anionic and a cationic membrane; the nanoporous glass membrane is placed in the middle of the cell. Two Luggin capillaries are used for measuring the potential difference across the glass membrane.

Results and Discussion

In a 0.01 M NaCl solution, no limiting current was observed in the case of 100 nm and 15 nm porous glass membranes. In a 0.001 M NaCl solution, the limiting current for all studied membranes was detected. This behaviour was predicted by Yaroshchuk A. (2012) model for nanoporous membranes: the limiting current may occur in more dilute solutions and may not occur in more concentrated ones. However, in a 0,0001 M NaCl solution no limiting current was observed due to high resistivity of the system.

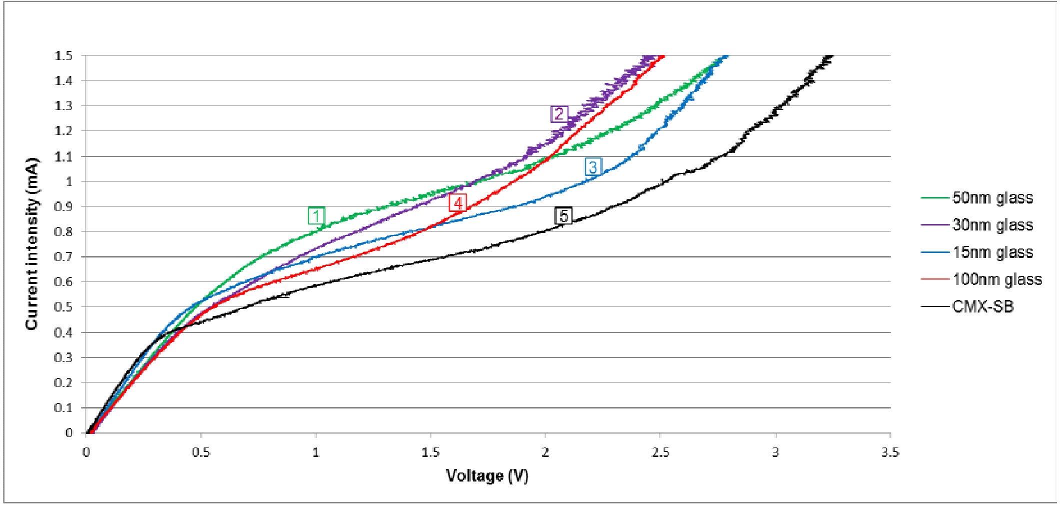

Figure 1. Voltammetry curves for a 0.001 M NaCl solution and different tested membranes. 1) 50nm porous glass membrane. 2) 30nm porous glass membrane. 3) 15nm porous glass membrane. 4) 100nm porous glass membrane. 5) CMX-SB homogeneous membrane

In the graph below the experimental I-V curves 0.001 M NaCl solutions are shown for a 15, 30, 50 and 100 nm porous glasses membranes and also for a CMX-SB homogeneous membrane to comparison.

Conclusion

Generally, it can be seen that the highest limiting current is observed for the 50 nm membrane, it decreases in the range: 50 > 30 > 15 > CMX-SB. This range may be explained by increasing membrane permselectivity: lower pore size reduces the fraction of pore space filled with uncharged solution. The case of 100 nm membrane presents an exception to the rule.

Acknowledgements

The authors are grateful to the European "CoTraPhen" project for financial support.

References

1. *Markovic A., Stoltenberg D., Enke D., Schlünder E.-U, Seidel- Morgenstern A.* Gas permeation through porous glass membranes. Part I. Mesoporous glasses- Effect of pore diameter and surface properties // Journal of Membrane Science, 2009. V 336, P 17-31.
2. *Enke D., Janowski F., Schwieger W.* Porous glasses in the 21th century- a short review // Microporous and Mesoporous Materials, 2003. V 60, P 19-30.
3. *Yaroshchuk A.* What makes a nano-channel? A limiting- current criterion // Microfluid Nanofluid, 2012. V 12, P 615-624.

MECHANISMS OF THE SURFACE FORCE ACTION IN CAPILLARY PHENOMENA

Vjacheslav Roldughin, Tat'yana Kharitonova
Frumkin Institute of Physical Chemistry and Electrochemistry of RAS, Moscow, Russia,
E-mail: roldugin@phyche.ac.ru

Introduction

The existing approaches to the description of capillary effects in some cases lead to paradoxical situations. Even classic findings of a number of well-known formulas may be in conflict with the general physical concepts of intermolecular interactions. We discuss different capillary phenomena, give some examples of paradoxes and resolve them at molecular-kinetic level. In this note we consider just one example.

Capillary rise of liquid

We start our analysis with an apparent contradictions associated with different derivation of the expression for the height of capillary rise of a liquid (Fig. 1). The well-known Jurin formula for the height of capillary rise H_G is (we neglect the density of air)

$$H_G = \frac{2\sigma\cos\theta}{\rho g R_c}, \quad (1)$$

where σ is the surface tension, ρ is the liquid density, R_c is the capillary radius, θ is the contact angle, g is the acceleration of gravity. Here and below we do not take into account many subtle effects associated with the detailed structure of the meniscus, simply accept that it is spherical.

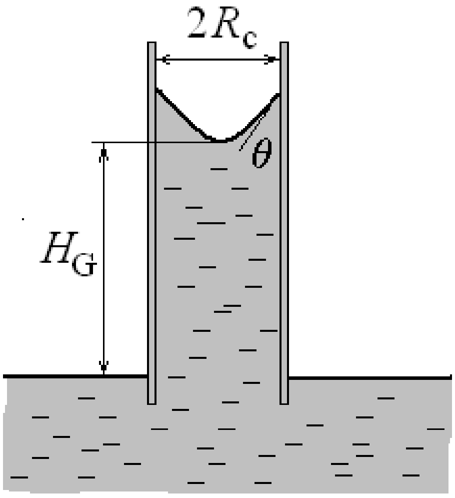

Figure 1. On the derivation of Jurin formula

Standard derivation of Eq. (1) is based on the consideration of hydrostatic pressure balance at the base level of liquid ($H = 0$) with the Laplace pressure reduction under the concave curved surface.

Consider another approach, which, at first glance, also gives Eq. (1). That is, we are talking about the so-called minimization of the free energy of the system. Free energy relating to the filling of the capillary with liquid, is given by

$$F(H) = \frac{1}{2}\rho g \pi R_c^2 H^2 + 2\pi R_c H(\sigma_{ls} - \sigma_s), \quad (2)$$

where H is the height of the liquid, σ_s is surface energy of the capillary material, σ_{sl} is the surface energy of the liquid-solid interface. Minimizing the free energy, we obtain

$$H_F = \frac{2(\sigma_s - \sigma_{ls})}{\rho g R_c}. \quad (3)$$

Using the Young formula

$$\cos\theta = \frac{\sigma_s - \sigma_{ls}}{\sigma}, \qquad (4)$$

we immediately arrive at the Jurin formula. Hence, the two approaches seem to yield the same result.

However, both approaches, as is easily seen, give the same result only if the

$$\frac{\sigma_s - \sigma_{ls}}{\sigma} \le 1 \qquad (5)$$

when from Eq. (4) the contact angle can actually be defined. But there are many situations, when the opposite inequality takes place

$$\frac{\sigma_s - \sigma_{ls}}{\sigma} > 1. \qquad (6)$$

In this case Eqs. (1) and (3) are in in conflict, and Eq. (3) predicts a higher capillary rise of the liquid.

There is also the question on the nature of forces lifting the liquid. The fact is that the pressure drop across the meniscus is related to the internal fluid forces. For this reason it cannot maintain the fluid in a gravitational field.

An explanation of the first problem

It is known that the condition (6) simply means that the liquid spreads over the surface of the solid, the contact angle is not formed, and may be formally set equal to zero. The question arises as to what height the liquid rises in this case. The answer is as follows. The height of the meniscus rise is determined by Eq. (1), but on the surface of the capillary wetting film is formed (Fig. 2), the height of the liquid film rise can greatly exceed the value given by the Jurin formula. Let us estimate the height of the liquid film rise.

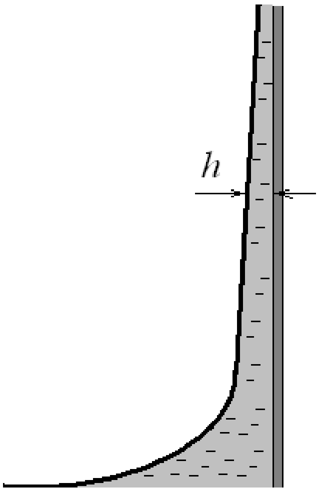

Figure 2. Profile of the liquid meniscus under condition of wetting film formation

The height of wetting film rise can be determined by well-known expressions for the disjoining pressure Π (h) as a function of film thickness h and height H. For a film on a vertical wall we have [1]

$$d\Pi(h) = \rho g dH\,. \qquad (7)$$

From this expression, it is clear that the height of the film rise is actually determined by the disjoining pressure at boundary thickness h_0, where the transition from wetting to adsorption film takes place.

$$H_R = \frac{\Pi(h_0)}{\rho g}. \tag{8}$$

We have put that at the level of the water surface or meniscus the disjoining pressure vanishes.

Let us estimate the characteristic values of the disjoining pressure. We use for the estimation the disjoining pressure in the wetting films corresponding to the dispersion forces

$$\Pi_m(h) = \frac{A}{6\pi h^3}, \tag{9}$$

where A is the Hamaker constant. It is well known that the disjoining pressure isotherm (9) is valid up to a thickness approximately equal to $h_0 = 0.8$ nm, where the film can be considered as a wetting one. We take this value as the lower limit for the thickness of wetting films and evaluate the appropriate height. After substituting in equation (8) expression (9) for the disjoining pressure we obtain the following height of the wetting film rise

$$H_{Rf} = \frac{\Pi_m(h_0)}{\rho g} = \frac{A}{6\pi\rho g h_0^3}. \tag{10}$$

Let us estimate the height value given by Eq. (10). For a film of water on a glass substrate the Hamaker constant $A = 1.1\times10^{-20}$ J. Substituting the values of A and h_0 results in the value of H_{Rf}, equal to about 10^2 m which is a very large quantity. For comparison, in a capillary with $R_c = 1$ μm, the water will rise, according to the formula Jurin, to a height of about 7-8 m. If we take into account the structural component of disjoining pressure [1]

$$\Pi_s(h) = K\exp(-h/l) + K_0\exp(-h/l_0), \tag{11}$$

then

$$H_{Rf} = [K\exp(-h/l) + K_0\exp(-h/l_0)]/\rho g, \tag{12}$$

and using the parameter of the structure component of disjoining for the water film on the quartz surface $K = 2\times10^7$ dyn/cm^2, $l = 2$ nm and $K_0 = 3\times10^9$ dyn/cm^2, $l_0 = 0.3$ nm, we get to the height of film rise (the film thickness 1 nm) the giant value of about 10^3 m.

The higher altitude of the wetting film rise as compared to the liquid column is due to the excess tangential stress (pressure) is spent on hold not the liquid column, but only the wetting film, as described by equation (7).

Conclusion

Our analysis shows that the liquid in the capillary is supported not by the pressure drop at the meniscus, but surface forces acting directly at the capillary walls. There is a number of examples showing that the classical treatment of capillary phenomena leads to paradoxes. Only a detailed analysis of the phenomena at the molecular level can give them a consistent interpretation.

References

1. *Derjaguin B.V., Churaev N.V., Muller V.M.* Surface Forces, Nauka, Moscow, 1985.

ON SOME PECULIARITIES OF THE GAS MIXTURE FLOW IN NANOSIZE CHANNELS

[1] Vjacheslav Roldughin, [1]Elena Sherysheva, [2]Vladimir Zhdanov
[1]Frumkin Institute of Physical Chemistry and Electrochemistry of RAS, Moscow, Russia,
E-mail: roldugin@phyche.ac.ru
[2]National Research Nuclear University “MEPhI”, 31, 115409, Moscow, Russia,
E-mail: VMZhdanov@mail.ru

Introduction

The effects of asymmetry for heterogeneous membrane systems have recently attracted the attention of researchers. The asymmetry effects were observed in the permeability of heterogeneous membranes and in catalytic processes in membranes. It should be noted that the observed effects are quite strong: the permeability coefficients for different orientations of the membrane coefficients can distinguished twice.

Different models have been proposed to explain the observed effects. It was in particular shown that the asymmetry of the permeability of bilayer membranes can be due to the surface diffusion, if one takes into account the dependence of surface diffusion coefficient on the degree of surface coverage. In the latter case it was possible to explain one and a half difference in the permeability coefficients of differently oriented membranes.

Binary mixture transfer in nanosize membranes

We begin our discussion with the analysis of transport of a binary gas mixture in nanosize channels when surface diffusion makes a significant contribution. We limit ourselves to the simplest situation of binary mixture flow through nanosize channels, taking into account the diffusion in the adsorbed layer. We assume that the adsorption of the components is described be Langmuir isotherm

$$\Gamma_i = \Gamma_{\max} \frac{p_i / \alpha_i}{1 + p_1/\alpha_1 + p_2/\alpha_2}, \tag{1}$$

Where $\Gamma_{\max}$ is the maximum adsorption Γ_i is adsorption of component *i*, p_i is its partial pressure, α_i are the parameters of the adsorption isotherm. We assume that the transfer of the components in the channel volume and the surface layer is independent and that the transfer in the adsorbed layer is associated with the gradient of the adsorption of the component. Then the component fluxes through a cylindrical channel of radius r are given by

$$J_i = \pi r^2 \frac{D_{vi}}{kT}\frac{dp_i}{dz} + 2\pi r D_{si}\Gamma_{\max}\frac{d}{dz}\left(\frac{p_i/\alpha_i}{1 + p_1/\alpha_1 + p_2/\alpha_2}\right), \tag{2}$$

where the *z* axis is directed along the axis of the channel, *k* is the Boltzmann constant, *T* is absolute temperature , D_{vi}, D_{si} are the coefficients of bulk and surface diffusion of component *i*.

There are no published data on the calculations of dependence of surface diffusion coefficient on surface coverage in the case of multicomponent systems. However, we can obtain the corresponding dependence using the following considerations. Diffusion flux is usually written in the form

$$J = -\frac{Dn}{kT}\nabla\mu, \tag{3}$$

where μ is the chemical potential of the diffusing component, *n* is its concentration. This form allows to take into account the interaction between the molecules at high concentration. In fact, it is a classical Fick's law, written using the Einstein relation between the mobility of the particles and their diffusion coefficient. The chemical potential gradient in this case, obviously, is the average force acting on the particle. As the gas in the bulk phase at pressures considered in this paper can be treated as ideal, the chemical potentials of the components can be represented in the form

$$\mu_i = kT\ln(p_i/p_0), \tag{4}$$

where p_0 is the normalization constant. Using the condition that the chemical potentials of the components in the bulk phase and in the adsorbed layer and the Langmuir isotherm can be obtained by the following relation between the equilibrium vapor pressure and surface coverage of components $\theta_i = \Gamma_i/\Gamma_{\max}$:

$$p_i = \frac{\alpha_i \theta_i}{1-\theta_1-\theta_2}. \tag{5}$$

Given the above relation the flux of *i*-th component in the channel can be represented as follows

$$J_i = \pi r^2 \frac{D_{vi}}{kT}\frac{dp_i}{dz} + 2\pi r D_{si}\Gamma_{\max}\theta_i \frac{d}{dz}\ln\left(\frac{\alpha_i\theta_i}{1-\theta_1-\theta_2}\right), \tag{6}$$

According to the above relations, we obtain the following expression for the component fluxes

$$J_i = \pi r^2 \frac{D_{vi}}{kT}\frac{p_{i\text{in}} - p_{i\text{out}}}{l} + \frac{2\pi r D_{si}\Gamma_{\max}}{l}\frac{p_{i\text{out}} + p_{i\text{in}}}{p_{1\text{out}} + p_{2\text{out}} + p_{1\text{in}} + p_{2\text{in}}}\ln\left[\frac{1+\dfrac{p_{1\text{in}}}{\alpha_1}+\dfrac{p_{2\text{in}}}{\alpha_2}}{1+\dfrac{p_{1\text{out}}}{\alpha_1}+\dfrac{p_{2\text{out}}}{\alpha_2}}\right], \tag{7}$$

where $p_{i_{\text{in}}}$, $p_{i_{\text{out}}}$ are the partial pressures at the membrane inlet and outlet, respectively.

Figure 1 shows the mutual influence of the components on their transport in nanosize channels.

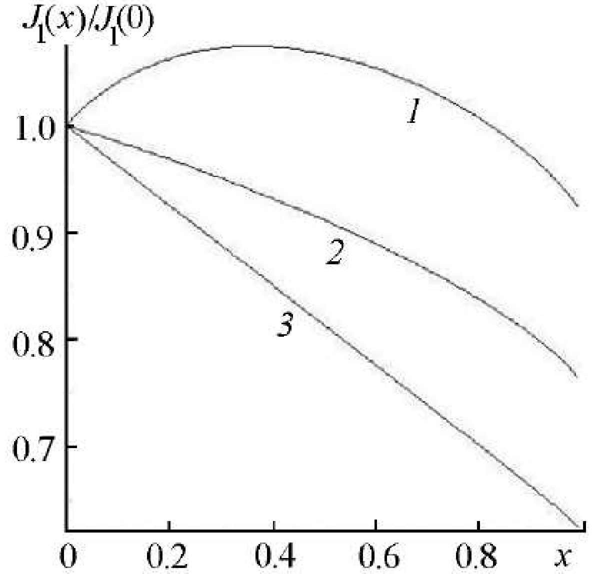

Figure 1. Dependencies $J_1(x)/J_1(0)$ taking into account the influence of components for 1– α1/α2 = 0.1, 2 – 1, 3– 10; x is the mole fraction of the second component

It should be noted not only quantitative but also a qualitative change in the mutual influence of components depending on the adsorption characteristics. In particular, if the second component more readily adsorbed, in the case of small its content the transfer of the first component increases. The second component displaces the first component to lower concentrations in the adsorption layer due to steric interactions. It is important to note here that the entrainment prevails the suppression of adsorption and reduction of transport in the adsorption layer. As a result of two competing processes reduction of adsorption of the first component and reducing its transfer into the adsorption layer and the entrainment, accelerating the transport of the first component, as a whole, the influence of the second component is less strong than in the absence of interaction between the components.

Consider now a binary pumping of the gas mixture through a membrane. In the steady state, the component fluxes remain constant in any section of the membrane module , including the inside of the porous membrane. The ratio fluxes of G_1 first and G_2 second components can be represented as

$$\frac{G_1}{G_2} = \frac{c_1}{1-c_2}, \tag{8}$$

where c_1 is the concentration of the first component at the membrane inlet.

To provide this flux ratio, before the membrane the concentration of the first component must be lowered (this component passes through the membrane faster). Let c_0 is the concentration of the first component just before the membrane. Figure 2 shows the dependence of the c_0 concentration on the ratio of pressures before (p_{in}) and behind (p_{out}) the membrane for α_1 = 5 atm and α_2 = 0.5 atm. There's also given the dependence calculated by the Knudsen formula. The difference between these curves characterizes the influence of surface diffusion on the separation factor (concentration c_0). We note the fundamental feature that the calculation by formula (7) results in two solutions. One is a "typical", that predicts a slightly smaller value of c_0, which is associated with a faster transfer of the first component due to its transport in the adsorption layer. The second solution predicts the opposite to the "typical" increase of the concentration of the “faster” component before the membrane. This is due to the nonlinear nature of the transport processes in nanosize channels, described by Eqs. (7). It is easy to explain the appearance of the second solution. Formally, adsorption of the “slower” is greater, so its transfer increases in the adsorption layer. A the same time it significantly suppress the transfer of the first component in the adsorption layer.

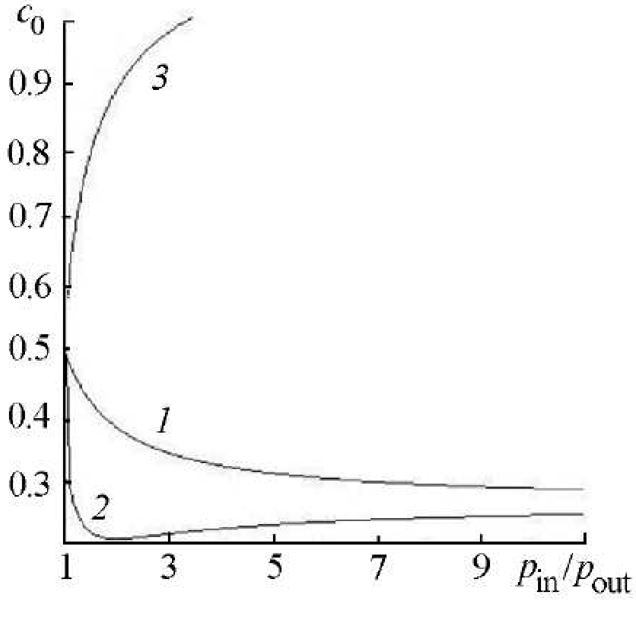

Figure 2. The concentration before the porous membrane vs. pressure ratio: 1 is the calculation by the Knudsen formula, 2, 3 – by Eqs. (7)

Conclusion

Thus, taking into account the gas transport in the adsorption layer the opposite effects can be realized. The mixture can be both enriches and impoverishes with one of the components. This is a consequence of the nonlinearity of transport processes in this case.

POTENTIOMETRIC DETERMINATION OF VITAMINS AND AMINO ACIDS IN THE RECONSTITUTED MILK USING PD-SENSORS BASED ON MEMBRANES MF-4SK

Elena Ryzhkova, Anna Parshina, Olga Bobreshova, Tatyana Titova
Voronezh State University, Voronezh, Russia, *E-mail: ryshkova-helen@mail.ru*

Introduction

In the process of production of powdered milk the thermal treatment of the product is used. This leads to reduction of the content of essential amino acids (lysine, cysteine) and vitamins (A, groups B, C) [1]. The powdered milk is used in the manufacture of infant formula. Lysine and thiamine (vitamin B1) are most wholesome and necessary for the nutrition and growth of children. Therefore, monitoring of their content in reconstituted milk is important. The aim of the work was the development of potentiometric multisensory systems with PD-sensors based on membranes MF-4SK for qualitative and quantitative analysis of reconstituted milk.

Experiments

As objects of research are solutions of reconstituted milk with 0.40-8.46 wt. % of the powdered milk. The following analytes of interest were dissolved in aqueous solutions: lysine monohydrochloride (LysHCl) and thiamine chloride (ThiaminCl). Concentrations of LysHCl and ThiaminCl in test solutions ranged from $1.0\cdot10^{-4}$ to $1.0\cdot10^{-1}$ M.

Multisensory systems for analysis of solutions of reconstituted milk included: PD-sensors, pH-selective electrode (pH ECK-10601/7), Ca-selective electrode (ELIT-041), NH_4-selective electrode (ELIT-051), Na-selective electrode (ELIC-112Na), silver chloride/silver reference electrode (EVL-1M3.1) and potentiometer. For organization PD-sensors perfluorinated sulphocation-exchange membranes MF-4SK in the K-type, H-type, $LysH_2$-type were used [2].

Results and Discussion

Potentiometric multisensory systems for the recognition of images of reconstituted milk with different amounts of powdered have been developed. The optimized radar chart of sensors responses in test solutions of reconstituted milk is presented in figure 1.

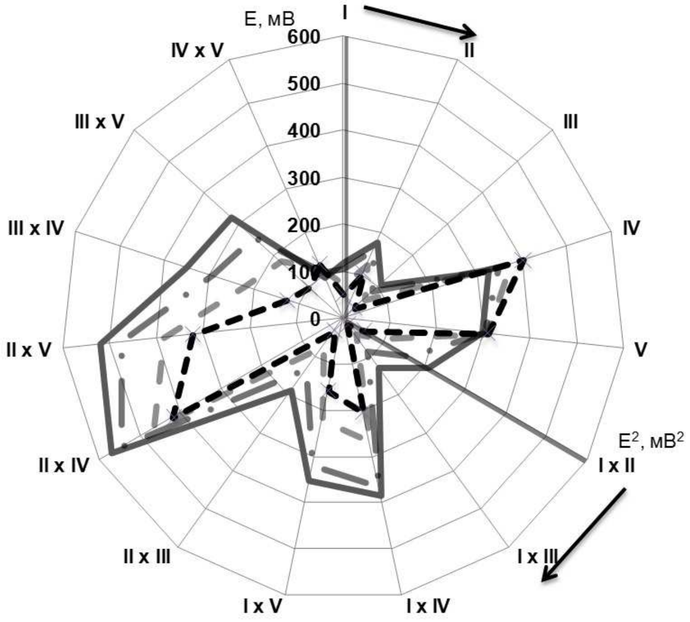

Figure 1. The optimized radar chart of sensors responses in the test solutions of reconstituted milk: I, II – PD-sensors based on membrane MF-4SK in K-type and H-type, respectively; III – Na-SE, IV – NH_4-SE, V – Ca-SE; the percentage of powdered:
——— *0,40 %;* — · — *1,30 %;* – – – *3,40 %;* ········ *8,46 %*

The sensitivity of PD-sensors based on membranes in the K-type, H-type, $LysH_2$-type in solutions containing powdered milk and LysHCl (or ThiaminCl) were investigated. The greatest sensitivity of PD-sensors to $LysH^+$ (or $Thiamin^+$ and $ThiaminH^{2+}$) in test solutions of reconstituted milk was for the membranes in the K-type (figure 2).

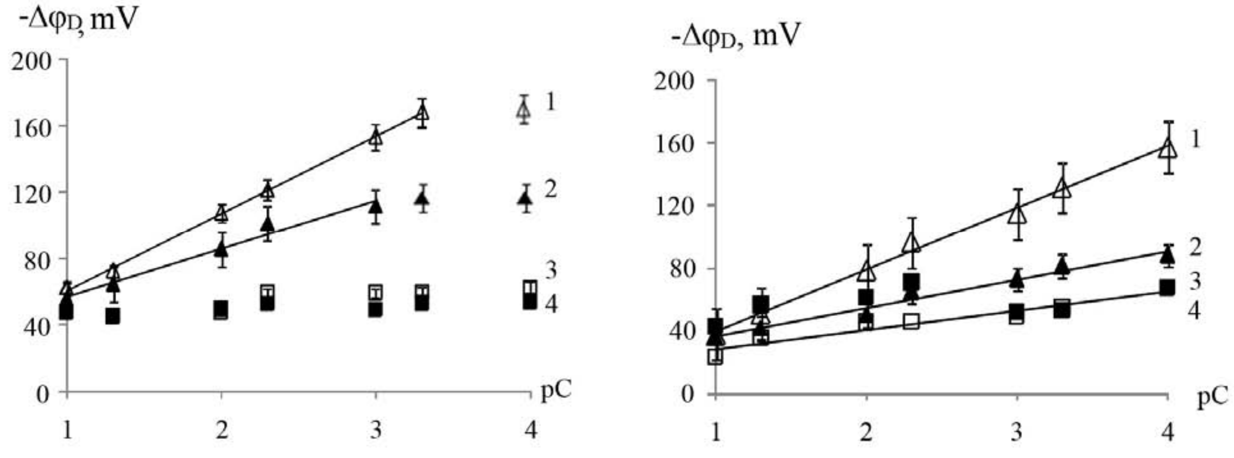

a *b*

Figure 2. The graduation of the PD-sensors based on membrane in K-type *in solutions containing LysHCl (a), ThiaminCl (b) and powdered milk: 1-0,40 %; 2-1,30 %; 3-3,40 %; 4-8,46 %*

The sensitivity of PD-sensors to $LysH^+$ in the test solutions containing 0.4 wt. % of powdered milk and $1.0\cdot10^{-3}$-$1.0\cdot10^{-1}$ M of LysHCl was 29 mV/pC for membranes in the K-type (figure 2.a). The sensitivity of PD-sensors to $Thiamin^+$ and $ThiaminH^{2+}$ in the test solutions containing from 0.4 to 4.4 wt. % of powdered milk and $1.0\cdot10^{-4}$-$1.0\cdot10^{-1}$ M of LysHCl was from 18 to 13 mV/pC for membranes in the K-type (figure 2.b). This sensitivity is sufficient for the quantitative determination of $LysH^+$ (or $Thiamin^+$ and $ThiaminH^{2+}$) in solutions of reconstituted milk.

Acknowledgements

This study was funded by the Russian Fund for Basic Research (12-08-00743-a, 12-08-31471/ mol_a) and P.Y.S.I.C. (project 10493p/16870, 08.06.2012).

References

1. *Prosenkov A.Y., Kopotkaya E.V., Mudrikova O.V.* Methods to determine reconstituted milk in liquid one // Dairy industry. 2010. V. 2. P. 49-50.
2. *Bobreshova O.V., Parshina A.V., Agupova M.V., Polumestnaya K.A.* Determination of amino acids, vitamins, and drug substances in aqueous solutions using new potentiometric sensors with Donnan potential as analytical signal // Russ. J. of Electrochem. 2010. V. 46, № 11. P. 1338-1349.

ELECTRICAL PROPERTIES LATENT TRACKS OF HEAVY IONS IN POLYMERS

[1]Konstantin Sabbatovskiy, [2]Aleksander Vilenskiy, [1]Vladimir Sobolev
[1]Frumkin Institute of physical chemistry and electrochemistry RAS, Russia, Moskow,
E-mail: sabbat07@mail.ru and vsobolev@phyche.ac.ru
[2]Shubnicov Institute of Crystallography RAS, Russia, Moskow

Introduction

A review of domestic and foreign works of recent years, where various points of view on the structure of tracks of heavy, high-energy ions in polymers. Analysis of published data and the results of our research show that the latent tracks of high-energy heavy ions in PET after contact with an aqueous solution can be regarded as an array of through nanocapillaries stripped from radiolysis products, which are suitable for studying electrical properties. In measuring the diameter of the tracks in polyethylene terephthalate krypton seepage (water and nitrogen gas) and conductometric methods.

Figure 1 shows the dependence of The average diameter of the core track is 3,9-4,1 nm. The values of the pore size calculated from the tracks of electric resistance of the film irradiated using 0.5 M KCl solution were 4,3-4,4 nm. As can be seen, the diameters of tracks defined in three different ways in good agreement with each other and with the literature datathe electrical conductivity of the electrolyte solution in the tracks of PET film to the bulk conductivity at the same electrolyte concentration, K/K0 the initial concentration of C solutions KCl, LiCl, $MgCl_2$ and $BaCl_2$. A significant excess of the measured values of the bulk value, due to the excessive presence of counterions in the tracks. For concentrations of 4.10 and 3.10 eq / l, this value was about 600-800 and 40-80, respectively, depending on the type of electrolyte. In comparison, for the etched tracks with a pore size of 13-17 nm, the maximum ratio K/K_0 were in the range 50-75 and 10-20 for a similar concentration of the electrolyte. Further, with increasing electrolyte concentration ratio K/K_0 predictably reduced to 1 at concentrations of 0.25 and 0.5 eq / l.

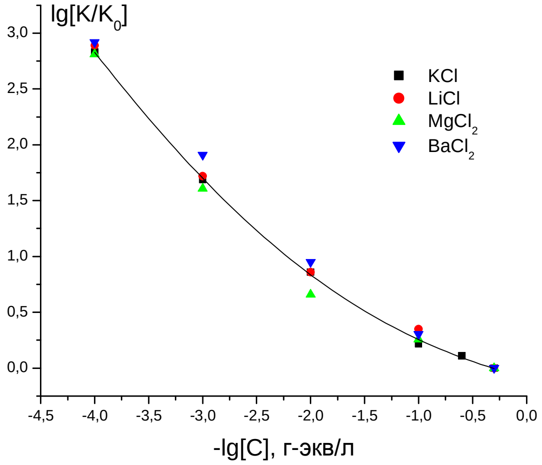

Figure 1. The ratio of the electrical conductivity of the electrolyte in the tracks of PET (D = 4,3 nm) to the bulk conductivity of the solution (k/k0) depending on the concentration of the electrolyte

For the concentration dependence of σ $BaC1_2$ and $MgCl_2$ (Fig. 2) there is a smooth decrease in the surface charge of the track surface with increasing concentration of the electrolyte. At the same time, depending on the concentration of σ $MgCl_2$ and $BaCl_2$ are different. So, for $BaCl_2$ observed recharge the track surface at a concentration of 2,5 $\times10^{-2}$ eq. Whereas for the entire range of $MgCl_2$ concentrations track surface retains a negative charge.

Depending on the pH of the potential flow of 0.01 N solutions $MgCl_2$ and $BaCl_2$ (Fig. 3) show a significant difference in the isoelectric points of the track surface using the above electrolyte. So, for $MgCl_2$ pI value -3.57, at the level of single-charged K^+ and Li^+, whereas $BaCl_2$ - 4,40, indicating a much higher adsorption capacity of the ion Ba^{2+} compared to Mg^{2+}. This allows you to understand the reasons for the lack of recharging the track surface in the case of $MgCl_2$.

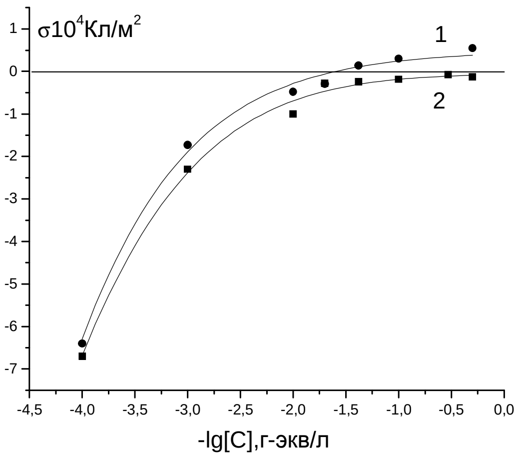

Figure 2. Dependence of the surface charge density σ PET tracks the electrolyte concentration C. The film thickness 10 microns. 1- $BaCl_2$, 2- $MgCl_2$

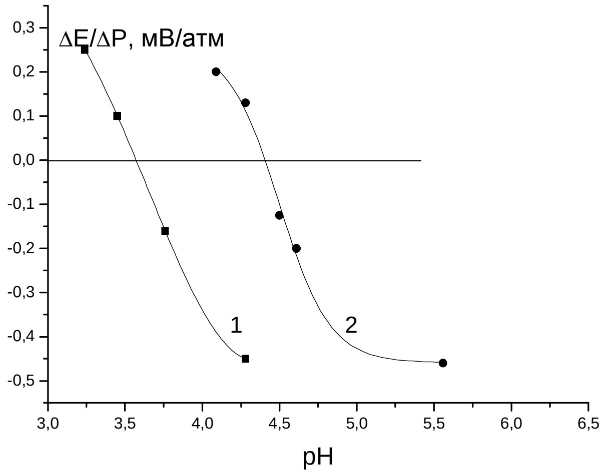

Figure 3. The dependence of the flow potential of the irradiated film pH 0,01 N solution 1 – $MgCl_2$, 2 – $BaCl_2$. PEP for $MgCl_2$ -3,57, for $BaCl_2$ - 4,40. Film thickness 10 microns

Thus, analysis of published data and the results of our research show that the latent tracks of high-energy heavy ions in PET after contact with an aqueous solution can be regarded as an array of through nanocapillaries suitable for the investigation of the electrophysical properties. A significant excess conductivity of electrolyte solutions (KCl, LiCl, $MgCl_2$ and $BaCl_2$) in the tracks compared to the bulk. The dependences of the surface charge σ tracks on the concentration of electrolytes and pH.

MORPHOLOGY OF COPPER PARTICLES CHEMICALLY DEPOSITED INSIDE ION-EXCHANGE MATRICES WITH VARIOUS NATURE OF FIXED GROUPS

[1]Ekaterina Sakardina, [1,2]Ekaterina Zolotukhina, [1]Tamara Kravchenko
[1]Voronezh State University, Voronezh, Russia, *E-mail: ks-chem@mail.ru*
[2]Institute for Problems of Chemical Physics RAS, Chernogolovka, Russia

Introduction

Chemical deposition of metals on (or into) various polymer surfaces (or matrices) is usually used for creation of nanocomposite materials. Polymer matrix can play the role either inert stabilizer of metal particles or electron- and ion-conductive system. In the last case formed nanocomposites have bifunctional properties [1]. Such systems establish a reputation as good catalysts, electrocatalysys and sorbents. In this work we study the morphology of copper particles chemically deposited inside the matrices with various nature of fixed groups and their volume distribution inside these matrices in dependence on mechanism of matrix interaction with metal ions: ion exchange, sorption, complex formation.

Experiments

Metallic copper was deposited by dynamic conditions inside macro- and microporous ion-exchange polymers in the form of granules: sulfo- and carboxyl-cation exchangers and strongly basic amino-anion exchangers (table 1).

Table 1. Ion-Exchange Matrices

№	Ionogenic centres	Porosity	Ion-exchange capacity, mmol/cm^3
Cation exchangers			
1	-SO$_3$–H$^+$	Macroporous	1.2
2	-SO$_3$–H$^+$	Microporous	1.8
3	-COOH	Macroporous	3.9
4	-COOH	Microporous	3.5
Anion exchangers			
5	-(R)$_3$N$^+$OH$^-$	Macroporous	2.5
6	-(R)$_3$N$^+$OH$^-$	Microporous	1.8

Reducer of neutral type (hydrazine) was used in the case of cation exchangers and of anion type (dithionite) was used in the case of anion exchangers to purpose of uniform distribution of copper along the radial direction of granules. Chemical deposition of copper was realized due to ion exchange saturation of matrices with copper ions interchanging with reduction with alkaline solution of reducer. For anion-exchange matrices this order of saturation was reversed: at first, ion exchange saturation with reducer solution was preformed and then solution containing copper ions was used. Such synthetic procedure was reiterated 5 times (N=5). Size and distribution of copper particles was controlled by SEM with EDS analysis.

Results and Discussion

Composites with various copper contents and different radial distribution were synthesized on the basis of granular ion-exchange matrices (table 2).

Table 2. Characteristics of Copper-Ion Exchanger Nanocomposites

Number of matrix from table 1	Ionic form	Copper capasity mmol/cm^3		Average size of copper aggregates inside of granule, *d*, nm		Distribution density of copper particles in radial direction, *ρ*	
		N=1	*N*=5	centre	surface	centre	surface
1	H$^+$	0.4	2.5	100-200	200-300	0.7	1.3
2	H$^+$	1.9	-	250-300	300-500	0.4	1.6
3	H$^+$	-	1.0	150-300	150-300	0.4	1.6
4	H$^+$	0.3	5.5	250-300	50-150	0.1	1.9
5	SO$_4^{2-}$	-	1.2	200-350	50-200	0.2	1.8
6	SO$_4^{2-}$	-	0.5	50-150	100-200	0.1	1.9

Difference between content and distribution of copper particles inside ion-exchange matrices can be refer to specific of interaction of metal ions, precursor ions (OH-) and reducer with functional groups of ion exchangers. Revealed morphological features of nanocomposites makes possible to represent the spatial pattern of the most important stages of chemical deposition of metal into the matrices with various nature of fixed groups: I – strongly acide, II – weakly acide, III – strongly basic (Fig. 1).

We can take into account only macroporous matrices in wich the principal stages are: 1 – ion exchange and non-equivalent sorption, 2 – chemical deposition of precursor, 3 – chemical reduction of precursor and formation of metal particles. The main feature of geleous (microporous) matrices is the great charge, diffusion and spatial restriction for chemical deposition process.

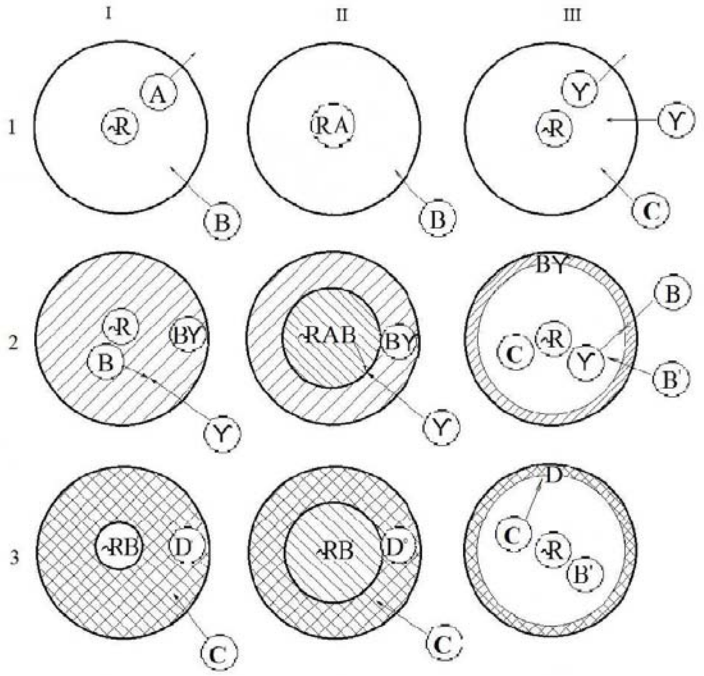

Figure 1. Scheme of chemical deposition of metal into ion-exchange matrices. Principle stages of process: 1 – ion-exchange saturation; 2 – chemical deposition of precursor; 3 – chemical reduction of metal. Types of matrices: I – strongly acid, II – weakly acid , III – strongly basic. Particles: ~R – fixed group, A – initial counterion, B – counterion from solution, v – co-ion, C – molecule, D_0 – metal particle.

I - $\sim R - SO_3^-$, A – H^+, B – Cu^{2+}, B' – Na^+, v – OH^-, C – N_2H_4, D^0 – Cu^0;

II - $\sim R - COOH$, A – H^+, B – Cu^{2+}, B' – Na^+, v – OH^-, C – N_2H_4, D^0 – Cu^0;

III - $\sim R - N^+(CH_3)_3$, A – OH^-, B – Cu^{2+}, C – S_2O_4, D^0 – Cu^0.

Stage (1) can be considered within the bounds of F.Helferich conception. Interaction mechanism between metal ions and ionogenic centres of matrix defined the degree of their fixation and the amount of independent ions in porous of polymer. The diffusion rate of reagents and their concentration in matrix depend on swelling index and porous size.

Next stage (2) is heterogeneous reaction of solid precursor formation ($Cu(OH_)2$) and the last stage (3) is solid-state reaction of precursor to metal nanoparticles transformation. The first solid product defined the size of metal particles. The area of metal ions and OH-anions interaction specify the type of metal particles volume distribution. The localization of this interaction depends on the nature of ionogenic centres of matrix and its porosity.

This work is supported by RFBR (project 13-08-00935).

References

1. *Zolotukhina E. V., Kravchenko T. A.* // Electrochimica Acta. 2011. V. 56. P. 3597-3604.

EVOLUTION OF TRANSPORT CHARACTERISTICS OF ION-EXCHANGE MEMBRANES USED IN ELECTRODIALYSIS TREATMENT OF TARTRATE CONTAINING SOLUTIONS

Veronika Sarapulova, Anastasia Gorobchenko, Marina Andreeva, Nataliya Pismenskaya
Kuban State University, Krasnodar, Russia. *E-mail: vsarapulova@gmail.com*

Introduction

At the present time the number of wineries that use electromembrane technology for wine conditioning is increasing. However, there are still many unresolved problems that restrain growing needs of the wine industry. The rapid deterioration of membranes and precipitate on an ion-exchange membrane's surface are the main problems of the electrodialysis (ED) treatment of wine. In this regard, stability of the anion-exchange membranes characteristics becomes a topical problem. Therefore, the objectives of this study are to investigate the mechanisms of the anion-exchange membrane aging and finding ways to their regeneration after operation in plants for electrodialysis demineralization of wine.

Experiments

The properties of heterogeneous and homogeneous membranes, which are currently used or are potentially interesting in ED of wine, were studied. Their main characteristics are presented in Table 1.

Table 1. Some of the characteristics of the membranes under study

Membrane	Manufacturer	Thickness, μm		Fixed groups	IE Capacity * mmole / mL
		NaCl	KHT		
AMX-sb	Astom (Tokuyama Soda)	140±10	150±10	$–N^+(CH_3)_3$	1,56
AX	Astom (Tokuyama Soda)	145±10	175±10	-	2,88
MA-41	JSC ShchekinoAzot	480±10	500±10	$–N^+(CH_3)_3$	1,25
MA-41P$_I$	JSC ShchekinoAzot	500±15	535±10	$–N^+(CH_3)_3$	0,92
MA-41P$_{II}$	JSC ShchekinoAzot	470±10	510±10	$–N^+(CH_3)_3$	1,11

* for the swollen membrane in the Cl^- form

We have studied the ageing of the membranes by soaking them in a wine model solution and a red wine for a certain time *t*. The initial chemical composition of the model solution was as follows:

tartaric acid	2 g/L;
KCl	0,4 g/L;
$CaCl_2$	0,36 g/L;
acetic acid	0,48 g/L;
lactic acid	1 g/L;
pH = 3,25.	

The measurements of electrical conductivity of membranes were carried out (after a time *t* of soaking) using the differential method [1, 2] with a clip-type cell and immittance measurement setup MOTECH MT4080 at AC frequency 1 kHz and temperature 25 ± 0,2 º C.

Results and Discussion

The membrane specific conductivity in wine model solution (a) and in red wine (b) as a function of the time of soaking is shown in Fig. 1. In the wine model solution, the specific conductivity of ***MA-41 P$_I$*** and ***MA-41 P$_{II}$*** is 1,5 times higher than that of the homogeneous

AMX membrane and, almost 3 times higher than the conductivity of commercially available MA-41 membrane.

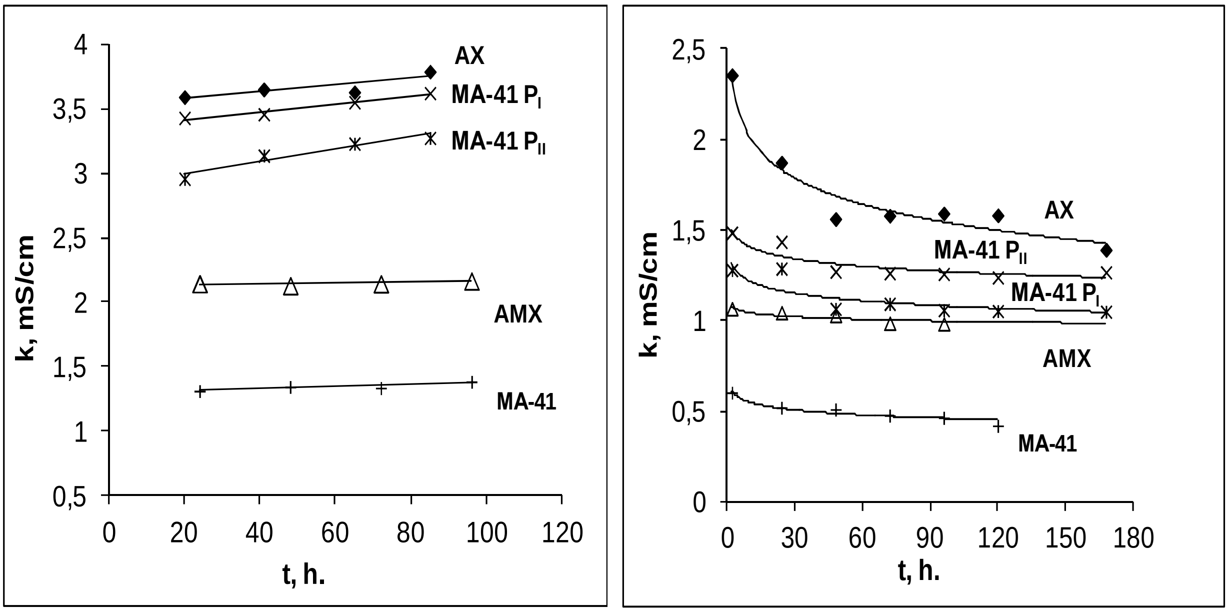

a *b*

Figure 1. Membrane electrical conductivity vs the time of their soaking in the wine model solution (a) and in a red wine (b)

However, almost the conductivity of all membranes in the red wine drops significantly in comparison with the wine model solution. Reduced conductivity has been observed in the first hour of contact with the wine and extends over the next 30-50 hours. The condutivity of ***MA-41 P_I*** and ***MA-41 P_{II}*** membranes decreases the most noticeably.

The analysis of photomicrographs of anion-exchange membranes ***MA-41 P_I*** in red wine, made using an optical microscope Zeiss Imager.Z1 (Fig. 2), shows that the precipitate is absent on the smooth surface of polyethylene. It is observed on the surface of ion-exchange particles and fills cavities on the surface of the membrane. Ion-exchange particles change their color, that indicates at the presence of fouling substances. Since the membranes are anion-exchange, the polyanions of poly-carboxylic acids and/or polysaccharides may be possible causes of their fouling [3].

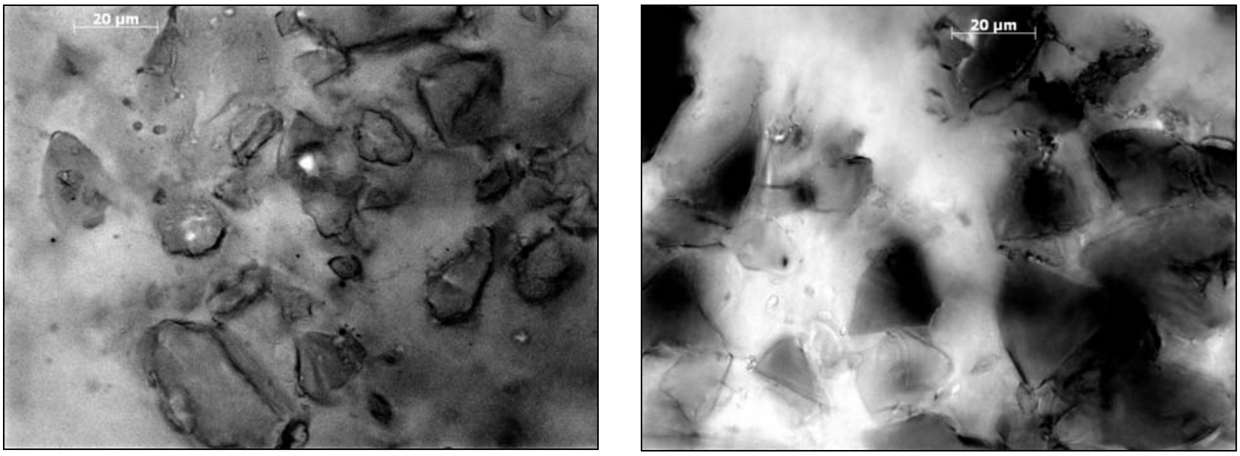

a *b*

*Figure 2. Photomicrography of the heterogeneous anion exchange membrane **MA-41 P_I** in NaCl solution (a) and in red wine (b)*

The possibility of regeneration of membranes by treating them with various agents (NaCl, HCl, NaOH , NH_4OH, $C_3H_4OH(COOH)_3$) (citric acid) и $KHC_4H_4O_6$ (KHT)) was experimentally evaluated on the second stage of the study. It is shown that the exposure to alkaline solutions leads to blackening of membranes and further reduces their conductivity. Treatment of the membranes with acidic solutions does not lead to improvement of their characteristics. Partial regeneration of the membranes is achieved after soaking them in a concentrated NaCl solution.

Conclusion

1. The characteristics of membranes do not change during their soaking in a wine model solution containing the mix of carboxylic acids. In a natural wine, the transport characteristics of membranes decay because of their poisoning.
2. Regeneration of membranes with alkaline or acidic solutions does not lead to positive effect. The partial regeneration of membranes is achieved by their treatment with NaCl solution.

Acknowledgement

The study was realized within French-Russian laboratory “Ion-exchange membranes and related processes”. We are grateful to CNRS, France, and to RFBR (grants 11-08-93107, 12-08-93106), Russia, as well as to FP7 Marie Curie Actions “CoTraPhen” project PIRSES-GA-2010-269135 for financial support.

References

1. *Lteif, R., Dammak L., Larchet C., Auclair B.* Conductivité électrique membranaire: étude de l'effet de la concentration, de la nature de l'électrolyte et de la structure membranaire // Europ. Polymer J. 1999. V. 7. P. 1187-1195.
2. *Karpenko L., Demina O., Dvorkina G., Parshikov S., Larcher C., Berezina N.* Comparative study of methods used for the determination of electroconductivity of ion-exchange membranes // Rus. J. Electrochem. 2001. V. 37. P. 287-293.
3. *Jackson R. S.* Chemical constituents of grapes and wine. In: Wine science: Principles and applications. N.Y.: Academic Press, 2008. Ch. 6. P. 418-519.

SIMULATION SWELLING KINETICS POWDERED CELLULOSE SECONDARY ACETATE IN LIQUID AND STEAM MEDIA

ValentinSedelkin, Olga Chirkova, Larisa Potehina, Catherine Goroholinskaya
Engels Technological Institute (branch) of the Saratov State Technical University, Engels, Russia,
E-mail: larisa_potehina@mail.ru

Introduction

To adjust the structure and the functional properties of polymeric filtration membranes is a promising source application modifying polymeric material.

This paper presents the results of a study of the kinetics of physical and chemical modification of liquid and steam environments, cellulose secondary acetate (CSA), which is widely used for the manufacture of micro-and ultrafiltration membranes.

Experiments

The study was conducted on an industrial powdered cellulose secondary acetate, main parameters are given in Table 1.

Origin of raw mate-rials	**Physical and chemical characteristics**						
	Thedegree of acetylation %	**Average molecular weight M, g/mol**	**The limiting viscosity number $[\eta]^{25}$, cm^3/g**	**Bulk density $\rho_н$, $g\times cm^{-3}$**	**Specific surface S_{sp}, m^2/g**	**Pore volume V_p, cm^3/g**	**Range of pore radius Δr_p, nm**
Cotton	55,4	7,8×104	1,65	1,32	11,5	0,05	1,5-40

As seen from Table 1, the powdery raw material CSA a change mesoporous pore radii ranging from 1,5 nm to 40 nm. This is the predominant region of small mesopores with pore radius range of variation from 1,5 to 10 nm, which is apparently characteristic of polymers based on cellulose. Swelling CSA conducted in liquid (water) and a steam (water vapor and aqueous-organic mixtures) environments. The process was characterized by the swelling degree of swelling of α:

$$\alpha = \frac{m - m_0}{m_0} \cdot 100\%,$$

Where: m and m_0 - weight of the polymer before and after swelling, respectively, g.

Results and discussion

To analyze the kinetics of swelling of the current value of speed (ω_τ) and constants (K_τ) swelling, as well as on the average of allocated sites ($\Delta\tau$) speeds ($\overline{\omega_{\Delta\tau}}$) and constants ($\overline{K_{\Delta\tau}}$) of swelling. Figure 1 and 2 shows the kinetic curves CSA swelling powder in water and steam media.

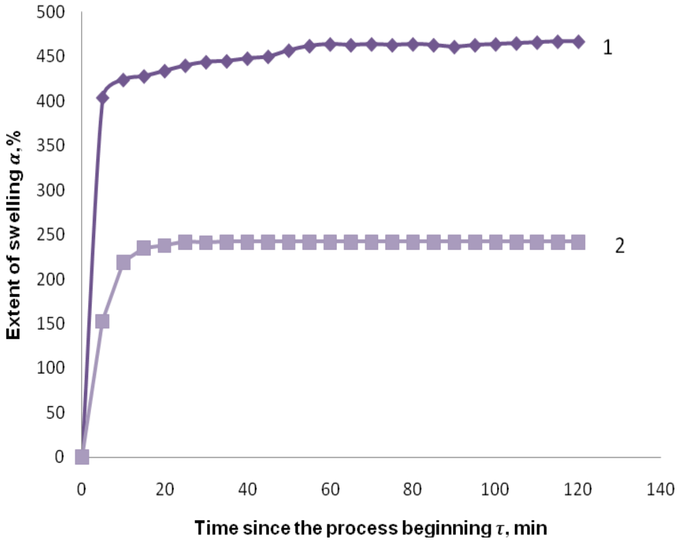

Figure 1. Kinetic curves of swelling CSA powder in water : 1- swelling in an unlimited amount of water in the natural decantation phase, 2- swelling in an unlimited amount of water followed by phase separation with a glass filter

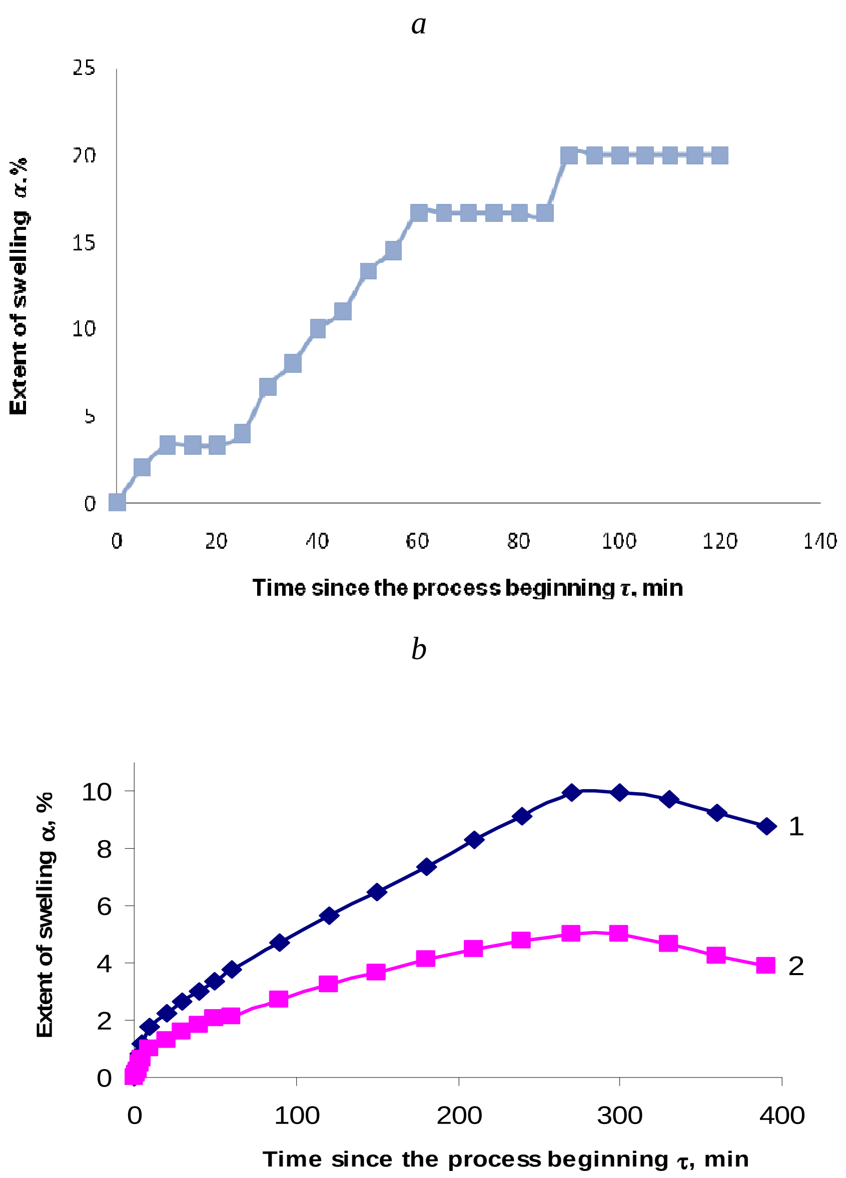

Figure 2. Kinetic curves of swelling powder CSA in steam environments: a - swelling in water vapor, b - swelling in aqueous-organic mixtures: 1 - vapor mixture of water and DMSO, 2 - a mixture of water vapor and DMAA

It is seen that the increase in mass of the polymer sample in time during swelling in liquid media and steam occurs with varying intensity. The degree of swelling increases over time, gradually approaching the maximum equilibrium value (α_{max}).The lowest values were obtained by the swelling α_{max} CSA powder in a mixture of H_2O vapor and DMAA, and the highest, with swelling of the sample in an unlimited amount of water in the natural decanting phases.

Analysis of experimental data has shown that the kinetics of swelling when CSA modification in different media is determined by many factors including porosity, physico-chemical characteristics of the medium - and of the modifier resin (nature and its crystal structure, chemical composition macromolecules structure and flexibility of the polymer chain, forces of interaction between macromolecules, etc.), the rate of diffusion processes.

CSA is a polymer powder swelling adsorbent. Therefore, when swelling in steam or liquid media volume sample will occur just before the chemisorption process. The mechanism and process steps presented us swelling CSA viewed. In the first stage by the forces of adhesion molecules occurs physical adsorption medium modifying the outer surface of the particles of the polymer powder and open pairs. The intensity of the processes taking place at this stage, can be estimated using known methods of adsorption-structural studies and calculations of physical adsorption.

In the second stage, after placement of sorbate molecules on the outer surface and open pores of the powder particles, the surface interaction begins modifying medium (hydrated molecules and ions) with acetyl groups and hydroxyl functional macromolecules CSA other through hydrogen bond (superficial chemisorption). Thus there is a so-called "disturbance" surface sorbate-sorbent interactions at the interface of the resulting polymer and the adsorption layer. At this stage of development begins solvation processes, the interaction and binding of the active groups of the polymer with the sorbate.

In the third stage, the diffusion component of the modifier-solute polymer frame and deep penetration of the swelling agent in the closed pores and supramolecular structures. As the number of penetrating into the polymer medium increases its mass and volume, as well as changing the internal structure. There is penetration of diffusing component between the macromolecules of the polymer, the distance between them gradually increases, which causes a chain and segmental conformational changes, as well as the weakening of inter-and intramolecular hydrogen bonds and other bonds.

In the third stage of swelling, other than diffusion processes will continue the process of solvation (hydration). Around the polymer macromolecules having hydration shells, which represent a specific connection (usually) undefined related to chemical groups CSA forces of different nature and intensity - from the weak intermolecular interaction forces to the forces of chemical bonds, determined by the activity of water in the solution, the role of Donnan equilibrium with swelling polymers in aqueous solutions, reactions between pairs of solvated ions component and the polymer swelling agents. In essence, the third stage of the swelling is still actively pursued chemisorption processes.

As seen from Figures 1 and 2, the degree of swelling in water vapor CSA higher than the water vapor in mixtures of organic solvents (DMSO and DMAA). This effect can be explained by the strong affinity of pure water vapor, compared with aqueous-organic vapor mixtures, to cellulose acetate.

In turn, the swelling powder in liquid water CSA faster and to a greater extent than in the steam. This is due, firstly, higher adhesive interaction with the surface of the liquid polymer particles and second diffusion coefficients large liquid compared with steam.

Conclusion

Thus, the experimental data suggest a complex, multi-step mechanism of the processes occurring during the swelling of polymers in liquid and steam environments. The results can be used to develop evidence-based theory of swelling polymers.

STRUCTURAL CHARACTERISTICS OF THE CELLULOSE SECONDARY ACETATE EXPOSED TO PHYSICAL AND CHEMICAL MODIFICATIONS

Valentin Sedelkin, Larisa Potehina, Olga Chirkova, Catherine Goroholinskaya, Elena Oleynikova

Engels Technological Institute (branch) of the Saratov State Technical University named after Yuri Gagarin, Engels, Russia, E-mail: larisa_potehina@mail.ru

Introduction

Cellulose secondary acetate (diacetates - CSA) is widely used as feedstock for the production of permselective membrane filtration. To isolate ingredients of multicomponent solutions of various molecular weights and particle sizes required membrane controlled distribution of pore radii have a particular structure and functional properties.

A promising approach to changing the characteristics of the membranes is a modification of polymeric materials by various physico-chemical methods.

Experiments

In this work, for this purpose, machining powder CSA pairs aqueous-organic mixtures [water + dimethylsulfoxide (DMSO)] and [water + dimethylacetamide (DMAA)]. For the experiments was chosen for optimum efficacy in modifying the ratio of a binary mixture of water-organic solvent equal to about 90:10 vol. %. In the first series of experiments by physical sorption-desorption of liquid nitrogen were determined parameters of the porous structure of powdered SCA before and after modification. Measurements were made using high speed computerized analyzer specific surface area and pore size "Quantachrome NOVA 1200e".

Determination of the structural characteristics of the samples was carried out on the basis of shot adsorption-desorption isotherms. Samples investigated polymer previously degassed under vacuum at 50 ° C for two hours.

Measurements showed that the adsorption isotherms for both samples differ in the initial linear portion, which is stored for the ratio of system pressure to the condensation pressure P/P_0 range from 0,05 to 0,7. This indicates that even in the adsorption inert towards SCA sorbate (nitrogen) is increased (previously inaccessible disclosure) of the surface is proportional to the amount of adsorption of the adsorbed matter. Found that the specific surface area polymeric adsorbents CSA types due to non-uniform distribution of the interfacial active sites of low and high energy absorption, such as polar and non-polar functional groups. On the porous structure and adsorption characteristics of cellulose acetate affect their molecular-mass polydispersity and molecular structure.

Using the linear shape of the adsorption isotherm (BET equation) specific surface area was calculated Ssp CSA powder before and after the modification, which was found to be respectively 11,5 m^2/g and 11,1 m^2/g. To determine the pore size distribution method was used BJH. The initial data for the calculation method used in this branch of the isotherm in the range of relative pressures P/P_0 = 0,400-0,967. Type of adsorption isotherms and pore volume distribution and specific surface area can be considered radially investigated samples CSA raw mesoporous pore radius range from 1,5 to 40 nm. The most representative area pore radius is small mesopore area in the range of 1,5 to 10 nm, which is apparently characteristic of the products based on cellulose.

In a second series of experiments directly related to the processing of powder CSA pairs of aqueous-organic mixtures investigated the intensity and the rate of swelling of the polymer samples from time to time. Since CSA is swellable absorbent polymer, when it absorbs water vapor and solvent (DMSO and DMAA) therein chemisorption processes begin. The intensity of the chemisorption processes in the samples was evaluated according to their degree of swelling α in pairssorbate. To analyze the kinetics of swelling α were determined according to the process time, and the current value of the speed ω_τ and constant of swelling K_τ.

Analysis of the kinetics of swelling in pairs CSA binary mixtures showed that the swelling curves can be divided into several time sections of differing speeds and constant swelling.

Identifies five such sites with different process time Δτ, average speeds in the area $\overline{\omega_{\Delta\tau}}$ average and average constant swelling $\overline{K_{\Delta\tau}}$.

Found that the most intense absorption of vapor mixtures polymeric adsorbent is in the initial stage of the process, and the maximum characterizing the equilibrium saturation vapor sample is obtained after about 270 minutes from the start of the experiment.

The results of experiments revealed major step chemisorption process modification CSA pairs of binary aqueous-organic mixtures: 1) physical adsorption of molecules on the surface of the mixture has a solid phase, and 2) the diffusion depth penetration with the polymeric backbone of these molecules in the macromolecular structure of the polymer, and 3) reacting the hydroxyl-sorbate and carbonyl functional groups of macromolecules CSA via hydrogen and other links with the formation of the chemisorption complexes CSA-agent sorbate.

Conclusions

Results from this study are used to analyze the structure and functional properties (permeability, selectivity, strength, etc.) of filtration membrane made from unmodified and modified cellulose secondary acetate.

KINETICS THE PHASEINVERSION OF PROCESSES OF FORMATION OF NANOPOROUS FILTRATIONAL MEMBRANES FROM HOMOGENEOUS AND HETEROGENEOUS POLYMERIC MIXTURES

Valentin Sedelkin, Larisa Potekhina, Olga Chirkova, Daria Mashkova
Engels Technological Institute (branch) of the Saratov State Technical University named after Yuri Gagarin, Engels, Russia, E-mail: larisa_potehina@mail.ru

Introduction

Application of membrane filtrational technologies is perspective for division and fractionation of multicomponent liquid mixtures in chemical, pharmaceutical, food and other industries. Basic element of any filtrational installation are the permeable membranes nanostructured selektively which are made by a method of inversion of phases of forming polymeric solutions.

In this work models of fazoinversionny processes with which use the kinetics of formation of porous filtrational membranes both from homogeneous, and from heterogeneous polymeric solutions is analysed in the dry way are offered.

Experiments and discussion

As initial polymeric raw materials for preparation of solutions it is used powdery cellulose secondary acetates (CDA) of a cotton origin. Acetone served as CDA solvent. Two groups of solutions were applied to formation of membranes: homogeneous and heterogeneous. The first group included the solutions representing single-phase liquid mixes (dissolved polimer+protofilny liquids). The second group was represented by the polymeric heterogeneous systems including except the liquid-phase environment a firm disperse phase. The thermoprocessed waste of the thresh of millet is used as a firm disperse phase. It is possible to receive on the basis of forming mixes of the second group the filled polymeric membrane compositions possessing expanded range of regulation of their structural and functional characteristics. The compounding of the offered polymeric composite mixes for formation of the nanostructured filtrational membranes is protected by the patent for the invention [1]. Research of kinetics of formation of the membranes conducted with use of a method of a range of a turbidity and as optical and electronic microscopy, showed that full dissolution of a polymeric skeleton of CDA to molecular and uniform level even in thermodynamic good solvents is unattainable. The crystallites not dissolved and not destroyed completely and their fragments form in solution associates (microgel particles – MGP) with big, than at polymer macromolecules, the sizes. Therefore forming solutions of the first group any more aren't about the structure zole 1 and phase inversion will take place according to the scheme: zole 2→gel, instead of according to the scheme: zole 1→zole 2→gel as was considered still [2]. Initial forming solution of the second group is the disperse system consisting of the liquid-phase dissolving environment with a disperse phase in the form of microgel particles and a firm disperse phase in the form of particles of a filler. Thus, at the initial moment of fazoinversionny process we will have zole with two disperse phases (liquid and firm) in uterine polymeric solution. Therefore transition process zole in gel in this system has to differ from process of phase inversion in purely polymeric liquid-phase system. Really, as showed shootings under a microscope, emergence in uterine solution of the second (firm) disperse phase leads to adsorption on particles of a filler of polymeric macromolecules and to formation of an external polymeric film that promotes formation of the specific combined porous structure of received membranes.

Conclusion

On the basis of results of the conducted research in work models of kinetics of the fazoinversionny processes happening at production of nanostructured filtrational membranes from homogeneous and heterogeneous polymeric solutions are offered.

References

1. Pat. RU 2426305 C1, IPC A01J 11/10. / *V.M. Sedelkin* [and others]. – Decl.. 24.02.2010, publl. 20.08.2011
2. *A.A Swittsov. M. Delhi* Introduction in membrane technologies. 2007. p. 208.

THE RESEARCH OF CELLULOSE ACETATE AND POLYAMIDE MEMBRANES AS ION-SELECTIVE INDICATORS

Valentin Sedelkin, Marina Pozdeeva, Larisa Potehina, Olga Chirkova, Elena Oleynikova
Engels Technological Institute (branch) of Saratov State Technical University, Engels, Russia
E-mail: Pozdeevamg@mail.ru

Introduction

Membrane ultrafiltration using cellulose acetate and polyamide membranes are increasingly used for complex processing of secondary raw milk (skim milk, whey and buttermilk). First of all, with serum proteins, with sizes d_b=5÷50 nm and a molecular weight of M=(10-50)10^3 Da extracted from the filtrate. Membranes with pore sizes of the corresponding set for the detention of such particles.

Experiments

In experimental studies, ultrafiltration cheese whey and buttermilk on our developed membranes of secondary cellulose acetate (SCA) and hollow-fiber polyamide membranes (PAM) revealed that there is a change in the filtration process, not only the concentration of protein, and mineral constituents, in particular ions Ca^{2+} and Cl^-. These ions, even in the presence of hydration shells have a size $d_{Ca}{}^{2+} \leq 0{,}2$ nm and $d_{Cl}{}^{-} \leq 0{,}052$ nm and should easily sifts through the pores of studied membranes, the size of were> 5 nm. Given that used in the experiments SCA and PAM membranes do not contain active ionic groups, it was assumed that the ions are transported in the pore volume and partially adsorbed on their walls. Adsorbed in the nano-capillary pores ions form a quasi-crystalline lattice with a specific ionic charge corresponding inside the membrane electrical potential φ, and can interact with the static elements of the charged chemical groups starting polymers.

In particular, the membranes of SCA contain in the surface layer of chain link carboxyl oxygen and hydroxyl group with a mobile hydrogen:

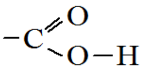

$$-C\begin{smallmatrix}\nearrow O \\ \searrow O-H\end{smallmatrix}$$

The electron density of the hydroxyl group, due to mobility of hydrogen, can be shifted to the carboxyl oxygen, which in turn can attract ions of the opposite sign from the solution. Polyamide membranes contain a group $-NH_2$, which is concentrated on the nitrogen negative charge. Nitrogen ions can also interact with oppositely charged ions of the filtered solution, facilitating their migration.

In the process of acetylation of cellulose is a small amount of free acetic acid, so the cellulose acetate membranes are a solid buffer solution containing a small amount of H^+ ions and hydrogen ions are exchanged for ions from a solution like the glass electrode. If we place the electrode in a solution containing hydrogen ions, it will be exchanged with hydrogen ions between the two phases - the solution and the membrane (glass): $H^+ \leftrightarrow H^+_{gl.}$, $H^+ \leftrightarrow H^+_{m.}$.

Ion of hydrogen transition from one phase to another is equivalent to the movement of a unit charge, that is, in the equation for the potential of the glass electrode n = 1. The same process is possible for membranes based on polyamide. Method of potentiometry was determined the potential of glass electrode to the silver chloride electrode in various media (alkaline, neutral and acidic). Then a glass electrode was replaced for membranes based on secondary cellulose acetate unfilled and filled - activated charcoal two fractions (85 microns and 160 microns) and polyamide fibers. The membrane was fixed on a copper wire and measured potential. The results are presented in the table 1 below.

As can be seen, the potential of the glass electrode is: in the acidic environment -0,060 V, in the neutral -0,410 V and -0,760 V in alkaline. Value of potential decreases during the transition from acidic to alkaline, the less potential, the lower the acidity of the medium. Acidity in a solution of HCl in the measurement of the membrane of cellulose acetate larger than when measured with a glass electrode. Consequently, the H^+ ions move from the membranes into the solution. With the introduction of active carbon in the membrane the potential decreases in acidic medium as compared to the membrane without coal. It can be assumed that the carbon block passage of ions H^+ from the membrane into the solution.

Table 1. The values of the potential of electrode in different condition depending on the type of electrode

Type of electrode	**Potential of electrode E, (V)**		
	NaOH	**H_2O**	**HCl**
Glass	-0,760	-0,410	-0,060
SCA-membrane	-0,600	-0,100	-0,380
SCA-membrane with activated carbon (85 microns)	-0,450	-0,180	-0,100
SCA-membrane with activated carbon (160 microns)	-0,350	-0,180	-0,050
Hollow polyamide membrane	-0,300	-0,170	-0,270

If you use a polyamide membrane, the equilibrium between the hydrogen ions in the solution and the membrane is more shifted towards transition of ions in the membrane and in the solution of their remains less. The proposed mechanism may explain the fact that hydrogen ions can interact with the amide groups $-NH_2$, forming ion - dipole coupling with nitrogen or other polar groups in the membrane structure.

The test of the membrane used as indicator electrodes for determining the concentration of acid in relation to the standard silver-silver chloride electrode. The figure 1 shows as an example titration curves of HCl with the indicator electrode from membranes of different composition.

The point of equivalence titration were identified:

- the membrane of polyamide fiber - 12.5 ml;
- cellulose acetate membrane without filler - 11.5 ml;
- cellulose acetate membrane filled with coal fines (85 microns) - 10.5 ml;
- cellulose acetate membrane filled with coal coarse (160 microns) - 9.5 ml.

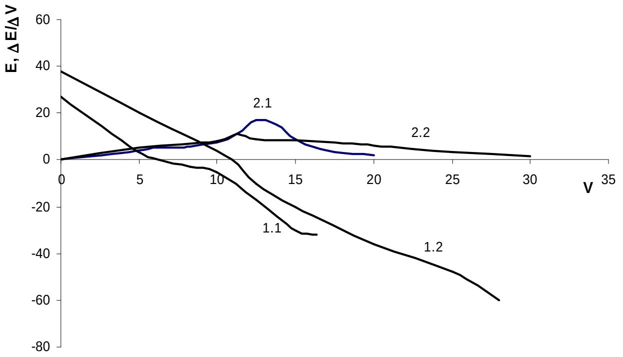

Figure 1. The integral (1) and differential (2) titration curves of hydrochloric acid with the indicator electrode of polyamide fibers (1) and cellulose acetate without filler (2)

Conclusion

The titration curves show that the investigated membranes can be used as indicator electrodes in acid-base interactions. Most accurately determine the concentration of the acid can be an indicator of a membrane based on cellulose acetate and cellulose acetate, filled with coal fines. Shown that the membrane based on SCA and SCA-modified activated carbon and polyamide fibers are capable of ion exchange with ion-containing environment. Therefore investigated membranes can be used as ion-selective indicators for acid-base titration.

INFLUENCE OF SLIGHTLY SOLUBLE D-METAL HYDROXIDES INTRODUCED INTO BIPOLAR MEMBRANE BY CHEMICAL METHOD AT ITS CHARACTERISTICS

Olga Shapovalova, Natalia Alpatova, Nikita Kovalev
Kuban State University, Krasnodar, Russia, *E-mail: sheld_nv@mail.ru*

Introduction

Bipolar ion-exchange membranes are made of two layers –anion and cation exchange, which are connected with each other. At the boundary of these layers the space charge region occurs in which dissociation of water molecules generates hydrogen and hydroxyl ions when an electric current flows. Use of such membranes allows obtain acid and alkali in the solutions adjacent to the bipolar membrane.

It is known that many slightly soluble heavy metal hydroxides increase the dissociation constant of water [1, 2]. In these studies, metal hydroxides were introduced in the membrane in powder form, or synthesized by electrochemical method. The first method does not allow obtain membranes with low voltage drop, the second is too laborious. At the same time it is known that metal hydroxides may be introduced into membranes chemically [3]. However, it is not known if the activity of metal hydroxides catalysts made by this method high enough. The aim of this work was to study catalytic activity of slightly soluble heavy metals hydroxides chemically introduced into heterogeneous bipolar membrane.

Experiments

The object of study was analogues to bipolar membrane MB-2, obtained by pressure of cation and anion exchange membranes Ralex CMH and Ralex AMH, produced in the Czech Republic, with prior chemical modification by metal hydroxides of Fe^{3+}, Cu^{2+}, Co^{2+}, Ni^{2+}.

To study the catalytic activity of slightly soluble hydroxides in modified bipolar membranes electrochemical impedance method was used as well as partial current-overvoltage characteristics and effective rate constants of water dissociation in the bipolar region in the absence of an electric field.

Virtual impedance meter – analyzer coupled with a computer was used to measure the frequency spectrum of the electrochemical impedance of the samples of membranes in 1 Hz - 1 MHz frequency range were AC frequency were distributed on a logarithmic scale. The amplitude of the alternating measuring voltage across the membrane was 50 mV. Relative error of impedance module was less than 5%.

In this work, the frequency spectrum of impedance of the bipolar membrane was measured at 25°C in flow electrochemical cell in 0.5 M HCl | 0.5 M NaOH system. The working area of the membrane was equal to 2.27 cm^2. The concentration of hydrochloric acid and sodium hydroxide was 0.5 mol/l. Resistance of bipolar region was calculated with $R_b = R_0 - R_\infty$ were R_0 – membrane resistance at "zero" frequency, R_∞ – membrane resistance when extrapolated to the "infinitely large" frequency. Next current-voltage characteristic of bipolar region was calculated on the dependence of the resistance of the bipolar region on current

$$\eta_b = \int_0^{I^*} R_b dI \qquad (1)$$

The effective rate constant of water dissociation at zero electric field was calculated by formula proposed in [1]:

$$i_{H^+,OH^-} = k_\Sigma \frac{\varepsilon\varepsilon_0}{\beta}\left[\exp\left(\beta E_m\left(\eta_Б\right)\right) - \exp\left(\beta E_m(0)\right)\right] \qquad (2)$$

Results and Discussion

Comparison of frequency spectra of electrochemical impedance (Figure 1*a*) shows that membranes modified by iron hydroxide (III) have the highest catalytic activity, and membranes modified by copper hydroxide (II) have the lowest activity. Overvoltage of bipolar region of bipolar membrane modified by iron hydroxide (III) is 0.7 V at 4.4 A/dm^2 current density. This is 10 times less than in the case of overvoltage at membranes modified by less catalytically active copper and nickel hydroxides. Current-voltage characteristic of bipolar region of bipolar membrane modified by iron hydroxide (III) is linear, which is typical for the best known industrial membranes (Figure 1*b*).

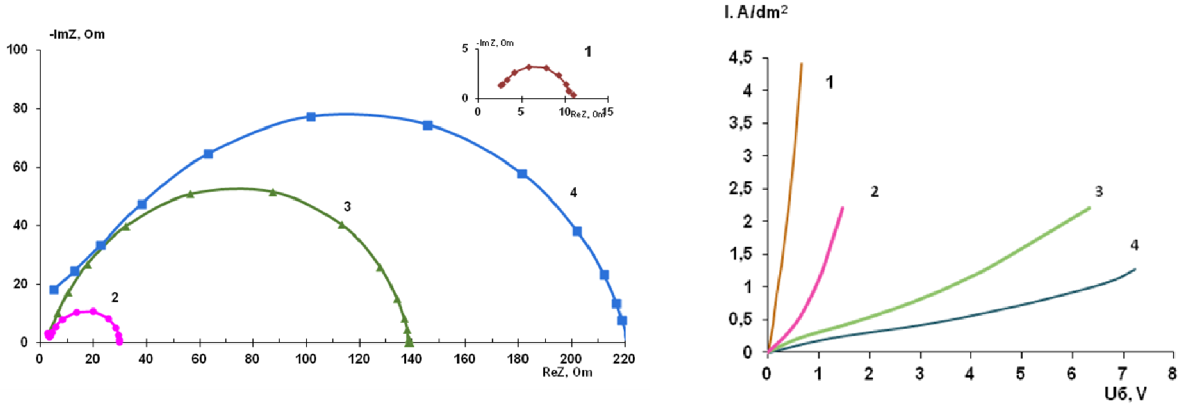

a *b*

Figure 1. Frequency spectra of electrochemical impedance (a) at 0.88 A/dm^2 current density and partial current-overvoltage characteristics (b) of bipolar membranes modified by hydroxides: 1 - iron (III), 2 - cobalt (II), 3 - nickel (II) and 4 - copper (II)

Figure 2 shows the frequency spectra of electrochemical impedance at different electric currents for the best bipolar membrane modified by iron hydroxide (III). Resistance of this bipolar membrane does not change on electric current density and indicates high catalytic activity of iron hydroxide.

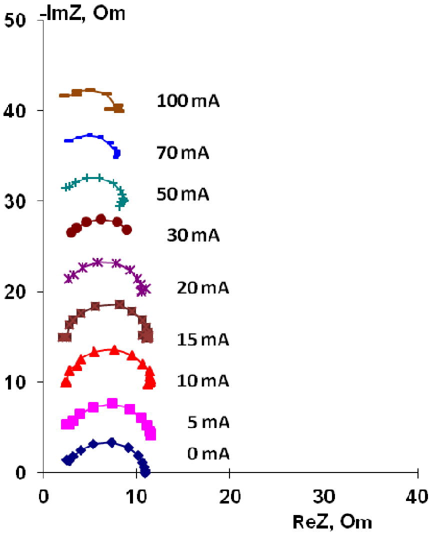

Figure 2. The dependence of the frequency spectrum of the electrochemical impedance of BPM modified by iron hydroxide (III), at different currents (the numbers near the curves)

Modified membranes in 0.5 M H_2SO_4 | 0.5 M NaOH system under 4 A/dm^2 remain stable during 60 hours (Figure 3).

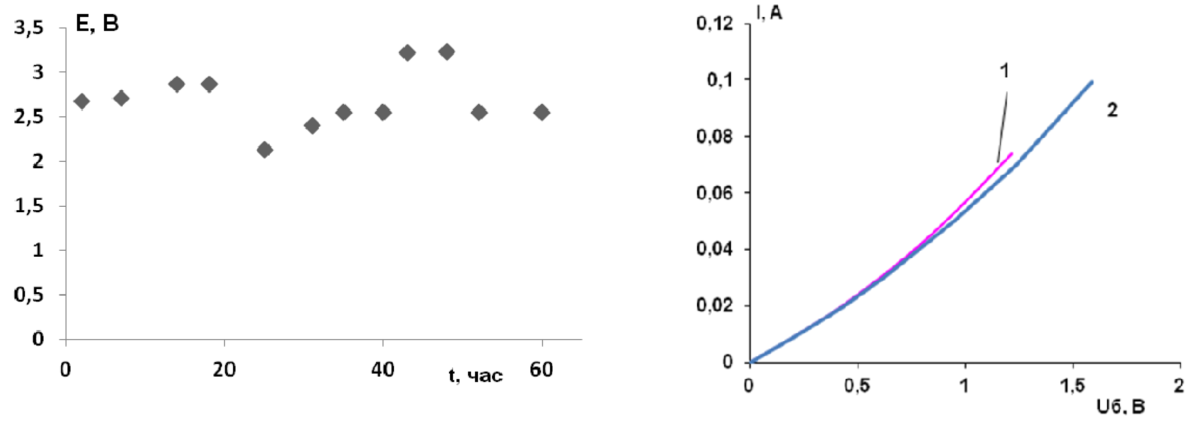

a *b*

Figure 3. Typical dependence of the voltage drop on MB-2 bipolar membrane modified by heavy metal hydroxide on time in 0.5 M H2SO4 | 0.5 M NaOH system under 4 A/dm2 electric current density (a). Partial current-overvoltage characteristics of bipolar region (b) of the membrane before testing (1) and after 60 h (2)

High catalytic activity of iron hydroxide (III) is confirmed by calculated effective rate constants for water dissociation in bipolar membranes modified heavy metals hydroxides (Table).

Table. Characteristics of water molecules dissociation in the space charge region of analog of MB-2 bipolar membrane chemically modified by heavy metals hydroxides and in original analog of MB-2

Membrane	**k∑,1/s**	**β, m/V**
MB-2, modified by:		
$Fe(OH)_3$	100,93	7,4
$Co(OH)_2$	14,45	7,3
$Ni(OH)_2$	42,43	2,4
$Cu(OH)_2$	21,97	2,3
MB-2	4,77	4,9

Based on this study one can construct a series of catalytic activity of slightly soluble metal hydroxides introduced into bipolar region of bipolar membrane by chemical method:

$$Cu\,(OH)_2 < Ni\,(OH)_2 < Co\,(OH)_2 < Fe\,(OH)_3.$$

Study was partially supported by Russian foundation for basic research, research project № 13-08-96529 r_yug_a.

References

1. *Mel'nikov S.S., Shapovalova O.V., Shel'deshov N.V., Zabolotsky V.I.* Effect of *d*-metal hydroxides in the water dissociation in bipolar membranes // Membranes and membrane technology, 2011. T. 1, № 2. P. 149-156.
2. *Shel'deshov N.V., Zabolotsky V.I., Ganych V.V.* Effect of insoluble metal hydroxides in water dissociation reaction rate to a cation exchange membrane // Electrochemistry. 1994. Vol. 30, № 12. P. 1458-1461.
3. *Simons R.* Preparation of a high performance bipolar membrane //J. Membr. Sci. 1993. V. 78. P. 13-23.
4. *Umnov V.V., Shel'deshov N.V., Zabolotsky V.I.* The current-voltage characteristics of the space-charge bipolar membrane // Electrochemistry. 1999. Vol. 35. № 8. P. 871-878.

INFLUENCE OF HEAVY METAL HYDROXIDES ON ELECTROCHEMICAL CHARACTERISTICS OF BIPOLAR MEMBRANES

Olga Shapovalova, Stanislav Melnikov, Nicolai Sheldeshov, Victor Zabolotsky
Kuban State University, Krasnodar, Russia, *E-mail: sheld_nv@mail.ru*

Introduction

Bipolar ion-exchange membranes are composed of two parts - cationite and anionite. When electric current flows through bipolar membrane dissociation of water occurs, which leads to the formation of hydrogen and hydroxyl ions on both sides of the membrane. The main characteristics determining the effective application of such membranes are bipolar region overvoltage and the total voltage drop across the membrane.

It is known that catalytic additives added to the contact area of cationite and anionite improves these characteristics. Introduction of additives may be performed in various ways: during manufacture of the membrane by hot pressing, by chemical and electrochemical methods. Such additives can be both organic and inorganic substances. In this work heavy metals hydroxides are selected as such catalyst additives.

Experiments

Objects of the study were bipolar membranes MB-2 modified by an electrochemical method, as well as analogs of MB-2 membranes obtained from the membranes Ralex CMH-PES membranes and Ralex AMH-PES by chemical method and by incorporation of a heavy metal hydroxide powder.

MB-2 modification by electrochemical deposition of chromium hydroxide (III), iron (III), nickel (II) was carried out in 4-chamber cell under the following conditions: concentration of salts and an alkali solution supplied to the cell was 0.1 M, the DC density - 5 mA/cm^2 deposition time - 16 min.

Chemical modification of the bipolar membranes obtained from the membranes Ralex CMH-PES membranes and Ralex AMH-PES was carried out by applying to the cation exchange membrane a solution of metal salts: iron (III), nickel (II), cobalt (II), copper (II) or cerium (III) followed by treatment of the membrane with sodium hydroxide.

Introduction of powder chromium hydroxide (III), iron (III), nickel (II), cobalt (II) and copper (II) to the same bipolar membrane was carried out by applying freshly prepared, dried and ground powders of metal hydroxides in the bipolar region.

Fequency spectrum of the electrochemical impedance samples were measured with virtual meter – impedance analyzer interfaced to a computer. The measurements were performed in a frequency range of 1 Hz - 1 MHz in the four-chamber flow cell with 2.27 cm^2 working area of membrane.

Differential resistance of bipolar region R_b was calculated from the frequency spectra of electrochemical impedance of the membrane. Current-voltage characteristic of bipolar region was calculated from dependence of R_b on electric current using the equation:

$$\eta_\mathrm{b} = \int_0^{I^*} R_\mathrm{b} dI$$

Total current-voltage characteristics of modified membranes were measured by voltammetry method under dynamic conditions with virtual meter-voltage characteristics analyzer interfaced to a computer at a speed of 0.02 mA/s. The potential difference across the membrane was measured with a standard silver chloride electrode.

Results and Discussion

Introduction heavy metal hydroxides in the bipolar membrane area of MB-2 or its analogs reduces bipolar region overvoltage of the samples (Figure 1) and the total voltage across the membrane (Figure 2), except nickel hydroxide (II), which significantly increases the voltage drop at the membrane (Figure 2 *a*, curve 3). The use of chemical and electrochemical methods of introducing of metal hydroxides allows to differentiate hydroxides according to their catalytic activity in the dissociation of water (Figure 1 *a*, *b*, Figure 2). Introduction hydroxide in powder form (Figure 1 *c*) does not allow to reach the same low values of bipolar overvoltage as using electrochemical and chemical methods. This difference may be due to the fact that hydroxides in a powder form lower catalytic activity due to their drying and partial dehydration which occur during drying and hot pressing of cation-exchange and anion-exchange layers.

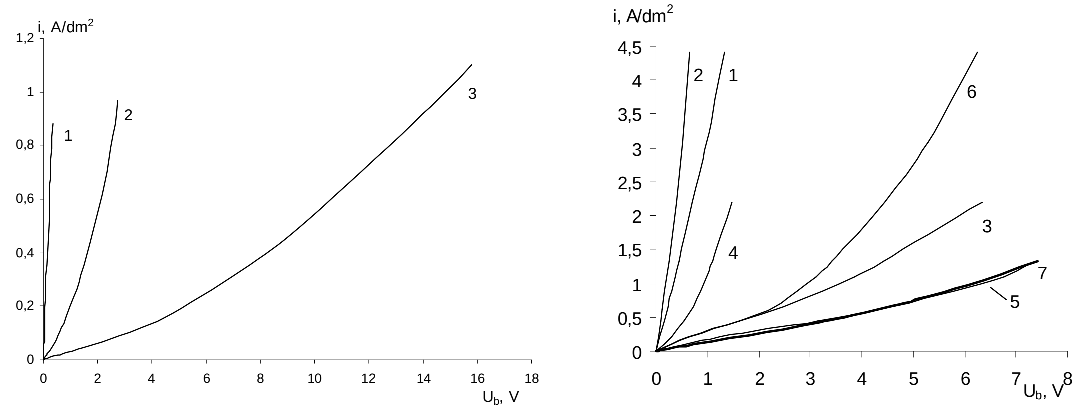

a *b*

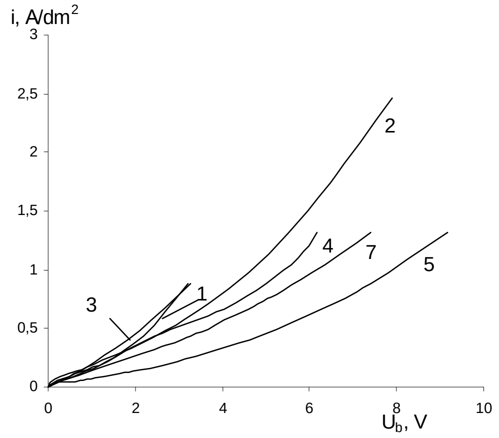

c

Figure 1. Partial current-voltage characteristics of the bipolar membranes modified by methods: electrochemical (a), chemical (b) and powder (c). Catalyst additive: 1 – $Cr(OH)_3$,, 2 – $Fe(OH)_3$,3 – $Ni(OH)_2$, 4 – $Co(OH)_2$, 5 – $Cu(OH)_2$, 6 – $Ce(OH)_3$. 7 – initial MB-2. Current-voltage characteristics were measured in the systems 0,01 M HCl | 0,01 M NaOH (a) and 0,5 M HCl | 0,5 M NaOH (b, c)

The rate constants k_1, k_2 of limiting steps of the reaction of water dissociation (1) – (2)

$$\mathrm{Me(OH)_n} \underset{k_{-1}}{\overset{k_1}{\rightleftarrows}} \mathrm{Me(OH)^+_{n-1}} + \mathrm{OH^-},\ K_1 \ (1) \qquad \mathrm{Me(OH)^+_{n-1}} + 2\mathrm{H_2O} \underset{k_{-2}}{\overset{k_2}{\rightleftarrows}} \mathrm{Me(OH)_n} + \mathrm{H_3O^+},\ K_2 \ (2)$$

in a bipolar region of modified membranes was calculated by the well-known thermodynamic and kinetic data by the method proposed in [1].

Effective dissociation rate constant of water k_Σ and entropy factor β were calculated using the equation $i_{H^+/OH^-} = k_\Sigma \frac{\varepsilon\varepsilon_0}{\beta}(\exp(\beta E_m(\eta_b)) - \exp(\beta E_m(0)))$ proposed in [2] for the partial voltage-current characteristics of the bipolar regions of the modified membranes. Current density of hydrogen and hydroxyl ions generated in the space charge region of bipolar membranes was calculated $i_{\mathrm{H^+,OH^-}} = iT_{\mathrm{H^+,OH^-}}$ using ion transport numbers of ions through bipolar membrane MB-2 and its analogues [3].

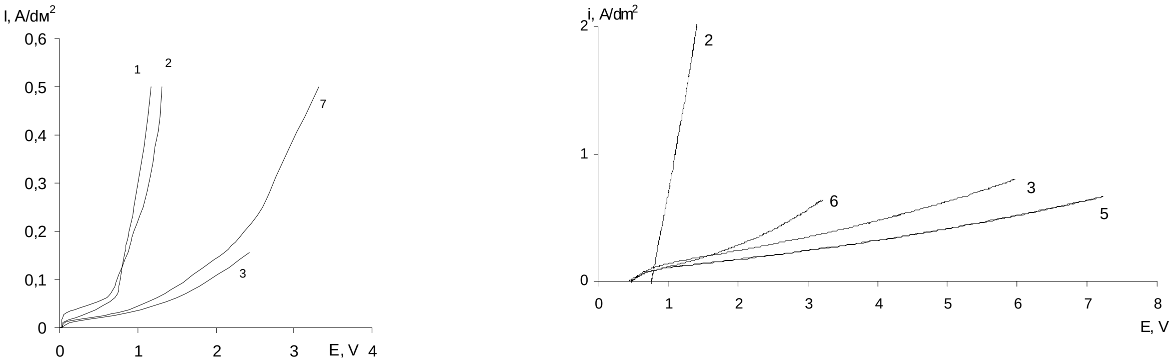

a *b*

Figure 2. Total current- voltage characteristics of the bipolar membranes modified by electrochemical (a) and chemical (b) methods. The catalytic additive: 1 – $Cr(OH)_3$, 2 – $Fe(OH)_3$, 3 – $Ni(OH)_2$, 4 – $Co(OH)_2$, 5 – $Cu(OH)_2$, 6 – $Ce(OH)_3$. 7 – initial membrane. Current-voltage characteristics were measured in the systems 0,1 M Na_2SO_4|0,1 M Na_2SO_4 (a) and 0,5 M HCl | 0,5 M NaOH (b)

Table shows that metal hydroxides in oxidation state (+3) exhibit a stronger catalytic effect on the dissociation of water molecules in the bipolar membranes than in oxidation state (+2)

Table. Thermodynamic and kinetic characteristics of the dissociation of water molecules in the space charge region of MB-2 bipolar membrane and its analogs obtained by chemical modification with hydroxides of heavy metals

Hydroxide	K_1, mol/l	K_2, mol/l	k_1, $M^{-1}c^{-1}$	k_2, $M^{-1}c^{-1}$	k_Σ, 1/c	β, м/V	U_b, V at 2 A/dм^2
$Fe(OH)_3$	5.12×10^{-9}	6.11×10^{-10}	16.2	19.3	101	7.43	0.3
$Cr(OH)_3$	3.73×10^{-8}	8.39×10^{-11}	119	2.65	366	3.33	0.6
$Co(OH)_2$	5.48×10^{-7}	5.71×10^{-12}	1.73×10^{3}	0.180	14.4	7.31	1.4
$Ce(OH)_3$	1.10×10^{-6}	2.84×10^{-12}	3.50×10^{3}	8.98×10^{-2}	15.7	4.16	4,2
$Ni(OH)_2$	8.95×10^{-4}	3.49×10^{-15}	2.83×10^{6}	1.10×10^{4}	42.4	2.41	6.0
$Cu(OH)_2$	2.25×10^{-8}	1.39×10^{-10}	71.1	4.40	22.0	2.28	9.0

Study was partially supported by Russian foundation for basic research, research project № 13-08-96529 r_yug_a.

References

1. *Shel'deshov N.V., Zabolotsky V.I., V.V. Ganych.* Effect of insoluble metal hydroxides in water dissociation reaction rate to a cation exchange membrane // Electrochemistry. 1994. Vol. 30, № 12. P. 1458-1461.
2. *Umnov V.V., Shel'deshov N.V., Zabolotsky V.I.* The current-voltage characteristics of the space-charge bipolar membrane // Electrochemistry. 1999. Vol. 35. № 8. P. 871-878.
3. *O.V.Shapovalova, N.V.Sheldeshov, V.I.Zabolotsky.* Study of electrochemical characteristics of modified bipolar membranes // International Conference Proceedings “Ion transport in organic and inorganic membranes” 28 May – 2 June Krasnodar 2012. P. 201 – 203.

RESEACH OF ELECTRO MASSTRANSFER IN SYSTEMS WITH PROTON EXCHANGING POLYVIYLIDENE FLUORIDE –SULFONATED POLYSTYRENE MEMBRANES BY THE METHOD OF ROTATING MEMBRANE DISK

[1]Mikhail Sharafan, [2]Ardalion Ponomarev, [2]Emil Abdrashitov, [3]Yury Dobrovol`sky, [1]Anastasia But, [1]Victor Zabolotsky

[1]Kuban State University, Krasnodar, Russia, *E-mail: Shafron80@mail.ru*
[2]Branch of Institute of Energy Problems for Chemical Physics of RAS, Chernogolovka, Russia;
[3]Institute of Problems of Chemical Physics of RAS, Chernogolovka, Russia

Introduction

Membranes intended for use in various low-temperature electrochemical devices, in particular, hydrogen and methanol fuel cells must have a certain combination of properties: high proton conductivity, good mechanical strength, chemical stability in the presence of oxidizing agents, low permeability of hydrogen and methanol. To a large extent these requirements are met by the perfluorinated membranes such as Nafion and MF-4SC. However, these membranes are not without drawbacks. They do not sufficiently retain the water at elevated temperature, which leads to significant deterioration of conductivity, and are quite expensive because of the complexity of the synthesis. To date, the desire to create new types of membranes based on various fluorinated polymers have a number of positive characteristics seem very urgent task. In [1, 2] authors study the possibility of thermal polymerization of styrene (St) in the PVDF film in contact with the monomer solution in toluene at elevated temperature (90 °C), the proton-conducting membrane and obtained by sulfonation of the embedded polysterene (PS) and studied their electrical transport properties and permeability by hydrogen, water and methanol. In this study, electrical transport properties of these membranes, their structure and properties at limiting currents regimes may be a separate issue to explore.

The aim of this work is to study the regularities of electromasstransfer, the dissociation of water, the stability of composite membranes based on sulfonated polyvinylidenefluoride in limiting currents modes by rotating membrane disc (AMD).

Experiments

The electrochemical characteristics of the samples of composite membranes based on PVDF film 90 microns thick containing 10% by weight. (IE = 0.75 mmol/g) and 23% by weight (IE = 1.52 mmol/g) of PS implanted in 0.01 M NaCl in a stabilized thickness of the diffusion layer on a device with a rotating membrane disc. The membrane samples were synthesized and provided by the Institute of Energy Problems of Chemical Physics, Chernogolovka. The experimental method used to study electromembrane system (EMS) in this work – rotating membrane disc method – is described in detail in [3, 4]. Effective transport numbers, general and partial current-voltage characteristics was measured in the present work. Based on them limiting current densities and diffusion boundary layer thicknesses for different RMD rotation speeds were calculated. A comparison of the experimentally measured values of the limiting current density with those calculated from the theory of Levich was made. It is shown that the nature of the limiting current in dilute solutions is not purely electrodiffusion.

Results and Discussion

The experimental current-voltage characteristics of the EMS - *PVDF-(10% PS-*SO_3H*)*|0,01 M solution of NaCl (fig. 1), approximated by equation [eq.(1) 4]. The results of the approximation lines are shown in the figure (point - experimental data).

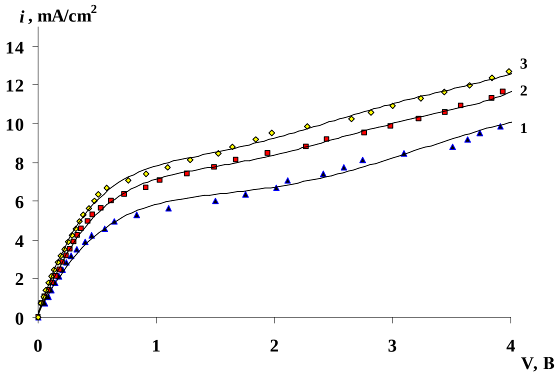

Figure 1. Total CVC for EMS - PVDF-(10% PS-SO$_3$H)/0,01 M NaCl, at different rotation speeds (rpm): 1 – 100; 2 – 200; 3 – 300

The experimentally found values of Hittorf transport numbers for the studied systems were built by partial CVC for Na$^+$ and H$^+$ - ions (Fig. 2). It can be seen that water dissociation can play a significant role in the overall masstransfer (up to 30% of total current is transferred by H$^+$-ions).

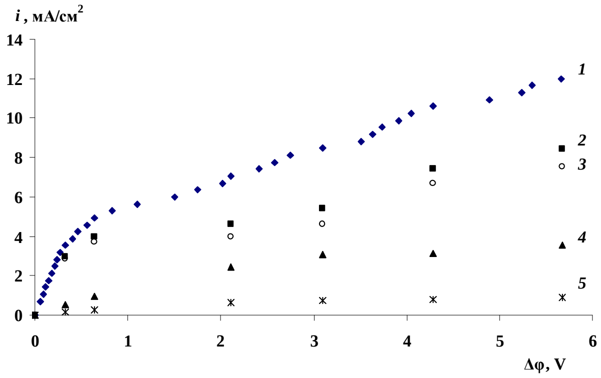

Figure 2. Total and partial CVC of EMS with PVDF-(10% PS-SO$_3$H) membrane in 0,01 M NaCl solution with the rotation speed of 100 rpm: 1 – total CVC, 2 – partial CVC for Na$^+$-ions, 3- partial CVC for Na$^+$-ions reduced by the exaltation current, 4 – partial CVC for H$^+$-ions, 5 – exaltation current Kharkats

A comparison of the experimental data was carried out by the characteristic linear dependence of $i_{\lim} - \sqrt{\omega}$, Fig. 3.

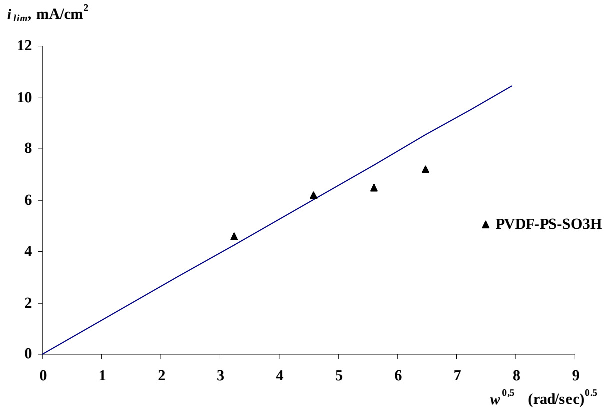

Figure 3. Total limiting current depended on the square root of the rotation angular velocity (dotted line – theory calculation by Levich, points – experimental data for (10% PS-SO$_3$H) – 0,01 M solution NaCl

Analysis of the dependence of the limiting currents found by the tangent method, from square root of the RMD angular velocity shows that obtained data deviates from the linear dependence

(Fig. 3). The values of the limiting currents lay below predicted by the theory of Levich. Such a course was previously detected in [5]. This result was attributed to the presence of the porous layer with less concentration of ionic groups on the surface of membrane.

Effective transport numbers were also measured and partial CVCs by hydrogen and sodium ions for EMS with PVDF-(23% PS-SO_3H)|0,01 M NaCl (Fig. 4).

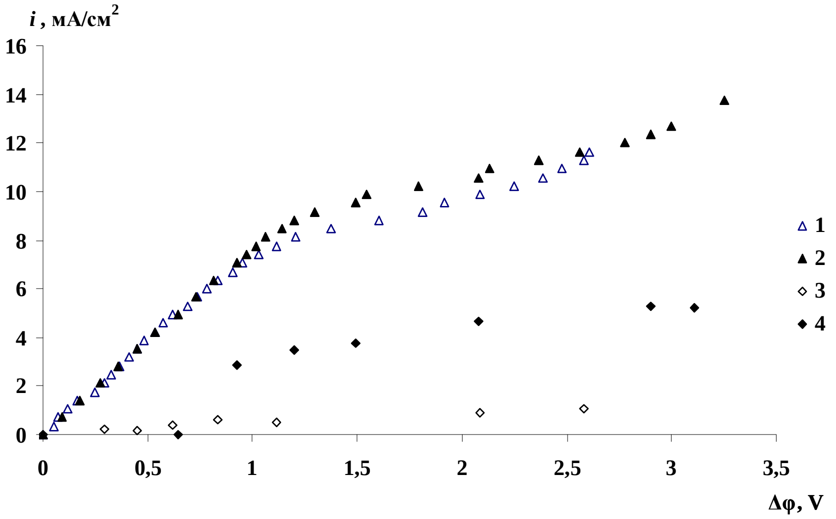

Figure 4. Total and partial CVC of EMS with PVDF-(23% PS-SO_3H) membrane in 0,01 M NaCl solution with the rotation speed of 100 rpm:
1– total CVC after 2 hours work under the current, 2 – total CVC after 20 hours work under the current, 3 – partial CVC for H^+-ions after 2 hours work under the current,
4 – partial CVC for H^+-ions after 2 hours work under the current

Figure 4 shows that the limiting current value for the membrane which had worked for 20 hours under overlimiting current $i > i_{\rm lim}$ are somewhat higher compared with the membrane subjected to two hours of polarization. The values of the partial currents by H^+-ions for the studied EMS also differs significantly. With increased exposure time part of the current carried by hydrogen ions increases from 15% to 40% of the total mass transfer. This indicates an increase in the water dissociation rateof the studied membrane. The angle of inclination of the initial part is unchanged, indicating stability of the conductive properties of the composite membrane.

References

1. *Abdrashitov E.F., Bokun V.Ch., Kritskaya D.A., Sanginov E.A., Ponomarev A.N., Dobrovol`ski Yu.A.* // Russian Journal of Electrochemistry, 2011, Vol. 47, № 4, P.387 – 394.
2. *Abdrashitov E.F., Kritskaya D.A., Voilov D.N., Dremova N.N., Sanginov E.A., Ponomarev A.N., Dobrovol`ski Yu.A.* // Membranes and membrane technology, 2011, V.1, № 4, P. 1 – 8.
3. Patent №78577 (RU) *M. Sharafan, V. Zabolotsky.*
4. *Zabolockii V.I., Shel'deshov N.V., Sharafan M.V.* // Russian Journ. Of Electrochemistry. 2006. Vol. 42. №12. P. 1494–1500.
5. *Kulincov P.I. Ph.D. thesis. Voronezh, 1988. 139 c.*

THE ROTATING MEMBRANE DISK IN ELECTROCHEMISTRY

Mikhail Sharafan, Victor Zabolotsky
Kuban State University, Krasnodar, Russia, *E-mail: Shafron80@mail.ru*

The report will discuss the most important problems of modern membrane electrochemistry: the study of ions transport patterns through membranes under high and ultra-high current densities, and new mechanisms for their delivery to membrane|solution interface, the role of concentration polarization phenomena and its impact on intensification of mass transfer in electromembrane systems (EMS). Progress in this direction has been made due to the fundamental works aimed at the study of the ions transport processes through membranes under intense current regimes, including usage of rotating membrane disc (RMD) method. RMD makes a unique tool to study the EMS because it provides a unique opportunity to apply a constant diffusion layer thickness on the entire surface of the ion exchange membrane, in accordance with the classical hydrodynamic theory by V.G. Levich. The RMD method was created based on the classic hydrodynamic theory by V.G. Levich, which was originally developed in the 40s for a system with a rotating disc electrode (RDE) [1]. The first attempt to use the method of the rotating disk for the study of EMS was made almost half a century ago in the work of the scientists of the Voronezh Institute of Chemical Technology, N.I. Isayev [2]. Further development of the RMD method was made in the works by A.I. Makai and I.C. Turner (1978) [3], D.A. Gough and J.K. Leypoldt (1979) [4], O.V. Bobreshova and co-authors (1987) [5], J.A. Manzanares et al. (1991) [6], E.A. Lukashev (2000) [7].

At high current densities, when numerous effects of concentration polarization complicate classical ions electrodiffusion transport phenomenon, it is insufficient only to register polarization characteristics of membranes. It is necessary to simultaneously measure ion fluxes (effective transport numbers of ions) with the registration of EMS current-voltage characteristics (CVC). Such a method and a system with RMD were first developed by the authors [8]. As a result we can obtain ion-exchange membrane CVC and Hittorf transport numbers simultaneously at a constant thickness of the diffusion layer, that fact strongly extends functionality of the RMD method.

The report presents the results of studies using the developed RMD method to address the major problems of membrane electrochemistry: the impact of the membrane surface morphology on transport of salt ions and water dissociation products, disclosure of EMS overlimiting state phenomenon, the role of conjugated phenomena of concentration polarization (water dissociation and conjoined exaltation effect, violations of electroneutrality of the solution and electroosmotic convection) for the various heterogeneous and homogeneous ion exchange membranes, the development of the concept of the catalytic water mechanism of the molecules dissociation in the membranes of different nature, regarding participation of the ionic groups. The report will also discuss the prospects for improving the method of RMD and the new possibilities of the method for solving urgent problems of membrane electrochemistry.

The present work is supported by the Russian Foundation for Basic Research (projects 12-08-93105-НЦНИЛ_а and 13-08-01460-а).

References

1. *Levich V.G.* Physico-chemical hydrodynamics. M.:(in Russia) 1959. 700 с.
2. *Isaev N.I.* // J. Phys. Chem. 1967. T. 41, № 4. C. 849.
3. *Makai A.I. Turner J.C.* // Chem. Soc. Faraday. Trans. 1978. Vol. 74, № 12. P. 2850.
4. *Gough D.A., Leypoldt J.K.* // J. Analytical Chemistry 1979 Vol. 51, № 3. P. 439
5. *Bobreshova O.V., Kulincov P.I.* // J. Phys. Chem 1987. T.61, № 1. C. 277–279.
6. *Lukashov E.A.* // Rus. J. Electrochem. 2000. T. 36. № 4. C. 414.
7. *Manzanares A., Kontturi K., Mafe S., & others* // Acta Chem. Scand. 1991. Vol. 45. P.115.
8. Patent №78577 (RU) *M. Sharafan, V. Zabolotsky.*

STABILITY AND CHAOS TRANSITION IN MICROFLOWS IN MEMBRANE APPLICATIONS

[1]Vladimir Shelistov, [2]Vladimir Kiriy

[1]Kuban State University, Krasnodar, Russia, *E-mail: shelistov_v@mail.ru*

[2]"Artre" Ltd, Krasnodar, Russia, *E-mail: vladimir@kiriy.ru*

Introduction

The work deals with one of the problems of microfluidics – stability of micro- and nanoflows in an electric field. When an external electric field induces ion flow to the selective surface (membrane, electrode, system of micro- or nanochannels), a new type of instability – electrokinetic instability – arises near that surface [1,2]. It enables convective transport mechanism of ions and leads to a supercritical bifurcation of the current-voltage characteristics (CVC). This effect has many practical applications: a) it is used to create asymmetric input and output characteristics of the current (for example, to create a hydrodynamic diode in nanochannels), b) electrokinetic instability detected by electrophoresis of the 2nd kind can be used for motion control microparticles, c) instability phenomenas have a significant impact on the separation of proteins according to their properties with the help of traveling electrical wave, and d) many others.

Theoretic Approach

Electrokinetic instability is investigated theoretically, using the methods of the theories of dynamical systems, bifurcations and hydrodynamic stability. A model of binary electrolyte between infinite cation-exchange membranes is considered, whose behavior is described by the Nernst-Planck-Poisson-Stokes equations. The dimensionless system is described by four parameters: the drop of potential ΔV, the double ionic layer thickness ν, the coupling coefficient κ and the concentration of cations in the membrane p. The latter, however, does not qualitatively affect the behavior of the system, so the number of parameters is reduced to three [3].

A one-dimensional solution becomes unstable for sufficiently large drops of potential. In a small vicinity of the critical point the solution of the system is obtained analytically, reducing it to the Ginzburg-Landau equation. For large supercriticalities, the study is conducted by numerical integration of the complete system; a special algorithm has been developed for that purpose. Numerical experiments have been performed on a supercomputer "Chebyshev" (Moscow State University).

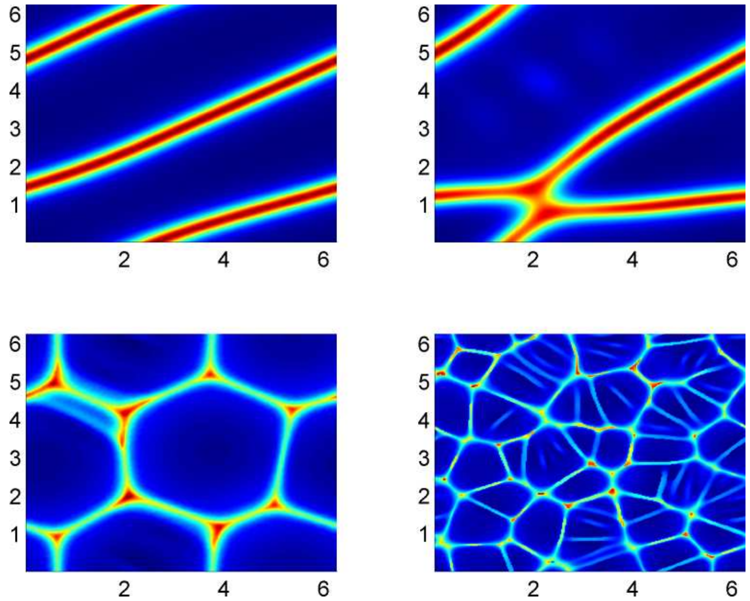

Figure 1. Charge density profiles for different drops of potential

Small sinusoidal perturbations are superimposed on the obtained solutions to calculate the linear growth coefficients. In addition to finding the boundaries of stability, an attempt was made to generalize Shilnikov's theory of the system under consideration.

Results and Discussion

The numerical experiments have shown that, despite the micro- and nano-scales of the phenomena, electrokinetic instability exhibits many of the characteristics of the classical hydrodynamic instability: the selection of disturbances with the characteristic length from the initial low-amplitude random noise, the presence of a cascade of bifurcations, leading to a “deterministic chaos” regime with coherent structures dominating in it. Shilnikov’s mechanism has been proven to be responsible for the chaos transition. The boundary of chaotic regimes and fractal dimension of the chaotic attractor have been found from the theory of Lyapunov exponents.

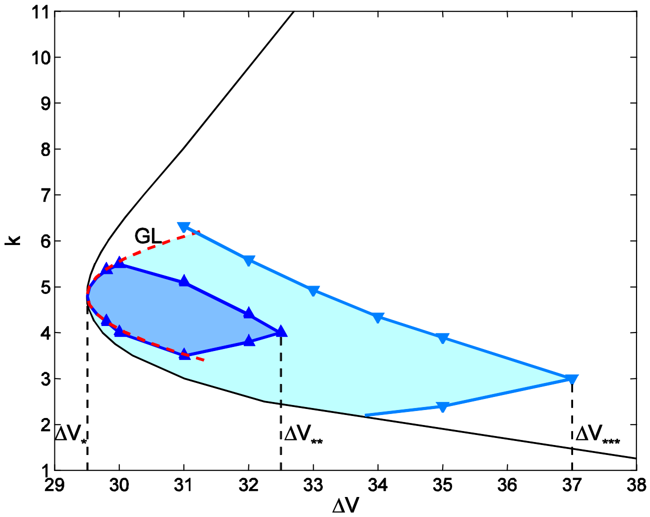

Figure 2. Stability ranges of the problem

It has been found that the distribution of the space charge near the selective surface takes the form of spikes, from which the fluid is pushed by the Coulombic force, which eventually leads to a supercritical bifurcation of the CVC. The self-similar nature of the solution in the vicinity of the spike has been shown; its angle has been calculated.

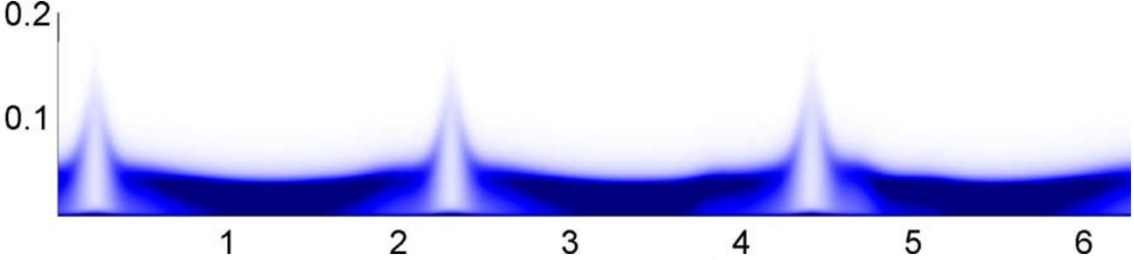

Figure 3. Two-dimensional spikes of charge density

These results have extended to more complex tasks: instability in microchannels, hydrophobicity and surface irregularities [4], etc.

Acknowledgements

The authors are grateful for the staff of Institute of Mechanics, Moscow State University, specifically for N.V. Nikitin and V.A. Polyanskiy, for fruitful preliminary discussion of the work. The work was supported by Russian Foundation for Basic Research, projects No 11-08-00480, 12-08-00924, 12-08-31544.

References

1. *Nikonenko V. V., Zabolotsky V. I., Gnusin N. P.* // Sov. Electrochem. 1989. V. 25, P. 301.
2. *Rubinstein I., Zaltzman B.* // Phys. Rev. E. 2000. V. 62. P. 2238.
3. *Demekhin E. A., Shelistov V. S., Polyanskikh S. V.* // Phys. Rev. E. 2011. V. 84. 036318.
4. *Chang H.-C., Demekhin E. A., Shelistov V. S.* // Phys. Rev. E. 2012. V. 86. 046319.

CONDITIONING INFLUENCE OF THE BASIC MEMBRANE ON THE PROPERTIES OF THE NANOCOMPOSITES MF-4SC/PAn

Svetlana Shkirskaya, Ninel Berezina, Mariya Kolechko, Ekaterina Nazyrova, Yanina Perepelitsa
Kuban State University, Krasnodar, Russia, *E-mail: shkirskaya@mail.ru*

In this study we investigated the MF-4SC s.29 “as received”, produced by "Plastpolimer" (St. Petersburg), MF-4SC sample that was created in the laboratory by alkaline hydrolysis of unsulphonated F-4SF matrix with 10% mass. solution of NaOH after that oxidation thermal preatreatment (OTP) of the sample was carried out, and the composites of MF-4SC with polyaniline (MF-4SC/PAn). Chemical synthesis is performed by sequential diffusion of protonated aniline ($C_6N_5NH_3^+$) solution and polymerization initiator $(NH_4)_2S_2O_8$ into the water. The contact time of the MF-4SC membrane with modification solution was 25 minutes [1]. After synthesis, the composite membrane MF-4SC/PAn has a gradient distribution of polyaniline across sample thickness. For visualization of polyaniline distribution in the composite membrane a number of photographs of the composite membrane cross-section were taken (Fig. 1). It can be seen that the polyaniline layer thickness in the composite membrane produced from MF-4SC s.29 is 25-30 µm, that is 1/4 of total membrane thickness. For the composite based on the MF-4SC (produced in the laboratory, OTP), the thickness of polyaniline layer is 130 microns (2/3 of the overall membrane thickness). Therefore, pretreatment of the initial matrix leads to expansion of the structural cavities in the perfluorinated membrane, which contributes to a more extended barrier polyaniline layer.

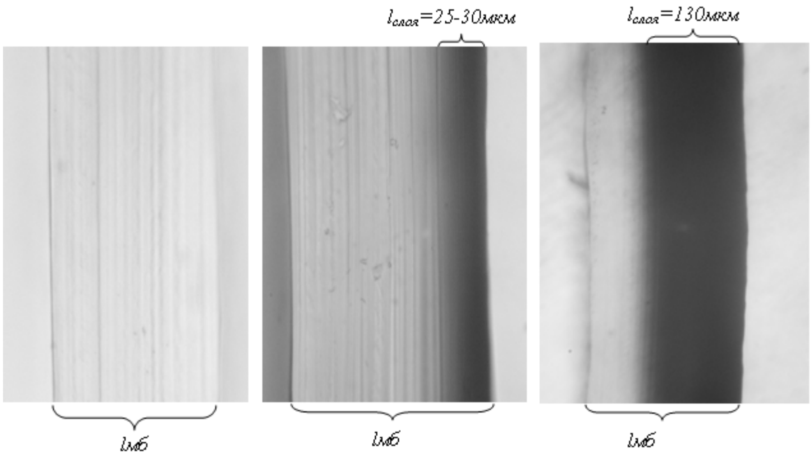

a b c

Figure 1. Microphotographs of the cross section of MF-4SC (a) and MF-4SC/PAn created on the basis of MF-4SC s. 29 (b) and MF-4SC (produced in the laboratory, OTP) (c)

To evaluate the transport properties of the MF-4SC/PAn composites concentration dependence of conductivity (k) and diffusion permeability (P) were studied in the same dyapason of HCl solution concentrations (Fig. 2). From the data obtained it follows that the conductivity after OTP increases by 15-20% compared with MP-4SK s. 29. As can be seen from the Figure 2 electrical conductivity decreases by 80 % for composite samples. It should be noted that the electrical conductivity of MF-4SC/PAn (produced in the laboratory, OTP) is two times higher compared with MF-4SC/PAn s. 29. From this follows that the expansion of the membrane matrix by oxidation and thermal pretreatment leads to the formation of extended structural cavities suitable for intercalation of polyaniline chains deposition and also leads to expansion of transport channels. Comparison of the diffusion permeability values for MF-4SC s. 29 before and after OTP (Fig. 2a, curves 1, 2), shows an increase of the diffusion permeability after OTP by 20%, which confirms the expansion of the transport channels after membranes boiling. Diffusion permeability is reduced by 50-70% for MF-4SC/PAn s. 29 and by 45-55% MF-4SC/PAn (produced in the laboratory, OTP) compared with the pristine membrane.

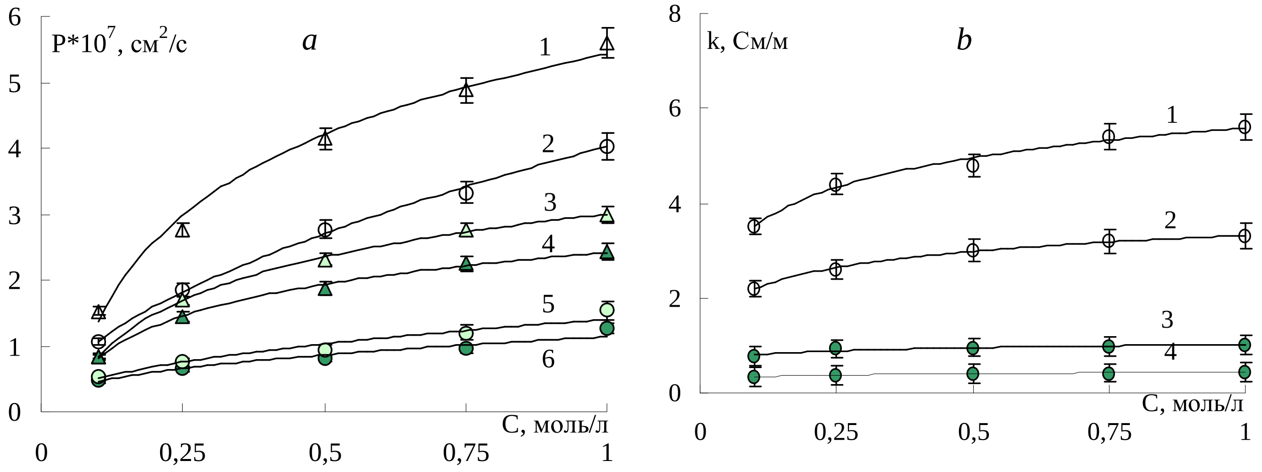

1 – MF-4SC (produced in the laboratory, OTP); 2 – MF-4SC s. 29; 3, 4 – MF-4SC/PAn (produced in the laboratory, OTP) oriented with unmodified and modified side towards electrolyte flux respectively; 5, 6 – MF-4SC/PAn s. 29 oriented with unmodified and modified side towards electrolyte flux respectively

1 – MF-4SC (produced in the laboratory, OTP); 2 – MF-4SC s. 29; 3 – MF-4SC/PAn (produced in the laboratory, OTP); 4 – MF-4SC/PAn s. 29

Figure 2. Integral diffusion permeability coefficients (a) and conductivity (b) of the studied membranes in dependence on the HCl solution concentration

Due to the fact that the resulting composite membrane had an anisotropic structure, study of the diffusion characteristics was conducted at different orientations to the flow of the electrolyte (Fig. 2a) and phenomenon of diffusive permeability asymmetry was found. The asymmetry of diffusion flux equals to 15% in the entire range of concentrations. Thus, the pretreatment of the initial membrane provides a composite membrane with a more extended polyaniline layer, but the introduction of polyaniline leads to approximately the same relative reduction of the electrical conductivity and the diffusion permeability compared to the initial membrane.

It was interesting to estimate electroosmotic permeability of the membrane samples before and after modification in NaCl solutions. It has been found that there is a significant reduction in water transport properties after modification with polyaniline. It should be noted that this effect is in quantitatively good agreement among themselves; the water transport number t_w is 4.5 for composite samples compared to 11.5 for the original membrane and is not dependent on the orientation of the membrane. It can be concluded that polyaniline surface layers play the key role in the deformation of the salt ions hydration shell. Obtained data shows that polyaniline surface layers plays a barrier role in transport of salt ions and water. Such properties allows to use the composite membranes MF-4SC/PAn in the process of electrolyte concentrating by electrodialysis.

This study was supported by the Russian Foundation for Basic Research.

References

1. *Berezina N.P., Shkirskaya S.A., Kolechko M.V., Popova O.V., Senchikhin I.N., Roldugin V.I.* Barrier effects of polyaniline layer in surface modified MF-4SK/Polyaniline membranes// Elektrokhimiya. 2011. Vol. 47. No. 9, P. 1066–1077.

BULK AND SURFACE CONDUCTIVITY OF AQUEOUS WETTING FILMS ON SOLID SURFACE

Vladimir Sobolev, Stanislav Itskov, Natalia Esipova
Frumkin Institute of Physical Chemistry and Electrochemistry RAS, Moscow, Russia,
E-mail: itskovs@rambler.ru

Introduction

Sustainability and the thickness of the wetting film is mainly determined by electrostatic forces. Known analytical solutions for electrostatic forces were obtained for two limiting cases, constant potential and constant charge, at both surfaces of the film subject to variation of thicknesses. The dependence of the conductivity on the thickness of the thin wetting films will determine the charges surfaces and to clarify the expression for the electrostatic component of the disjoining pressure.

Experiments

A novel method for investigation of electrical properties of thin wetting films was developed. The original method allows to indirectly determine the bulk and surface conductivity of wetting films in the range of thicknesses 10 -100 nm by measuring the electrical resistance of an annular wetting film being in contact with the meniscus of bulk liquid. The scheme of experimental cell is shown in fig.1.

The measuring cell is made of the glass cylinders of different diameter arranged concentrically. The cylinder walls are cut off in one plane in the lower part of the cell. In the upper part of the cell, the cylinder walls become conical and are welded together forming two working chambers – the outer chamber **1** and the inner chamber **2** that are separated by an air chamber being connected with atmosphere. The inner and outer chambers have pipe-bends that are connected with working vessel by means of flexible silicone hoses.

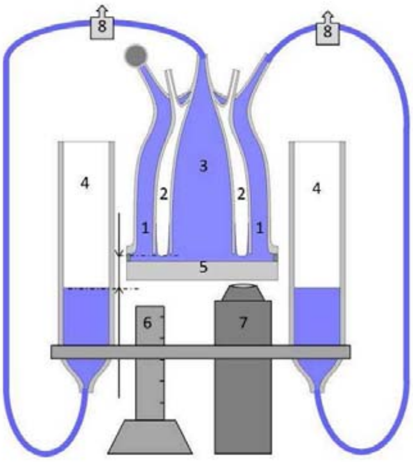

Figure 1. Experimental cell

The glass cell is placed on the surface of polished quartz plate **5** through a 50 mkm Teflon insert contacting with the lower slice of an outer cylinder. The outer and the inner working chambers are associated through a gap between the lower slices of cylinders and the quartz plate. The cell is filled with the experimental solution with the help of working vessels **4**. Lowering the liquid level in the working vessels by moving the holder of cathetometer **6** in the vertical axes, the solution is withdrawn from the cell until an annular wetting film contacting with meniscuses on the outer and inner walls of an air chamber is formed. The glass cell filled with experimental solution is put on a metallographic interference microscope Olympus GX51, equipped by a digital camera **7**.

The thickness of a formed annular wetting film is defined by the disjoining pressure value that is assigned by a difference between vertical positions of the film surface and the surface of solution in working vessels. For thickness determination an earlier developed [1,2] method, modified by the use of a digital camera was applied. The width of an annular wetting film was also measured.

For the determination of electrical properties of a wetting film, the experimental cell was affiliated to the electrical scheme by means of two electrodes **8**, placed in hoses between corresponding working chambers an working vessels. An electric scheme is shown in fig.2. The experimental cell was engaged in electrical scheme parallel with current source switched through a resistance unit $\mathbf{R_0}$, with resistance value close to the resistance of an annular wetting film $\mathbf{R_l}$. To exclude the effect of asymmetry potential of electrodes used, the polarity of current was reversed during the experiment. To obtain the resistance of a wetting film, the resistance value of a cell with a film formed was subtracted from that of a cell filled with experimental solution.

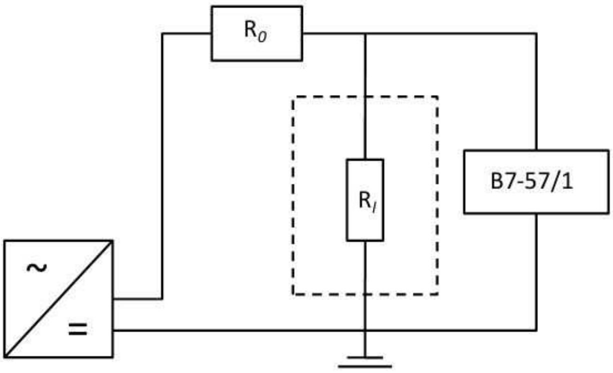

Figure 2. Electric scheme

The following equation was applied to define the resistance of a wetting film.

$$R_l = R_0\left(\frac{2U_1}{2U_1 - U_{1el} + U_{2el}}\right) - R_0$$

U_1 – voltage of a current source, U_{1el}, U_{2el} – voltages measured by a voltmeter **B7-57/1**, when the polarity of current is changed.

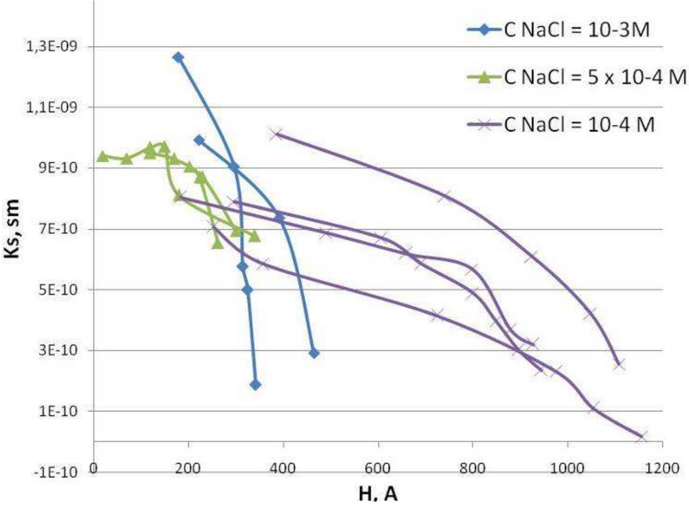

Figure3. Experimental data of surface conductivity of NaCl solutions on quartz surface

The obtained values of surface conductivity of NaCl solutions in the concentration range 10^{-3} ~10^{-4} M on quartz surface is between $8\text{x}10^{-10}$ Cm and $1.3\text{x}10^{-9}$ Cm that is lower than the previously published data.

This work was supported by the Russian Foundation for Basic Research, project no. 13-08-00674

References

1. *Derjaguin B.V., Zorin Z.M., Churaev N.V., Shishin V.A.* / Wetting, spreading and Adhesion. L.:Acad. Press, 1977, p.201-212
2. *Sheludko A., Platikanov D.* // Kolloid. Zeit. -1961. -B.175 -N2. -S.150

AN EXPRESSION FOR THE DIFFERENTIAL RESISTANCE OF THE DIFFUSION BOUNDARY LAYER IN ELECTRODIALYSIS OF ITACONIC ACID

Jan Stodollick, Robert Femmer, Said Abdu, Matthias Gloede, Matthias Wessling, Thomas Melin
RWTH Aachen University, Aachen, Germany

Nowadays fuels are mainly produced from oil. Therefore oil reserves are starting to run low. To preserve the remaining reserves of oil, other sources for fuels have to be found. To this end, biofuel production is gaining importance. At RWTH Aachen University the Excellence-Cluster “Tailor Made Fuels from Biomass” interdisciplinary research on biofuel production is carried out. Itaconic acid (IA) can be produced by fermentation and used as a platform chemical for biofuel production. As one step in the continuous production of IA, EDBM is used as purifying step and for pH control of the fermenter.

EDBM processes for acidification are operated at overlimiting current densities. The resistance of a diffusion boundary layer and consequently mass transfer under these conditions are not fully understood yet. In a first modeling approach, a differential resistance was assumed to describe the current-voltage behavior of an Anion Exchange Membrane. Experiments on a single membrane test cell under stationary conditions were carried out to measure IV-curves for different bulk phase compositions. Special attention was given to the influence of pH and ionic strength. It could be shown that the resistance at overlimiting currents follows an exponential law and that it depends on pH and ionic strength only with regards to the absolute level of the current. An expression for the resistance is proposed based on the Schmidt-Number, acknowledging the hydrodynamic character of electroconvection. Further it could be shown that the non-ideal behavior of the system can not be neglected and activity coefficients have to be considered.

STUDY OF POROUS STRUCTURE ACETATE MEMBRANES

Antonina Surkova, Valentin Sedelkin, Olga Pachina, Ilya Bogenko
Engels Technological Institute (branch) of Saratov state Technical University, Engels, Russia,
E-mail:pochta-mpp@mail.ru

Introduction

Derivative celluloses are widely used as a feedstock for making of porous filtration membranes. For a selection from multicomponent solutions of ingredients with the different molecular masses and sizes of necessary membranes with the managed distribution of pores on their radiuses, possessing a certain structure and functional properties. The most perspective going near adjusting of descriptions of membranes is a change of compounding of molding solutions. In this paper used for these purposes introduction polymer solution of the pore-forming additives $NaHCO_3$.

Experiments

A polymeric feedstock the powdery diacetate of cellulose served as for making of membranes (DAC). The solvent is selected acetone, which is the most cost effective and solvent power DAC. For making of membranes from polymer solutions used dry spinning process. The study of the porous structure of the membranes was measured by the standard contact porometry [1,2]. In experiments in the swollen membranes were operational. On figure 1-3 resulted the characteristics of pores membranes made from 7%% solutions of DAC in an acetone without addition of $NaHCO_3$ and with addition of 1% $NaHCO_3$.

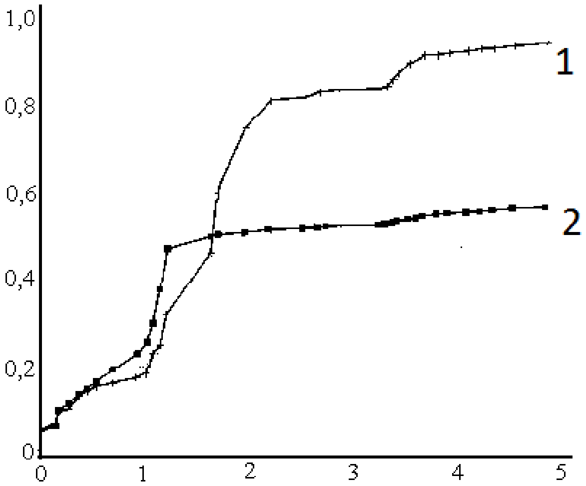

Figure 1. Integral curves of the distribution of pore radius in the membranes: 1- with the addition of 1% $NaHCO_3$, 2 - no added of 1% $NaHCO_3$.

Evidently, that the introduction of the polymer solution of sodium bicarbonate results in an increase of the pore volume and the total porosity of the membranes. The main contribution to the increase of porosity make small ($r_p = 1 \div 10$ nm) and average ($r_p = 10 \div 100$ nm) mesopores.

Analogical influence is rendered by addition of $NaHCO_3$ and on the change of integral specific surface of pores on their radiuses. The maximal values of this surface arrive at a 149 м^2/g and 176 м^2/g accordingly for membranes without addition and with addition of $NaHCO_3$.

The analysis of differential curves of change of specific surface of pores shows on radiuses (fig.3), that in membranes with the bicarbonate of natrium the specific surface of mesopore (r_p=1÷10 нм) is more developed, than in membranes without additions.

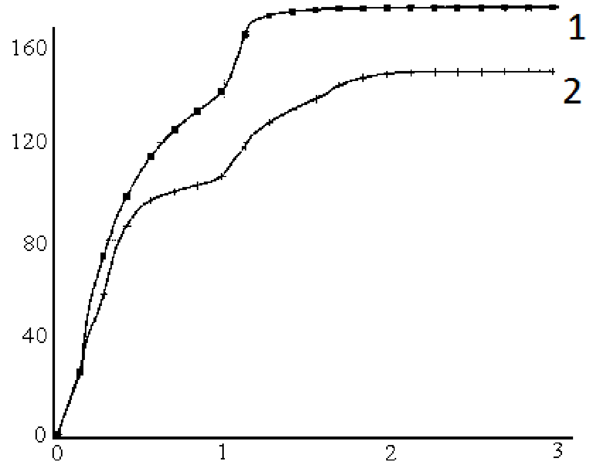

Figure 2. The integral distribution curves of the surface of the pore radius in the membranes 1- with the addition of 1% $NaHCO_3$, 2 - no added of 1% $NaHCO_3$

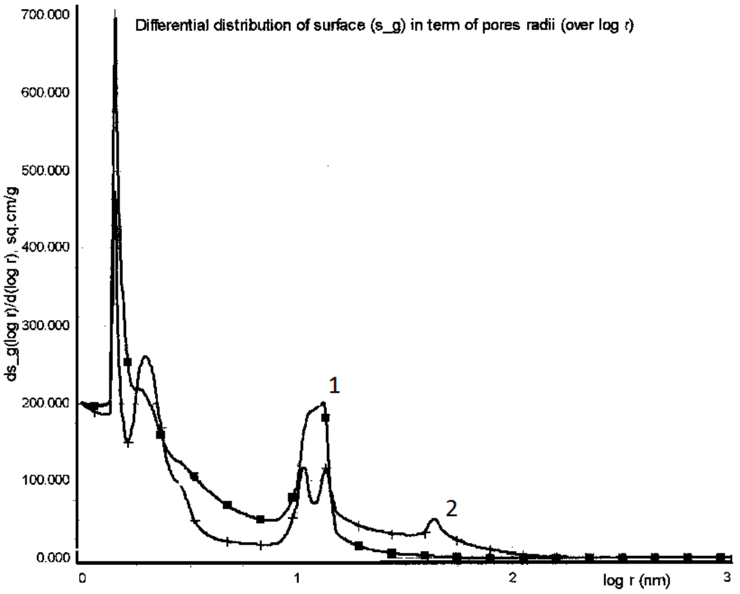

Figure 3. Differential distribution curves of the surface of the pore radius in the membranes 1- with the addition of 1% $NaHCO_3$, 2 - no added of 1% $NaHCO_3$

Conclusion

Thus, research of porous structure of acetate membranes showed that a bicarbonate of natrium was effective of porous addition in compounding of pilchard mixtures, allowing to regulate a porous structure, and consequently, permeability and selectivity of filtration membranes.

References

1. *Volfkovich U.* // Electrochemistry.-1984.-V.5-T.XX.-P.656-664.
2. *Kononenko N.* // Applied chemistry.-1985.-V.LVIII.-№10.-P.2199-2203.

METHODS OF EXPERIMENTS DESIGN AND TECHNOLOGICAL PARAMETERS OPTIMIZATION AT SYNTHESIS OF MULTICOMPONENT CHEMISORBTIONS MATERIALS «POLYCON K»

[1,2]Denis Terin, [1]Marina Kardash, [1]Ivan Tyurin
[1]Engels Technological Institute of Saratov State Technical University, Engels, Russia
[2]Saratov State University, Saratov, Russia

Introduction

The aim of the investigations is revealing the mathematical description of concatenation between technology factors of fabrication of a material «Polycon K», its properties and parameters of process, using the received experimental data [1-3] in the chosen factorial space.

Experiments

We aimed in searching the material possessing the best ion exchange characteristics. The static exchange capacity for objects «Polycon K» on polyacrylonitrile (PAN), oxidized PAN, carbon (CF) fibres and fabrics on the basis of novolak fibres (NLF) was investigated. Mix of monomers - waxsulphoacid (α) with formalin (β) was used in quality dipping compound.

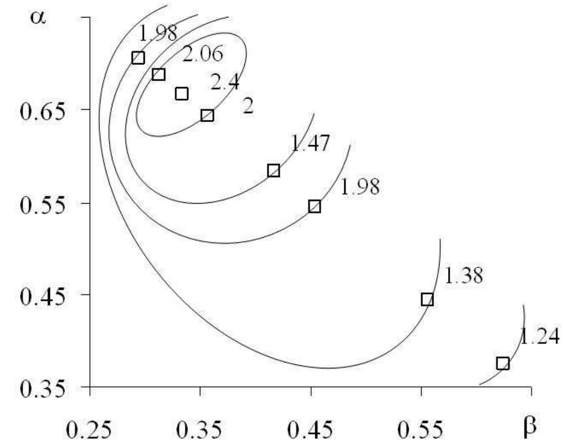

Figure 1. Dependence of static exchange capacity of dipping compound from relationship monomers volume fraction in mix

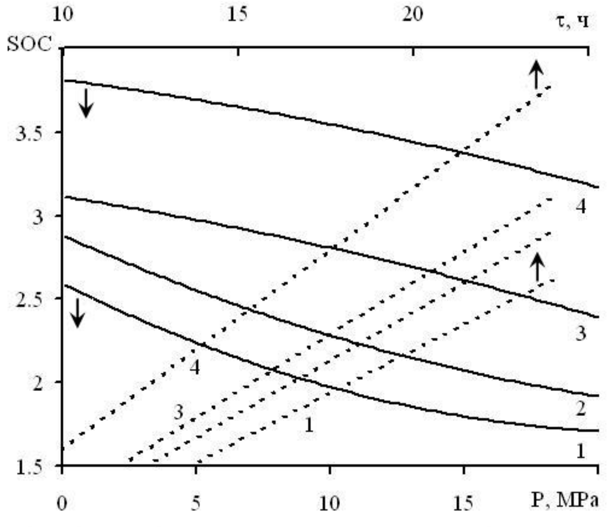

Figure 2. Influence of technological parameters on static exchange capacity (1 - PAN, 2 - oxidized PAN, 3 - CF, 4 - NLF)

Optimum relationship of monomers at fabrication of dipping compound having the best exchange capacity in hardened condition (fig. 1) was founded. The problem of composition development is the choice of relationship - fibre and polymeric matrix, within different types of fibres, using various hardening time (τ, hour) of structure and compacting pressure (P, MPa) (fig. 2).

As identification methods of object research methods of experiment design were selected (DEM). Now static selected design of experiments methods have become wide spread they suppose using the ready plans of experiment [4, 6]. The apparatus of regression analysis is the basis for models construction of these methods [4]. We understand under complete factorial experiment- the realization of all possible not repeating combinations of levels of factors variation. The ones changing at two levels and designated conditionally as +1 and -1. The number of possible combinations of factors levels determines the quantity of experimental points o f a plan and is calculated by formula N=2n, where N - the quantity of experimental points of a plan (the number of possible combinations of levels factors variation); 2- the number of variation levels of each factor; n - the number of factors.

We believe that the researched object has linear characteristics of out parameter which depend on input variables and so in our case it is necessary to use complete factorial (1).

$$\begin{aligned} Y = b_0 + \sum_{i=1}^{n} b_i x_i + \sum_{i<j}^{n} b_{ij} x_i x_j + \sum_{i=1}^{n} b_{ii} x_i^2 + \sum_{i\prec j\prec k}^{n} b_{ijk} x_i x_j x_k + \sum_{i\neq j}^{n} b_{ijj} x_i x_j^2 + \sum_{i=1}^{n} b_{iii} x_i^3 + \\ + \sum_{i\prec j\prec k\prec l}^{n} b_{ijkl} x_i x_j x_k x_l + \sum_{i\prec j\prec k}^{n} b_{ijkk} x_i x_j x_k^2 + \sum_{i\prec j}^{n} b_{iijj} x_i^2 x_j^2 + \sum_{i\neq j}^{n} b_{ijjj} x_i x_j^3 + \sum_{i=1}^{n} b_{iiii} x_i^4 + \ldots, \end{aligned} \tag{1}$$

where Y- response function (out parameter); x_i - input variables, factors (controlled parameters); b_0, b_i, b_{ij} - constant coefficients; n - number of input variables. On the basis of complete factorial, it is possible to estimate coefficients of regression equation, using first three items from (1):

$$Y = b_0 + b_1 X_1 + b_2 X_2 + b_3 X_3 + b_{12} X_1 X_2 + b_{13} X_1 X_3 + b_{23} X_2 X_3 \tag{2}$$

Optimization parameter is static exchange capacity, mg-eqv/g (Y), under the influence of the following factors: a ratio of fibre and dipping compound (X1), compacting pressure, MPa (X2) and hardening time, h (X3). For factors the following levels (the basic - Xio, bottom - Xiн (-1), top - Xiв (+1)) and intervals of a variation ΔXio have been chosen.

Table 1. Factor levels and variability interval (*-factor X1 of NLF)

Characteristics	X_1	X_1^*	X_2	X_3
X_{io}	0.5/0.5	0.5/0.5	10	15
$X_{iн}$	0.9/0.1	0.6/0.4	20	5
$X_{iв}$	0.1/0.9	0.4/0.6	0.1	25
ΔX_{io}	0.4	0.1	10	10

Experiment for check of experiences reproducibility was simulated. Processing of results was conducted by algorithm [7]. After model adequacy check the result was represented as regression equation in the coded form (Table 2).

Table 2. Regression equations of materials «Polycon K»

Subject of inquiry	Model
PAN	$Y = 1.738 + 0.236X_1 - 0.114X_2 + 0.1887X_3 + 0.338X_1X_2 + 0.286X_1X_3 + 0.036X_2X_3$
oxidized PAN	$Y = 1.86 + 0.086X_1 - 0.121X_2 + 0.1888X_3 - 0.089X_1X_2 + 0.511X_1X_3 + 0.3636X_2X_3$
CF	$Y = 1.889 + 0.311X_1 - 0.161X_2 + 0.638X_3 - 0.339X_1X_2 + 0.111X_1X_3 + 0.038X_2X_3$
NLF	$Y = 3.04 + 0.569X_1 - 0.118X_2 + 0.094X_3 - 0.21X_1X_2 + 0.069X_1X_3 + 0.081X_2X_3$

Results and Discussion

Thus, in the investigated area static exchange capacity for objects «Polycon K» on PAN, oxidized PAN, CF and NLF depends not unequivocally [5]. For materials on PAN and CF the greatest influences has the ratio of fibre and dipping compound in composition structure, and with the increasing of its quantity the value of optimization parameter will grow. Decreasing of optimization parameter is substantially caused by growth of compacting pressure. Duration of hardening time has smaller influence, that is especially typical for a material on NLF though on CF the influence of this parameter is shown more critically not in regular intervals, in comparison with the factor responsible for ratio of fibre and dipping compound.

Influence of double factors on optimization parameter is caused by chemical nature and topological structure of investigated objects and by irregular intervals changing speeds of chemical reactions competing during synthesis. For one-valued interpretation and accounting of influence of these factors further inquiry on the increasing of regression equation at the minimal numbers of experimental points is supposed.

References

1. *M.M.Kardash, Aleksandrov G.V., Kononenko S.G.* Technology principles of preparing Polikon materials based on sulfonated cloths //Fibre Chemistry. 2012. Vol. 43, №5. P.353 – 355.
2. *M.M.Kardash, Tyurin I.A., Terin D.V., Oleinik D.V.* Modification of Polikon K materials by ultradispersed inorganic additives // Fibre Chemistry. 2012. Vol. 44, № 1. P.6-9.
3. *M.M.Kardash, Tyurin I.A., Terin D.V., Oleinik D.V.* Prospects for creating new "Polikon" nanopolymer materials //Fibre Chemistry. 2012. Vol. 44, № 4. P. 242-248
4. *A. Filipov* Mathematical modeling of the membranes processes, Conf. proc. Ion transport in organic and inorganic membranes, Krasnodar, 2012, p.67.
5. *A. Yaroslavtsev* Hibrid membrane materials: properties and perspective of applicaton Conf. proc. Ion transport in organic and inorganic membranes, Krasnodar, 2012, p.250-252.
6. *A. Filipov, S. Dolgopolov, N. Kononenko* Mathematical model of anisotropic nanocomposite membranes for estimation of asymmetry of current-voltage curve parameters, Conf. proc. Ion transport in organic and inorganic membranes, Krasnodar, 2012, p.68-70.
7. *Win Nyi Nyi, V.D.Chalyj* Increase of effective experiments for the construction of complete and incomplete models // Scientific session of Moscow engineering physics Institute - 2008. Collection of scientific works. - 2008. Vol.11, P.162-163.

INVESTIGATIONS OF NANO-POLYMERIC FIBROUS ION-EXCHANGE COMPOSITE MATERIALS ”POLYCON K”

[1,2]Denis Terin, [1]Ivan Tyurin, [1]Marina Kardash
[1]Engels Technological Institute of Saratov State Technical University, Engels, Russia
[2]Saratov State University, Saratov, Russia

Introduction

The perfection of modern ion-exchange materials is an actual scientific problem. One of the ways of perfection development is formation of new materials with a complex of the preset properties manufactured by directive regulation of structure [2, 3]. It is possible to regulate the structure by changing technological parameters of manufacturing, and also by embedding of modifying agents as nanopowders [4, 5]. This type of modification realizes not only thedirected regulation of structure, but also brings to polymericmaterials new properties. New and perspective direction of ion-exchange materials manufacture is the formation of composite chemisorptions fibrous materials (CCFM) ”Polycon K” on the basis of nonwoven fabric by polycondensation filling method. It is known, that manufactured polymeric composites with application of nanostructures, possess with unique properties. Application of nanoparticles is complicated since they are highly active systems with strongly adanced surface. It causes course of spontaneous and frequently rather undesirable processes of sintering. Aim of

this work is the establishment of features of structural characteristics of composite chemisorptions materials ”Policon K” with embed nanocomponents in a polymeric matrix at a stage of synthesis and their influence on ionic selectivity (on operating characteristics).

Experiments

PAN folded character disappears. Areas with spherulitic inclusions could be observed (Fig.1).

We havemanufactured of high-performance, cation-exchange chemosorbtion fibrous materials on basis of phenol, formaldehyde, sulfuric acid, polyacrylonitrile fiber ”Polycon K” - CCFM with a directed controlled structure. CCFM have a high complex of operational properties, by means of implantation of the modifying additive in monomerization structure at a stage of ionite synthesis with which fibrous filler was later impregnated. Synthesis and condensation of ionite matrixes was carried out on surface and in structure of a fibre of the various chemical nature and textile structure.

The given work is the continuation of a complex work on creation of perspective polymeric composite filling compounds of channels deionization electrodialysis complexes.

There is a problem of high electric resistance membranes at electrodialysis of dilute solutions electrolits. Therefore, it is necessary to decrease the resistance of membranes by interchannel fillers implantation. Materials of interchannel fillers should have low electric resistance, should not increase power inputs of electrodialysis process, possess sufficient physicomechanical strength, good hydrophily and save geometrical sizes at swelling.

We have shown, that ultradisperse Fe and Si components implantation results in decreasing of electric resistance of the whole polymeric system and to formation of the additional lacing centers at formation of a polymeric matrix. Iron and silicon nanopowders produced by the method based on the plasma technology had specific surface area SSA -18 and 62 m2/gr. (Specific surface area of producted iron nanopowder was determined with the method of nitrogen thermal desorption).

By results of electronic-microscopic research it has been stated, that ultradisperse powders have the form close to spherical particles and the size does not exceed 50 nm. The element structure of ultradisperse particles has been investigated by EDX method. Application of nanoparticles is difficult as they represent highly active systems with strongly advanced surface. It causes the existence of spontaneous and rather undesirable sintering processes. To delete sintering processes nanoparticles were oxidized additionally. It has allowed to keep their structure, the individual sizes and thereof a uniform distribution of Fe and Si nanoparticles in volume of a composite was obtained. Introduction of ultradisperse particles during synthesis of sulfonic cation matrixes makes essential changes to thermodynamics and kinetics proceeding processes that proves to be true with the data differential-scanning calorimetry (fig. 1).

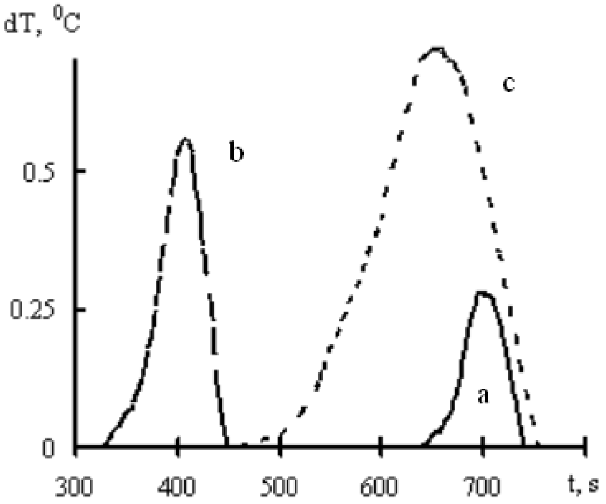

Figure 1. Data of differential-scanning calorimetry CCFM "Polycon K" on polyacrylic fiber with superdispersed additives, %: a-0; b - 1.5 Fe; c-1.5 Si.

The presence of ultradisperse additives increases not only the speed of synthesis, but also the speed of further structurization of a polymeric matrix as it has been shown. The increase in thermal effect of condensation reaction and displacement of thermal peak in lower temperature area was revealed.

Character of influence of nanostructure additives on the formation of ramified three-dimensional lace of polymeric matrix on polyacrylic fiber is submitted on fig. 2. Comparative analysis of surfaces morphology of investigated materials showed, that with implantation of nanopowders of metals the structure of a polymeric matrix becomes more dense and homogeneous. At the same time the quantity of channels in a matrix is not reduced, as they are responsible for delivery of water and tap of products to what high parameters of moisture capacity and exchange capacity testify.

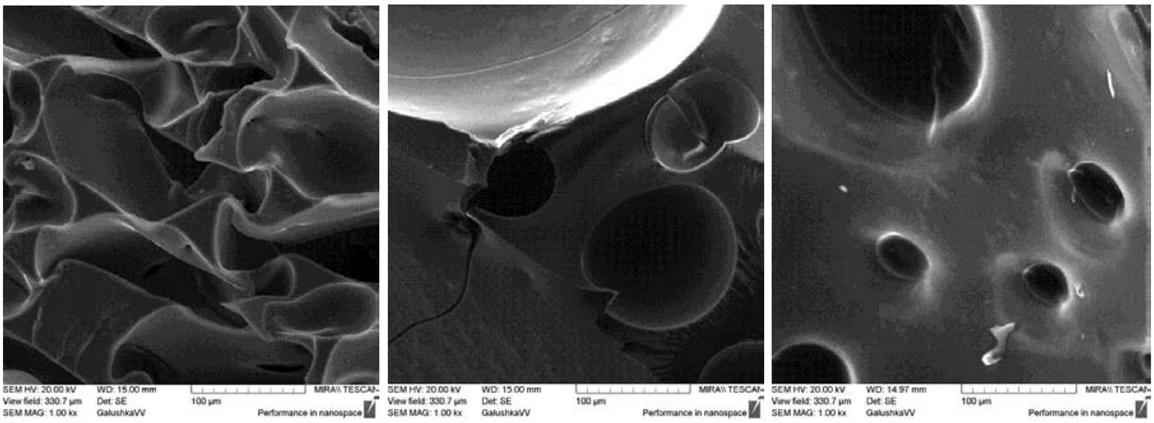

a *b* *c*

Figure 2. SEM images CCFM "Polycon K" on polyacrylic fiber with superdispersed additives, a - 0 ; b - 1.5% Fe; c- 1.5 %Si

We investigated porous material "Polycon K" and have estimated influence nanoparticles on quantity and sizes pores.

Results and Discussion

New and perspective direction of creating composite fibrous ion-exchange material is the method of polycondensation filling, consisting in synthesis of matrix polymer at the presence of organic fibers, allowing to eliminate defects of existing technologies and having by a number of essential advantages.

Basing on a complex research of regularities of the polymeric matrix synthesis processes in presence of fibrous fillers of different chemical nature and the revealed peculiazities of polymers structurization in such systems, the interrelation of CCFM structure and properties is established.

The opportunity of the directed regulation of CCFM structure and properties is shown. The interrelation of textile CCFMstructure, topological features of fibrous surfaces, the chemical nature of fibres with processes of synthesis and structurization ion-exchanger polymeric matrixes, structure and sorption properties is established.

Research of influence of technological parameters of CCFM production on their structural characteristics, hydrophilic hydrophobic, ion selective, ion conductiv and sorption properties is arried out.

Qualitative and quantitative characteristic are kept in all types of investigated reinforcement systems. The method of contact reference porometry was used for out complex research of porous structure, hydrophilic-hydrophobic and sorption properties of membranes ”Polycon” received on polyacrylonitrile, carbon and polyester fibres and their mix compositions at various pressure of pressing.

From porometric curves characteristics of porous structure are calculated. Within the framework of performance of the given project correlation between parameters of porous structure membrane materials and their ionic selectivity has been established. It is shown, that in a row carbon - polyacrylonitrile -polyester fiber one can see an increase in transfer numbers 0.79 for carbon up to 0.92 for polyester, thus observed law of decrease in transfer number with growth of pressure of pressing of a membrane at its manufacturing is kept for all types of the used reinforcement fibers.

The obtained information on structural, ion selective, conductive and sorption properties of CCFM depending on technological conditions of their manufacturing and the nature of fibrous stuff enables the directed regulation of properties of these materials for various special-purpose designation.

References

1. *M.M. Kardash, A.I. Shkabara, N. B. Fedorchenko, V.V. Khaprenko, V.V. Pavlov, I.A. Tyurin* // Fibre Chemistry. 2008. V.40, № 1. P. 66.
2. *M.M. Kardash, A.V. Pavlov, A.I. Shkabara* // Fibre Chemistry. 2007. V.39, № 1. P. 37.
3. *M.M. Kardash, N.B. Fedorchenko, A.V. Pavlov, A.I. Shkabara, M.E. Yasko, O.V. Nikiforova* // Fibre Chemistry. 2007. V.39, № 4. P. 327.
4. *Kardash M.M., Tyurin I.A., Terin D.V., Oleinik D.V.* // Fibre Chemistry. 2012. Vol. 44, № 1. P.6.
5. *Kardash M.M., Tyurin I.A., Terin D.V., Oleinik D.V.* // Fibre Chemistry. 2012. Vol. 44, № 4. P. 242.

PREPARATION AND CONDUCTIVITY OF TUNGSTOVANADOSILICIC HETEROPOLY ACID WITH KEGGIN STRUCTURE AND POLYVINYL ALCOHOL COMPOSITE MEMBRANE

[1]Naiqin Tian, [1]Wen Wu, [1]Xia Tong, [1*]Qingyin Wu, [2]Andrei Yaroslavtsev
[1]Zhejiang University, Hangzhou, PR China, *E-mail: qywu@zju.edu.cn*.
[2]Kurnakov Institute of General and Inorganic Chemistry, Moscow, Russia
E-mail: yaroslav@ igic.ras.ru

Introduction

Heteropoly acids (HPAs) are multifunctional materials because of their intriguing structures and diverse properties. They have a good potential for applications in the fields of catalysis, surface science and materials science. HPAs are superionic conductors at room temperature. The most advantageous feature is their tree-dimentional proton conductivity, chemical and thermal stability. They exist in the crystalline state, and are often processed into a thin film thus avoiding the obvious drawbacks of pellets for application as solid electrolytes. Since the high proton conductivity of HPAs was reported by Nakamura in 1979, some binary and ternary HPAs with Keggin structure have been frequently investigated, and HPA-containing hybrid materials were suggested as promising electrolytes for fuel cells and supercapacitors [1-6].

The proton conductivity of HPAs is based on their strong acidity. There are two types of protons in heteropoly acid crystals: one is the dissociated and hydrated proton that is combined with the HPA anion; the other is the unhydrated proton that is located on the bridge-oxygen in the HPA anion. The high conductivity is determined by the good mobility of dissociated protons, which correlates to the component elements in HPA and their structures.

Vanadium substituted HPAs have more negative charge of the heteropolyanion, and thus the larger number of protons in their structure. These characteristics have important influence on the proton conductivity. Recently, we have synthesized tungstovanadosilicic heteropoly acid $H_5SiW_{11}VO_{40}\cdot 15H_2O$ with Keggin structure ($SiW_{11}V$) by the stepwise acidification and the stepwise addition of element solutions. The HPA exhibits fairly good performance of proton conductivity. In this paper, we incorpotated it into polymer matrix to improve its stability. Polyvinyl alcohol (PVA) have desired characteristics, such as good thermo-stability and film-forming capability, insulating property and low conductivity, chemical resistance and gas barrier properties. Here we reported the preparation and conductivity of PVA composite membrane with 75wt. % $SiW_{11}V$.

Experiments

PVA was dissolved in boiling water, then $H_5SiW_{11}VO_{40}\cdot 15H_2O$ was added to the solution (1:3 weight ratio). The mixture was stirred at 60℃ until homogeneous solution was obtained. The viscous solution was equably spread over the plastic flat and dried at room temperature. The membrane was cut into 4.50 cm length and 1.10 cm width, and the thickness is 43μm.

Results and Discussion

IR spectra confirmed the existence of $SiW_{11}V$ in the composite membrane (Fig. 1). The results indicate the existence of Keggin structure in PVA/$SiW_{11}V$ composite membrane. The proton conductivity of PVA/$SiW_{11}V$ composite membrane calculated from the impedance measurement is 1.37×10^{-3} S.cm^{-1} at 15 ℃ with an activation energy of 14.4 kJ·mol^{-1} for proton conduction. The proton conduction mechanism is Grotthuss mechanism. The conductivity of PVA/$SiW_{11}V$ composite membrane is higher than pure PVA (3.72×10^{-7} S.cm^{-1}), which is the result of the increased proton density and water content in the composite membrane. When the heteropoly acid was incorporated into PVA, the connectivity of the hydrogen-bonding network was strengthened because of the acid doping and increased water retention, which resulted in the decrease of activation energy for proton conduction.

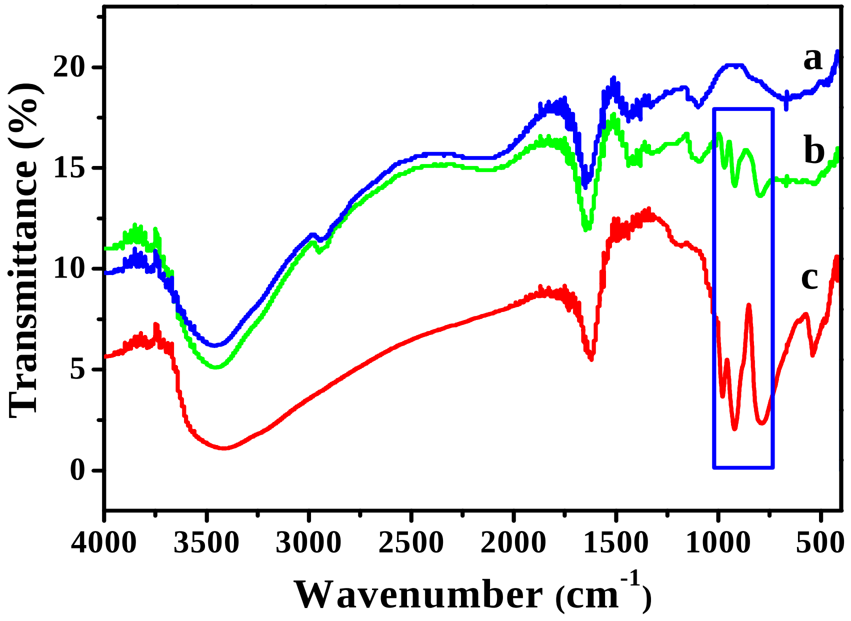

Figure 1. IR spectra of samples: (a) pure PVA film; (b)PVA membrane with 75 wt.% $SiW_{11}V$; (c) pure $SiW_{11}V$

Acknowledgements

This work is financially supported by the National Nature Science Foundation of China (21071124, 21173189) and the Foundation of NSFC-RFBR (21211120160, 12-08-91161).

References

1. *Denisova, T. A.; Leonidov, O. N.; Maksimova, L.G. Zhuravlev, N.* A. // Russ. J. Inorg. Chem. 2001. V. 46. P. 1553-1558.
2. *Sachdeva, S.; Turner, J. A.; Horan, J. L.; Herring, A. M.* // Struct. Bond. 2011. V. 141. P. 115-168.
3. *Tong, X.; Tian, N.Q.; Wu, W.; Zhu, W.M.; Wu Q.Y.; Cao, F.H.; Yan, W.F.; Yaroslavtsev, A. B.* // J. Phys. Chem. C, 2013. V. 117. P. 3258-3263.
4. *Tong, X.; Wu, X.F.; Wu Q.Y.; Zhu, W.M.; Cao, F.H.; Yan, W.F.* // Dalton Trans. 2012. V. 41. P. 9893-9896.
5. *Tong, X.; Wu, W.; Zhou, S.M.; Wu Q.Y.; Cao, F.H.; Yaroslavtsev, A. B.* // Funct. Mater. Lett. 2012. V. 5. P. 1250040 (1-5).
6. *Tong, X.; Tian, N. Q.; Zhu, W. M.; Wu, Q. Y.; Cao, F. H.; Yan, W. F. //* J. Alloys Compd. 2012. V. 544. P. 37-41.

DETERMINATION OF GLYCINE BY PD-SENSORS BASED ON ZIRCONIA-MODIFIED MEMBRANES IN ALKALINE SOLUTION

[1]Tatyana Titova, [1]Olga Bobreshova, [1]Anna Parshina, [2]Ekaterina Safronova
[1]Voronezh state university, Voronezh, Russia, *E-mail: titova_tatyana@mail.ru*
[2]Kurnakov Institute of general and inorganic chemistry RAS, Moscow, Russia

Introduction

Introduction of ZrO_2 into membrane changes its nanostructure and sorption conditions, so analysis of sensitivity to organic and inorganic ions of PD-sensors based on this membrane of great interest to us [1].

Experiments

The following analytes of interest were dissolved in aqueous solutions: glycine (Gly) and KOH. Concentrations of Gly and KOH in test solutions ranged from $1.0\cdot10^{-4}$ to $5\cdot10^{-2}$ M. The pH of the solutions are changed in the range from 10,7 to 14,0. The membranes in K-form were used to identify sensitivity of PD-sensor (sensors, analytical signal of which is the Donnan potential) to anion in alkali solutions. One end of membrane is volume-modified ZrO_2, and the other is unmodified polymer.

Results and Discussion

To estimate sensitivity distribution over the ions on the response of PD-sensors calibration equation was selected taking into account the influence of the sensor's response on three factors: the negative logarithm of concentrations of cations of potassium (pK), pH and the negative logarithm of total concentrations anions and zwitterions of glycine (pGly):

$$\Delta\varphi_D=b_0+b_1\cdot pK+b_2\cdot pH+b_3\cdot pGly \qquad (1)$$

where $\Delta\varphi_D$ is response of PD-sensor (mV), b_0 is free term of calibration equations (mV); b_i is coefficient (mV/pC) of sensitivity of PD-sensor to corresponding ions.

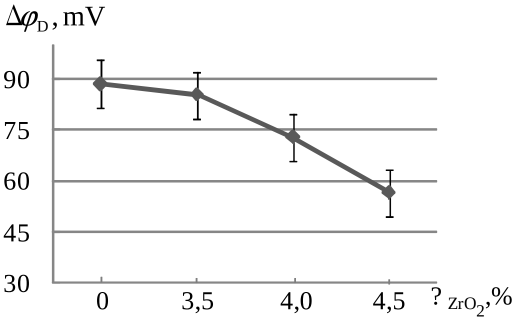

Figure 1. Dependence of the average values of responses PD-sensors on the concentrations of ZrO_2 in the modified end in the range from 10,7 to 14,0

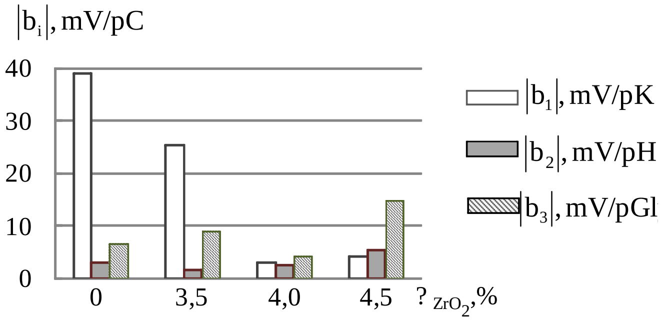

Figure 2. Coefficients of calibration equations PD-sensors, which characterizes the sensitivity of the sensor to the respective components

It was found that with increasing concentration of ZrO_2 in the membranes decreases the sensor response, increases sensitivity PD-sensor to Gly^- and $Gly^\pm$ and decreases sensitivity to K^+ and OH^-. This may be due to a decrease pore space while introducing the dopant and with increase of its concentration. Therefore, the anions Gly^- falling into the membrane with non-exchange-sorbed solution block the pore space and reduce the impact on the sensor response of inorganic ions. The greatest increase in sensitivity of PD sensor to Gly^- and $Gly^\pm$ was obtained for membranes with 4.5 wt.% of ZrO_2 (in 3.7 times greater in comparison with K^+).

This present work was supported by the Russian Foundation for Basic Research (projects №12-08-00743-a, №12-08-31471/ mol_a).

References

1. *Bobreshova O.V., Parshina A.V., Polumestnaya K.A., Safronova E.Yu., Yankina K.Yu., Yaroslavtsev A.B.* // Mendeleev Communications. 2012. Vol. 22. № 2. P. 83.

STUDY OF STABILITY STRONG BASIC ANION EXCHANGE MEMBRANES DURING ELECTRODIALYSIS WITH A DILUTE SOLUTION OF SODIUM CHLORIDE

Stanislav Utin, Ruslan Chermit, Mikhail Sharafan, Victor Zabolotsky
Kuban state university, Krasnodar, Russia, *E-mail: vizab@chem.kubsu.ru*

Introduction

Increased interest of researchers to the anion exchange membranes is not only due to the fact that functional groups of anion exchange membranes are less stable during the electrodialysis than most cation exchange membranes. [1-3]. Also of interest is linked to the possibility of transforming the amine of anion exchange membrane during operation, resulting in a change in the contribution of conjugate concentration polarization effects in the mass transfer of salt ions and water molecules dissociation products. Also known to date in the literature studies show that at high current densities, the rate of dissociation of water at the interface anion exchange membrane / solution is more intense than on the border of the cation exchange membrane / solution [4].

Objects and methods

The objects of study were strongly basic membrane MA-41P (experimental batch of weakly-bonded porous membranes produced by JSC "Shchekinoazot", Russia) and the Ralex AMH produced by Mega, Czech Republic. Research of the electrodialysis process with membranes was conducted in the solution of 0.01 M sodium chloride in a galvanostatic mode at the same flow rate of solution through the chamber (3 l / h). For this reason the electrochemical cell was assembled, membrane package which (Fig. 1) consists of 5 independent flow chambers: 2 investigated camera (1 - camera concentration (CC), 2 - camera desalination (CO)), two buffer chambers (3 and 4) , two electrode chambers (5 and 6). Intermembrane distance was 1 mm, the working area of the membranes - 30 cm^2. To prevent release of chlorine in the electrode chambers and discharge of the solution which is circulated through sodium sulfate.

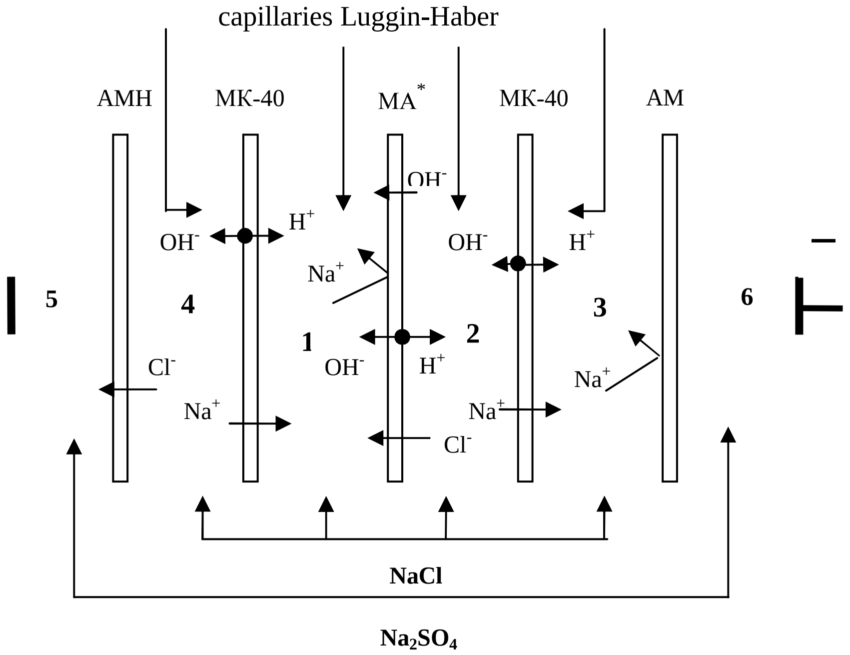

*Figure 1. Diagram of an electrodialysis cell for desalination. * MA - studied anion-exchange membrane*

Results and discussion

To assess the stability of anion exchange membranes were measured their current-voltage characteristics in the electrodialysis dilute solution of sodium chloride before and after working for 3 hours under a current at a current density of 10 mA/cm^2. pH change at the output of the desalination chambers formed by the studied membranes and mass transfer coefficients also were evaluated . The limiting current is on the membranes were measured by shear [5].

Main characteristics of the investigated mass transfer anion exchange membranes in electrodialysis before and after study energized for 3 hours are shown in Table 1.

Table 1. Main characteristics of the investigated mass transfer anion exchange membranes

Anion exchange membrane	Mass transfer characteristics of the membranes in the electrodialysis process of desalting					
	before the electrodialysis process			after the electrodialysis process		
	i_{lim}, mA/cm^2	pH in KK ($i = 2i_{lim}$)	k, dm/h ($i = 2i_{lim}$)	i_{lim}, mA/cm^2	pH in KK ($i = 2i_{lim}$)	k, dm/h ($i = 2i_{lim}$)
MA-41P	3,36	10,7	6,6	4,45	11,6	4
Ralex AMH	4,15	11,2	9,9	3,9	11,7	8,5

The figures show the current-voltage characteristics of the membrane MA-41p of the initial (Fig. 2a, curve 1) and after treatment under the current density of 10 mA cm -2 in the process of electrodialysis (Fig. 2a, curve 2). In the current-voltage characteristic of the used membrane MA-41P observed reduction limiting current plateau length, which indicates a partial transfer of quaternary ammonium base by thermal hydrolysis in the tertiary amino catalyzes the reaction of dissociation of water and allow for more rapid onset overlimiting state. For a membrane-MA-41P maximum density was determined in the electrodialysis demineralization 0.01M sodium chloride: for an initial membrane it was 3.36 mA/cm2 for the membrane that has undergone further processing energized for 3 hours - 4 45 mA/cm2. A similar study was conducted for the membranes Ralex AMH (Fig. 2b). Based on the definition of the limiting current was found that, unlike the membrane MA-41P, the limiting current density on the membrane AMH during electrodialysis demineralization is not changed so significantly - up processing energized it was 4.15 mA/cm2 (Fig. 2b curve 1), after treatment - 3.9 mA/cm2 Fig. 2b, curve 2).

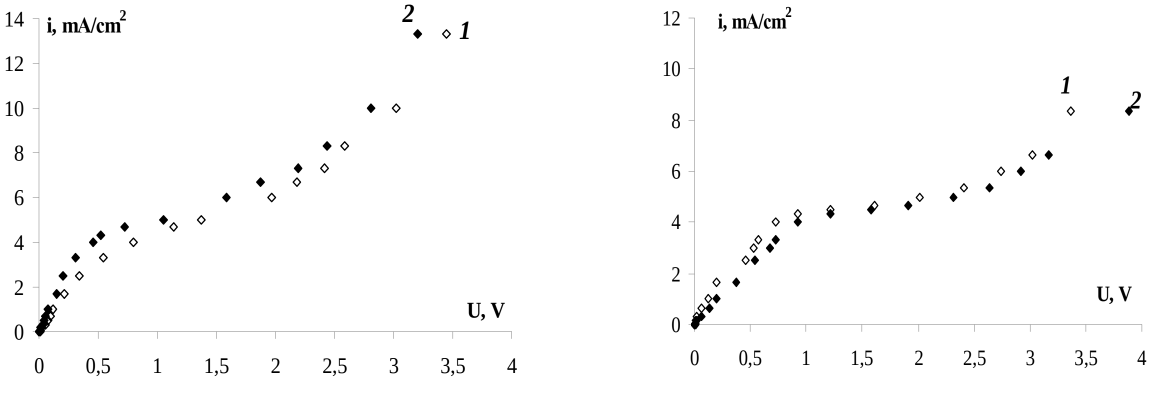

а *б*

Figure 2. The current-voltage characteristics of anion-exchange membranes in electrodialysis desalination of 0.01 M sodium chloride solution: a - the membrane MA-41P, b - the membrane Ralex AMH; 1 - the original membrane, 2 - the membrane after working under the current (i = 10 mA/cm2) for 3 hours

Found that the maximum density in the electrodialysis process of desalination of 0.01M sodium chloride solution for the initial MA-41P membrane was 3.36 mA/cm2 for the membrane that has undergone further processing current for 3 hours - 4.45 mA/cm2. In addition, the current-voltage characteristic in addition used membrane MA-41P a decrease in the length of the plateau of the limiting current, indicating that the partial transition of quaternary ammonium compounds by thermal hydrolysis in the tertiary amine groups which will cause a more rapid onset of overlimiting state. Unlike membrane MA-41P, the limiting current density on the membrane AMH during electrodialysis demineralization changes insignificantly - before treatment energized it was 4.15 mA/cm2 after treatment - 3.9 mA/cm2. Insignificant change the current limit, as well as smaller compared with the membrane MA-41P pH shift confirms the higher chemical stability of the anion exchange membranes Ralex AMH. The higher rate of mass transfer of salt ions to the membrane Ralex AMS compared with the membrane MA-41P, apparently associated with a greater proportion of the conductive surface.

This work was supported by RFBR grant № 12-08-93105-НЦНИЛ_a, grant № 12-08-31277 mol_a and №13-08-01460 A

References

1. *M. A. Min to, G. J. Moody, J. D. R. Thomas,* Lab. Pract., 21, 797, 1972
2. *Yasunori Iwai, Toshihiko Yamanishi*. Thermal stability of ion-exchange Nafion N117CS membranes // Polymer Degradation and Stability. 2009. V. 94 P. 679
3. *Cheng Chen, Thomas F. Fuller*. The effect of humidity on the degradation of Nafion membrane // Polymer Degradation and Stability. 2009. V. 94 P. 1436
4. *Tanaka, Y.* The concentration polarization and dissociation of water in ion-exchange membrane electrodialysis. V. The acceleration of ionic transport on the membrane surface / Y. Tanaka, M. Seno // Denki kagaku. – 1983. – Vol. 51, № 2. – P. 267–277
5. *D.Q. Cowan, I.W.* Brown Effect of turbulence in limiting current in electrodialysis cell //Ind. Eng. Chem. 1959. Vol.51, N 2. P.1445-1449.

STUDY OF PH CORRECTION PROCESS OF BICARBONATE SOFTENED WATER IN LONG CHANNELS OF ELECTRODIALYZERS WITH BIPOLAR MEMBRANES

Stanislav Utin, Victor Zabolotsky, Konstantin Lebedev
Kuban State University, Krasnodar, Russia, E-mail: utinstanislav@mail.ru

Introduction

The theoretical and experimental studies of the reagent-free pH correction of dilute mixed chloride-hydrocarbonate solution by means of electrodialysis with bipolar membranes were reported in [1]. It was shown that this process is complicated by chemical reactions between solution containing components and H^+ and OH^- ions, generating in bipolar membranes. In this paper we experimentally investigate the process of pH correction of bicarbonate softened water in the enlarged electrodialyzer with bipolar membranes and show the practicability of using bipolar electrodialysis technology for alkalization of feed water for boiler.

Experiments

The object of investigation is electrodialyzer with long channels length. The acidic and alkaline chambers of electrodialyzer were formed by bipolar membranes MB-3 and anion-exchange membranes MA-40. The working length of the electrodialyzer was 40 cm, the width 10 cm, and the intermembrane distance 0,8 mm. Electrodialyzer contains a 10 cell pairs. The pH correction process of softened bicarbonate water is investigated at different flow rates (W=5, 10 and 15 l/h) through acidic and alkali chambers of electrodialyzer. The composition of softened water is presented in table 1. The concentrations of all components at the outlet of analyzed chambers determinate according to methods, describing in [1].

Table 1. Components content in softened water

Initial components in softened water	Cl^-	HCO_3^-	H_2CO_3	SO_4^{2-}	Na^+
Concentration, mg/l	55	261	7	80	168

Results and Discussion

As it shown in figure 1 the pH of softened water at the outlet of acidic and alkaline chambers is increase with decrease of flow rate through these chambers. When the initial pH value is 8 it is possible to change a pH value up to 10 at outlet of alkaline chambers and to 6 at outlet in acidic chambers.

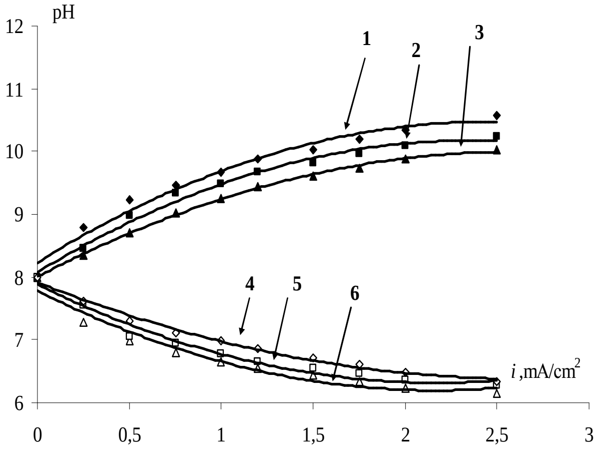

Figure 1. Dependences of pH on average current density: 1,2 and 3 – in alkaline chamber; 4,5 and 6 –in acidic chamber at different flow rates through each chamber: 1 and 4 –5 l/h, 2 and 5 – 10 l/h, 3 and 6 – 15 l/h

In contrast to electrodialysis of sodium chloride solution, where decrease of the ions concentration in alkaline chamber is exactly equal to its increase in acidic chamber, when flow rates through these chambers are identical, in case of bicarbonate softened water such equality is observed only for chloride and sulfate ions not taking part in chemical reactions with products of water molecules dissociation (figure 2).

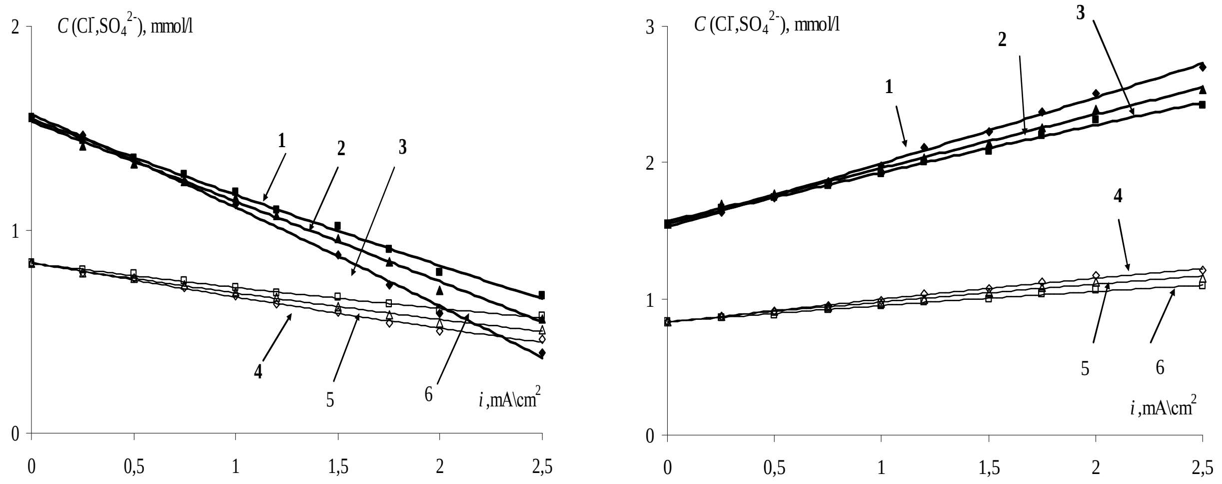

a *b*

Figure 2. Dependences of concentrations on average current density: a – chloride ions (1,2,3) and sulfate ions (4,5,6) in alkaline chamber; b – chloride ions (1,2,3) and sulfate ions (4,5,6) in acidic chamber at different flow rates through each chamber: 1 and 4 – 15 l/h, 2 and 5 – 10 l/h, 3 and 6 – 5 l/h

The experimental dependences of concentrations of carbon acid different forms in acidic and alkaline chambers on average current density (in long channels current density change over the channel length) at different flow rates are presented in figure 3. Asymmetric values diminution of bicarbonate ions concentration in alkaline chamber and it increment in acidic chamber are concerned with chemical reactions of bicarbonate ions with water dissociation products generated in bipolar membranes.

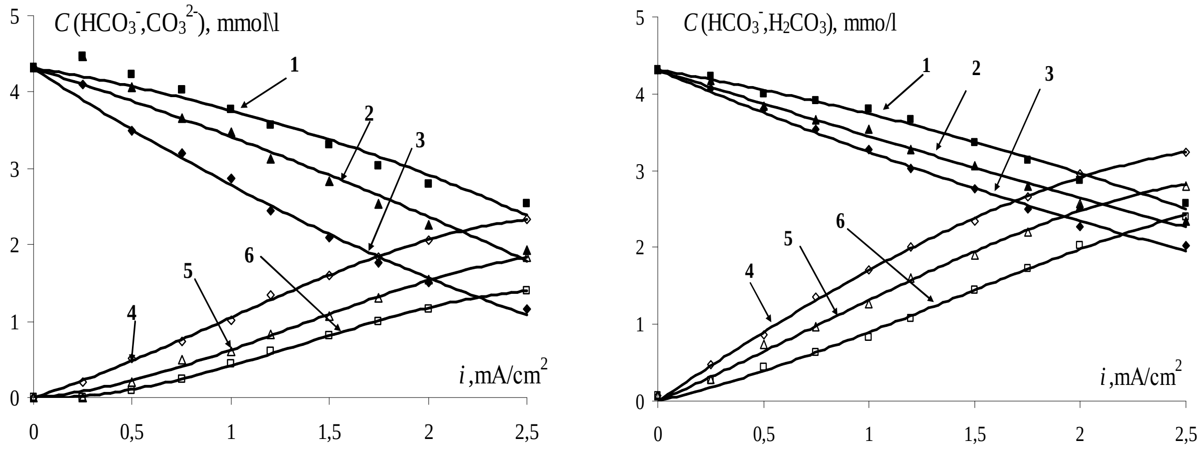

a *b*

Figure 3. Dependences of concentrations on average current density: a – bicarbonate ions (1,2,3) and carbonate ions (4,5,6) in alkaline chamber; b – bicarbonate ions (1,2,3) and carbonic acid (4,5,6) in acidic chamber at different flow rates through each chamber: 1 and 4 – 15 l/h, 2 and 5 – 10 l/h, 3 and 6 – 5 l/h

As example of possibility to use the electrodialysis with bipolar membranes at real industrial conditions for pH correction of water after reverse osmosis the dependence of water pH on continued operation time of electrodialyzer with productivity of 5 m^3/h is presented in figure 4.

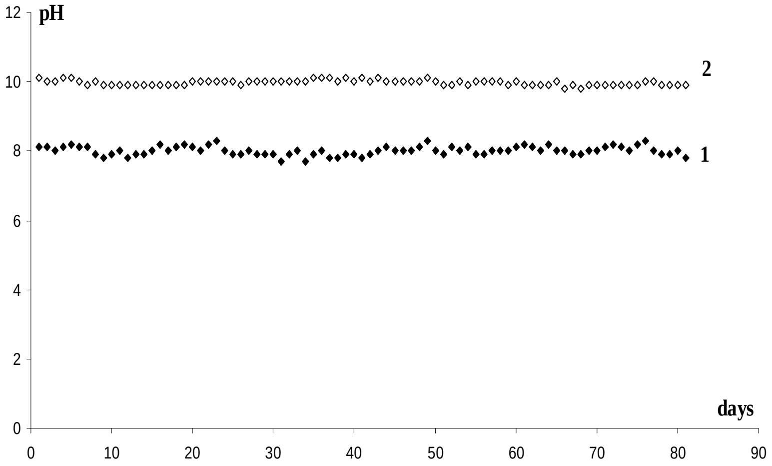

Figure 4. Dependence of treatment water pH on operation time of electrodialyzer with channels length of 70 cm and productivity of 5 m^3/h: 1 – initial pH value, 2 – pH value at the outlet of alkaline chambers of electrodialyzer

This data obtained in real industrial conditions confirm the applicability of electrodialysis with bipolar membranes for achievement the water pH value more then 9 which is necessary for feed to boiler.

This work was supported by RFBR grants: №11-08-00718-a and №12-08-31277_mol_a.

References

1. *Zabolotsky V.I. Utin S.V., Lebedev K.A., Vasilenko P.A., Shel'deshov N.V.* // Russian Journal of Electrochemistry. 2012. V. 48. №7. P. 767.

MATHEMATICAL MODELING OF ELECTROCONVECTION IN MEMBRANE SYSTEMS. CHANGES OF A SPACE CHARGE WITH INCREASING POTENTIAL DROP

[1]Aminat Uzdenova, [2]Anna Kovalenko, [2]Mahamet Urtenov, [2]Victor Nikonenko
[1] Karachaevo-Cherkessky State University named after U.D. Aliev, Karachaevsk, Russia,
E-mail: *uzd_am@mail.ru*
[2] Kuban State University, Krasnodar, Russia, *E-mail*: *urtenovmax@mail.ru*

Introduction

Electroconvection is a phenomenon which is essential in a number of research areas, such as intensification of electromembrane processes, development of micro- and nanofluidic devices, and others. This paper, which is a continuation of our earlier papers [1-3], studies new features of electroconvection in flow-through electrodialysis membrane cells, namely, the changes of the space charge value and the size of the space charge region with increasing potential drop.

Theory

In [1-3], a mathematical model of electroconvection for potentiodynamic mode in membrane systems based on the Nernst-Planck, Poisson and Navier-Stokes equations involving the body electric force have been proposed; the causes and main features have been identified. This model uses only first-principles laws and the most common boundary conditions, there are no adjustable parameters. For this reason, it was called "basic" model [3]. We have shown that the cause of electroconvection is the rotational nature of the electric body force $\vec{f} = \rho\vec{E}$, where ρ is the electric charge density, and $\vec{E}$ is the electric field strength. For the occurrence of an electroconvective vortex, it is necessary that $\left\| curl\, \vec{f} \right\| \geq P_0$, where P_0 is a threshold pressure required to overcome the viscous resistance of the solution. Since $curl\, \vec{E} = 0$, $curl\, \vec{f} = \rho\, curl\, \vec{E} + \nabla\rho \times \vec{E} = \nabla\rho \times \vec{E}$. Hence, the rate of electroconvection is determined by the gradient of space charge density and by the electric field strength. Therefore, it is interesting to follow the rate of the charge density variation in space, that is the value of ρ and the size of the space charge region (SCR) as functions of the applied potential drop.

Results and Discussion

In this paper, we present some results of numerical calculations using the 2D non-stationary “basic” model [1-3] for an electrodialysis flow-through cell. The space charge density is expressed in dimensionless form as $\rho=(c_1 - c_2)/c_0$, where c_1 and c_2 are the concentrations of cations and anions, respectively, c_0 is the inlet electrolyte concentration. We restrict ourselves to the charge density distribution near a cation-exchange membrane (CEM), which forms the cell together with an anion-exchange membrane. The values of $\rho(x)$ are given in a cross-section at the distance y=1900 μm from the channel inlet, for different potential drops over the cell (Fig. 1). A Neumann type boundary condition is used at the CEM: $(\partial c_1 / \partial x)_{x=h}=0$, which signifies that the conditional boundary between the solution and the CEM passes through the point within the SCR where the cation (counterion) concentration attains its minimum value. Thus, we ignore the equilibrium double electric layer at the CEM, but the extended SCR is taken into account. The calculation starts for the case where no potential drop is applied (Fig. 1, curve 0). Since no extended SCR occurs in this case, $\rho(x)=0$ for all x. The case 0.4 V relates to the nearly limiting current density: $c_2(h)$ is not negligible in comparison to $c_1(h)$, hence, $(\partial\rho / \partial x)_{x=h} \neq 0$, while $(\partial c_1 / \partial x)_{x=h}=0$. With increasing potential drop, $c_2(h)$ becomes negligible in comparison to $c_1(h)$, and $\rho \approx c_1/c_0$. At potential drops > 0.4 V, a local maximum of the space charge density arises within the extended SCR as in the case of 1D Rubinstein model [4, 5]. However, the development of electroconvection results in quantitative and qualitative deformation of space charge distribution. At 1.5 and 1.8 V, a local minimum of $\rho(x)$ appears near the external edge of the SCR (Fig. 1). Under these potential drops, oscillations of concentrations, charge density, electric field and velocity occur.

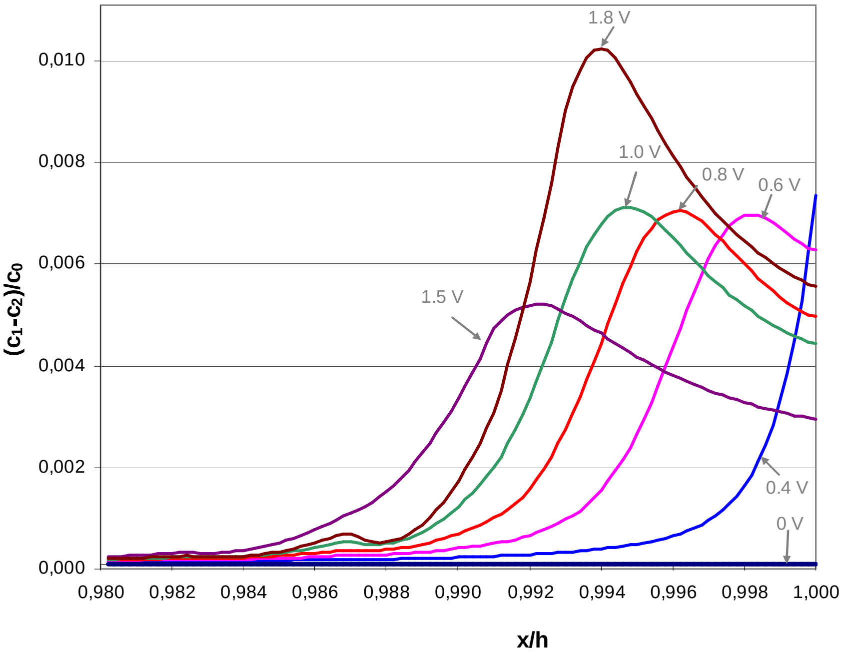

Figure 1. The charge distribution near a CEM in the cross section y=1900 μm at for different values of the potential drop

The local minimum of $\rho(x)$ and 1.5 and 1.8 V is due to an electroconvective vortex, which occurs at the CEM in the region of the cross section y=1900 µm and turns clockwise (Fig. 2).

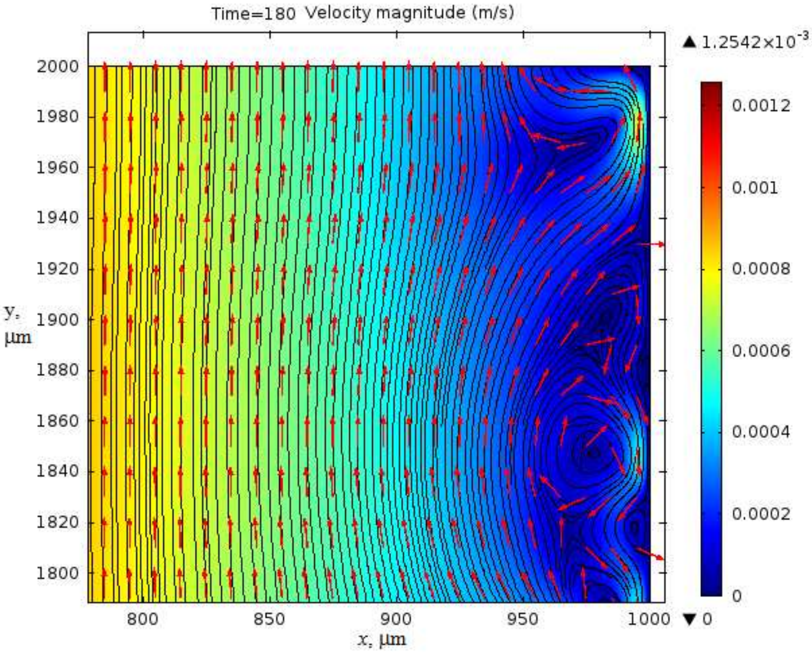

Figure 2. Fluid velocity streamlines at the potential drop 1.8 V

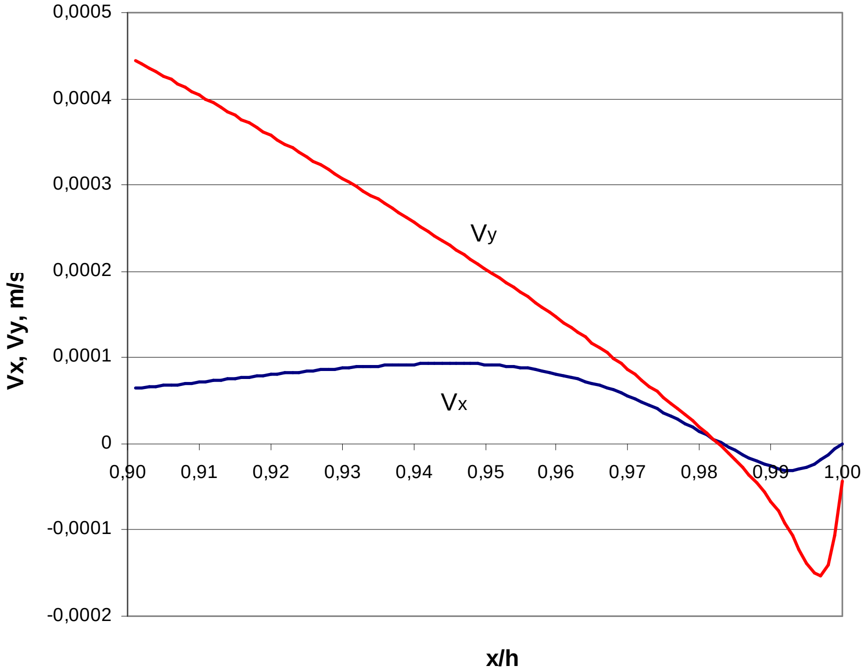

Figure 3. The velocity components distribution in the cross section near the CEM at $y=1900\mu m$ for the potential drop 1.8 V

A fresh portion of electrolyte solution is carried along by this vortex (at about x=970 µm, y=1900 µm). Then this portion of solution makes a half-turn and reappears in the section y=1900 µm in the vicinity of x=990 µm (Figs. 2, 3), just where the local minimum of $\rho(x)$ takes place. Certainly, during the way, the electrolyte concentration within this portion of solution decreases. However, it remains higher than in the neighbor regions with lower velocity, and that is expressed in the appearance of the local minimum of $\rho(x)$.

Thus we see that at small potential drops prior to occurrence of unstable electroconvection, the distribution of $\rho(x)$ is qualitatively similar to that obtained with help of the 1D model. With emergence of electroconvection, the space charge behavior is considerably more complicated.

Acknowledgments

This investigation was realized within French-Russian laboratory "Ion-exchange membranes and related processes". The authors are grateful to CNRS, France, and to RFBR, Russia (grants 11-08-00599-a, 11-08-93107_NCNIL, 12-08-00188-a, 12-08-31535, 13-08-01168, 13-08-00464), as well as to FP7 Marie Curie Actions "CoTraPhen" project PIRSES-GA-2010-269135 for financial support.

References

1. *Uzdenova A.M., Kovalenko A.V., Urtenov M.Kh.* Mathematical models of electroconvection in membrane systems. Karachaevsk, 2011.
2. *Nikonenko V., Kovalenko A., Urtenov M., Uzdenova A., Pismenskaya N., Vasil'eva V.* Theoretical and experimental study of overlimiting mass transfer in electrodialysis // Ion transport in organic and inorganic membranes: Materials Proceedings International Conference. 2012. P. 147-149.
3. *Urtenov M.K., Uzdenova A.M., Kovalenko A.V., Nikonenko V.V., Pismenskaya N.D., Vasil'eva V.I., Sistat P., Pourcelly G.* Basic mathematical model of overlimiting transfer in electrodialysis membrane systems enhanced by electroconvection // J. Membr. Sci. 2013, submitted to publication.
4. *Rubinstein I., Shtilman L.* Voltage against current curves of cation exchange membranes // J. Chem. Soc., Faraday Trans. 75. 1979. P. 231-246.
5. *Urtenov M.Kh.* Boundary value problems for the system of the Nernst-Planck-Poisson. Krasnodar, 1999.

CORRELATION OF THE DIMENSIONS FOR THE REGION OF ELECTROCONVECTIVE INSTABILITY AND I-V CURVE IN THE ELECTROMEMBRANE SYSTEMS WITH ANION-EXCHANGE MEMBRANES

[1]Vera Vasil'eva, [1]Anna Zhiltsova, [1]Mikhail Malykhin [2]Victor Zabolotsky,
[2]Konstantin Lebedev, [2]Ruslan Chermit
[1]Voronezh State University, Voronezh, Russia, *E-mail: viv155@mail.ru*
[2] Kuban State University, Krasnodar, Russia, *E-mail: vizab@chem.kubsu.ru*

Introduction

The aim of the present work was to study influence of ionogenic groups for the membranes with different catalytic activity relative to heterolytic reaction of water dissociation on the dynamics of the progress and dimensions of the region of electroconvective instability under high-intensive current modes by laser interferometry.

Experiments

The objects of investigations were heterogeneous anion-exchange membranes with different catalytic activity relative to heterolytic reaction of water dissociation. Anion-exchange membrane MA-40 modified with bi-functional polyelectrolyte complex involving certain amount of carboxylic groups and aliphatic chains with the tertiary amino-groups [1] were used as a sample membrane with virtually complete suppression of the catalytic activity relative to heterolytic reaction of water dissociation. Membranes of MA-40M10% and MA-40M15% correspond to the samples chemically modified in organic solutions containing 10% and 15% of copolymer, respectively. Strong-base membrane MA-41 is hydrolyzed under high current density due to alkalization and Joule heating at the interphase boundary. In order to enhance the chemical and thermal stability of this membrane its surface was modified with polyelectrolyte complex [2] (membrane MA-41M).

Experiments were performed in the electrochemical cell divided into seven compartments with the use of cation-exchange and anion-exchange membranes. The investigated central compartment consisted of one-type membranes and it was located horizontally. Under horizontal orientation of the electrodialyzer in the gravitation field the current directed in such a way that counter-ions moved up and the depleted diffusion layer was under the investigated membrane (a stable concentration-temperature stratification). The height of membrane channel L was of $4{,}2\cdot10^{-2}$ m, width was of $2{,}4\cdot10^{-2}$ m, intermembrane distance was $h = 2{,}0\cdot10^{-3}$ m. Sodium chloride solutions with the initial concentration of $2{,}0\cdot10^{-2}$ M were supplied with the rate of $1{,}3\cdot10^{-3}$ m/s, that corresponds to laminar flow (Re=2). Electrodialysis was performed in galvanostatic mode.

In order to make direct experiments on visualization of the progress in convective instability inside electrodialyzer cell laser interferometry method was applied with the use of interferometric module of Mach-Zender type. Visualization of the interferometric pattern in solution at the interphase boundaries allows to find localization area and to determine the characteristic size of the region of convective instability. Thickness of convective instability region d was determined as the distance from membrane surface where the interference band and concentration profile, respectively, are of non-stationary, oscillation character.

Results and Discussion

Fig. 1 represents I-V characteristics obtained experimentally as well as the dimensions of convective instability region for the system of anion-exchange membrane MA-41 – 10^{-2}M solution of sodium chloride. A specific feature of I-V characteristics in electromembrane systems is the presence of a secondary uprise of the current (III) that is usually related to the appearance of additional current carriers in the solution, namely H^+ and OH^- ions due to heterolytic reaction of water molecules dissociation and appearance of electroconvective mixing at the interphase boundary.

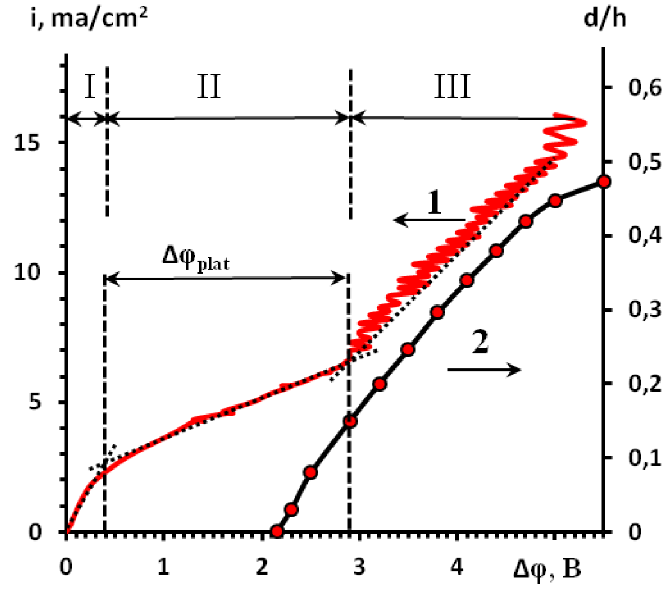

Figure 1. I-V curves (1)and thickness of the region of convective instability (2) in the solution at the boundary with anion-exchange membrane MA-41 under stable stratification of the system in gravitation field: $C_0(NaCl)=2,0\cdot10^{-2}M$, $h=2,0\cdot10^{-3}m$, $V=1,34\cdot10^{-3}m/s$

Experimental results (fig. 2) demonstrate the fact of less developed electroconvective mixing of solution with an increase of catalytic activity of ionogenic groups in ion-exchange membranes relative to the reaction of water dissociation.

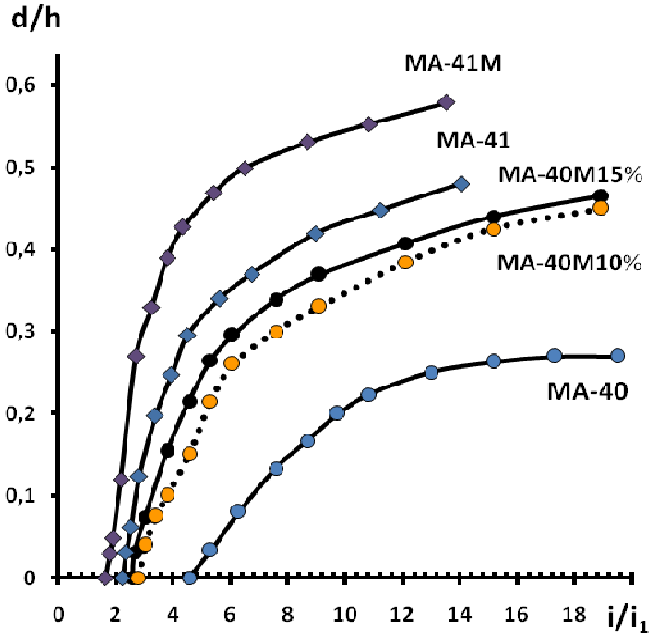

Figure 2. Influence of the nature of ionogenic groups in anion-exchange membranes on the thickness of convective instability region under stable stratification of the system in gravitation field: $C_0(NaCl)=2,0\cdot10^{-2}M$, $h=2,0\cdot10^{-3}m$, $V=1,34\cdot10^{-3}m/s$

Comparison between the sizes of the regions of electroconvective instability made it possible to compose the following sequence: MA-41M>MA-41>MA-40M>MA-40 (1). Minimal dimensions of the convective instability region are characteristic of the weak-base membrane MA-40, where heterolytic reaction of water dissociation proceeds in the most active manner. Decrease of amount of the secondary and ternary amino-groups on the surface of membrane MA-40 due to the PEC modification resulted in almost complete suppression of H^+ and OH^- ions emerging at the interphase boundary that promoted an abrupt progress of electroconvection. As compared to the original membrane MA-40 the current of registration of convective instability for the sample MA-40M is reduced by 2,5 times, while the sizes of convective mixing region increase by 1,5-2 times.

Under the exploitation of strong-base membrane MA-41 for the case of high-intensive current values tertiary amino-groups are known to be transformed into the ternary ones [2] as a result of thermal hydrolysis according to Hoffman reaction, which possess a high catalytic activity relative to the water dissociation reaction. The result of the surface modification of the membrane MA-41 with tetraalkylammonium groups chemically stable to thermal hydrolysis is the maximum size of the region of convective instability and minimal values of the registration current related to its appearance as compared with the investigated samples of anion-exchange membranes.

In our work a negative correlation was revealed between the thickness of the convective instability region and the length of plateau for the limiting current in I-V curves of the investigated anion-exchange membranes. The more was the length of the plateau the less was the size of the region of electroconvective mixing in a solution at the boundary of the membrane (fig. 3). The length of the plateau for the limiting current value that is a measure of electroconvection intensity increased in the sequence (1). Mathematical processing of the obtained dependence with the use of regression analysis made it possible to summarize the derived experimental data and represent them by the straight line with correlation coefficient r = 0,980.

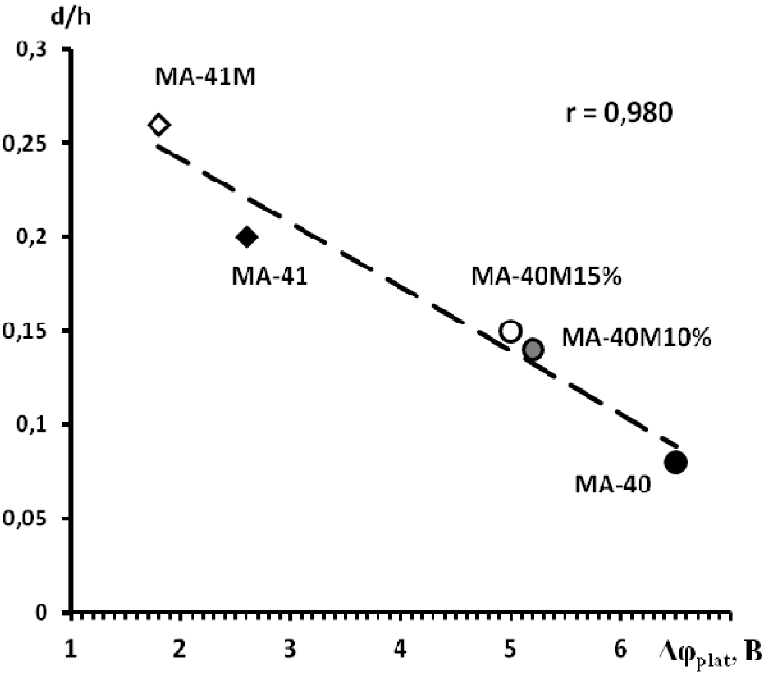

Figure 3. Correlation between a thickness of the convective instability region and the length of I-V curve plateau in the systems with anion-exchange membranes; R is correlation coefficient

The work was performed under financial support of the RFBR grant 12-08-93105-NTsNIL_a.

References

1. *Zabolotskii V.I., Fedotov Yu.A., Nikonenko V.V., Pis'menskaya N.D., Belova E.I., Lopatkova G. Yu.* Patent 2008141949 (Russia). 2008.
2. *Zabolotskii V.I., Bugakov V.V., Sharafan M.V., Chermit R.Kh.* // Russ. J. Electrochem. 2012. V.48. №6. P.650.

IMPACT OF CO_2 LOADING ON EFFICIENCY OF ALKANOLAMINE REGENERATION BY ELECTRODIALYSIS

Vladimir Vasilevsky, Evgeniya Grushevenko, Edouard Novitsky, Vladimir Volkov
Topchiev Institute of Petrochemical Synthesis RAS, Moscow, Russia
E-mail: ednov@ips.ac.ru, vvvolkov@ips.ac.ru

Introduction

Optimization of sorption-desorption stage remains a major problem for the process of CO_2 capture from various gas streams by aqueous solutions of alkanolamines. The disadvantage of operating systems is low level of utilization of alkanolamine solution capacity which is typically 50%. Thus, in case of monoethanolamine (MEA), CO_2 concentration in the rich solution, leaving the absorber, was 8.6% wt. (0.4 mol CO_2/mol MEA), while the concentration in the lean solution, leaving the desorber was 4.3% (0.4 mol CO_2/mol MEA) [1]. Finer cleaning is not performed to avoid heat stable salt (HSS) formation. This work is focused on the research of impact of CO_2 loading on efficiency of MEA and DEA water solutions regeneration by electrodialysis.

Experiments

The research was carried out on kinetics if CO_2 recovery from 30% wt. aqueous solutions of MEA and DEA with loadings 2,2-4% and 3,8-5.7% respectively to simulate the real process. Lab-scale apparatus was used with single membrane package with crossection area 50 cm^2 and 10 static-type concentration chambers. The apparatus worked at current 0.8 A and voltage 25 V. Carbon dioxide concentration in solutions was determined from values of specific volume conductivity (mS/cm) and gravimetrically by nomogram of density change in the solution.

Results and Discussion

Fig. 1 represents the data on CO_2 recovery from solutions which simulate the composition of real absorbent liquid after thermal regeneration. Fig. 2 represents the data on CO_2 recovery from solutions which simulate minimum permissible content of CO_2 assuming the possibility of thermal recovery to a residual content of MEA 2.2% (0.1 mol CO_2/mol MEA) and DEA 3.8% (0.3 mol CO_2/mol DEA).

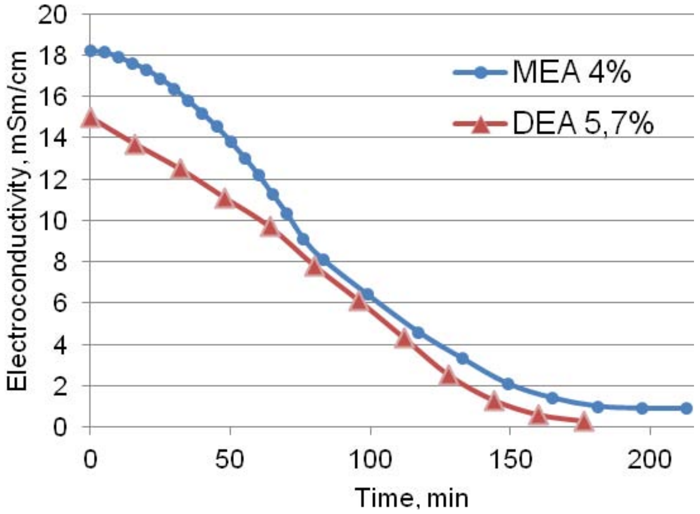

Figure 1. Kinetics of CO_2 ED-recovery from solutions after thermal regeneration

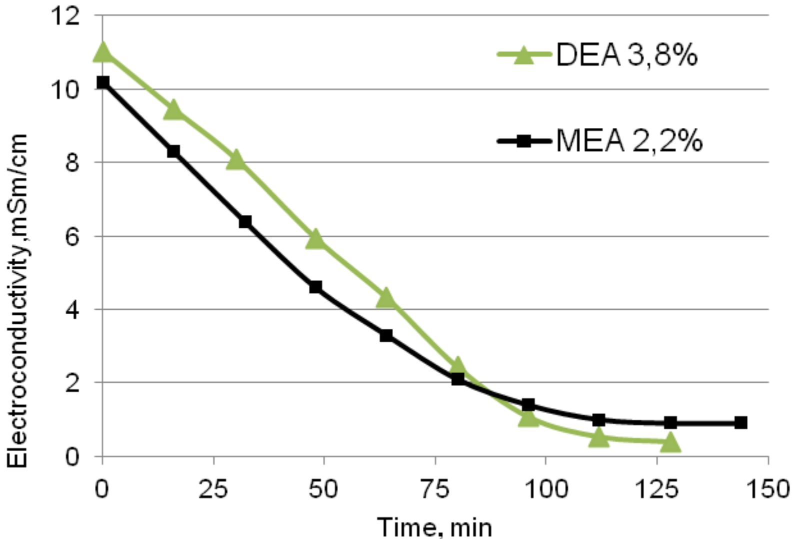

Figure 2. Kinetics of CO_2 ED-recovery from solutions with reduced concentration

From fig. 1 and 2 it is seen that in both cases fine cleaning from CO2 (conductivity of 30% aqueous MEA solution is 0.8 mS/cm and for DEA is 0.3 mS/cm) and obtaining pure amine solutions is possible. However, when implementing processes, presented on fig. 1, significant loss (up to 15-20%) of amines to the concentrate occurs, which is unacceptable. When processing solutions with reduced content of carbon dioxide the amine loss was less than 10%. Considering that the specific energy consumption during such cleaning for MEA was 1.7 kWh/kg and DEA was 1.1 kWh/kg carbon dioxide captured and that selected process is carried out at mild temperature conditions (not more than 40 ℃) such configuration of absorbent regeneration step can be efficient. Another effect of the latter process proposed is that the absorption capacity of amines is realized by almost 100%. It means that after cleaning lean solution of amine will have only insignificant traces of CO2.

The authors gratefully acknowledge the support RFBR grant #13-08-00767.

References

1. *L. Dumée, C. Scholes, G. Stevens, S. Kentish,* // International Journal of Greenhouse Gas Control, 10 (2012) 443–455

CAPSULE WITH A FRACTAL CORE IN A VISCOUS LIQUID

[1]Sergey Vasin, [2]Tatiana Kharitonova, [3]Tamara Philippova
[1]Gubkin Russian State University of Oil and Gas, Moscow, Russia,
E-mails: s.vasin@rambler.ru, a.filippov@mtu-net.ru
[2]Frumkin Institute of Physical Chemistry and Electrochemistry RAS, Moscow, Russia
[3]Moscow State University of Food Production, Moscow, Russia

The formation of microcapsules and the study of their physicochemical characteristics have become an important field of modern colloid chemistry [1]. Capsules are used for synthesis of particles and delivery of drug media, as containers for anticorrosive reagents, etc.

The hydrodynamic behavior of capsules is of great practical significance. Moreover, they have begun to play an important role of working elements in microfluidics [2]. Attempts are made to use them to govern hydrodynamic flows, study the boundary conditions at liquid–solid interfaces, and regulate motion of droplets.

In this work we shall consider the problem of a hydrodynamic flow around a porous capsule containing a fractal aggregate inside it. The main attention will be focused on the distribution of hydrodynamic flows in the capsule and a viscous force applied to it.

Let us consider a viscous liquid flow around a capsule of radius $\tilde{b}$, that represents a uniform porous shell enveloping a fractal aggregate of radius $\tilde{a}$, with a monolithic primary particle of radius occurring in the aggregate center (Fig. 1).

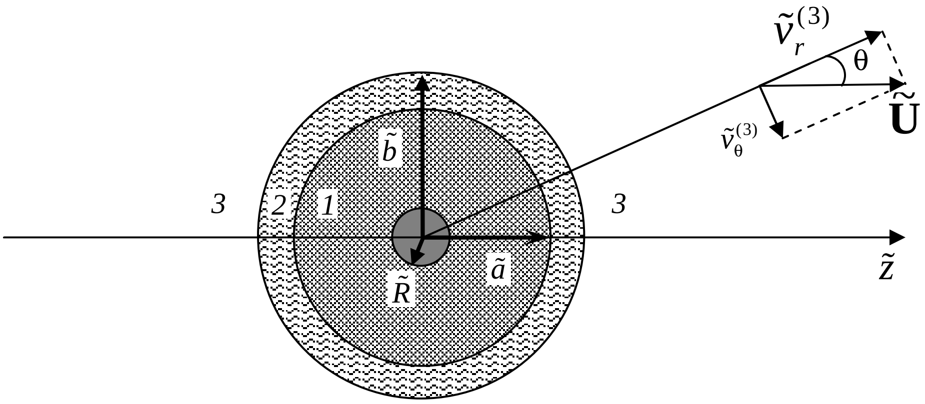

Figure 1. Schematic representation of a capsule containing a fractal core and flowed around by a viscous flow

At small Reynolds numbers, the motion of the liquid outside the capsule $\left(\tilde{b} < \tilde{r} < \infty\right)$ will be described by the Stokes and continuity equations as follows:

$$\begin{cases} \tilde{\nabla}\tilde{p}^{(3)} = \tilde{\mu}^{(3)}\tilde{\Delta}\tilde{\mathbf{v}}^{(3)}, \\ \tilde{\nabla}\cdot\tilde{\mathbf{v}}^{(3)} = 0. \end{cases} \tag{1}$$

The motion in the porous layer $\left(\tilde{a} < \tilde{r} < \tilde{b}\right)$ and in the medium with a fractal structure $\left(\tilde{R} < \tilde{r} < \tilde{a}\right)$ will be determined by the Brinkman and continuity equations [3] presented below:

$$\begin{cases} \tilde{\nabla}\tilde{p}^{(i)} = \tilde{\mu}^{(i)}\tilde{\Delta}\tilde{\mathbf{v}}^{(i)} - \tilde{k}^{(i)}\tilde{\mathbf{v}}^{(i)}, \\ \tilde{\nabla}\cdot\tilde{\mathbf{v}}^{(i)} = 0. \end{cases} \quad (i = 1, 2) \tag{2}$$

In Eqs. (1) and (2) and below, the tilde refers to dimensional values; the superscript (i) denotes the number of a region to which a value is relevant; $\tilde{\mu}^{(i)}$ refers to the viscosity coefficients of the liquid and the Brinkman medium, which are assumed to be different; $\tilde{p}^{(i)}$ refers to pressures; $\tilde{\mathbf{v}}^{(i)}$ refers to velocity vectors; and $\tilde{k}^{(i)}$ is the Brinkman parameter, which is inversely proportional to the specific permeability of the porous layer.

The external porous layer (region 2) is assumed to be uniform, and Brinkman parameter $\tilde{k}^{(2)}$, which characterizes the drag to the flow, is assumed to be constant.

The density of the fractal aggregate (region 1) with dimensionality D ($2 \le D \le 3$) is determined by the following relation [4, 5]:

$$\tilde{\rho}(\tilde{r}) = const\left(\frac{\tilde{R}}{\tilde{r}}\right)^{3-D}. \tag{3}$$

Brinkman parameter $\tilde{k}^{(1)}$ characterizing the drag of the fractal aggregate will be considered to be proportional to local density $\tilde{\rho}(\tilde{r})$

$$\tilde{k}^{(1)} = \tilde{k}_0\left(\frac{\tilde{R}}{\tilde{r}}\right)^{3-D}, \tag{4}$$

where $\tilde{k}_0$ is the value of the Brinkman parameter on the surface of the solid core ($\tilde{r} = \tilde{R}$).

In order to formulate the boundary problem for Eqs. (1) and (2), it is necessary to specify the boundary conditions. At infinity from the capsule, we specify a uniform flow as follows:

$$\tilde{\mathbf{v}}^{(3)} \to \tilde{\mathbf{U}}, \tilde{r} \to \infty \tag{5}$$

At the external liquid–porous layer interface ($\tilde{r} = \tilde{b}$), the continuity conditions of velocity, normal stresses $\tilde{\sigma}_{rr}$, and tangential stress jump $\tilde{\sigma}_{r\theta}$ are specified in the following form [6, 7]:

$$\begin{gathered} \tilde{\mathbf{v}}^{(3)} = \tilde{\mathbf{v}}^{(2)}, \\ \tilde{\sigma}^{(3)}_{rr} = \tilde{\sigma}^{(2)}_{rr}, \qquad \text{at } \tilde{r} = \tilde{b}. \\ \tilde{\sigma}^{(3)}_{r\theta} - \tilde{\sigma}^{(2)}_{r\theta} = \beta v^{(3)}_{\theta}\sqrt{\tilde{k}^{(2)}\mu^{(3)}}, \end{gathered} \tag{6}$$

where β is a parameter that characterizes the jump in the tangential stress and varies in the range of 0 to 1.

At the fractal–porous layer interface ($\tilde{r} = \tilde{a}$), the continuity conditions of velocity and tangential $\tilde{\sigma}_{r\theta}$ and normal $\tilde{\sigma}_{rr}$ stresses are preset as follows:

$$\begin{gathered} \tilde{\mathbf{v}}^{(1)} = \tilde{\mathbf{v}}^{(2)}, \\ \tilde{\sigma}^{(1)}_{rr} = \tilde{\sigma}^{(2)}_{rr}, \quad \text{at } \tilde{r} = \tilde{a}. \\ \tilde{\sigma}^{(1)}_{r\theta} = \tilde{\sigma}^{(2)}_{r\theta}. \end{gathered} \tag{7}$$

The following sticking condition is imposed on the surface of the central particle ($\tilde{r} = \tilde{R}$)

$$\tilde{\mathbf{v}}^{(1)} = 0. \tag{8}$$

The system of equations (1, 2) with boundary conditions (5) – (8) was solved analytically. Velocity and pressure distributions were determined.

An important characteristic of the problem under consideration is force $\tilde{F}$ applied to the capsule by the external liquid:

$$\tilde{F} = \oiint\limits_{S} \left(\tilde{\sigma}^{(3)}_{rr}\cos\theta - \tilde{\sigma}^{(3)}_{r\theta}\sin\theta\right)ds = -4\pi\, b_2\, \tilde{a}\, \tilde{\mu}^{(3)}\, \tilde{U}, \tag{6}$$

where the integration is carried out over the surface of the porous layer.

Dimensionless force Ω is determined by the ratio of force $\tilde{F}$ to the Stokes force $\tilde{F}_{\mathrm{st}} = 6\pi\,\tilde{a}\,\tilde{\mu}\tilde{U}$. Force $\Omega\left(R, b, m_1, m_2, \sigma, s_{20}, D, \beta\right)$ is a function of eight arguments. Parameter $R = \tilde{R}/\tilde{a}$ is the radius of primary particles; $b = \tilde{b}/\tilde{a}$ is the capsule radius; $m_1 = \tilde{\mu}^{(1)}/\tilde{\mu}^{(3)}$ and $m_2 = \tilde{\mu}^{(2)}/\tilde{\mu}^{(3)}$ are the viscosity ratios; $\sigma = \tilde{a}/\sqrt{\tilde{\mu}^{(3)}/\tilde{k}_0}$ and $s_{20} = \tilde{a}/\sqrt{\tilde{\mu}^{(3)}/\tilde{k}^{(2)}}$ are the dimensionless Brinkman coefficients characterizing the drags of the fractal aggregate and uniform porous layer, respectively; D is the fractal dimension; and parameter β is the characteristic the tangential stress jump at the liquid–porous medium interface.

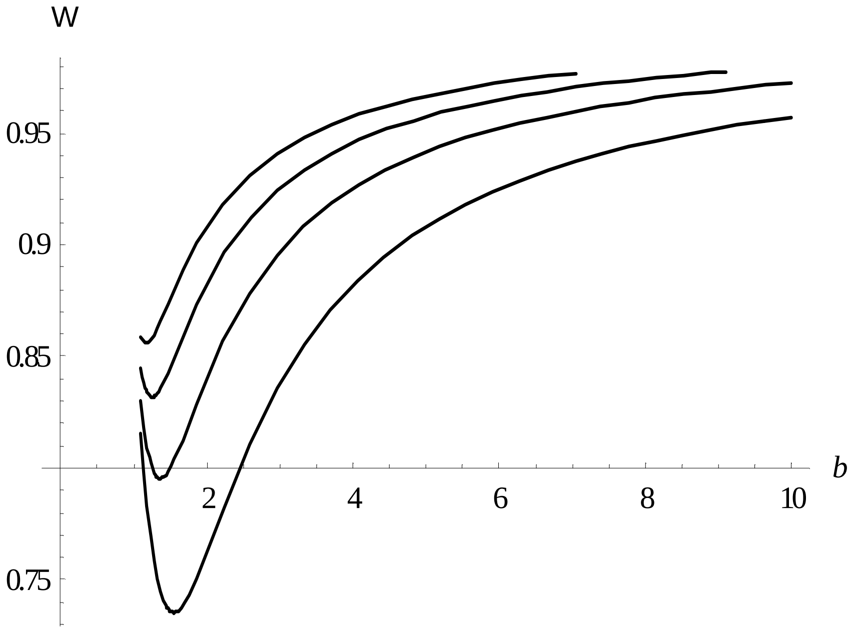

Figure 2. Dependences of dimensionless force Ω on dimensionless radius b of the capsule at R = 0.3, m_1 = 1, m_2= 1.2, σ = 10, β = 0.2, D = 2.7, and s_{20} = 2, 3, 4, and 5, parameter s_{20} increases from bottom to top

Figure 2 exhibits the dependences of dimensionless force Ω on dimensionless capsule radius *b* at different values of parameter s_{20}, which characterizes the drag of the external porous shell. The dependences have an extremal character that is explained as follows. The value of Ω is the ratio of a force applied to a capsule with radius *b* to the Stokes force applied to a solid particle of radius b. Dimensionless Brinkman radius $1/s_{20}$ determines the depth to which the flow penetrates into the porous shell. Therefore, due to liquid filtration, dimensionless force Ω decreases with a change in the porous layer thickness ($\delta = b - 1$) from 0 to $1/s_{20}$ (Fig. 2). As the thickness of the external porous layer further grows, the depth of the flow penetration into the capsule remains constant and the hydrodynamic force increases.

This work was supported by the Russian Foundation for Basic Research, project no. 11-08-00807_a.

References

1. *Bedard, M.F., De Geest, B.G., Skirtach, A.G., Mohwald, H., and Sukhorukov, G.B.* // Adv. Colloid Interface Sci., 2010, vol. 158, p. 2.
2. *Tabeling, P.* // Phys. Fluids, 2010, vol. 22, p. 021302.
3. *Brinkman, H.* // Appl. Sci. Res. A, 1947, vol. 1, p. 27.
4. *Roldughin, V.I.* // Usp. Khim., 2003, vol. 72, p. 931.
5. *Roldughin, V.I.*, Fizikokhimiya poverkhnosti (Surface Physical Chemistry), Dolgoprudnyi: Izd. Dom “Intellekt”, 2008.
6. *Ochoa-Tapia J.A., and Whitaker, S.* // Int. J. Heat Mass Transfer. 1995. V. 38. P. 2635.
7. *Ochoa-Tapia J.A., and Whitaker, S.* // Int. J. Heat Mass Transfer. 1995. V. 38. P. 2647.

CAPACITIVE DEIONISATION OF WATER SOLUTION AND SURFACE CONDUCTIVITY OF POROUS ELECTRODES

Yurii Volfkovich, Daniil Bograchev, Alexey Mikhalin, Alexey Rychagov
Frumkin Institute of Physical Chemistry and Electrochemistry of RAS, Moscow, Russia,
E-mail: yuvolf40@mail.ru

Introduction

Capacitive deionization technology (CDT) is an effective new method of desalinating of brackish water [1,2]. In CDT, a brackish water stream flows between pairs of high surface area carbon electrodes that are held at a potential difference $\supseteq$ 1.0 V. The ions and other charged particles are attracted to and held on the electrode of opposite charge. The negative electrode adsorbs cations, while the positive electrode adsorbs anions. Eventually the electrodes become saturated with ions and must be regenerated. The applied voltage is removed, and since takes place desorption of ions from electrodes and from the system, producing a more concentrated brine stream. In practice, for a gallon of water fed to the a CDT process, more than 80% emerges as fresh, deionized potable water, and the remainder is discharged as a concentrated brine solution containing virtually all of the salts in the feed. The main advantage of CDT is its low operating cost, which is about one third that of the main competitor, reverse osmosis. This is important because operating costs dominate the cost of desalination. Mechanism of the CDT operation is founded on charge - a discharge of electric double layer (EDL), as well as in electric double layer supercapacitor.

The purpose of this work was scientific research, development and verification of mathematic model of water capacitive deionization (CDI) process and also CDI regime optimization. Up present it is absent the adequate mathematical model of the process of CDI. On the other hand, they exist the models of electrochemical supercapacitors, in porous carbon electrodes which also take place the processes of ion elctrosorption and electrodesorption ion Processes of the ion transport along thickness of porous electrodes and separator are taken into account in these model as well as a process of charge – discharge of a EDL. However in these models also is not taken into account a hydrodynamic flow of water along external electrode surface. In CDI method the water flow is directed along of external of the surfaces of the electrodes, and so it is necessary to solve the two-dimensional problem: distribution of the processes both along, and across external of the surfaces of the electrodes and a porous spacer.

Mathematical model

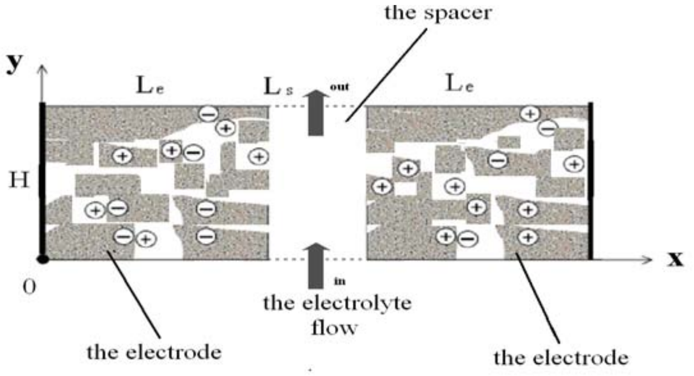

Figure 1. Scheme of the functioning the dynamic cell

As a result of our studies we have made a conclusion that process deionization of solution is very complex. In models we have taken into account following processes: charge- discharge of electric double layer (EDL); transport ion processes along of electrode and spacer thickness (x – direction) are diffusion and migration; transport ion process along of electrode external surface (y-direction) : hydrodynamic flux; specific adsorption; characteristics of porous structures; characteristics of hydrophilic – hydrophobic properties; convective flux of electrolyte; surface conductivity. The ion surface conductivity in EDL of carbon electrodes is longitudal conductivity of EDL in high dispersed material. Our model has been based on the following assumptions: 1) The convective diffusion of electrolyte can be described by the average equations of mass-transfer based on dilute-solution theory in porous media. 2) The hydrodynamic velocity is precalculated, i.e. it can be treated as a given value.3) The effective diffusion coefficients and effective electrolyte conductivities are calculated by the Arch's law. 4) The electrolyte can be presented as binary one with effective concentration in gram/mol dimension. 5) The full conductivity is sum of electrolyte conductivity as linear function of concentration and surface conductivity.6) The diffusion can be neglected in all directions except x-direction along of electrode thickness . 7) The capacity of electrode is accepted as constant, i.e. it does not depend on potential. 8) In the equation of the potential, the derivative of potential in y directions can be neglected. 9) The porous electrode can be treated as having uniform potential; it means that the Ohm losses of the electrons can be neglected.

The equations for potential and concentration can be presented in the electrode region as follows:

$$C_S\frac{\partial \Phi-\Phi_C}{\partial t}=\frac{\partial}{\partial x}\left(k_E\frac{\partial\Phi}{\partial x}\right)+\frac{\partial}{\partial x}\left(k_E(t_+-t_-)\frac{RT}{F}\frac{\partial\log c}{\partial x}\right) \qquad (1)$$

$$\varepsilon_E\frac{\partial c}{\partial t}+v_y\frac{\partial c}{\partial y}=D_E\frac{\partial^2 c}{\partial x^2}-\frac{C_S}{F}A_E\frac{\partial\Phi-\Phi_C}{\partial t}-k_A c \qquad (2)$$

where C_S - specific capacity, Φ_C - potential of electrode, Φ - potential of electrolyte, t_+ and t_- are the cation and anion transfer numbers , ε_E -porosity in the electrodes, $k_E = k_{E\lambda}c + k_{surf}$ - electrolyte conductivity in the electrodes, $k_{E\lambda}$ - equivalent electrolyte conductivity in pores, k_{surf} - surface conductivity of electrode, $D_E = D\varepsilon_E^{\,n}$ -effective diffusion coefficient in electrodes, (the exponent n is defined by property of porous media) k_A - specific adsorption coefficient, $A_E=(t_+\frac{dq_+}{dq}+t_-\frac{dq_-}{dq})\approx\pm\frac{1}{2}$ -electric adsorption coefficient , v - vector of hydrodynamic velocity.

And the equations in the spacer region can be written:

$$\frac{\partial}{\partial x}\left(k_S\frac{\partial\Phi}{\partial x}\right)+\frac{\partial}{\partial x}\left(k_S(\frac{t_+-t_-}{f})\frac{\partial\log c}{\partial x}\right)=0 \qquad (3)$$

$$\varepsilon_S\frac{\partial c}{\partial t}+(v_x\frac{\partial c}{\partial x}+v_y\frac{\partial c}{\partial y})=D_S\frac{\partial^2 c}{\partial x^2} \qquad (4)$$

where ε_S - spacer porosity , $k_S = k_{S\lambda}c$ - electrolyte conductivity in the spacer, $k_{E\lambda}$ - reference electrolyte conductivity in spacer, $D_S = D\varepsilon_S^{\,n}$ -effective diffusion coefficient in spacer. Porosimetric characteristics of electrodes and spacer were measured by the method of standard contact porosimetry [3].

Surface conductivity

We at first have developed the method for measurement of surface conductivity for porous electrodes at controlled potentials. We have developed the two chamber five electrode electrochemical cell for this method (Fig. 2). Fig. 3 shows dependence conductivity on KCl concentration for carbon cloth electrode CH900 (made in Japan). This figures illustrates extrapolation obtaining of surface conductivity value. Extrapolation value of surface conductivity for solution concentration equal zero (C= 0) is defined by value of exchange capacity of its surface groups for a porous carbon electrode (Fig. 3).

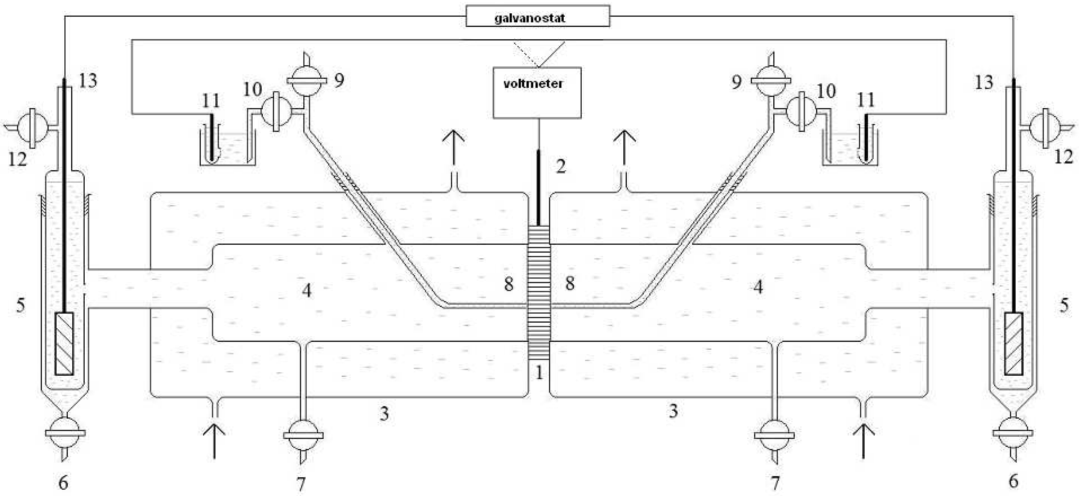

Figure 2. Electrochemical cell for measurement of surface conductivity. 1 – test electrode (carbon cloth), 2 – platinum current collector, 3- the chambers for a termostating, 5 –two counter electrodes, 8- two Luggin capillaries of reference electrodes 11 – two reference electrodes

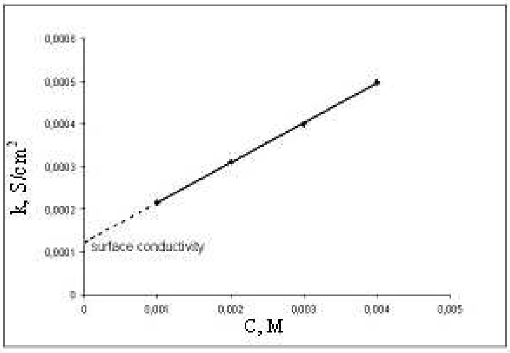

Figure 3. Dependence conductivity on KCl concentration for carbon cloth CH-900

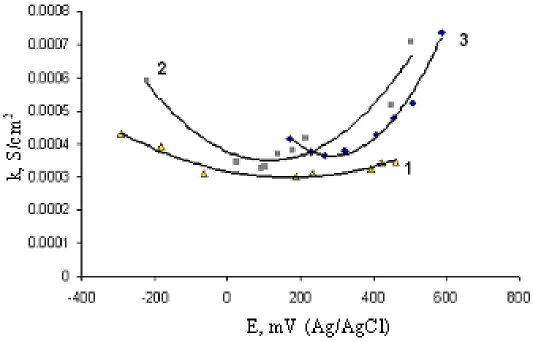

Figure 4. Dependences of surface conductivity of carbon cloth electrode conductivity on potential for different KCl concentrations:1- 0.002 M, 2- 0.003 M, 3- 0.004 M

According to measurements the values of exchange capacity for carbon electrodes CH900 and SAIT (Korea) equals 1.14 and 0.37 mg-equiv/g accordingly. The values of surface conductivities are 1.25x10^{-4} and 0.4x10^{-4} S/cm^2 accordingly. Thus surface conductivity at C= 0 is proportional to exchange capacity. This is surface conductivity caused by surface groups ($k_{surf\ group}$). Fig 4 shows the measured dependences of surface conductivity of carbon cloth on potential for different KCl concentrations. In our opinion minima on these curves correspond to potentials of a zero charge. Total surface conductivity k_{surf} is sum of $k_{surf\ group}$ and longitudal conductivity of usual electrostatic EDL ($k_{electrostatic}$). Thus method of measurement of surface conductivity is a new method for studying of a electrode double electric layer for porous electrodes.

The measured values of surface conductivity were used for calculations with the above described model. Fig. 5 demonstrates calculated fluxes concentration in the outlet of the cell vs. time for adsorption and desorption stages for different voltages, and Fig. 6 demonstrates corresponding concentration field.

Verification of the model

We have carried out the capacitive deionization measurements by using the Samsung Electronics Co. (Korea) installation (see Fig. 7). This installation contains: an electrochemical cell, the pump for water pumping, conductometer, pH – meter, and the computer with the display. As electrodes in the cell were used activated carbon clothes CH900 with sizes 100x100x0.5 mm and with specific surface area 1500 m^2/g.

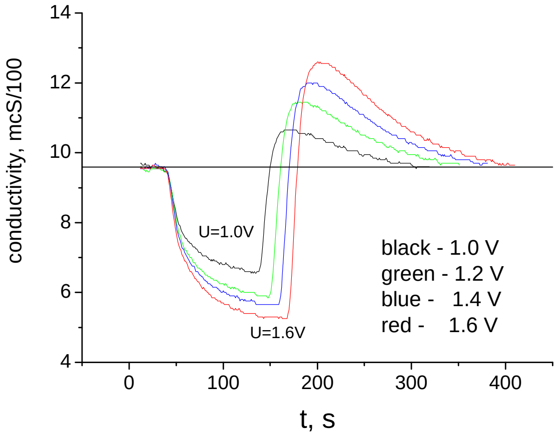

Figure 5. The dimensionless flux concentration in the outlet of the cell vs. time (20ml/min) for adsorption and desorption stages for different voltages and for carbon electrodes SAIT type

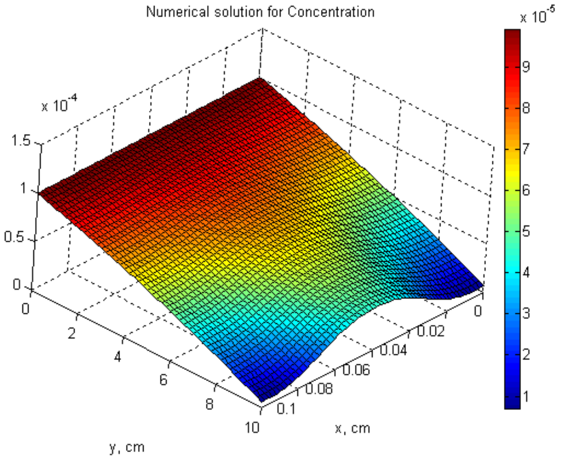

Figure 6. Concentration field; v=0.1 cm/s, t=99s

Figure 7. Installation for capacitive deionization made by Samsung Electronics Co

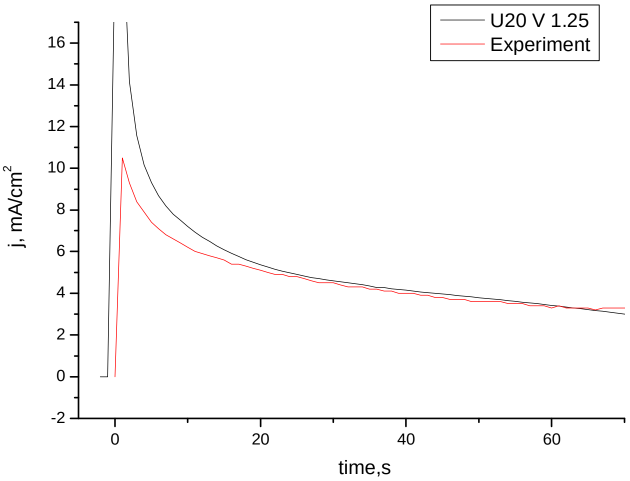

Figure 8. Experimental and modeling time-current dependences at flow rate 20ml/min and voltage 1.25V

The Fig.8 shows the satisfactory consent between calculated and experimental curves. Some differences model curve from experimental one for very small times are explained that we could not take into account the contact resistance between electrodes and current collectors. The satisfactory consent between calculated and experimental curves confirms a correctness of the developed mathematical model. Using model, we have calculated optimal regimes of adsorption and desorption stages for the minimization of energy consumption demanded for receiving of pure water.

References

1. *M.A. Anderson, A.L. Cudero* // J. Palma. Electrochimica Acta, 55 (2010) 3845.
2. *Y. Oren* // Desalination, 228 (2008) 10.
3. *Yu.M.Volfkovich, V.S.Bagotzky*. // J. Power Sources, 48 (1994) 327, 339.

AFM STUDY OF CONDUCTING POLYMER FILMS NEAR ELECTRODE'S EDGE OR GROWN ON MICROBAND ELECTRODE

[1,2,3]Mikhail Vorotyntsev, [3]Dmitry Konev, [4]Ulrich Lang, [5]Yuriy Tolmachev, [6]Magdalena Skompska

[1] ICMUB-UMR 6302 CNRS, Universite de Bourgogne, Dijon, France
[2]Lomonosov Moscow State University, Moscow, Russia; *E-mail: mivo2010@yandex.com*
[3] Institute for Problems of Chemical Physics of RAS, Chernogolovka, Russia
[4] University of Regensburg, Institute of Analytical Chemistry, Regensburg, Germany
[5] Ftorion, Inc., Boston, USA
[6] Faculty of Chemistry, University of Warsaw, Warsaw, Poland

Electric conductivity represents one of the principal characteristics of various materials. For powders or films on an insulating background the conductance may be measured by the conventional 4-probe technique where the material under study is placed as a layer between two insulating surfaces, with 4 point electrodes in electric contact with the layer (two of them used to pass electric current along the layer while two others measure the induced potential difference). The subsequent calculation of the specific conductivity is possible if the layer thickness is known.

The situation is more complicated for thin films on a conducting substrate, in particular deposited electrochemically. Their detachment from the electrode results generally in a damage of the film. Another disadvantage of this method is the necessity to grow the film on a relatively large electrode surface while it is much more difficult to ensure its uniformity at this scale. Besides, the above 4-probe technique is inevitably ex situ (unlike its electrochemical variant discussed below) so that it is realized under an uncertain oxidation/doping level of the material.

The most largely used in situ method to measure the film resistance directly in contact with the electrode surface and for various oxidation levels of the film is based on the microband technique proposed by M.S.Wrighton [1] and used later in several tens of publications. In most cases it is a planar electrochemical setup which includes two closely-spaced electrodes separated by an insulating gap. They may represent two straight bands (see e.g. [2,3]), or possess a complicated shape (e.g. arrays) to increase their length (see e.g. [4,5]), i.e. the sensitivity. The widths of both bands and the gap belong in most cases to the interval from 5 to 200 micrometers, or even larger.

The film under study must cover this whole system including the insulating gap. For electrodeposited layers they are generated by imposing equal (or almost equal) potentials at both electrodes. The film grows initially up from their surfaces, covering progressively the insulating gap. Then, one can measure the current between two band electrodes via the coating induced by a small-amplitude potential difference. Their ratio gives effective film conductance as a function of the average of the electrode potentials or of the average oxidation level of the film.

Calculation of the specific conductivity of the film from this resistance requires determining "the geometrical constant" of the system which is frequently estimated from the hypothesis that the coating above the gap represents a uniform layer, see e.g. [2,3,5]. It might be justified in the case where the layer thickness exceeds significantly the width of the gap. However, real measurements are typically carried out for much thinner films. In these conditions the above hypothesis might still be valid if the film is propagating along the insulating surface much faster than it grows upward from the electrode surface.

To clarify the applicability of this assumption we have studied the growth of films of the electron-conducting polymer, polypyrrole (PPy), for a single-band or a double-band electrode configuration (Fig.1) by means of the ex situ large-scale (up to 100 μm) AFM technique. The polymer deposition was carried out in conditions ensuring the maximal uniformity of the deposited film, in particular its minimal surface roughness: potentiostatic regime (0.7 V vs Ag/0.01 M Ag+ in acetonitrile, AN) in 1 mM pyrrole + 0.1 M TBAPF6 + AN solution.

Fig.2 shows cross-sections of the bare single band (300 nm high, 8-9 μm in width) and of polymer films of various thicknesses deposited on this electrode (point A in Fig.1 left). The initial growth (up to about 200 nm in thickness, two thinner films) takes dominantly place on the upper part of the electrode surface. The further polymerization combines the vertical growth with film extension along the insulator surface. At last for the most voluminous film in Fig.2 its dimensions are about 1.2 µm above the centre of the band, 1.7 µm above its edges and about 2.4 µm along the insulator. Thus, the propagation in the horizontal direction becomes somewhat faster than that in the normal one for sufficiently thick films while an opposite effect is observed for thinner film.

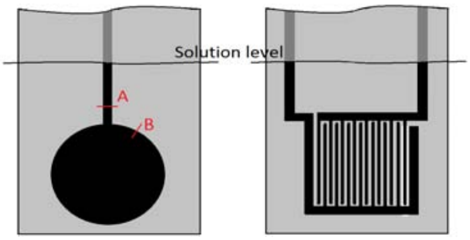

Figure 1. Schematic pictures of electrodes. Left: single band (point A) and macrodisk (0.38 mm^2, point B). Right: double-band electrode

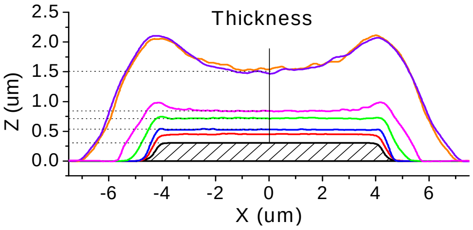

Figure 2. Cross-sections of the bare single-band electrode (point A in Fig.1) and polymer films deposited on its surface

In order to achieve coverage of 5-µm gaps by films growing from neighboring bands, the thickness of the polymer layer deposited over each of band electrodes for conductance measurements was 2-2.5 µm. Formation of a conducting bridge across insulating gaps is confirmed by optical image presented in Fig. 3a as well as by the current flown between the band electrodes in the potential range corresponding to the oxidized form of the polymer (Fig. 3b).

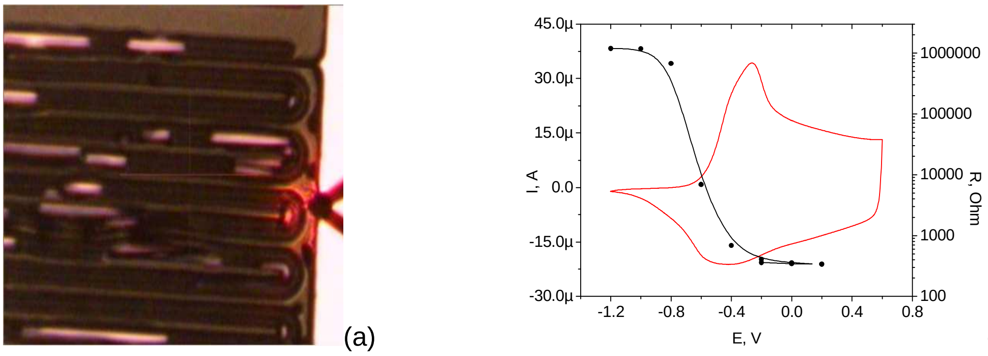

(a)

(b)

Figure 3. (a) Optical image as well as (b) cyclic-voltammetry (red line) and resistance (black line) responses of the thick film (2-2.5 µm) formed on the double-band electrode

However, even for such thick films the wells present in the AFM image (dark lines in Fig. 4a) as well as in the height profile (Fig. 4b) above the former insulating gaps indicate that the "bridge" between the bands cannot be considered as a uniform layer. Additionally, the film thickness varies also along the gaps.

Moreover, the optical image (Fig.3a) demonstrates exfoliation of some parts of this film. One may expect that this effect will become even stronger for thicker films. According to AFM images for various film thicknesses over double-band electrodes, the local structure of the film surfaces becomes much looser for thicker films. All these factors make impossible a reliable determination of the specific conductivity of the deposited PPy material on the basis of such conductance/resistance data.

This conclusion confirms intuitive expectations of many users of the microband technique (see e.g. [1,4,6]) who discussed properties of films immediately on the basis of the resistance (or conductance) as a function of the average potential. However, it is frequently overlooked that the resistance determined with the double-band technique includes not only the contribution of the bulk film but also those of two band/film interfaces (see review [7] for discussion). It has been proposed to separate these contributions with the use of an analog of the 4-probe method, i.e. 4-band electrodes where two extreme electrodes play the role of current suppliers while two central ones represent reference electrodes to measure the contact-free potential difference [7]. As a result, this configuration provides both the bulk-film and contact resistances for each film oxidation level.

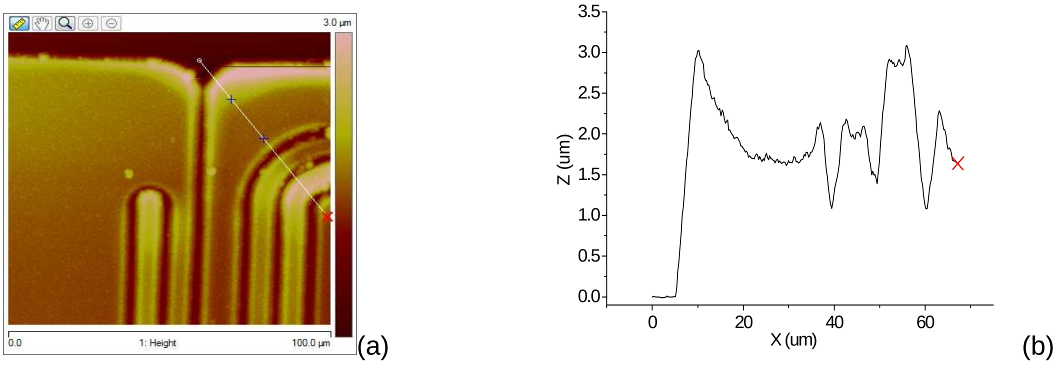

(a) (b)

Figure 4. Large-scale AFM image (a) and height profile (b) of a relatively thick film (about 2-2.5 µm over the electrode surface) deposited on the double-band electrode. Light color in Fig.4a corresponds to higher areas (above the electrodes) while the wells are shown as dark

As for the problem to determine the bulk-film specific conductivity one can circumvent it by combining this double- or four-band technique with an alternative approach based on the chronopotentiometric method for a disc electrode [8] which can be applied for thin films and for which the geometrical constant can be easily estimated with a good precision.

Acknowledgements: Support of the Russian Ministry of Education and Research (Federal Program 2012–1.5, project 8644), the Russian Foundation for Basic Research (projects 12-03-01119-a and 12-03-00797-a) as well as CNRS, Conseil Régional de Bourgogne and Université de Bourgogne is acknowledged.

References

1. *E. W. Paul, A. J. Ricco, M. S. Wrighton*, Resistance of polyaniline films as a function of electrochemical potential and the fabrication of polyaniline-based microelectronic devices // J. Phys. Chem. 1985, 89, 1441
2. *G. Schiavon, S. Sitran, G. Zotti*, A simple two-band electrode for in situ conductivity measurements of polyconjugated conducting polymers // Synth. Met., 1989, 32, 209
3. *M. C. Morvant, J. R. Reynolds*, In situ conductivity studies of poly(3,4-ethylenedioxythiophene) // Synth. Met. 1998, 92, 57
4. *A. Smie, A. Synowczyk, J. Heinze, R. Alle, P. Tschuncky, P. Gotz, P. Bauerle*, β,β-Disubstituted oligothiophenes, a new oligomeric approach towards the synthesis of conducting polymers // J. Electroanal. Chem., 1998, 452, 87
5. *J. Hjelm, R.W. Handel, A. Hagfeldt*, Conducting Polymers Containing In-Chain Metal Centers: Electropolymerization of Oligothienyl-Substituted {M(tpy)2} Complexes and in Situ Conductivity Studies, M = Os(II), Ru(II) // Inorg. Chem., 2005, 44, 1073
6. *M. Skompska, J. Mieczkowski, R. Holze, J. Heinze*, In situ conductance studies of p- and n-doping of poly(3,4-dialkoxythiophenes) // J. Electroanal. Chem., 2005. 577, 9
7. *U. Lange, V.M. Mirsky* Chemiresistors based on conducting polymers: A review on measurement techniques // Analyt. Chim. Acta, 2011, 687, 105
8. *M. A. Vorotyntsev, D. V. Konev* Primary and secondary distributions after a small-amplitude potential step at disk electrode coated with conducting film // Electrochim. Acta, 2011, 56, 9105

HYDRODYNAMIC PERMEABILITY OF A MEMBRANE BUILT UP BY POROUS DEFORMED SPHEROIDAL PARTICLES

[1]Pramod Kumar Yadav, [2]Satya Deo, [3]Manoj Kumar Yadav, [4]Anatoly Filippov
[1]Motilal Nehru National Institute of Technology, Allahabad, India, *E-mail: pramod547@gmail.com*
[2]University of Allahabad, Allahabad, India
[3]National Institute of Technology Patna, Patna, India
[4]Gubkin Russian State University of Oil and Gas, Moscow, Russia, *E-mail: a.filippov@mtu-net.ru*

Introduction

This work concerns the slow viscous flow of an incompressible fluid past a swarm of identically oriented porous deformed spheroidal particles, using particle-in-cell method. The Brinkman's equation in the porous region and the Stokes equation for clear fluid region in their stream function formulations are used. Explicit expressions are investigated for both the inside and outside flow fields to the first order in a small parameter characterizing the deformation. The flow through the porous oblate spheroid is considered as the particular case of the porous deformed spheroid. The hydrodynamic drag force experienced by a porous oblate spheroid and permeability of a membrane built up by porous oblate spheroids having parallel axis are evaluated. The dependence of the hydrodynamic drag force and the hydrodynamic permeability on particle volume fraction, deformation parameter and viscosities of porous and fluid medium are also discussed. Four known boundary conditions on the hypothetical surface are considered and compared: Happel's, Kuwabara's, Kvashnin's and Cunningham's (Mehta-Morse's condition). Some previous results for hydrodynamic drag force and hydrodynamic permeability have been verified. The model suggested can be used for evaluation of changing hydrodynamic permeability of a membrane under applying unidirectional loading in pressure-driven processes (reverse osmosis, nano-, ultra- and microfiltration).

Mathematical Formulation of the Problem

In the mathematical model, we will represent a disperse system (membrane) by a periodic net of identical porous deformed spheroidal particles each of them is enveloped by a concentric spheroid, named as cell surface (Fig. 1).

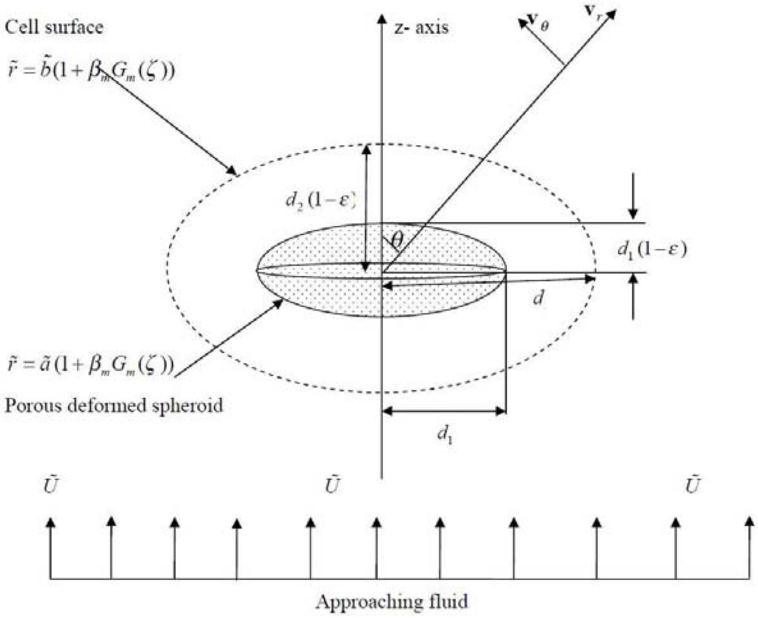

Figure 1. Physical model and co-ordinate system of the problem

Let us assume that these porous deformed spheroidal particles are identical and their axes are parallel and hence the porous medium shall become homogeneous and isotropic. The problems of such kind are arising when extended in a plane porous medium (for example thin membrane) which is consisted from spherical particles undergoes deformable loading in the same direction.

Actually all membranes during pressure-driven processes are working under such loading. Therefore our goal here is to take into account how is the membrane permeability changed under dynamic loading. Let us now consider that porous deformed spheroidal particles are stationary and steady axisymmetric flow has been established around and through it by uniform velocity $\tilde{\mathbf{U}}$ ($|\tilde{\mathbf{U}}| = \tilde{U}$) directed along the positive z-axis.

Let the surface S_p of a spheroid which departs but a little in shape from a sphere $\tilde{r} = \tilde{a}$ be

$$\tilde{r} = \tilde{a}\,(1+\beta_m G_m(\zeta)), \qquad \tilde{a} = \mathrm{d}_1(1-\varepsilon). \tag{1}$$

The equation of correspondingly outer cell surface, i.e., hypothetical surface S_H be

$$\tilde{r} = \tilde{b}(1+\beta_m G_m(\zeta)), \qquad \tilde{b} = \mathrm{d}_2(1-\varepsilon). \tag{2}$$

Further, assuming that the coefficients β_m is sufficiently small, so that squares and higher powers may be neglected i.e.

$$\left(\frac{r}{a}\right)^n \approx 1 + n\beta_m G_m(\zeta), \tag{3}$$

where, n may be positive or negative, $\zeta = \cos\theta$ and $G_m(\zeta)$ being the Gegenbauer function of first kind. The flow in the outside region of the porous deformed spheroid is governed by the Stokes equation with continuity condition:

$$\tilde{\nabla}\tilde{p}^o = \tilde{\mu}^o\,\tilde{\Delta}\tilde{\mathbf{v}}^o,\ \tilde{\nabla}.\tilde{\mathbf{v}}^o = 0. \tag{4}$$

For the region inside the porous deformed spheroid, we assume that the flow is governed by the Brinkman equation and the continuity condition:

$$\tilde{\nabla}\tilde{p}^i = \tilde{\mu}^i\,\tilde{\Delta}\,\tilde{\mathbf{v}}^i - \tilde{k}\,\tilde{\mathbf{v}}^i, \tilde{\nabla}.\tilde{\mathbf{v}}^i = 0, \tag{5}$$

where o and i are superscript, which mark flow outside the porous deformed spheroid and inside the porous deformed spheroid, respectively; tilde over a symbols marks dimensional values; $\tilde{\mathbf{v}}^o, \tilde{\mathbf{v}}^i$ and $\tilde{p}^o, \tilde{p}^i$ are velocity and pressure in the outside and inside of the porous region; $\tilde{\mu}^o$ and $\tilde{\mu}^i$ are viscosities in the outside and inside of the porous region; $\tilde{k}$ is the hydrodynamic resistance of the porous region.

By using the following dimensionless variables

$$\frac{1}{\gamma} = \frac{\tilde{b}}{\tilde{a}}, r = \frac{\tilde{r}}{\tilde{a}}, \nabla = \tilde{\nabla}.\tilde{a}, \Delta = \tilde{\Delta}.\tilde{a}^2, p = \frac{\tilde{p}}{\tilde{p}_o}, \tilde{p}_o = \frac{\tilde{U}.\tilde{\mu}^o}{\tilde{a}}, s = \frac{s_o}{\lambda}, s_o = \frac{\tilde{a}}{\tilde{R}_b}, \lambda^2 = \frac{\tilde{\mu}^i}{\tilde{\mu}^o},$$

$$\lambda^2 = \frac{\tilde{\mu}^i}{\tilde{\mu}^o}, \mathrm{v} = \frac{\tilde{\mathbf{v}}}{\tilde{U}},\ k = \frac{\tilde{k}}{\tilde{a}^2},\ \tilde{R}_b = \sqrt{\frac{\tilde{\mu}^o}{\tilde{k}}}, \tag{6}$$

the system of governing equations (4) and (5) in dimensionless form becomes:

$$\begin{cases} \nabla p^o = \Delta \mathrm{v}^o, \\ \nabla.\mathrm{v}^o = 0 \end{cases} \qquad \left(1 \le r \le \frac{1}{\gamma}\right), \tag{7}$$

$$\begin{cases} \nabla p^i = \lambda^2 \Delta \mathrm{v}^i - s_0^2 \mathrm{v}^i, \\ \nabla.\mathrm{v}^i = 0 \end{cases} \qquad (r \le 1). \tag{8}$$

In order to solve (7)-(8) we employ the stream dimensionless functions $\psi^{o,i} = \dfrac{\tilde{\psi}}{\tilde{U}\,\tilde{a}^2}$ both in the porous spheroid and clear liquid. To match the solution at the porous-liquid interface ($r = 1+\beta_m G_m(\zeta)$), we use along with the continuity of velocity components; continuity of normal stress and continuity of shear stress [1]. The continuity of the radial components of fluid velocity on the outer cell and one of four special boundary conditions (Happel – the tangential stress vanishes on the outer cell surface; Kuwabara – the curl of velocity ($\tilde{\mathbf{v}}^o$) vanishes on the outer cell surface; Kvashnin – a symmetry condition and Cunningham/Mehta-Morse – homogeneity of the flow on the outer cell surface) were also applied. We have determined the explicit expressions for the stream function for the flow inside and outside of the porous deformed sphere.

Results

The dependence of hydrodynamic permeability L_{11} of a membrane built up by porous spheroidal particles on viscosity ratio λ of porous and fluid medium and deformation parameter ε are presented graphically in Fig.2 and Fig.3, correspondingly.

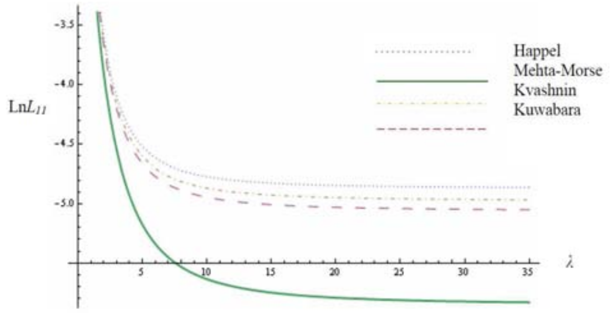

Figure 2. Variation of natural logarithm of the dimensionless hydrodynamic permeability L_{11} *with the parameter* λ *at* $\gamma = 0.8$, $s = 5$ *and* $\varepsilon = 0.1$.

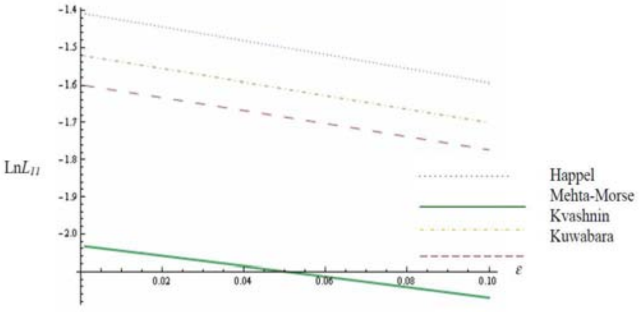

Figure 3. Variation of $\ln L_{11}$ *with the deformation parameter* ε *at* $\gamma = 0.6$, $s = 5$ *and* $\lambda = 2$

Fig.2 shows that the dependence of dimensionless hydrodynamic permeability L_{11} of a membrane decreases with viscosity ratio λ, i.e., the flow through membrane becomes difficult with the increase of inner viscosity. Fig.3. shows that the dependence of dimensionless hydrodynamic permeability of a membrane L_{11} also decreases with increasing deformation parameter ε.

Conclusion

From our analysis, we conclude that the dependencies of L_{11} on various parameters for all four cell models are extremely close to each other except for the Mehta-Morse boundary condition for which the value of hydrodynamic permeability is significantly lower than the other models, signifying its non-suitability to model the hydrodynamic permeability of a membrane. So only three models suggested here can be used for evaluation of changing hydrodynamic permeability of a membrane under applying unidirectional loading in pressure-driven processes (reverse osmosis, nano-, ultra- and microfiltration). The problems considered here are arising when extended in a plane porous medium (for example thin membrane), which is consisted from spherical particles, experiences deformable loading in the same direction. In fact all membranes during pressure-driven processes are working under such loading. Moreover cake or gel-layer which is often formed on the membrane surface from retarded particles also undergoes deformation and changes their permeability during filtration process. Therefore, for the first time, the cell models, suggested in the present paper, take into account how is the membrane system permeability changed under dynamic loading.

This work is supported by the Russian Foundation for Basic Research (project no 13-08-92695-Ind).

References

1. *Yadav P.K., Deo S., Yadav M.K., Filippov A.N.* On Hydrodynamic Permeability of a Membrane Built up by Porous Deformed Spheroidal Particles // Colloid J. 2013. V. 75 (in press).

POTENTIOMETRIC MULTISENSORY SYSTEMS WITH PD-SENSORS BASED ON MEMBRANES CONTAINING ZrO_2 FOR DETERMINATION OF ANIONS AND CATIONS IN AQUEOUS SOLUTIONS

[1]Kristina Yankina, [1]Olga Bobreshova, [1]Anna Parshina, [1]Tatiana Denisova,
[2]Ekaterina Safronova, [2]Andrey Yaroslavtsev
[1]Voronezh State University, Voronezh, Russia, E-mail: olga1@box.vsi.ru
[2]Kurnakov Institute of General and Inorganic Chemistry RAS, Moscow, Russia

Introduction

In [1] we have suggested to use potentiometric sensors, analytical signal of which is the Donnan potential (PD-sensors) at the ion-exchange membrane / electrolyte solution interface, for the determination of some bioactive substances in polyionic solutions. The use of membrane MF-4SC and Nafion containing ZrO_2 for PD-sensor revealed the sensitivity of the sensor to anions in solutions of amino acids [2]. The aim of this paper was the development of multisensory systems for the quantitative determination of anions and cations in multiionic aqueous solutions.

Experiments

The following analytes of interest were dissolved in aqueous solutions: hydrochloride novocaine (NovHCl), hydrochloride lidokaine (LidHCl), cysteine (Cys) and inorganic electrolytes (KOH, KCl). Concentrations of test solutions ranged from $1.0\cdot10^{-4}$ to $1.0\cdot10^{-1}$ M. The ionic composition of solutions of NovHCl and LidHCl is represented mainly singly charged ions $NovH^+$ (or $LidH^+$) and Cl^- (pH ranged from 4.38±0.05 to 5.91±0.05). The ionic composition of solutions of NovHCl+KCl and LidHCl+KCl is represented mainly singly charged ions $NovH^+$ (or $LidH^+$), K^+ and Cl^- (pH ranged from 4.26±0.05 to 6.18±0.05). The ionic composition of solutions of Cys+KOH is presented by ions CH_3COCOO^-, HS^-, OH^-, K^+ and NH_4^+ (pH ranged from 8.22±0.05 to 10.50±0.05).

The samples of membranes MF-4SC and Nafion with 2.0-5.0 wt.% of ZrO_2 were investigated. One half of membrane contains nanoparticles of ZrO_2. This half of membrane contacted with test solution. Other half of a membrane was not modified and contacted with reference solution of PD-sensor. The procedure for obtaining of membranes containing ZrO_2 is described in [3].

Results and discussion

Cross-sensitive PD-sensors for quantitative determination of ions $NovH^+$ and $LidH^+$ in aqueous solutions. Results of the study of cross-sensitivity of PD-sensor in solutions of NovHCl and LidHCl the following. Sensitivity of PD-sensors to ions $NovH^+$ and $LidH^+$ increased for membranes with 2.0-2.4 wt.% of ZrO_2 in comparison with the unmodified membranes (by a factor of 2 or 1.6 for the $NovH^+$ or $LidH^+$ respectively). Sensitivity of PD-sensors to ions H_3O^+ decreased for these membranes (by a factor of 3.6 or 1.5 for solutions NovHCl or LidHCl respectively). Sensitivity of PD-sensors to ions $NovH^+$ and $LidH^+$ in comparison with ions H_3O^+ for membranes with 2.8-5.0 wt.% of ZrO_2 decreased.

Results of the study of cross-sensitivity of PD-sensor in solutions of NovHCl+KCl and LidHCl+KCl the following. Assumed that three factors influence on the response of sensors (1). The first factor is variation of concentration of ions $NovH^+$ (or $LidH^+$) in test solutions. The second factor is variation of concentration of ions K^+ in test solutions. The third factor is variation of pH of the test solutions.

$$\Delta\varphi_D = b_0 + b_1 \cdot pC_{NovH^+(LidH^+)} + b_2 \cdot pC_{K^+} + b_3 \cdot pH \qquad (1)$$

where $\Delta\varphi_D$ is response of PD-sensor (mV); $pC_{NovH^+(LidH^+)}$ is negative decimal logarithm of concentration of ions $NovH^+$ (or $LidH^+$); pC_{K^+} is negative decimal logarithm of concentration of ions K^+; b_1, b_2, b_3 are coefficients of sensitivity of PD-sensor to corresponding ions (mV/pC).

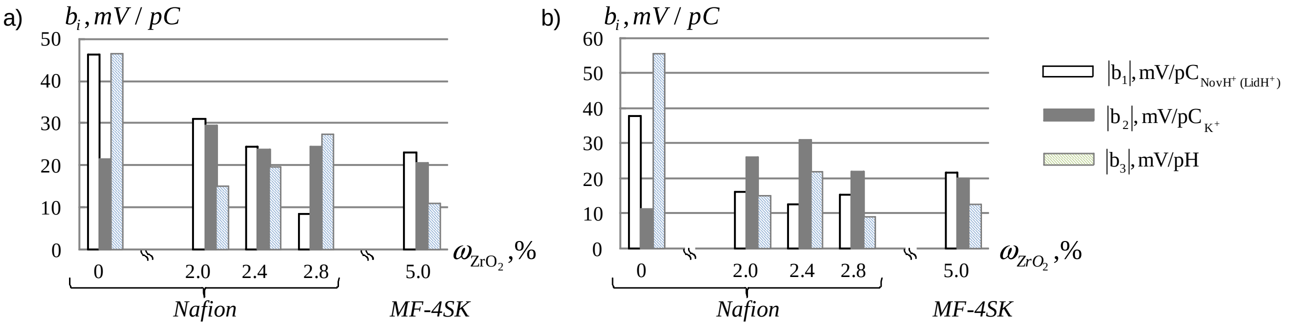

Figure 1. Coefficients of calibration equations of PD-sensors based on membranes MF-4SC and Nafion in solutions of NovHCl+KCl (a) and LidHCl+KCl (b)

The greatest sensitivity of PD-sensors to $NovH^+$ in comparison with ions H_3O^+ was for the membranes containing 2.0 and 5.0 wt.% of ZrO_2 (Figure 1, a). The greatest sensitivity of PD-sensors to $LidH^+$ in comparison with ions H_3O^+ was for the membranes containing 5.0 wt.% of ZrO_2 (Figure 1, b). Therefore these membranes for quantitative determination of ions $NovH^+$ and $LidH^+$ in solutions of NovHCl+KCl and LidHCl+KCl were chosen.

Multisensory systems for quantitative analysis of solutions of NovHCl+KCl and LidHCl+KCl included: PD-sensor, potassium selective electrode (K-SE), glass electrode for measurement pH, silver chloride/silver reference electrode and potentiometer. Calibration equations of PD-sensors and K-SE in solutions of NovHCl+KCl and LidHCl+KCl are shown on figures 2 and 3 respectively. Accuracy of analysis are defined by method "input/ found" (figures 2, 3).

a)

$$\begin{cases} -\Delta\varphi_D = -142 - 46\cdot pC_{NovH^+} - 21\cdot pC_{K^+} + 46\cdot pH; \\ E_{K-SE} = 301 - 36\cdot pC_{NovH^+} - 60\cdot pC_{K^+} + 43\cdot pH \end{cases}$$

Input C, M		**Found C, M**		**s_r**	
$NovH^+$	**K^+**	**$NovH^+$**	**K^+**	**$NovH^+$**	**K^+**
$1,0\cdot10^{-4}$	$1,0\cdot10^{-4}$	$1,0\cdot10^{-4}$	$1,1\cdot10^{-4}$	0,3	0,2
$5,0\cdot10^{-3}$	$1,0\cdot10^{-4}$	$7,0\cdot10^{-4}$	$9,3\cdot10^{-5}$	0,13	0,09
$5,0\cdot10^{-4}$	$1,0\cdot10^{-3}$	$4,3\cdot10^{-4}$	$9,1\cdot10^{-4}$	0,11	0,98
$1,0\cdot10^{-4}$	$1,0\cdot10^{-2}$	$1,3\cdot10^{-4}$	$1,1\cdot10^{-2}$	0,09	0,12

b)

$$\begin{cases} -\Delta\varphi_D = 78 - 23\cdot pC_{NovH^+} - 20\cdot pC_{K^+} - 11\cdot pH; \\ E_{K-SE} = 301 - 36\cdot pC_{NovH^+} - 60\cdot pC_{K^+} + 43\cdot pH. \end{cases}$$

Input C, M		**Found C, M**		**s_r**	
$NovH^+$	**K^+**	**$NovH^+$**	**K^+**	**$NovH^+$**	**K^+**
$1,0\cdot10^{-4}$	$1,0\cdot10^{-4}$	$1,0\cdot10^{-4}$	$1,2\cdot10^{-4}$	0,07	0,5
$5,0\cdot10^{-3}$	$1,0\cdot10^{-4}$	$3,4\cdot10^{-3}$	$1,4\cdot10^{-4}$	0,12	0,09
$5,0\cdot10^{-3}$	$1,0\cdot10^{-3}$	$5,2\cdot10^{-2}$	$8,1\cdot10^{-3}$	0,3	0,2
$1,0\cdot10^{-3}$	$1,0\cdot10^{-2}$	$9,7\cdot10^{-4}$	$9,8\cdot10^{-3}$	0,3	0,2

Figure 2. Quantitative determination of compounds in solutions of NovHCl+KCl for membranes containing 0 wt. % (a) and 5.0 wt. % (b) of ZrO_2

a)

$$\begin{cases} -\Delta\varphi_D = 328 - 38\cdot pC_{LidH^+} - 11\cdot pC_{K^+} - 55\cdot pH; \\ E_{K-SE} = 575 - 19\cdot pC_{LidH^+} - 48\cdot pC_{K^+} - 28\cdot pH \end{cases}$$

Input C, M		**Found C, M**		**s_r**	
$LidH^+$	**K^+**	**$LidH^+$**	**K^+**	**$LidH^+$**	**K^+**
$1,0\cdot10^{-4}$	$1,0\cdot10^{-4}$	$1,1\cdot10^{-4}$	$8,1\cdot10^{-5}$	0,11	0,87
$5,0\cdot10^{-3}$	$1,0\cdot10^{-4}$	$6,7\cdot10^{-3}$	$9,4\cdot10^{-5}$	0,12	0,10
$1,0\cdot10^{-4}$	$1,0\cdot10^{-2}$	$1,3\cdot10^{-4}$	$1,2\cdot10^{-2}$	0,01	0,03
$1,0\cdot10^{-3}$	$1,0\cdot10^{-2}$	$1,5\cdot10^{-3}$	$8,4\cdot10^{-3}$	0,3	0,10

b)

$$\begin{cases} -\Delta\varphi_D = 36 - 15\cdot pC_{LidH^+} - 22\cdot pC_{K^+} - 9\cdot pH; \\ E_{K-SE} = 575 - 19\cdot pC_{LidH^+} - 48\cdot pC_{K^+} - 28\cdot pH \end{cases}$$

Input C, M		**Found C, M**		**s_r**	
$LidH^+$	**K^+**	**$LidH^+$**	**K^+**	**$LidH^+$**	**K^+**
$5,0\cdot10^{-3}$	$1,0\cdot10^{-4}$	$4,1\cdot10^{-3}$	$1,1\cdot10^{-4}$	0,2	0,08
$5,0\cdot10^{-4}$	$1,0\cdot10^{-3}$	$5,5\cdot10^{-4}$	$1,1\cdot10^{-1}$	0,5	0,3
$5,0\cdot10^{-4}$	$1,0\cdot10^{-2}$	$6,7\cdot10^{-2}$	$1,0\cdot10^{-3}$	0,4	0,10
$1,0\cdot10^{-3}$	$1,0\cdot10^{-2}$	$1,2\cdot10^{-3}$	$9,1\cdot10^{-3}$	0,5	0,3

Figure 3. Quantitative determination of compounds in solutions of LidHCl+KCl for membranes containing 0 wt. % (a) and 5.0 wt. % (b) of ZrO_2

The relative error of determination for unmodified membranes and membranes with 5.0 wt. % of ZrO_2 did not exceed 4 and 2 % respectively. Thus use membranes containing ZrO_2 leads to decreases error determination of ions $NovH^+$, $LidH^+$, K^+ in comparison with the unmodified membranes.

Cross-sensitivity of PD-sensor in alkaline solutions. Results of the study of cross-sensitivity of PD-sensor based on membranes Nafion containing 2.0-2.8 wt.% of ZrO_2 the following. Assumed that three factors influence on the response of sensors (2). The first factor is variation of concentration of ions K^+ and NH_4^+ in test solutions. The second factor is variation of pH of the test solutions. The third factor is variation of concentration of ions CH_3COCOO^- and HS^- in test solutions.

$$\Delta\varphi_D = b_0 + b_1 \cdot pC_{K^+,NH_4^+} + b_2 \cdot pH + b_3 \cdot pC_{CH_3COCOO^-,HS^-} \qquad (2)$$

where pC_{K^+,NH_4^+} is negative decimal logarithm of total concentration of ions K^+ and NH_4^+; $pC_{CH_3COCOO^-,HS^-}$ is negative decimal logarithm of total concentration of ions CH_3COCOO^- and HS^-.

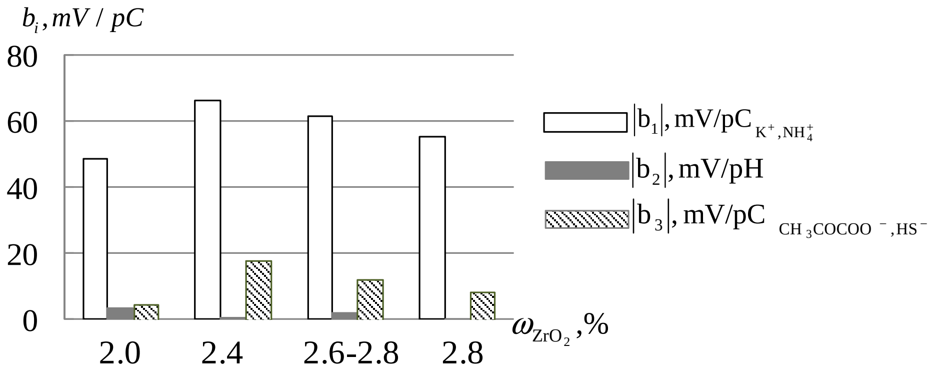

Figure 4. Coefficients of calibration equations of PD-sensors based on membranes Nafion in alkaline solutions

The greatest sensitivity of PD-sensors to anions CH_3COCOO^- and HS^- in comparison with ions K^+, NH_4^+ and OH^- was for the membranes containing 2.4 wt.% of ZrO_2. It can be because of presence of large organic ions (CH_3COCOO^-) into the pores of modified membrane, which reduces the interaction of the inorganic ions with -SO_3^--groups.

Acknowledgements

This study was funded by the Russian Fund for Basic Research (12-08-00743-a, 12-08-31471/mol_a) and P.Y.S.I.C. (project 8080r/14016, 30.04.2011).

References

1. *Bobreshova O.V., Parshina A.V., Agupova M.V., Polumestnaya K.A.* // Russ. J. of Electrochem. 2010. V. 46, № 11. P. 1338-1349.
2. *Bobreshova O.V., Parshina A.V., Polumestnaya K.A., Safronova E.Yu., Yankina K.Yu., Yaroslavtsev A.B.* // Mendeleev Communications. 2012. V. 22, № 2. P. 83-84.
3. *Voropaeva E.Yu., Stenina I.A., Yaroslavtsev A.B.* // Russ. J. Inorg. Chem. 2008. V. 53, № 11. P. 1677-1680.

INFLUENCE OF DOPANT SURFACE NATURE ON THE TRANSPORT PROPERTIES OF HYBRID MEMBRANES

[1,2]**Andrei Yaroslavtsev**

[1]Kurnakov Institute of General and Inorganic Chemistry RAS, Moscow, Russia, *E-mail: yaroslav@igic.ras.ru*

[2]Topchiev Institute of Petrochemical Synthesis. RAS, Moscow, Russia

Progress of modern technologies demands more and more energy. Technologies of the future will be based on the clean and safe energy sources. One of the most promising is hydrogen energy which is based on the membrane technology [1]. This report is devoted to some achievements in their development deals with hybrid membranes.

The best membranes for fuel cells are perfluorinated Nafion membranes [2]. They contain pores including water and protons formed due to dissociation of functional groups. But they have some disadvantages. Its necessary to maintain high humidity for high proton conductivity. In addition, these membranes can not be heated above 100°C. At this temperature platinum catalyst is irreversibly poisoned by the trace amounts of carbon monooxide which is the main admixture to cheap hydrogen, formed by means of carboncontaining products conversion [1].

It is known that the introduction of nanoparticles can improve proton conductivity of membranes, their permeability, strength and some other parameters. It’s a new directions, which was based abut twenty years ago.

Ionic conductivity

Membranes for fuel cells should have high proton conductivity. Proton conductivity of MF-4SK membranes modified by silica is higher than the conductivity of the initial sample. The dependence of conductivity on the dopant content is passes through a maximum. To explain the reasons of conductivity increase during the modifications we have proposed a model of "limited elasticity" of the membrane pore walls, which is based on the Gierke model of membrane structure [3].

The dopant nanoparticles use a part of pore volume and replace water molecules. But membrane water uptake is determined by the osmotic pressure and strong interaction of protons of functional groups with water molecule. Proton concentration varies very slightly after modification. So water uptake should remain the same or increases slightly due to additional water adsorption on the surface of the hydrophilic particles. The increase in the pore size results in the increase of the size of connecting channels. This leads to the acceleration of proton transport through narrow channels and membrane conductivity increase. But further increase in the nanoparticle size leads to a decrease in water uptake and membrane conductivity.

According to Hooke's law the more the deformation the more is elastic force necessary for pore expansion. So for the large particle size the osmotic pressure became insufficient to maintain the same water uptake. So the additional obstacles are formed between the pore wall and the dopant particles surface. This is equivalent to the formation of new narrow "channels" limiting the conductivity.

The comparison of the NMR data and the conductivity of hybrid membranes can be considered as the evidence of proposed model. The diffusion coefficients of protons obtained from the NMR relaxation data, is determined by the migration of protons and water molecules in large pores, within which the most of the protons are located. These values are much higher than the proton diffusion coefficients calculated from the conductivity data, which is limited by the proton migration through the narrow channels. The rate of NMR relaxation in hybrid membranes can be more or less then for the initial system, while the conductivity of hybrid membranes is always higher. This shows that the increase in the ionic conductivity of hybrid membranes takes place due to the influence of the dopant particles on the ion transport in channels [4].

Selectivity of the transport processes

One of the most important properties of membranes is their selectivity or the decrease in their permeability to gases and methanol. Low permeability to methanol makes such membranes extremely effective for use in direct methanol fuel cells. Selectivity is also determined by the ability to selective transport of individual ions. Cation exchange membrane should transfer cations, whereas the transport of anions should carry out much more slowly. The selectivity of such membranes is determined by transport numbers. An decrease in transport numbers of anions is typical for a number of hybrid membranes.

The heterogeneity of cations and anions distribution is determined by the presence of significant negative charge on the pore walls due to the presence of fixed ions. So double electric layer should be formed in the pores. The most of the protons are locolised within the thin Debye layer with the size of the order 1 nm. In contrast, anions are excluded from it [5]. In the center of the pore almost electrically neutral solution is localized, whose composition is close to the composition of the outside solution.

Proton conductivity of such membrane is determined mainly by the transfer in the Debye layer along the pore walls, and anions and non-polar molecules (or molecules containing large non-polar fragments) move mainly through "free" solution, which is localized in the centers of the pores. But formation of hydrophilic nanoparticles takes place in the center of pores due to electrostatics forces. Therefore, these particles replace "free" solution from the pores and did not affect thin Debye layer, localized near the walls. Their proton conductivity remains the same or even increases but anions and neutral molecules transfer decreases. This is the reason of selectivity increase in hybrid membranes [5].

The influence of the dopant nature

Dopant nature can change the water uptake of the membranes and carrier concentration. Both factors significantly affect the conductivity. Dopants with hydrophilic surface (silica, zirconia) increases water uptake and membrane conductivity as a rule.

The second factor, (carrier concentration) is more important. Proton carriers in membrane are interstices (additional protons, located in the abnormal, additional positions). So it seems better to increase the acidity of the dopant by means of acids modification.

This modification is likely have a double effect. On the one hand, it leads to an increase in the number of carriers [5]. On the other hand, the water uptake of the membranes is determined by the amount of acid groups. Increasing the number of acid groups we increase osmotic pressure and water uptake. Furthermore, the selectivity of these membranes should increase because we get two Debye layer with similar charges in a pore, which should replace anions and organic molecules from the pores, because the polarity of molecule even for alcohol is much smaller than that of water [5].

This affect is the most important for the low humidity, than the particle surface takes place in proton transfer too. An excellent example of such systems is membrane doped with silica nanoparticles and heteropolyacids. Their proton conductivity even at low humidity remains very high. They are of several orders of magnitude higher than the conductivity of initial membrane and the membrane doped by silica only.

In the case of particles modified by amino groups the effect should be reversed, because they give the positive charge of the pore walls after dissociation. We inoculate organic chains containing amino groups to the surface of silica nanoparticles. As expected, the ion-exchange capacity and water content of the membranes decreases in both cases with increasing of such groups' content dew to the ionic bonds formation with the walls of the pores. However, the exchange capacity for the membranes with particles with two amino groups decreased less. This indicates that the amino groups of the aromatic ring are less available.

Surprise for us was the fact that the conductivity of the membranes increased with the concentration of inoculated fragments [6]. This fact can be explained in terms of increasing of the dopant particles. But diffusion permeability and interdiffusion pass trough the maximum in the membranes at low fragments concentration, and then increases sharply. Obviously, with a high concentration of these groups the destruction of membrane structure takes place, as noted above. But at low concentration, the decreasing of interstitial solution volume takes place due to the attraction of the pore walls, which leads to an increase in the selectivity. Moreover, in some areas the crosslinking of the pore wall and the surface of the dopant could take place.

Mechanical properties

Another unusual feature is the change in the mechanical strength of the hybrid membranes. It would seem that the introduction of the nanoparticles, which increases the size of the pores and connecting channels should lead to membranes strength reduction. The exception might take place in the case of one-dimensional nanoparticles introduction, such as carbon nanotubes. The strength of the membrane increases at their low concentration really [7]. While with increasing of its concentration it decreases again sharply. The surprise was the increase of membrane strength after the introduction of a small amount of silica particles. The increase in Young's modulus takes place because we have to stretch the membrane which was deformed before. The increase in tensile strength seems a little surprising. Here, the research is in progress.

This study was funded by the Russian Fund for Basic Research (11-08-93105-НЦНИЛ_a) and Ministry of Education and Science of RF (project № 8024).

References

1. *Yaroslavtsev A.B., Dobrowolski Yu.A., Shaglaeva N.S., Frolova L.A., Gerasimova, E., Sanginov EA* // Rus.Chem.Rev. 2012. V.81. № 3. P.191-220.
2. *Kreuer K.D., Paddison S., Spohr E., Schuster M.*// Chem. Rev. 2004. V. 104. P.4637-4678.
3. *Ярославцев А.Б., Караванова Ю.А., Сафронова Е.Ю.* // Membranes and membrane technology 2011. V. 1. № 1. P. 3-10.
4. *Safronova E.Yu., Stenina I.A., Pavlov A.A., Volkov V.I., Yurkov G.Yu., Yaroslavtsev A.B.* / J. Inorganic. Chem. 2011. V. 55. P. 187.
5. *Yaroslavtsev A.B.* // Rossiyskie Nanotechnologii., 2012, V.7, №9-10. P. 8-18.
6. *Mikheev A.G., Safronova E.Yu., Yurkov G.Yu., Yaroslavtsev A.B.* // Mendeleev Commun., 2013, V.23, №2, p. 66-68.
7. *Perepelkina A.I., Safronova E.Yu., Shalimov A.S., Yaroslavtsev A.B.* // Membranes and membrane technology 2012. V. 2. № 1. P. 27-32.

SYNTHESIS AND DIFFUSION PROPERTIES OF CATION-EXCHANGE MEMBRANE BASED ON MC-40, MF-4SC AND POLYANILIN

Polina Yurova, Yulia Karavanova
Kurnakov Institute of General and Inorganic Chemistry, Moscow, Russia, *E-mail: polina31415@mail.ru*

Introduction

Ion-exchange membranes are nanoporous polymer materials, which functional properties are determined by ions transport in the channels and pores with charged walls. They are used for different fields, for example, the creation of a cells fuel [1], water purification, separation and purification of liquids [2]. Membrane should have a high ion selectivity, chemical stability, mechanical strength and be able to work in different temperature regimes. But ion-exchange membranes with the best characteristics are quite expensive and the variety of industrial materials is limited. There is a great interest in synthesis new ion exchange materials and finding ways to modify existing [3,4]. In this work asymmetric cation exchange materials based on industrial membrane MC-40, which surface was modified by thin layer of MF-4SC with polyaniline introduction, were obtained. Applying a thin layer of more expensive but more permeable membrane MF-4SC can significantly improve the diffusion parameters of the MC-40 and slightly increase the cost. Introduction of polyaniline can increase defects of structure and lead to increased rate of cation transport.

Experiments

In the study, samples at 0, 1, 2 and 3% of polyaniline content in the MF-4SC matrix on the surface of MC-40 membrane were obtained. Diffusion parameters was study for these samples, including diffusion permeability, interdiffusion and ionic conductivity of the membranes in various mixed-alkali H^+ / Na^+ forms and for different temperatures. Based on these data we have calculated the activation energy of ionic conductivity and diffusion coefficients of H^+ and Na^+ in the membranes.

Results and Discussion

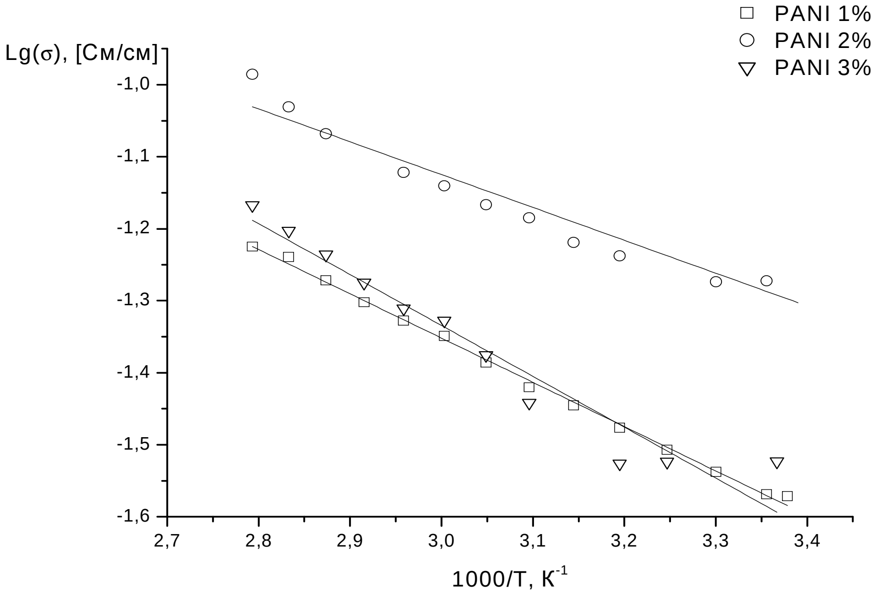

Figure 1. Dependence ionic conductivity membranes on temperature

Introduction of polyaniline in a MF-4SC matrix leads to some decrease, and then, with increasing polyaniline content, an increase of cations diffusion coefficients. At the same time diffusion permeability is reduced markedly, that corresponds to an increase of selectivity.

Impedance spectroscopy showed conductivity increase in the main part of modified samples. Membrane PANI 2% have shown maximum ionic conductivity of the corresponds to a model of limited elasticity of the membrane pores.

These results shows perspectivity this method of material modification for electrodialysis water treatment.

References

1. *Prater K.,* J. Power Sources, *1994.*
2. *Yaroslavtsev A., Zabolotskij V., Niconenko V.,* // Russian Chemical 2003. V.72. №5. P. 438.
3. *M.A. Hickner. H. Ghassemi. Y.S. Kim. B.R. Einsla. J.E. McGrath* // Chem. Rev. 2004. V. 104. P. 4587
4. *Yaroslavtsev A. B., Nikonenko V. V.* // Ross. Nanotekhnologii [Russian Technologies]. 2009. V. 3. P. 8.

HYBRID BARO-ELECTROMEMBRANE UNIT FOR BOILER FEED WATER PRODUCTION

[1,2]Victor Zabolotsky, [1]Stanislav Melnikov, [1]Vyacheslav Bugakov
[1]Kuban State University, Krasnodar, Russia
[2]LLC «Innovative Enterprise «Membrane Technology», Krasnodar, Russia

Introduction

An important factor influencing the corrosion resistance of steam generators material, except mineral impurities, is pH of the feed water. The requirements for the pH is strictly regulated in the requirements for boiler feed water, but often do not meet the necessary requirements for salt content and pH. To solve this problem, electrodialysis with bipolar membranes may be used for pH shifting to the alkaline side coupled with reverse osmosis used for desalination.

Experiments

To produce water for the steam generator with pH> 8,6 electrodialysis module (ED) with bipolar membranes is used. Membrane stack of said module has 2-chamber elementary cell (acid and alkali chambers), which consists of alternating bipolar membranes and anion exchange membranes MA-41. Scheme of the membrane stack is shown on Figure 1, andsome of its properties is shown in Table 1. Flow rates for alkali and acidic chambers is 100 and 50 L/h, respectively. Acidic solution is used to wash electrode chambers from gases and then goes to waste. Boiler feed water obtained by mixing of alkali solution and reverse osmosis permeate in proportions from 1:10 to 1:5 goes into storage tank (2 m^3). Total TDS and pH of the water in storage tank is periodically controlled.

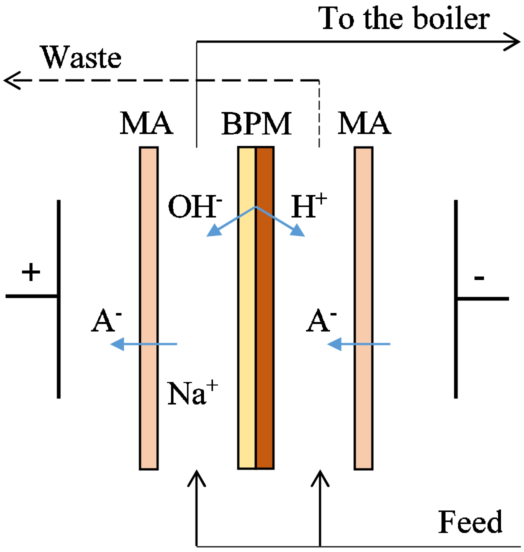

Figure 1. Scheme of membrane stack of bipolar electrodialysis module used to produce boiler feed water

Table 1. Properties of electrodialysis module

Number of elementary cells	25 pieces
Membranes	
Bipolar	MB-1
Anion-exchange	MA-40
Materials	
anode	RuO_2/Ti
cathode	Stainless steel
spacers	PE
Chanel dimensions	
length	400 mm
width	100 mm
heigth	0,9 mm

ED works in the hybrid baro-electromembrane unit (HBEU-1) for production of boiler feed water in polypropylenes carpet funicular workshop in JSC “Kamenskvolokno”. The principal scheme of the HBEU-1 is shown on Figure 2.

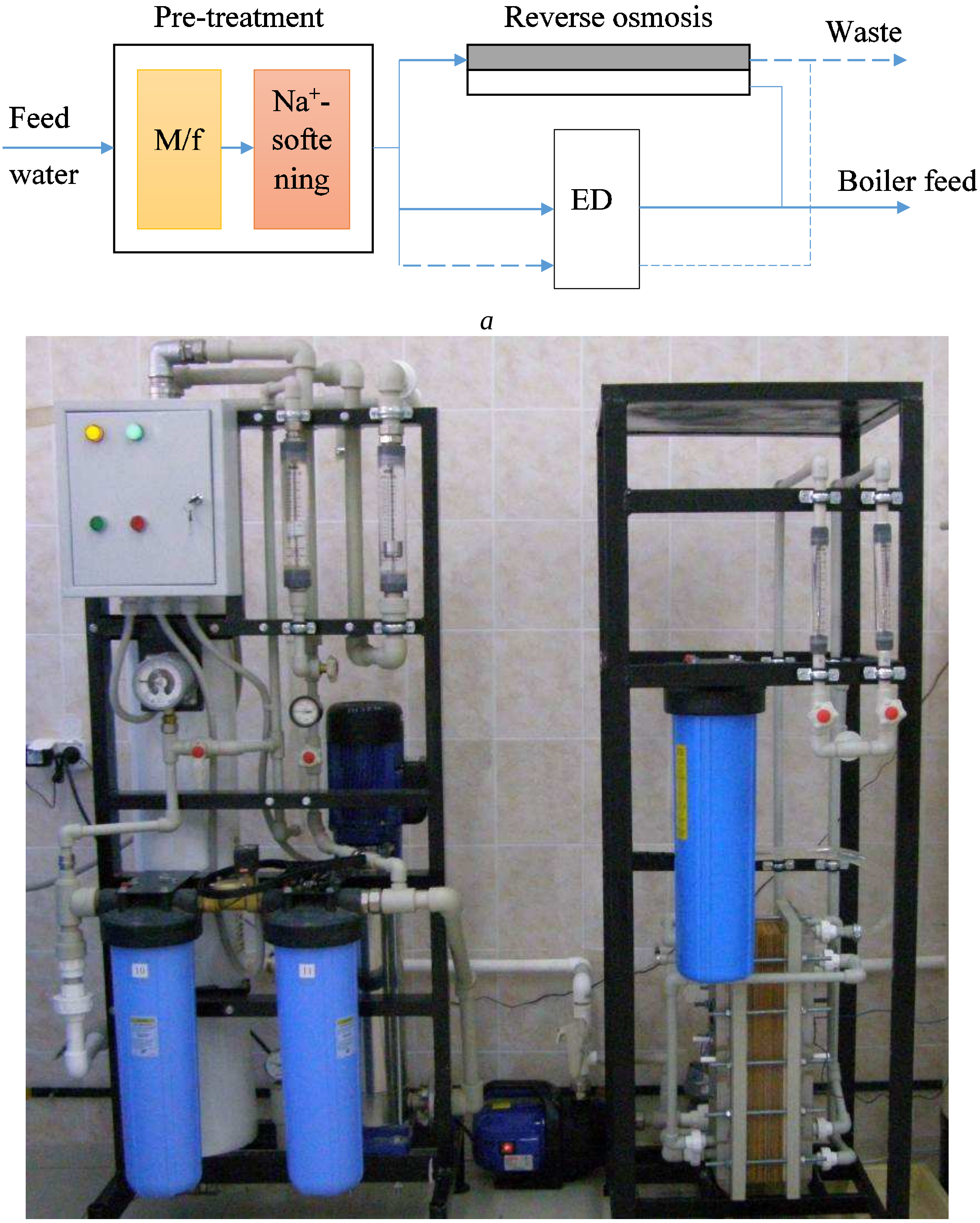

a

b

Figure 2. Principal scheme (a) and photo of complete HBEU-1 (b)

Pre-treatment module include mechanical and micro filtration, Na^+-softening and removal of bacteria and free chlorine on activated carbon. After pre-treatment module, the feed water splits to two independent streams one of which goes to deep desalination on reverse osmosis, and the other goes to pH correction on ED with bipolar membranes.

Results and Discussion

Compositions of the feed water and of solutions after softening (before HBEU-1), and solution in the storage tank (after HBEU-1) are shown in Table 2.

Table 2. Feed and treated solutions composition

Parameter	Feed	Softened feed	Boiler feed
pH	6,5-8,0	6,5-8,0	>8,6
Mineralization, mg/L	< 1400	< 1400	< 100
Hardness, m-eq/L	< 13,5	< 0,08	< 0,02
Alkalinity, m-eq/L	< 6	< 6	< 1
Chloride, mg/L	< 300	< 300	< 30
Sulfates, mg/L	< 400	< 400	< 50
Iron (III), mg/L	< 0,1	< 0,08	< 0,02

As seen from the table, feed water has a high alkalinity which is not removed after softening. Comparison of this data with feed water pH value leads to the conclusion that high alkalinity is presented due to high concentration of hydrocarbonate ions in the feed water. Their presence leads to a buffering capacity of the solution, as generated by the bipolar membrane hydroxyl ions will first be spent in the chemical reaction with hydrocarbonate ions and only after that the pH of the solution will rise. Given the feed water mineralization, alkalinity and pH it os easy to calculate that we need to produce as much as 0,6 mol/h of OH^- -ions. From these data the characteristics of ED with bipolar membranes were calculated (Table 1).

Figure 3 shows results of HBEU-1 work in the long period of time.

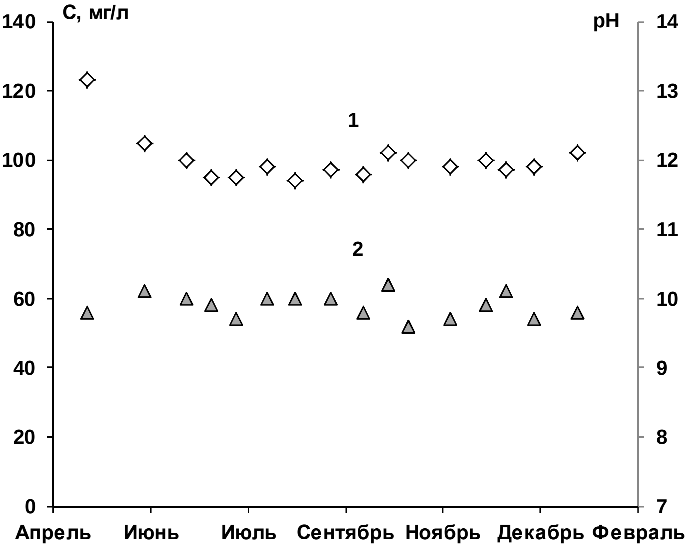

Figure 3. Main characteristics of boiler feed water after HBEU-1. 1- total mineralization, 2 – pH. Data shown was acquired in the period from April 2011 to February 2012

HBEU-1 showed very good results in terms of stability of the boiler feed water main characteristics (total mineralization and pH). The HBEU-1 allows to obtain a given salt content (<100 mg/L) and pH> 8.6 with the simultaneous removal of free and bound carbon dioxide.

Acknowledgments

The reported study was partially supported by Russian foundation for basic research, research projects No. 11-08-00718-a.

SPECTRAL COMPOSITION OF THE CONCENTRATION FIELD FLUCTUATIONS IN SOLUTIONS AT THE BOUNDARY WITH ANION-EXCHANGE MEMBRANES UNDER OVERLIMITING CURRENT DENSITY

Anna Zhiltsova, Vladimir Kolganov, Vera Vasil'eva
Voronezh State University, Voronezh, Russia, E-mail: *viv155@mail.ru*

Introduction

This work is aimed at the determination of spectral composition of the concentration field fluctuations in solutions within the stratified electromembrane systems of different nature under high-intensive current operation conditions with the use of Fourier-analysis.

Experiments

Experiments were made in electro-dialyzer divided into seven compartments with alternating cation-exchange and anion-exchange membranes. Membranes with different chemical nature of the fixed groups were selected as the objects of investigation: anion-exchange membrane MA-40 and its sample MA-40M modified with copolymer of acrylonitrile and dimethyl-diallyl-ammonium chloride (DDAACl), involving tertiary ammonium bases [1]. Such modification does not break original structure of the surface and bulk of membrane and thus it results in the instant decrease of amount of secondary and ternary amino-groups on the surface of membrane. Anion-exchange membrane MA-41 was applied just as its sample where the surface was modified with tetraalkylammonium groups in order to enhance chemical and thermal stability.

The study of concentration field in a solution at the boundary with the membrane was performed by laser interferometry with the use of interferometric module of Mach-Zender type. The obtained interferograms were presented as separate subject videos. Interference band represented the profile of the refractive index and concentration, respectively.

The height of membrane channel L was of $4{,}2\cdot10^{-2}$ m, width of $2{,}4\cdot10^{-2}$ m, intermembrane distance was $h = 2{,}0\cdot10^{-3}$ m. Sodium chloride solutions with the initial concentration of $2{,}0\cdot10^{-2}$ M were supplied with the rate of $1{,}3\cdot10^{-3}$ m/s, that corresponds to laminar flow (Re=2). Electrodialysis was performed in galvanostatic mode.

While performing laser-interferometric dynamic analysis the results of measurements of the fluctuations for the interference bands were recorded in the form of time series with the length of $(2\text{-}3)\cdot 10^3$ samplings. To digitize results we applied software based on the registration of the changes in colour intensity in the local points and presentation of the information in the digital form. The process of digitizing comprised of two stages: 1 – formation of the graphical image representing dynamics of the changes in the position of the intensity peaks for several interference bands; 2 – digitizing of the graphical images. The advantage of this kind of the program includes the possibility of simultaneous digital description of the fluctuations for several interference bands in the arbitrary space point.

Results and Discussion

According to the results of the investigations it was found that with an increase of the current density amplitude and frequency of oscillations for the interference band increased as well (fig. 1).

These values were considerably greater for MA-40M membrane at the currents exceeding the limiting diffusion value of i_{lim} by 5-15 times as compared with MA-40 membrane. Quantitative calculation of the amplitude and mean frequency demonstrated that the amplitude of oscillations for the modified membrane MA-40M exceeded the corresponding value of amplitude for MA-40 membrane by 3 times while the mean value of frequency – by 1,5 times. It means more developed convective instability in case of MA-40M membrane. Probably, it is connected with modification of the surface for MA-40 membrane with polyelectrolyte complex that resulted in a decrease of the amount of secondary and ternary amino-groups on the surface of MA-40 membrane and thus caused almost complete suppression of H^+ and OH^- ions emerging at the interphase boundary promoting in a sudden development of electroconvection. Modification of

MA-41 membrane did not result in considerable changes of the fluctuation picture for the interference band as compared with the original sample of MA-41 membrane.

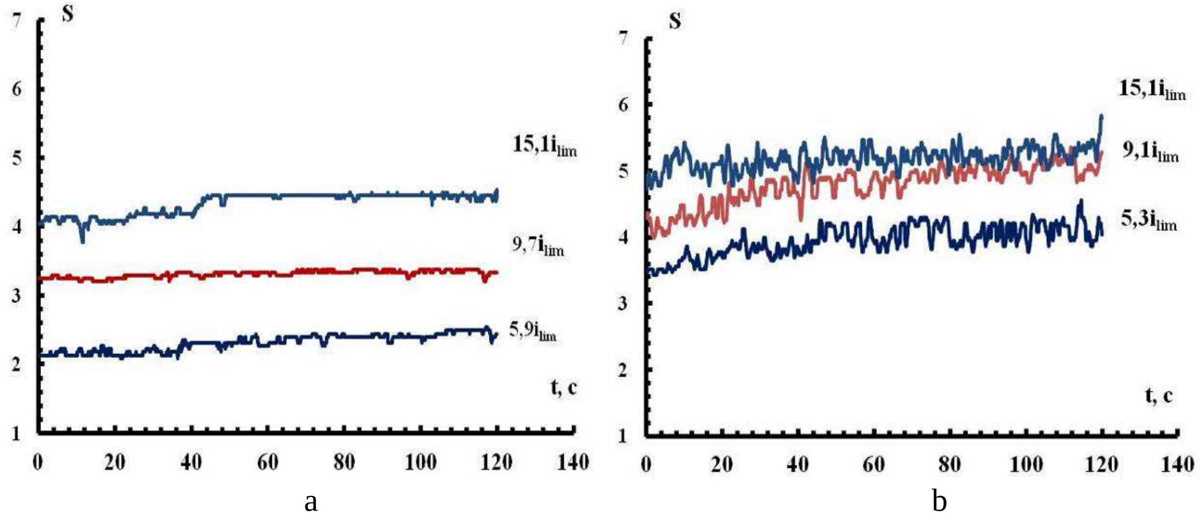

a b

Figure 1. Shift of the interference band with time in solution at the boundary with anion-exchange membrane MA-40 (a) and MA-40M (b); $C_0(NaCl)=2,0\cdot10^{-2}M$*,* $h=2,0\cdot10^{-3}$ *m,* $V=1,34\cdot10^{-3}$ *m/s*

Fourier-analysis that is usually applied for the investigation of noise can provide in making conclusion on the frequency composition of noise averaged over all the time of record for the oscillation process. Calculations of the spectral density *P(f)* was made basing on fast Fourier transform (FFT) for time series of the interference bands fluctuations and the band itself had n characteristic “flicker-noise” dependence of $P(f) \sim f^{-n}$ type. Parameter *n*, characterizing transition in the liquid motion from the laminar flow down to the limit of turbulized one with an increase of the current density was determined as a slope ratio for the high-frequency part of the spectrum. This parameter can vary within the values from 1 to 3; for *n* = 3 a turbulent mixing of solution usually takes place.

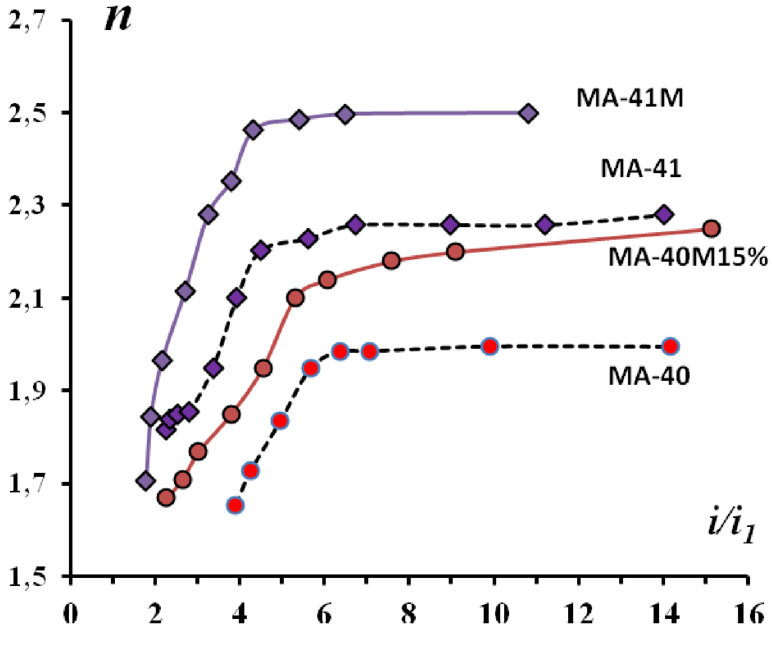

Figure 2. Comparison of the dependences for the parameter n on the overlimiting current density for the membranes of different nature; $C_0(NaCl)=2,0\cdot10^{-2}M$*,* $h=2,0\cdot10^{-3}m$*,* $V=1,34\cdot10^{-3}$ *m/s*

Under increase of the overlimiting current density an increase of the characteristic slope for the part of spectrum was observed as well as an increase of the exponential power *n*.

Comparison of dependences for parameter n on the overlimiting current density for the membranes of different nature demonstrated that the maximum degree of turbulence was observed for the sample of MA-41M membrane modified with polyelectrolyte complex (fig. 2).

The work was performed under financial support of the RFBR grant 12-08-93105-NTsNIL_a.

References

1. *Zabolotskii V.I., Fedotov Yu.A., Nikonenko V.V., Pis'menskaya N.D., Belova E.I., Lopatkova G. Yu.* Patent 2008141949 (Russia). 2008.

COMPARISON OF SINGLE-, OLIGO- AND MANY-PORE ASYMMETRIC MEMBRANES PRODUCED USING SURFACTANT-CONTROLLED ETCHING

[1,2]Katarzyna Zielinska, [1]Alina Gapeeva, [1]Oleg Orelovitch, [1,3]Pavel Apel
[1]Flerov Laboratory of Nuclear Reactions, JINR, Dubna, Russia; *E-mail: apel@nrmail.jinr.ru*
[2]Faculty of Chemistry, Nicolaus Copernicus University, Torun, Poland
[3]The International University "Dubna", Dubna, Russia

Introduction

Nanochannels fabricated in ion-tracked PET membranes have been widely used for resistive-pulse sensing. These structures are able to detect e. g. DNA, proteins and viruses. Among the biological nanopores used for sensing experiments, special attention should be paid to the α-hemolysin. A great reproducibility and unfortunately fragile nature of the lipid bilayer membranes containing the α-hemolysin channel contributed to the development of artificial nanopore alternatives. Studies of the reproducibility of the pores of different geometries and sizes have established that the symmetric track-etched pores are highly homogeneous, conical pores produced using one-step pore-etching process are heterogeneous and conical pores produced using two-step pore-etching procedure are highly homogeneous [1-6]. Formation of asymmetric pores using the surfactant-controlled etching has another specificity, so in this work the issue of asymmetric pores uniformity was studied.

Experiments

Polyethylene terephthalate (Hostaphan RE 5 and RN 12, 5 and 12 μm thick respectively) films were irradiated with Kr, Xe and Au ions of energy 11.4 MeV/u at UNILAC linear accelerator (GSI). The ion-track membranes were subjected to physicochemical treatment. First, the samples were pretreated with UV radiation and then etched chemically in surfactant-doped 5 mol/L NaOH for 6 min 30 sec at 60°C. The etched samples were examined using a JSM-840 and LEO-1530 scanning electron microscopes. Pore profiles were determined via imaging of fractures of membranes. Current-voltage characteristics of the samples were determined using an electrolytic cell with Ag/AgCl electrodes. Each half-cell was filled with KCl solution. The working area of the sample was 0.44 cm^2. The electric current was measured by stepping the voltage between +2 and -2 V with a PC-controlled Hioki 5322 LCR-meter equipped with a shunt resistor.

Results and Discussion

The irradiation of PET membranes with various number of ions and surfactant enhanced etching with asymmetrical pretreatment allowed fabrication of single-, 10- and $1.5 \cdot 10^3$-pores (Fig. 1) in which the tip is bullet-like in shape and the rest of the channel is a cylinder (Fig. 2).

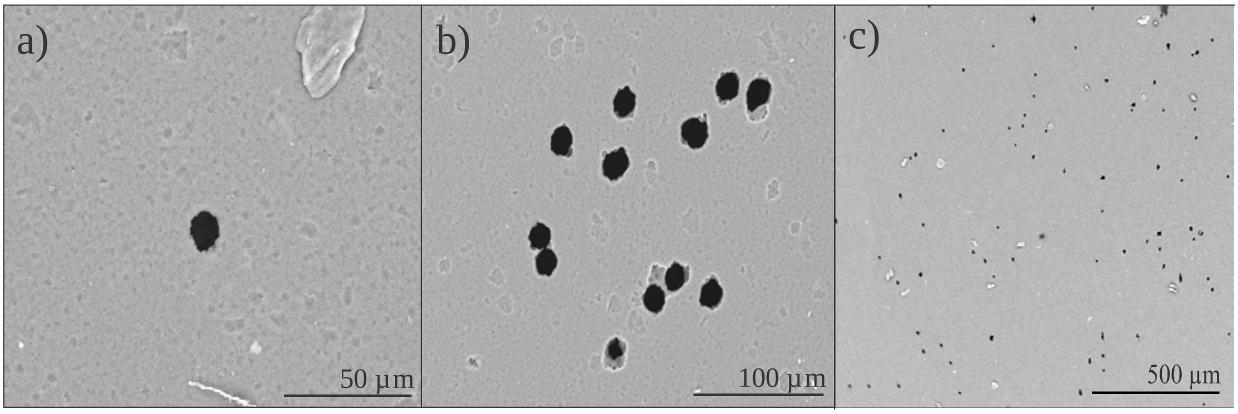

Figure 1. SEM images of the surfaces of a single- (a), 12-pore- (b) and $1.5 \cdot 10^3$-pore (c) membranes with thickness of 12 μm

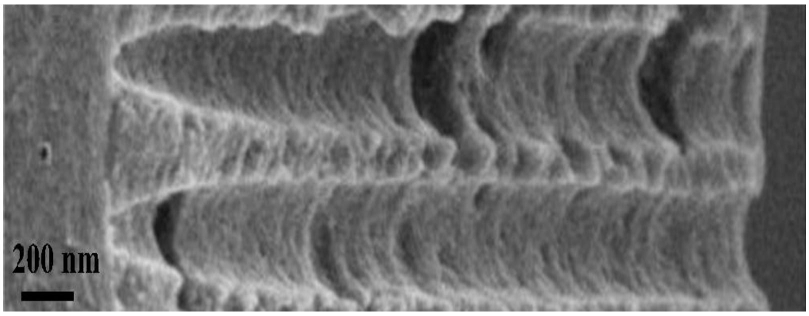

Figure 2. Cross-section of channels etched in 5 M NaOH for 6 min 30 sec at 60ºC. The pore density of membrane is $5 \cdot 10^7$ pores/cm^2 and the foil thickness is 5 μm. The sample is tilted at an angle of 60º

It is known, that the base diameter of nanopores is independent of the track density and for all samples prepared under the same conditions is identical. For samples etched in surfactant-doped 5 mol/L NaOH for 6 min 30 sec the base diameter determined from the SEM images was found equal to 230 nm [7]. At low and moderate KCl concentrations, the individual pores with bullet-like tip exhibit substantially heterogeneous, non-linear current-voltage characteristics. At high electrolyte concentrations, almost symmetric current-voltage responses were recorded. The maximum rectification ratio for all membranes was observed at electrolyte concentrations of 0.07-0.2 mol/L. This indicates that the tip diameter of the pore is mainly responsible for the ionic selectivity. In comparison with the membranes containing many pores [7], the single-pore samples showed the higher rectification effect. It is probably due to structural defects (large pores) in the many-pore samples which lower the ionic selectivity.

Table 1. Rectification ratios I(-1V)/I(+1V) at different KCl concentrations and effective pore diameters (d_{eff}) for 10- and $1.5 \cdot 10^3$-pore membranes with thicknesses of 12 μm. The effective pore diameter is defined as the diameter of a cylindrical pore having the same electrical conductance in 1 mol/L KCl at ±0.1 V

	rectification ratio (r)							
C_{KCl} [mol/L]	10-pore membranes			$1.5 \cdot 10^3$-pore membranes				
	1	2	3	1	2	3	4	5
0.01	9.9	5.2	2.2	2.9	6.6	6.9	4.0	5.0
0.03	27.3	17.2	4.3	6.6	12.3	10.8	7.9	7.3
0.05	30.7	21.8	5.3	12.6	15.5	11.5	12.6	8.1
0.07	34.0	21.2	6.8	15.7	15.0	10.4	14.4	9.2
0.1	30.6	20.4	9.2	20.0	15.9	10.2	15.4	9.4
0.2	26.2	14.6	8.2	15.7	11.5	6.2	11.1	6.9
0.4	19.9	6.8	4.4	9.3	6.8	3.4	5.7	4.6
1.0	5.6	2.1	1.5	3.4	2.7	1.8	2.2	2.3
3.0	1.9	1.6	1.6	1.3	1.3	1.2	1.3	1.3
d_{eff} [nm]	**213**	**249**	**217**	**275**	**247**	**259**	**256**	**242**

In this work we also studied the ionic transport properties of PET membranes with thickness of 5 μm containing one and $2.5 \cdot 10^3$ pores. Compared with data obtained for 12-μm-thick membranes (Table 1), the higher scatter of rectification ratios and effective pore diameter was observed for thinner membranes. It means that in the shorter channels the highly-tapered tip of the nanopore has greater contribution to the resistance. The rectification ratio values for single- and multi-pore membranes in all electrolyte concentrations were lower than in the case of single- and multi-pore ones with thickness of 12 μm. It is because of the reduction in the pore length which is associated with a decrease in geometric asymmetry [6].

As it can be seen, a surfactant-controlled etching method used in this work for the creation of asymmetric nanopores in single-, few- and multi-pore membranes allows to control with good reproducibility the base diameter of the nanopore. The scatter of rectification ratios at different KCl concentrations for all investigated single-pore membranes can be caused by e. g. the differences in pore mouth diameter, the differences in the form of the pore or heterogeneous surface charge distribution in the nanochannels. It can be attributed to irregularities in polymer, which is known to consist of both crystalline and amorphous regions of the nanoscale dimensions. Previous study [7] has noticed that even small differences in the tip diameter of the pore (Fig. 3) can lead to the large differences in the rectification ratio values. The aim of our future work is to find a correlation between the rectification ratio and tip diameter of the pore.

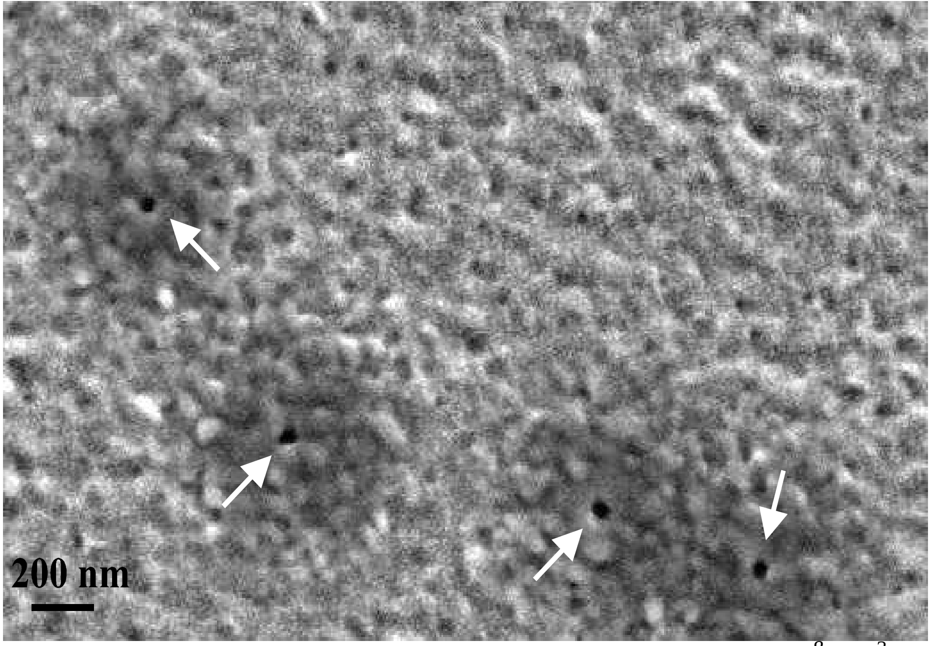

Figure 3. FESEM image of membrane selective side (pore density of $1 \cdot 10^8$ cm^{-2}). The arrows indicate pore openings

Partial financial support from the Russian Ministry of Education and Science (contract No 14.513.11.0063) and JINR grant no. 13-502-01 is appreciated. The authors thank the Material Research group (GSI) for providing irradiated samples.

References

1. *Wharton J. E., Jin P., Sexton L. T, Horne L. P., Sherrill S. A., Mino W. K., Martin C. R.* // Small 2007. V. 3. P. 1424-1430.
2. *Maglia G., Restrepo M. R., Mikhailova E., Bayley H.* // Proc. Natl. Acad. Sci. U.S.A. 2008. V. 105. P. 19720.
3. *Apel P. Y., Korchev Yu. E., Siwy Z., Spohr R., Yoshida M.* // Nucl. Instr. Meth. Phys. Res. B. 2001. V. 184. P. 337-346.
4. *Kowalczyk S. W., Blosser T. R., Dekker C.* // Trends Biotechnol. 2011. V. 29. P. 607-614.
5. *Kasianowicz J. J., Brandin E., Branton D., Deamer D. W.* // Proc. Natl. Acad. Sci. U.S.A. 1996. V. 93. 13770.
6. *Zhou Y., Chen Ch., Baker L. A.* // Anal. Chem. 2012. V. 84. P. 3003-3009.
7. *Apel P. Y., Blonskaya I. V., Orelovitch O., Ramirez P., Sartowska B.* // Nanotechnology 2011. V. 22. P. 175302.

DETERMINATION OF NANOFILTRATED MEMBRANE MASS TRANSFER RESISTANCE AFTER SEPARATION OF WHEY

Yuriy Zmiyevskiy, Ivanna Kyrychuk, Valeriy Myronchuk
National University of Food Technologies, Kyiv, Ukraine, *E-mail: yrazm@meta.ua*

Introduction

Nanofiltration is a baromembrane process which is widely used in various industries, particularly in the food industry. If to compare it with reverse osmosis it is characterized by high performance, lower power consumption and, moreover, it allows separating monovalent ions of polyvalent and macromolecular compounds [1]. Such advantage is the main reason for development of new whey processing technologies by using nanofiltration [2, 3]. While concentrating solids partial demineralization of whey, first of all, reduces the amount of moisture evaporated in a vacuum evaporator, and with its further processing improves the crystallization of lactose [4], which, in turn, reduces energy consumption during its spray drying [5], and secondly, treating this whey on electrodialysis for deep demineralization is recommended [6], as it increases the electrical conductivity and decreases the liquid volume which requires a smaller pump that positively affects the power consumption of such treatment [7].

However, fouling of membrane during separation of liquid medias is unavoidable, this leads to growing of membrane mass transfer resistance and, consequently, to decreasing its effectiveness. The reason for this, in most cases, is the concentration polarization, adsorption, gelling, sealing or blocking of pores [8]. There is no data in the scientific literature concerning mass transfer resistance of nanofiltrated membrane OPMN-P after separation of whey, which requires a special research.

Therefore, the aim of this paper was to determine the value of mass transfer resistance of nanofiltrated membrane OPMN-P after separation of whey because this is an important indicator in assessing the level of membrane fouling.

Experiments

Pretreatment of the new membrane OPMN-P (JSC STC "Vladipor", Russia) was by filtering distilled water at the operating pressure of 2.5 MPa to adjust a stable performance. Experiments were conducted on a laboratory unit. The effective membrane area was $4{,}3 \cdot 10^{-3}$ m^2.

Results and Discussion

The distilled water flux of the new membrane at a pressure of 2.5 MPa was 190.24 $dm^3/(m^2h)$. Dynamic viscosity of water at 20°C was $1004\ 10^{-6}$ Pa s. Resistance membrane R_m, was calculated, which was $4{,}7\ 10^{13} m^{-1}$for membrane OPMN-P under the mention conditions.

It was found out that whey flux of the new membrane was lower; this can be explained by sorption of whey components and by active formation of dynamic membrane on it. After reaching a concentration factor value of 1.25 the flux started to decrease more slowly due to the established dynamic equilibrium in the system. After the experiment the unit was filled by distilled water and was left for 10 minutes with mixer on. The distilled water was refilled and the flux volume was determined. It was around 30.44 $dm^3/(m^2h)$ under those conditions. This value was slightly lower than the initial flux while whey separation. General resistance, R_t, and mass transfer resistance, R_f, of adsorbed components of whey on membrane were calculated. Their values were $R_t = 29{,}5 \cdot 10^{13}$ m^{-1}, $R_f = 24{,}7 \cdot 10^{13}$ m^{-1}. As we can see, whey components had almost 5 times more resistance than membrane. Then this membrane was removed and washed, the surface was cleaned manually under running distilled water, and flux was tested again, on both distilled water and whey. Those procedures were repeated twice after which the active layer of membrane was damaged. The data are presented in Table. 1.

Based on the data achieved, we see that the flux of nanofiltrated membranes was considerably restored after mechanical cleaning. Obviously, most of the contaminants are adsorbed on the membrane surface and only a small portion enters into the pores. However, this assumption is not confirmed experimentally. During whey separation on the washed membrane we noticed that the flux was larger. It is obvious that the new membrane has a certain surface charge which leads to intense absorption of the dissolved components which in turn creates significant resistance of mass transfer. By mechanical cleaning we washed the fouling layer that was not in direct contact with the membrane surface; that affects the redistribution of the membrane surface charge and the subsequent intensity of the whey separation adsorption process. However, to confirm the above additional studies are needed to be conducted.

Table 1. Specific Membrane Capacity And Mass Transfer Resistance Values

	J, $dm^3/(m^2 h)$	**R_t, m^{-1}**	**R_f, m^{-1}**
New membrane	190,24	4,7·1013	0
After nanofiltration of whey	30,44	29,4·1013	24,7·1013
After nanofiltration of whey + mechanical cleaning	170,83	5,2·1013	0,5·1013
After 2 cycles of nanofiltration of whey + 2 cycles of mechanical cleaning	139,51	6,4·1013	1,7·1013
After 3 cycles of nanofiltration of whey + 3 cycles of mechanical cleaing	149,47*	6,0·1013	1,3·1013

*active layer of membrane was damaged

Repeated washing showed that R_f was increased almost three times (Table 1), although the flux of separating whey remained at the same level. The authors [9] also noticed the increase in mass transfer resistance when ultrafiltrating coconut water by number of repeated experiments. Therefore, an important step in the developing industrial technologies is a study of nanofiltrated membranes regeneration process by chemical reagents, for instance.

Summary

It was found out that mass transfer resistance of the new nanofiltrated membrane OPMN-P (JSC STC "Vladipor, Russia") at the pressure of 2.5 MPa is $R_m = 4,7 \cdot 10^{13}$ m^{-1}, however, this figure rises to 6.25 times after whey separation and the overall mass transfer resistance reaches $Rt = 29,4 \cdot 10^{13}$ m^{-1}. Mechanical cleaning of the membrane surface, though, restores the flux but leads to rapid membrane damage. The study of nanofiltrated membranes regeneration process after whey separation using chemical reagents is promising.

Referenes

1. *Encyclopedia of membranes*: at 2 v / [comp. Bryk M.T.]. - K.: Vyd. Dim "Kiev-Mohyla Academy", 2005. - Vol.1. - 2005. - 658 p.
2. *Hinkova A., Zidova P., Pour V., Bubnik Z., Henke S., Salova A., Kadlec P.* // Procedia Engineering. 2012. V. 42. P. 1554-1565.
3. *Atra R., Vatai G., Bekassy-Molnar E., Balint A.* // J. Food Engineering. 2005. V. 67. P. 325-332.
4. *Guu Y. K., Zall R.* // Journal of Food Science.1992. V.57 (3). P. 735-739.
5. *Kong F., Liu L., Sun Z., Li H., Lu J.* // Nongye Gongcheng Xuebao/Transactions of the Chinese Society of Agricultural Engineering, 2010. V. 26(12). P. 363-366 (in Chinese).
6. *Simova H., Kysela V., Cernin A.* 2010. // Desalination and Water Treatment. 2010. V.14. P. 170-173.
7. *Bazinet L.* 2005. // Critical Reviews in Food Science and Nutrition. 2005. V.45 (4). P. 307-326.
8. *Mulder M.* Introduction to membrane technology [Trans. from English., edited by Yampolskiy Y.P. and Dubyaga V.P.]. - Moscow: Mir. - 1999. - 513 p.
9. *Jayanti V.K., Rai P., Dasgupta S., De S.* // Journal of Food Process Engineering. 2010. V. 33. P. 128–143.

ONE-STEP AND ONE-POT METHOD FOR SYNTHESIS OF HYBRID COMPOSITE METAL-POLYPYRROLE-CARBON (ME/PPY/C) NANOMATERIALS AND THEIR APPLICATION IN CATALYSIS

[1]Ekaterina Zolotukhina, [1,2,3]Mikhail Vorotyntsev, [3]Igor Bezverkhyy,
[4]Veronika Zinovyeva, [1]Andrey Belmesov
[1]Institute of Problems of Chemical Physics Russian Academy of Sciences, Chernogolovka, Russia
E-mail: ks-chem@mail.ru
[2]Moscow State University, Moscow, Russia
[3]University of Burgundy, Dijon, France
[4]University of Paris 11, Paris, France

Introduction

A one-step and one-pot method to design composite nanomaterials based on conjugated polymer, polypyrrole, and palladium nanoparticles by the redox-reaction of the monomer and a palladium salt in non-aqueous and aqueous media was described previously in the works of our team [1-3].

These composite materials were successfully tested as heterogeneous catalysts for the most known organic syntheses (Suzuki reaction, direct C–C conjugation, Sonogashira reaction, etc.) and showed excellent catalytic activity. This fact made such materials interesting for further investigation. On the other hand, monodisperse palladium and platinum nanoparticles incorporated inside electroactive polymers are most interesting materials for electrochemical applications in fuel cells, sensor devices etc.

The aim of this work is to develop a one-step and one-pot method for preparing hybrid composite materials that combine the advantages of palladium (or platinum)-polypyrrole composite materials and microscopic size of the support, carbon nanoparticles and nanotubes.

Experiments, Results and Discussion

For the synthesis of palladium-polypyrrole-carbon particles (Pd/PPy/C) or carbon nanotubes (Pd/PPy/CNT) hybrid materials, we used the carbon powder (30-40 nm particles according to AFM data) or carbon nanotubes (Bayer, diameter of multiwall nanotubes was 10-25 nm according to TEM), solution of tetraamminepalladium(II) dichloride, and aqueous pyrrole solution. The reaction mixtures were ultrasonicated for 5 days, for 5 h a day. Then, the mixtures were kept under stationary conditions at ambient temperature until spontaneous precipitation of colloids on the tenth day.

The amount of carbon powder (and nanotubes) was selected so that the carbon support surface was completely covered with a composite material layer 10-15 nm thick taking into account previously obtained data on the formation of palladium-polypyrrole composites in the absence of carbon particles.

The formation of colloidal solutions of composite and hybrid materials was monitored by UV-Vis spectroscopy. The spectrum of the oxidant in the presence or in the absence of carbon nanoparticles in solution indicates that the possible adsorption of palladium (II) complex onto the carbon particle surface does not change markedly its concentration in solution. Furthermore, this solution is unstable, and sedimentation of carbon particles is observed during several hours after exposure to ultra-sound has been ceased; similar picture is observed for nanotubes. The low stability of colloidal solution of reaction mixture is explained by the low values of zeta potential obtained by dynamic light scattering.

The IR-spectra of hybrid composite materials and palladium-polypyrrole composites without carbon support are similar. This fact indicates that the redox-reaction between Pd(NH3)4Cl2 and pyrrole in the presence of carbon particles leads to formation of polypyrrole with the same structural features as in the absence of carbon particles.

The morphology of resultant composite materials was studied by transmission electron microscopy (Fig.1). The surface of initial carbon particles is completely coated with a layer of the palladium–polypyrrole composite. The composite shell of carbon powder is large: the composite layer on the surface of carbon particles is an agglomerate of globules of ~40–50 nm in diameter. The strong agglomeration of globules provides no opportunity to accurately determine their size. The ~10-nm thick composite layer surrounds the carbon particles and their agglomerates that are less permeable for electrons. Palladium particles with average size of 1.8 nm in diameter are present inside the modified layer. A slightly different situation is observed for carbon nanotubes. The palladium–polypyrrole composite produces a 10-nm thick layer that evenly surrounds a separate nanotube. The average size of palladium particles in this case remains unchanged. Table shows the data of elemental HCNS analysis for powders of hybrid composite materials.

Table. Elemental Composition of Palladium–Polypyrrole–Carbon Support Composites (wt %)

System	C	N	H	Pd
Pd/PPy	33.0	13.3	3.4	33.5
Pd/PPy/C	41.4	13.6	2.8	28.0
Pd/PPy/CNT	46.8	10.3	2.3	26.0

It is seen that the nitrogen and hydrogen percentages in two samples, which indicate the polypyrrole content, differ insignificantly. The change in the element content as compared with the palladium-polypyrrole composite without carbon support appears mainly as a growth of carbon content.

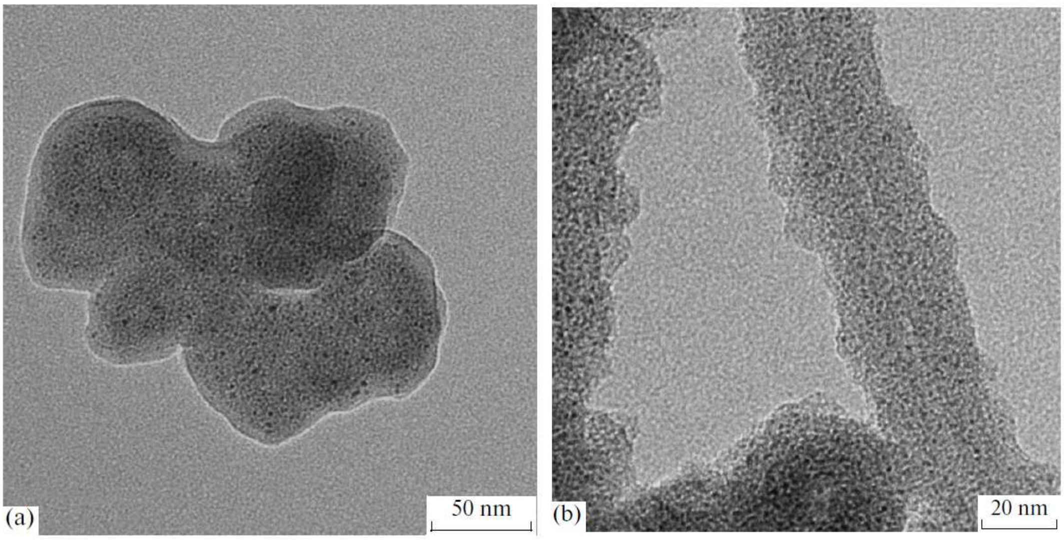

Figure 1. TEM Images of Hybrid Nanocomposites (a) Pd/PPy/C and (b) Pd/PPy/CNT [4]

The presence of palladium (or platinum) and the absence of chlorine in the studied materials are confirmed by energy-dispersive analysis and X-ray photoelectron spectroscopy.

The same synthetic procedure was used for preparation of Pt/PPy composites. In this case the time of synthesis was longer (about 15 days). Colloid solutions without carbon particles are more stable for palladium containing composites whereas sedimentation of Pt-containing composition is much faster. The amount of Pt inside of polypyrrole globules (according to TGA) was 22-25 wt %.

Thus, we have developed the procedure of one-step and one-pot synthesis of hybrid composite metal–polypyrrole–carbon particles nanomaterials where the metal–polypyrrole composite forms layer on the surface of the carbon support in the course of redox polymerization. The composite layer on the carbon support surface in the resulting hybrid materials has the same structure and chemical composition as composites prepared without carbon particles. At the same time, the considerably larger size of the support (the length of carbon nanotubes is in the micrometer range) allows the obtained composites to sediment quickly from solution.

Acknowledgments

This work was supported by the Ministry of Education and Science of the Russian Federation (project no. 2012-1.1-12-000-1012-441, agreement 8373) and the Russian Foundation for Basic Research (projects no. 12-03-00797 and 12-03-31746). The authors also thank Conseil Regional de Bourgogne, CNRS, and Universite de Bourgogne for support.

References

1. *Vasilyeva, S.V., Vorotyntsev, M.A., Bezverkhyy, I.*, et al. // J. Phys. Chem. C. 2008. V. 112. P. 19878-19885.
2. *Zinovyeva, V.A., Vorotyntsev, M.A., Bezverkhyy, I.*, et al. // Adv. Funct. Mater. 2011. V. 21. P. 1064-1075.
3. *Magdesieva, T.V., Nikitin, O.M., Levitsky, O.A.*, et al. // J. Mol. Catal. A: Chem. 2012. V. 50. P. 353-354.
4. *Zolotukhina E.V., Vorotyntsev M.A., Zinovyeva V.A.*, et al. // Doklady Physical Chemistry. 2013. V. 449 (2). P. 63-65.

EFFECT OF THERMAL OR CHEMICAL TREATMENT ON HYDROPHOBICITY OF ION-EXCHANGE MEMBRANES

[1]Kseniya Nebavskaya, [1]Nataliya Pis'menskaya, [1]Nadezhda Mel'nik, [2]Vera Vasil'eva, [1]Andrei Nebavskii, [1]Veronika Sarapulova, [2]Elmara Akberova

[1]Kuban State University, Krasnodar, Russia. Email: littlegreenchemist@yandex.ru

[2]Voronezh State University, Voronezh, Russia

Introduction

The hydrophilic-hydrophobic balance on the surface of materials has an important effect on their properties. In particular, increasing surface hydrophobicity facilitates the slip of fluid over the membrane surface that results in enhancing ion transfer in membrane system. There are numerous methods of membrane surface treatment, which leads to providing specific properties including an increase in hydrophobicity [1]. Among these methods, there are membrane treatment under elevated temperatures, by using acid or alkali solutions. While the response of membrane properties on such type of treatment were already studied extensively [2], there is still not enough understanding of the mechanisms of changes in membrane characteristics.

The aim of this work is to study the effect of membrane treatment under elevated temperature and/or with aggressive solutions on the hydrophobicity of several commercial ion exchange membranes.

Experiments

Commercial Nafion 117 membrane and some other Nafion materials, as well as a MK-40 membrane and anion exchange MA-40 and MA-41 membranes were studied. The Nafion materials besides an unmodified native Nafion 117 membrane, included a Nafion 117 membrane modified with Nafion film layer doped with carbon nanotubes [1], and Nafion film on polymethylmethacrylate (PMMA). The Nafion film was created by casting 5% Nafion solution in isopropyl alcohol on polished and degreased PMMA surface. All membranes were initially dry and then transferred in Na^+ form using standard salt pretreatment.

The contact angles were measured according to the early developed method [3]; electrochemical properties were studies using the experimental apparatus and method, described in [1]. Micrographs of surface of MA-40 and MA-41 membranes were obtained using raster electron microscopy at JSM-6380 LV microscope (Japan) equipped with energy dispersive spectrometer and regulated pressure (EDS RP).

The kinetic dependencies of contact angles were measured for the samples in the following conditions: dry native sample, hydrated native sample, sample after thermal treatment at 100^oC, and sample treated with aggressive media – Nafion membranes underwent oxidizing-thermal treatment as described in [2], MA-40 and MA-41 were boiled in 5.0 M NaOH solution or 2.5 M H_2SO_4 solution during 50 hrs.

Results and Discussion

From all studied native membranes Nafion was the most hydrophobic with contact angle 82^o, followed by MA-41 (59^o), MK-40 (52^o) and MA-40 (48^o). This is understandable, since Nafion membrane is homogeneous and it contains highly hydrophobic perfluorinated matrix while the MA-41 and MA-40 are heterogeneous with polyethylene used as an inert binding agent. Nafion film on PMMA possesses much higher contact angle of 100^o. Nafion membranes modified with highly hydrophobic carbon nanotubes (contact angle 130^o) were found highly hydrophilic with contact angle 51^o. Hydrated samples were less hydrophobic, with contact angle of Nafion 117, MA-41, MK-40, MA-40 membranes and Nafion film becoming equal to 68^o, 50^o, 60^o, 44^o and 68^o, correspondingly. It should be noted that neither for dry nor for hydrated native samples no contact angle dependence on duration of experiment was found.

After the boiling the contact angles for all samples significantly decreased. This way contact angles for dry Nafion 117, MA-41, MK-40 and MA-40 membranes and Nafion film became equal to 68^o, 30^o, 30^o, 34^o and 86^o, correspondingly. It is of interest that Nafion film became crannied after the boiling and completely deteriorated after the swelling of sample. Moreover, in case of membranes the contact angle value becomes dependent on the time of measurement: it drops rapidly during the first 5 seconds of measurements, reaching later a plateau; it isn't observed in case of film.

To explain these facts let us consider the nature of ion exchange materials. It is widely known that they all possess a microstructure: hydrophilic fixed groups are united in hydrophilic clusters, while hydrophobic clusters are forming crystallites. From the principle of minimization of free surface energy it is possible to conclude that at the standard conditions materials are covered with a thin layer of hydrophobic (low-energy) groups. Low mobility of polymer chains at ambient temperatures prevents the quick access to hydrophilic groups. However, during the boiling of membrane its chains can reorient, so some of hydrophilic groups start facing the external media.

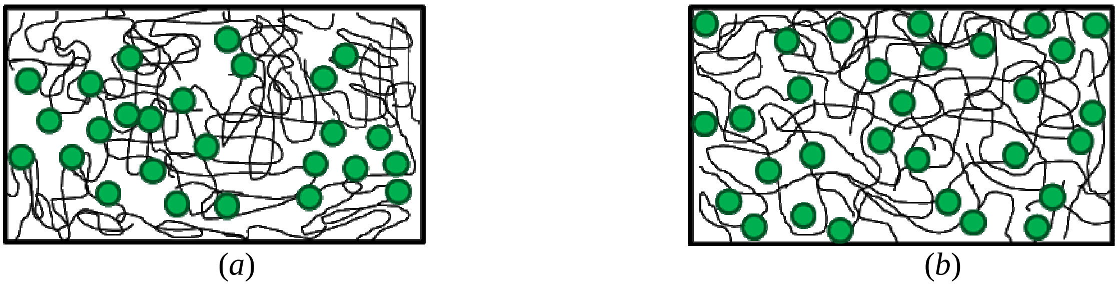
(*a*) (*b*)

Figure 1. Distribution of hydrophobic chains (dark lines) and hydrophilic groups (green circles) in ion exchange material before (a) and after (b) its boiling

Moreover, structural changes in the boiled membrane facilitate the movement of chains, so for the treated samples the process called the reorientation of polymer chains becomes possible. During this process the hydrophilic groups became drawn to droplet of water, applied at the surface of the sample.

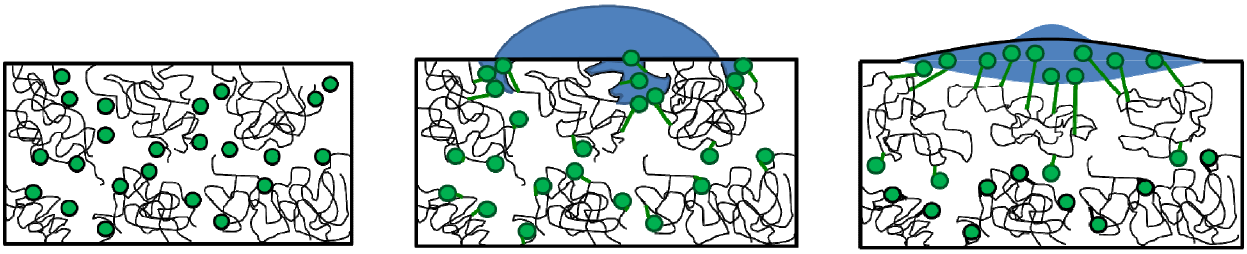

Figure 2. Scheme of polymer reorientation. From left to right: boiled sample; boiled sample during the first 5 s of contact angle measurements; boiled sample after prolonged contact with droplet of liquid

Similar orientation of polymer chains occurs in case of modified membrane. When nanotubes are dispersed in Nafion solution, they are covered with hydrophobic segments of Nafion chains. Hence, the hydrophilic groups are faced to outside media and stay there during the drying of modifier, so the hydrophobicity of modified membrane decreases compared to native one. When such membrane functions in an electrodialysis apparatus, however, the polymer chains become washed away from the surface of nanotubes, exposing them and raising the hydrophobicity of membrane, making its contact angle equal 81^{o}.

These data agree well with our theory [2] that the overlimiting mass transfer rate through an ion-exchange membrane is strongly affected by the degree of its surface hydrophobicity. Generally the more hydrophobic the surface, the more intensive is the overlimiting transfer, as it shown in Figure 3.

The reason of differences of properties of Nafion film lays in its thickness. Its chains can't move in all three directions equally even after boiling, hence no reorientation occurs for this sample. When the film becomes heated, its 2D structure becomes unstable, leading to degradation of film.

In case of treatment of membranes with acidic and alkaline solutions no changes in contact angle were observed for the MA-40 and MA-41 membranes boiled in 5 M NaOH solution during 50 hrs. However, for the same membranes boiled in 2.5 M H_2SO_4 significant change in a kinetic dependence of contact angle was observed. The liquid quickly permeated the membrane, so after the first ten seconds of experiment no sign of applied drop could be observed. As suggested, this change could be connected with the increased porosity of the membranes, namely the gain in the radius of macropores. Using the methodic [4] and micrographs of surface of samples it was found that the weighted mean radius of macropores at the membrane surface increased on 55% compared to native surface.

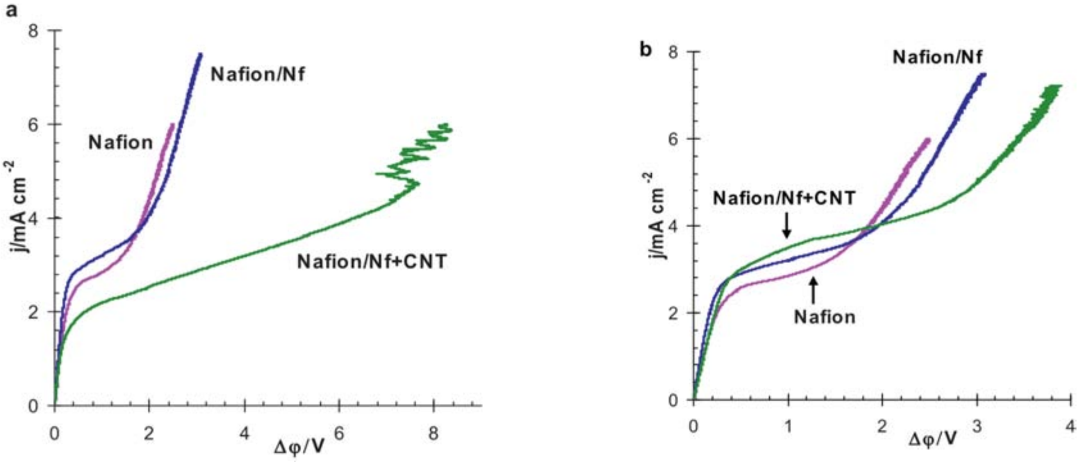

Figure 3. Current–voltage characteristics of a commercial Nafion^{TM} 117 membrane and its modifications: (a) “fresh” membranes not operated under electric current; (b) membranes after 100 h of operation under a current density $i = 1.5i_{lim}$.

This way it was found that the behavior of ion exchange material at its contact with water depends on conditions of material pretreatment. During the thermal treatment of an ion exchange materials mobility of their chains increases, decreasing their hydrophobicity and enabling their reorientation.

Acknowledgements

Part of this investigation was realized within French-Russian laboratory "Ion-exchange membranes and related processes". The authors are grateful to RFBR, Russia (grants 12-08-00188-a, 13-08-01168)

References

1. *E.D. Belashova, N.A. Melnik, N.D. Pismenskaya, K.A. Shevtsova, A.V. Nebavsky, K.A. Lebedev, V.V. Nikonenko*. Overlimiting mass transfer through cation-exchange membranes modified by Nafion film and carbon nanotubes // Electrochim. Acta. 2012. V. 59, P. 412-423.
2. *N.P. Berezina, S.V. Timofeev, N.A. Kononenko*. Effect of conditioning techniques of perfluorinated sulphocationic membranes on their hydrophylic and electrotransport properties // J. Membr. Sci. 2002. V. 209. P. 509–518.
3. Patent № 124786, IPC (8) G01B11/26 (2006.01) G01N13/00 (2006.01). / *Nebavskaya K.A., Nebavsky A.V., Nikonenko V.V., Belova E.I.* (Krasnodar, RF); the applicant and the patent owner: Kuban State University, RU; 20.09.2012.
4. *E.A. Sirota, V.I. Vasil’eva, E.M. Akberova*. Certificate of state registration of PC program. 2012619723 (Ru). Government Funded Organisation of Higher Professional Education «Voronezh State University». 26.10.2012.